PB80-226723

Sediments of Southern Lake Huron Elemental Composition and Accumulation Rates

Michigan Univ.
Ann Arbor

Prepared for

Environmental Research Lab.
Duluth, MN

Aug 80

U.S. Department of Commerce
National Technical Information Service
NTIS

United States
Environmental Protection
Agency

Environmental Research
Laboratory
Duluth MN 55804

EPA-600/3-80-080
August 1980

Research and Development

PB80-226723

EPA

Sediments of Southern Lake Huron

Elemental Composition and Accumulation Rates

REPRODUCED BY
NATIONAL TECHNICAL
INFORMATION SERVICE
U. S. DEPARTMENT OF COMMERCE
SPRINGFIELD, VA. 22161

RESEARCH REPORTING SERIES

Research reports of the Office of Research and Development, U.S. Environmental Protection Agency, have been grouped into nine series. These nine broad categories were established to facilitate further development and application of environmental technology. Elimination of traditional grouping was consciously planned to foster technology transfer and a maximum interface in related fields. The nine series are:

1. Environmental Health Effects Research
2. Environmental Protection Technology
3. Ecological Research
4. Environmental Monitoring
5. Socioeconomic Environmental Studies
6. Scientific and Technical Assessment Reports (STAR)
7. Interagency Energy-Environment Research and Development
8. "Special" Reports
9. Miscellaneous Reports

This report has been assigned to the ECOLOGICAL RESEARCH series. This series describes research on the effects of pollution on humans, plant and animal species, and materials. Problems are assessed for their long- and short-term influences. Investigations include formation, transport, and pathway studies to determine the fate of pollutants and their effects. This work provides the technical basis for setting standards to minimize undesirable changes in living organisms in the aquatic, terrestrial, and atmospheric environments.

This document is available to the public through the National Technical Information Service, Springfield, Virginia 22161.

1A

TECHNICAL REPORT DATA

(Please read Instructions on the reverse before completing)

1. REPORT NO.
EPA-600/3-80-080

2.

3. RECIPIENT'S ACCESSION NO.
PB 80 226723

4. TITLE AND SUBTITLE
Sediments of Southern Lake Huron: Elemental Composition and Accumulation Rates

5. REPORT DATE
August 1980 Issuing Date.

6. PERFORMING ORGANIZATION CODE

7. AUTHOR(S)
John A. Robbins

8. PERFORMING ORGANIZATION REPORT NO.

9. PERFORMING ORGANIZATION NAME AND ADDRESS
Great Lakes Research Division
The University of Michigan
Ann Arbor, Michigan 48109

10. PROGRAM ELEMENT NO.
1BA769

11. CONTRACT/GRANT NO.
Grant R 803086

12. SPONSORING AGENCY NAME AND ADDRESS
Environmental Research Laboratory-Duluth
Office of Research and Development
U.S. Environmental Protection Agency
Duluth, Minnesota 55804

13. TYPE OF REPORT AND PERIOD COVERED
Final

14. SPONSORING AGENCY CODE
EPA/600/03

15. SUPPLEMENTARY NOTES
Project Officer: Michael D. Mullin, ERL-Duluth, Grosse Ile, MI 48138

16. ABSTRACT

It is widely recognized that most metal contaminants in lakes are primarily associated with particulate matter and are conveyed to underlying deposits in association with fine-grained materials such as organic debris, hydroxides of iron, and manganese or clay minerals. In the Great Lakes the fine-grained sediments and associated contaminants are not deposited uniformly over the bottom but are confined to "pockets" or depositional basins which are of more limited extent and generally found in deeper areas of each lake. This report describes the composition and rates of accumulation of metal contaminants in the depositional basins of southern Lake Huron.

Results of this study include: (1) recognition of the role of sediment mixing by benthic organisms in modifying metal contaminant and radioactivity profiles, (2) estimates of the rates of accumulation of metal contaminants in these depositional basins, (3) identification of which metals are contaminants and their degree of surface enrichment, and (4) limited comparisons of accumulation rates with lake loadings.

17. KEY WORDS AND DOCUMENT ANALYSIS

a. DESCRIPTORS	b. IDENTIFIERS/OPEN ENDED TERMS	c. COSATI Field/Group
Sediments Benthos Metals	Lake Huron Particulate matter Depositional basins Accumulation rates Loading rates	08/H

18. DISTRIBUTION STATEMENT
Release to the public

19. SECURITY CLASS *(This Report)*
Unclassified

20. SECURITY CLASS *(This page)*
Unclassified

21. NO. OF PAGES

22. PRICE

EPA Form 2220-1 (9-73)

☆ U.S. GOVERNMENT PRINTING OFFICE: 1980--657-155/[illegible]

EPA-600/3-80-080
August 1980

SEDIMENTS OF SOUTHERN LAKE HURON:
ELEMENTAL COMPOSITION AND ACCUMULATION RATES

by

John A. Robbins
Great Lakes Research Division
The University of Michigan
Ann Arbor, Michigan 48109

Grant No. R803086

Project Officer

Michael D. Mullin
Large Lakes Research Station
Environmental Research Laboratory-Duluth
Grosse Ile, Michigan 48138

ENVIRONMENTAL RESEARCH LABORATORY--DULUTH
OFFICE OF RESEARCH AND DEVELOPMENT
U.S. ENVIRONMENTAL PROTECTION AGENCY
DULUTH, MINNESOTA 55804

i3

DISCLAIMER

This report has been reviewed by the Environmental Research Laboratory-Duluth, U.S. Environmental Protection Agency, and approved for publication. Approval does not signify that the contents necessarily reflect the views and policies of the U.S. Environmental Protection Agency, nor does mention of trade names or commercial products constitute endorsement or recommendation for use.

FOREWORD

The presence of hazardous materials in the environment is a topic of major interest to the Environmental Protection Agency. Most metal contaminants in lakes are primarily associated with particulate matter and are conveyed to underlying deposits in association with fine-grained materials such as organic debris, hydroxides of iron, and manganese or clay minerals. In order to develop an understanding of this sedimentation process, it is necessary to determine the amounts and locations of these sediments.

This report describes the composition and rates of accumulation of metal contaminants in the depositional basins of southern Lake Huron. Appendix A appears in a separate volume, which is available from National Technical Information Services (NTIS).

Norbert Jaworski, Ph.D
Director
Environmental Research Laboratory
Duluth

ABSTRACT

It is widely recognized that most metal contaminants in lakes are primarily associated with particulate matter and are conveyed to underlying deposits in association with fine-grained materials such as organic debris, hydroxides of iron, and manganese or clay minerals. In the Great Lakes the fine-grained sediments and associated contaminants are not deposited uniformly over the bottom but are confined to "pockets" or depositional basins which are of more limited extent and generally found in deeper areas of each lake. This report is the first in a series of three comprehensive reports which describes the composition and rates of accumulation of metal contaminants in the depositional basins of Lake Huron. This first report deals with the two principal depositional basins in southern Lake Huron: the Port Huron basin and the Goderich basin.

Over a period of a year (1974-1975) nearly 100 sediment cores were taken within these two basins. Cores were carefully sectioned aboard ship and subsequently analyzed for large number of elements using state-of-the-art methods. Elements determined include Al, As, Ba, Br, Ca, Cd, Ce, Co, Cr, Cs, Cu, Eu, Fe, K, La, Lu, Hg, Hf, Mg, Mo, Mn, Na, Ni, P, Pb, Rb, Sb, Sc, Si, Sm, Sn, Sr, Ti, Th, U, V, Yb and Zn. Most of the known or potential metal contaminants are included in this list. Many of the cores were dated by radiometric methods using lead-210 and cesium-137. In addition, for a limited set of cores the distribution of dissolved substances was determined to estimate possible exchanges with overlying water.

Results of this study include: (1) greatly improved estimates of sediment accumulation rates, (2) recognition of the role of sediment mixing by benthic organisms in modifying metal contaminant and radioactivity profiles, (3) estimates of the rates of accumulation of metal contaminants in these depositional basins, (4) identification of which metals are contaminants and their degree of surface enrichment (in particular, the discovery of tin as a contaminant metal), and (5) limited comparisons of accumulation rates with lake loadings. The extent of contamination of sediments relative to natural levels is greatest for Hg and then, in decreasing order Sn, Pb, Sb, As, Cd, Zn, Ni, U, Cu, and Br. Data presented include: (1) contour maps of surface concentrations of major and trace constituents, enrichment factors, total anthropogenic metal accumulation since about 1800, vertically integrated cesium-137, depth of sediment mixing, mass and mean linear sedimentation rates, the intrinsic time resolution, rates of accumulation of major constituents and contaminant metals, (2) vertical distributions of major, trace, and dissolved constituents, (3) models for the behavior of cesium-137 in water, sediment mixing, and silicon dissolution in sediments, (4) area-wide loadings of major and trace constituents plus contaminant metals.

CONTENTS

Page

Foreword iii

Abstract iv

Figures viii

Tables xvi

Acknowledgments xx

Introduction 1

Conclusions and Recommendations 8

Methods 14

- Field Methods 14
  - Sediment collection 14
  - Sample processing 14
- Laboratory Methods 20
  - Wet Sediment 20
    - Bulk density 20
    - Zoobenthos 20
  - Dry Sediment 20
    - Fraction dry weight 20
    - Cesium-137 23
    - Trace elements (NAA) 23
    - Total and inorganic carbon 24
  - Acid-peroxide extracts 25
    - Soluble fraction 25
    - Trace elements (AAS) 25
    - Lead-210 26
  - Base Extracts 28
    - Amorphous silicon 28

Pore Water 29
    Soluble reactive PO_4 and Si 29
    Other constituents 29

Accuracy of Results 29

Neutron activation analysis 29

Timed Extractions 33
    Metals (AAS) 33
    Amorphous silicon 36

Pore water air-exposure effect 40

Results and Discussion 43

Physical properties of sediments 43

Composition of surface sediments 48

Average composition 64
Distribution and interelement associations 67
    Major constituents 67
    Trace constituents 88

Vertical distribution of elements 118
    Major constituents 122
    Trace constituents 131
    Cores at station 18 140

Enrichment factors 159

Vertically integrated concentrations 183

Sediment mixing and sedimentation rates 195
    Cesium-137 195
    Lead-210 213
    Stable lead 223
    Time resolution in cores 234

Rate of accumulation of sedimentary constituents 244
    Computation 244
    Distribution 246
    Mean and total accumulation rates 253
    Comparison with external loadings 265

Vertical distribution of dissolved constituents 277

Literature Cited 301

Publications and presentations receiving EPA support 308

Appendix

FIGURES

Number		Page
1	Surficial sediment distribution in Lake Huron	2
2	Sediment coring locations in Lake Huron	4
3	Southern Lake Huron study area	5
4	Surficial sediment distribution in southern Lake Huron	7
5	Shipboard collection and processing scheme	17
6	Cross-sectional view of cassette sediment squeezer	19
7	Sample analysis scheme	21
8	A comparison of analytical precision and accuracy in determination of trace element composition of standard lake sediment via neutron activation analysis	33
9	Elemental concentration ascribed to standard lake sediment versus extraction time	35
10	Silicon released from standard lake sediment versus extraction time	39
11	Concentration of selected elements in successive 3 ml aliquots of pore water	41
12	Fraction dry weight of sediment versus bulk density for 540 sediment samples	45
13	Vertical distribution of porosity in selected cores (Saginaw and Port Huron Basins)	46
14	Vertical distribution of porosity in selected cores (Goderich Basin)	47
15	Vertical distribution of porosity in two contrasting cores	49
16	Distribution of surface porosity	50
17	Distribution of porosity at depth	51

18 Distribution of compaction parameter 52

19 Relative variability of element concentrations in surface sediments 65

20 Distribution of inorganic carbon in surface sediments 71

21 Distribution of calcium in surface sediments 73

22 Distribution of magnesium in surface sediments 74

23 Distribution of fraction soluble component in surface sediments 75

24 Relation between calcium and inorganic carbon in surface sediments 76

25 Relation between magnesium and inorganic carbon in surface sediments 77

26 Relationship between calcium and magnesium in surface sediments 78

27 Distribution of dolomite in surface sediments 80

28 Distribution of organic carbon in surface sediments 83

29 Distribution of iron in surface sediments 84

30 Relation between the fraction soluble component (corrected for dolomite contributions) and organic carbon 85

31 Relation between observed and predicted values of dolomite-corrected fraction soluble content of surface sediments 87

32 Relation between iron and organic carbon in surface sediments 89

33 Distribution of manganese in surface sediments 90

34 Distribution of phosphorus in surface sediments 91

35 Distribution of potassium in surface sediments 92

36 Distribution of sodium (NAA) in surface sediments 93

37 Relation between iron (NAA) and cobalt (NAA) in surface sediments 94

38 Relation between zinc and copper in surface sediments 95

39 Degree of correlation of element concentrations with the organic carbon content of surface sediments 97

40 Distribution of antimony (NAA) in surface sediments 99

41 Distribution of arsenic (NAA) in surface sediments 100

42 Distribution of bromine (NAA) in surface sediments 101

43 Distribution of cadmium in surface sediments 102

44 Distribution of chromium in surface sediments 103

45 Distribution of copper in surface sediments 104

46 Distribution of lead in surface sediments 105

47 Distribution of mercury in surface sediments 106

48 Distribution of nickel in surface sediments 107

49 Distribution of thorium (NAA) in surface sediments 108

50 Distribution of tin in surface sediments 109

51 Distribution of uranium (NAA) in surface sediments 110

52 Distribution of zinc in surface sediments 111

53 Hierarchical trees resulting from cluster analysis of surface sediment concentrations 113

54 Association of calcium family and related constituents based on principal components analysis 114

55 Association of non-calcium family elements in the most complete data set based on principal components analysis 115

56 Results of principal components analysis of complete data set including calcium-family elements 116

57 Hierarchical tree resulting from cluster analysis of the complete set plus additional non-enriched elements 117

58 Vertical distribution of the fraction soluble component for selected cores from the Port Huron and Saginaw Depositional Basins ... 123

59 Vertical distribution of the fraction soluble component for selected cores from the Goderich Basin 124

60 Vertical distribution of calcium in selected Port Huron and Saginaw Basin cores 125

61 Vertical distribution of calcium in selected Goderich Basin cores 126

62 Vertical distribution of iron in selected Port Huron and Saginaw Basin cores 127

63 Vertical distribution of iron in selected Goderich Basin cores 128

64 Vertical distribution of magnesium in selected Port Huron cores 129

65 Vertical distribution of magnesium in selected Goderich Basin cores 130

66 Vertical distribution of mercury in a Goderich Basin core 132

67 Vertical distribution of manganese in selected Port Huron and Saginaw Basin cores 133

68 Vertical distribution of manganese in selected Goderich Basin cores 134

69 Vertical distribution of phosphorus in selected Port Huron and Saginaw Basin cores 135

70 Vertical distribution of phosphorus in selected Goderich Basin cores 136

71 Vertical distribution of potassium in selected Port Huron and Saginaw Basin cores 137

72 Vertical distribution of potassium in selected Goderich Basin cores 138

73 Vertical distribution of amorphous silicon in selected Goderich Basin cores 139

74 Vertical distribution of cadmium in a Port Huron basin core 141

75 Vertical distribution of chromium in selected Port Huron Basin cores 142

76 Vertical distribution of chromium in selected Goderich Basin cores 143

77 Vertical distribution of copper in selected Port Huron and Saginaw Basin cores 144

78 Vertical distribution of copper in selected Goderich Basin cores 145

79 Vertical distribution of lead in selected Port Huron and Saginaw Basin cores 146

80 Vertical distribution of lead in selected Goderich Basin cores 147

81 Vertical distribution of nickel in selected Port Huron and Saginaw Basin cores 148

82 Vertical distribution of nickel in selected Goderich Basin cores 149

83 Vertical distribution of tin in a Goderich Basin core 150

84 Vertical distribution of zinc in selected Port Huron and Saginaw Basin cores 151

85 Vertical distribution of zinc in selected Goderich Basin cores 152

86 Vertical distribution of major elements (NAA) in Goderich Basin core (74-18-2) 156

87 Vertical distribution of minor elements (NAA) in Goderich Basin core (74-18-2) 157

88 Vertical distribution of elements in Goderich Basin core (74-18-2) possessing a significant degree of enrichment 158

89 Distribution of the cadmium enrichment factor 175

90 Distribution of the calcium enrichment factor 176

91 Distribution of the copper enrichment factor 177

92 Distribution of the lead enrichment factor 178

93 Distribution of the manganese enrichment factor 179

94 Distribution of the nickel enrichment factor 180

95 Distribution of the zinc enrichment factor 181

96 Relationship between the mean enrichment factor and the degree of unrelatedness between surface and underlying element concentrations 182

97 Enrichment factors for elements in the fine-grained sediments of southern Lake Huron 184

98 Distribution of vertically integrated excess manganese 186

99 Distribution of vertically integrated excess copper 187

100 Distribution of vertically integrated excess nickel 188

101 Distribution of vertically integrated excess lead 189

102 Distribution of vertically integrated excess zinc 190

103 History of cesium-137 deposition in Lake Huron 197

104 Vertical distribution of cesium-137 in selected cores (74:3-8) 200

105 Vertical distribution of cesium-137 in selected cores (74:9-13, 19) 201

106 Vertical distribution of cesium-137 in selected cores (74:14-18) 202

107 Vertical distribution of cesium-137 in selected cores (74:20-32) 201

108 Vertical distribution of cesium-137 in selected cores (74:33-36) 202

109 Vertical distribution of cesium-137 in a series of cores at station 14 collected in 1974 (14-1,2) and in 1975 (14A-2, SC) 203

110 Relation between the expected and observed distribution of cesium-137 at station 14 (Core 14A-2) 205

111 Relation between the depth of sediment mixing as indicated by either cesium-137 or lead-210 and the depth above which 90% of benthic macroinvertebrates occur (Z_{90}) 207

112 Distribution of mixed depth based on cesium-137 210

113 Distribution of vertically integrated cesium-137 activity 211

114 Vertical distribution of lead-210 and cesium-137 in core 74-13 217

115 Vertical distribution of lead-210 and cesium-137 in core 74-12 218

116 Vertical distribution of excess lead-210 in selected Port Huron and Saginaw Basin cores 219

117 Vertical distribution of excess lead-210 in Goderich Basin cores (75-53, 63) 220

118 Vertical distribution of lead-210 and cesium-137 in cores from stations 14 and 18 221

119 Distribution of vertically integrated excess lead-210 (standing crop) 222

120 Relationship between the mass sedimentation rates estimated from cesium-137 and lead-210 224

121 Estimated regional atmospheric emissions of lead from the combustion of coal and leaded fuel additives 226

122 Vertical distribution of major elements in core EPA-SLH-75-18A 227

123 Vertical distribution of trace elements in core EPA-SLH-75-18A 228

124 Vertical distribution of lead in selected radiometrically dated cores 229

125 Relationship between the mass sedimentation rates calculated from stable lead and lead-210 profiles 231

126 Rate of accumulation of fine-grained sedments in southern Lake Huron 237

127 The average linear sedimentation rate in the upper ten cm of sediment in southern Lake Huron 238

128 The effect of rapid steady-state mixing on the sedimentary record of two events occurring ten years apart 242

129 The approximate time-resolution expected in sampling cores in southern Lake Huron 243

130 The rate of accumulation of organic carbon in surface sediments 247

131 The rate of accumulation of iron (AAS) in surface sediments 248

132 The rate of accumulation of chromium (AAS) in surface sediments 249

133 The rate of accumulation of inorganic carbon in surface sediments 250

134 The rate of accumulation of calcium in surface sediments 251

135 The rate of accumulation of magnesium in surface sediments 252

136 The distribution of the factor converting surface concentrations to present (1980) values 254

137 Rate of accumulation of anthropogenic antimony (adjusted to 1980) 255

138 Rate of accumulation of anthropogenic copper (adjusted to 1980) 256

139 Rate of accumulation of anthropogenic mercury (adjusted to 1980) 257

140 Rate of accumulation of anthropogenic lead (adjusted to 1980) 258

141 Rate of accumulation of anthropogenic nickel (adjusted to 1980) 259

142 Rate of accumulation of anthropogenic tin (adjusted to 1980) 260

143 Rate of accumulation of anthropogenic zinc (adjusted to 1980) 261

144 Vertical distribution of dissolved barium in selected cores 280

145 Vertical distribution of dissolved calcium in selected cores ... 281

146 Vertical distribution of dissolved iron in selected cores 282

147 Vertical distribution of dissolved magnesium in selected cores 284

148 Vertical distribution of dissolved manganese in selected cores 285

149 Vertical distribution of dissolved reactive phosphate in selected cores 287

150 Vertical distribution of dissolved potassium in selected cores 289

151 Vertical distribution of dissolved silicon in selected cores ... 290

152 Vertical distribution of dissolved sodium in selected cores 291

153 Vertical distribution of dissolved strontium in selected cores 292

TABLES

Number Page

1 Area of surficial sediments in Lake Huron 6

2 Southern Lake Huron stations 15

3 A summary of physical and chemical parameters determined 22

4 Composition of standard sediment determined via nutron activation analysis 30

5 Results of repeated analysis of standard lake sediment and U.S.G.S. samples 32

6 Composition of standard lake sediment determined via atomic absorption spectrophotometry 37

7 Extraction efficiencies for selected trace elements 38

8 Composition of pore water with and without air exposure 42

9 Composition of surface sediments 53

10 A summary of surface concentration data 59

11 Correlation matrix for surface concentration data 60

12 Mercury and tin in surface sediments 62

13 Regression data for mercury 68

14 Regression data for tin 69

15 Comparison of mean surface concentration data with other reported values 70

16 Concentration of dolomite in surface sediments 81

17 Multiple regression coefficients for FSOL* versus organic carbon plus iron plus manganese 86

18 Comparison of acid soluble and whole sediment element concentrations 96

19 Results of principle components analysis 119

20 Significant interelement associations 120

21 Summary of vertical distribution measurements 121

22 Vertical distribution of major elements in whole sediment (station 18) 153

23 Vertical distribution of minor elements in whole sediment (station 18) 154

24 AAS to NAA element concentration ratios 160

25 Mean whole-sediment element concentrations in surface and in underlying sediments. Station EPA-SLH-74-18(2) 161

26 Vertical distribution of elements in the acid-soluble fraction (AAS). Station EPA-SLH-75-18A(2) 162

27 Concentration of major elements (AAS) in surface and in underlying sediments 165

28 Concentration of minor elements (AAS) in surface and in underlying sediments 168

29 Correlations between enrichment factors 172

30 Summary of mean concentration ratios and enrichment factors 173

31 Comparison of mean enrichment factors by depositional basin 174

32 Vertically integrated excess element concentrations 185

33 Correlations between total excess deposition of selected elements 191

34 Storage of anthropogenic elements in sediments of southern Lake Huron 193

35 Inventory of cesium-137 in southern Lake Huron 194

36 Vertically integrated activity of cesium-137 and mixing-model parameters 208

37 Values of the mixing depth versus hypothetical sediment losses 212

38 Summary of lead-210 data, sedimentation rates, and mixed-depths 216

39 Sedimentation rates derived from stable lead profiles 230

40 Exponential source function parameters 233

41 Summary of sedimentation rate data 235

42 Summary of mixed depth estimates 239

43 Mean and total accumulation of fine-grained sediments and non-enriched elements 262

44 Coefficients used to estimate missing background concentrations of enriched elements 264

45 Accumulation rates of enriched elements Port Huron Basin 266

46 Accumulation rates of enriched elements Goderich Basin 267

47 Accumulation rates of enriched elements southern Lake Huron 268

48 Sensitivity of mean accumulation rates to changes in estimated background levels 269

49 Comparison of element composition of dolomitic sediment with the composition of Canadian Lake Huron shoreline materials 272

50 Comparison of mean anthropogenic element accumulation rates with other loading data 274

51 Summary of dissolved element concentration data 278

52 Comparison of accumulation rates of amorphous silicon with regeneration rates 294

APPENDIX TABLES

A-1 Physical properties of sediment cores A1

A-2 Vertical distribution of metals A71

A-3 Vertical distribution of amorphous silicon A138

A-4 Vertical distribution of cesium-137 .... A139

A-5 Vertical distribution of lead-210 .... A147

A-6 Vertical distribution of benthic macrofauna A153

A-7 Vertical distribution of dissolved species A163

A-8 Coefficients associated with pair-wise regression of surface sediment concentration data A174

ACKNOWLEDGMENTS

It would not have been possible to do this work without the generous help from a great many individuals. I should like to thank James Murphy, Captain of the R/V Laurentian and his crew, and Richard Thibault, Captain of the R/V Laurentian and his crew for their dedicated and effective help in the collection of samples from southern Lake Huron. I am especially grateful to John Krezoski and Kjell Johansen for their long-standing commitment to this work and the help they have given in so many ways both in the field and in the laboratory. Thanks are due K. Remmert for her help in the preparation and analysis of samples and to J. Jones and the staff of the Phoenix Memorial Laboratory for help in Neutron Activation Analysis. I wish to thank W. Ullman and L. Hess for their help in data reduction and J. Gustinis for the assistance in the design and fabrication of the sediment pore water extraction system. Thanks are due M. Barron for the cadmium analyses and to V. Hodge for the mercury and tin analyses.

Finally a tribute to those whose contributions too often go unrecognized: the people who have had to read my handwriting and convert it into recognizable English prose. I wish to thank L. Ayers, J. Thomas, L. Trost, L. Gardner, and B. McClellan for their help in manuscript preparation. Special thanks go to S. Schneider for his patience and help in producing this document.

INTRODUCTION

This is the first in a series of three reports dealing with the composition of recent sediments of Lake Huron and the rate of accumulation of metal contaminants. The aims of the series are many and include: (1) determination of recent sedimentation rates by both radiometric and other means, (2) identification of elemental contaminants by examination of concentration profiles in dated sediment cores, (3) development of contour maps for the Lake which show the concentration of metal contaminants and their historical and present rates of accumulation, (4) estimation of the total amount of various contaminants stored in the sediments, (5) identification of the origins of metal contaminants in selected cases and (6) recognition and quantitative treatment of processes affecting sedimentary records of radioactivity and metal contaminants and the exchange of substances between sediments and overlying water. The results of the research reported in this Lake Huron sediment series represent a natural extension of the work of Thomas et al. (1973) who provided the first extensive and systematic mapping of the surficial sediments of Lake Huron and that of Kemp and Thomas (1976b) who provided the first limited exploratory study of the distribution of metal contaminants in pollen-dated cores from this Lake.

On the basis of extensive grab sampling and echo sounding, Thomas et al. (1973) identified several major lithological units in Lake Huron: (1) glacial till and bedrock; (2) glaciolacustrine clay; (3) postglacial mud and (4) sand. The areas of sand, bedrock, till and glaciolacustrine clay are considered as non-depositional. These areas are not currently receiving any long-term input of sediments. Fine-grained materials entering the lake at the present time accumulate primarily in the comparatively limited areas of the Lake as shown in Figure 1. This is a very general feature of sedimentation in the Great Lakes: accumulation is not uniform over the Lake bottom. Instead, there is strong sediment focusing (cf. Lehman, 1975; Kamp-Nielsen and Hargrave, 1978). In Lake Huron, less than half and perhaps as little as a third of the area, receives modern sediments (see Table 1). Postglacial muds occur in basins of three distinct types as indicated in Fig. 1: (1) Type A. Regular basins in which mud forms a continuous cover; (2) Type B. Irregular basins with undulating bottom topography. Mud cover is greater than 50%; (3) Type C. As for Type B but with mud cover less than 50%. Postglacial mud accumulation is continuous in the southern basins of the Lake due to the gentle relief of the Lake bottom. In the northern region of the Lake, mud accumulation is discontinuous due to the undulating nature of the Lake bottom. Mud fills the hollows leaving glacio-lacustrine clay exposed at the top of undulations in this region. As most metal and other contaminants are associated with the fine-grained sedimentary materials, they preferentially accumulate in the depositional basins in combination with

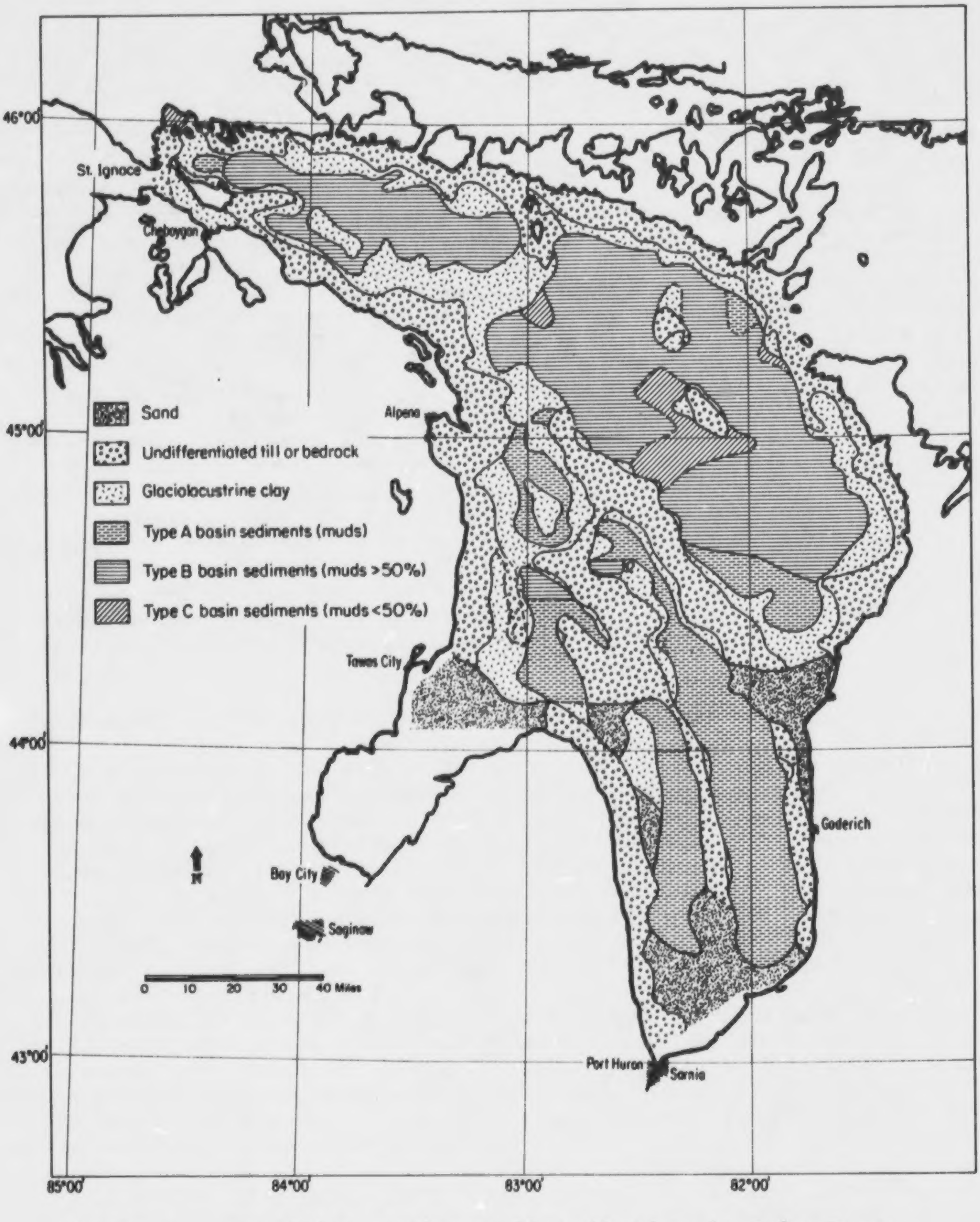
46°00'
45°00'
44°00'
43°00'
85°00'
84°00'
83°00'
82°00'
St. Ignace
Cheboygan
Alpena
Tawas City
Bay City
Saginaw
Goderich
Port Huron
Sarnia
N
Sand
Undifferentiated till or bedrock
Glaciolacustrine clay
Type A basin sediments (muds)
Type B basin sediments (muds >50%)
Type C basin sediments (muds <50%)
0 10 20 30 40 Miles

Figure 1. Surficial sediment distribution in Lake Huron.

postglacial muds. For this reason, emphasis is placed in the reports on the composition of sedimentary materials within these depositional basins.

Each of the three reports deals with a specific area of Lake Huron as indicated in Fig. 2. This report is concerned with southern Lake Huron as defined by the enclosed rectangular region in Fig. 2. The second report in the series is devoted to the sediments of lower Saginaw Bay and the third report treats recent sediments of northern Lake Huron as indicated in each case by the enclosed rectangular regions. The symbols in Figure 2 indicate the locations of sediment sampling sites where, in general, multiple cores were taken.

Within the southern Lake Huron study area, there are two principal depositional basins, the Port Huron basin to the west having a mean depth of 88 m and the Goderich basin to the east, having a mean depth of 119 m (Fig. 1). As can be seen in Fig. 3, these two basins reflect the bathymetry of this part of the Lake and are separated by a mid-Lake, north-south trending escarpment referred to as the Ipperwash scarp (Thomas et al., 1973). Along the escarpment there is no significant accumulation of postglacial muds, and surficial deposits are characterized as a narrow band of undifferentiated till and bedrock. Included within the southern Lake Huron study area is a small portion of a lesser basin termed the Saginaw basin located just beyond the entrance to Saginaw Bay. In southern Lake Huron about 40% of the bottom is covered by Type A mud. Approximately 13% of the total area corresponds to the Port Huron basin, which is contained entirely within the study area. Approximately 27% of the area of southern Lake Huron corresponds to the Goderich basin and approximately 90% of this basin is contained within the study area (See Table 1). As can be seen in Fig. 4, the sediment sampling sites have been chosen to provide extensive coverage of the two primary depositional basins within the southern Lake Huron study area. In comparison with previous work in this part of the Lake, the present study represents a considerable advance. Kemp and Thomas (1976) based a whole-lake contaminant metals inventory on only three dated cores from Lake Huron of which only one was taken from the southern part. It is the intent of this study to provide sufficient coverage of the depositional basins that there can be an improved understanding of the variability of composition of sediments within depositional basins and an improved accuracy and comprehensiveness in mass-balance calculations for major and minor sedimentary constituents and for metal contaminants in particular.

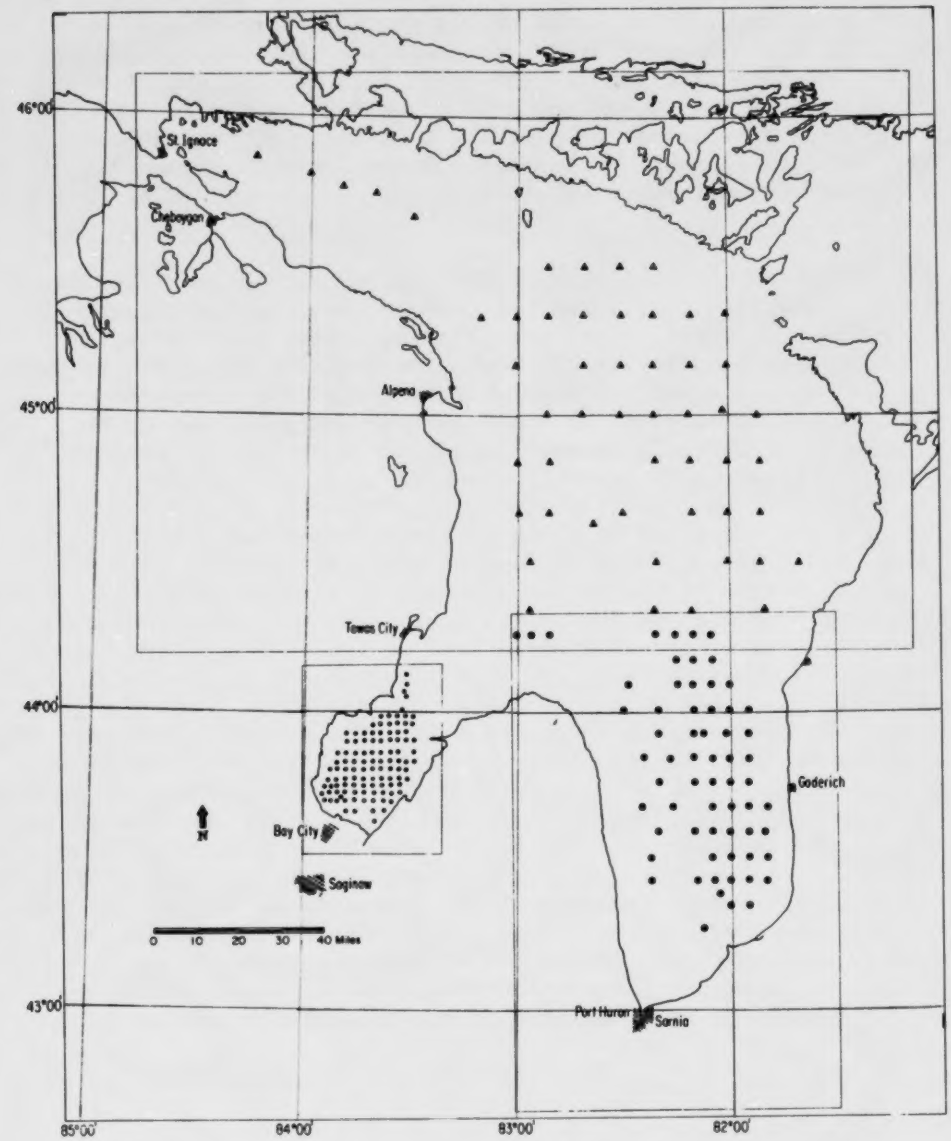
46°00'
St. Ignace
Cheboygan
45°00'
Alpena
Tawas City
44°00'
Bay City
Saginaw
Goderich
N
0 10 20 30 40 Miles
43°00'
Port Huron
Sarnia
85°00'
84°00'
83°00'
82°00'

Figure 2. Sediment coring locations in Lake Huron.

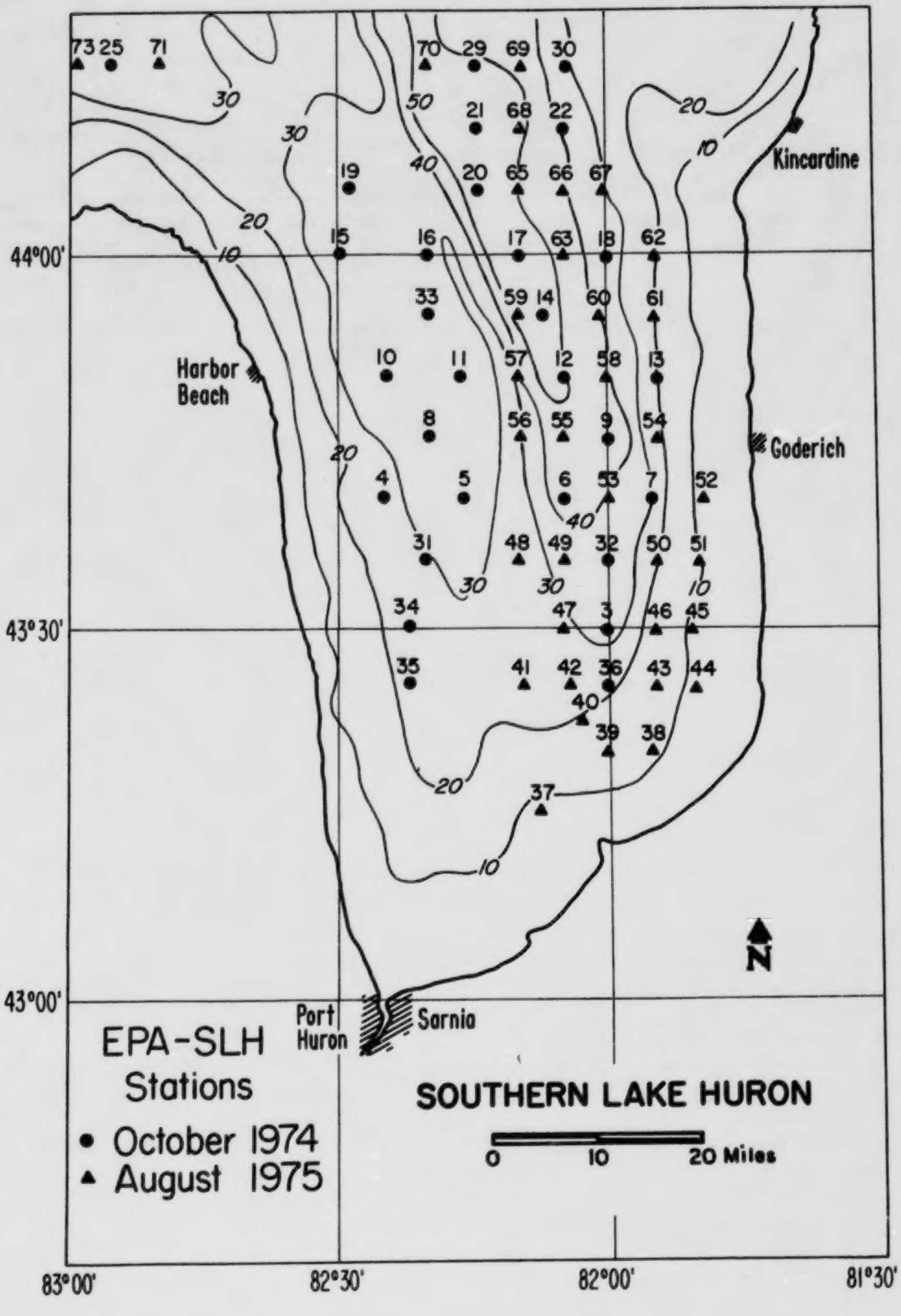

EPA-SLH
Stations
● October 1974
▲ August 1975
SOUTHERN LAKE HURON
0 10 20 Miles
N
Kincardine
Goderich
Harbor Beach
Port Huron
Sarnia
44°00'
43°30'
43°00'
83°00'
82°30'
82°00'
81°30'

Figure 3. Southern Lake Huron study area.

TABLE 1. AREA OF SURFICIAL DEPOSITS IN LAKE HURON (IN UNITS OF 10^{13} cm^2).

Sediment type[1]	Northern Lake Huron[2]	Southern Lake Huron[2]	Georgian Bay[3]	Saginaw Bay[4]	Total
Sand	0.3	2.6	-	2.5	5.4
Undifferentiated till or bedrock	9.0	2.5	5.31[7]	0	16.8
Glaciolacustrine clay	6.2	0.6	8.20	0	15.0
Postglacial muds:					
Type A	2.6	3.8[6]	-	0.36	6.8
Type B	9.5	0	-	0	9.5
Type C	0.9	0	-	0	0.9
Undifferentiated	-	-	5.29	-	5.29
Total areas	28.5	9.5	18.8	2.8	59.6[5]

---

[1] Based on the classification of Thomas et al. (1973).

[2] Northern and southern portions divided along latitude 44° 15'N. Data of Thomas et al. (1973).

[3] Data from IJC (1977) p. 354.

[4] Based on the data of this study.

[5] The total surface area of Lake Huron is 23,000 sq. mi. or $5.96 \times 10^{14} cm^2$. U. S. Dept. of Commerce, NOAA-National Ocean Survey, General Great Lakes Chart 0.

[6] The area of the Port Huron Basin is $1.22 \times 10^{13} cm^2$, and the area of the Goderich Basin is $2.59 \times 10^{13} cm^2$.

[7] $1.84 \times 10^{13} cm^2$ glacial till, plus $3.47 \times 10^{13} cm^2$, melange, bedrock, till and glaciolacustrine clay.

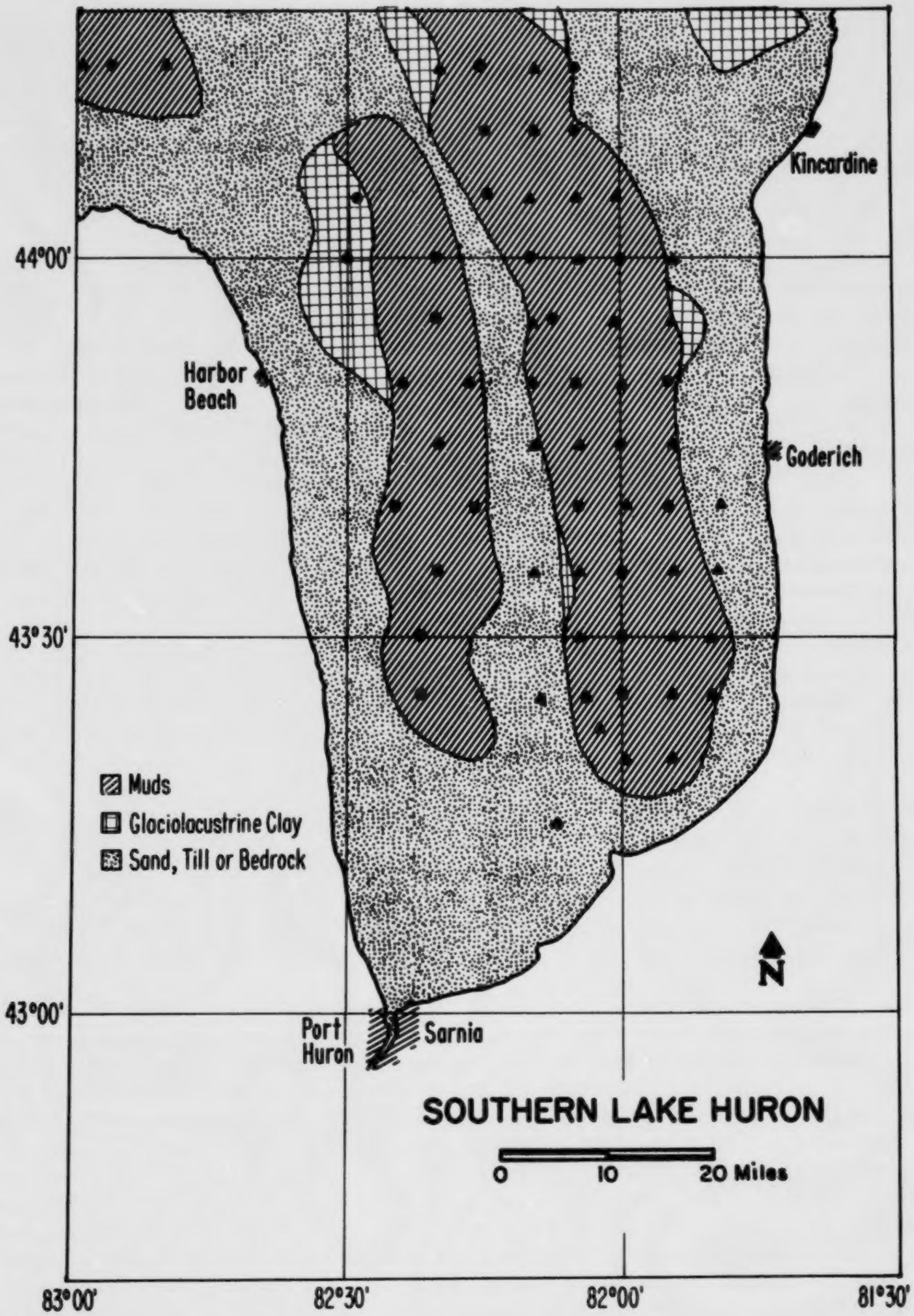
Kincardine
Harbor Beach
Goderich
Port Huron
Sarnia
44°00'
43°30'
43°00'
83°00'
82°30'
82°00'
81°30'
▨ Muds
▦ Glaciolacustrine Clay
▩ Sand, Till or Bedrock
N
SOUTHERN LAKE HURON
0
10
20 Miles

Figure 4. Surficial sediment distribution in southern Lake Huron.

CONCLUSIONS AND RECOMMENDATIONS

Intensive coring combined with radiometric and multielement analysis of carefully-sectioned cores has led to an improved view of the patterns and processes of accumulation of sedimentary constituents in the two principal depositional basins of southern Lake Huron. As a result of a combination of factors including bathymetry, hydrodynamics, and the distribution of source materials, the two basins are very different in character. The Port Huron basin is comparatively inefficient as a collector of fine-grained materials and associated metal contaminants. This is due partly to its lesser size and to much lower sedimentation rates. In contrast, the Goderich basin is roughly five times more efficient in accumulation of sediments. In addition, there is a considerable degree of systematic variability in concentrations and accumulation rates within this basin, partly as a result of the markedly enhanced deposition of silt-sized materials toward the eastern margin. The preferential deposition of fine-grained materials in limited areas of the lake bottom, or sediment focusing, has been clearly demonstrated by the work of Thomas and Kemp (1973). This report shows that rate of accumulation of certain sedimentary constituents is even more sharply focused within depositional basins. These general features are apparent in many of the conclusions which follow.

Porosity profiles are generally exponential in shape within depositional basins but tend to show discontinuities toward basin margins. Surface sediments are least consolidated toward the escarpment side of the depositional basins, and possess a maximum porosity of 0.9 or greater. In the Goderich basin surface sediments are considerably more consolidated toward the eastern margin and may have porosities as low as 0.6 or less.

The mean concentration of elements (37) determined in this study are generally consistent with the limited concentration data published by others. However, mean concentrations of contaminant elements tend to be somewhat higher than previously reported and this is shown to be due to improvements in the sampling methods adopted for this study. An exception is mercury, which is found to be significantly less in the Port Huron basin than previously reported. If not due to analytical or methods differences, this result could imply a decrease in the amount of mercury stored in this basin during the five-year period between surveys. Two major groups of elements occur in surface sediments: the calcium family elements and those associated with organic carbon and other fine-grained constituents. The calcium family elements (Ca, Mg, and IOC) are strongly associated with each other and occur in proportions which indicate dolomite as their primary source. The amount of material which dissolves on acid treatment is principally composed of dolomite plus organic carbon and iron compounds. In the Goderich basin up to 92% of the acid-soluble fraction is composed of dolomite. Subtraction of the dolomite fraction from the total amount which is acid-soluble leaves a residual fraction which correlates well with the organic carbon and iron content of surface sediments. Multiple linear regression of the residual fraction soluble on iron and organic carbon concentrations indicates the mean composition of organic carbon as CH_2O. A very high degree of correlation exists between organic carbon and iron and other minor and trace constituents. Hydrodynamic as well as geochemical processes result in the co-deposition of trace constituents with fine-grained materials such as clay minerals, organic carbon, and iron compounds. As a result, considerable redundancy exists in the distribution of most non-calcium family elements in surface sediments of the two depositional basins. The distribution in surface concentrations of such elements as As, Br, Cd, Cr, Cu, Pb, Hg, Ni, Th, Sn, U, and Zn are very similar and are highest toward the escarpment sides of the depositional basins where sediments are least consolidated. In contrast, the calcium family elements have the highest concentration in surface sediments toward the eastern margin of the Goderich basin.

Of the 37 elements determined only a few exhibit an enrichment of surface concentrations above background levels. Elements enriched in surface sediments are, in decreasing order, Hg, Sn, Pb, Mn, Sb, As, Cd, Zn, Si, Ni, U, Cu, and Br. The enrichment of Mn is confined to the upper 1 to 2 cm in all cores and is probably the result of natural diagenesis. The enrichment of Si (amorphous) may be either natural or the result of enhanced fixation of soluble silicon in overlying water. Enrichments of the other elements probably are due to recent anthropogenic loadings to the lake. The concentration of Hg is four to five times higher in surface sediments than in background sediments. Tin (Sn) is second only to Hg in terms of enrichment and has a maximum concentration in surface sediments of about 6 ppm. On the basis of profiles in dated cores, tin is recognized as a significant contaminant. This study represents the first reported observation of tin as a metal contaminant in sediments of the Great Lakes. As recent sediments of Lake Huron are in general relatively less contaminated with metals than sediments of lakes such as Michigan, Erie, and Ontario, it is likely that appeciably higher concentrations may be found in certain sediments of these other lakes. The degree of enrichment shows a systematic variation within the depositional basins similar to that for surface concentrations of non-calcium family elements. Hence, the degree of enrichment of elements is not a unique characteristic of the lake or even of depositional basins but shows nearly as much spatial variability as do element concentrations.

With the exception of Mn and possibly Si, concentrations of enriched elements are subdivided into natural levels corresponding to concentrations deep in cores (generally below about 15 cm) and anthropogenic concentrations taken as the amount above natural levels. Vertically integrated anthropogenic concentrations in individual cores indicate the total amount of an element accumulated at a location resulting from human activity. The greatest vertically integrated concentrations occur toward the center of the Goderich basin. There has been relatively little accumulation of anthropogenic elements in the Port Huron basin. The total storage of anthropogenic elements in southern Lake Huron as of 1975 was 700, 2400, 1000, and 3000 metric tons of Cu, Pb, Ni, and Zn respectively. For cesium-137, a radionuclide produced by nuclear testing in the atmosphere, the total stored was about 400 Curies. This amount is less than the relatively well-known decay-corrected deposition on the southern part of the lake since the mid 1950s (950 Curies). Over half the cesium-137 deposited on the lake surface did not accumulate in underlying sediments. Without an inventory of the entire lake, it is not possible to tell if this deficit is located in other parts of the lake. An alternative possibility is that there is storage over nondepositional areas. Only a few tenths gram of material per cm^2 in the water column overlying nondepositional areas is sufficient to achieve the proper materials balance for this radionuclide.

Analysis of cesium-137, lead-210, and stable lead profiles in a large number of sediment cores generally leads to self-consistent estimates of recent sedimentation rates. The mean sedimentation rate in the Goderich basin is 35.7 $mg/cm^2/yr$, while the mean rate in the Port Huron basin is 12.8 mg/cm^2yr. These values imply that about 1 million metric tons of fine-grained sediments are deposited annually, corresponding to a mean area-wide sedimentation rate of 11.4 mg/cm^2yr. Thus the mean accumulation rate in southern Lake Huron is not greatly different from the main lake average of 10 $mg/cm^2/yr$ reported by Kemp et al. (1974). A considerable fraction (20%) of the material accumulating in the southern Lake Huron basins is dolomite. Mass sedimentation rates on the eastern side of the Goderich basin are very high as a result of intense deposition of dolomite. Within this basin rates toward the escarpment side are under 20 $mg/cm^2/yr$ while values on the eastern side may exceed 100 $mg/cm^2/yr$. High mass sedimentation rates are associated with sediments which are relatively consolidated. As a result, the distribution of the linear sedimentation rate (cm/yr) is very different. Because of compaction, the linear rate is not uniquely defined in a given sediment core but is taken in this report to be the average rate over the upper 10 cm of sediment. This rate is very low in the Port Huron basin (0.5-1 mm/yr) and also in the southern half of the Goderich basin. Highest values are around 1.5 mm/yr in the northern section of the Goderich basin.

Both radioactivity and anthropogenic element profiles often possess a zone at the sediment-water interface where concentrations are essentially constant. This feature is interpreted as being due to the mixing of sediment solids. A model developed for this report of rapid steady-state mixing over a zone of well-defined depth accounts satisfactorily for observed profiles. The vertical distribution of benthic macroinvertebrates in a series of replicate cores from two locations (as well as data from Saginaw Bay) indicates that benthos can be the active agents in sediment mixing (bioturbation). Ninety percent of the benthos are located within the zone of mixing as determined radiometrically. Because of sediment mixing, profiles of cesium-137 are of limited usefulness in determining sedimentation rates. The greatest depth of sediment mixing tends to occur toward the escarpment sides of the depositional basins where sediments are least consolidated.

Sediment mixing may be the principal determinant of the resolution attainable in reconstruction of historical events from sedimentary records. The resolution is given approximately by the residence time of particles within the mixed zone (the ratio of the mixed depth in g/cm^2 to the sedimentation rate g/cm^2yr). On the average this time is about 20 years in southern Lake Huron. The resolution varies systematically in the Goderich basin, decreasing to values less than 10 years in certain areas contiguous with the eastern margin. Sediment mixing serves to increase the contact time between contaminated sediments and overlying water. In the absence of additional metal contaminant fluxes to sediments, concentrations in surface sediments would be expected to decrease by about 5% per year according to the steady-state mixing model. Because of sediment mixing, it is not likely that any recent improvements in water quality will have as yet had a measurable effect on sedimentary profiles in this area of the lake.

Stable lead profiles have been given particular attention in this report and it has been shown that stable lead can be used as a geochronological tool. Since lead profiles in radiometrically dated cores exhibit the same time- dependence from one location to another, the local rate of deposition may evidently be expressed in terms of separated variables: one part containing the spatial dependence and the other containing the time variable. This latter part is referred to as the source function. The source function for lead is shown to be given in terms of the regional lead loadings reconstructed from emissions inventories based on combustion of coal and leaded fuel additives. This source function is essentially exponential over the pertinent time period (from about 1900) and indicates a twenty year doubling time for anthropogenic lead inputs. Application of the exponential source function formalism to other anthropogenic element profiles indicates that anthropogenic Cu, Sn, and Zn also have doubling times of about twenty years. Anthropogenic Ni has a 14 year doubling time which may not be significantly different. Mercury, on the other hand, has a 40 year doubling time. This higher value is probably an artifact resulting from migration of the element within sediments.

The rate of accumulation of an anthropogenic element is computed as the product of the anthropogenic element concentration and the mass sedimentation rate. Because the anthropogenic concentration has been increasing over time, accumulation rates must be referred to a specific date. By means of the steady-state mixing model and use of the exponential source functions, metal contaminant profiles are adjusted so as to provide estimates of 1980 accumulation rates. To convert measured concentrations (1-2 cm interval) to surface values (1975), the typical adjustment for the effects of sediment mixing and finite-interval sampling is about 40%. Another 20% increase is due to adjustment of values from 1975 to this report date (1980). The mean anthropogenic accumulation rates (µg/cm^2/yr) for southern Lake Huron are: As (0.32); Br (0.24); Cd (0.022); Cu (0.24); Hg (0.002); Ni (0.42); Pb (0.94); Sb (0.014); Si (79); Sn (0.047); Zn (1.3). Values refer to amounts deposited per unit area of southern Lake Huron. The mean accumulation rates are generally comparable to measured or estimated loadings from the atmosphere. Direct municipal and industrial discharges as estimated by the International Joint Commission (IJC, 1977) are far too low to be of importance while tributary inputs often far exceed the measured accumulation rates. Differences are undoubtedly due both to analytical problems with tributary measurements and to insufficient distinction of chemical and physical forms of the elements in the water samples. In general, anthropogenic element accumulation rates tend to be highest toward the center of the Goderich basin and show limited variability within the Port Huron basin. The mean rate of accumulation of anthropogenic bromine is consistent with the lead data and suggests combustion of fuel additives as the primary source. Because of the high degree of variability in the anthropogenic element concentrations and accumulation rates within the Goderich basin especially, inventories based on a single core or on a few cores can lead to considerable error. On the other hand, because of the high degree of correlation of anthropogenic constituents with organic carbon and iron, a sampling and analysis scheme can be devised which takes optimal account of these correlations in estimating anthropogenic sediment loadings.

The concentration of several elements in pore water are sensitive to exposure to air. In addition to those of known sensitivity such as Fe, PO_4 and Mn, additional sensitive elements include Co, La and Sb. Profiles of some dissolved elements (Fe, Mn, PO_4 and Si) exhibit large gradients either at or just below the sediment-water interface. Very rough comparisons of upward fluxes based on gradients at $z=0$ with excess accumulation rates suggest a steady-state diagenetic cycle involving burial, dissolution, upward migration and reprecipitation for Fe, Mn, and possibly PO_4. The PO_4 data are of marginal quality because of air exposure effects. Careful calculations of soluble reactive silicon fluxes (SRS) based on interstitial gradients at $z=0$ imply fluxes ranging from 750 to 1700 μg Si/cm^2/yr. Such fluxes are consistent with values obtained in postglacial muds of northern Lake Huron (for the third in this report series) ranging from about 1000-2000 μg Si/cm^2/yr. If such fluxes are representative of annual average releases of silicon to overlying water, then the sediments are a major source of SRS in the water column. In two cores the outward SRS flux is matched by the downward supply of available (amorphous) silicon. In two other cores the outward SRS flux considerably exceeds the supply of available silicon. Reasons for the imbalance are unclear. Relations between amorphous (available) Si and that dissolved in pore water suggest a theoretical treatment developed for marine sediments which can be modified to take account of the finite range of bioturbation as encountered in sediments of the Great Lakes.

The postglacial deposits of the Great Lakes serve as repositories for particle-bound contaminants entering the Lakes. As seen in this report, the sediments provide a literal "ground truth" for attempts to develop contaminant mass balances and play an important role in some of the nutrient cycles in the lakes. For these reasons the recent sediments should be accorded considerable attention and effort should be made to obtain accurate sedimentation rate information in cores in combination with measurements of the vertical distribution of metal contaminants and available nutrient elements such as PO_4 and Si. Because of the recognition that the fate of many toxic organic substances are also transported in association with particulate matter, the distribution of organic constituents in carefully dated sediment cores should also be undertaken not only for purposes of reconstructing the history of organic pollutant accumulation (where diagenesis may be neglected) but so as to properly model the role of the sediments in the exchange of substances with overlying water.

This study has demonstrated the desirability of using several methods in combination to obtain information on sedimentation rates and sediment mixing. Of particular interest is the lead-lead-210 pair. As these two forms of lead have significantly different sources but probably the same geochemistry and hydrodynamics in the lakes, lead-210 has the potential ability to serve as a tracer for atmospheric lead contributions. This property should be exploited not only in order to understand the behavior of lead contaminants in the lakes but for the wider implications. Use of stable-radioactive element pairs as well as radionuclides such as cesium-137 can play a very important role in the calibration of ecosystems models of other pollutants such as toxic organics. The preliminary mass balance for the cesium-137 suggests that nondepositional areas of the lake should be examined for possible boundary layer storage of contaminants.

The phenomenon of sediment mixing as identified previously in Lake Michigan (Robbins and Edgington, 1975) is also occurring in sediments of Lake Huron. As sediment mixing serves to prolong the contact time between sediments and overlying water, this process may be an important factor in the ability of lakes to resolve themselves following implementation of pollutant abatement strategies. Laboratory studies should be undertaken to define the role of natural benthos communities on the mixing of sediments and exchange of substances across the sediment-water interface. Of particular interest would be laboratory simulations of the role of benthos and sediment mixing on the long-term exchange of contaminants with water.

As tin is shown to be a significant sedimentary contaminant, further studies of the concentration and distribution of tin in selected areas of the Great Lakes should be undertaken. Since tin can be converted to biologically active organotin compounds by bacterial action, the chemical forms of tin in sediments, water and biota should be investigated as should the potential effect of such compounds on sensitive members of the biota in the Lakes.

Because of the importance of the sediments in the cycling of silicon in the lake, realistic models of particulate and soluble silicon in sediments need to be developed. Such models sould be tested by careful laboratory studies of the kinetics of silicon dissolution as well as by concurrent measurements of pore water concentration profiles and fluxes of silicon (SRS) across the sediment-water interface.

METHODS

FIELD METHODS

Sediment Collection

Sediment samples were collected at 65 stations in southern Lake Huron (Table 2) during October 1974 and August 1975. The locations of sediment sampling stations, shown in Figure 3, cover with considerable detail most of the corable areas of southern Lake Huron. This can be seen in Figure 4 which shows the location of stations in relation to the distribution of major types of surficial sediments (Thomas et al., 1973). The locations are largely within the two depositional basins (Port Huron, and Goderich basins) which contain recently deposited muds with only a few stations located where there are glaciolacustrine clays, or sandy and coarser deposits. Most of the cores were taken in the Goderich Basin and only three were taken in the Saginaw Basin (25, 71, 73) which mostly lies outside the study area (Figure 4). In areas with coarse-grained deposits samples were collected by means of a Ponar grab. Elsewhere, core samples were recovered using a 3-inch diameter (7.6 cm) gravity core (Benthos, Inc., N. Falmouth, Massachusetts). The inner diameter of the core liners is 6.66 ± 0.03 cm. (Area = 34.8 cm^2). To minimize disturbance of the surface sediments which are often extremely loosely consolidated and flocculent, several steps were taken. The plastic core liners were outfitted with a butterfly valve which presents little resistance to water flow through the tube during descent of the corer through the water column and during impact with the sediments. In addition, the corer was lowered to a position 5-10 meters above the sediments before allowing it to fall freely. Free fall from this position allowed the corer to penetrate sediments at velocities over 1 m/sec. For cores of this diameter minimum core distortion occurs for velocities over 1 m/sec. (Hongve and Erlandsen, 1979). These procedures aided in the retreival of cores possessing an interface remarkably intact. In some cases the delicate detrital mounds produced by tubificid worms or by Chirononid larvae were present in recovered cores (see also Robbins et al., 1977).

Sample Processing

The shipboard processing of cores and grab samples is summarized in Figure 5. Sediment cores contained in plastic liners were placed on a hydraulic extruding stand. The sediment column within the liner was forced upward by filling the bottom of the liner with water under pressure. A precisely controlled amount of sediment (± 0.1 cm) was extruded into a

TABLE 2. SOUTHERN LAKE HURON STATIONS

STATION NUMBER	LOCATION		WATER DEPTH (METERS)	GROSS SEDIMENT CHARACTERISTICS
EPA-SLH-74-3	43° 30.0' N	82° 00.0' W	58	Gray Mud
EPA-SLH-74-4	43° 40.0'	82° 25.0'	51	--
EPA-SLH-74-5	43° 40.0'	82° 16.3'	61	--
EPA-SLH-74-6	43° 40.0'	82° 04.0'	77	--
EPA-SLH-74-7	43° 40.0'	81° 55.0'	51	--
EPA-SLH-74-8	43° 45.0'	82° 20.0'	63	--
EPA-SLH-74-9	43° 45.0'	82° 00.0'	80	--
EPA-SLH-74-10	43° 50.0'	82° 25.0'	62	--
EPA-SLH-75-10A	43° 50.3'	82° 28.5'	54	--
EPA-SLH-74-11	43° 50.0'	82° 16.0'	69	--
EPA-SLH-74-12	43° 50.0'	82° 05.0'	91	--
EPA-SLH-74-13	43° 50.0'	81° 55.0'	40	--
EPA-SLH-74-14	43° 55.0'	82° 07.5'	96	Dr. Gray Silt
EPA-SLH-74-15	44° 00.0'	82° 30.0'	67	Red Sandy Clay
EPA-SLH-74-16	44° 00.0'	82° 19.0'	69	Dk. Gray Silt
EPA-SLH-74-17	44° 00.0'	82° 10.0'	102	Dr. Gray Silt
EPA-SLH-74-18	44° 00.0'	82° 00.0'	68	Dk. Gray Sandy Silt
EPA-SLH-74-19	44° 05.0'	82° 29.0'	70	Lt. Gray Sandy Mud
EPA-SLH-74-20	44° 05.0'	82° 15.0'	96	Dk. Gray Silt
EPA-SLH-74-21	44° 10.0'	82° 15.0'	63	Dk. Gray Silt
EPA-SLH-74-22	44° 10.0'	82° 05.0'	77	Pink Sandy Mud
EPA-SLH-74-25	44° 15.0'	82° 55.0'	62	Gray Silt
EPA-SLH-74-29	44° 15.0'	82° 15.0'	95	Dk. Gray Silt
EPA-SLH-74-30	44° 15.0'	82° 05.0'	64	Tan Sandy Clay
EPA-SLH-74-31	43° 35.0'	82° 20.0'	53	Gray Sandy Silt
EPA-SLH-74-32	43° 35.0'	82° 00.0'	69	Lt. Gray Sandy Mud
EPA-SLH-74-33	43° 55.0'	82° 20.0'	69	Gray Silt
EPA-SLH-74-34	43° 30.0'	82° 22.5'	44	--
EPA-SLH-74-35	43° 25.0'	82° 22.5'	40	--
EPA-SLH-74-36	43° 25.0'	82° 00.0'	42	Gray Sandy Mud
EPA-SLH-75-37	43° 15.4'	82° 07.4'	20	Sand
EPA-SLH-75-38	43° 20.0'	81° 55.0'	21	Brown Silty Sand
EPA-SLH-75-39	43° 20.0'	82° 00.0'	24	Olive Sandy Mud
EPA-SLH-75-40	43° 22.5'	82° 02.9'	40	--
EPA-SLH-75-41	43° 25.0'	82° 09.2'	43	Sand
EPA-SLH-75-42	43° 25.0'	82° 02.6'	43	Gray Mud
EPA-SLH-75-43	43° 25.0'	81° 55.0'	27	Olive Sandy Mud
EPA-SLH-75-44	43° 25.0'	81° 50.0'	18	Gray Sandy Clay
EPA-SLH-75-45	43° 30.0'	81° 50.0'	21	Gray Sandy Clay
EPA-SLH-75-46	43° 30.0'	81° 55.0'	37	Gray Sandy Mud
EPA-SLH-75-47	43° 30.0'	82° 05.0'	52	Dk. Gray Sandy Silt

(continued)

TABLE 2. (continued)

STATION NUMBER	LOCATION		WATER DEPTH (METERS)	GROSS SEDIMENT CHARACTERISTICS
EPA-SLH-75-48	43° 35.0'	82° 10.0'	46	--
EPA-SLH-75-49	43° 35.0'	82° 05.0'	58	Brown Mud
EPA-SLH-75-50	43° 35.0'	81° 55.0'	43	Gray Sandy Mud
EPA-SLH-75-51	43° 35.0'	81° 50.0'	21	Gray Sandy Clay
EPA-SLH-75-52	43° 40.0'	81° 50.0'	21	--
EPA-SLH-75-53	43° 40.0'	82° 00.0'	73	Brown Gravelly Mud
EPA-SLH-75-54	43° 45.0'	82° 55.0'	46	Gray Clayey Silt
EPA-SLH-75-55	43° 45.0'	82° 05.0'	73	Dk. Gray Sandy Silt
EPA-SLH-75-56	43° 45.0'	82° 10.0'	64	--
EPA-SLH-75-57	43° 50.0'	82° 10.0'	76	Dk. Gray Sandy Silt
EPA-SLH-75-58	43° 50.0'	82° 00.0'	64	Brown Clayey Sand
EPA-SLH-75-59	43° 55.0'	82° 10.0'	67	Brown Sandy Silt
EPA-SLH-75-60	43° 55.0'	82° 00.9'	76	Gray Sandy Mud
EPA-SLH-75-61	43° 55.0'	81° 55.0'	40	Gray Silt
EPA-SLH-75-62	44° 00.0'	81° 55.0'	37	Gray Sandy Silt
EPA-SLH-75-63	44° 00.0'	82° 05.0'	73	Gray Sandy Silt
EPA-SLH-75-65	44° 05.0'	82° 10.0'	91	Gray Sandy Silt
EPA-SLH-75-66	44° 05.0'	82° 05.0'	82	Gray Sandy Silt
EPA-SLH-75-67	44° 05.0'	82° 00.0'	55	Gray Mud
EPA-SLH-75-68	44° 10.0'	82° 10.0'	91	Gray Brown Sandy Silt
EPA-SLH-75-69	44° 15.0'	82° 10.0'	82	Gray Sandy Silt
EPA-SLH-75-70	44° 15.0'	82° 20.0'	91	Dk. Gray Sandy Mud
EPA-SLH-75-71	44° 15.0'	82° 50.0'	61	Gray Sandy Silt
EPA-SLH-75-73	44° 15.0'	83° 00.0'	58	Gray Sandy Mud

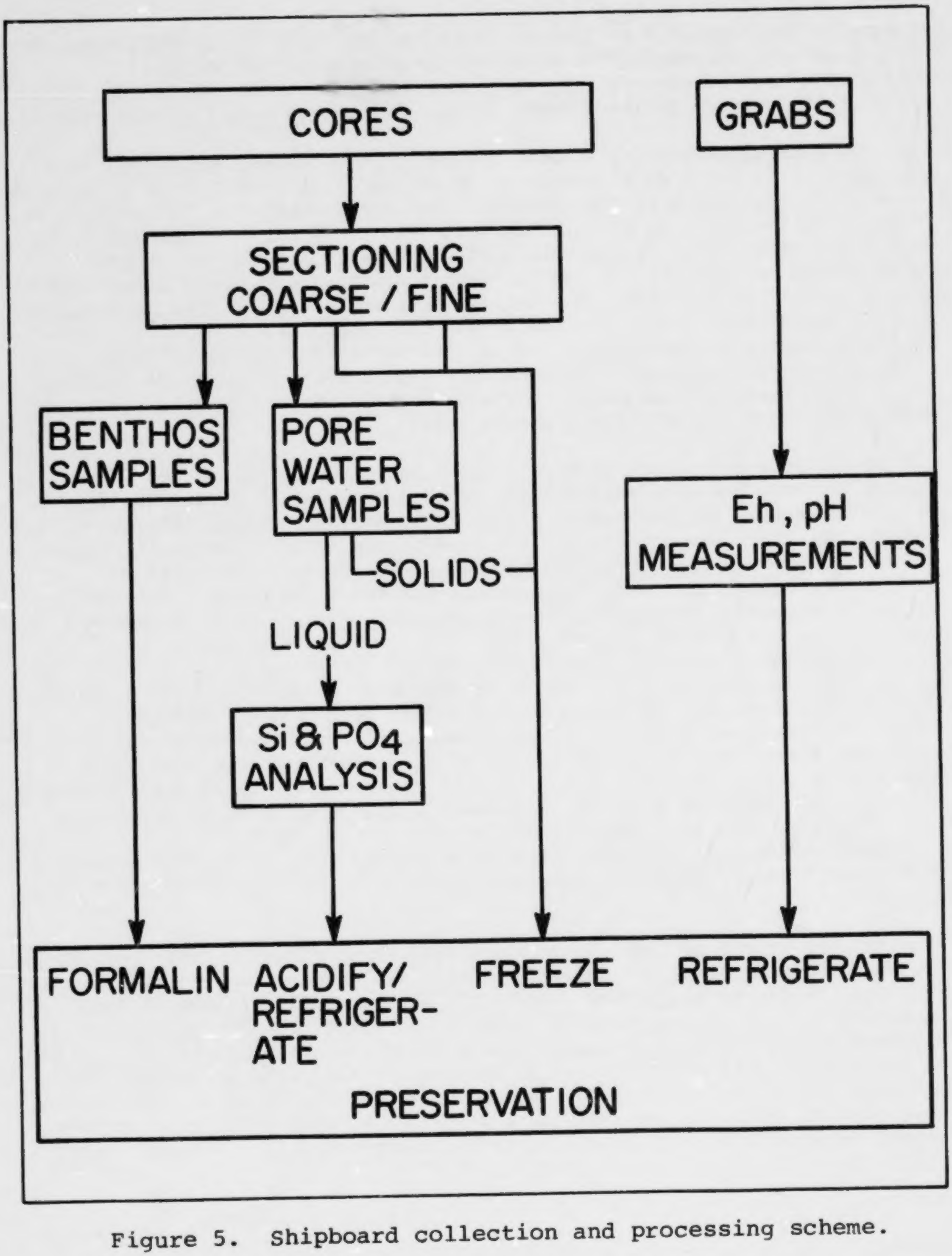
CORES
GRABS
SECTIONING
COARSE / FINE
BENTHOS
SAMPLES
PORE
WATER
SAMPLES
SOLIDS
LIQUID
Si & PO4
ANALYSIS
Eh, pH
MEASUREMENTS
FORMALIN
ACIDIFY/
REFRIGER-
ATE
FREEZE
REFRIGERATE
PRESERVATION

Figure 5. Shipboard collection and processing scheme.

plastic collar made of a section of liner having centimeter graduations. By this means even unconsolidated material could be sectioned without appreciable loss of material and with adequate preservation of the relationship between sediment depth and cumulative dry mass per unit area.

Two general sectioning schemes were used: (1) coarse sectioning; 1 cm intervals to 14 cm, 2 cm intervals to 30 cm, and 5 cm intervals to a depth of 60 cm or to the bottom of the core; (2) fine sectioning; 0.5 cm intervals to 10 cm, 1 cm intervals to 20 cm, 2 cm intervals to 30 cm, and 5 cm intervals to a depth of 60 cm or to the bottom of the core. Recovery of sediment was quantitative for all one and two centimeter sections while only about half of each 5 cm section was kept. The maximum time cores were allowed to stand at ambient temperature before sectioning was one hour. Expansion of the cores or the formation of gas pockets during this period was not significant although such problems are significant in high sedimentation areas such as the eastern basin of Lake Erie. Sediment sections were stored in preweighed polyethylene bottles and frozen aboard ship.

Cores from four stations were sampled for interstitial water. The method is described here very briefly as it has already been described in detail by Robbins and Gustinis (1976). Immediately following collection, the core in its liner was mounted on an extruding stand and a set of insulated copper coils was slipped over the outside of the liner. The coils were cooled by circulating a mixture of antifreeze and water using a constant temperature pumping system (Lauda model K-2/RD). Sediments were extruded into a glove box (550 cc volume) filled with nitrogen supplied by a pressure-building dewar of liquid nitrogen which provided about 10^5 l of N_2 gas at STP. Within the glove box, sediments were transferred to a modified (Robbins and Gustinis, 1976) gas-operated diaphragm squeezer (Reeburgh, 1967). A cross-sectional view of the squeezer is shown in Fig. 6. Pore water was forced through a 0.45 micron 90 mm dia. Millipore filter under about 100 p.s.i.g pressure. Approximately 30 ml of pore water was obtained within 20 minutes from each one centimeter sediment section. A portion of this sample was analyzed immediately for reactive Si and PO_4 by spectrophotometric methods described below while the remainder was acidified with about 1 ml of ULTREX concentrated nitric acid and refrigerated for later analysis.

At each of two stations in southern Lake Huron (EPA-SLH-75-14 and 18) twelve cores were taken for determination of the composition, density and vertical profile of zoobenthos. Each core was hydraulically extruded and sectioned in 1 cm intervals to 10 cm within 30 minutes of collection. It is presumed that short storage times reduced the extent of migration of animals in response to altered conditions of temperature and light intensity. The effect of coring and storage on the vertical distribution of benthos was not investigated. Sediment sections were preserved with buffered formalin and stored in plastic bags for analysis in the laboratory.

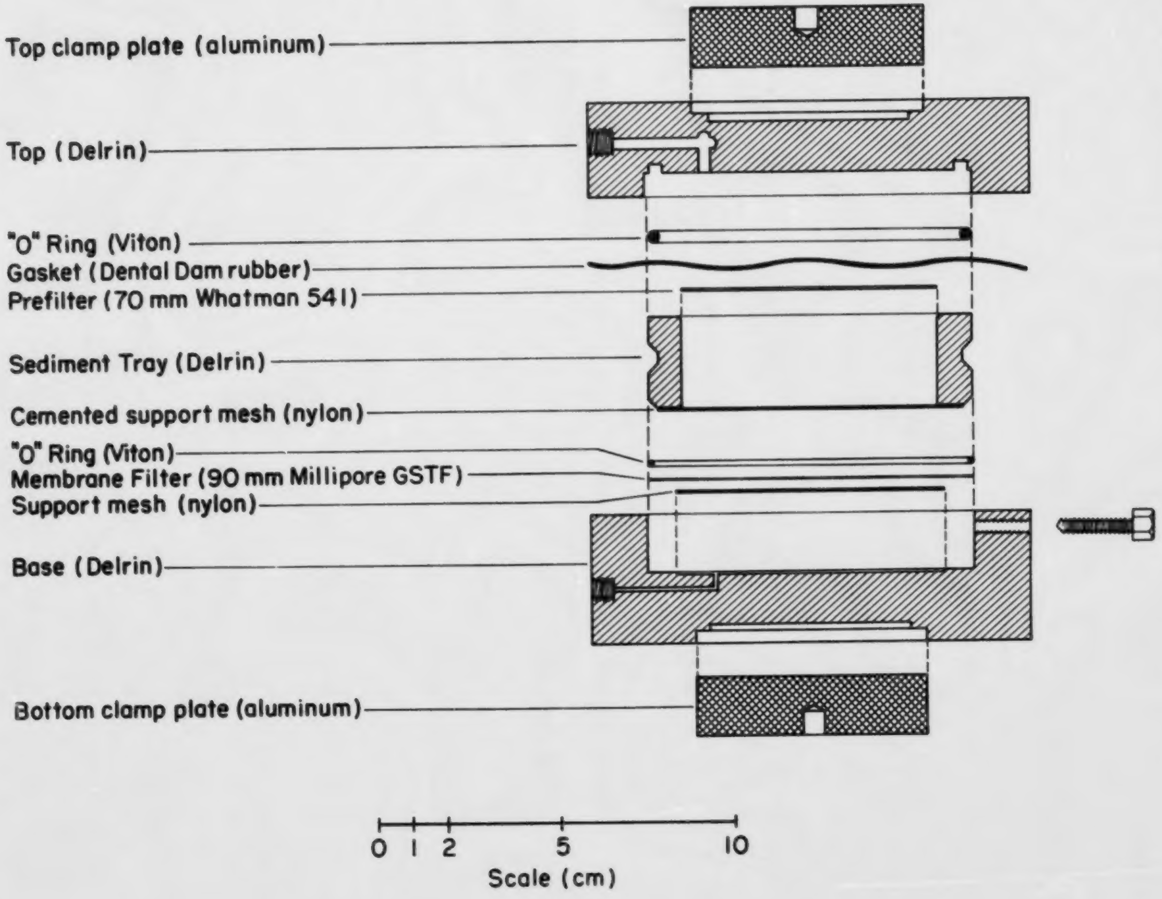
Top clamp plate (aluminum)
Top (Delrin)
"O" Ring (Viton)
Gasket (Dental Dam rubber)
Prefilter (70 mm Whatman 541)
Sediment Tray (Delrin)
Cemented support mesh (nylon)
"O" Ring (Viton)
Membrane Filter (90 mm Millipore GSTF)
Support mesh (nylon)
Base (Delrin)
Bottom clamp plate (aluminum)
0 1 2 5 10
Scale (cm)

Figure 6. Cross-sectional view of cassette sediment squeezer.

LABORATORY METHODS

In the laboratory sediment samples were processed according to the scheme indicated in Fig. 7. The analytical methods and measured quantities are summarized in Table 3. Description of the methods below is organized by sediment phase.

Analysis of Wet Sediment

Bulk Density

The bulk density of wet sediment was determined by weighing tared bottles containing frozen sediments. Uncertainty in the bulk density is largely due to inaccuracies in specifying the section thickness (± 0.1 cm). Hence the uncertainty is around 10% for 1 cm sections and 5% for 2 cm sections. The data are provided in Table A-1 of the Appendix.

Zoobenthos

Formalin-preserved wet sediment samples were suspended in approximately one liter of tap water and sieved using a No. 10 Nitex screen (mesh size: 0.15mm). Organisms were isolated under 10X or greater magnifications. Chironoimids and oligochaetes were identified under a compound microscope. Additional information on methods can be found in Robbins et al. (1977) and Krezoski et al. (1978). Based on previous sampling experience with oligochaetes in deeper parts of the Great Lakes (S.C. Mozley, personal communication) the estimated standard error in the vertically integrated density is about 20% for analysis of twelve cores. This precision is desirable for studies of benthic invertebrates (Elliot, 1971). Zoobenthos data are given in Table A-6 of the Appendix. Standard errors in estimating the vertical distribution of benthos can be very large (>100%) at some depths because of the very low benthos densities and the large variability between replicate cores.

Dry Sediment

Fraction Dry Weight

Weighed frozen sediment samples in preweighed polyethylene bottles were freeze-dried for at least 4-5 days. Samples remained frozen during removal of moisture even when additional heat was applied via hot plate to facilitate drying. Following freeze-drying, samples were again weighed to obtain the fraction dry weight, the cumulative dry weight per unit area of the core and, by inference, the sediment porosity. Uncertainties in the estimate of the fraction dry weight are less than 5%. Uncertainties in calculation of the cumulative dry weight are around 10% or less provided the error in estimating section thickness is truly random. Any systematic error involved in sectioning the core will result in an increasing absolute error in the estimate of the cumulative dry weight of sediment. The error in estimating the porosity which is calculated from the fraction dry weight assuming a constant density of sediment solids ($\rho_s = 2.54\ g/cm^3$) is 15% or less.

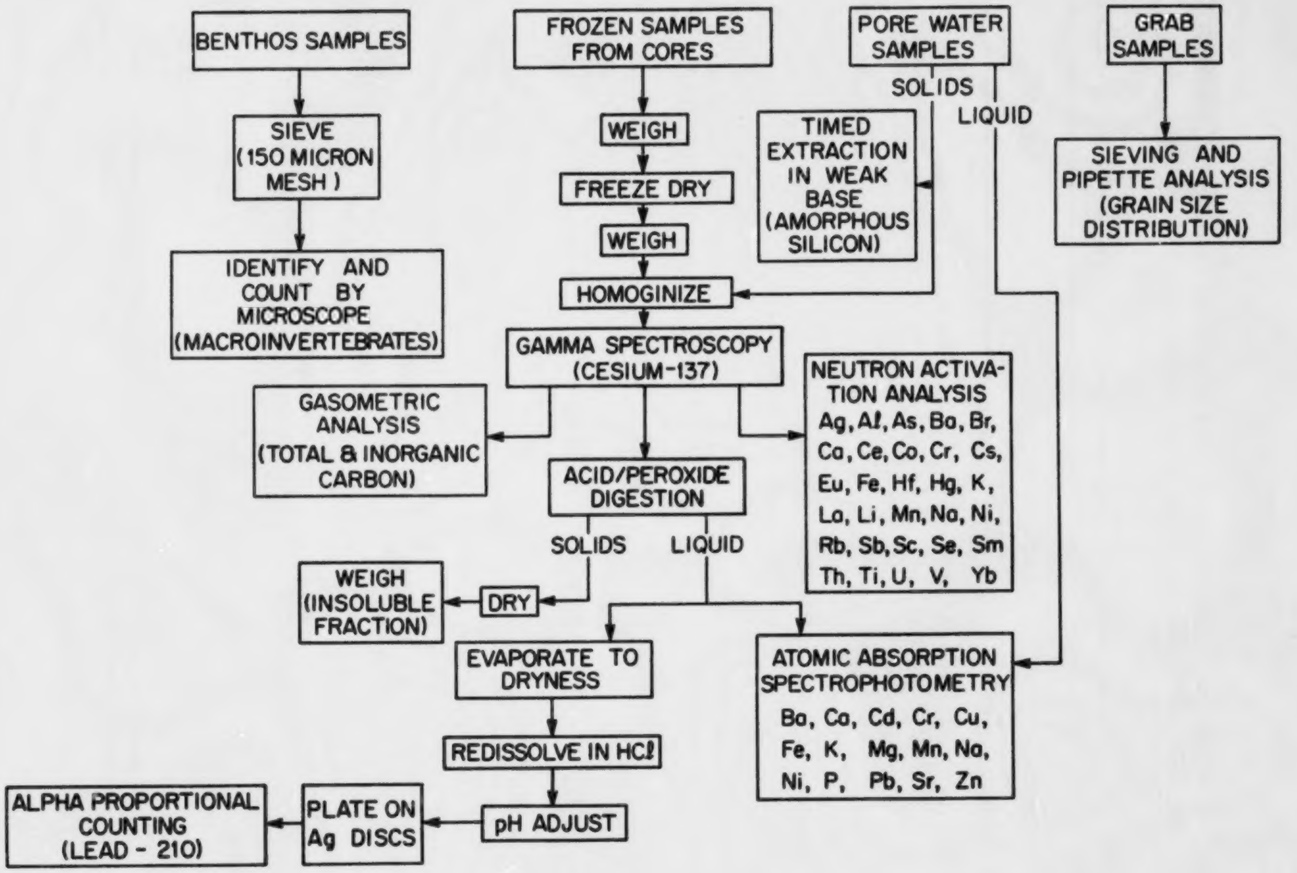
BENTHOS SAMPLES
SIEVE (150 MICRON MESH)
IDENTIFY AND COUNT BY MICROSCOPE (MACROINVERTEBRATES)
FROZEN SAMPLES FROM CORES
WEIGH
FREEZE DRY
WEIGH
HOMOGINIZE
GAMMA SPECTROSCOPY (CESIUM-137)
GASOMETRIC ANALYSIS (TOTAL & INORGANIC CARBON)
ACID/PEROXIDE DIGESTION
SOLIDS
LIQUID
DRY
WEIGH (INSOLUBLE FRACTION)
EVAPORATE TO DRYNESS
REDISSOLVE IN HCl
pH ADJUST
PLATE ON Ag DISCS
ALPHA PROPORTIONAL COUNTING (LEAD - 210)
PORE WATER SAMPLES
SOLIDS
LIQUID
TIMED EXTRACTION IN WEAK BASE (AMORPHOUS SILICON)
NEUTRON ACTIVATION ANALYSIS
Ag, Al, As, Ba, Br, Ca, Ce, Co, Cr, Cs, Eu, Fe, Hf, Hg, K, La, Li, Mn, Na, Ni, Rb, Sb, Sc, Se, Sm, Th, Ti, U, V, Yb
ATOMIC ABSORPTION SPECTROPHOTOMETRY
Ba, Ca, Cd, Cr, Cu, Fe, K, Mg, Mn, Na, Ni, P, Pb, Sr, Zn
GRAB SAMPLES
SIEVING AND PIPETTE ANALYSIS (GRAIN SIZE DISTRIBUTION)

Figure 7. Sample analysis scheme.

TABLE 3. A SUMMARY OF THE PHYSICAL AND CHEMICAL PARAMETERS DETERMINED FOR SEDIMENTS OF SOUTHERN LAKE HURON AND SAGINAW BAY

Sediment Fraction	Parameter	Method
1. Wet sediment	a. bulk density	weighing
	b. zoobenthos	sieving/microscopic study
	c. Eh/pH*	electrode
	d. grain size*	sieving/pipette
2. Dry sediment	a. fraction dry weight, cumulative mass per unit area	weighing
	b. cesium-137	gamma spectroscopy
	c. Trace elements Ag, Al, As, Ba, Br, Ca, Ce, Co, Cr, Cs, Eu, Fe, Hf, Hg, K, La, Lu, Mn, Na, Ni, Rb, Sb, Sc, Se, Sm, Th, Ti, U, V, Yb	neutron activation analysis (NAA)
	d. Organic/Inorganic Carbon	gasometric
3. Acid-peroxide extracts	a. Fraction soluble	centrifuging/weighing
	b. Trace elements: Ba, Ca, Cd, Cr, Cu, Fe, Hg, K, Mg, Mn, Na, Ni, P, Pb, Sn, Sr, Zn	atomic absorption spectrophotometry (AAS)
	c. lead-210	alpha proportional counting
4. Base extracts	a. Amorphous silicon	colorimetric
5. Pore water	a. Reactive Si and PO_4	colorimetric
	b. Trace elements: Ba, Ca, Fe, Mg, Mn, K, Na, Sr, Zn	(AAS)

*for Saginaw Bay samples only

Fraction dry weight, cumulative dry weight and porosity data are given in Table A-1 of the Appendix.

Cesium-137

The cesium-137 activity of sediment samples was determined by gamma spectroscopy using a well-shielded 3x5 inch NaI(Tl) crystal gamma detector connected to a multichannel analyzer (Nuclear Data 100). Prior to counting, sediment samples were ground by mortar and pestle and compacted into a cylindrical plastic container. Standardization of the sample geometry is necessary for accurate measurement of absolute activity. The cylindrical configuration of sediment was placed concentrically on the axis of the detector several millimeters from the crystal face and counted for times ranging from 2 to 60 hours. Standards of the same geometry were prepared by doping inactive sediments with known amounts of cesium-137 (Amersham Searle Corp.). Doped samples were then counted to obtain the counting efficiency of the system for different sample volumes (variable height, constant cross-sectional area). The total activity of cesium-137 (vertically integrated) is given in Table 36 while vertical distribution data are given in Table A-4 of the Appendix. Uncertainties indicated refer only to the Poisson statistical error in counting the sample. Other sources of error are negligible.

Trace Elements (via neutron activation analysis, NAA)

Up to 25 trace elements were determined in portions of freeze dried sediments via non-destructive neutron activation analysis using the Ford Nuclear Reactor at the Phoenix Memorial Laboratory (University of Michigan, Ann Arbor, Michigan). Both pneumatic-tube and in-pool irradiations were carried out. The pneumatic tube method is applicable to measurement of elements with half lives the order of a few hours or less where short exposure times are required. In-pool irradiations involve insertion of samples into the core of the reactor to obtain maximal thermal neutron fluxes. This method is used to achieve long exposure times for measuring elements with long half lives.

For the pneumatic-tube irradiations, 50-75 mg splits of each sample, ground well to avoid homogeniety problems, were weighed into small polyethylene vials. For each four such samples, two comparative standards were prepared: U.S. Geological Survey Standard Rock Sample USGS-BCR-1; (See Flanagan, 1973) and PML primary standard. Samples and standards were initially irradiated for 25 seconds at a thermal neutron flux at about 10^{12} n/cm^2/sec, allowed to undergo decay for 20 minutes, and counted for 30 seconds. When all residual activity from the 25 second irradiation had decayed (in 3 to 4 days), four samples and two standards were again irradiated, this time for 10 minutes, allowed to decay for 12 hours and counted for 400 seconds. The first irradiation yielded data for Al, Ca, Mn, Ti and V. The second provided a measurement of K, Na and Mn.

For the in-pool irradiations, 60-70 mg portions of four sediment samples and two standards were weighed into ultra-pure Synthetic quartz tubing (Suprasil T-21, Amersil, Inc., Hillside, New Jersey). Standards used were U.S.G.S. rock samples, USGS-BCR-1 and USGS-RGM-1. The quartz tubes containing sediments or standards were flame-sealed and groups of seven were irradiated for ten hours within the core at a thermal neutron flux of about

10^{13} n/cm^2/sec. then allowed to decay for eight days. Following this "cooling" period, samples were separated, the outside surface of the quartz tubes cleaned, dried and counted for 1800 seconds. After two weeks, following decay of the intermediate lived isotopes, the samples were counted for 7200 seconds to obtain data for the long-lived constituents. The first counting yielded data for Ag, As, Ba, Br, La, Lu, Na, Ni, Rb, Sc, Sm, Th, Yb and U. Second counting provided a measurement of Ce, Co, Cr, Cs, Eu, Fe, Hf, Hg, Sb, Sc and Se.

A specially prepared sample of standard lake mud (SLM-1) was analyzed via this method (NAA) to ascertain the reproducibility of the method. A large (>10 1) sample consisting of the upper 20 cm of several cores of fine-grained sediment from Lake Michigan was placed in a multilayered polyethylene bag and homogenized thoroughly by kneading the outside of the bag. The sample was then frozen and on return to the laboratory was freeze-dried, ground in a mortar and pestle, sieved to 250 mm mesh size and split into sixteen subsamples using a conventional riffle sample splitter. Two subsamples, SLM-1-1 and SLM-1-10 were further subdivided into 4 and 3 splits respectively for a total of 7 replicate NAA analyses. In each case about 200 mg of sample was irradiated. These original analyses were completed in early 1976; in Jan. 1978 a 200 mg sample of SLM-1-1 was re-analyzed by the method thus providing another replicate sample.

Gamma spectra were obtained using an lithium-drifted germanium detector (Ortec, Inc., Oak Ridge, Tenn.) having a resolution of 2.0 - 2.3 Kev fwhm for the 1332 KeV cobalt-60 gamma ray. Intrinsic detector efficiency is about 12-15%. The detector was interfaced to a semiautomated nuclear data 4420 minicomputer pulse height analysis system. Spectral data were stored on magnetic disk immediately following the end of each counting period and subsequently reduced by computer. Details of the irradiation procedures, sources of uncertainty, corrections for interferences and data reduction methods are given by Dams and Robbins (1970). The reliability of the method is discussed further below.

Total and Inorganic Carbon

A gasometric technique was used to obtain the total and inorganic carbon content of the sediment samples. Total carbon was determined by combustion of 2-3 grams of sediment. The CO_2 evolved is assumed to result from complete oxidation of organic carbon and conversion of inorganic carbonate to CO_2. The procedure was carried out using the LECO carbon analyzer (Furnace Model No. 507-100 and Volumetric System Model No. 572-200). Inorganic carbon was determined on the same system by titrating the sediment with acid to evolve $CO2$ from the carbonate phases. The organic carbon content is inferred to be the difference between total and inorganic carbon.

The precision of the method (e.g. Kolpack and Bell, 1968; Bien, 1952) was examined by analyzing 15 standard lake mud samples (SLM-1-8). The average value of total organic carbon was 5.45 ± 0.15 percent by weight. Thus the standard deviation in the estimate of the mean is about 3% (Table 6). There is an additional source of uncertainty which must be built in to the overall error which results from variable uptake of moisture by sediments. Before processing, sediments were first dried at 100° C for 24 hours. The reduction in weight for Standard Lake Mud (SLM-1-8) was 1.5%. This was not corrected for in estimating the total carbon concentration because the re-uptake of moisture after drying but before combustion was not determined. Hence the overall error (including calibration errors) in estimating the total carbon content of a single sample is probably less than 10%.

The method for inorganic carbon analysis follows that described by Kolpack and Bell (1968) with the following exceptions: (1) 10 ml of 2N HCl were added per gram of sample, (2) 4 ml of 5% $FeSO_4$ were added to each sample and (3) a temperature of 70-80° was maintained throughout digestion. Analyses of $CaCO_3$ and standard lake mud samples indicate the overall error in estimating inorganic carbon in a single sample to be less than 5%. The mean concentration of inorganic carbon in six replicate samples was 3.26 ± 0.07 percent by weight.

All measurements were corrected for temperature and pressure variations. The organic and inorganic carbon data are given in Table 9.

Acid - peroxide Extracts

Soluble Fraction

A slurry of 2-3 g of ground freeze-dried sediment and 25 ml of distilled water was prepared in 250 ml glass beakers. 25 ml of conc. HNO_3 are added slowly to control the extent of foaming. After foaming subsided, 5 ml of 30% H_2O_2 were carefuly added. The beakers were then covered with watch glasses and placed in an 90-95° C water bath for 96 hours. 5 ml 30% H_2O_2 were added every 24 hours. Following this sequence, the watch glasses were removed and the mixture was evaporated to near but not complete dryness (i.e. about 2 mm of solution on top of settled sediment). Evaporated samples were removed from the bath, allowed to cool and combined with 10% HNO_3 into 50 ml pre-weighted (±0.0001 g) centrifuge tubes. The tubes were spun for 20 min at 1800 rpm, the supernatant decanted and the sediment residue resuspended with a few ml of HNO_3 and the mixture recentrifuged. The rinse supernatant was combined with the original supernatant and the entire volume was diluted to 100 ± 0.02 ml with 10% HNO_3. Half of this solution was set aside for AAS analysis while the remaining solution was bottled separately for lead-210 analysis. The sediment residues in the centrifuge tubes were dried at 100° C overnight, weighed (± 0.0001 g) and stored in labeled Whirlpack$^{(TM)}$ bags.

The fraction soluble is computed as the ratio of the original sample weight minus the weight of this residue divided by the original sample weight. The uncertainty in the estimate of the fraction soluble can be as high as 15% because of the uncertainties in recovery and in weighing the sample residue. Data on the fraction soluble are given in Table 9.

Trace Elements (via Atomic Absorption Spectrophotometry, AAS)

The concentration of up to 16 elements (Ba, Ca, Cd, Cr, Cu, Fe, K, Mg, Mn, Mo, Na, Ni, P, Pb, Sr, and Zn) in sediment acid extracts and up to 11 elements (Ba, Ca, Fe, K, Mg, Mn, Ni, P, Si, Sr, and Zn) in interstitial waters were determined by Atomic Absorption Spectrophotometry.

Determinations of all elements except Cd were made on a Perkin-Elmer, Model 403 Spectrophotometer according to the standard conditions recommended for flame atomization in the Perkin-Elmer Operating manual (Perkin-Elmer Corp., Norwalk, Connecticut). Where necessary, dilution of extracts were made using 10% HNO_3. Cd concentrations were obtained by flameless atomization using a Varian Technion Model 1200 Atomic Absorption Spectrophotometer with a Model 60 Carbon Rod Atomizer (Varian Inc., Palo Alto, California).

Phosphorus concentrations were measured by the addition of an ammonium molybdate tetrahydrate solution to the acid extracts and the subsequent extraction of the resulting phosphomolybdic acid by iso-butyl acetate. The concentration of phosphorus could then be determined by measuring the absorption of Mo by AAS. This method is described in detail by Ramakrishna et al. (1969).

Toward the completion of this report it became feasible to analyze a number of samples for two additional elements, mercury and tin. New portions of freeze-dried material were allowed to leach in 6M HCl for about one month. Comparison of lead concentrations in samples from core 18A determined from 50% HNO_3 leaches made in 1977 with those determined in recent (Marc, 1980) 6 M HCl extraction gave the following results:

$$\text{Pb (1980 HCl leach)} = 1.010 \times \text{Pb (1977 } HNO_3 \text{ leach)} - 3.9$$
$$\text{with } r = 0.995 \text{ and } N = 10.$$

On the average there was a 6 ($\pm$5) percent difference in concentrations of lead as determined in separate portions of samples extracted by different methods, and analyzed by different people on different atomic absorption instruments. Concentrations of mercury were determined by means of the cold-vapor method described by Lawrence et al. (1980). One ml of the lechate was sonicated after addition of $SnCl_2$ and Hg vapors produced by this method were flushed into a cold vapor tube for analysis via AAS. Concentrations of tin were determined by reaction of the lechate with $NaBH_4$ to produce volatile tin hydrides which are detected via AAS. The method is essentially interference-free and capable of determining subnanogram quantities of Sn(IV) and the halides of many organotin compounds. As used here, the method gave values for total Sn(IV) concentrations. The method is described in detail by Hodge et al. (1979). Concentrations of mercury and tin in surface sediments are given in Table 12. Atomic absorption data for the other elements are given in Table 9 and in A-2 of the Appendix. Concentrations of dissolved constituents determined primarily via AAS are given in Table A-7.

Lead-210

The lead-210 activity of the sediment samples was determined by measurement of the alpha activity of its daughter, polonium-210. It is assumed that polonium-210 and lead-210 are in secular equilibrium in each sediment sample so that the activity of polonium-210 is exactly equal to the activity of lead-210. In most samples this condition will be met automatically because the age of the sample is large in comparison with the half-life of polonium-210 (138 days) and because neither lead-210 nor polonium-210 have appreciable mobility in the sedimentary column. Therefore in physically undisturbed sediments, each layer (subsample) is a closed system with respect to these two isotopes (see Robbins, 1978). Eakins and Morrison (1974) found evidence of polonium-210/lead-210 disequilibrium in near surface sediments but the effect is small. The long storage time of isolated sediment sections prior to analysis (about 1 year) favors establishment of secular equilibrium even in sections where the possibility exists of a small degree of in situ disquilibrium.

The method of determining the activity of polonium is adapted from the procedure of Holtzman (1963), Flynn (1968), and Robbins and Edgington (1975) which takes advantage of the ability of polonium to selectively self-plate onto polished silver discs. The 50 ml extract of the sample (in 10% HNO_3) set aside for Pb-210 analysis, was dried at a temperature of 90° C. Then 10 ml of concentrated HCl and a few drops of H_2O_2 were added and the sample re-evaporated to dryness. Caution was taken to keep the temperature at or below 90° C. Polonium chloride sublimes at 190° C. The steps of adding HCl and H_2O_2 and evaporation were repeated twice for a total of three evaporations to dryness with HCl to thoroughly eliminate traces of NO_3 ions. Their presence in strong acid will cause etching of the silver disc and prevent complete self-plating of polonium. The extract was then dissolved in 10 ml of hot 10% HCl, and 1.0 gram of ascorbic acid plus 10 ml of distilled water was added. The pH was adjusted to 1.4 ± 0.1 by addition of concentrated NH_4OH via pipette. This solution of less than 40 ml final volume was then transferred to plating containers made from 8 ounce "Nalgene" square linear polyethylene wide-mouth bottles. A 1 ml Eppendorf pipette tip inserted through a hole in one of the bottom corners of the bottle served as a stopper and vent.

Approximately 1/8 inch of bottle tip was removed and smoothed by pressing on a hot plate, trimmed and ground flat with 0.7 micron abrasive. A washer intended for 3/4 in bolts inside the bottle cap served to press a 0.005 inch thick 1.5" diameter silver disc against the ground surface to create a seal. The silver discs (Handy and Harmon Corp., New York, New York) were polished by means of a slurry of 0.3 micron "Alpha Micropolish" (Bueler Inc.). Each container was rinsed with distilled water and then with 10% HCl prior to filling with pH adjusted extracts. The plating containers (15) were installed in a water bath shaker (Eberbach, Co.) and shaken for two hours at 85-90° C. Efficiency of plating was occasionally checked by replating the solution. The ratio of the activity on second plating to that on first plating indicated an efficiency consistently better than 90%. Then containers were disassembled and silver discs were rinsed first with distilled water, then with methanol and counted on a 2-pi gas-flow proportional counter (NMC Model DS-2P, Scaler and PCC-11T proportional counter, Nuclear Measurements Corporation, Indianapolis, Ind.). The efficiency of the counter was determined using a standard lead-210 (polonium-210) source. Raw counts are corrected for decay of polonium following plating and converted into absolute activity per unit weight of sediment (pCi/g). Lead-210 data are given in table A-5 of the Appendix. Uncertainties indicated refer only to the Poisson statistical error in counting the sample. The overall uncertainty is significantly larger because of the variability in plating efficiency. The estimated error introduced by this factor combined with other sample processing errors yields a 10% error which must be combined with the counting error provided in table A-5.

Basic Extracts

Amorphous Silicon

To determine the amorphous silicon content of the sediments a modified version of the method of Mckeys et al. (1974) was used. The method takes advantage of the differing rates of dissolution for various forms of silicon. Authigenic particulate silica, diatoms and possibly other non-crystalline (amorphous) phases (see Nriagu, 1977) dissolve rapidly (within one to two hours) in 0.5N NaOH at room temperature. In contrast, silicon associated with clay mineral dissolves under such conditions at a very much slower rate, while silicon as quartz is resistant to dissolution to any significant degree over time periods of 6 hours or so.

In the method of McKeys et al., sediment samples are treated alternatively with strong acid and weak base. They found that alternating acid-base treatment dissolved more amorphous silica than the base treatment alone. McKeys et al. conjectured that strong acid removes iron and other metal coatings on surfaces of amorphous silica which hinder dissolution (see also Hurd, 1973). Because of time constraints, the alternating acid-base treatment was not followed. Rather, samples were pre-treated with acid as a one shot exposure. It was found that the difference between a one shot exposure and alternate acid-base treatments was not large. The latter treatment dissolved about 10% more amorphous silicon than the single acid treatment (SLM-1-8).

30 mls of 8N HCl were added to poly-propylene centrifuge tubes containing 0.1-0.4 g crushed dried sediment previously squeezed to obtain pore water. After 30 minutes, the mixture was centrifuged, the supernatant discarded and the sediment washed with distilled water and transferred to a polyethylene bottle with 200 ml 0.5N NaOH. The bottle was tightly capped and agitated on a rotary arm shaker at room temperature. Approximately each hour, 4 ml of solution were removed via polyethylene syringe, filtered through a 0.45 micron filter and stored at 40° C.

After about six hours a suite of filtered samples were analyzed for reactive dissolved silicon colorimetrically (Bausch and Lomb Spec 100 Spectrophotometer) using the method outlined by Strickland and Parsons (1960). The method was modified for use with 0.5N NaOH rather than water. Analysis of replicate samples indicated an overall error of about 10% in estimating the amount of reactive dissolved silicon in solution.

The amorphous silicon concentration was estimated by extrapolating the amount of silicon dissolved per gram of dry sediment back to zero time. Error in replicating of the amorphous silicon content is around 15%. Limits to the acccuracy of the method are discussed below.

Pore Water

Reactive Si and PO_4.

The concentration of dissolved reactive phosphate and silicon in pore water was determined colorimetrically by the method of Sutherland et al. (1966). Samples were stored under refrigeration (4° C) for not more than about two hours following sediment "squeezing". A mixed reagent of ammonium molybdate and potassium antimony tartrate was used to form a blue phosphomolybdate complex for the determination of phosphate. Absorbance was measured at 690 nm. An ammonium molybdate solution was used to complex the reactive dissolved silicon. The absorbance of the resulting yellow silicomolybdic complex was measured at 400 nm. Shipboard colorimetric determinations were made on a Bausch and Lomb Spectronic 100 Spectrophotometer (Bausch and Lomb, Rochester, New York). Analytical uncertainty in silicon and phosphate concentrations are generally around 10% and 15% respectively. Limitations in the accuracy of the methods are further discussed below.

Other Constituents

The concentrations of Ba, Ca, Fe, Mg, Mn, K, Na, Sr and Zn were determined using Atomic Absorption Spectrophotometry (Perkin Elmer 403 spectro- photometer). As sample volumes were extremely limited, replicate analyses were not possible. However the approximate uncertainty of replication can be inferred from comparison of concentrations in a set of contiguous pore water samples toward the bottom of sediment cores where real variations should be negligible. Analysis of 1-6 such samples shows that the replication error is roughly 20% for Ba, 5% for Ca, 10% for Fe, under 5% for Mg and Mn, about 30% for PO_4, 10% for K, under 5% for Si, about 5% for Sr and over 40% for Zn. The high uncertainties for Ba and Zn arise because concentrations are near the limits of detection. The high value for PO_4 is probably at least in part due to air exposure effects discussed further below.

Accuracy of Results

Neutron Activation Analysis

The results of analysis of seven replicate standard lake mud samples are given in Table 4. It can be seen that the precision of the analytical results is excellent for most elements. The percent deviation from the mean is mostly under 10% and only a few elements have concentrations deviating by more than 20% from the mean. With 7 replicate analyses, the error in estimating mean concentration of most elements is better than 5% and all elements are determined to better than 10%. There is no significant difference between mean concentration of split 1 and split 10 for any specific element. However, taken as a whole, mean concentrations are 2% higher in split 10 (weighted average) than in split 1. As the samples were analyzed randomly it is unlikely that this systematic variation arises from differential treatment of samples or standards. Most likely it is the result of sample inhomogeneity.

The reproducibility of the neutron activation method was further

TABLE 4. COMPOSITION OF STANDARD LAKE MUD SAMPLES (SLM-1-1 AND SLM-1-10) DETERMINED VIA NEUTRON ACTIVATION ANALYSIS (CONCENTRATIONS IN μg/g DRY WEIGHT)

	SLM-1-1						SLM-1-10					Combination			
	Subsample						Subsample								
Element	1	2	3	4	Mean N=4	Standard dev.	1	2	3	Mean N=3	Standard dev.	Mean N=7	Standard dev.	% dev.	% error in ave. est.*
Al	53596	52375	48332	53193	51874	2415	53135	54175	53839	53716	530	52700	2000	4	1.4
As	3.64	7.97	<10.0	<10.3	8.0	3.0	<10.5	<10.4	6.82	9.2	2.1	6.14	2.24	36	12.5
Ag	<2.38	<1.94	<2.00	<2.02	-	-	<2.08	<2.05	<2.02	-	-	-	-	-	-
Ba	439	361	526	290	400	100	498	566	370	475	98.7	434	99	23	8.0
Br	46.2	38.4	40.8	38.5	41.	4.0	42.7	43.0	37.4	41.0	3.15	41.0	3	8	2.8
Ca	70397	62846	70321	77576	70310	6055	74349	69417	65871	69879	4257	70100	5000	7	2.5
Ce	53.4	51.7	51.5	48.1	51.2	2.2	51.1	52.7	54.6	52.8	1.75	51.9	2.0	4	1.4
Co	11.94	11.79	11.95	11.64	11.8	0.15	12.45	12.13	12.08	12.2	0.20	12.0	0.3	2	0.7
Cr	81.7	97.3	87.9	87.9	88.7	5.4	92.8	88.9	85.2	89.0	3.8	88.8	5	6	2.1
CR	4.38	5.23	4.86	4.38	4.71	0.41	4.94	4.82	4.08	4.61	0.47	4.67	0.4	9	3.2
Eu	0.99	0.89	0.94	0.87	0.92	0.05	0.92	0.91	0.89	0.91	0.02	0.91	.04	4	1.4
Fe	33288	32347	33912	32598	33036	706	34522	33392	32921	33612	822	33300	800	2	0.7
Hf	4.37	4.08	4.22	4.10	4.19	0.13	4.65	4.32	3.60	4.19	0.54	4.19	0.3	8	2.8
Hg	<0.10	<1.17	<1.39	<1.41	-	-	<1.43	<1.43	<1.07	-	-	-	-	-	-
K	22088	16442	23754	21734	21005	3167	24277	29496	26668	23814	3112	22200	3000	15	5.3
La	25.8	27.0	27.4	26.1	26.6	0.8	27.4	28.3	27.7	27.8	0.46	27.10	0.9	3	1.1
Lu	0.36	0.36	0.51	0.45	.42	0.08	0.57	0.54	0.31	0.47	0.15	0.44	0.1	22	7.7
Mg	37381	26225	27113	25865	29145	5515	27364	27898	28716	27993	681	28700	4000	14	4.9
Mn	600	572	689	597	539	53.0	558	666	689	674	12.7	654	50	7	2.5
Na	5003	4702	4754	4614	4768	167	4704	4535	6670	5303	1187	5000	800	15	5.3
Ni	<64.3	<35.1	<72.1	<72.3	-	-	<74.17	<74.4	<56.8	-	-	-	-	-	-
Rb	100.6	76.6	57.5	70.4	76.3	18.0	73.9	66.0	73.39	71.1	4.4	74.1	13	18	6.3
Sb	1.00	1.08	1.76	1.85	1.42	0.44	1.90	2.21	1.25	1.79	0.49	1.58	0.5	29	10.1
Sc	9.54	9.23	9.52	9.27	9.39	0.16	9.83	9.51	9.38	9.56	0.25	9.46	0.2	2	0.7
Sc	9.54	9.55	9.43	9.28	9.45	0.13	9.58	9.53	9.55	9.55	0.03	9.25	0.8	8	2.8
Se	<5.5	2.99	<2.77	<2.81	-	-	<2.83	<2.86	2.75	-	-	-	-	-	-
Sm	4.66	4.73	4.52	4.45	4.6	0.1	5.15	5.05	4.47	4.89	0.37	4.72	0.3	6	2.2
Th	7.04	8.45	7.10	6.76	7.3	0.8	7.59	7.48	7.16	7.41	0.22	7.37	0.6	8	2.8
Ti	2344	3656	3402	3312	3229	554	4290	2905	4382	3879	793	3510	700	21	7.4
U	2.26	3.94	4.68	3.68	4.0	1.0	3.34	3.41	5.57	4.11	1.27	3.84	1.0	27	9.5
V	76.86	68.9	60.7	75.0	68.3	5.7	73.4	83.1	104.9	87.1	16.1	76.4	14	19	6.7
Yb	2.35	2.85	1.99	1.94	2.3	0.4	2.04	2.00	2.22	2.09	0.12	2.20	0.3	15	5.3

*100 * ($\sqrt{N-1}/N$) * Standard Deviation/mean investigated by reanalysis of the standard lake mud sample (SLM-1-1) two years later. The results are summarized in Table 5. In general, the long term reproducibility is good. Agreement with the mean concentrations is usually better than 10%. Thus the level of precision survives variability in laboratory techniques, use of new standards and minor modifications in analysis of raw data over a two year period. Only for one element, Lu, is the reproducibility poor. Reasons for the significantly lower value on reanalysis are obscure but are probably due to use of new PML or USGS standards in combination with interferences which affect the accuracy of the results.

To investigate the accuracy of the method five USGS, rock standards other than BCR-1 and RGM-1 were analyzed as unknowns. The "unknowns" were two samples of USGS-GSP-1, two USGS-G-2 and one sample of USGS-AGV-1. A measure of the accuracy of the determination is given as

$$Q_A = (100/N) \sum_{i=1}^{N} (C_i - C_A) / C_A \qquad (1)$$

where C_i is the measured concentration of a given element in the i^{th} standard while C_A is the accepted concentration of the i^{th} standard (N=5). Thus Q_A is the mean percent deviation from accepted values. This value may be compared with the mean deviation of the concentration of a given element (C_i) in SLM-1 samples (N=7) from the mean concentration (C)

$$Q_P = (100/N) \sum_{i=1}^{N} (C_i - C) / C \qquad (2)$$

This measure of the precision is compared with the measure of accuracy in Figure 8. It can be seen that for most elements both Q_A and Q_P are under 10%. Exceptions occur for Ba and Lu where the precision is significantly less than the accuracy of the method and for Cr, Sb, and particularly for U where the accuracy of the method is considerably poorer than the precision. For these elements there are probably significant uncompensated interferences which limit the validity of the results. There may be an accuracy problem with Br as well. In most rock standards values of Br are unspecified. Results of an additional analysis of AGV-1 given in Table 5 show a dramatically higher measured concentration than the accepted value. Yet, bromine can be determined via NAA without interferences. Moreover contamination is unlikely to have occurred. Furthermore analysis of Br in SLM-1 samples gives a mean concentration (41 ppm) which is very comparable to

TABLE 5. RESULTS OF A SECOND ANALYSIS OF STANDARD LAKE MUD (SLM-1-1) AND OF A U.S. GEOLOGICAL SURVEY ROCK STANDARD (AGV-1) BY NEUTRON ACTIVATION ANALYSIS

	Concentration (Mg/g)					
	SLM-1-1			AGV-1		
Element	1975 Analysis[1]	1978 Analysis[2]	% difference	Accepted[3]	Measured[2]	% difference
As	<8	<6	-	0.8	<6	-
Ag	<2	<1.2	-	-	-	-
Bu	400+100	390+28	3	1208	1300±50	7
Br	41±4	39±0.4	5	0.6	2.3±0.4	300
Ce	51±2	49±.2	4	63	53±0.2	16
Co	11.8±0.2	10.0±0.07	16	14.1	11.8±0.1	16
Cr	89±6	83.2±1	7	12.2	9.9±0.5	19
Cs	4.7±0.4	3.8±.07	21	1.4	1.1±0.1	21
Eu	0.92±0.05	0.89±0.02	3	1.7	1.4±0.02	18
Fe	3300±700	2900±100	13	47300	36000±100	24
Hf	4.2±0.1	4.4±0.06	5	5.2	4.6±0.06	11
Hg	<1.4	<.5	-	-	-	-
La	26.6+0.8	27.0+0.2	2	35	38.7±0.2	11
Lu	0.42±0.08	0.20±.01	66	0.28	0.14±0.01	50
Na	4800±200	408±50	1	31600	30000±100	5
Ni	<72	<35	-	18.5	<35	-
Rb	76+1.8	77±2	1	67	57±2	15
Sb	1.4±0.4	1.4±0.06	0	4.5	3.7±0.1	18
Sc	9.4±0.1	9.9±0.03	5	13.4	12.0±0.03	11
Se	<3	<1.5	-	-	-	-
Sm	4.6+0.1	4.4+0.02	4	5.9	5.0±.02	15
Th	7.3±0.8	7.2±0.1	1	6.4	6.0±0.1	6
U	4.0±1.0	2.7±0.3	9	1.88	2.3±.28	22
Zn	-	86±2	-	84	30±1	64

---

[1] mean and standard deviation from analysis of four subsamples.

[2] analytical error associated with a single analysis.

[3] USGS standard values (Flannagan et al. 1973).

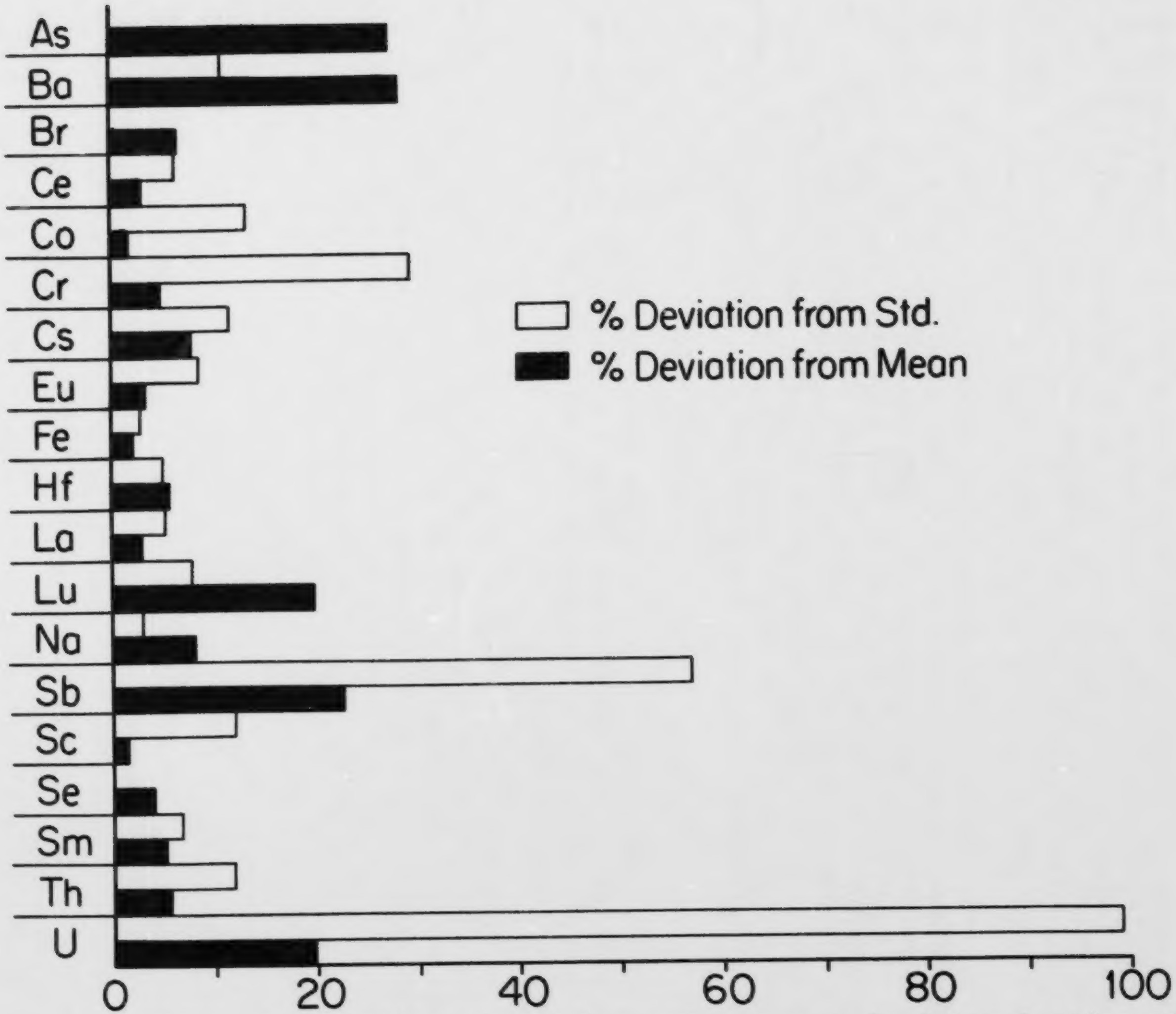

Figure 8. A comparison of analytical precision and accuracy in determination of trace element composition of standard lake sediment via neutron activation analysis.

concentrations reported by Shimp et al. (1971) for sediments collected in the same area of the lake. Therefore it is likely that the published value of Br is incorrect in this case. The inaccuracy in the Zn value is due to the presence of Sc. It is very difficult to properly correct for Sc interference and for this reason no NAA results are reported for Zn. The measured concentrations of elements in the AGV-1 sample (Table 5) are systematically too high by 10% primarily due to error in weighing small sample as well as to sample homogeneity. A comparison of the percent difference between first and second analyses for Lu (66%) and the apparent accuracy (AGV-1, 50%) indicates the possibility of significant inaccuracies in the determination of this element even though Q_A and Q_P defined above (Fig. 8) are under 20%.

No determination of the accuracy of measuring the concentration of the elements corresponding to short-lived isotopes (i.e. Al, Ca, Mg, Ti, V) was made. For most of these elements the interference corrections are negligible (see Dams and Robbins, 1970). However there is a major interference in the determination of magnesium due to fast neutron production of Mg^{27} through the (n,p) reaction on aluminum. That is, if the gamma-emitting isotope Mg^{27}, which serves as the measure of the amount of the Mg present can be produced either by Mg^{26} (n,γ) Mg^{27} or by Al^{27} (n,p) Mg^{27}. The interference correction is given approximately by (Dams & Robbins, 1970)

$$[Mg]_{actual} = [Mg]_{observed} - 0.15\,[Al] \qquad (3)$$

As [Al] = 53,000 ppm roughly 0.15 x 53,000 = 8000 ppm of the measured concentration or about 8000/29,000 = 25% is due to an interference. As the interference correction is only approximate, the values for Mg may be in error by as much as 20%.

In summary, neutron activation analysis is a precise and accurate method for the determination of many elements in sediments. Exceptions occur for U, Lu and possibly Cr, Sb and Mg where the data may be of limited accuracy because of uncompensated interferences. The multiple analysis of SLM-1 splits makes it a useful standard for intercomparison of analytical methods and results in laboratories undertaking metal analysis of lacustrine sediments. Portions of this material are available from our laboratory on request.

Timed Extractions

Metals (AAS)

The standard procedure for extracting sediments involved treatment in hot 50% HNO_3 (+ H_2O_2) for 96 hours. The efficiency of this method was checked by determining the release of metals from standard lake mud for shorter treatment times and for the alternative, more conventional, treatment with 50% HCl (+ H_2O_2). (Samples were extracted in HNO_3 to provide chloride-free extracts for neutron activation analysis. Chloride is a major interference in the determination of shortlived elements via NAA.) The results are illustrated in Figure 9. For most elements the release is complete within a few hours. Included in the rapid release group are Ca, Cr, Cu, Fe, Mg, Mn, Ni, Pb, Sr and Zn. For sodium the release is considerably

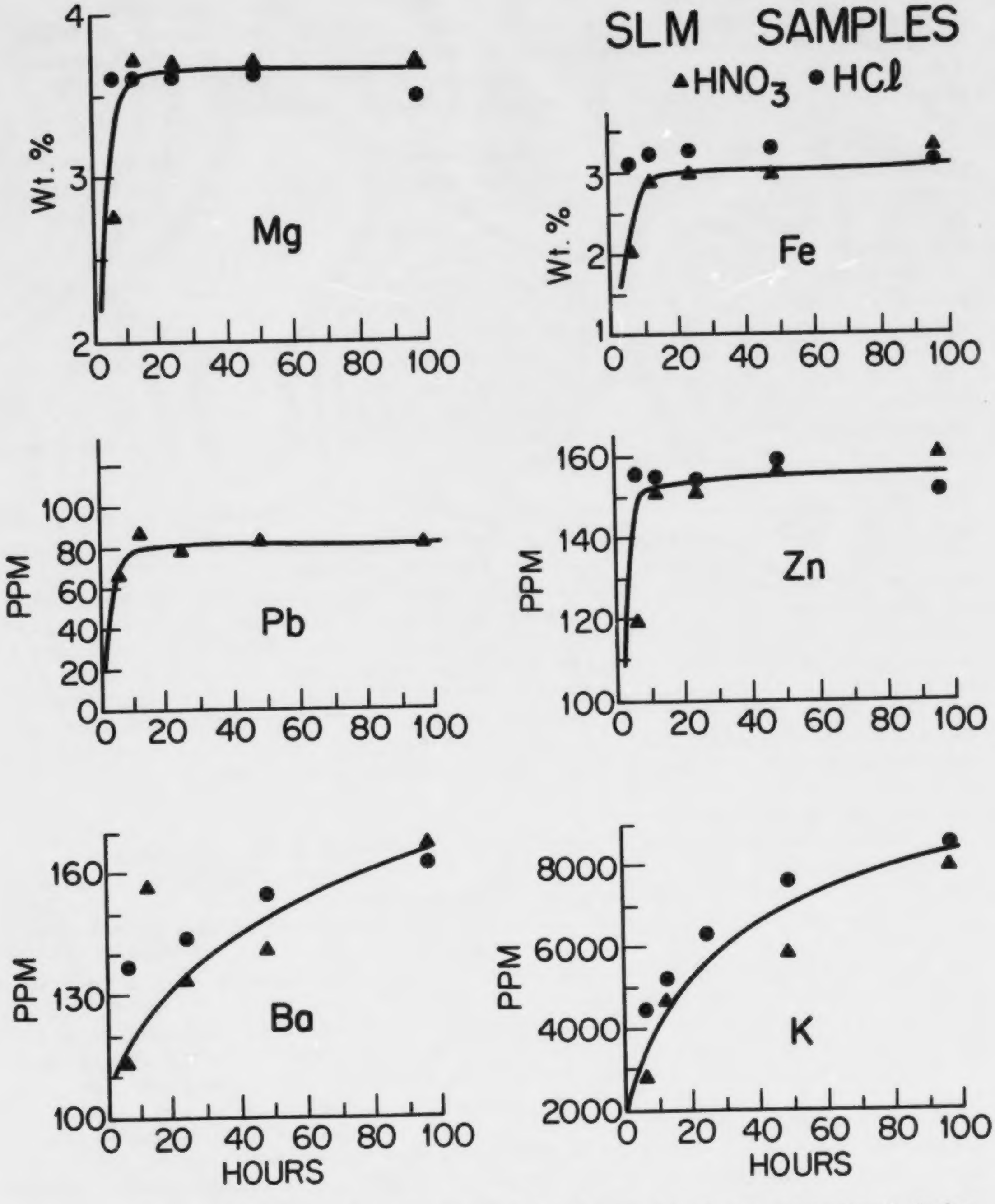

Figure 9. Elemental concentration ascribed to standard lake sediment versus extraction time.

slower but nevertheless complete by the end of the four day extraction period. For two elements, K and Ba, the extraction is evidently not complete even after four days. This result is understandable since K is a principal constituent of the clay minerals which resist dissolution on acid treatment. That Ba is also in the incomplete category indicates that a considerable fraction of it too is bound in the resistant clay mineral phase.

There are significant differences between HNO_3 and HCl treatments. The biggest effect is for Cu. The HNO_3 treatment is about 25% more efficient for extraction of copper. It is also slightly more efficient for Ni and Zn ($\leq$10%). For Mg there is no significant difference in treatment. An independent analysis of six replicate SLM-1 samples in this laboratory (R. Rossmann, personal communication) was undertaken using 2 g of sediment ground in a mixer mill extracted in 10% HCl with repeated additions of 30% H_2O_2 (R. Rossmann, 1975). Samples were allowed to extract for a 48 hour period at 90° C and extracts analyzed via AAS. These results are given in Table 6. For most elements (Ca, Fe, Mg, Mn, Zn) the agreement is satisfactory (10% or better). However the 10% HCl extraction yields significantly higher concentrations (about 20%) of Cr, Ni and Sr. Reasons for this effect have not been investigated.

For selected elements there are both NAA results for whole sediment as well as for acid-peroxide extracts. These data provide a measure of the efficiency of the extraction method. Results are summarized in Table 7. For calcium and magnesium,the efficiency is essentially 100%; for the transition elements Fe, Mn and Cr the efficiency is over 80% while for Ba, K and Na the efficiency is below 40%. These latter elements are in good part contained in resistant clay minerals. The low efficiencies are very consistent with the results of the timed extraction study discussed above. An important result for this study is that the transition elements are efficiently extracted by the acid-peroxide treatment. It is therefore likely that efficiency of extracting the anthropogenic components is essentially 100%.

Amorphous Silicon

The results of a timed extraction of a standard sediment sample (fine-grained mud) and a standard sample of illite (see Robbins et al., 1977) are given in Fig. 10. The rapid increase in dissolved silicon in 0.5 m NaOH during the first ten minutes or so corresponds primarily to the dissolution of amorphous silica. The slower, essentially constant rate of dissolution of the silicon in mud samples beyond about one hour corresponds to the release of the element from clay minerals. The rate of dissolution of "pure" illite, a principal clay constituent of these muds, is essentially the same beyond an hour. According to McKeyes et al. (1974) the amorphous silicon content may be inferred by linear extrapolation of the concentration time curve for ($t > 1$ hr) back to $t = 0$. This is an accurate method only if the release rate of Si from the clay mineral fraction is constant over the initial extraction period. The illite extraction curve shows that this is not true. More rapid release occurs during the first 10 minutes. If this rapid initial increase is not due to contamination of the illite sample with "amorphous" materials, but due to release of silica from illite, then the linear extrapolation is probably underestimating the amount of silica in the 0.5N NaOH attributable to clay minerals. From Figure 10, it can be seen that the

TABLE 6. COMPOSITION OF REPLICATE STANDARD LAKE MUD SAMPLES
(SLM-1-3; SLM-1-7; SLM-1-8)
DETERMINED BY GASOMETRIC OR ATOMIC ABSORPTION ANALYSIS (AAS)

Element	Concentration (µg/g)								
	30% HNO_3 extract			30% HCl extract			10% HCl extract[1]		
	Mean	%	N	Mean	%	N	Mean	%	N
Ba	-	-	-	-	-	-	-	-	-
Ca*	7.5±0.14	1.9	4	-	-	-	7.18±0.05	0.7	6
Cu	41.8±0.9	2.2	12	31.2±0.5	1.6	5	42.3±0.1	0.2	6
Cr	64.5±2.6	4	5	-	-	-	78.9±1.7	2.2	6
Fe*	3.0±0.1	3	12	3.2±0.1	3	5	3.1±0.2	6.5	6
K	-	-	-	-	-	-	0.87±0.04	4.6	6
Mg*	3.77±0.05	1	12	3.64±0.08	2	5	3.66±0.03	0.8	6
Mn	540±6	1.1	12	610±4	0.7	5	605±3	0.5	6
Na*	-	-	-	-	-	-	0.09±0.007	7.8	6
Ni	37.2±0.5	1.3	8	33.3±0.7	2.1	5	46.9±0.1	0.2	6
Pb	96±2	2	8	-	-	-	-	-	-
Sr	42.0±0.7	1.7	12	-	-	-	51.0±0.9	1.8	6
Zn	163±5	3	12	155±2	1	5	168±14	8.3	6
C (total)	5.45±.15*	3	15						
C (inorganic)	3.26±.07*	2	6						

---

[1] Independent analysis of six SLM-1 samples by R. Rossmann (pers. comm.).
* Concentrations in percent by weight.

TABLE 7. EFFICIENCY OF EXTRACTION OF SELECTED TRACE ELEMENTS VIA ACID-PEROXIDE TREATMENT (SLM-1 SAMPLES)

	Concentration (µg/g)		
Element	Whole Sediment[2] (NAA)	Acid-Peroxide Extract (Mean)	Efficiency (%)
Ba	434	176	40
Ca	7.00*	7.3*	>100[3]
Cr	88.8	71.7	81
Fe	3.33*	3.10*	93
K	2.20*	0.87*	40
Mg	2.87*	3.7*	>100[4]
Mn	654	578	88
Na	0.50*	0.09	18

* Concentration in percent by weight

[1] 100 x concentration from acid-peroxide extract/whole sediment concentration

[2] Data from table 3

[3] >100 because of statistical uncertainties

[4] >100 because of interference effects in NAA analysis for Mg (see text)

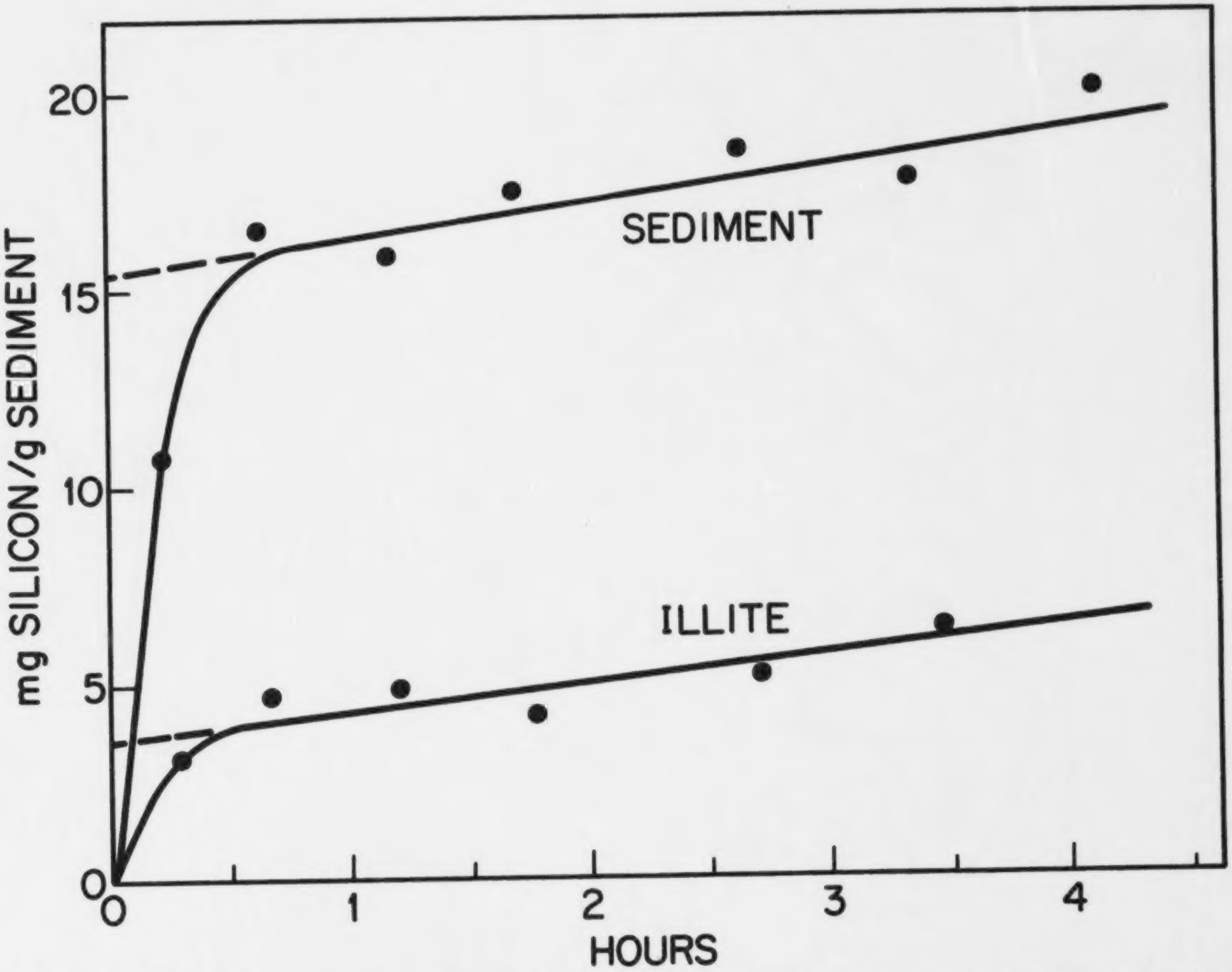

FIGURE 10. Silicon released from standard lake sediment versus extraction time.

amount of Si released by clay minerals could be as much as 4 mg/g lower than that implied by a linear extrapolation. For this particular sample, which is fairly representative, corresponds to a (3.5/(15.4-3.5)) * 100 = 30% effect. As the actual data cannot be corrected accurately for such effects, the inaccuracy in the results could be as much as about 30% and will increase for low measured amorphous Si values. The precision of the method is far better, around 15%.

Pore water air-exposure effects

It is now well-known that even very limited exposure of anoxic sediments to air prior to sampling for pore water can have a drastic effect on the concentration of certain dissolved species (phosphate: Bray et al., 1973; Weiler, 1973; iron: Troup et al., 1974). Using the method described above and in Robbins and Gustinis (1976), the sensitivity of the concentration of the elements Ba, Ca, Fe, K, Mg, Mn, Na, P, Si and Sr has been studied.

A 5 cm section of fine grained anoxic sediment was split under nitrogen. Half the sample was squeezed in an inert nitrogen atmosphere. The other half was exposed to air for 15 seconds. As the sediment plug was fairly well-consolidated the sectioned pieces retained their shape and limited surface area was in momentary contact with air. Following exposure to air, the section was returned to the nitrogen-filled glove box, loaded into the cassettes and squeezed. In squeezing the unexposed sample, care was taken to eliminate traces of air within the squeezer system by purging it with nitrogen using a rubber diaphragm with a pin hole leak (see Robbins and Gustinis, 1976). Application of N_2 pressure to the assembled, clamped squeezer forced nitrogen through the system eliminating traces of air as well as nitrogen-purged distilled water used to clean the parts. For the exposed section, the system was not purged with N_2. Therefore it necessarily contained both traces of air and residual distilled water. On squeezing, aliquots of pore water were taken from each of the squeezers after each 3 ml had been produced.

The results for the elements showing the greatest sensitivity to air exposure are shown in Figure 11. The concentration of Si is reduced by about 8% on brief exposure to air. The initial low values in the concentration of Si in pore water from exposed sediment is due to residual distilled water in the system. For Mn the reduction on air exposure is about 14%. For both Fe and PO_4 the effect is drastic. Concentrations of these constituents never reach an equilibrium value during squeezing. By the end of squeezing, the concentration of Fe in pore water remains approximately half of the value obtained from squeezing unexposed samples. For PO_4 the reduction is nearly a factor of 4. In normal operation, the first six mls of pore water are discarded as they contain some distilled water. The subsequent 20-25 mls are collected. Therefore in such an integrated sample, brief exposure of consolidated sediments to air and squeezing in an incompletely purged system can result in nearly order of magniture decreases in the concentration of PO_4 and Fe. There were no measurable effects for Ba, Ca, K, Mg or Sr. These results are of importance for interpreting interstitial profiles of Si, Mn, Fe and PO_4. Radical departures from smooth variations in contiguous samples

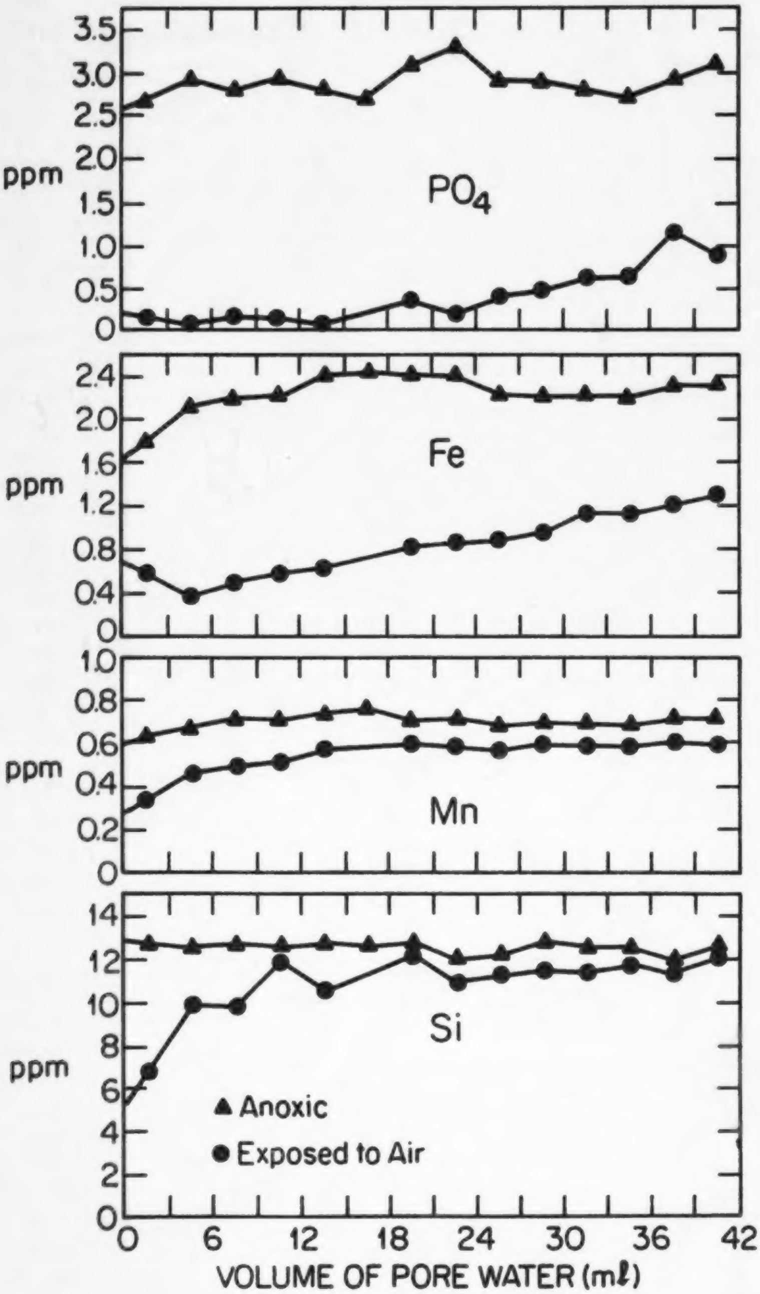

Figure 11. Concentration of selected elements in successive 3 ml aliquots of pore water. For some elements brief exposure of sediments to air drastically reduces dissolved concentrations.

are likely to result from inadvertent contamination with air. The effects of limited air exposure on concentrations of the above elements and others in pore water are summarized in Table 8.

TABLE 8. CONCENTRATION OF SELECTED ELEMENTS IN PORE WATER SAMPLES WITH AND WITHOUT BRIEF EXPOSURE TO AIR

	Concentration (ppm)			
Element	Unexposed	Exposed	Ratio (%)[1]	Method
Ba	0.51	0.59	>100	AAS
Br	0.091	0.085	93	NAA
Ca	25.4	26.1	∿100	AAS
Ca	22.6	30.0	>100	NAA
Co	6.4*	<1.0*	<16	NAA
Fe	2.3	0.89	39	AAS
Fe	3.0	0.80	27	NAA
K	1.2	1.3	∿100	AAS
La	5.7*	2.5*	44	NAA
Mg	8.8	8.2	93	AAS
Mn	0.71	0.59	83	AAS
Na	5.7	5.0	88	AAS
Na	6.3	6.7	>100	NAA
PO_4	2.9	0.46	16	COLOR
Sb	2.7*	0.76*	28	NAA
Si	12.5	11.6	93	COLOR
Sr	0.11	0.14	>100	AAS

* Concentration in ppb

[1] Ratios >100% reflect analytical and other errors.

RESULTS AND DISCUSSION

PHYSICAL PROPERTIES OF SEDIMENTS

To develop an accurate estimate of the flux of metal contaminants to sediments it is necessary to know the mass per unit area as a function of depth in individual cores. This has been accomplished in two ways: (1) by direct measurement of the mass per unit area and (2) by determination of the fraction of the total sediment section weight which is due to solids, the fractional dry weight, f. The direct measurement would suffice if it were not for the fact that some sediment is occasionally lost on sampling, so that the actual volume of sediment recovered in sectioning is less than the volume corresponding to a section of thickness dz in the core liner of cross-sectional area A. If the wet weight of sediment is w then the directly measured bulk density is:

$$\rho_b = w / (A\ dz) \qquad (4)$$

and if D is the dry weight of sediment in the section, the mass per unit area is:

$$dm = D / (A\ dz) \qquad (5)$$

the second measure of dm may be obtained from determination of:

$$f = D / w \qquad (6)$$

Clearly the measured value of f does not depend on loss of sediment during sampling. The fraction dry weight of a section is related to dm in the following way. If the mean density of sediment solids, ρ_s, is essentially constant within the depositional basins then the porosity of sediment is given by:

$$\phi = v_\ell / (v_\ell + v_s) \qquad (7)$$

and

$$f = v_s \rho_s / (v_s\rho_s + v_\ell\rho_\ell) \qquad (8)$$

where v_ℓ and v_s are the partial volumes of liquid and solids in a given section (ρ_ℓ = density of water = 1). From there it can be seen that (eliminating v_s and v_ℓ)

$$\phi = \rho_s (1 - f) / (\rho_s (1 - f) + f) \tag{9}$$

and since

$$dm = (1 - \phi) \rho_s dz \tag{10}$$

subtracting Eq. 9,

$$dm = f \rho_s dz / (f + \rho_s (1 - f)) \tag{11}$$

furthermore the bulk density of sediment is given either by Eq. 4 above or by

$$\rho_b \equiv (\rho_s v_s + \rho_\ell v_\ell) / (v_s + v_\ell) = \rho_s / (\rho_s (1 - f) + f) \tag{12}$$

In figure 12 values of ρ_b (the bulk density) are plotted against f for 2 cm thick sediment sections where sediment losses on sectioning are minimal. The line shown is the relationship expected if ρ_s is about 2.5 ± 0.2 g/cm^3. The large uncertainty in the estimate of ρ_s primarily reflects the insensitivity of ρ_b and f to changes in the value. Comparison of the two measures of ρ_b provides an estimate of loss of material. This comparison is provided in the Appendix (Table A-1). For five centimeter sections $\rho_b/\rho_b^* = 1/2$ since approximately 1/2 of the section was discarded on sampling the core. In compiling the cumulative mass,

$$M = \int_o^z dm \tag{13}$$

Eq. 11 was used. Physical properties of approximately sixty cores are tabulated in the Appendix (Table A-1).

Examples of the vertical distribution of porosity are shown in Fig. 13 for stations 5, 10, 19 from the Port Huron basin and 25 from the Saginaw basin. In Fig. 14 are shown porosity profiles for stations 14A, 18A, 53 and 63 in the Goderich Basin. Because of the very large number of profiles determined, only selected examples are illustrated in the report. The above eight stations will serve to illustrate not only the vertical dependence of physical properties but the vertical dependence of chemical and radioactivity parameters as well.

Smoothly decreasing porosity (and f) profiles are found throughout most of the depositional areas with discontinuities such as those seen at stations 10, 14A and 53 occurring generally toward basin margins. Smoothly varying profiles are characterized by an approximately exponential porosity profile (5, 25, 14A, 18A, 63) described by the equation

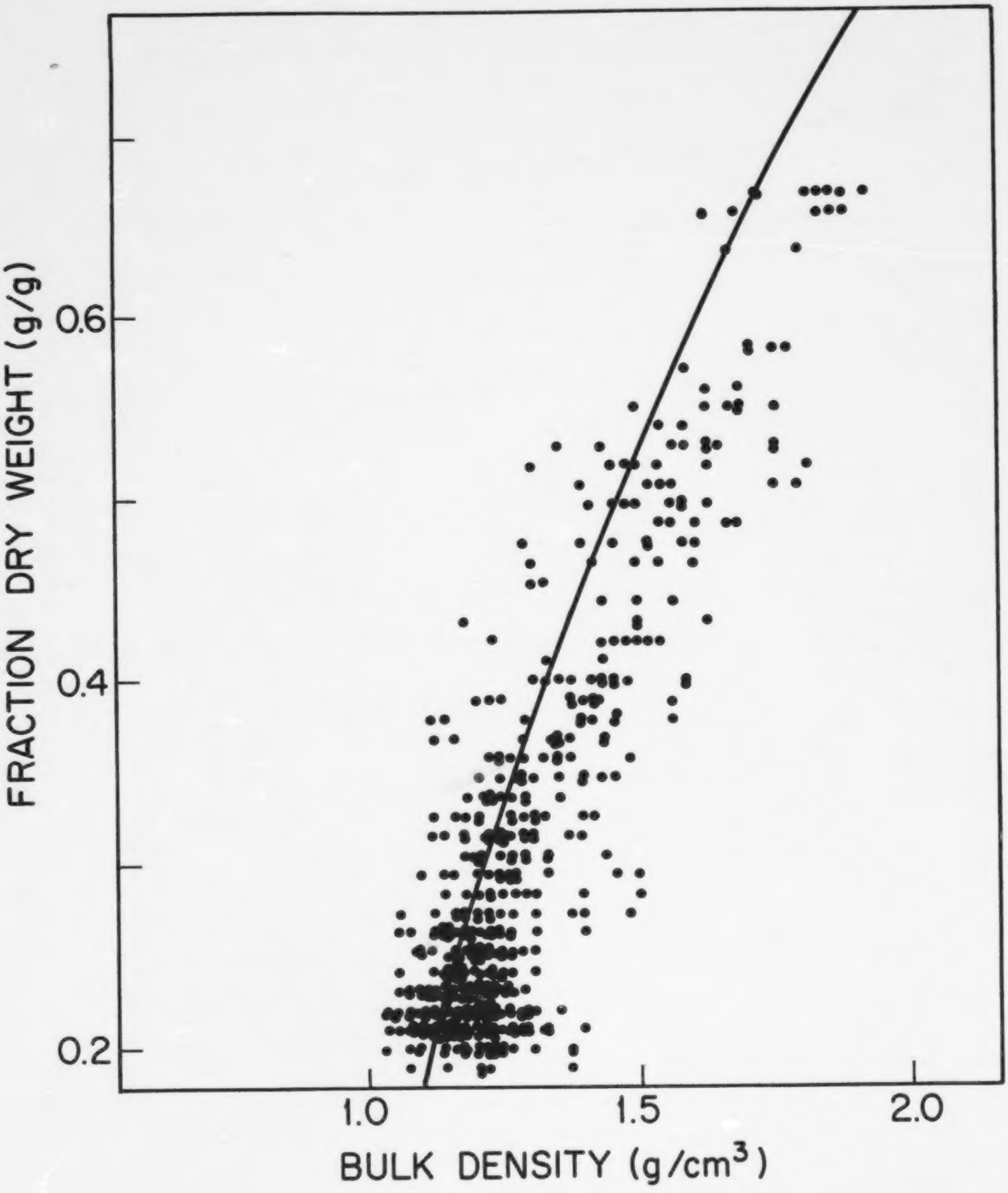

Figure 12. Fraction dry weight of sediment versus bulk density for 540 sediment samples. Solid curve expected if all samples have the same density of solids (2.54 g/cm^3).

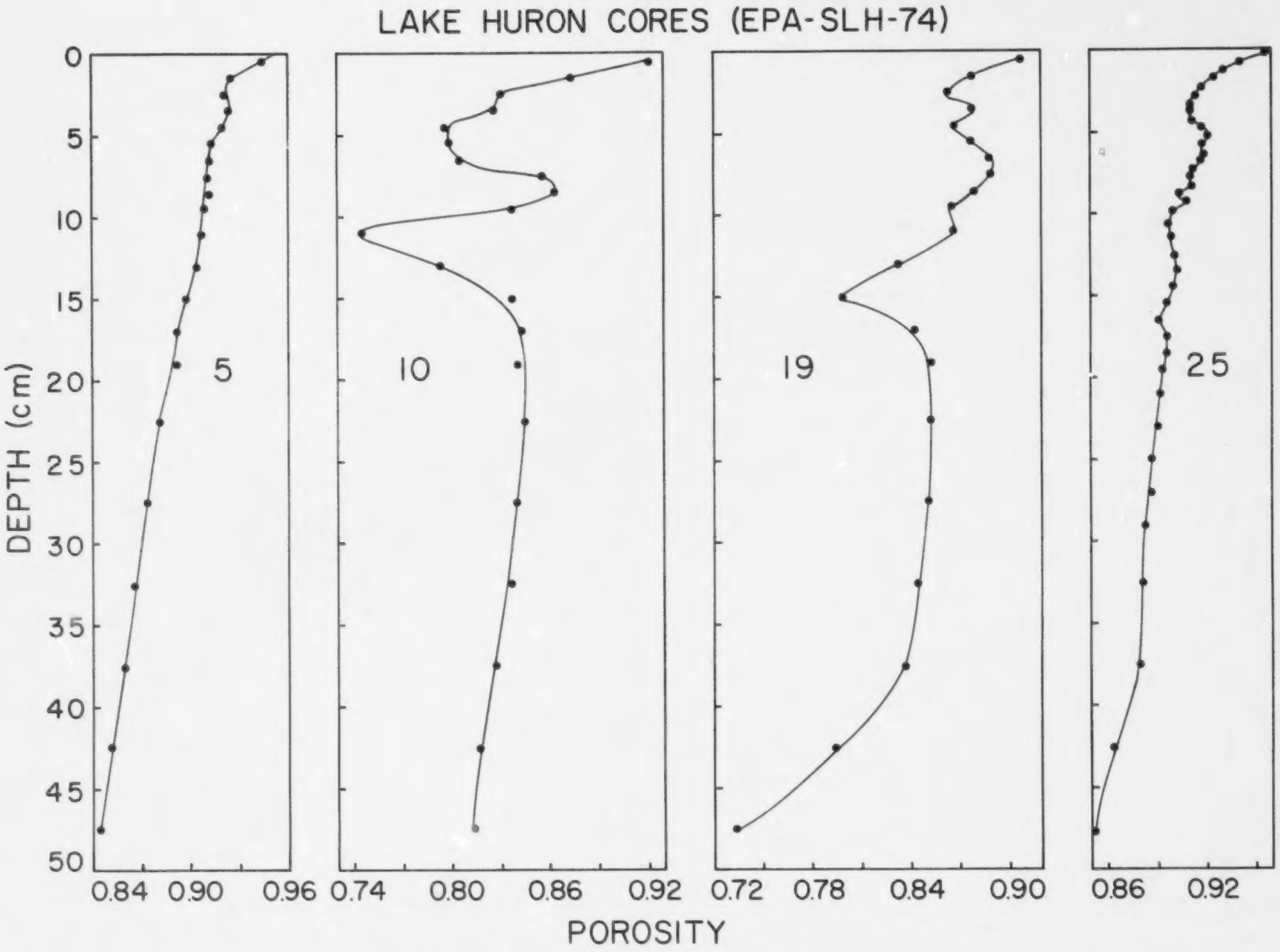

Figure 13. Vertical distribution of porosity in selected cores (Saginaw and Port Huron Basins).

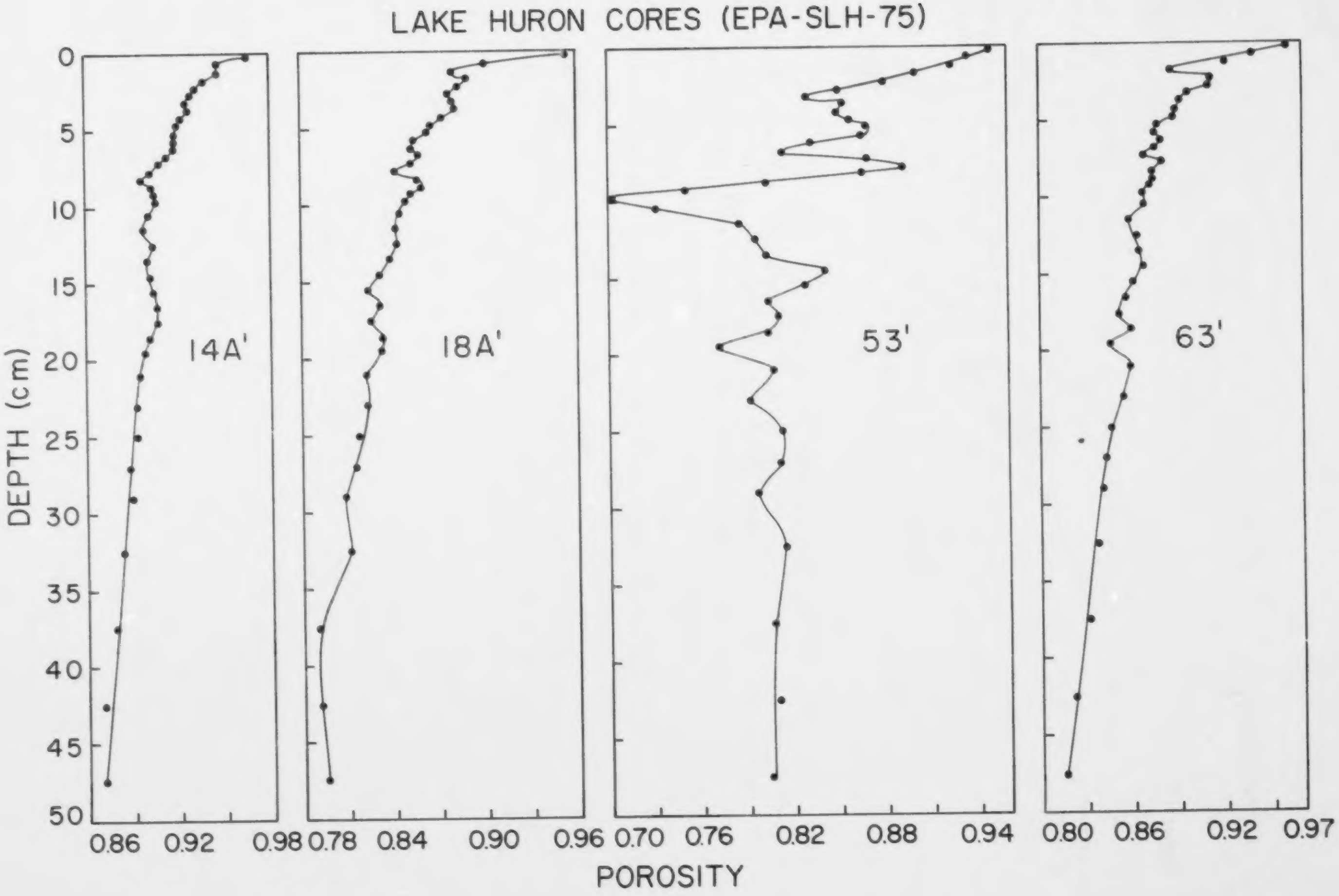

Figure 14. Vertical distribution of porosity in selected cores (Goderich Basin).

$$\phi = (\phi_o - \phi_f)\, e^{-\beta z} + \phi_f \quad (14)$$

Where $\phi = \phi_o$ at $z = o$ and $\phi = \phi_f$ at sufficiently great depths. Units of the compaction parameter β are cm^{-1}. Within the upper few cm, the water content (porosity) is generally somewhat underestimated by this relationship (Eq. 7) as can be seen in Fig. 15 which shows a least squares fit to porosity profile in a core from Station 18 using Eq. 14. Also shown is a contrasting irregular profile, having no meaningful description in terms of Eq. 14, for another marginal location (station 22; see Figs. 3 and 4). Eq. 14 predicts a surface porosity of 0.90 while the measured value is 5% higher. (Note that Hongve and Erlandsen (1979) found that the water content of cores were not affected by coring compression during sampling.) Because ϕ is essentially discontinuous at $z=0$, Eq. 14 has been used to obtain an average ϕ, roughly over the 1-2 cm interval for purposes of illustrating the systematic variation over the depositional areas. In cases where discontinuities occur ϕ_o and ϕ_f have been estimated from actual values around $z=1$-2 cm and $z=50$ cm without aid of Eq. 14.

Shown in Figures 16 and 17 are values of ϕ_o and ϕ_f for the two depositional basins in southern Lake Huron. Variations are similar for both ϕ_o and ϕ_f are quite systematic. High porosity sediments tend to occur in deepest parts of the basins, mid lake toward the central escarpment and in fine grained, organic rich deposits. Particularly within the Goderich Basin, sediments are considerably more consolidated toward the eastern, shoreward margin in areas of high inorganic carbon deposition (Thomas et al., 1973). The variation in the compaction parameter, β (cm^{-1}), with location is less systematic as can be seen from Fig. 18. However, β tends to be highest in marginal areas not either toward the escarpment nor in the area of highest inorganic carbon deposition (see Fig. 17). A large β, indicates a comparatively rapid decrease in sediment porosity with depth.

COMPOSITION OF SURFACE SEDIMENTS

The composition of surface sediments (1-2 cm) is given for 62 cores in Table 9. Concentrations of mercury and tin are given separately in Table 12. Concentrations based on neutron activation analysis are given for 39 of the 62 cores. Care should be exercised in using this table as the AAS data refer to acid-extractable element concentrations while the NAA data are for whole sediments. Quantities starred in Table 9 are NAA data. Also where confusion could arise, acid-soluble (AAS) concentrations are given the suffix 1 whereas whole sediment (NAA) concentrations are given the suffix 2. Thus, for example, Na1 refers to acid-soluble sodium while Na2 refers to whole-sediment sodium. Unless explicitly stated in the text element concentrations refer to acid-soluble quantities.

Since as many as 36 parameters have been determined in these sections, the data set is the largest and most complete elemental analysis of sediments in this part of the lake yet available. In Table 9 Fsol (g/g) refers to the fraction of dry sediment soluble by acid-perioxide treatment. IOC and OC refer respectively to inorganic and organic carbon in weight percent. Cs37

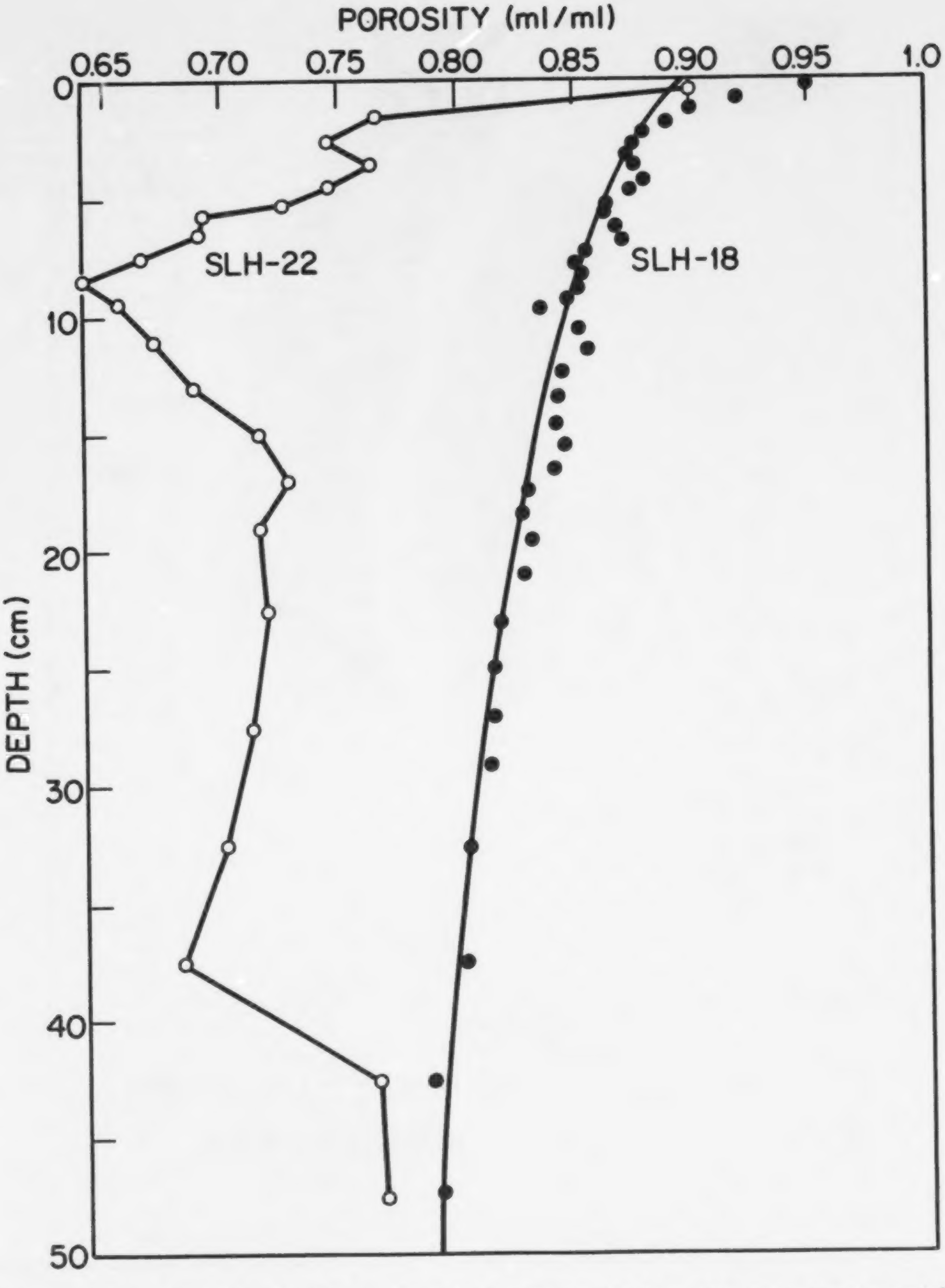

Figure 15. Vertical distribution of porosity in two contrasting cores.

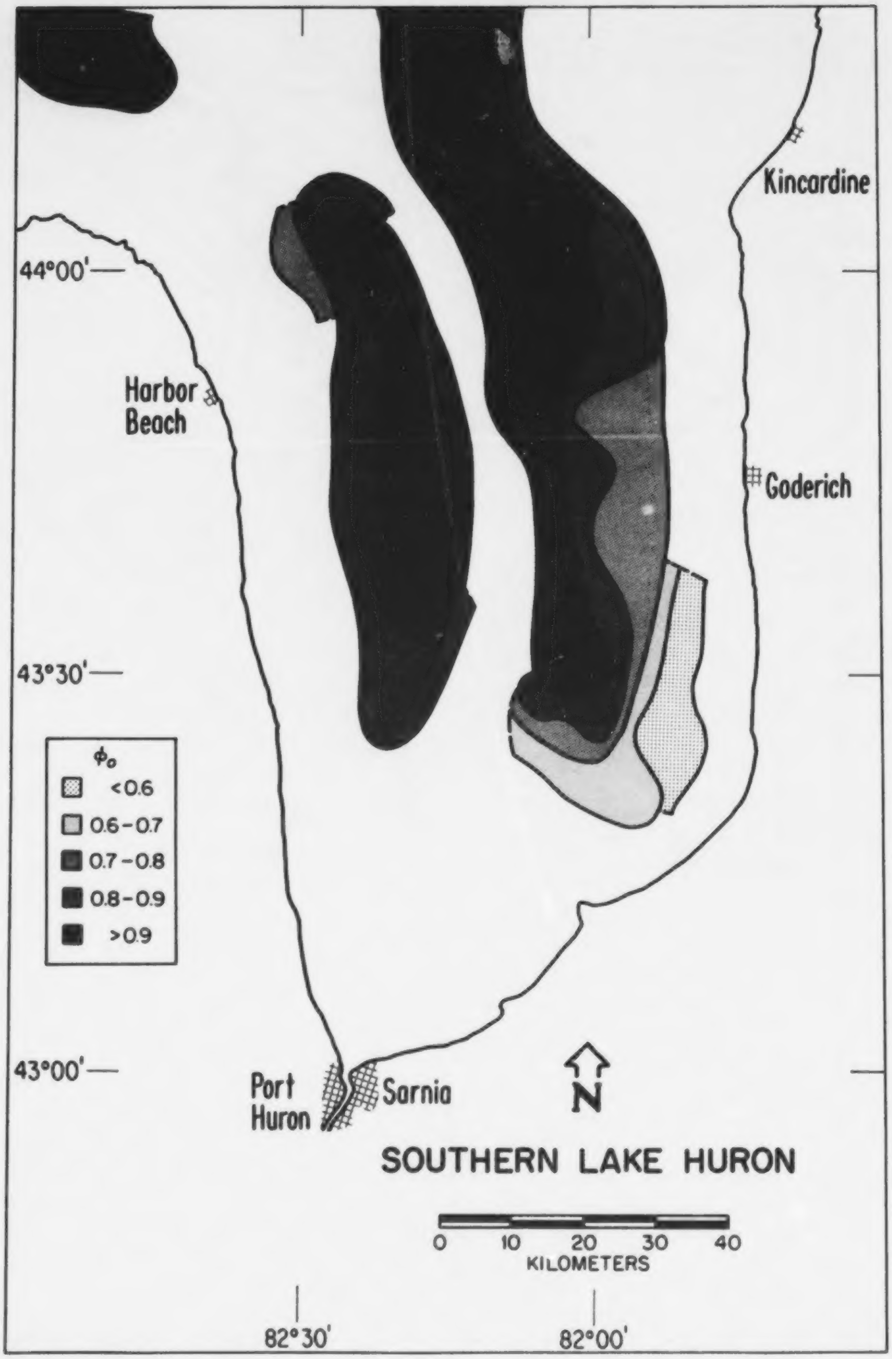
Kincardine
44°00'
Harbor Beach
Goderich
43°30'
φ₀
<0.6
0.6-0.7
0.7-0.8
0.8-0.9
>0.9
43°00'
Port Huron
Sarnia
N
SOUTHERN LAKE HURON
0 10 20 30 40
KILOMETERS
82°30'
82°00'

Figure 16. Distribution of surface porosity.

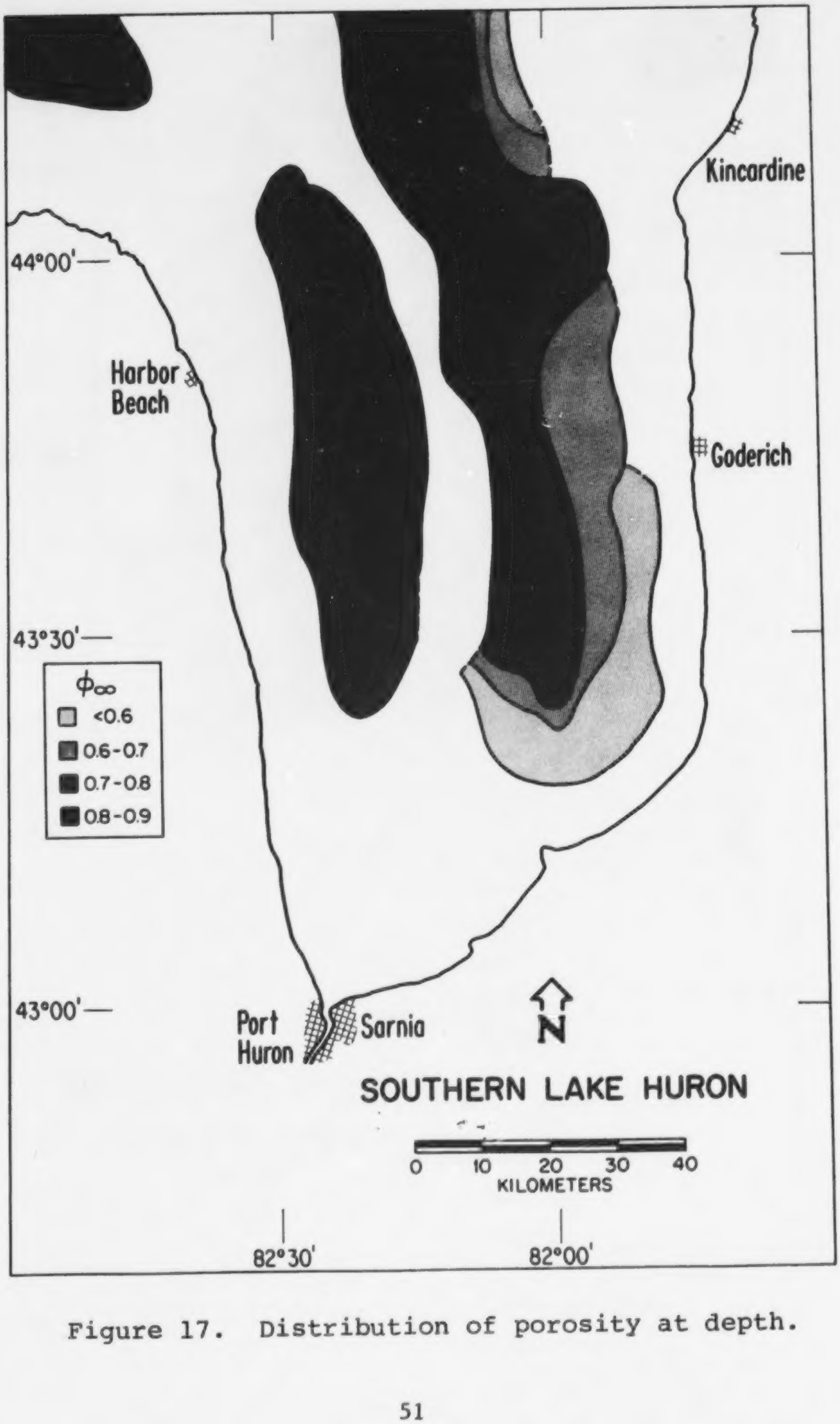
Kincardine
44°00'
Harbor Beach
Goderich
43°30'
ϕ_∞
<0.6
0.6-0.7
0.7-0.8
0.8-0.9
43°00'
Port Huron
Sarnia
N
SOUTHERN LAKE HURON
0
10
20
30
40
KILOMETERS
82°30'
82°00'

Figure 17. Distribution of porosity at depth.

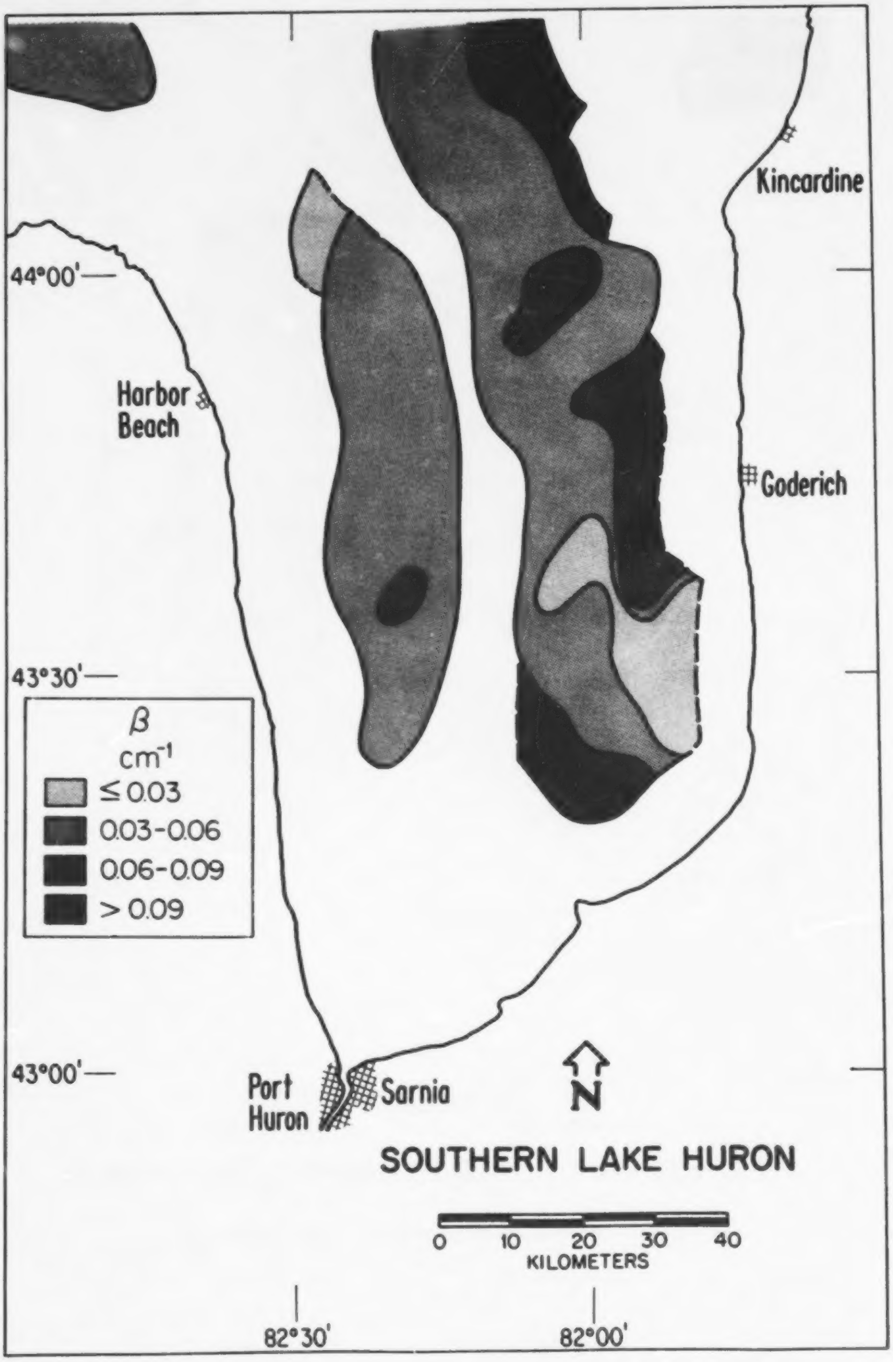
Kincardine
Goderich
Harbor Beach
44°00'
43°30'
43°00'
β
cm⁻¹
≤0.03
0.03-0.06
0.06-0.09
> 0.09
Port Huron
Sarnia
N
SOUTHERN LAKE HURON
0 10 20 30 40
KILOMETERS
82°30'
82°00'

Figure 18. Distribution of compaction parameter (see text).

TABLE 9. COMPOSITION OF SURFACE (1-2 CM) SEDIMENTS IN SOUTHERN LAKE HURON*

STN	FSO	IOC (%)	OC (%)	AS* (PPM)	BA1 (PPM)	BA2* (PPM)	BR* (PPM)
3.	0.243	-	-	17.2	-	471.	22.8
4.	-	-	-	-	-	-	-
5.	0.260	0.10	4.54	20.7	138.1	442.	26.2
6.	-	-	-	-	-	-	-
7.	0.428	4.78	0.63	-	66.5	457.	12.6
8.	0.260	0.09	4.91	24.8	-	458.	22.1
9.	0.283	2.41	2.48	-	-	433.	16.0
10.	-	-	-	-	-	-	-
11.	-	-	-	-	-	-	-
12.	0.326	1.21	4.11	21.6	147.2	366.	23.3
13.	0.463	4.85	1.22	-	90.2	358.	13.5
14.	0.317	0.95	4.27	21.2	256.4	391.	31.3
15.	-	-	-	-	-	-	-
16.	0.250	0.14	4.73	24.9	177.4	370.	27.9
17.	0.318	0.64	4.16	22.9	171.3	398.	27.5
18.	0.354	2.37	3.44	-	122.9	420.	63.0
19.	-	-	-	-	-	-	-
20.	-	-	-	-	-	-	-
21.	-	-	-	-	-	-	-
22.	-	-	-	-	-	-	-
29.	0.317	0.78	4.11	24.2	189.4	418.	27.7
30.	-	-	-	-	-	-	-
31.	0.187	0.10	3.70	16.2	-	474.	18.4
32.	-	-	-	-	-	-	-
33.	0.262	0.16	4.94	28.1	-	593.	118.1
34.	-	-	-	-	-	-	-
35.	-	-	-	-	-	-	-
36.	-	-	-	-	-	-	-
37.	-	-	-	-	-	-	-
38.	-	-	-	-	-	-	-
39.	-	-	-	-	-	-	-
40.	0.242	2.67	0.55	-	58.3	297.	14.7
41.	-	-	-	-	-	-	-
42.	0.212	1.08	3.92	23.1	121.9	443.	81.4
43.	-	-	-	-	-	-	-
44.	0.452	5.39	1.44	-	109.2	231.	9.4
45.	0.397	4.71	0.67	-	77.3	339.	11.8
46.	0.375	4.40	0.80	-	88.6	366.	16.2
47.	0.303	0.27	5.35	50.2	198.5	468.	157.8
48.	-	-	-	-	-	-	-
49.	0.311	0.26	5.77	54.0	172.5	501.	165.2
50.	0.401	4.68	0.99	-	91.7	279.	14.8
51.	0.411	4.72	-	-	93.6	397.	8.1
52.	-	-	-	-	-	-	-
53.	-	-	-	-	-	-	-
54.	0.434	4.68	1.93	-	122.0	327.	23.1
55.	0.296	0.32	4.91	48.8	221.2	463.	106.3
56.	-	-	-	-	-	-	-
57.	0.270	-	-	22.5	213.0	540.	97.4
58.	0.211	1.67	1.62	-	79.6	298.	31.7
59.	0.278	-	-	33.8	134.8	500.	106.4
60.	0.322	-	-	14.7	156.2	480.	59.5
61.	0.430	-	-	-	-	409.	30.6
62.	0.391	3.36	2.78	-	140.7	363.	38.1
63.	0.276	1.30	3.91	23.6	164.8	504.	79.0
65.	0.272	0.61	4.66	23.9	201.9	547.	96.2
66.	0.327	-	-	17.6	182.7	521.	78.4
67.	0.306	2.13	3.01	-	173.8	530.	45.8
68.	0.297	-	-	27.7	192.9	503.	88.7
69.	0.310	-	-	20.4	-	428.	82.5
70.	0.205	-	-	31.9	202.3	528.	100.4
71.	0.267	-	-	27.8	192.9	538.	106.6

(continued)

*Values are either in PPM = µg/gram whole dry sediment or in % = percent by weight. Starred values refer to neutron activation analysis or whole sediments. Other metal concentrations based on acid-peroxide extracts.

TABLE 9 (continued)

STN	CA (%)	CD (PPM)	CE* (PPM)	CO* (PPM)	CR1 (PPM)	CR2* (PPM)	CS* (PPM)
3.	2.00	2.81	54.8	10.4	52.5	67.1	3.62
4.	0.11	-	-	-	20.1	-	-
5.	0.47	3.06	65.8	11.8	64.8	75.6	4.08
6.	0.64	-	-	-	52.3	-	-
7.	7.37	-	41.3	6.7	21.9	56.8	2.30
8.	0.62	-	65.6	12.3	60.0	79.4	4.65
9.	3.99	2.00	41.3	7.6	35.9	48.8	2.46
10.	0.47	-	-	-	33.9	-	-
11.	0.54	-	-	-	48.6	-	-
12.	2.33	-	63.0	12.6	49.4	74.0	4.32
13.	7.68	-	37.9	6.1	29.7	42.8	2.22
14.	2.46	3.30	62.9	12.5	52.0	86.4	4.27
15.	0.15	-	-	-	15.3	-	-
16.	0.64	2.83	64.9	13.3	51.0	73.7	4.87
17.	1.37	3.22	62.6	13.7	64.6	73.7	4.72
18.	4.21	1.51	-	14.4	47.4	86.0	5.30
19.	0.38	-	-	-	39.0	-	-
20.	1.07	-	-	-	55.9	-	-
21.	1.29	-	-	-	58.1	-	-
22.	0.67	-	-	-	31.7	-	-
29.	1.68	3.02	64.4	13.9	63.9	77.7	4.39
30.	0.65	-	-	-	16.7	-	-
31.	0.64	2.11	55.2	9.1	52.9	61.8	3.22
32.	0.55	-	-	-	40.5	-	-
33.	0.59	3.86	59.2	13.1	53.2	84.1	4.48
34.	0.40	-	-	-	31.1	-	-
35.	0.28	-	-	-	18.6	-	-
36.	3.33	-	-	-	42.5	-	-
37.	2.78	-	-	-	40.9	-	-
38.	6.66	-	-	-	32.4	-	-
39.	2.68	-	-	-	27.2	-	-
40.	4.18	2.05	26.9	4.6	24.6	37.1	1.18
41.	1.18	-	-	-	45.2	-	-
42.	1.84	2.54	-	11.0	51.2	68.7	3.28
43.	6.66	-	-	-	24.4	-	-
44.	9.44	3.19	-	5.1	30.4	32.8	1.66
45.	8.33	2.77	-	3.8	24.6	44.3	0.75
46.	7.51	3.14	-	5.2	28.5	35.2	1.36
47.	0.87	3.16	-	14.5	76.7	85.0	4.91
48.	0.45	-	-	-	32.6	-	-
49.	0.82	2.97	-	14.0	72.8	86.2	4.89
50.	7.17	2.54	33.6	4.8	30.2	35.2	1.64
51.	8.33	3.08	25.5	4.0	25.9	31.9	0.78
52.	2.85	-	-	-	22.0	-	-
53.	1.95	-	-	-	62.4	-	-
54.	7.97	3.47	38.2	6.0	35.5	43.4	2.40
55.	1.08	4.27	63.0	14.3	77.4	84.5	5.23
56.	0.27	-	-	-	37.2	-	-
57.	0.85	4.24	65.8	14.3	80.9	84.2	4.83
58.	2.86	1.55	37.9	6.7	36.3	42.9	1.91
59.	0.69	2.06	67.6	14.4	55.3	85.4	4.77
60.	3.78	2.44	50.9	10.6	55.2	63.2	3.70
61.	6.24	4.22	42.4	8.3	51.0	55.6	2.94
62.	5.80	2.70	51.5	9.4	62.4	62.1	3.52
63.	2.22	2.57	59.3	12.5	80.2	73.1	4.63
65.	1.44	3.28	65.2	14.2	70.5	85.6	5.08
66.	2.80	2.84	59.5	12.7	61.5	74.6	4.27
67.	3.33	2.45	57.8	11.3	55.7	65.1	3.83
68.	1.84	2.81	65.6	13.9	66.8	85.4	4.78
69.	2.05	2.93	61.7	13.6	81.9	76.7	4.79
70.	0.87	2.98	63.0	14.8	82.6	84.1	5.41
71.	1.09	2.57	62.7	13.5	71.8	85.2	4.33

(continued)

TABLE 9 (continued)

STN	CS37 (pCi/g)	CU (PPM)	EU* (PPM)	FE1 (%)	FE2 * (%)	K (%)	LA * (PPM)
3.	9.60	47.5	1.30	2.42	3.02	0.52	32.0
4.	-	7.38	-	0.94	-	-	-
5.	7.70	65.4	1.42	3.32	3.54	0.85	39.1
6.	-	64.4	-	4.06	-	-	-
7.	1.70	16.5	0.92	1.27	2.09	0.25	23.0
8.	8.30	62.0	1.54	3.01	3.76	0.69	40.5
9.	3.60	-	0.98	2.01	2.20	0.32	23.5
10.	-	37.7	-	1.92	-	-	-
11.	-	61.1	-	3.80	-	-	-
12.	9.90	51.3	1.29	3.33	3.80	0.72	35.5
13.	2.60	22.8	0.86	1.38	1.78	0.37	20.6
14.	12.50	49.9	1.28	3.26	3.58	0.73	36.1
15.	-	5.56	-	0.85	-	-	-
16.	6.90	63.3	1.33	3.83	4.00	0.56	38.4
17.	10.50	62.2	1.43	3.67	3.84	0.84	37.3
18.	9.90	41.3	1.34	2.43	4.00	0.62	30.7
19.	-	31.6	-	1.98	-	-	-
20.	-	62.9	-	3.78	-	-	-
21.	-	57.9	-	3.56	-	-	-
22.	-	16.4	-	1.90	-	-	-
29.	11.80	59.3	1.16	3.99	4.09	0.87	38.3
30.	-	8.25	-	1.27	-	-	-
31.	6.30	45.7	1.14	2.22	2.61	0.45	32.4
32.	-	35.5	-	2.30	-	-	-
33.	7.80	55.9	1.40	3.53	3.98	0.70	40.7
34.	-	22.9	-	1.61	-	-	-
35.	-	9.48	-	1.28	-	-	-
36.	-	31.7	-	1.77	-	-	-
37.	-	22.1	-	2.11	-	-	-
38.	-	9.86	-	1.00	-	-	-
39.	-	12.2	-	1.27	-	-	-
40.	1.07	10.4	0.74	0.92	1.23	0.26	18.3
41.	-	27.9	-	1.82	-	-	-
42.	6.01	39.7	1.02	2.24	2.79	0.62	29.6
43.	-	8.86	-	0.89	-	-	-
44.	0.12	12.2	0.65	1.16	1.46	0.37	17.9
45.	0.60	6.29	0.69	0.87	1.39	0.15	16.9
46.	2.34	12.6	0.70	1.14	1.39	0.31	16.5
47.	17.74	71.1	1.26	3.59	3.91	1.19	37.4
48.	-	22.4	-	1.37	-	-	-
49.	8.75	65.3	1.30	3.52	3.98	0.57	39.7
50.	1.63	16.5	0.75	1.19	1.43	0.28	17.5
51.	1.18	8.63	0.59	0.87	1.15	0.20	13.0
52.	-	3.26	-	0.89	-	-	-
53.	-	46.1	-	2.67	-	-	-
54.	4.32	21.7	0.82	1.43	1.79	0.51	20.3
55.	14.60	63.1	1.32	3.96	4.31	1.26	39.2
56.	-	21.1	-	1.45	-	-	-
57.	9.00	67.2	1.37	4.10	4.14	0.93	39.7
58.	2.94	20.6	0.75	1.53	1.80	0.40	19.2
59.	12.50	45.2	1.38	2.46	4.11	0.71	39.8
60.	9.90	38.3	1.04	2.60	2.93	0.85	29.4
61.	5.90	26.2	0.95	1.92	2.30	0.57	25.2
62.	5.40	32.5	1.10	2.13	2.54	0.71	29.4
63.	10.50	49.5	1.19	3.28	3.72	0.94	34.6
65.	13.40	59.0	1.27	3.79	4.01	1.21	38.6
66.	10.70	49.6	1.29	3.19	3.43	1.11	34.2
67.	3.13	41.4	1.22	2.71	3.11	0.94	33.8
68.	11.80	53.9	1.27	3.32	3.82	1.03	36.9
69.	13.20	49.6	1.24	3.71	3.77	0.77	36.8
70.	14.00	61.2	1.33	3.91	4.30	-	40.2
71.	11.80	63.4	1.24	3.45	3.94	1.09	38.8

(continued)

TABLE 9 (continued)

STN	LU* (PPM)	MG (%)	MN (%)	NA1 (%)	NA2 * (%)	NI (PPM)	P (%)
3.	0.35	1.46	0.075	-	0.749	53.5	0.120
4.	-	0.16	0.020	-	-	8.4	-
5.	0.35	0.82	0.048	0.205	0.799	46.8	-
6.	-	0.76	0.231	-	-	76.2	-
7.	0.26	5.19	0.023	0.111	0.778	25.8	-
8.	0.40	0.86	0.119	-	0.846	60.4	0.199
9.	0.27	3.06	0.068	-	0.772	42.2	0.142
10.	-	0.46	0.192	-	-	62.8	-
11.	-	0.66	0.409	-	-	74.6	-
12.	0.36	1.96	0.250	0.148	0.664	62.7	-
13.	0.23	5.41	0.038	0.121	0.668	34.1	-
14.	0.34	2.10	0.180	0.330	0.715	63.5	0.230
15.	-	0.12	0.031	-	-	5.3	-
16.	0.34	0.87	0.245	0.075	0.738	71.7	-
17.	0.38	1.46	0.227	0.203	0.671	87.1	-
18.	0.32	3.17	0.045	0.114	0.650	51.5	0.220
19.	-	0.55	0.034	-	-	38.6	-
20.	-	1.14	0.309	-	-	96.6	-
21.	-	1.28	0.234	-	-	87.3	-
22.	-	0.66	0.116	-	-	31.1	-
29.	0.36	1.73	0.351	0.180	0.678	85.6	-
30.	-	0.25	0.569	-	-	26.2	-
31.	0.33	0.36	0.032	-	0.869	45.5	0.180
32.	-	0.61	0.102	-	-	42.2	-
33.	0.44	0.89	0.127	-	0.795	53.0	0.210
34.	-	0.40	0.198	-	-	50.9	-
35.	-	0.25	0.038	-	-	22.5	-
36.	-	2.59	0.045	-	-	42.5	-
37.	-	1.67	0.041	-	-	34.4	-
38.	-	3.91	0.040	-	-	22.0	-
39.	-	1.72	0.036	-	-	24.2	-
40.	0.26	2.93	0.018	0.254	0.875	30.2	0.049
41.	-	0.91	0.061	-	-	38.1	-
42.	0.36	1.49	0.153	0.156	0.719	81.5	0.079
43.	-	4.27	0.026	-	-	36.0	-
44.	0.20	5.00	0.033	0.160	0.728	23.9	0.040
45.	0.26	5.18	0.026	0.154	0.843	21.4	0.108
46.	0.21	4.68	0.036	0.154	0.830	24.8	0.059
47.	0.40	1.05	0.242	0.384	0.668	85.2	0.131
48.	-	0.38	0.078	-	-	31.7	-
49.	0.41	1.01	0.273	0.300	0.735	74.7	0.159
50.	0.22	4.97	0.024	0.204	0.791	31.0	0.063
51.	0.17	4.58	0.029	0.165	0.838	21.6	0.085
52.	-	1.66	0.014	-	-	14.0	-
53.	-	1.73	0.140	-	-	64.1	-
54.	0.25	5.30	0.034	0.156	0.672	34.7	0.068
55.	0.43	1.23	0.273	0.259	0.701	82.1	0.175
56.	-	0.32	0.095	-	-	29.6	-
57.	0.39	1.27	0.149	0.409	0.713	81.3	0.172
58.	0.23	2.18	0.064	0.163	0.866	37.0	0.062
59.	0.30	0.83	0.188	0.150	0.710	54.2	0.111
60.	0.36	3.11	0.150	0.171	0.672	54.7	0.111
61.	0.25	4.38	0.045	-	0.652	48.1	0.130
62.	0.29	4.38	0.038	0.265	0.641	44.3	0.091
63.	0.37	2.04	0.122	0.181	0.685	72.1	0.210
65.	0.32	1.49	0.243	0.240	0.688	79.5	0.239
66.	0.35	2.47	0.159	0.221	0.653	64.9	0.245
67.	0.31	2.76	0.043	0.161	0.685	52.8	0.226
68.	0.34	1.77	0.258	0.169	0.672	70.3	0.144
69.	0.38	1.83	0.225	-	0.655	72.8	0.240
70.	0.41	1.14	0.245	0.184	0.709	80.6	0.159
71.	0.44	1.24	0.106	0.268	0.794	67.6	0.205

(continued)

TABLE 9 (continued)

STN	PB (PPM)	PB21 (pCi/g)	SB* (PPM)	SC * (PPM)	SM * (PPM)	SR (PPM)	TH * (PPM)
3.	90.0	8.9	0.94	11.1	5.42	-	8.20
4.	-	-	-	-	-	-	-
5.	98.5	7.4	1.13	13.4	6.51	37.2	10.08
6.	123.0	-	-	-	-	-	-
7.	39.4	2.4	0.34	8.2	4.16	48.0	6.01
8.	110.0	5.4	1.13	13.8	6.57	-	10.48
9.	65.5	5.0	0.54	8.6	4.20	-	6.00
10.	55.7	-	-	-	-	-	-
11.	105.0	-	-	-	-	-	-
12.	115.0	14.0	0.78	13.1	6.15	43.4	9.83
13.	49.8	2.9	0.43	7.9	3.84	55.6	5.13
14.	96.9	12.6	0.79	12.9	6.24	44.9	8.93
15.	9.7	-	-	-	-	-	-
16.	109.5	0.2	0.90	13.4	6.19	36.2	10.19
17.	100.3	8.2	0.78	13.6	6.24	45.2	9.65
18.	88.2	8.8	1.44	11.7	5.36	38.8	8.55
19.	19.5	-	-	-	-	-	-
20.	112.0	-	-	-	-	-	-
21.	114.0	-	-	-	-	-	-
22.	26.7	-	-	-	-	-	-
29.	125.0	-	1.00	14.0	6.23	41.1	10.14
30.	50.6	-	-	-	-	-	-
31.	83.8	4.3	0.80	11.2	5.39	-	8.42
32.	66.7	-	-	-	-	-	-
33.	95.3	7.9	1.26	14.2	6.66	-	10.83
34.	55.3	-	-	-	-	-	-
35.	22.0	-	-	-	-	-	-
36.	68.0	-	-	-	-	-	-
37.	36.3	-	-	-	-	-	-
38.	31.8	-	-	-	-	-	-
39.	38.8	-	-	-	-	-	-
40.	35.4	-	0.41	5.8	3.09	36.1	4.35
41.	50.3	-	-	-	-	-	-
42.	83.1	-	0.78	10.5	5.16	32.7	8.18
43.	35.8	-	-	-	-	-	-
44.	31.1	-	0.21	6.4	2.86	49.5	4.17
45.	33.9	1.5	0.17	5.9	3.11	46.5	4.49
46.	41.3	-	0.33	5.8	2.80	42.2	3.86
47.	140.0	-	1.39	13.6	6.10	47.9	9.78
48.	44.5	-	-	-	-	-	-
49.	133.0	-	1.49	14.5	6.38	43.1	10.94
50.	39.4	2.2	0.39	6.3	3.07	45.1	5.55
51.	33.8	2.4	0.26	4.9	2.74	45.4	3.96
52.	14.1	-	-	-	-	-	-
53.	92.2	-	-	-	-	-	-
54.	51.4	-	0.40	7.5	3.80	49.6	5.14
55.	120.0	-	1.36	14.2	7.02	47.3	10.96
56.	40.1	-	-	-	-	-	-
57.	121.0	6.2	1.19	14.6	6.93	48.4	10.60
58.	46.9	-	0.42	6.8	3.07	42.7	5.08
59.	80.8	-	1.15	14.4	6.32	29.5	10.94
60.	81.3	-	0.89	11.1	5.34	42.9	7.44
61.	64.1	3.7	0.50	9.4	4.69	-	7.07
62.	69.0	-	0.80	11.1	5.05	49.2	8.97
63.	57.3	11.4	0.95	12.8	6.17	42.5	9.33
65.	112.0	-	1.11	14.0	6.46	46.6	10.32
66.	94.8	-	0.99	12.6	5.32	46.4	10.56
67.	64.8	-	1.09	12.7	5.22	43.9	8.66
68.	105.0	-	1.37	13.6	5.80	44.6	8.93
69.	109.0	7.3	0.92	13.4	6.10	41.0	9.43
70.	114.0	-	1.30	14.5	5.98	41.6	9.64
71.	108.4	-	1.63	13.0	6.38	43.6	10.76

(continued)

TABLE 9 (continued)

STN	U* (PPM)	ZN
3.	2.65	139.2
4.	–	20.7
5.	3.17	184.9
6.	–	196.8
7.	2.35	55.6
8.	3.96	175.3
9.	2.22	96.2
10.	–	117.0
11.	–	158.5
12.	2.98	155.5
13.	2.04	78.0
14.	2.56	171.7
15.	–	8.2
16.	3.80	192.7
17.	2.91	173.8
18.	2.48	140.6
19.	–	61.2
20.	–	199.2
21.	–	182.1
22.	–	40.8
29.	3.89	193.0
30.	–	35.1
31.	3.30	133.0
32.	–	102.8
33.	3.62	183.7
34.	–	96.5
35.	–	45.1
36.	–	98.9
37.	–	72.1
38.	–	45.8
39.	–	54.4
40.	2.27	47.2
41.	–	78.4
42.	2.09	122.7
43.	–	32.1
44.	2.21	27.8
45.	1.68	22.0
46.	1.91	74.3
47.	2.98	201.1
48.	–	62.2
49.	3.78	190.2
50.	2.72	54.2
51.	1.24	34.6
52.	–	9.1
53.	–	145.7
54.	1.94	68.8
55.	1.86	190.8
56.	–	52.9
57.	2.05	203.4
58.	2.55	62.5
59.	4.22	135.9
60.	1.69	120.0
61.	1.68	96.5
62.	2.88	126.1
63.	2.34	163.7
65.	2.90	188.0
66.	4.16	156.2
67.	4.17	131.0
68.	3.91	152.4
69.	3.07	199.2
70.	3.49	204.3
71.	2.95	178.3

TABLE 10. SUMMARY OF SURFACE CONCENTRATION DATA

	Range					
	Minimum	Maximum	Average	Standard Deviation	Ratio*	N
FSOL (g/g)	0.19	0.46	0.31	0.07	0.23	39
IOC (%)	0.09	5.4	2.1	1.9	0.90	29
OC (%)	0.55	5.8	3.2	1.6	0.52	28
As	14.7	54.0	26.7	10	0.39	24
Ba1	58.3	256	148	51	0.34	32
Ba2	231	593	432	84	0.19	39
Br	8.1	118	51.2	37	0.72	39
Ca (%)	0.11	9.4	2.67	2.6	0.98	62
Cd	1.5	4.3	2.87	0.66	0.23	35
Ce	25.5	67.6	54.3	13	0.23	32
Co	3.8	14.8	10.6	3.6	0.34	39
Cr1	15.4	82.6	47.1	19	0.39	62
Cr2	31.9	86.4	66.5	18	0.28	39
Cs	0.75	5.41	3.64	1.4	0.38	39
Cs137 (pCi/g)	0.12	17.7	7.73	4.6	0.59	39
Cu	3.3	71.1	37.0	21	0.57	61
Eu	0.59	1.54	1.12	0.26	0.23	39
Fe1 (%)	0.85	4.10	2.37	1.1	0.46	62
Fe2 (%)	1.15	4.30	3.06	1.0	0.34	39
K (%)	0.15	1.26	0.68	0.31	0.45	38
La	13.0	40.7	31.1	8.7	0.28	39
Lu	0.18	0.45	0.33	0.072	0.22	39
Mg (%)	0.12	5.4	2.00	1.6	0.79	62
Mn (%)	0.014	0.57	0.13	0.11	0.87	62
Na1 (%)	0.075	0.41	0.20	0.076	0.38	32
Na2 (%)	0.64	0.88	0.73	0.072	0.98	39
Ni	5.3	96.7	50.6	23	0.45	62
P (%)	0.40	0.25	0.15	0.064	0.44	32
Pb	9.7	140	73.6	35	0.48	61
Pb210 (pCi/g)	1.5	14.0	6.54	3.6	0.55	20
Sb	0.17	1.63	0.87	0.40	0.46	39
Sc	4.9	14.6	11.2	3.1	0.28	39
Sm	2.7	7.02	5.23	1.3	0.26	39
Sr	29.5	55.6	43.6	5.2	0.12	33
Th	3.86	11.0	8.24	2.4	0.29	39
U	1.24	4.2	2.79	0.81	0.29	39
Zn	8.2	204	116	63.	0.54	62

Values in μg/g unless indicated. * Ratio = SD/mean.

TABLE 11. CORRELATION COEFFICIENTS BASED ON PAIR-WISE LINEAR REGRESSION OF SURFACE SEDIMENT CONCENTRATION DATA

	FSOL	IOC	OC	AS	BA1	BA2	BR	CA	CD	CE	CO	CR1	CR2	CS	CS37	CU	EU	FE1	FE2
FSOL	1.00	0.83	-0.53	0.15	-0.43	-0.48	-0.41	0.85	0.29	-0.48	-0.53	-0.50	-0.51	-0.48	-0.44	-0.59	-0.54	-0.52	-0.52
IOC	0.83	1.00	-0.90	-0.30	-0.73	-0.61	-0.57	0.99	-0.12	-0.83	-0.85	-0.80	-0.83	-0.81	-0.76	-0.91	-0.84	-0.87	-0.85
OC	-0.53	-0.90	1.00	0.82	0.85	0.66	0.67	-0.87	0.40	0.95	0.94	0.89	0.92	0.92	0.84	0.97	0.90	0.94	0.93
AS	0.15	-0.30	0.82	1.00	0.19	0.16	0.59	-0.45	0.30	0.48	0.60	0.43	0.62	0.58	0.46	0.55	0.19	0.35	0.55
BA1	-0.43	-0.73	0.85	0.19	1.00	0.63	0.64	-0.71	0.52	0.82	0.83	0.85	0.82	0.83	0.83	0.85	0.78	0.90	0.83
BA2	-0.48	-0.61	0.66	0.16	0.63	1.00	0.73	-0.65	0.19	0.62	0.70	0.67	0.74	0.67	0.60	0.67	0.69	0.65	0.70
BR	-0.41	-0.57	0.67	0.59	0.64	0.73	1.00	-0.61	0.22	0.58	0.74	0.75	0.74	0.71	0.72	0.64	0.57	0.66	0.71
CA	0.85	0.99	-0.87	-0.45	-0.71	-0.65	-0.61	1.00	-0.01	-0.84	-0.85	-0.36	-0.84	-0.82	-0.75	-0.51	-0.86	-0.51	-0.85
CD	0.29	-0.12	0.40	0.30	0.52	0.19	0.22	-0.01	1.00	0.27	0.17	0.31	0.19	0.19	0.22	0.26	0.17	0.35	0.21
CE	-0.48	-0.83	0.95	0.48	0.82	0.62	0.58	-0.84	0.27	1.00	0.97	0.82	0.96	0.96	0.84	0.95	0.95	0.92	0.97
CO	-0.53	-0.85	0.94	0.60	0.83	0.70	0.74	-0.85	0.17	0.97	1.00	0.88	0.97	0.98	0.90	0.94	0.92	0.94	0.99
CR1	-0.50	-0.80	0.89	0.43	0.85	0.67	0.75	-0.36	0.31	0.82	0.88	1.00	0.83	0.88	0.85	0.89	0.78	0.89	0.86
CR2	-0.51	-0.83	0.92	0.62	0.82	0.74	0.74	-0.84	0.19	0.96	0.97	0.83	1.00	0.95	0.88	0.91	0.93	0.90	0.97
CS	-0.48	-0.81	0.92	0.58	0.83	0.67	0.71	-0.82	0.19	0.96	0.98	0.88	0.95	1.00	0.88	0.93	0.93	0.93	0.98
CS37	-0.44	-0.76	0.84	0.46	0.83	0.60	0.72	-0.75	0.22	0.94	0.90	0.85	0.88	0.89	1.00	0.84	0.78	0.85	0.88
CU	-0.59	-0.91	0.97	0.55	0.85	0.67	0.64	-0.51	0.26	0.95	0.94	0.89	0.91	0.93	0.84	1.00	0.92	0.97	0.94
EU	-0.54	-0.84	0.90	0.19	0.78	0.69	0.57	-0.86	0.17	0.95	0.92	0.78	0.93	0.93	0.78	0.92	1.00	0.87	0.94
FE1	-0.52	-0.87	0.94	0.35	0.90	0.65	0.66	-0.51	0.35	0.92	0.94	0.89	0.90	0.93	0.85	0.97	0.87	1.00	0.95
FE2	-0.52	-0.85	0.93	0.55	0.83	0.70	0.71	-0.85	0.21	0.97	0.99	0.86	0.97	0.98	0.88	0.94	0.94	0.95	1.00
K	-0.35	-0.71	0.83	0.50	0.86	0.66	0.77	-0.68	0.32	0.79	0.95	0.90	0.81	0.84	0.85	0.83	0.73	0.86	0.83
LA	-0.59	-0.89	0.96	0.50	0.85	0.72	0.67	-0.90	0.24	0.98	0.96	0.87	0.95	0.95	0.83	0.96	0.96	0.94	0.97
LU	-0.59	-0.86	0.91	0.46	0.78	0.70	0.70	-0.84	0.26	0.92	0.86	0.83	0.87	0.84	0.78	0.89	0.95	0.87	0.87
MG	0.87	0.99	-0.86	-0.38	-0.65	-0.61	-0.58	0.98	-0.00	-0.76	-0.80	-0.24	-0.78	-0.76	-0.71	-0.39	-0.81	-0.39	-0.80
MN	-0.37	-0.68	0.75	0.48	0.74	0.40	0.57	-0.48	0.28	0.71	0.78	0.42	0.72	0.74	0.79	0.56	0.60	0.63	0.78
NA1	-0.25	-0.41	0.43	0.38	0.54	0.30	0.48	-0.38	0.48	0.22	0.33	0.53	0.38	0.30	0.44	0.44	0.31	0.41	0.31
NA2	-0.26	0.09	-0.34	-0.10	-0.56	-0.20	-0.36	0.09	-0.27	-0.36	-0.51	-0.47	-0.42	-0.55	-0.51	-0.34	-0.36	-0.44	-0.46
NI	-0.53	-0.81	0.86	0.42	0.83	0.58	0.68	-0.42	0.28	0.84	0.90	0.85	0.84	0.87	0.85	0.91	0.77	0.92	0.88
P	-0.32	-0.68	0.71	-0.20	0.76	0.72	0.49	-0.61	0.13	0.75	0.73	0.65	0.75	0.74	0.62	0.71	0.76	0.76	0.75
PB	-0.53	-0.87	0.96	0.65	0.85	0.62	0.66	-0.43	0.29	0.92	0.93	0.87	0.91	0.92	0.89	0.95	0.86	0.94	0.93
PB21	-0.48	-0.66	0.72	0.10	0.74	0.22	0.37	-0.64	-0.01	0.72	0.77	0.57	0.75	0.75	0.84	0.67	0.69	0.74	0.78
SB	-0.53	-0.80	0.88	0.69	0.74	0.76	0.80	-0.80	0.09	0.85	0.90	0.83	0.91	0.89	0.80	0.88	0.85	0.82	0.90
SC	-0.52	-0.86	0.95	0.54	0.85	0.72	0.69	-0.87	0.25	0.98	0.97	0.88	0.96	0.97	0.85	0.95	0.95	0.95	0.98
SM	-0.52	-0.87	0.94	0.44	0.84	0.72	0.65	-0.87	0.31	0.96	0.94	0.86	0.95	0.94	0.84	0.95	0.95	0.94	0.96
SR	0.63	0.49	-0.25	0.14	0.05	-0.13	-0.18	0.47	0.53	-0.27	-0.28	-0.10	-0.25	-0.21	-0.16	-0.17	-0.26	-0.14	-0.26
TH	-0.52	-0.87	0.95	0.51	0.81	0.71	0.69	-0.86	0.24	0.96	0.94	0.86	0.94	0.93	0.81	0.94	0.94	0.92	0.95
U	-0.43	-0.64	0.60	0.11	0.42	0.43	0.34	-0.62	-0.19	0.62	0.60	0.44	0.57	0.58	0.41	0.58	0.65	0.54	0.59
ZN	-0.56	-0.89	0.96	0.44	0.87	0.68	0.66	-0.45	0.30	0.94	0.95	0.90	0.92	0.94	0.86	0.98	0.91	0.97	0.95

(continued)

TABLE 11 (continued)

	K	LA	LU	MG	MN	NA1	NA2	NI	P	PB	PB21	SB	SC	SM	SR	TH	U	ZN
FSOL	-0.35	-0.58	-0.59	0.87	-0.37	-0.25	-0.26	-0.53	-0.32	-0.53	-0.48	-0.53	-0.52	-0.52	0.63	-0.52	-0.43	-0.56
IOC	-0.71	-0.89	-0.86	0.99	-0.68	-0.41	0.09	-0.81	-0.68	-0.87	-0.66	-0.80	-0.86	-0.87	0.49	-0.87	-0.64	-0.89
OC	0.83	0.96	0.91	-0.86	0.75	0.43	-0.34	0.86	0.71	0.96	0.72	0.88	0.95	0.94	-0.25	0.95	0.60	0.96
AS	0.50	0.50	0.46	-0.38	0.48	0.38	-0.10	0.42	-0.20	0.65	0.10	0.69	0.54	0.44	0.14	0.51	0.11	0.44
BA1	0.86	0.85	0.78	-0.69	0.74	0.54	-0.56	0.83	0.76	0.85	0.74	0.74	0.85	0.84	0.05	0.81	0.42	0.87
BA2	0.66	0.72	0.70	-0.61	0.40	0.30	-0.20	0.58	0.72	0.62	0.22	0.76	0.72	0.72	-0.13	0.71	0.43	0.68
BR	0.77	0.67	0.70	-0.58	0.57	0.48	-0.36	0.68	0.49	0.66	0.37	0.80	0.69	0.65	-0.18	0.69	0.34	0.66
CA	-0.68	-0.90	-0.84	0.98	-0.48	-0.38	0.09	-0.42	-0.61	-0.43	-0.64	-0.80	-0.87	-0.87	0.47	-0.86	-0.62	-0.45
CD	0.32	0.24	0.26	-0.00	0.28	0.48	-0.27	0.28	0.13	0.29	-0.01	0.09	0.25	0.31	0.53	0.24	-0.19	0.30
CE	0.79	0.98	0.82	-0.78	0.71	0.22	-0.36	0.84	0.75	0.92	0.72	0.85	0.98	0.96	-0.27	0.96	0.62	0.94
CO	0.85	0.96	0.86	-0.80	0.78	0.33	-0.51	0.90	0.73	0.93	0.77	0.90	0.97	0.94	-0.28	0.94	0.60	0.95
CR1	0.90	0.87	0.83	-0.24	0.42	0.53	-0.47	0.85	0.65	0.87	0.57	0.83	0.88	0.86	-0.10	0.86	0.44	0.90
CR2	0.81	0.95	0.87	-0.78	0.72	0.38	-0.42	0.84	0.75	0.91	0.75	0.91	0.96	0.95	-0.25	0.94	0.57	0.92
CS	0.84	0.95	0.84	-0.76	0.74	0.30	-0.55	0.87	0.74	0.92	0.75	0.89	0.97	0.94	-0.21	0.93	0.58	0.94
CS37	0.85	0.83	0.78	-0.71	0.79	0.44	-0.51	0.85	0.62	0.89	0.84	0.80	0.85	0.84	-0.16	0.81	0.41	0.86
CU	0.83	0.96	0.89	-0.39	0.56	0.44	-0.34	0.91	0.71	0.95	0.67	0.88	0.95	0.95	-0.17	0.94	0.58	0.98
EU	0.73	0.96	0.85	-0.81	0.60	0.31	-0.36	0.77	0.76	0.86	0.65	0.85	0.95	0.95	-0.26	0.94	0.65	0.91
FE1	0.86	0.94	0.87	-0.39	0.63	0.41	-0.44	0.92	0.76	0.94	0.74	0.82	0.95	0.94	-0.14	0.92	0.54	0.97
FE2	0.83	0.97	0.87	-0.80	0.78	0.31	-0.46	0.88	0.75	0.93	0.78	0.90	0.98	0.96	-0.26	0.95	0.59	0.95
K	1.00	0.81	0.76	-0.62	0.69	0.51	-0.55	0.83	0.64	0.83	0.73	0.83	0.84	0.81	0.02	0.82	0.44	0.83
LA	0.81	1.00	0.90	-0.85	0.73	0.37	-0.37	0.85	0.74	0.92	0.69	0.88	0.99	0.98	-0.26	0.98	0.67	0.96
LU	0.76	0.90	1.00	-0.80	0.66	0.46	-0.26	0.82	0.66	0.88	0.65	0.85	0.88	0.90	-0.18	0.88	0.46	0.89
MG	-0.62	-0.85	-0.80	1.00	-0.44	-0.37	-0.00	-0.30	-0.55	-0.32	-0.61	-0.76	-0.82	-0.82	0.52	-0.82	-0.60	-0.33
MN	0.69	0.73	0.66	-0.44	1.00	0.25	-0.46	0.66	0.45	0.63	0.71	0.60	0.75	0.71	-0.19	0.70	0.46	0.58
NA1	0.51	0.37	0.46	-0.37	0.25	1.00	-0.07	0.41	0.27	0.47	0.19	0.40	0.36	0.39	0.23	0.38	0.00	0.44
NA2	-0.55	-0.37	-0.26	-0.00	-0.46	-0.07	1.00	-0.51	-0.34	-0.41	-0.49	-0.33	-0.46	-0.40	-0.21	-0.39	-0.13	-0.40
NI	0.83	0.85	0.82	-0.30	0.66	0.41	-0.51	1.00	0.61	0.92	0.70	0.75	0.87	0.85	-0.19	0.83	0.43	0.93
P	0.64	0.74	0.66	-0.55	0.45	0.27	-0.34	0.61	1.00	0.67	0.74	0.66	0.74	0.75	0.07	0.74	0.48	0.75
PB	0.83	0.92	0.88	-0.32	0.63	0.47	-0.41	0.92	0.67	1.00	0.77	0.85	0.93	0.92	-0.15	0.91	0.52	0.96
PB21	0.73	0.69	0.65	-0.61	0.71	0.19	-0.49	0.70	0.74	0.77	1.00	0.60	0.73	0.73	-0.45	0.70	0.38	0.71
SB	0.83	0.88	0.85	-0.76	0.60	0.40	-0.33	0.75	0.66	0.85	0.60	1.00	0.88	0.85	-0.23	0.88	0.58	0.86
SC	0.84	0.99	0.88	-0.82	0.75	0.36	-0.46	0.87	0.74	0.93	0.73	0.88	1.00	0.99	-0.22	0.97	0.65	0.96
SM	0.81	0.98	0.90	-0.82	0.71	0.39	-0.40	0.85	0.75	0.92	0.73	0.85	0.98	1.00	-0.21	0.97	0.54	0.95
SR	0.02	-0.26	-0.18	0.52	-0.19	0.23	-0.21	-0.19	0.07	-0.15	-0.45	-0.23	-0.22	-0.21	1.00	-0.25	-0.33	-0.19
TH	0.82	0.98	0.88	-0.82	0.70	0.38	-0.39	0.83	0.74	0.91	0.70	0.88	0.97	0.97	-0.25	1.00	0.66	0.93
U	0.44	0.67	0.46	-0.60	0.46	0.00	-0.13	0.43	0.48	0.52	0.38	0.58	0.65	0.54	-0.33	0.66	1.00	0.57
ZN	0.83	0.96	0.89	-0.33	0.58	0.44	-0.40	0.93	0.75	0.96	0.71	0.86	0.96	0.95	-0.19	0.93	0.57	1.00

TABLE 12. MERCURY AND TIN IN SURFACE SEDIMENTS OF SOUTHERN LAKE HURON (μg/g)

Station	Mercury	Tin
3	0.18	4.2
4	N.D.	N.D.
5	-	4.0
6	-	5.0
7	-	2.0
8	0.14	4.1
9	-	1.8
10	-	3.3
11	-	3.8
12	-	6.4
13	-	1.5
14	-	4.0
15	0.04	0.3
16	-	3.8
17	-	4.0
18	0.16	3.1
19	0.05	0.7
20	-	3.7
21	-	4.6
22	-	1.0
29	0.18	4.1
30		0.8
31		3.7
32		2.0
33		2.0
34	0.07	1.6
35	0.03	0.8
36		2.0
37	0.07	1.5
38	-	1.0
39	-	1.4
40	0.05	1.3
41	-	1.4
42	0.13	2.3
43	-	1.2
44	0.06	0.6
45	0.05	1.0
46	-	1.2
47	0.20	5.0
48	-	1.7
49	0.17	3.6
50	-	0.8

(continued).

TABLE 12. (continued).

Station	Mercury	Tin
51	-	0.6
52	-	0.2
53	-	2.4
54	0.07	1.3
55	0.22	4.4
56	0.07	1.5
57	0.19	4.2
58	-	1.2
59	-	-
60	-	2.2
61	-	1.6
62	-	1.8
63	-	3.4
65	-	4.4
66	-	4.0
67	-	2.1
68	-	4.0
69	-	3.7
70	-	4.4
Min	0.03	0.2
Max	0.22	6.4
Avg.	0.11	2.5
SD	0.06	1.5
SD/Mean	0.59	0.60
N	19	59

N.D. Not Detectable

refers to the average activity of cesium-137 within the thickness of sediment where it is found.

i.e.,

$$\text{Cs37} = \frac{1}{z\ \text{max}} \int_{o}^{z\ \text{max}} \text{Cs-137}(z)dz \qquad (15)$$

Contour maps showing the spatial variation in surface sediment concentration values are in subsequent figures. To conserve space, concentration isopleths are shown for only about half of the elements. This does not represent a significant limitation because of the considerable redundancy in the concentration data.

Average Composition

The average concentrations of elements in surface sediments within the two depositional basins in southern Lake Huron given in Tables 10 and 12 are compared with other concentration data in Table 15. The relative variability of element concentrations in surface sediments is illustrated in Fig. 19. Anthropogenically or diagenetically enriched elements generally exhibit a high degree of variability within depositional basins as do the calcium family elements. Surface concentration data are given in terms of each depositional basin based upon the study of Kemp and Thomas (1976) and reported by the International Joint Commission (1977). Also given in Table 15 are average elemental concentration values for fine-grained sediments of Lake Michigan (Shimp et al. 1971). Concentrations in the single core (115) refer to the upper ten centimeters of sediment (Frye and Shimp 1973). This core was taken from a depositional environment in the eastern part of southern Lake Michigan possessing characteristics comparable in many respects to the Goderich Basin in Lake Huron.

Most of the major elements determined in this report have concentrations which are comparable to values reported by IJC (1977). Note that the calcium values in the Goderich Basin as reported by the IJC are significantly higher than those in the Port Huron Basin. The observation is consistent with the results of this study (see below) which indicate significantly (order of magnitude) higher dolomite deposition in the Goderich Basin. Note also that potassium values are roughly a factor of four lower in this study. Values reported by the International Joint Commission are for whole sediment while those reported here are for the acid-soluble fraction. Similarly the silicon concentrations reported by the International Joint Commission are for whole sediment while the values reported here are for amorphous silicon. On the average approximately 4% of the total silicon of the fine-grained sediments is in an amorphous, easily-leached form.

Some discrepancies are apparent on comparison of previously reported concentrations of trace elements with the results of this study. The present study indicates arsenic concentrations of 27 ± 10 ppm whereas the IJC reports 1 ± 2 ppm for the Goderich Basin. As can be seen from inspection of Table 5, neither the accuracy nor the precision of the method of instrumental activation analysis is particularly good for determination of this element. Moreover Walter et al. (1974) report surface concentrations of arsenic of

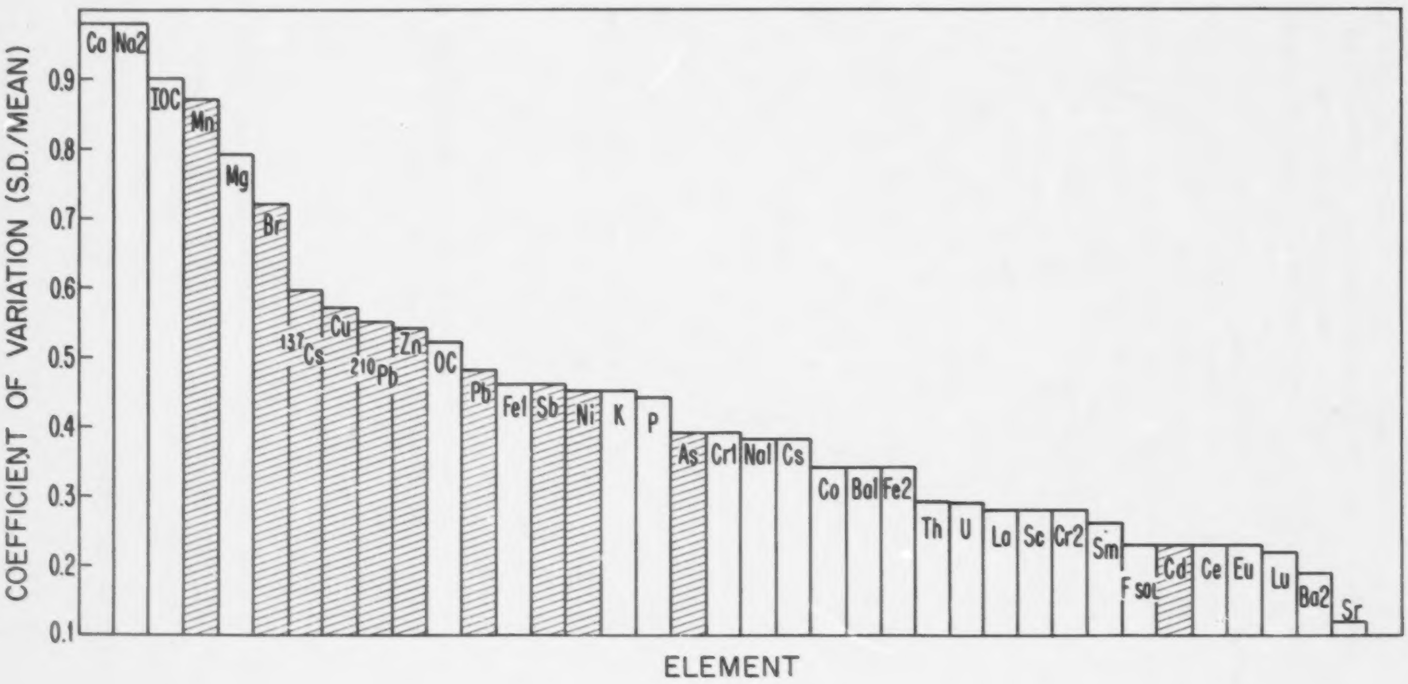

Figure 19. Relative variability of element concentrations in surface sediments. Anthropogenically or diagenetically enriched elements (shaded regions) generally exhibit a high degree of variability within depositional basins.

around 1 - 2 ppm for Lake Erie sediments and values no higher than 10 ppm even in grossly polluted harbor sediments. These results suggest that the As levels reported here are too high, perhaps because of unidentified interferences. On the other hand, surface sediments from comparable depositional environments in Lake Michigan indicate values of around 15 ppm (Frye and Shimp 1973). Furthermore Ruch et al. (1970) found that recent sediments in Lake Michigan had concentrations ranging from 5 to 30 ppm. As they used radiochemical separation procedures following neutron activation analysis, their results should be interference-free. The results reported here for southern Lake Huron are quite consistant with the Lake Michigan data. Reasons for this situation are not yet clear. Other elements reported here are also higher on the average than values reported by IJC. The ratios of mean concentration in surface sediments for the Goderich Basin as determined here to those determined by IJC are 2.9, 1.5, 1.3, and 1.9 for Cd, Ni, Pb, and Zn respectively. Levels of Cd reported by Walters et al. (1974) for recent sediments of Lake Erie range from about 1 to 4 ppm. Values reported by Barron (1976) for recent sediments of Lake Michigan average about 4 ppm. While part of the difference in surface concentrations of Cd reported here and by IJC may be due to analytical inaccuracies, at least part is probably due to the sampling methods. The data reported by IJC are based on analysis of the upper 3 cm of sediments collected by Shipex grab sampler. Losses of surface sediment by grab samplers can significantly reduce the measured concentration of enriched (see below) elements in what is defined as surface sediments. It is easy to see how the approximately 50% higher levels of Ni, Pb and Zn reported here could result from a slight loss of surface sediments. Consider the case of lead. For purposes of illustration suppose that the real concentration, C_o, at the surface ($z = 0$) is 100 ppm and that the natural level C_f is 30 ppm. It is shown below that the anthropogenic loading of lead to the Lake has an approximate 20 year doubling time. Thus, the actual profile of lead in sediments would then have the form:

$$C = C_o\, e^{-\beta t} + C_f = C_o\, e^{-\beta z/\bar{\omega}} + C_f \qquad (16)$$

where $\beta = 0.69315/20$ years and $\bar{\omega}$ is the mean linear sedimentation rate about 0.08 cm/yr. The concentration of lead in the section from 0 - 3 cm (used by Kemp and Thomas, 1976) is then

$$C_{0-3} = \frac{1}{3}\int_o^3 C(z)\, dz = 69.5 \quad \text{(ppm)} \qquad (17)$$

If there were just a 1 cm loss of sediment the expected concentration would be

$$\text{"}C_{0-3}\text{"} = \frac{1}{3}\int_1^4 C(z)\, dz = 55.8 \quad \text{(ppm)} \qquad (18)$$

A two cm loss of material would give:

$$\text{"}C_{0-3}\text{"} = \frac{1}{3}\int_2^5 C(z)\, dz = 46.9 \quad \text{(ppm)} \qquad (19)$$

Thus for realistic sedimentation rates and doubling times, just a two cm loss of sediment would reduce the apparent concentration of lead by a factor of 1.5. Clearly the effect of sediment loss of other sediment disturbance by Shipex sampling depends on the degree of enrichment of the element over background levels. The determination of elements possessing a significant degree of enrichment will be sensitive to losses of surface material. For non-enriched elements measured concentration are insensitive to sediment disturbances.

In contrast with most enriched elements, concentration of mercury as determined for this report are significantly less than those reported by the IJC and by Thomas (1973). Mean surface concentrations of mercury for the Port Huron and Goderich Basins are not significantly different and average 0.11 ppm. Values reported by IJC are 0.44 and 0.25 for these respective depositional basins. The analytical method used here is interference-free and values obtained agree with those reported by Kemp and Thomas (1976) for a core in the Goderich Basin. In their core the surface concentration (0-2 cm) was found to be 0.20 ppm whereas in two adjacent cores (Stn. 55 and 57) collected for this report surface (1-2 cm) concentrations were .22 and .19 ppm respectively. To some degree the distribution of mercury in surface sediments as found for this report are the mirror image of the distribution reported by Thomas (1973). In the sediments collected in 1969, Thomas found highest concentrations of mercury in the Port Huron Basin. Values were not only generally lower in the Goderich Basin but there was an indication that the areas identified in this report as being high in organic carbon were somewhat depleted in mercury. In contrast, in this present study mercury concentrations in surface sediment were found to follow the same general pattern as do concentrations of iron, organic carbon and most other trace elements and contaminants associated with fine-grained sedimentary materials. Like mercury, strontium concentrations are found to be lower significantly than previously reported by IJC. The reasons for these differences are not clear but are probably due at least in part to analytical inaccuracies. An intriguing alternative explanation is that there has been a net movement of mercury out of the Port Huron Basin and into the Goderich Basin during the five year period between the two sample collection dates; 1969 and 1974-1975. Additionally there could perhaps have been a net loss of mercury from sediments during this period.

Distribution and Interelement Associations

Major Constituents

Inspection of the correlation matrix (Table 10) shows that many elements are extremely well-correlated with each other. Linear regression coefficients are tabulated in Table A-8 of the Appendix. Regression coefficients for mercury and tin are given in Tables 13 and 14 respectively. An outstanding feature seen in looking the correlation matrix is the appearance of a set of elements correlated well with each other but negatively correlated with most other elements. This group is comprised of the calcium family elements, Ca, Mg, IOC and to a lesser extent Fsol, Sr, and Na2. In Figure 20 are shown the isopleths for inorganic carbon (IOC). This distribution is consistent with that found by Thomas et al. (1973) both in terms of absolute values and the strong trend toward high carbonate carbon

TABLE 13. RESULTS OF PAIRWISE REGRESSION ANALYSIS OF MERCURY SURFACE CONCENTRATION DATA

		Intercept		Slope		
Element	N	Value	Standard Error*	Value	Standard Error*	Correlation Coefficient
FSOL	13	0.258	0.10	-0.379	0.30	-0.47
IOC	11	0.184	0.02	-0.026	0.01	-0.85
OC	11	0.029	0.02	0.030	0.01	0.91
AS	8	0.145	0.04	0.001	0.00	0.47
BA1	11	-0.024	0.03	0.001	0.00	0.92
BA2	13	-0.106	0.06	0.001	0.00	0.86
BR	13	0.081	0.03	0.001	0.00	0.73
CA	19	0.128	0.03	-0.006	0.01	-0.29
CD	12	0.052	0.10	0.029	0.03	0.35
CE	7	-0.051	0.07	0.004	0.00	0.89
CO	13	-0.006	0.02	0.014	0.00	0.94
CR1	19	-0.022	0.02	0.003	0.00	0.94
CR2	13	-0.046	0.03	0.003	0.00	0.92
CS	13	0.013	0.02	0.035	0.01	0.92
CS-137	13	0.055	0.02	0.011	0.00	0.93
CU	19	0.019	0.01	0.003	0.00	0.94
EU	13	-0.059	0.05	0.177	0.04	0.86
FE1	19	-0.006	0.02	0.052	0.01	0.92
FE2	13	-0.010	0.02	0.048	0.01	0.94
K	13	0.028	0.03	0.159	0.03	0.89
LA	13	-0.046	0.04	0.006	0.00	0.92
LU	13	-0.114	0.06	0.738	0.17	0.88
MG	19	0.124	0.03	-0.007	0.01	-0.18
MN	19	0.059	0.02	0.454	0.14	0.73
NA1	11	0.055	0.06	0.346	0.26	0.53
NA2	13	0.462	0.22	-0.440	0.30	-0.53
NI	19	0.000	0.02	0.002	0.00	0.89
P	12	0.040	0.5	0.747	0.32	0.71
PB	19	0.013	0.01	0.001	0.00	0.95
PB-210	5	0.046	0.05	0.016	0.01	0.86
SB	13	0.033	0.02	0.115	0.02	0.90
SC	13	-0.041	0.03	0.016	0.00	0.93
SM	13	-0.057	0.03	0.037	0.01	0.93
SN	19	0.017	0.01	0.039	0.00	0.97
SR	11	0.106	0.23	0.001	0.01	0.06
TH	13	-0.033	0.03	0.021	0.00	0.93
U	13	0.065	0.08	0.028	0.03	0.37
ZN	19	0.016	0.01	0.001	0.00	0.95

[Hg] = intercept + slope [element] * 90% confidence limits.

Note: regression data for other element pairs in Table A-8 of Appendix.

TABLE 14. RESULTS OF PAIRWISE REGRESSION ANALYSIS OF TIN SURFACE CONCENTRATION DATA

		Intercept		Slope		
Element	N	Value	Standard Error*	Value	Standard Error*	Correlation Coefficient
FSOL	37	6.092	1.32	-10.035	4.05	-0.51
IOC	29	4.085	0.38	-0.641	0.13	-0.79
OC	28	0.469	0.53	0.734	0.15	0.81
AS	22	3.490	0.75	0.016	0.03	0.18
BA1	30	-0.480	0.78	0.023	0.00	0.77
BA2	37	-0.979	1.55	0.009	0.00	0.52
BR	37	2.009	0.51	0.019	0.01	0.46
CA	57	3.337	0.36	-0.264	0.09	-0.47
CD	33	1.487	1.51	0.466	0.51	0.22
CE	30	-2.202	0.83	0.098	0.02	0.86
CO	37	-0.643	0.56	0.340	0.05	0.85
CR1	57	-0.366	0.50	0.062	0.01	0.77
CR2	37	-1.482	0.70	0.067	0.01	0.84
CS	37	-0.204	0.52	0.869	0.14	0.84
CS-137	37	0.889	0.35	0.270	0.04	0.85
CU	56	0.155	0.26	0.065	0.01	0.90
EU	37	-2.327	0.82	4.700	0.72	0.84
FE1	57	-0.339	0.34	1.211	0.13	0.87
FE2	37	-0.698	0.53	1.202	0.17	0.86
HG	19	-0.247	0.28	23.609	2.17	0.97
K	36	0.567	0.59	3.428	0.79	0.72
LA	37	-1.490	0.66	0.144	0.02	0.85
LU	37	-2.313	1.03	16.061	3.08	0.78
MG	57	3.342	0.43	-0.356	0.16	-0.38
MN	57	1.648	0.36	7.032	2.02	0.55
NA1	30	1.484	1.06	7.035	4.94	0.35
NA2	37	8.470	3.23	-7.592	4.40	-0.38
NI	57	-0.292	0.38	0.056	0.01	0.84
P	30	0.603	0.65	14.706	4.13	0.69
PB	57	-0.309	0.27	0.039	0.00	0.92
PB-210	20	0.820	0.62	0.333	0.08	0.80
SB	37	0.601	0.56	2.762	0.61	0.73
SC	37	-1.490	0.66	0.399	0.06	0.85
SM	37	-1.871	0.73	0.925	0.14	0.85
SR	31	5.036	3.69	-0.048	0.08	-0.15
TH	37	-1.311	0.69	0.521	0.08	0.83
U	37	0.341	1.07	0.938	0.37	0.51
ZN	57	0.030	0.28	0.022	0.00	0.89

[Sn] = intercept + slope [element] * 90% confidence limits.
Note: regression data for other element pairs in Table A-8 of Appendix.

TABLE 15. COMPARISON OF MEAN SURFACE CONCENTRATION DATA WITH OTHER REPORTED VALUES

Element	Mean Concentration				
		IJC, 1977		(Frye and Shimp, 1973) Lake Michigan	
	This Report Basins Combined[a]	Port Huron Basin	Goderich Basin	Core 115	Average
Major (%)					
Al	(5.9)[b]	5.5 ± 0.6	4.6 ± 1.3	5.0	-
Ca	2.7 ± 2.7	0.93 ± 0.07	3.9 ± 3.3	6.7	5.6
K	0.68 ± 0.3	2.7 ± 0.2	2.3 ± 0.6	2.0	-
Mn	0.13 ± 0.11	0.08 ± 0.05	0.08 ± 0.03	0.06	0.06
Na2	0.73 ± 0.07	0.7 ± 0.04	0.72 ± 0.06	0.45	-
P	0.15 ± 0.06	0.06 ± 0.01	0.08 ± 0.02	0.15	0.07
Si	1.2	31 ± 1.9	28 ± 3.1	22	25
Ti	(0.30)	0.33 ± 0.03	0.31 ± 0.07	0.31	-
Fe2	3.1 ± 1.0	3.2 ± 0.6	3.0 ± 1.2	3.1	2.6
Minor (ug/g)					
As	27 ± 10	-	1 ± 2	15	14
Cd	2.9 ± 0.7	1 ± 0.4	1 ± 0.5	-	4.9[c]
Co	11 ± 4	14 ± 7	22 ± 21	15	13
Cr	47 ± 19	36 ± 8	29 ± 11	80	77
Cu	37 ± 21	42 ± 11	30 ± 16	45	37
Hg	0.11 ± 0.06	0.44 ± 0.17	0.25 ± 0.13	0.24	0.20
Ni	51 ± 23	43 ± 8	35 ± 17	40	34
Pb	74 ± 35	38 ± 27	58 ± 12	125	88
Sr	44 ± 5	74 ± 17	79 ± 26	-	-
V	(90)	56 ± 19	40 ± 23	66	48
Zn	120 ± 60	50 ± 27	63 ± 37	270	206

[a] The mean is dominated by values from the Goderich Basin. [b] Values in parenthesis for a single core.
[c] Value from Barron (1976).

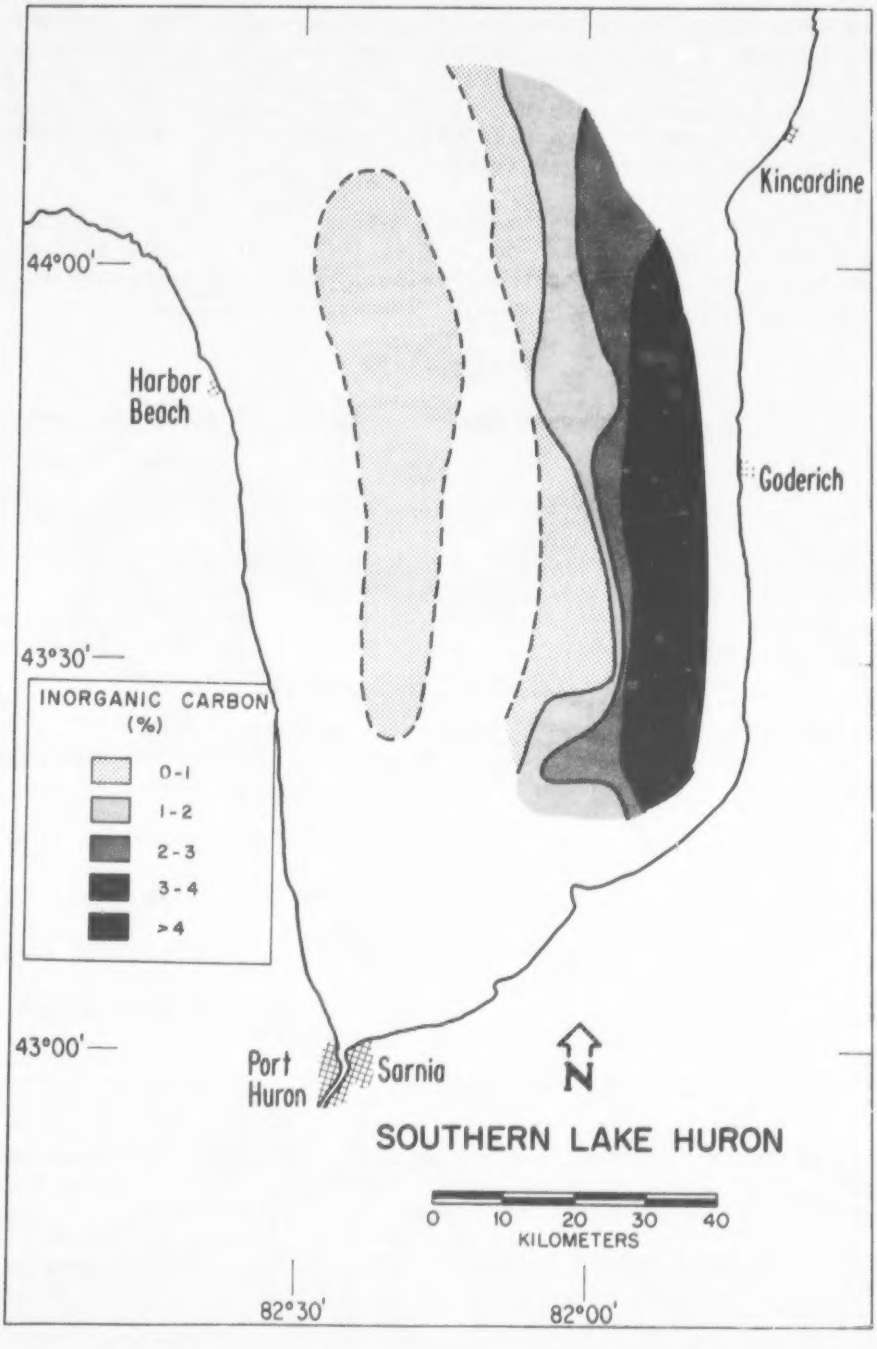
44°00'
43°30'
43°00'
82°30'
82°00'
Kincardine
Harbor Beach
Goderich
Port Huron
Sarnia
N
SOUTHERN LAKE HURON
0
10
20
30
40
KILOMETERS
INORGANIC CARBON (%)
0-1
1-2
2-3
3-4
>4

Figure 20. Distribution of inorganic carbon in surface sediments.

deposition along the eastern side of Lake Huron. Thomas et al. attribute the high carbonate values on the eastern side of the Lake to the proximity of carbonate bedrock of the Bruce Peninsula and the shoreline exposures of glacial sediments on the eastern shore. Their x-ray diffraction studies indicate that the carbonate in the eastern portion of the lake consists predominantly of dolomite with subsidiary calcite. The calcium family element data support that observation.

Both calcium (Fig. 21) and magnesium (Fig. 22) as well as Fsol (Fig. 23) have distributions very similar to that of IOC. The scatter plot of Ca vs. IOC shown in Fig. 24 indicates the excellent degree of correlation between these quantities (R = 0.995; N = 29). The regression equation is

$$\mathrm{Ca} = 0.39 + (1.58 \pm .04)\ \mathrm{IOC}. \qquad (20)$$

If the calcium and IOC were due entirely to dolomite, the expected ratio would be

$$\mathrm{Ca/IOC} = 40/24 = 1.66 \qquad (21)$$

if the composition of dolomite is taken to be $\mathrm{CaMg(CO_3)_2}$. The 4% difference between the observed and expected slopes is within experimental uncertainties. Hence the relationship between Ca and IOC suggest that essentially all the inorganic carbon present is due to non-substituted dolomite.

The magnesium data are also consistent with this analysis. A scatter plot of Mg vs. IOC (Fig. 25) shows that provided Mg > 1% the correlation with IOC is excellent. Regression analysis of all data yields

$$\mathrm{Mg} = 0.824 + (0.829 \pm .04)\ \mathrm{IOC} \qquad r = 0.987 \qquad N = 34 \qquad (22)$$

whereas regression on data for which Mg> 1% yields:

$$\mathrm{Mg} = 0.87 + (0.89 \pm .05) \times \mathrm{IOC} \qquad r = 0.98 \qquad N = 29. \qquad (23)$$

This latter slope may be compared with that expected if both Mg and IOC were due exclusively to dolomite:

$$\mathrm{Mg/IOC} = 24/24 = 1.00. \qquad (24)$$

Again the observed slope is consistent with expectation, although some Mg is evidently associated with non-dolomitic material. Similarly the regression of Ca on Mg (Fig. 26) for Mg > 1% yields

$$\mathrm{Ca} = -0.95 + 1.72\ \mathrm{Mg} \qquad r = 0.97 \qquad N = 42 \qquad (25)$$

while the expected slope is

$$\mathrm{Ca/Mg} = 40/24 = 1.65.$$

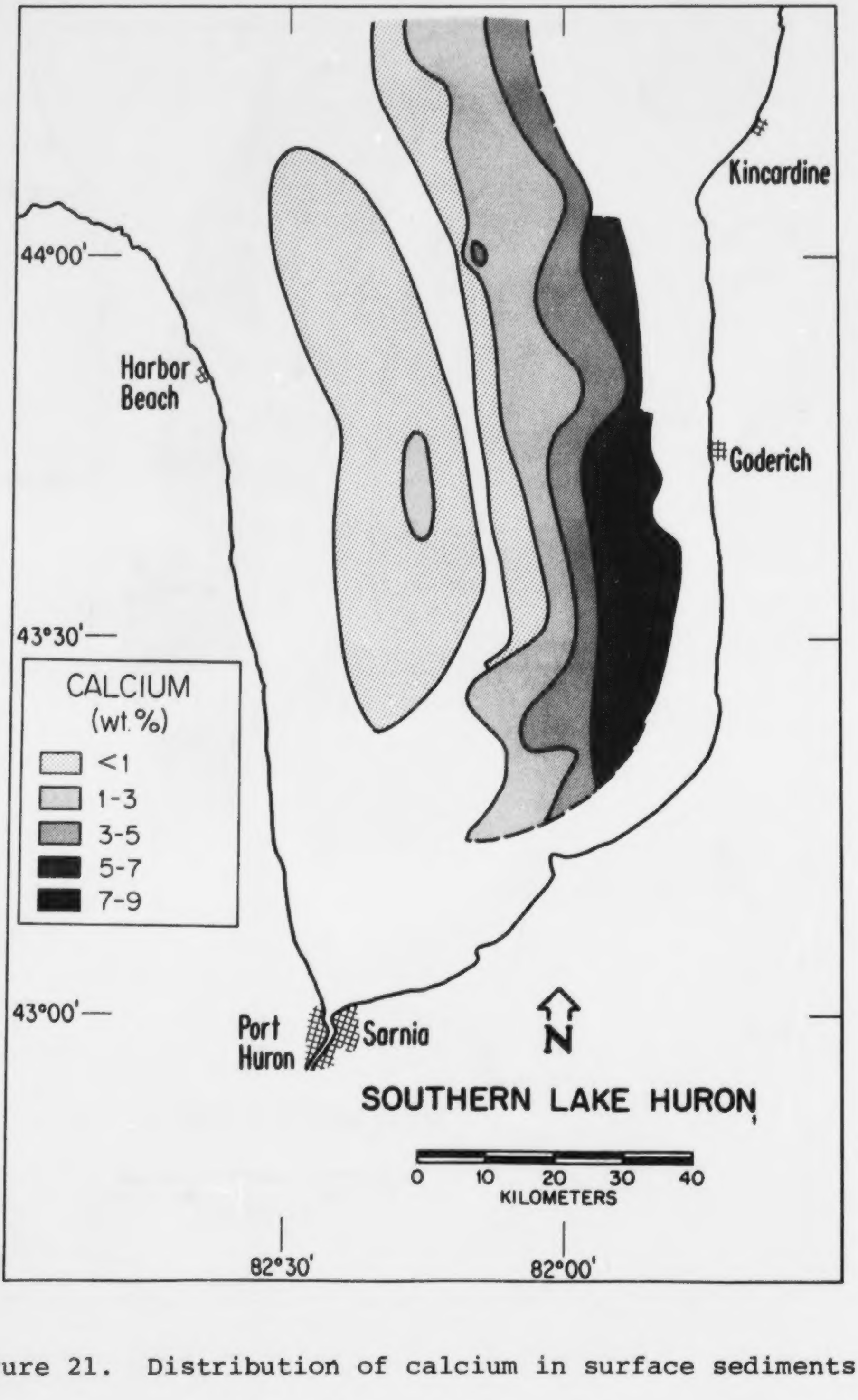
Kincardine
44°00'
Harbor Beach
Goderich
43°30'
CALCIUM (wt.%)
<1
1-3
3-5
5-7
7-9
43°00'
Port Huron
Sarnia
N
SOUTHERN LAKE HURON
0 10 20 30 40
KILOMETERS
82°30'
82°00'

Figure 21. Distribution of calcium in surface sediments.

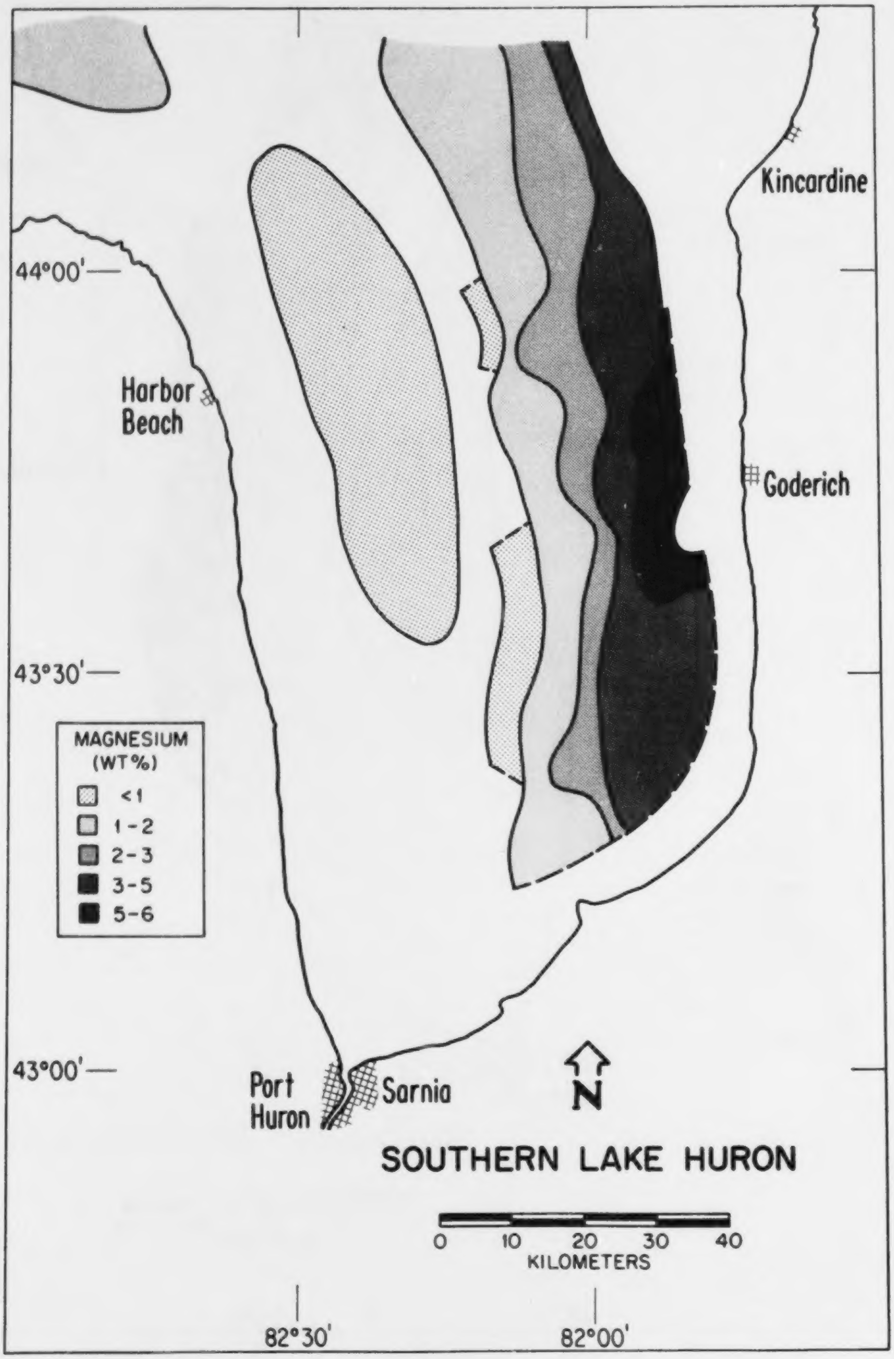
Kincardine
44°00'
Harbor Beach
Goderich
43°30'
MAGNESIUM (WT%)
<1
1-2
2-3
3-5
5-6
43°00'
Port Huron
Sarnia
N
SOUTHERN LAKE HURON
0 10 20 30 40
KILOMETERS
82°30'
82°00'

Figure 22. Distribution of magnesium in surface sediments.

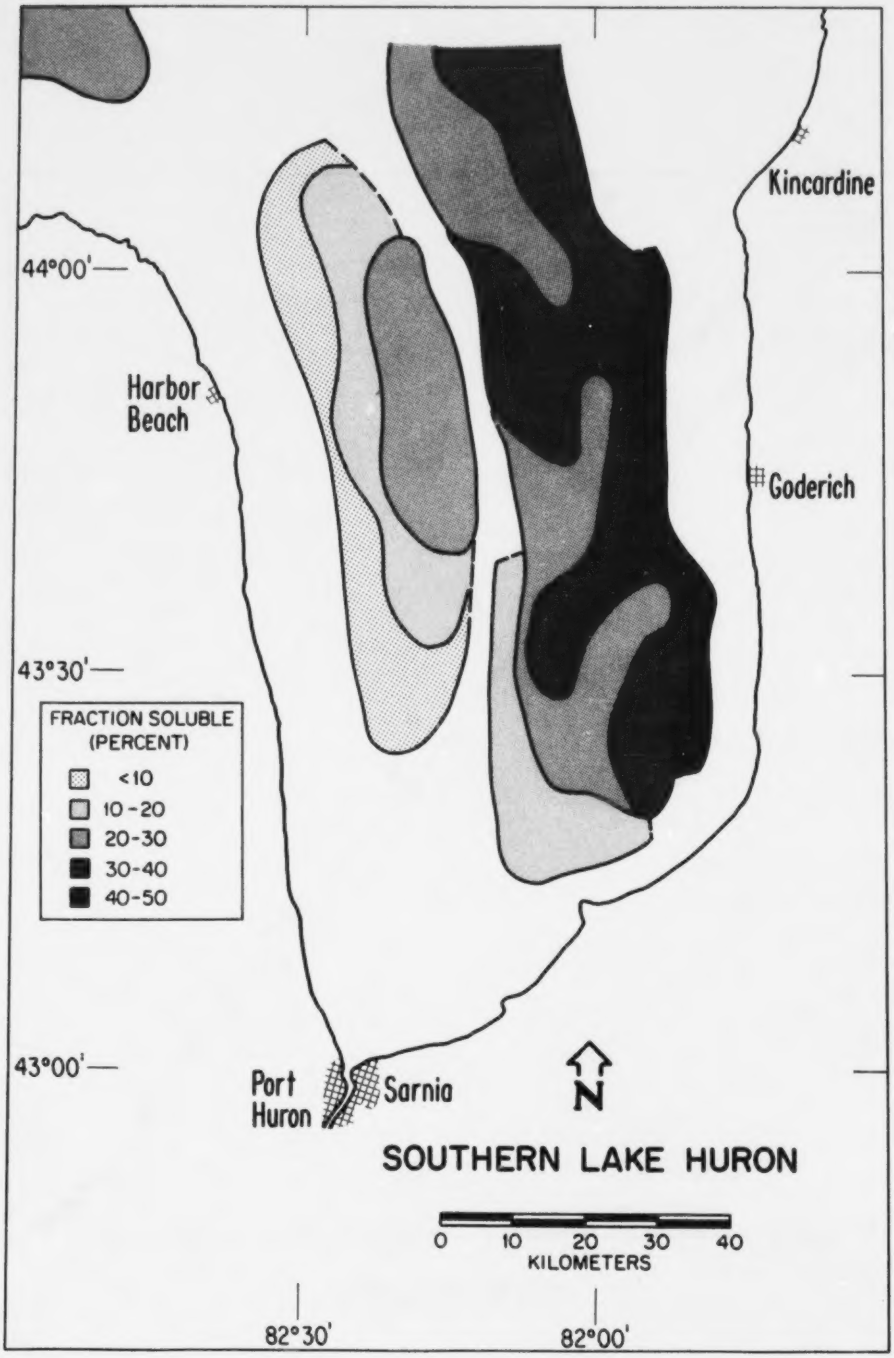

Kincardine
44°00'
Harbor Beach
Goderich
43°30'
FRACTION SOLUBLE (PERCENT)
<10
10-20
20-30
30-40
40-50
43°00'
Port Huron
Sarnia
N
SOUTHERN LAKE HURON
0 10 20 30 40
KILOMETERS
82°30'
82°00'

Figure 23. Distribution of fraction soluble component in surface sediments.

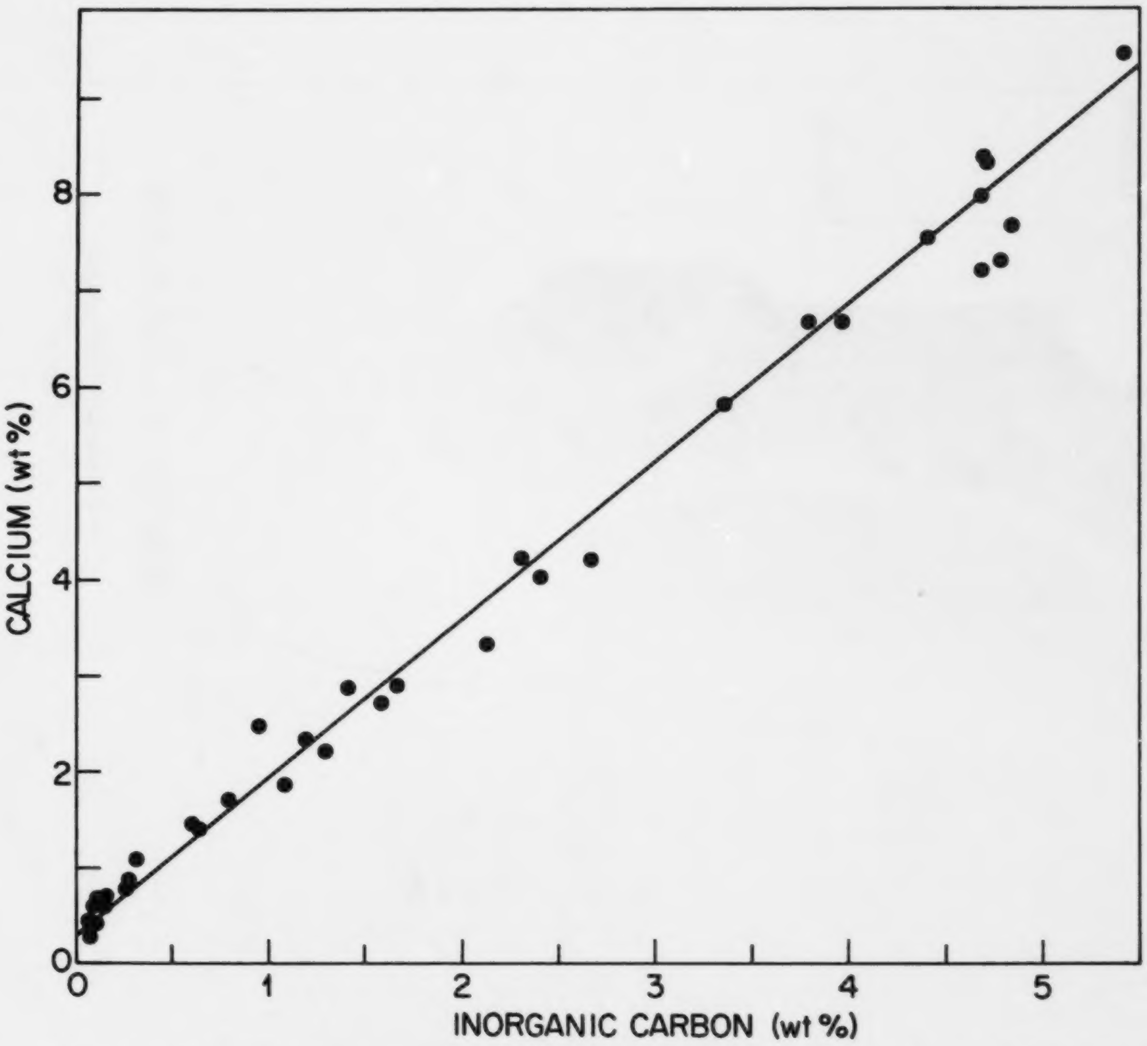

Figure 24. Relation between calcium and inorganic carbon in surface sediments.

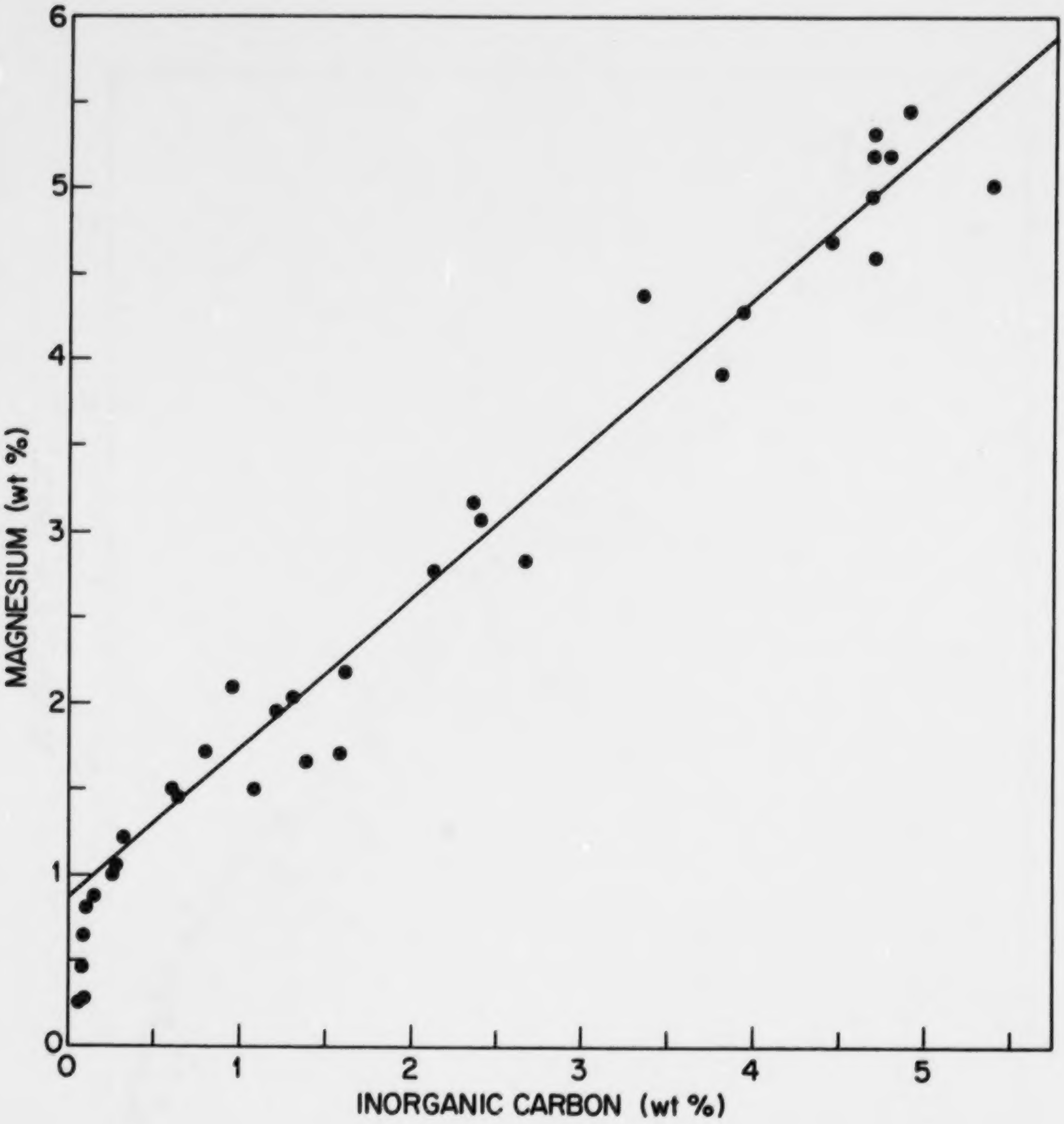

Figure 25. Relationship between magnesium and inorganic carbon in surface sediments.

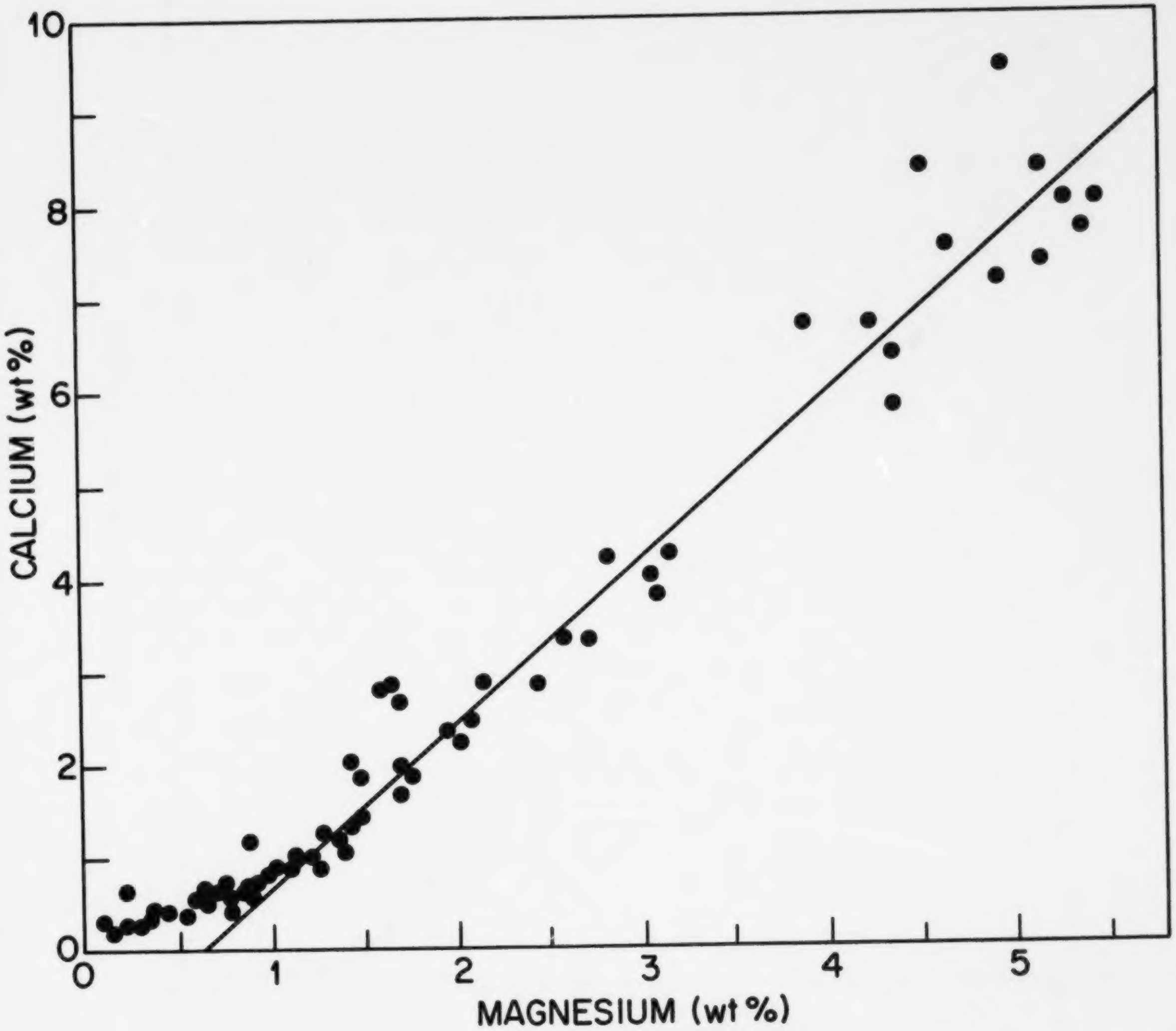

Figure 26. Relation between calcium and magnesium in surface sediments.

As can be seen from inspection of the correlation matrix and regression Table (A-8), the correlation of Sr with major calcium family constituents is significant but considerably poorer:

$$Sr = 40.59 + 0.86\ Ca \qquad r = 0.47 \qquad N = 33. \qquad (26)$$

The strontium associated with calcium occurs in the ratio of:

$$Sr/Ca = 0.86 \times 10^{-4}\ (g/g).$$

The three independent estimators of dolomite, Ca, Mg, and IOC, are used in Table 16 to obtain the best estimate of dolomite in surface sediments. The resulting distribution of dolomite is shown in Fig. 27. Toward the eastern margin of the Goderich Basin dolomite can account for over 40% of the total weight of dry sediment.

It is therefore, not surprising that Fsol is well-correlated with the calcium family elements. Much of what goes into solution on acid-peroxide treatment is evidently due to dissolution of dolomite. Regression of Fsol on Ca gives:

$$Fsol = 0.241 + 0.022\ Ca \qquad r = 0.85 \qquad N = 39. \qquad (27)$$

As Fsol must include dissolution of nondolomitic materials as well, its correlation with Ca is predictably less than major calcium family and IOC inter-correlations. Given in Table 16 is the fraction of dry sediment which dissolves on acid treatment which is not due to dolomite dissolution, Fsol*:

$$Fsol^* = Fsol - (Dolomite\ (wt.\ \%)\ /\ 100.0) \qquad (28)$$

The ratio Fsol*/Fsol, also shown in Table 16 is the fraction of sediment dissolved which is non-dolomitic. At some stations such as 44 where Fsol*/Fsol = 0.06, 94% of the material in solution is due to dissolution of dolomite. In contrast at Station 5 where Fsol*/Fsol = 0.92, 92% of the material dissolved is not due to dolomite.

With the dolomite contributions removed from Fsol by introducing Fsol*, this latter quantity should correlate strongly with the complementary major sedimentary constitutents which go into solution, organic carbon and iron. Their isopleths are shown in Figures 28 and 29 respectively. A scatter plot of Fsol* versus OC, shown in Figure 30, shows that Fsol* is well-correlated with organic carbon (and Fe).

Pair-wise regression analysis yields:

$$Fsol^* = +\ 0.001 + 0.048OC \qquad r = 0.96 \qquad N = 28. \qquad (29)$$

Fsol* is also well-correlated with iron:

$$Fsol^* = -\ 0.033 + 0.074\ Fe \qquad r = 0.96 \qquad N = 28. \qquad (30)$$

As Fsol* is most certainly made up of contributions from both Fe and OC

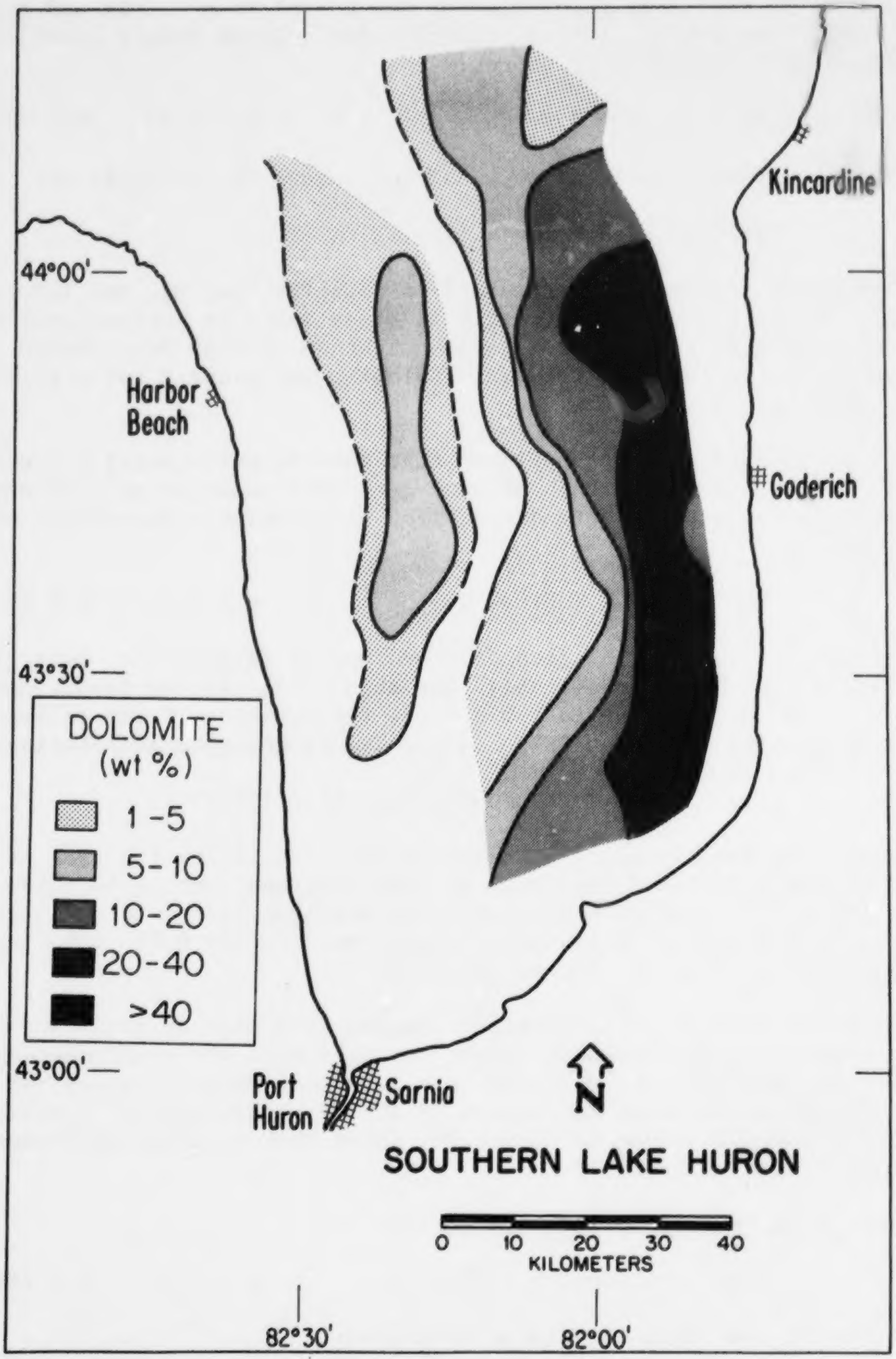
Kincardine
44°00'
Harbor Beach
Goderich
43°30'
DOLOMITE (wt %)
1-5
5-10
10-20
20-40
>40
43°00'
Port Huron
Sarnia
N
SOUTHERN LAKE HURON
0 10 20 30 40
KILOMETERS
82°30'
82°00'

Figure 27. Distribution of dolomite in surface sediments. Values are based on analysis of calcium, magnesium and inorganic carbon content.

TABLE 16. CONCENTRATION OF DOLOMITE IN SURFACE SEDIMENTS BASED ON CALCIUM, MAGNESIUM AND INORGANIC CARBON CONTENT (WT %)

Station	Calcium	Magnesium	IOC	Dol(Ca)	Dol(Mg)	Dol(IOC)	Dol	Fsol	Fsol*	Fsol*/Fsol
3	2.01	1.47		9.3	7.2		8.2	0.243	0.161	0.662
4	0.11	0.17		0.5	0.0		0.3			
5	0.48	0.82	0.10	2.2	2.1	2.2	2.2	0.260	0.238	0.917
6	0.64	0.77		3.0	1.7		2.3			
7	7.37	5.19	4.78	34.0	36.7	37.8	36.1	0.428	0.067	0.156
8	0.62	0.87	0.09	2.9	2.5	2.1	2.5	0.260	0.235	0.905
9	4.00	3.06	2.41	18.4	19.3	19.8	19.3	0.283	0.090	0.317
10	0.48	0.47	0.08	2.2	0.0	2.0	1.4			
11	0.54	0.67		2.5	0.9		1.7			
12	2.33	1.96	1.21	10.7	11.1	10.6	10.8	0.326	0.218	0.668
13	7.68	5.42	4.85	35.4	38.4	38.3	37.4	0.463	0.089	0.193
14	2.46	2.11	0.95	11.4	12.3	8.7	10.6	0.317	0.209	0.661
15	0.16	0.12		0.7	0.0		0.4			
16	0.64	0.88	0.14	3.0	2.5	2.5	2.7	0.250	0.223	0.893
17	1.38	1.47	0.64	6.3	7.2	6.3	6.6	0.318	0.252	0.792
18	4.22	3.17	2.37	19.4	20.7	19.4	19.9	0.354	0.155	0.439
19	0.39	0.55		1.8	0.0		0.9			
20	1.08	1.14		5.0	4.6		4.8			
21	1.30	1.29		6.0	5.8		5.9			
22	0.68	0.67		3.1	0.9		2.0			
29	1.69	1.73	0.78	7.8	9.3	7.4	8.1	0.317	0.236	0.743
30	0.65	0.26	0.10	3.0	0.0	2.2	1.7			
31	0.64	0.73		3.0	1.4		2.2	0.187	0.165	0.883
32	0.55	0.61		2.6	0.4		1.5			
33	0.60	0.90	0.16	2.8	2.7	2.6	2.7	0.262	0.235	0.897
34	0.40	0.40		1.8	0.0		0.9			
35	0.29	0.26	0.08	1.3	0.0	2.0	1.1			
36	3.33	2.60		15.3	16.1		15.7			
37	2.79	1.62		12.8	8.4		10.6			
38	6.66	3.92	3.79	30.7	26.6	30.2	29.2			
39	2.69	1.72	1.59	12.4	9.2	13.5	11.7			

(continued)

TABLE 16. (continued)

Station	Calcium	Magnesium	IOC	Dol(Ca)	Dol(Mg)	Dol(IOC)	Dol	Fsol	Fsol*	Fsol*/Fsol
40	4.18	2.83	2.67	19.3	18.0	21.7	19.7	0.242	0.045	0.188
41	1.19	0.91		5.5	2.8		4.1			
42	1.84	1.50	1.08	8.5	7.4	9.6	8.5	0.212	0.127	0.598
43	6.66	4.27	3.93	30.7	29.4	31.3	30.5			
44	9.45	5.01	5.39	43.5	35.2	42.4	40.4	0.452	0.048	0.107
45	8.34	5.18	4.71	38.4	36.6	37.2	37.4	0.397	0.023	0.058
46	7.51	4.68	4.40	34.6	32.6	34.9	34.0	0.375	0.035	0.092
47	0.88	1.05	0.27	4.0	3.9	3.5	3.8	0.303	0.265	0.874
48	0.46	0.39		2.1	0.0		1.0			
49	0.82	1.01	0.26	3.8	3.6	3.4	3.6	0.311	0.275	0.884
50	7.17	4.97	4.68	33.0	34.9	37.0	35.0	0.401	0.051	0.128
51	8.34	4.58	4.72	38.4	31.8	37.3	35.9	0.411	0.052	0.128
52	2.85	1.66	1.41	13.1	8.8	12.1	11.4			
53	1.95	1.73		9.0	9.3		9.1			
54	7.97	5.31	4.68	36.7	37.5	37.0	37.1	0.434	0.063	0.145
55	1.09	1.23	0.32	5.0	5.3	3.9	4.7	0.296	0.249	0.840
56	0.28	0.32		1.3	0.0		0.6			
57	0.85	1.28		3.9	5.7		4.8	0.270	0.222	0.822
58	2.86	2.19	1.67	13.2	12.9	14.1	13.4	0.211	0.077	0.365
59	0.77	0.92		3.5	2.9		3.2	0.278	0.246	0.885
60	3.79	3.12		17.4	20.3		18.8	0.322	0.134	0.415
61	6.25	4.38		28.8	30.3		29.5	0.430	0.135	0.313
62	5.81	4.38	3.36	26.7	30.3	27.0	28.0	0.391	0.111	0.284
63	2.22	2.04	1.30	10.2	11.7	11.3	11.1	0.276	0.165	0.598
65	1.44	1.50	0.61	6.6	7.4	6.1	6.7	0.272	0.205	0.753
66	2.81	2.48		12.9	15.2		14.1	0.327	0.186	0.570
67	3.33	2.76	2.13	15.3	17.4	17.6	16.8	0.306	0.138	0.451
68	1.84	1.78		8.5	9.6		9.1	0.297	0.206	0.695
69	2.05	1.83		9.5	10.1		9.8	0.310	0.212	0.685
70	0.88	1.14		4.0	4.6		4.3	0.205	0.162	0.788
71	1.21	1.39		5.6	6.6		6.1	0.267	0.206	0.773
73	1.08	1.40		5.0	6.7		5.8			

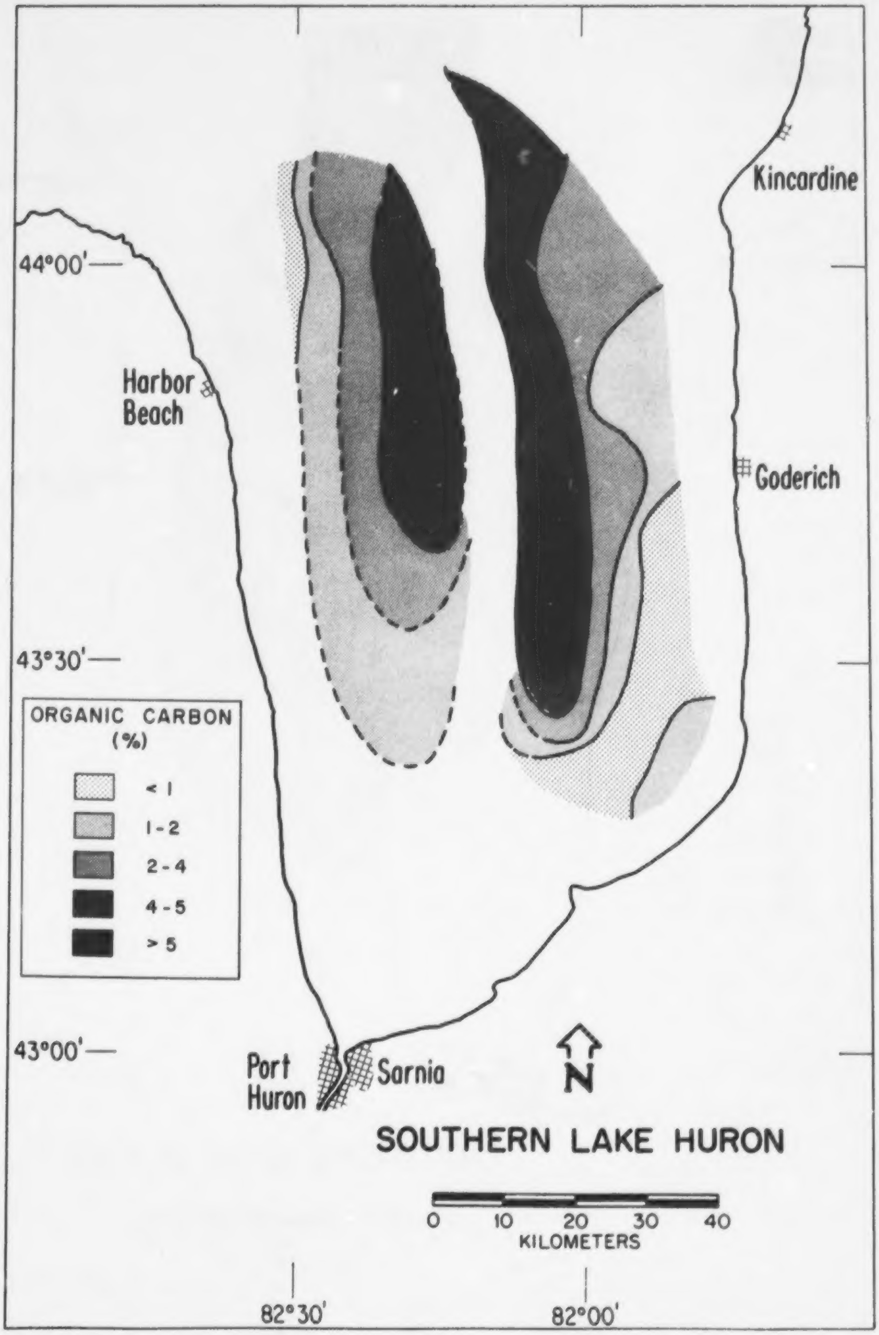

44°00'
43°30'
43°00'
82°30'
82°00'
Kincardine
Harbor Beach
Goderich
Port Huron
Sarnia
N
ORGANIC CARBON (%)
< 1
1 - 2
2 - 4
4 - 5
> 5
SOUTHERN LAKE HURON
0
10
20
30
40
KILOMETERS

Figure 28. Distribution of organic carbon in surface sediments.

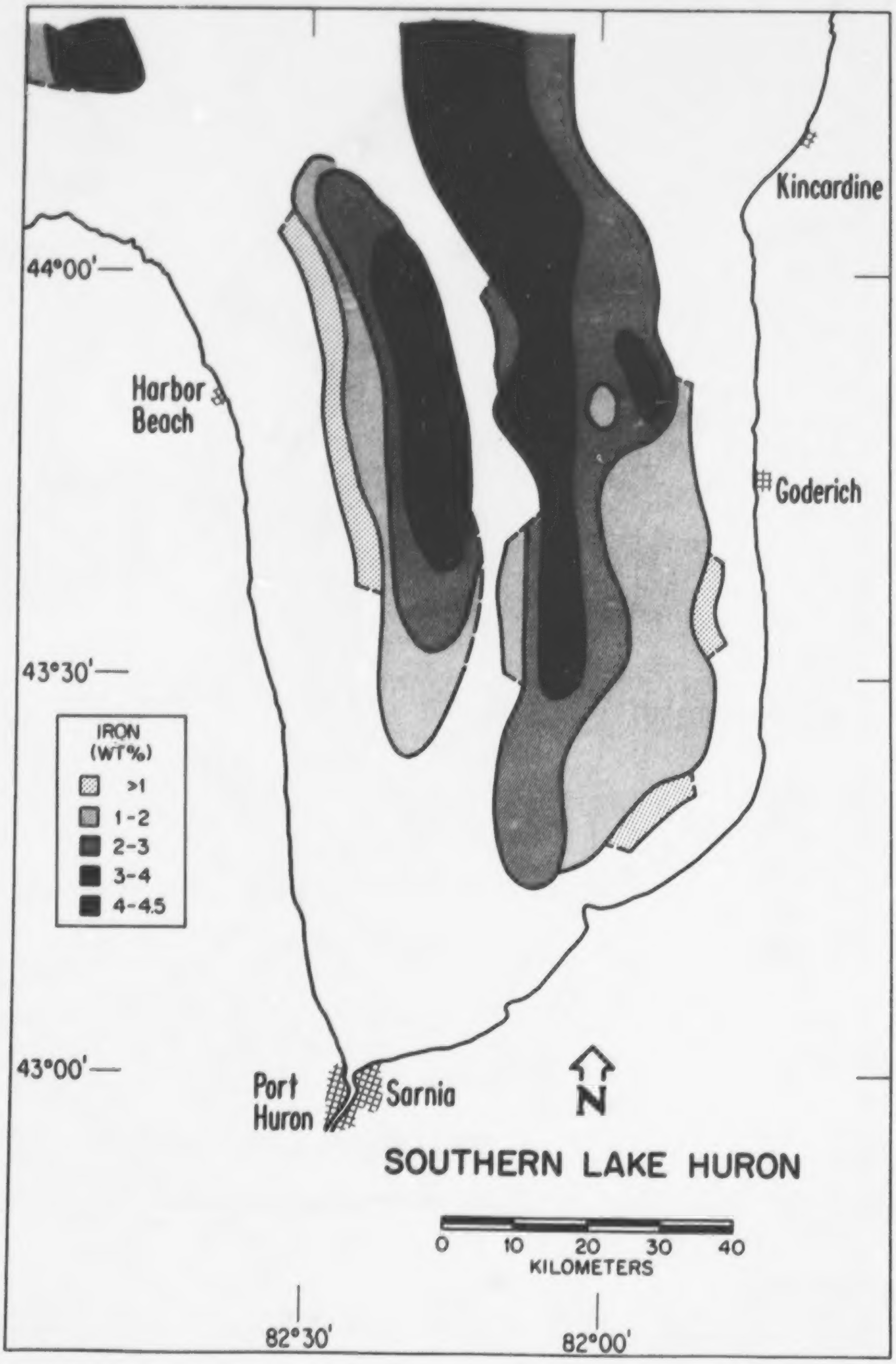
Kincardine
44°00'
Harbor Beach
Goderich
43°30'
IRON (WT%)
>1
1-2
2-3
3-4
4-4.5
43°00'
Port Huron
Sarnia
N
SOUTHERN LAKE HURON
0
10
20
30
40
KILOMETERS
82°30'
82°00'

Figure 29. Distribution of iron in surface sediments.

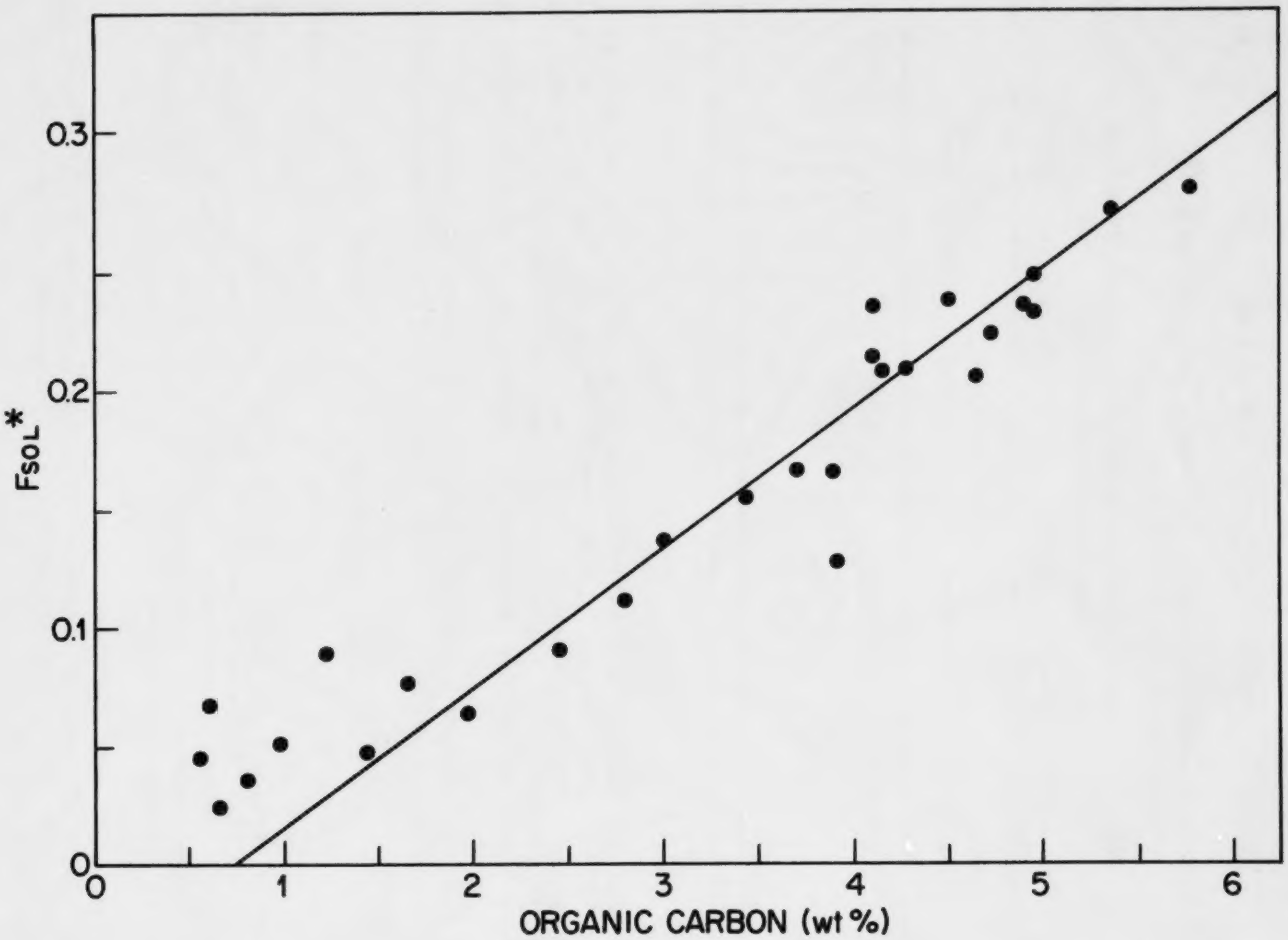

Figure 30. Relation between the fraction soluble component (corrected for dolomite contributions) and organic carbon.

as well as Mn to a lesser extent it should be best described in terms of a linear combination of these elements; i.e.,

$$\text{Fsol}^* = \alpha + \beta\ \text{OC} + \gamma\ \text{Fe} + \delta\ \text{Mn} \qquad (31)$$

multiple regression analysis yields the values given in Table 17.

TABLE 17. COEFFICIENTS FROM MULTIPLE LINEAR REGRESSION OF FSOL* VS OC, FE AND MN

Coefficient	Value		Standard Error	Level of Significance
α	- 0.0202	$\pm$	0.012	0.1
β (OC)	0.0251	$\pm$	0.007	0.001
γ (Fel)	0.0358	$\pm$	0.013	0.01
δ (Mn)	0.0207	$\pm$	0.072	0.8

N = 28

Most of the significance is determined by OC and Fe. The unexplained variance and the contribution of manganese to the proper description of Fsol* are negligible. The parameters, α and β, have associated uncertainties of 28% and 36% respectively. The relationship between Fsol* determined by dolomite subtraction and that predicted by equation 26 is shown in Figure 31.

If the contribution of organic carbon to Fsol* were due solely to compounds having the empirical formula, $(CH_2O)_n$ (sugars, cellulose, etc.)

$$\text{Fsol}^*(\text{org.C}) = \frac{12 + 18}{12} \times \frac{1}{100} = 0.025\ \text{OC} \qquad (32)$$

This is precisely the value found from the regression analysis. Thus the above empirical formula is consistent with the inferred contribution of organic carbon to the acid-peroxide extractable material in sediments. Such close agreement between the value of beta and that in Eq. 32 above is undoubtedly accidental, however.

Values of γ and δ are consistent with the assumption that the principal forms of iron and manganese in surface sediments are high oxidation state hydroxides such as $Fe(OH)_3$ and $Mn(OH)_4$. Compounds of these forms contribute to Fsol* as

$$\text{Fsol}^*\ (\text{Fe}) = \frac{55.9 + 3 \times 17}{54.93}\ \frac{1}{100} = 0.019\ \text{Fe}(\%) \qquad (33)$$

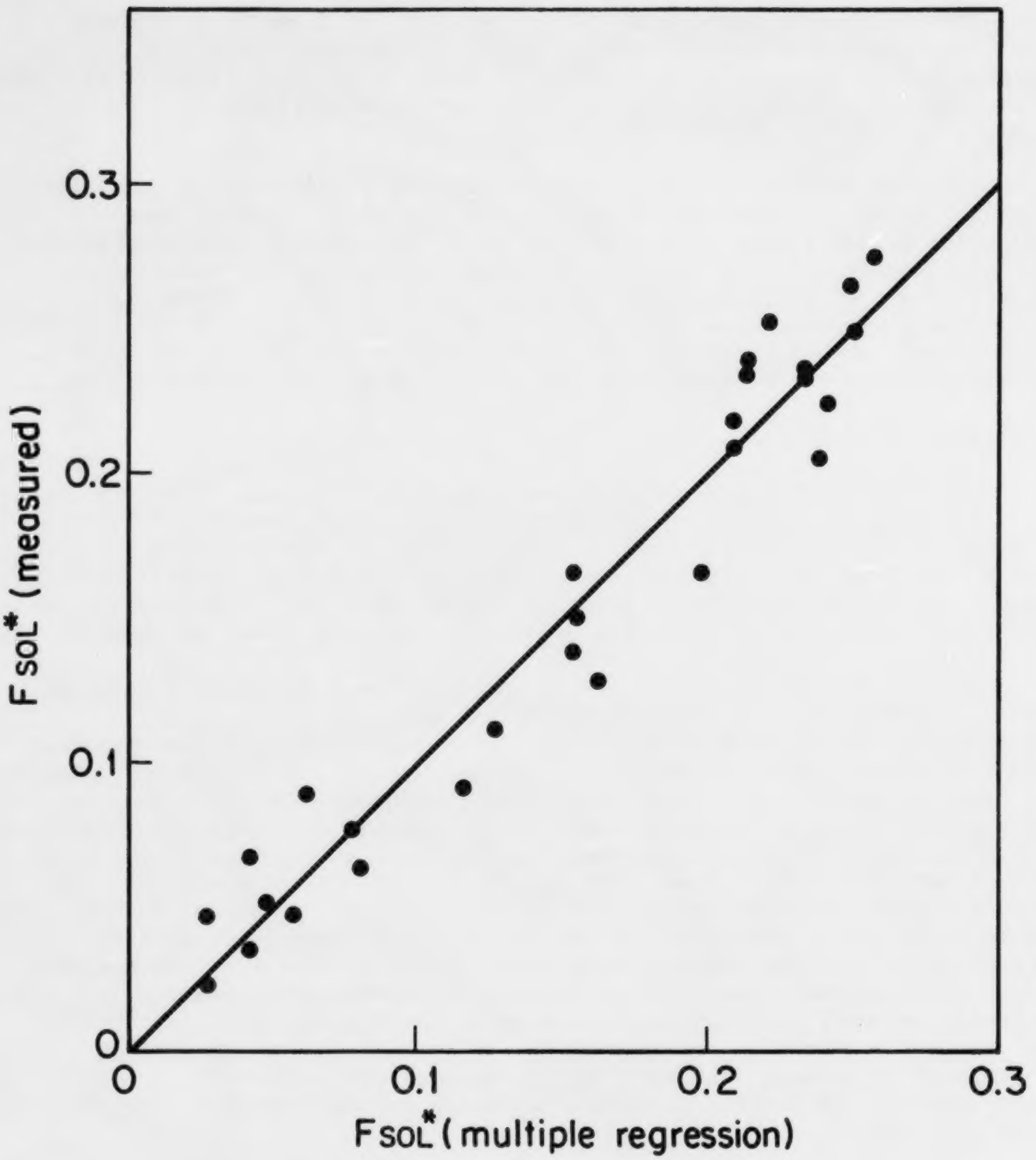

Figure 31. Relation between observed and predicted values of dolomite-corrected fraction soluble content of surface sediments.

$$\text{Fsol*}(\text{Mn}) = \frac{54.93 + 4 \times 17}{54.93} \; \frac{1}{100} = 0.022 \; \text{Mn} \; (\%) \cdot \qquad (34)$$

Both values are consistent with those obtained from the regression analysis within experimental errors, 0.036 ± 0.013 and 0.02 ± 0.07 respectively. The coefficient in Eq. 33 would increase for contribution from iron compounds having less iron by weight per molecule, such as iron phosphates and iron in humic materials.

The distribution of organic carbon in surface sediments is consistent with the observations of Thomas et al. (1973) both in terms of absolute value and trend toward higest concentrations in deeper parts of each depositional basin. As shown in Fig. 32, Fe and organic carbon are well-correlated. Distributions of other major elements are shown in Figures 33-36. Mn, acid-soluble P and K have distributions similar to those of OC and Fe. The distribution of Na2 (NAA) tends to follow that of the calcium family elements with highest concentrations along the eastern margin of the Goderich Basin.

Trace Constituents

Many of the 27 trace elements are intercorrelated to a very high degree as can be seen by inspection of the correlation matrix (Table 11). The highest correlation occurs for the pair, Fe2(NAA) - Co(NAA), with r = 0.99 for N = 39 (Fig. 37). Among acid-extracted elements, the highest correlation occurs for Zn and Cu with r = 0.98 and N = 61 (Fig. 38). Many other element pairs have correlations exceeding 0.90 for a sizeable number of observations.

On the other hand, trace element concentrations in the acid soluble sediment fraction and in whole sediment are not necessarily as well-correlated. The results of pair-wise linear regression analysis of AAS and NAA data are in Table 18 for Ba, Cr, Fe, and Na. If the dependent variable is taken to be the acid-extractable element concentration (AAS) and the independent variable is taken as the whole sediment concentration (NAA) then the slope derived from the regression analysis is a measure of the average extraction efficiency. This value may be directly compared with the value obtained from replicate analysis of standard sediment given in Table 6. From Table 18 it can be seen that for Ba, Cr and Fe the average extraction efficiencies are very comparable to those obtained using standard sediment. For Na, the average extraction efficiency is significantly smaller than for standard sediment although there is a large uncertainty in estimating the value. Particularly in the case of Ba and Na, AAS values are poorly, correlated with those obtained from NAA because the portion which is acid-leachable is largely unrelated to the Ba and Na present in the unleached sediment matrix.

Nearly all of the trace elements have a significant degree of correlation with organic carbon (and iron) and most correlations are very high as can be seen in Fig. 39. In this figure elements are ordered according to their degree of correlation with organic carbon. Cu, Pb and Zn plus the rare earth elements as well as Co, Fe, Sc and Th all have

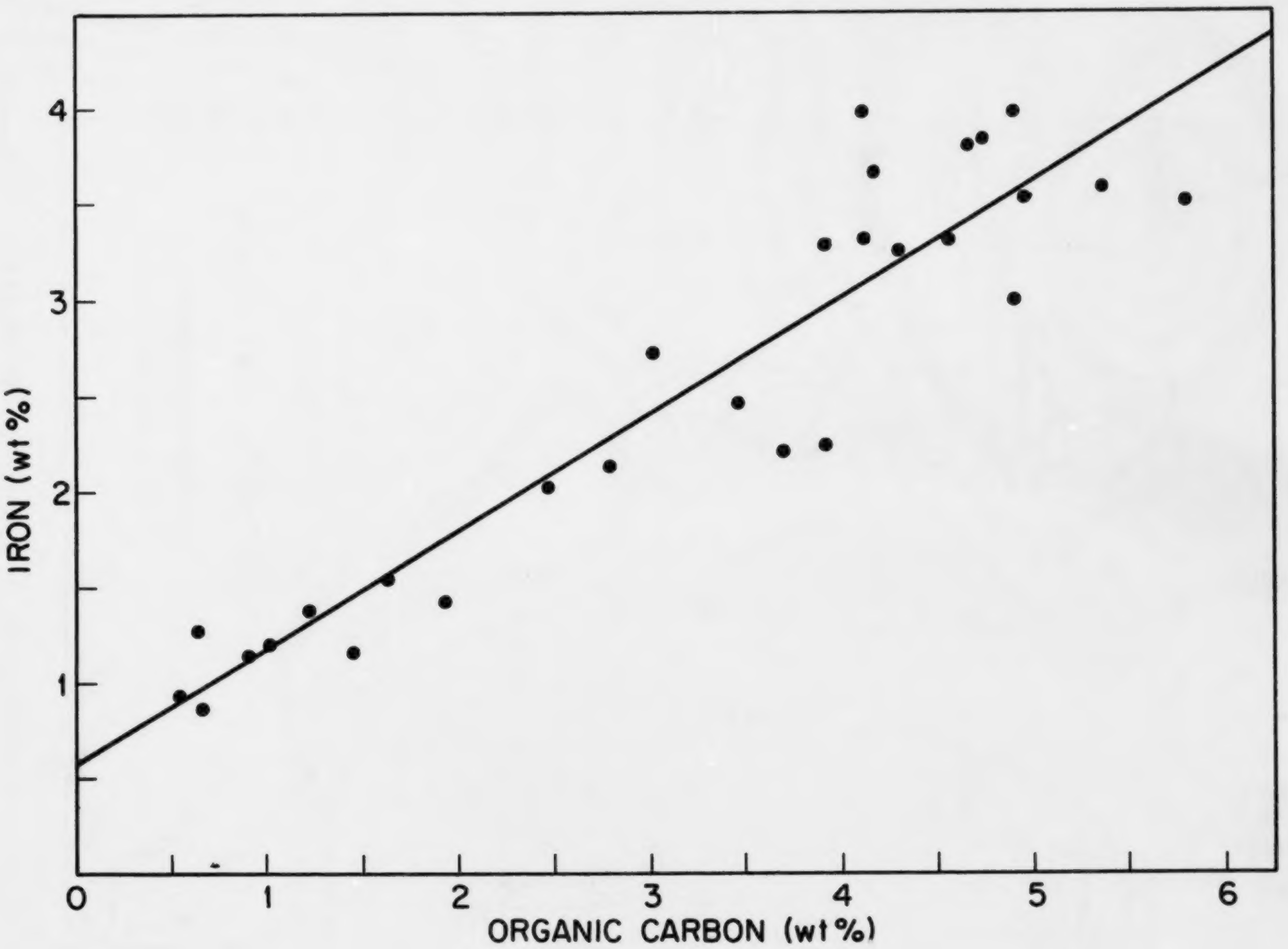

Figure 32. Relation between iron and organic carbon in surface sediments.

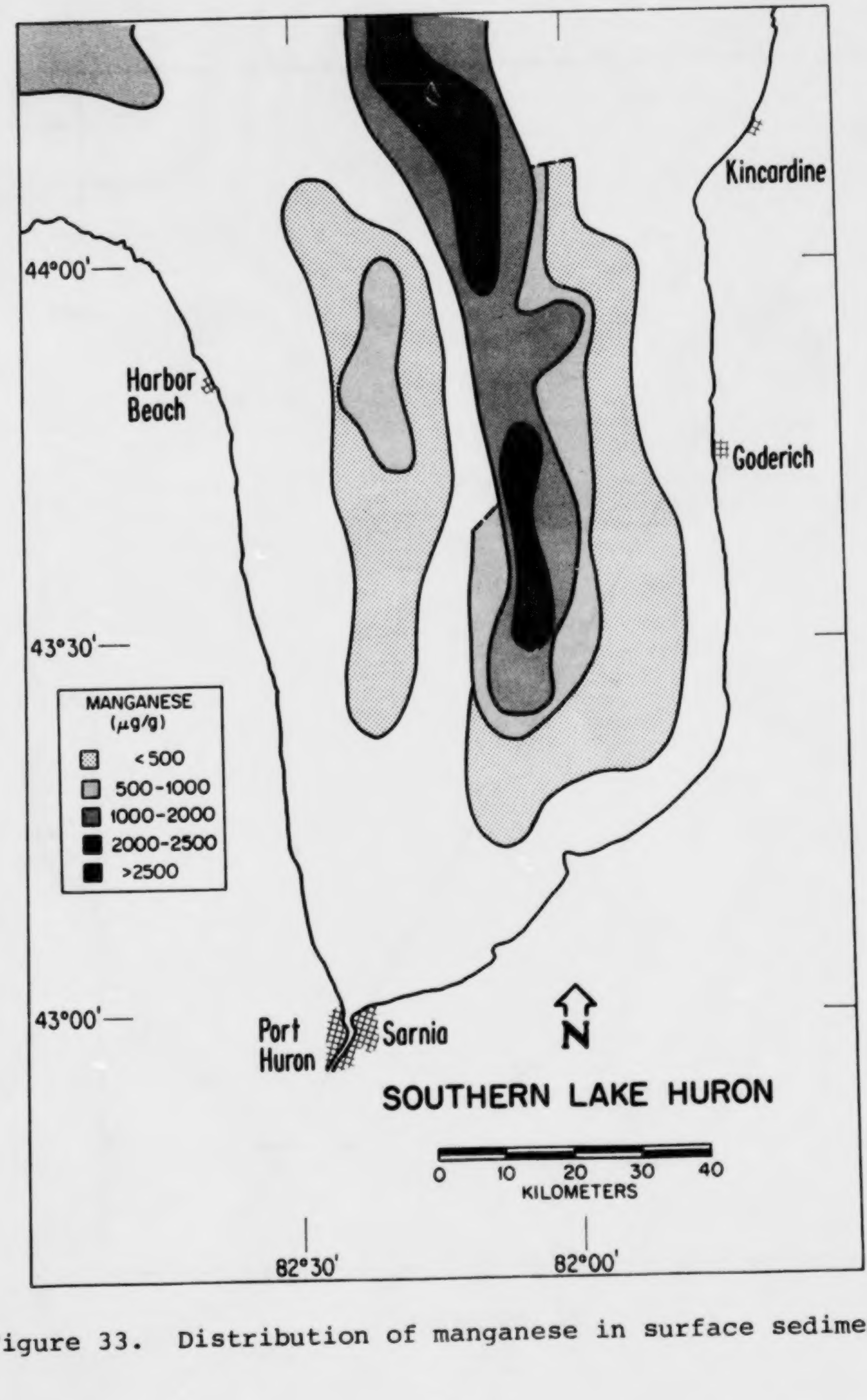
Kincardine
Harbor Beach
Goderich
44°00'
43°30'
43°00'
MANGANESE (μg/g)
<500
500-1000
1000-2000
2000-2500
>2500
Port Huron
Sarnia
N
SOUTHERN LAKE HURON
0
10
20
30
40
KILOMETERS
82°30'
82°00'

Figure 33. Distribution of manganese in surface sediments.

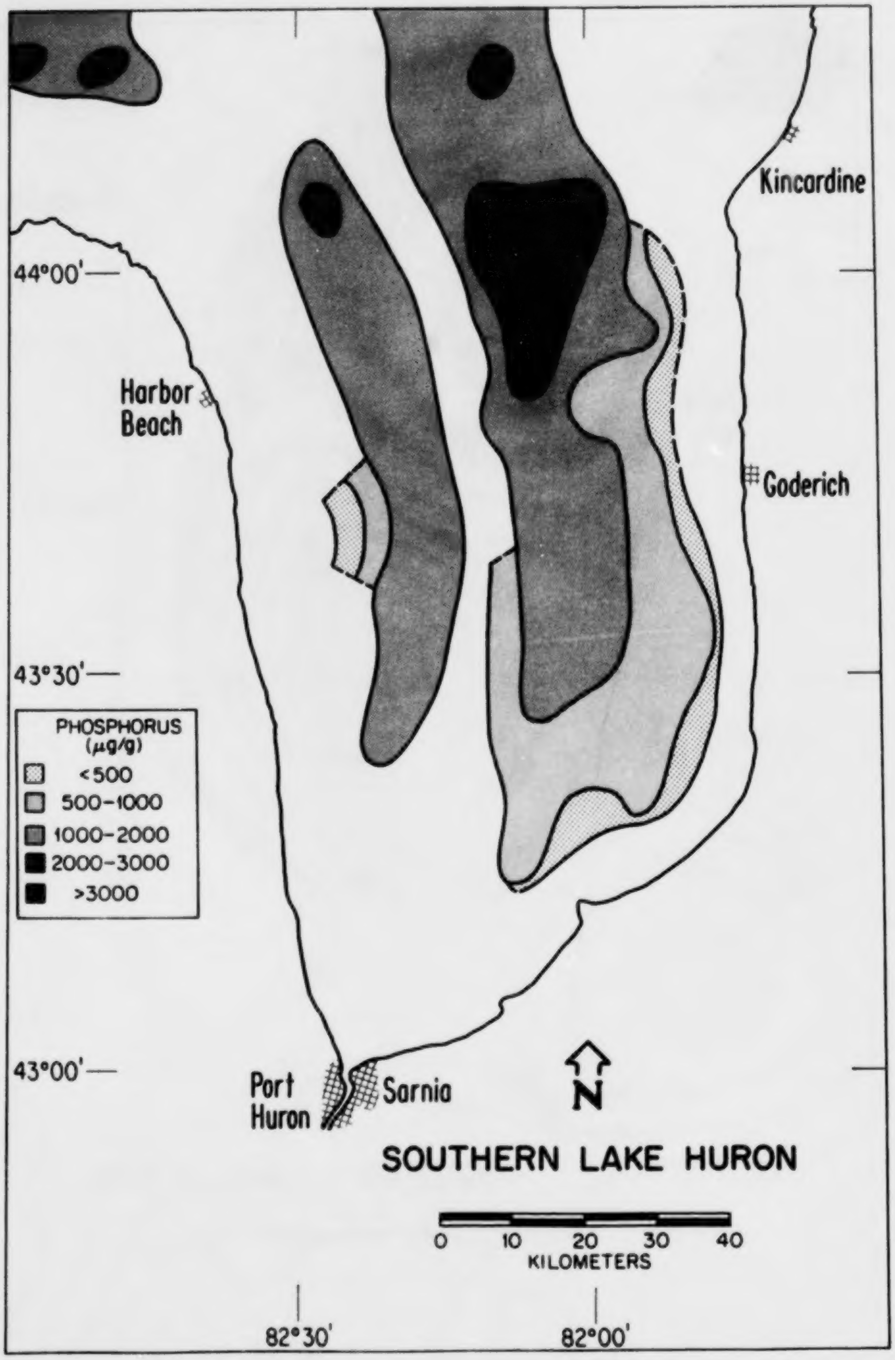
Kincardine
44°00'
Harbor Beach
Goderich
43°30'
PHOSPHORUS (μg/g)
<500
500-1000
1000-2000
2000-3000
>3000
43°00'
Port Huron
Sarnia
N
SOUTHERN LAKE HURON
0 10 20 30 40
KILOMETERS
82°30'
82°00'

Figure 34. Distribution of phosphorus in surface sediments.

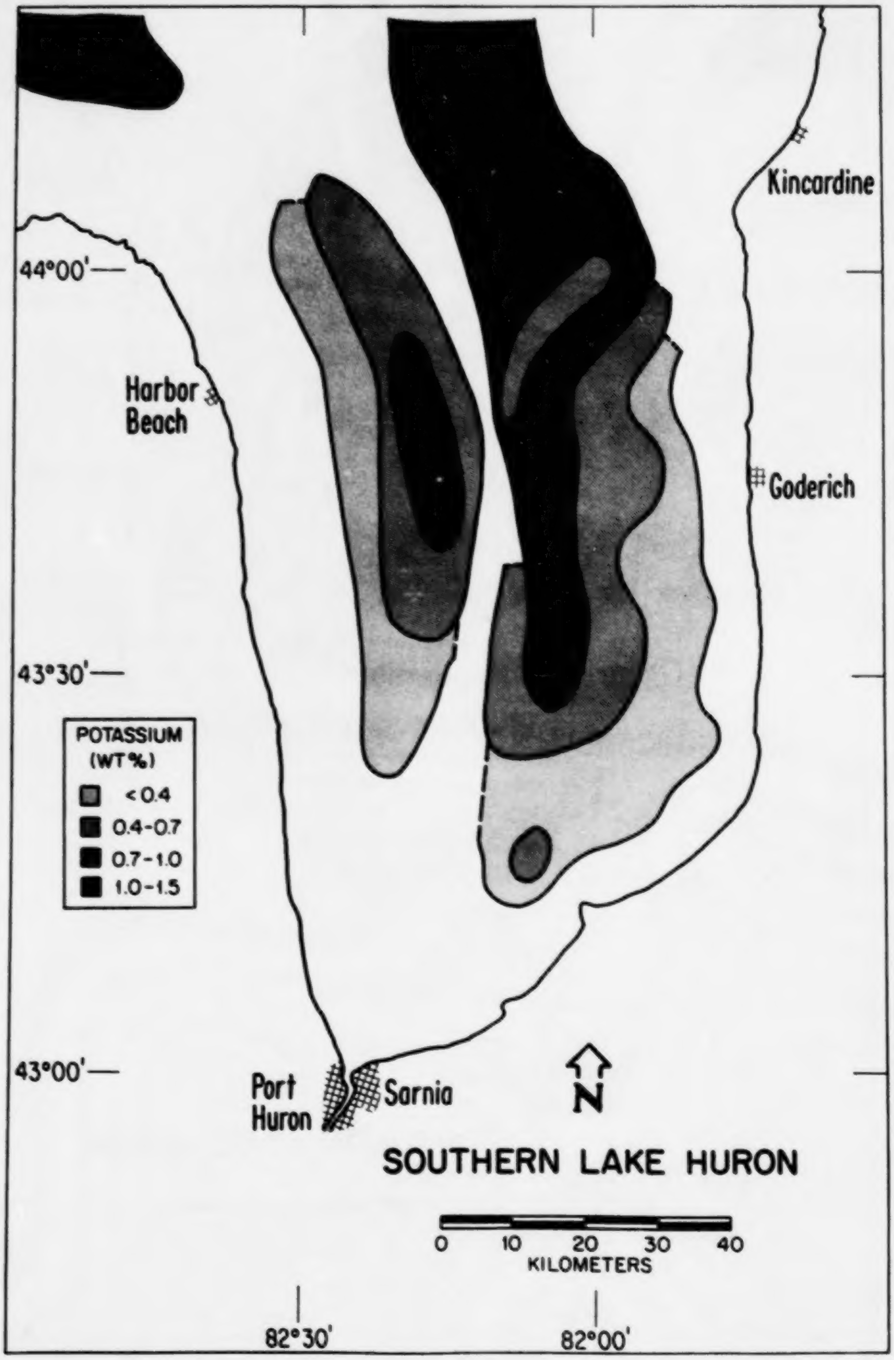
Kincardine
44°00'
Harbor Beach
Goderich
43°30'
POTASSIUM (WT %)
< 0.4
0.4-0.7
0.7-1.0
1.0-1.5
43°00'
Port Huron
Sarnia
N
SOUTHERN LAKE HURON
0 10 20 30 40
KILOMETERS
82°30'
82°00'

Figure 35. Distribution of potassium in surface sediments.

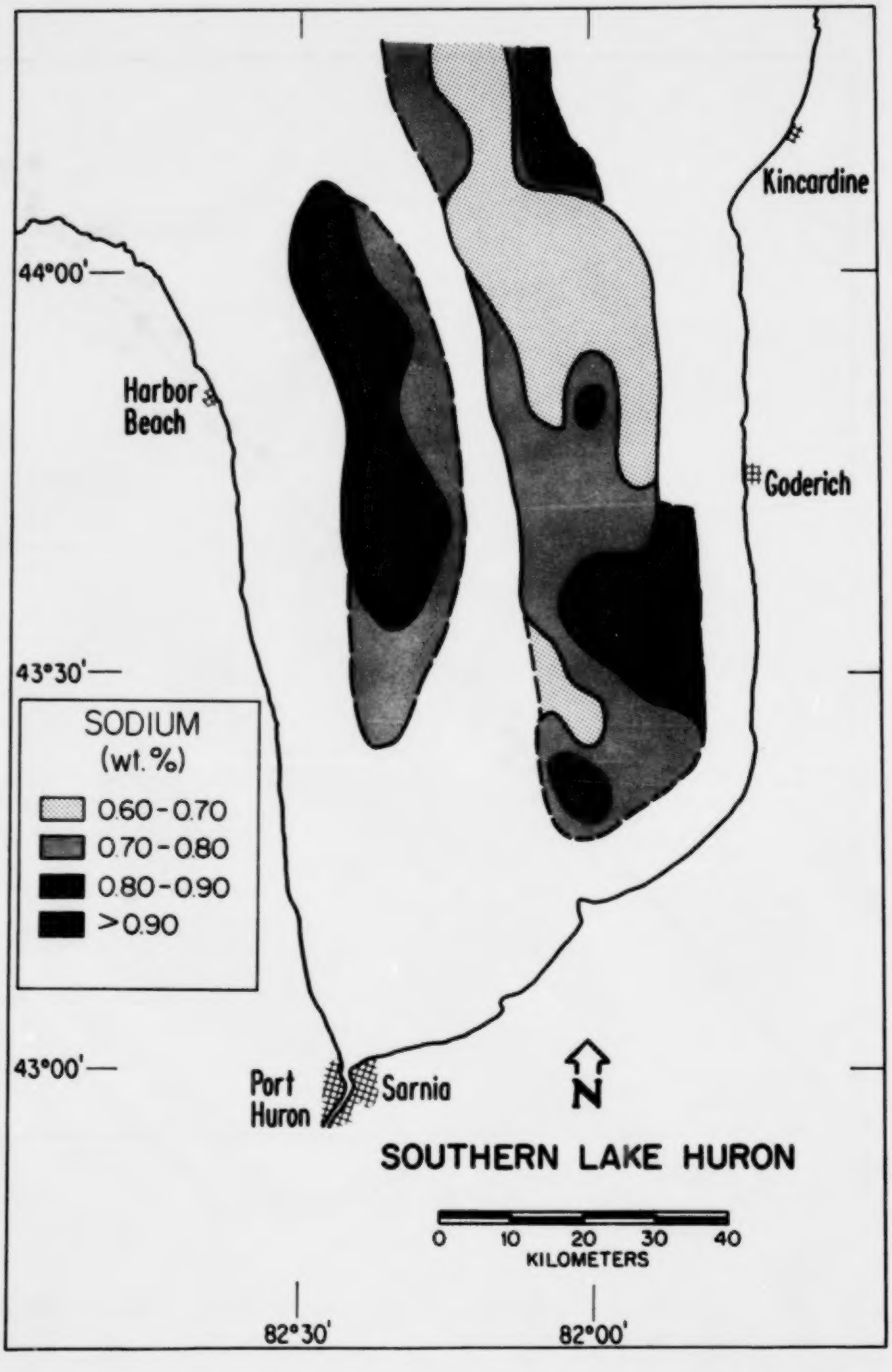

Kincardine
44°00'
Harbor Beach
Goderich
43°30'
SODIUM (wt.%)
0.60-0.70
0.70-0.80
0.80-0.90
>0.90
43°00'
Port Huron
Sarnia
N
SOUTHERN LAKE HURON
0 10 20 30 40
KILOMETERS
82°30'
82°00'

Figure 36. Distribution of sodium (NAA) in surface sediments.

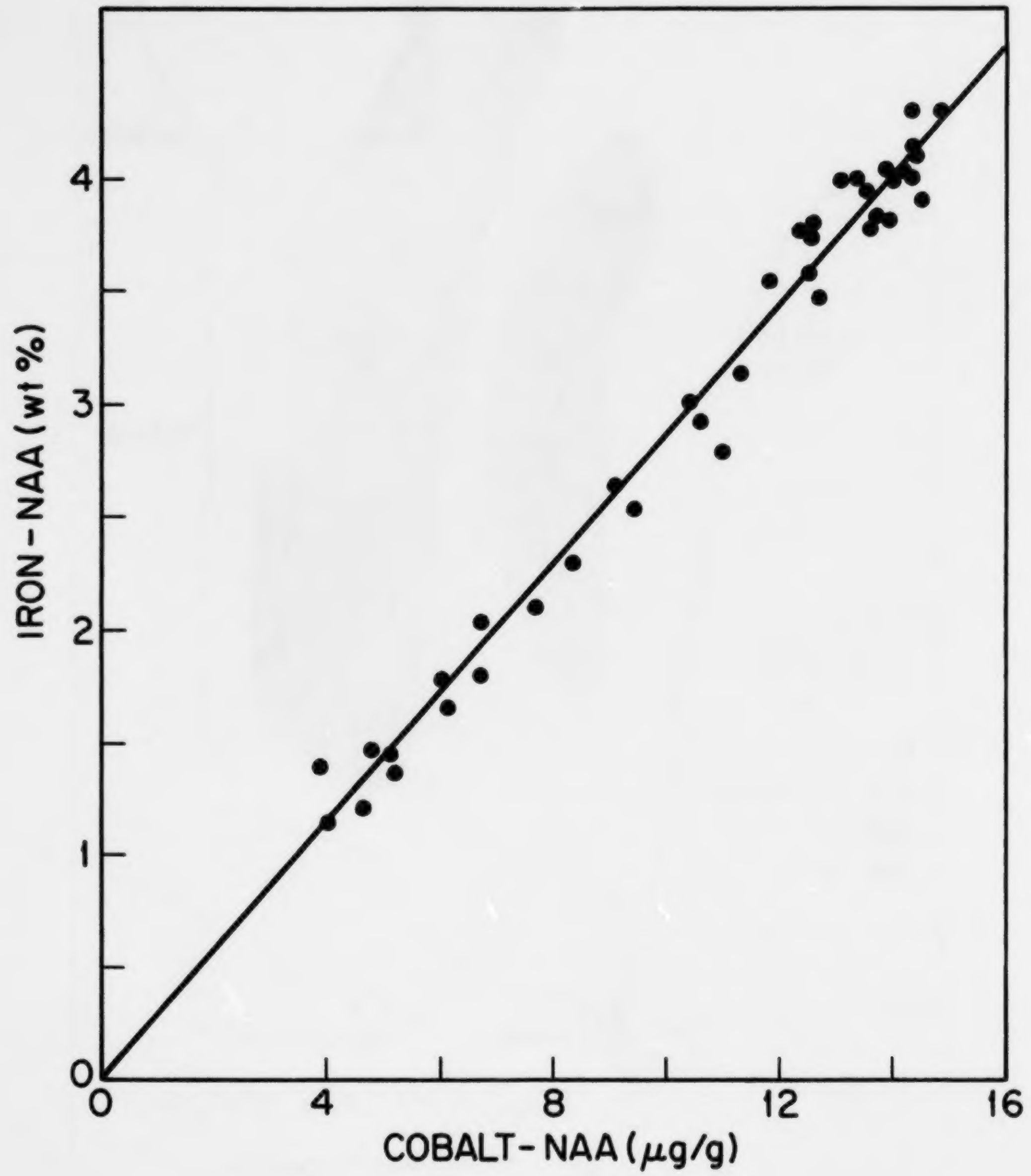

Figure 37. Relation between iron (NAA) and cobalt (NAA) in surface sediments.

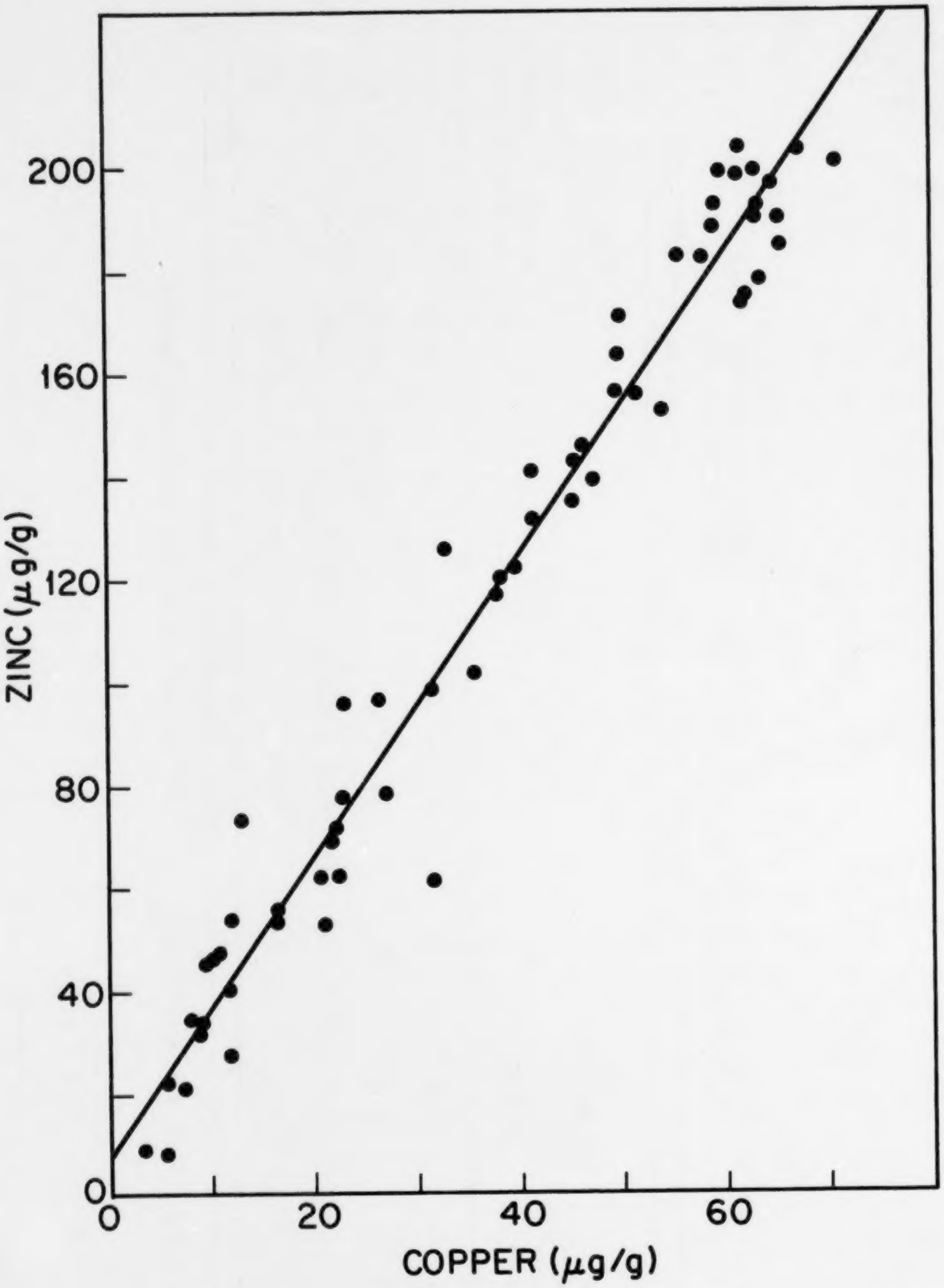

Figure 38. Relation between zinc and copper in surface sediments.

TABLE 18. COMPARISON OF ACID-SOLUBLE (AAS) AND WHOLE SEDIMENT (NAA) ELEMENT CONCENTRATIONS USING PAIR-WISE LINEAR REGRESSION ANALYSIS

Dependent Variable (Element via AAS)	Independent Variable (Element via NAA)	N	Regression Parameters*		Extraction Efficiency (%)		
			Intercept	Slope r	r	Average This Data	Standard Sediment (Table 6)
Ba1	Ba2	32	- 9.1 ± 50**	0.37 ± 0.11	0.63	37	40
Cr1	Cr2	39	- 1.5 ± 9	0.83 ± 0.13	0.83	83	81
Fe1	Fe2	39	- 0.28 ± 0.23	0.95 ± 0.07	0.95	95	93
Na1	Na2	32	0.26 ± 0.2	- 0.08 ± 0.3	- 0.07	0	18

* From Table A-8 of the Appendix.

**Standard error (90% confidence limits).

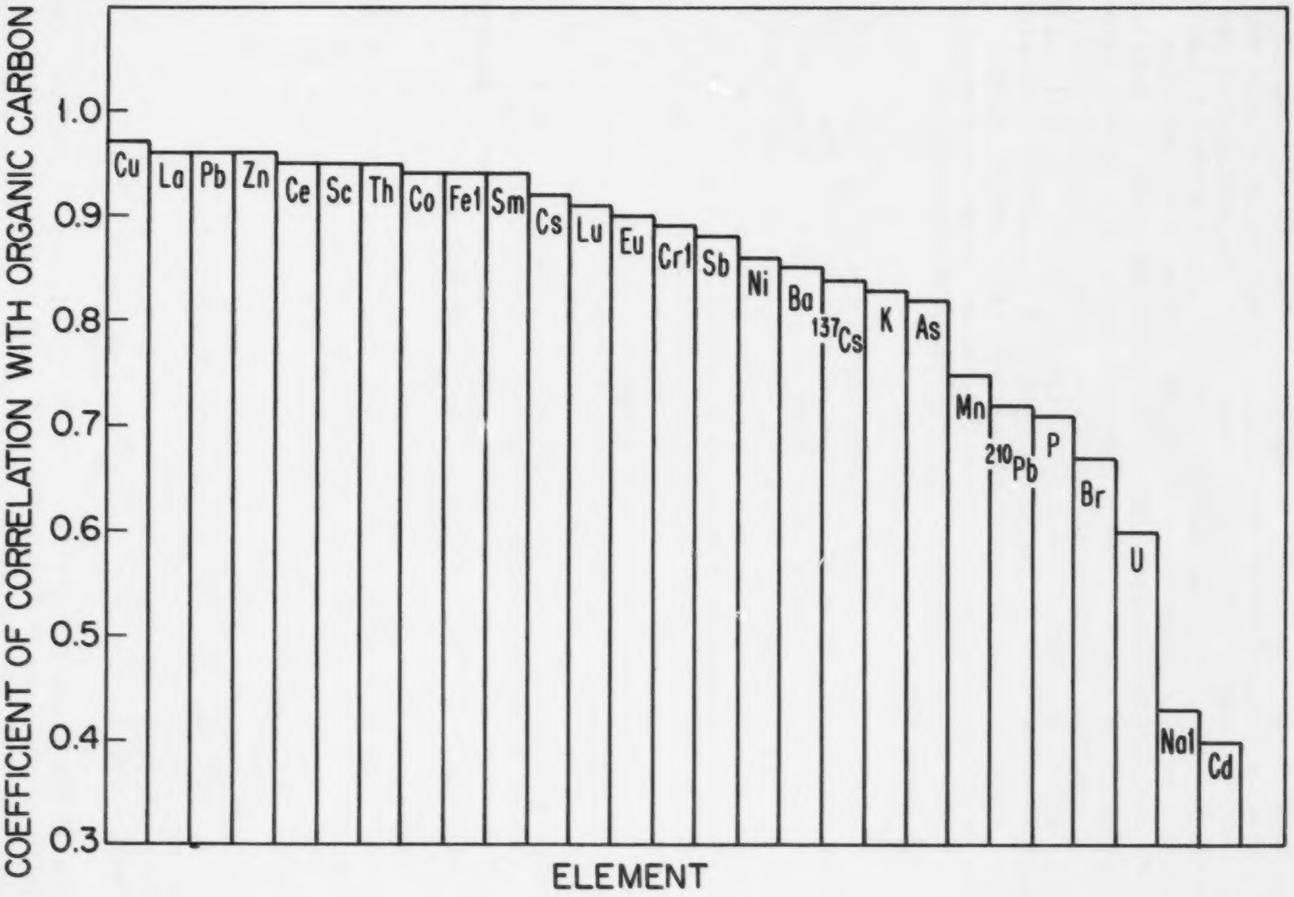

FIGURE 39. Degree of correlation of element concentrations with the organic carbon content of surface sediments.

correlation coefficients of 0.90 or greater. Hence distributions of most trace elements conform to that of organic carbon, exhibiting highest concentrations in the fine-grained sediments occurring in the deeper areas of each depositional basin. It should be emphasized that the high degree of correlation between trace elements and organic carbon (or iron) does not necessarily mean a chemical affinity in every case. The correlation results from a combination of geochemical and hydrodynamic processes which result in the codeposition of trace elements with organic carbon, iron, and clay minerals. The selective deposition of fine-grained sediments in restricted, low energy areas of lakes, or sediment focusing, as it is popularly termed is coming to be recognized as a general feature of sediment transport and deposition in lakes (cf. Kamp-Nielsen and Hargrave, 1978). In most cases, trace constituents are found to be codeposited with fine-grained materials (cf. Clay and Wilhm, 1979). As considerable redundancy exists in the distribution of trace elements only those for several selected elements, particularly those shown later to be anthropogenically enriched, are presented in Figures 40-52.

While a detailed discussion of interelement associations is beyond the scope of this report, a limited statistical analysis reveals some important relationships. In this report, we have examined the data in terms of cluster analysis and principle components analysis. In cluster analysis, elements are grouped according to the degree of similarity in their behavior. While several alternative measures of similarity have been developed, we have chosen to base the degree of similarity on the correlation coefficient. The degree of similarity is taken to be, 1 - r, where r is the correlation coefficient. Clustering is performed by stepwise addition of elements to the set. Principle components analysis provides a means of identifying a set of independent variables, a linear combination of which provides a statistically adequate representation of measured concentration values. In the present case the number of truly independent variables is far less that the number of elements determined. Like cluster analysis, principal components analysis provides a means of summarizing the associations between elements. Because of the frequency of missing observations the two statistical methods were applied to subsets of the data. Nine elements (Ca, Cr1, Cu, Fe1, Mg, Mn, Ni, Pb, Zn) comprise the most complete set of data of 60 observations with no missing data. Other sets including those with either OC, IOC or neutron activation data are more limited, consisting of about 30 observations. Five subsets of data examined are:

1. IOC set (IOC, Ca, Mg, Fsol, Sr, Na2, Ba1; N = 25)
2. OC set (OC, Cu, Zn, Fe1, Pb, Ni, Cr1, Mn; N = 27)
3. Complete data set (N = 60)
4. Complete data set plus surface-enriched elements (N = 22)
5. Complete data set plus non-enriched elements (N = 30)

Results of the cluster analysis are shown in Figures 53 and 57. From the discussion of the calcium family elements in the earlier section, it should be expected the IOC, Ca and Mg would bear a close relation to each other, while Fsol, being comprised of both dolomitic and non-dolomitic contributions, would be less strongly related. The cluster analysis illustrates this relationship in terms of a hierarchical tree (Fig. 53, IOC

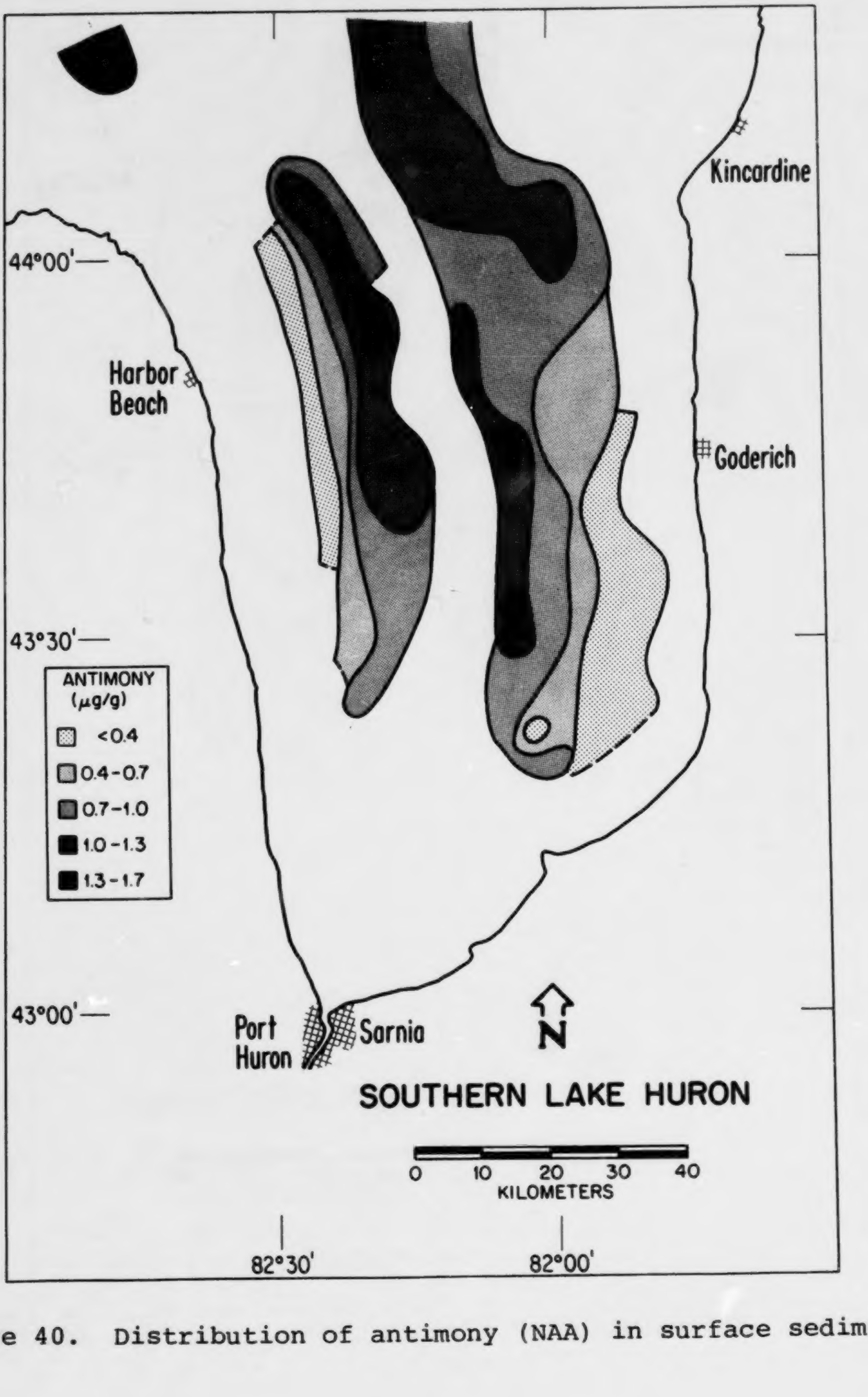
Kincardine
44°00'
Harbor Beach
Goderich
43°30'
ANTIMONY (µg/g)
<0.4
0.4-0.7
0.7-1.0
1.0-1.3
1.3-1.7
43°00'
Port Huron
Sarnia
N
SOUTHERN LAKE HURON
0 10 20 30 40
KILOMETERS
82°30'
82°00'

Figure 40. Distribution of antimony (NAA) in surface sediments.

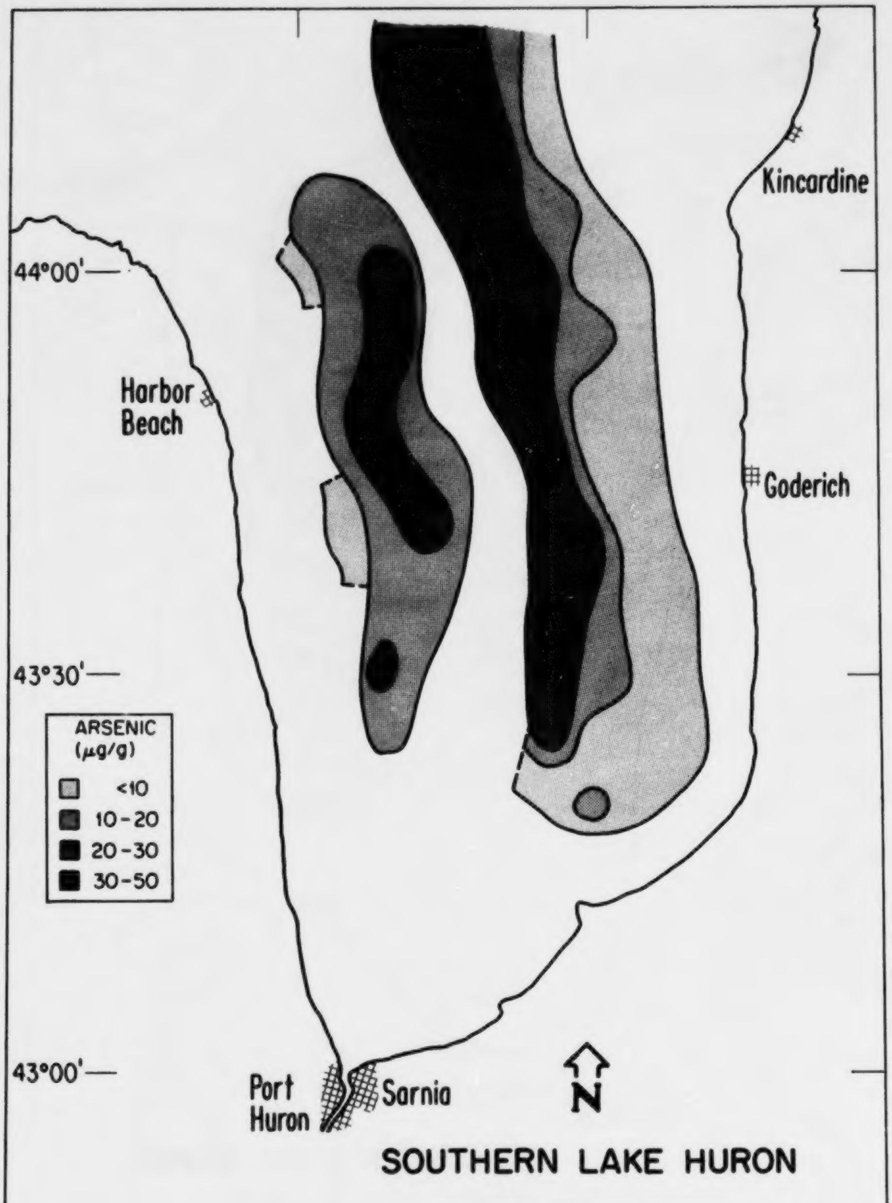
Kincardine
44°00'
Harbor Beach
Goderich
43°30'
ARSENIC (µg/g)
<10
10-20
20-30
30-50
43°00'
Port Huron
Sarnia
N
SOUTHERN LAKE HURON
0 10 20 30 40
KILOMETERS
82°30'
82°00'

Figure 41. Distribution of arsenic (NAA) in surface sediments.

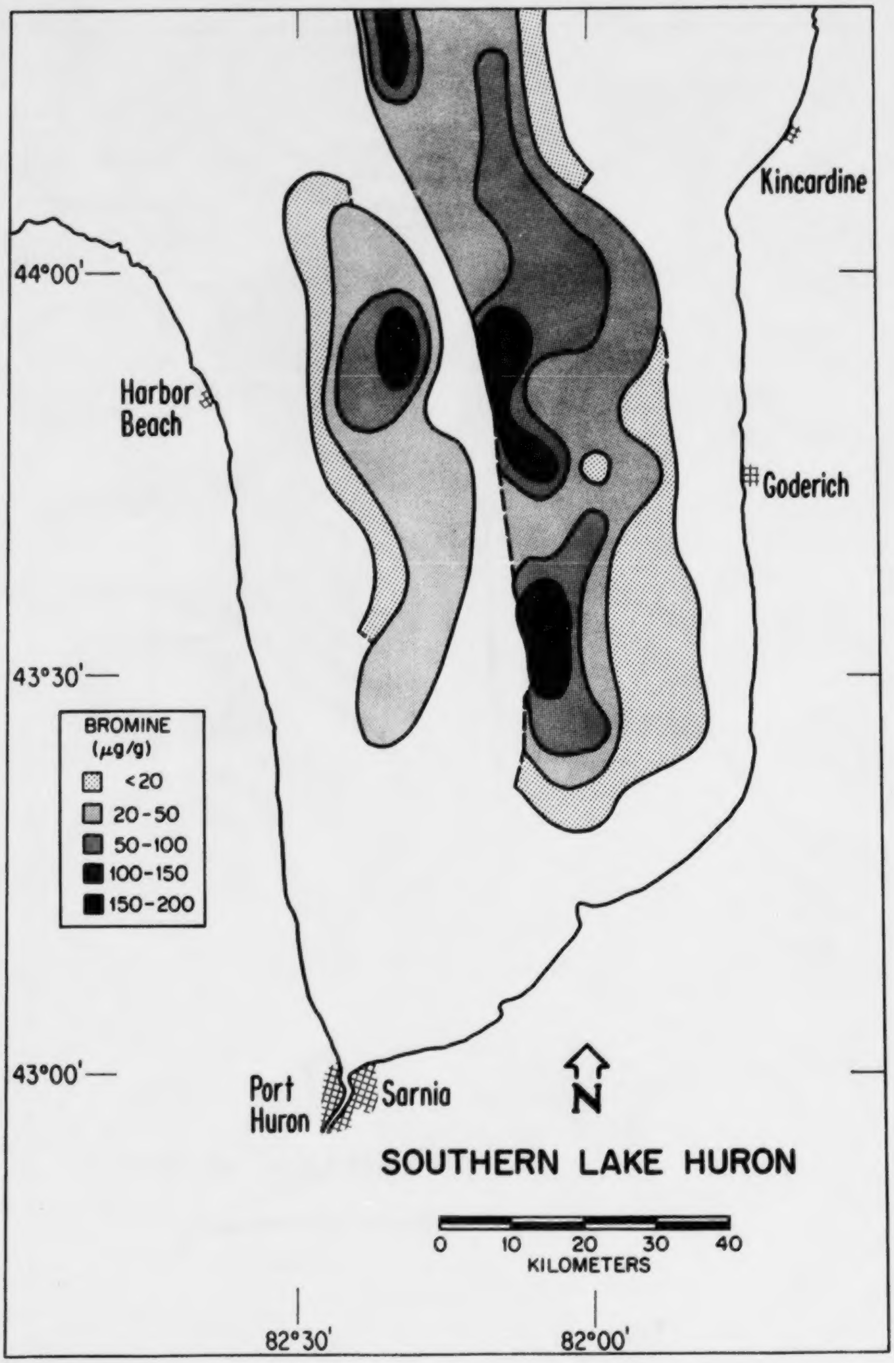
Kincardine
44°00'
Harbor Beach
Goderich
43°30'
BROMINE (μg/g)
<20
20-50
50-100
100-150
150-200
43°00'
Port Huron
Sarnia
N
SOUTHERN LAKE HURON
0 10 20 30 40
KILOMETERS
82°30'
82°00'

Figure 42. Distribution of bromine (NAA) in surface sediments.

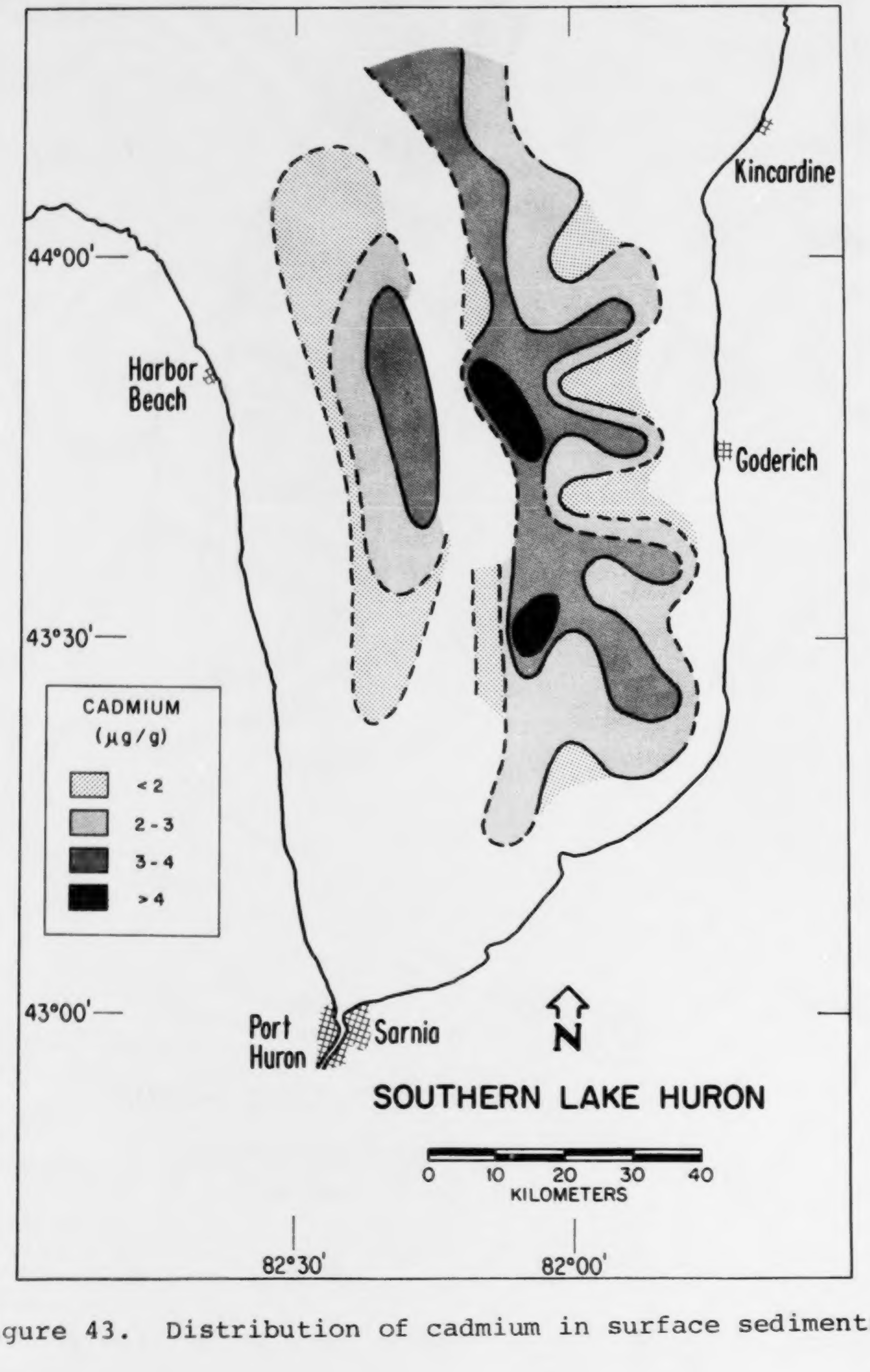
Kincardine
44°00'
Harbor Beach
Goderich
43°30'
CADMIUM
(μg/g)
< 2
2 - 3
3 - 4
> 4
43°00'
Port Huron
Sarnia
N
SOUTHERN LAKE HURON
0 10 20 30 40
KILOMETERS
82°30'
82°00'

Figure 43. Distribution of cadmium in surface sediments.

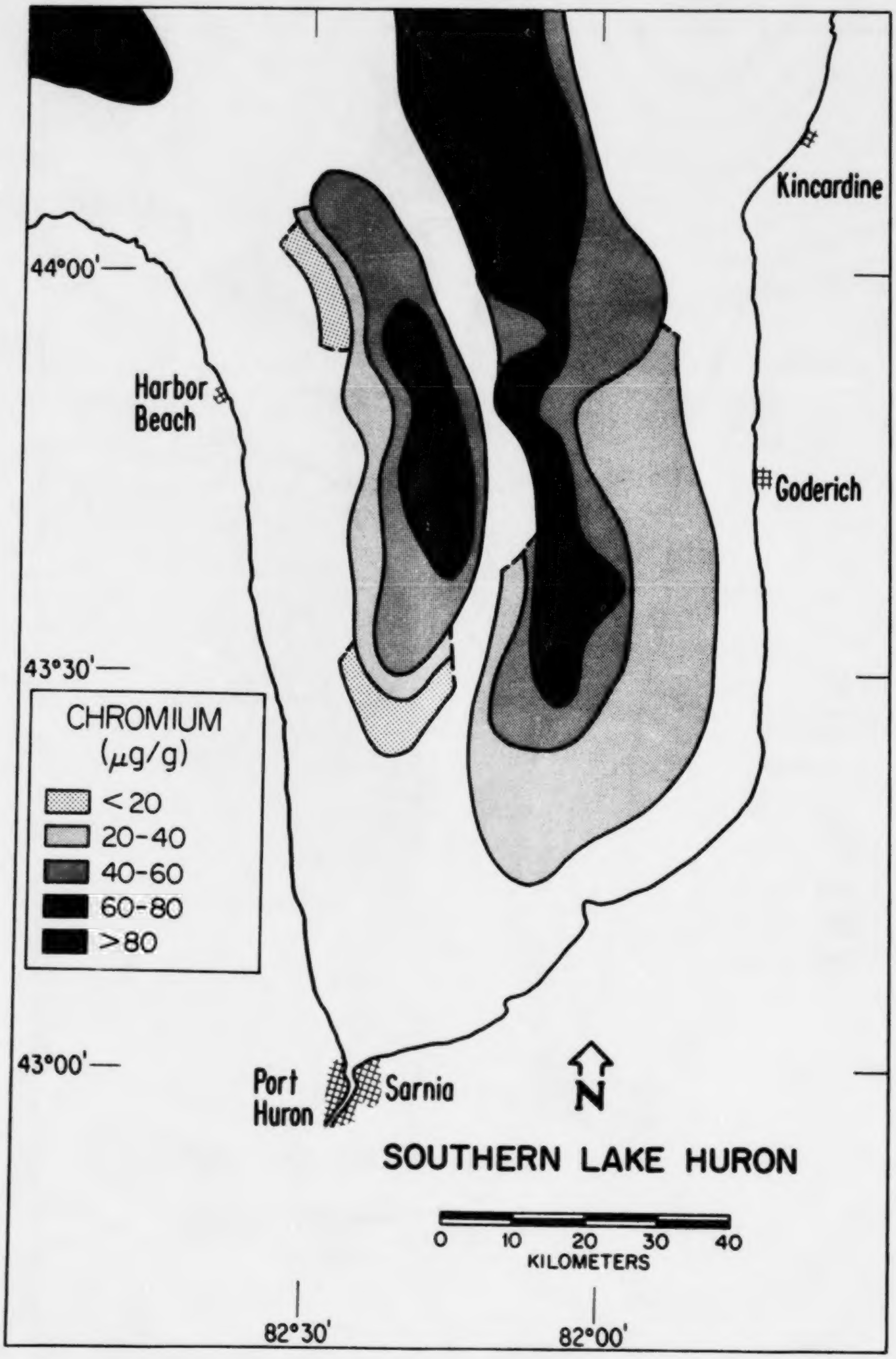

Kincardine
44°00'
Harbor Beach
Goderich
43°30'
CHROMIUM (μg/g)
< 20
20-40
40-60
60-80
>80
43°00'
Port Huron
Sarnia
N
SOUTHERN LAKE HURON
0 10 20 30 40
KILOMETERS
82°30'
82°00'

Figure 44. Distribution of chromium in surface sediments.

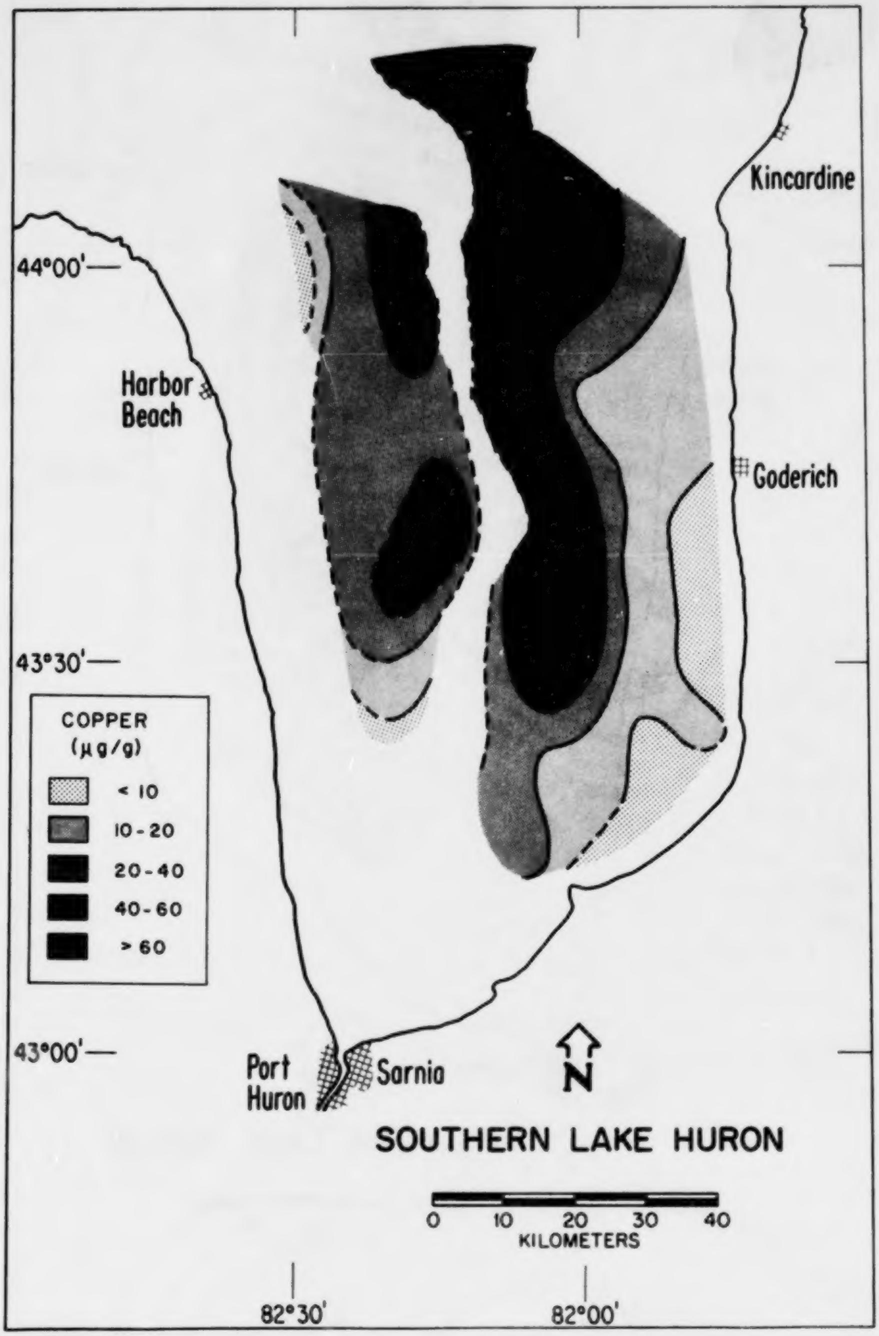
Kincardine
44°00'
Harbor Beach
Goderich
43°30'
COPPER (μg/g)
< 10
10-20
20-40
40-60
> 60
43°00'
Port Huron
Sarnia
N
SOUTHERN LAKE HURON
0 10 20 30 40
KILOMETERS
82°30'
82°00'

Figure 45. Distribution of copper in surface sediments.

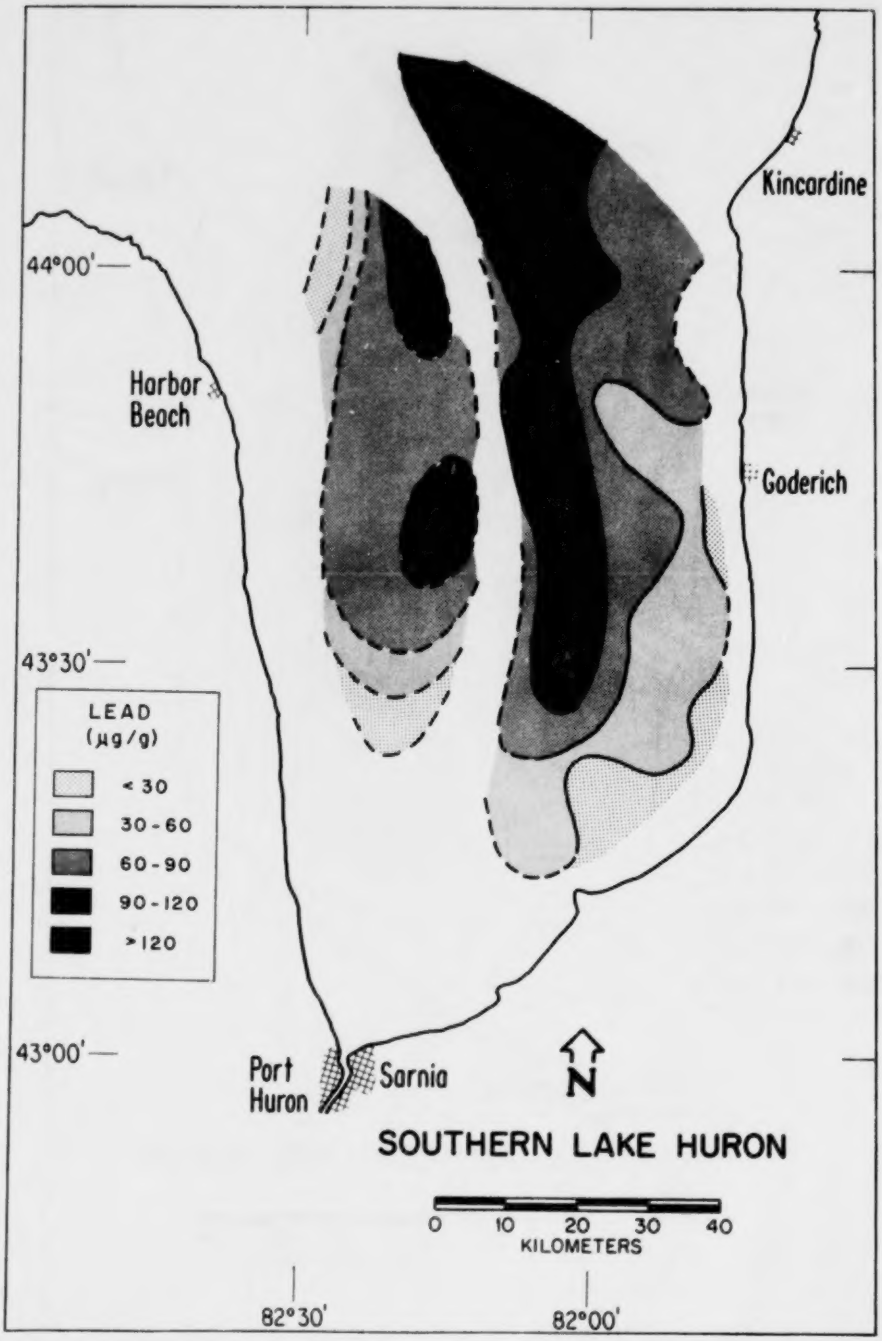

Kincardine
Harbor Beach
Goderich
44°00'
43°30'
43°00'
LEAD (µg/g)
< 30
30-60
60-90
90-120
>120
Port Huron
Sarnia
N
SOUTHERN LAKE HURON
0 10 20 30 40
KILOMETERS
82°30'
82°00'

Figure 46. Distribution of lead in surface sediments.

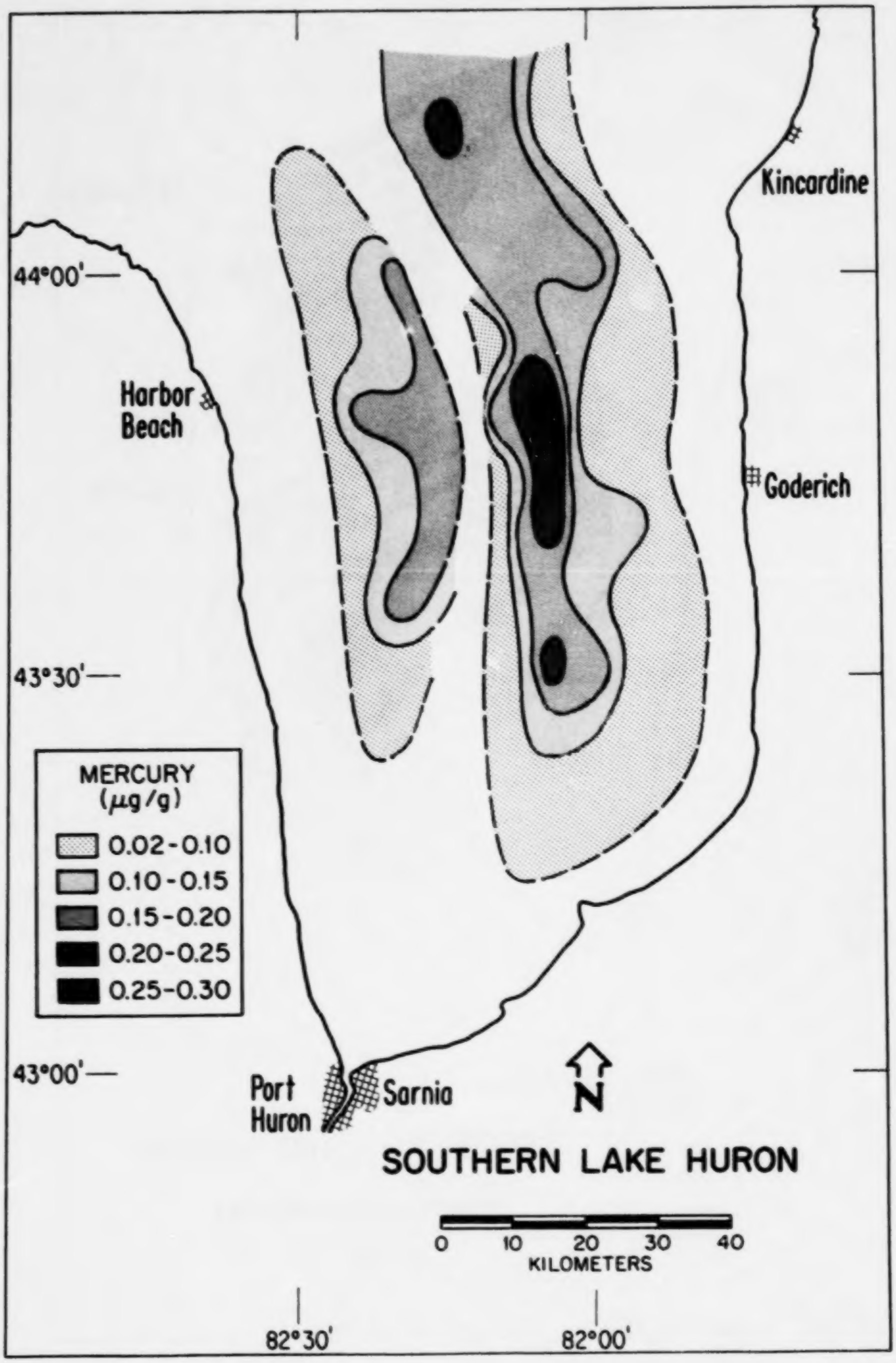

Kincardine
44°00'
Harbor Beach
Goderich
43°30'
MERCURY
(μg/g)
0.02-0.10
0.10-0.15
0.15-0.20
0.20-0.25
0.25-0.30
43°00'
Port Huron
Sarnia
N
SOUTHERN LAKE HURON
0
10
20
30
40
KILOMETERS
82°30'
82°00'

FIGURE 47. Distribution of mercury in surface sediments.

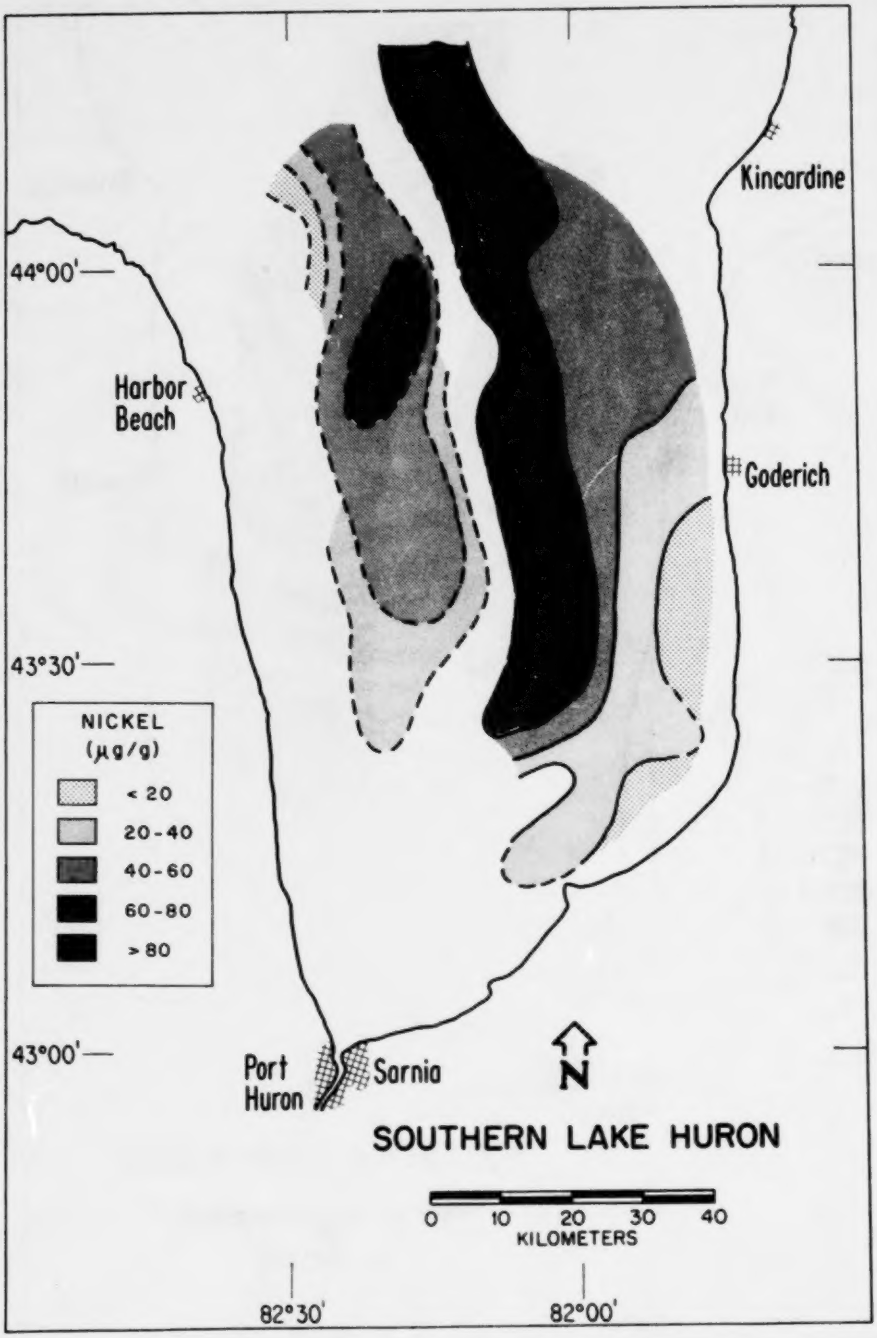
Kincardine
44°00'
Harbor Beach
Goderich
43°30'
NICKEL (µg/g)
< 20
20-40
40-60
60-80
> 80
43°00'
Port Huron
Sarnia
N
SOUTHERN LAKE HURON
0 10 20 30 40
KILOMETERS
82°30'
82°00'

FIGURE 48. Distribution of nickel in surface sediments.

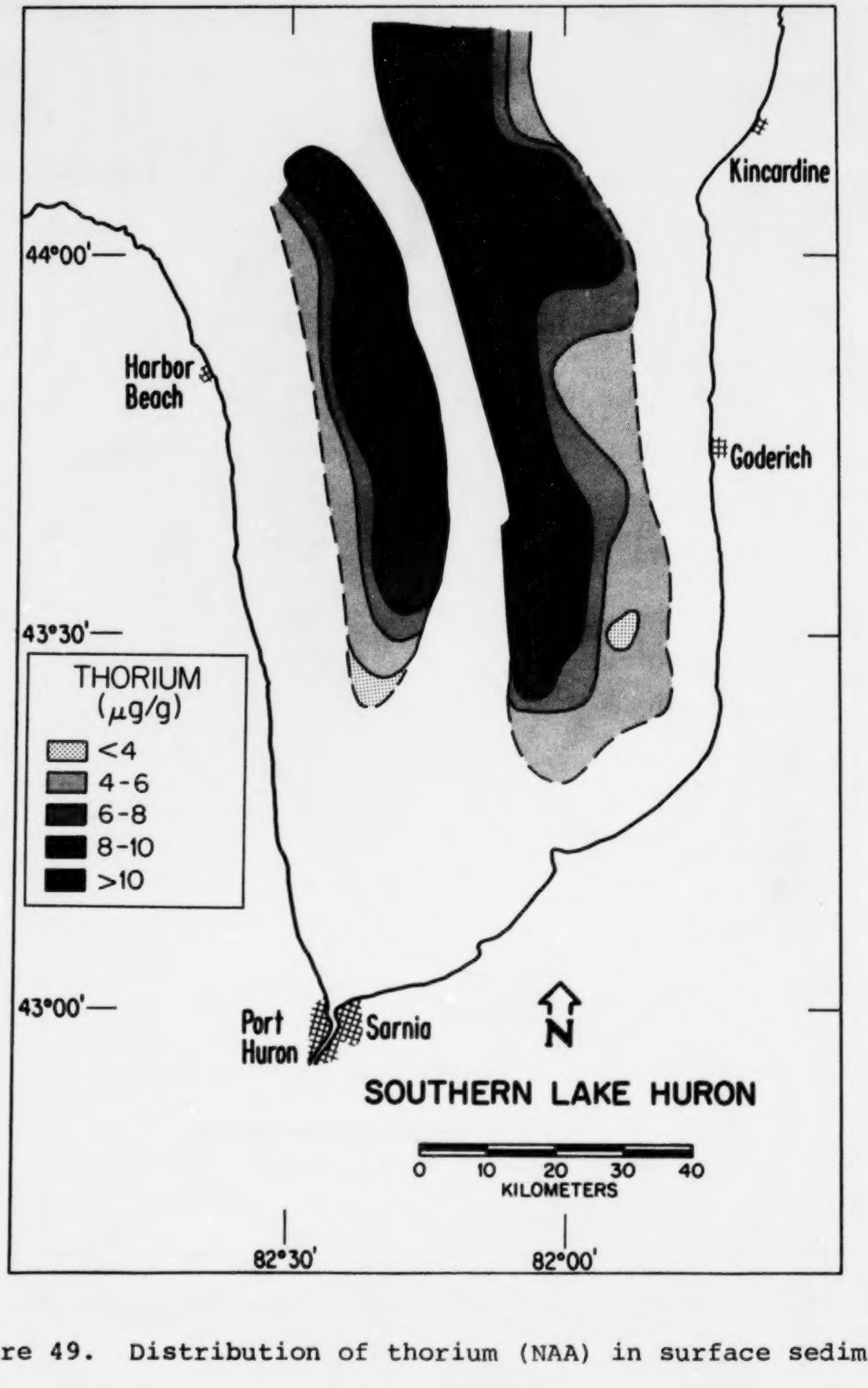

Kincardine
44°00'
Harbor Beach
Goderich
43°30'
THORIUM (µg/g)
<4
4-6
6-8
8-10
>10
43°00'
Port Huron
Sarnia
N
SOUTHERN LAKE HURON
0 10 20 30 40
KILOMETERS
82°30'
82°00'

Figure 49. Distribution of thorium (NAA) in surface sediments.

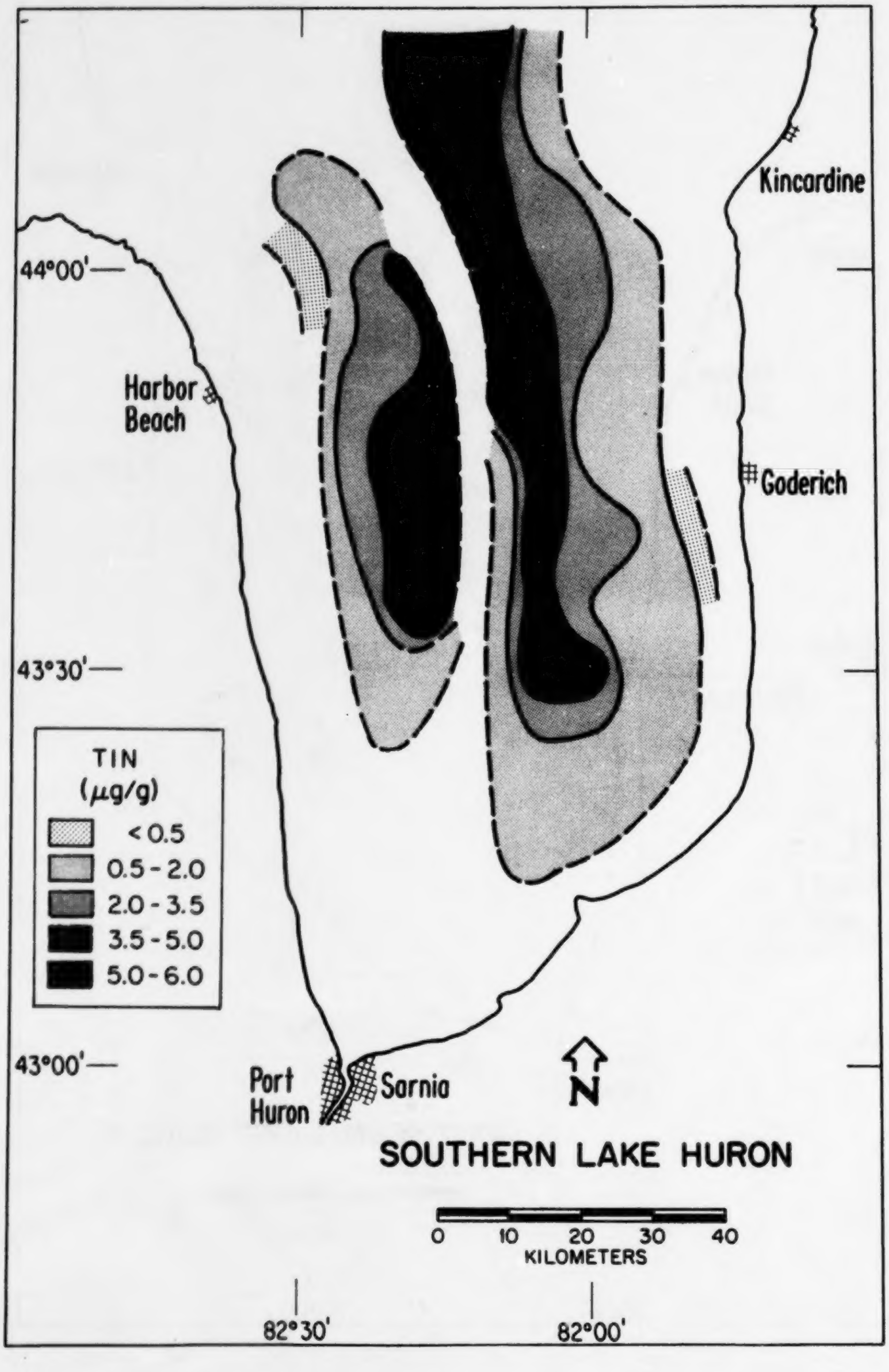
Kincardine
Goderich
Harbor Beach
Port Huron
Sarnia
44°00'
43°30'
43°00'
82°30'
82°00'
TIN
(μg/g)
< 0.5
0.5 - 2.0
2.0 - 3.5
3.5 - 5.0
5.0 - 6.0
N
SOUTHERN LAKE HURON
0
10
20
30
40
KILOMETERS

FIGURE 50. Distribution of tin in surface sediments.

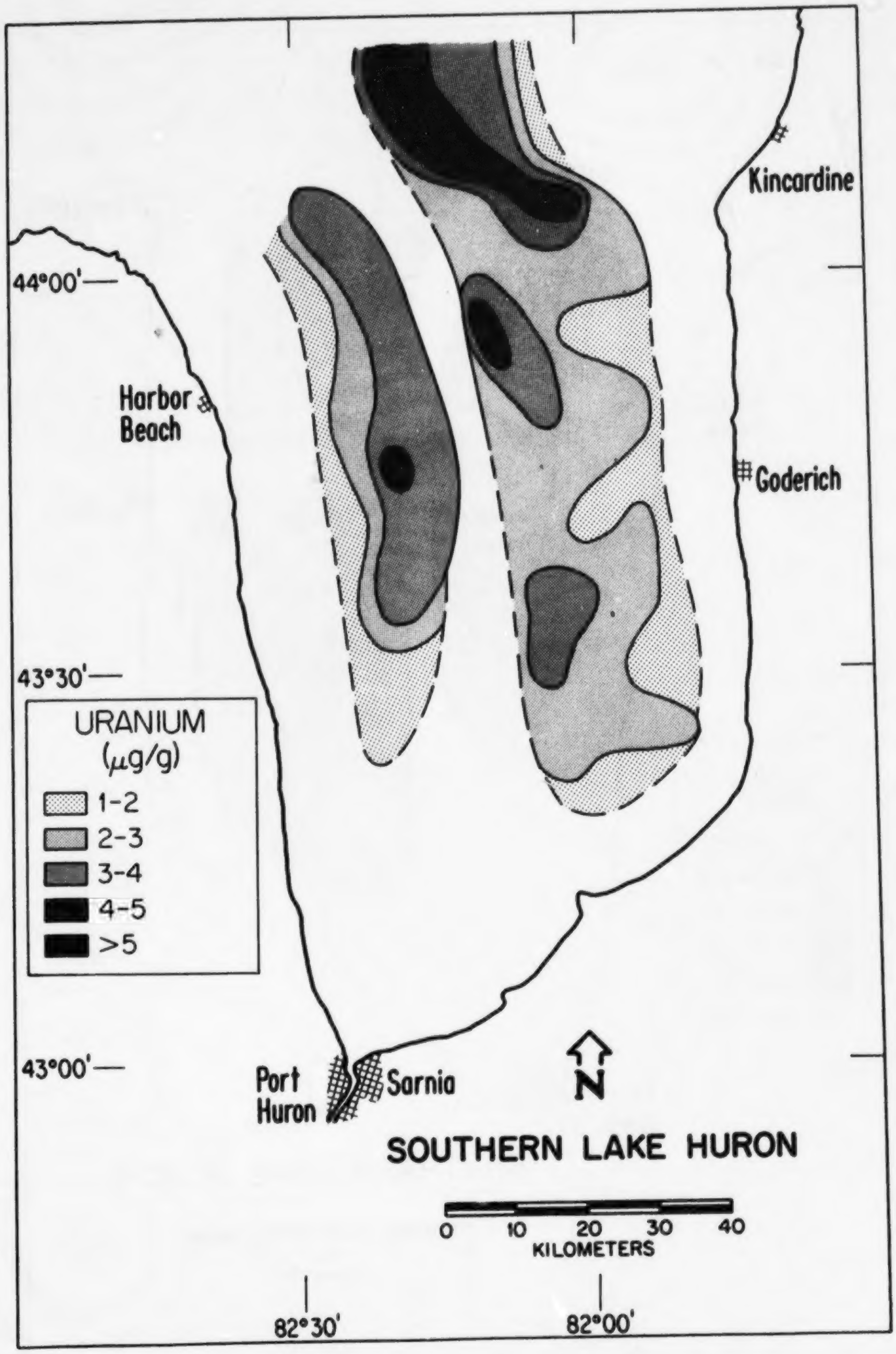
Kincardine
44°00'
Harbor Beach
Goderich
43°30'
URANIUM (μg/g)
1-2
2-3
3-4
4-5
>5
43°00'
Port Huron
Sarnia
N
SOUTHERN LAKE HURON
0 10 20 30 40
KILOMETERS
82°30'
82°00'

Figure 51. Distribution of uranium (NAA) in surface sediments.

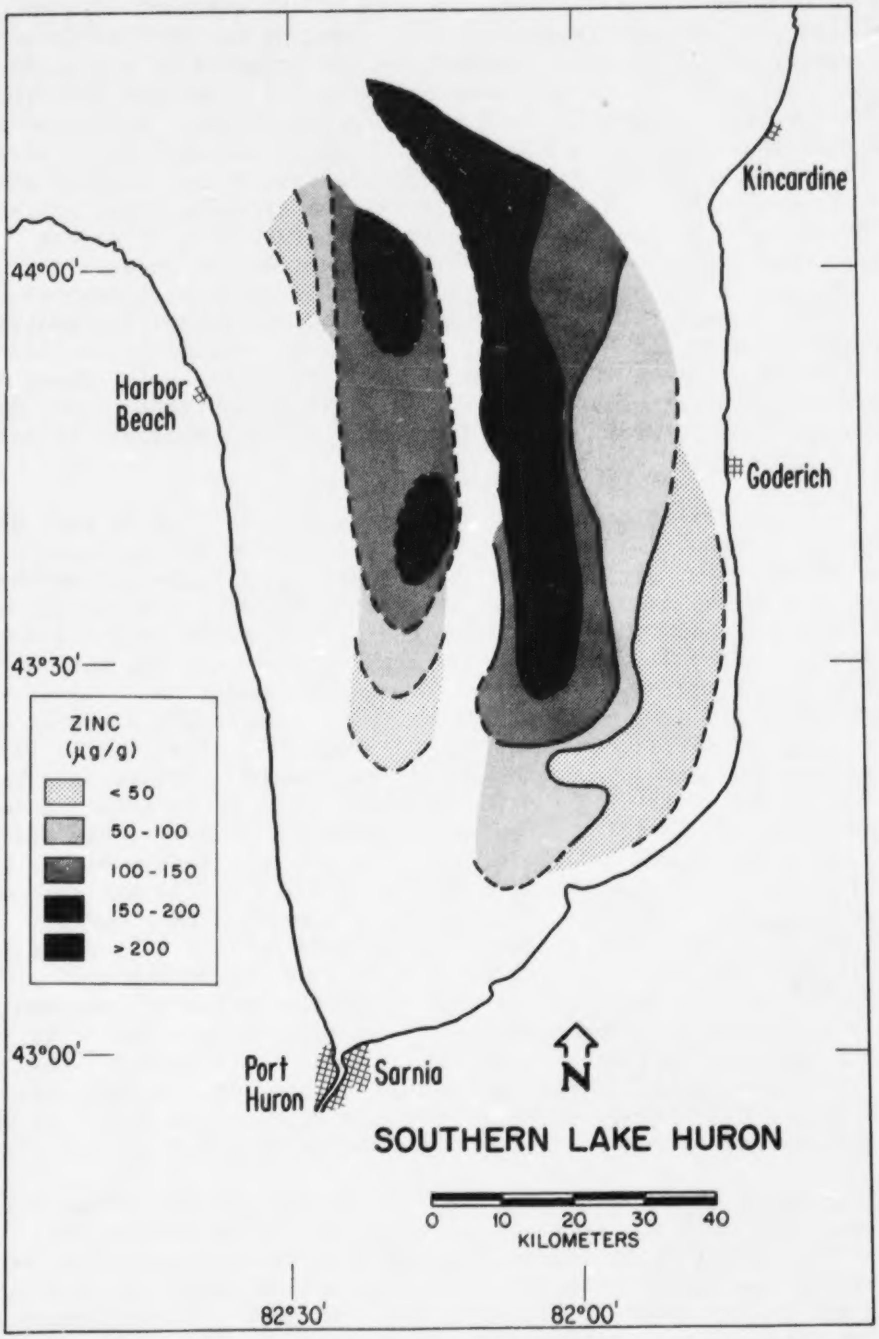
Kincardine
44°00'
Harbor Beach
Goderich
43°30'
ZINC
(µg/g)
< 50
50 - 100
100 - 150
150 - 200
> 200
43°00'
Port Huron
Sarnia
N
SOUTHERN LAKE HURON
0
10
20
30
40
KILOMETERS
82°30'
82°00'

Figure 52. Distribution of zinc in surface sediments.

set). In successive stages elements are attached to discreet clusters. At the first stage, Ca is associated with IOC. Next Mg is added to form a three element cluster. Fsol, while added next, is not attached to a specific element, but rather to the three element cluster. Sr, Na2 and particularly Bal, are weakly coupled to this group. Inspection of the correlation matrix shows that Bal should not even be included in the "calcium family" element group. Na2 should be included in this group because it was a small but positive correlation with Ca. Use of alternative distance (similarity) measures (Euclidean, Minkowski, etc.) does not result in a different clustering. This configuration is stable with respect to changes not only in association measures but with respect to weighting given to neighboring data points. Similar results are obtained using principal components analysis. Two components account for over 95% of the variance. Elements are located in the plane defined by these two components as shown in Fig. 54. Groupings can be seen to be consistent with the results of cluster analysis. IOC, Ca, and Mg are tightly grouped; Fsol is more distant as are the elements Sr and Na1 while Bal is essentially unrelated.

Because the correlation between organic carbon and iron is very high the possibility of using statistial techniques to determine the relative importance of these two variables in the deposition of trace contaminants is marginal at best. The only hope lies in examination of a limited set of variables including both OC and Fe. For the nine elements in the complete set, replicate samples were run and they are therefore the set with minimum experimental uncertainties. To further provide a separation in terms of cluster and principle components analysis the calcium family elements were left out of the set while organic carbon was included. The results (Fig. 53, OC set) show that Cu and Zn form the principle cluster. Fel is attached to this cluster at the next level and at the third level OC is attached to this three-element group. Beyond that point elements are progressively added to this single cluster in the order: Pb, Ni, Crl, and Mn. Trials with other measures of association show that the pair Zn - Cu is stable but that OC and Fe may "trade places". This is reflected in the results of principle components analysis (Fig. 51) where two components suffice to account for 95% of the variance. As can be seen in Fig. 55, Zn, Cu and OC are most closely associated while Fel is somewhat removed. Lead, while further removed is principally described by component 1. In contrast, Mn is principally described in terms of component 2 and is, in fact, the reason for the existence of a two-component description of the data set. On balance, there is a trend toward association of Zn and Cu with OC but even with very high quality data such as this, the distinction between OC and Fe is marginal.

The clustering of elements revealed by treatment of data subsets is preserved when the complete data set is used. As can be seen in Fig. 53 (complete set), Ca and Mg are strongly associated and form a cluster which is only remotely connected to other elements. Cu and Zn again are most strongly associated and Fel is added at the third stage to form a three-element cluster. To this cluster are added Pb and Ni in order, while Mn is essentially an independent element. Similar relationships are seen on principle components analysis (Fig. 56). The anthropogenically enriched elements (see below) form a close association (Pb, Zn, Ni, Cu). Crl and Fel are slightly removed from this group while both Mn and Ca + Mg are distant

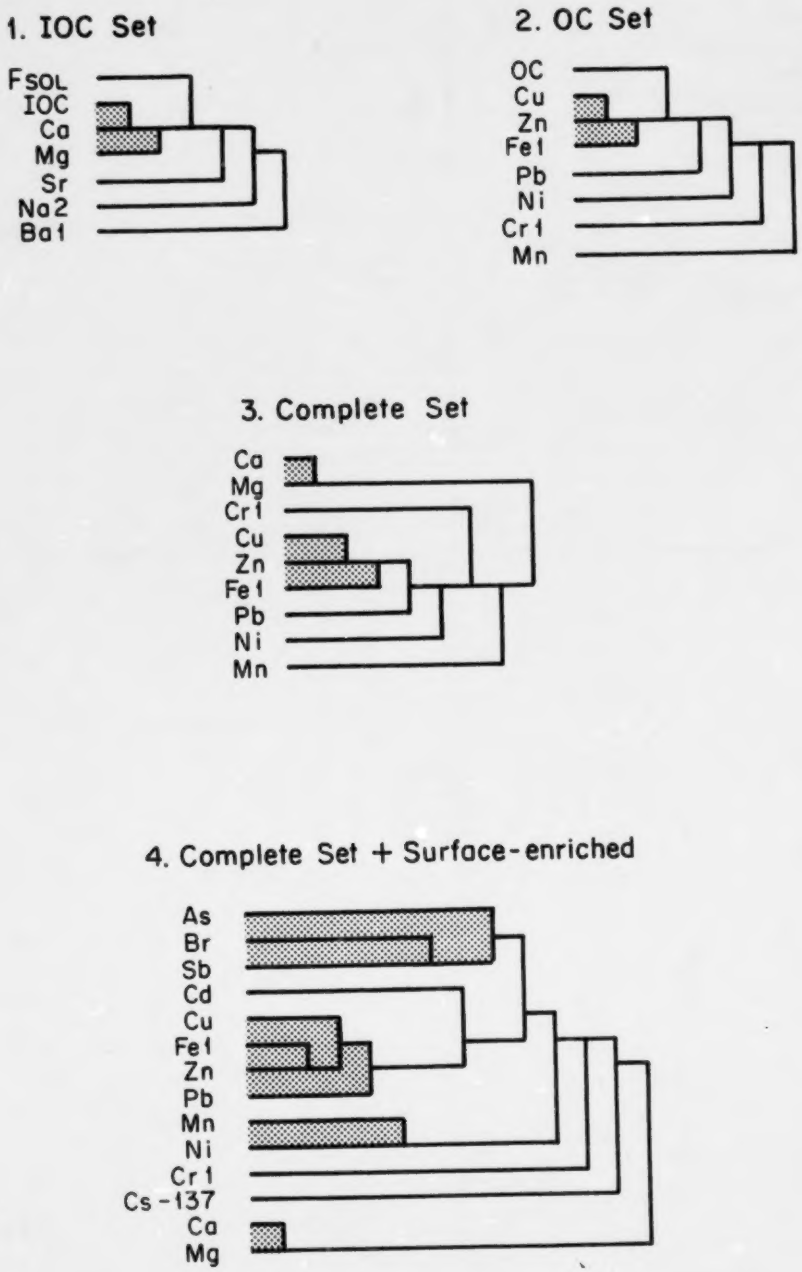
1. IOC Set
FSOL
IOC
Ca
Mg
Sr
Na2
Ba1
2. OC Set
OC
Cu
Zn
Fe1
Pb
Ni
Cr1
Mn
3. Complete Set
Ca
Mg
Cr1
Cu
Zn
Fe1
Pb
Ni
Mn
4. Complete Set + Surface-enriched
As
Br
Sb
Cd
Cu
Fe1
Zn
Pb
Mn
Ni
Cr1
Cs-137
Ca
Mg

Figure 53. Hierarchical trees resulting from cluster analysis of surface sediment concentrations.

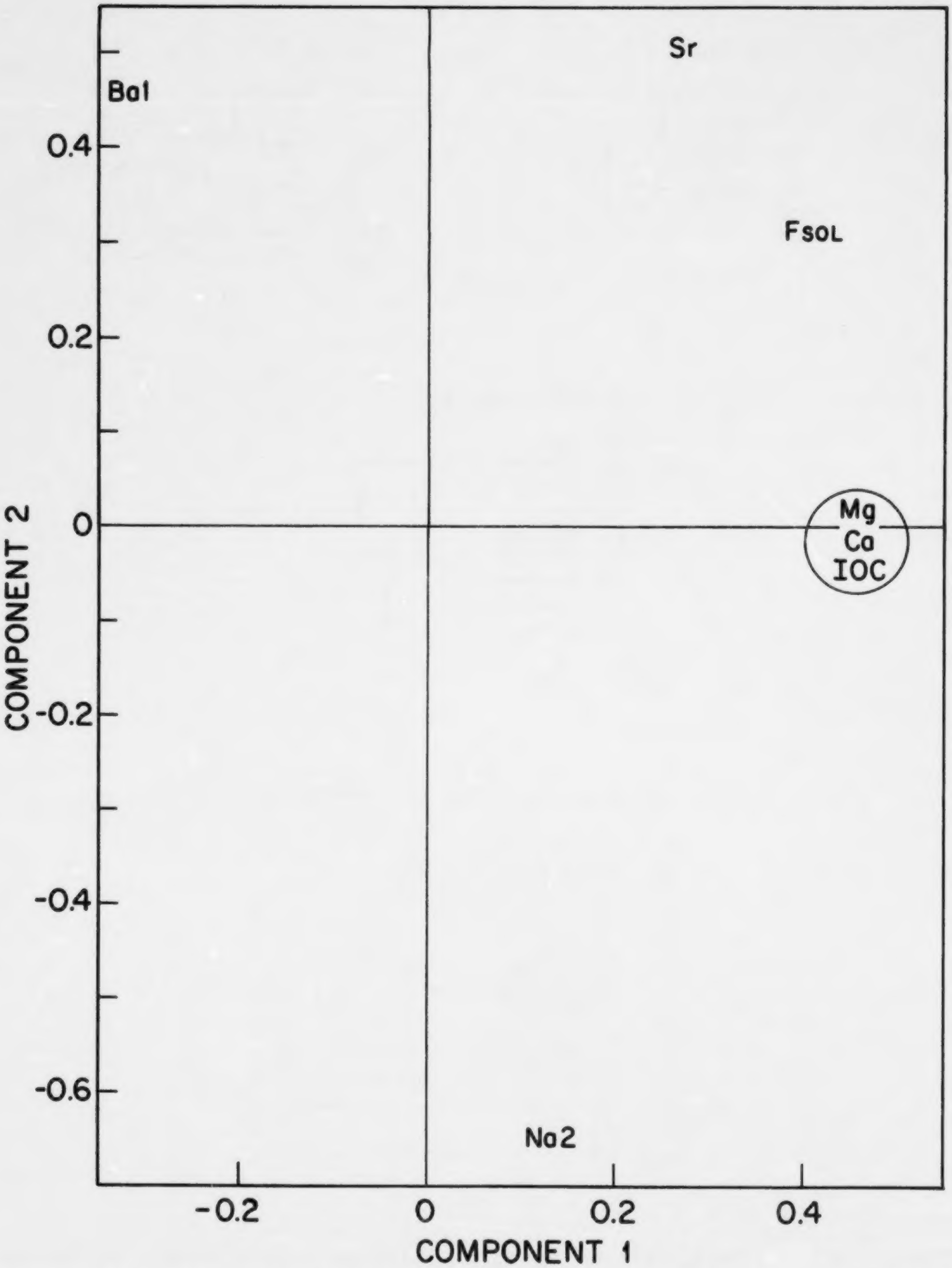

Figure 54. Association of calcium family and related constituents based on principal components analysis.

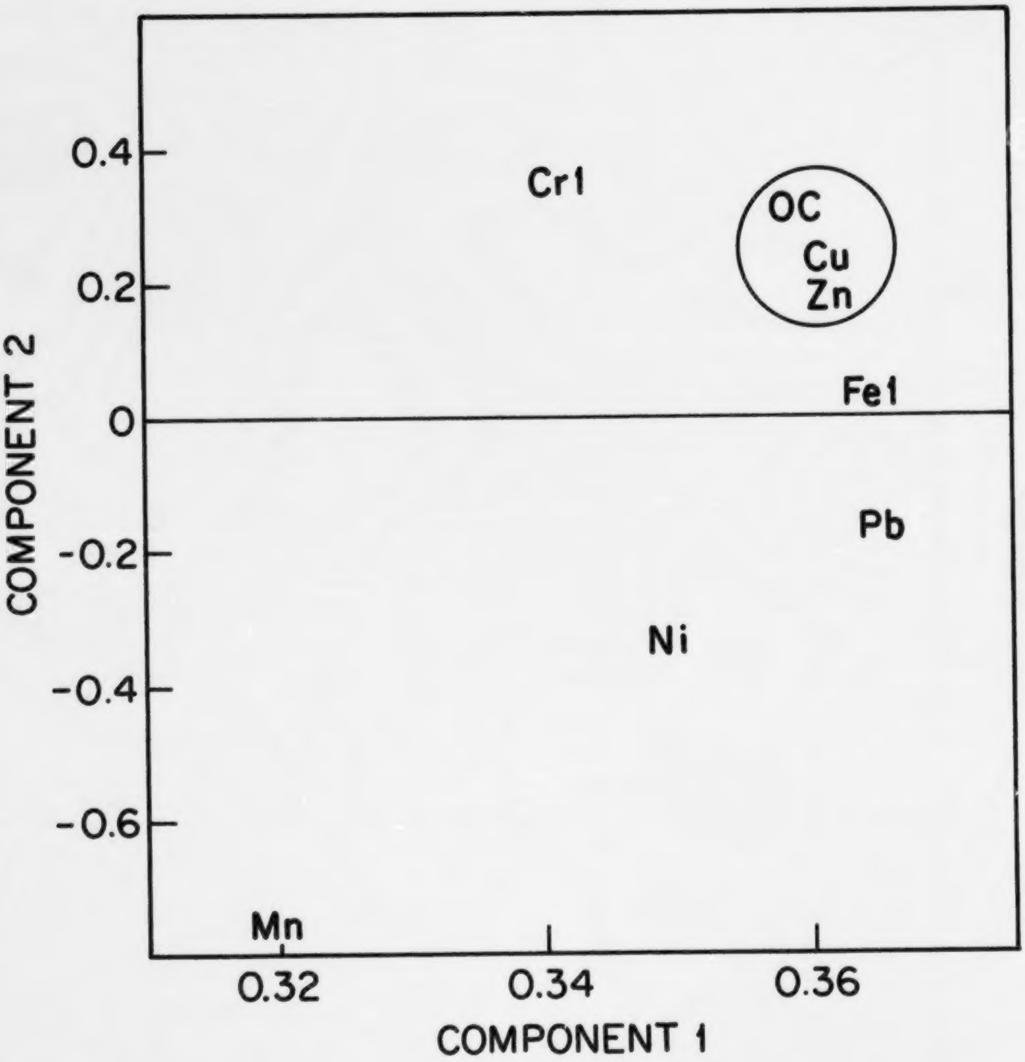

Figure 55. Association of non-calcium family elements in the most complete data set based on principal components analysis.

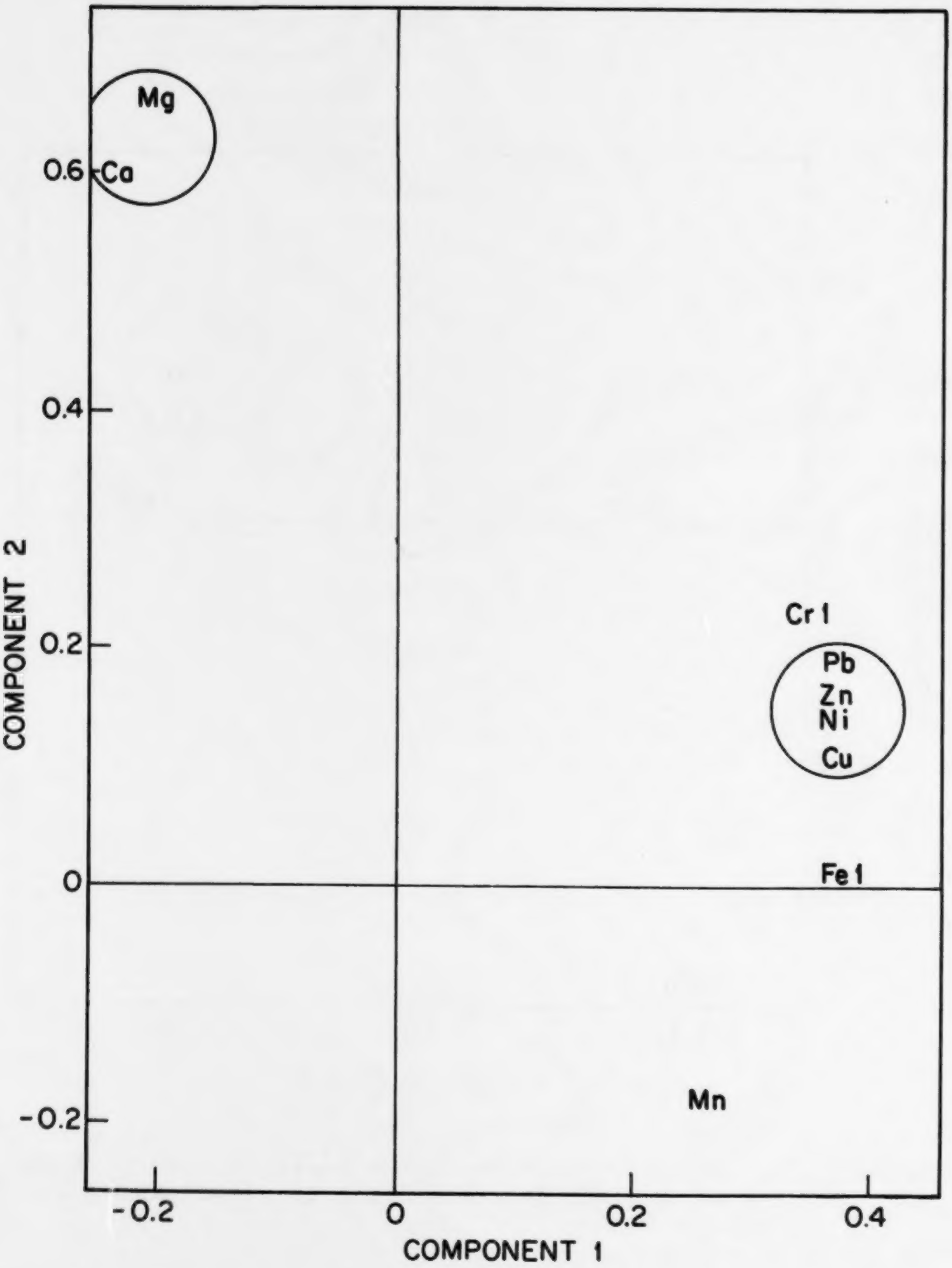

Figure 56. Results of principal components analysis of complete data set including calcium-family elements.

5. Complete Set + Non-enriched

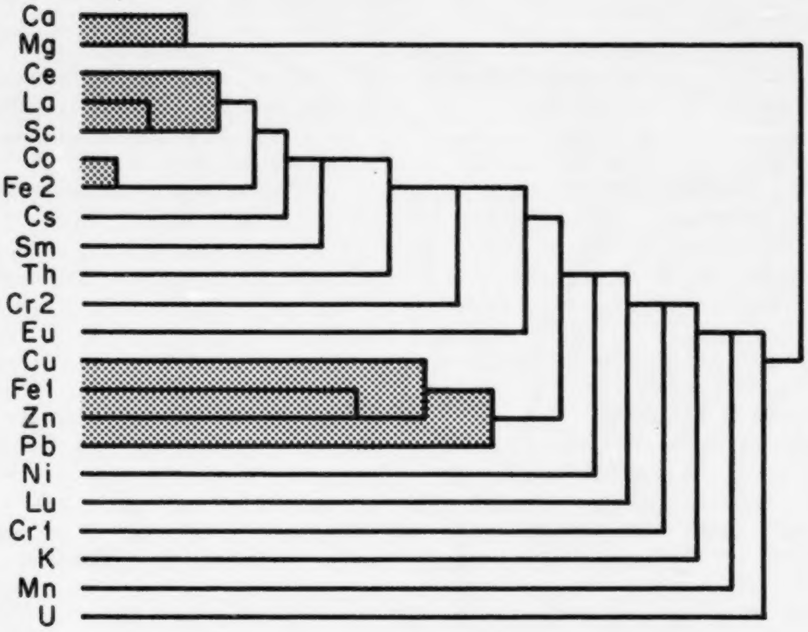
Ca
Mg
Ce
La
Sc
Co
Fe2
Cs
Sm
Th
Cr2
Eu
Cu
Fe1
Zn
Pb
Ni
Lu
Cr1
K
Mn
U

Figure 57. Hierarchical tree resulting from cluster analysis of the complete data set plus additional non-enriched elements.

elements. On the basis of the complete (N = 60) data set the principle components analysis recognizes three components accounting for 96% of the variance. The first and second, used to locate elements in Fig. 56, correspond to the transition metal group + lead and to calcium family elements respectively. The third component corresponds to Mn. The uniqueness of Mn may be attributed to its ability to undergo diagenetic remobilization in near-surface sediments. This attribute would not normally be revealed on application of multivariate techniques to gross sediment samples. The uniqueness of Mn is emphasized as a result of using a sediment section close to the surface whose Mn concentration is often dominated by the remobilized fraction. This effect may be better appreciated by comparison of manganese concentration profiles with those of other elements (see below). The results of principle components analysis on the complete set are summarized in Table 19.

If all surface-enriched elements are added to the complete data set, an additional group emerges from cluster analysis as can be seen in Fig. 53. In addition to the groups (Cu, Zn, Fel, Pb) and (Ca - Mg) there is (As-Br-Sb). Reasons for this association are not clear although As and Sb, at least, are in the same chemical family and might reasonably be expected to have similar geochemical behavior. Elements such as Cd, Crl, and Cs-137 are not strongly related to any group although they are clearly not associated with calcium family elements. The association of Ni with Mn is unstable and does not survive changes in the measure of similarity.

The hierarchical tree resulting from cluster analysis of the non-enriched elements plus the basic data set is shown in Fig. 57. Two new associations are apparent. In addition to the Cu-Zn-Pb-Fel and the Ca-Mg groups, there are Ce-La-Sc and Co-Fe2. Both of these latter sets involve elements determined via NAA on whole sediments. With the exception of Fe2 these elements are primarily lattice-bound constituents not readily leached by acid. Both sets are probably characteristic of the clay minerals present and are themselves connnected together early on in the stepwise clustering process. To the larger cluster defined by Ce-La-Sc-Co-Fe2 are progressively added the other rare earth elements (Sm, Eu) and Cs, Cr2 and Th. Elements loosely connected to any cluster are Ni, Crl, K, Mn, U and the rare earth element, Lu. Thus with the exception of Lu, the rare earth elements are a part of a major cluster (Ce, Sm, Eu) which includes La, Sc, Co, Fe2, Cs, Th, and Cr2.

In summary, five principal groupings of elements are identified: (1) IOC Group: IOC-Ca-Mg-Fsol; (2) OC group: OC-Fel-Cu-Zn-Pb-(Ni); (3) Diagenetic Group: Mn only; (4) Sb-As group: Sb-Br-As; and (5) Clay mineral group: two sub groups A = Ce-La-Sc and B = Co-Fe2 which in turn are connected so that the major cluster is A-B-Cs-Sm-Th-Cr2-Eu. These results are presented in Table 20.

VERTICAL DISTRIBUTIONS OF ELEMENTS

Vertical distribution of metals and radioactive constituents have been measured in 32 cores as summarized in Table 21. NAA elements were determined in only one of the cores at Station 18 (Tables 22, 23). The vertical

TABLE 19. RESULTS OF PRINCIPLE COMPONENTS ANALYSIS OF COMPLETE DATA SET*

	Component			
Element	1.	2.	3.	4.
Ca	-0.252	0.601	0.207	0.019
Crl	0.343	0.234	-0.304	-0.840
Cu	0.378	0.108	-0.158	0.337
Fel	0.380	0.097	-0.037	0.121
Mg	-0.211	0.669	0.171	0.210
Mn	0.269	-0.181	0.887	-0.217
Ni	0.367	0.146	0.109	0.012
Pb	0.371	0.189	0.056	0.190
Zn	0.377	0.159	-0.085	0.285
Cumulative Explained Variance (%)	73	90	96	98

*N = 60.

TABLE 20. SIGNIFICANT INTERELEMENT ASSOCIATIONS IN SURFACE SEDIMENTS OF SOUTHERN LAKE HURON

Group		Elements in order of decreasing degree of association
I.	Inorganic Carbon	IOC-CA-Mg-Fsol ----- Sr-----Na2
II.	Organic Carbon/ Iron	Cu-Zn-(Fe1-OC)-Pb--Ni---------Cr1
III.	Diagenic	Mn only
IV.	Sb-As	Sb-Br-As
V.	Clay Mineral	A: La-Sc-Ce B: Co-Fe2
		$\left.\begin{matrix}A\\B\end{matrix}\right\rangle$ Cs-Sm-Th-Cr2-Eu

TABLE 21. A SUMMARY OF VERTICAL DISTRIBUTION MEASUREMENTS IN CORES FROM SOUTHERN LAKE HURON.

Station	Physical Properties	AAS Elements	NAA Elements	Cesium-137	Lead-210	Amorphous Silicon	Dissolved[1] Elements	Benthic Invertebrates
3	x	x		x	x			
4	x	x		x	x			
5	x	x		x	x			
6	x	x		x	x			
7	x	x		x	x			
8	x	x		x	x			
9	x	x		x	x			
10	x	x		x	x			
12	x	x		x	x			
13	x	x		x	x			
14	x	x		x	x	x	x	x
15	x	x		x				
16	x	x		x	x			
17	x	x		x	x			
18	x	x	x	x	x	x	x	x
19	x	x		x	x			
25	x	x		x	x			
29	x	x		x				
31	x	x		x	x			
33	x	x		x	x			
35	x	x		x	x			
38	x	x		x	x			
39	x	x		x	x			
41	x	x		x	x			
45	x	x		x	x			
50	x	x		x	x			
51	x	x		x	x			
53	x	x		x	x	x	x	
57	x	x		x	x			
61	x	x		x	x			
63	x	x		x	x	x	x	
69	x	x		x	x			

---

[1] Pore water concentrations. A complete listing of vertical profile data is contained in the Appendix (Table A-2).

distributions of amorphous silicon and dissolved elements were determined for 4 cores (Stns. 14A, 18A, 53 and 63) and the distributions of zoobenthos were determined at two locations (Stns. 14A and 18A) with a high degree of replication. Discussion of the vertical distribution of zoobenthos is deferred to the section on radioactivity profiles. To conserve space, only eight locations are selected for illustration. The stations include 5, 10 and 19 in the Port Huron Basin; 25 from the Saginaw Basin and stations 14A, 18A, 53, and 63 in the Goderich Basin. As can be seen from Table 21, these stations in the Goderich Basin are particularly well-characterized. As the primary focus of this report is the characterization of anthropogenic elements in sediments, their increase in concentration and rates of deposition, the discussion below emphasizes trends in element concentration profiles and the significance of concentration increases toward the sediment-water interface. The general behavior of concentration profiles is expressed in terms of the ratio of the concentration of an element of near surface sediments (1-2 cm) to its average concentration in deeper sections of the cores where variations with depth are usually minimal. For cores in southern Lake Huron, element concentrations are generally constant below about 20 cm except in cores from stations located in basin margins and possessing a high degree of inhomogeniety. Surface-to-depth concentration ratios for the entire set of cores is given in Table 27 and summarized in Table 30 and 31. Values are given also for the enrichment factor defined below.

Major Constituents

Vertical profiles of major constituents are shown in Figs. 58-85. Each profile is accompanied by a trend line to facilitate visualization. As can be seen in Figs. 58 and 59, Fsol is essentially constant with depth within experimental errors for most stations except 25 and 53 where there is a slight but systematic increase over the upper 5 cm or so. In contrast, Fsol is lower at the surface at station 19. This core is inhomogeneous with respect to grain size, possessing a lens of sandy mud in the upper 7 cm. On the average, as can be seen in Table 27, Fsol is about 10% higher in surface sediments than in deeper sections of cores. Calcium profiles (Figs. 60, 61) are essentially constant for Stations 5, 10, 19, 14A, and 18A. Cores at stations 25 and 53 exhibit a small increase in Ca concentration near the surface while at 63 there is a small subsurface maximum at around 10 cm. On the average the concentration of calcium is about 30% higher in surface sediments (Table 27). Iron consistently shows a slight increase in concentration within the upper 5 cm or so as can be seen in Figs. 62 and 63. The exception is the core at the marginal station, 19, where surface iron concentrations are reduced. The average surface-to-depth concentration for iron (Table 27) is similar to that of Fsol, about 1.08, indicating an 8% increase in surface values. For Mg, concentration profiles at stations 5, 8, 16, and 14A are remarkably constant while those at 18A and 63 exhibit small, broad subsurface maxima but are otherwise essentially constant (Fig. 64 and 65). Alternative stations were selected for Mg because no measurements were made at 10, 19 or 25 for this element. Stations 8, 15 and 16 are all located in the Port Huron Basin. The core at station 15 is grossly inhomogenous with respect to sediment type, possessing a 5 cm section of fine sand which grades into glaciolacustrine clay with increasing sediment depth. This progressive

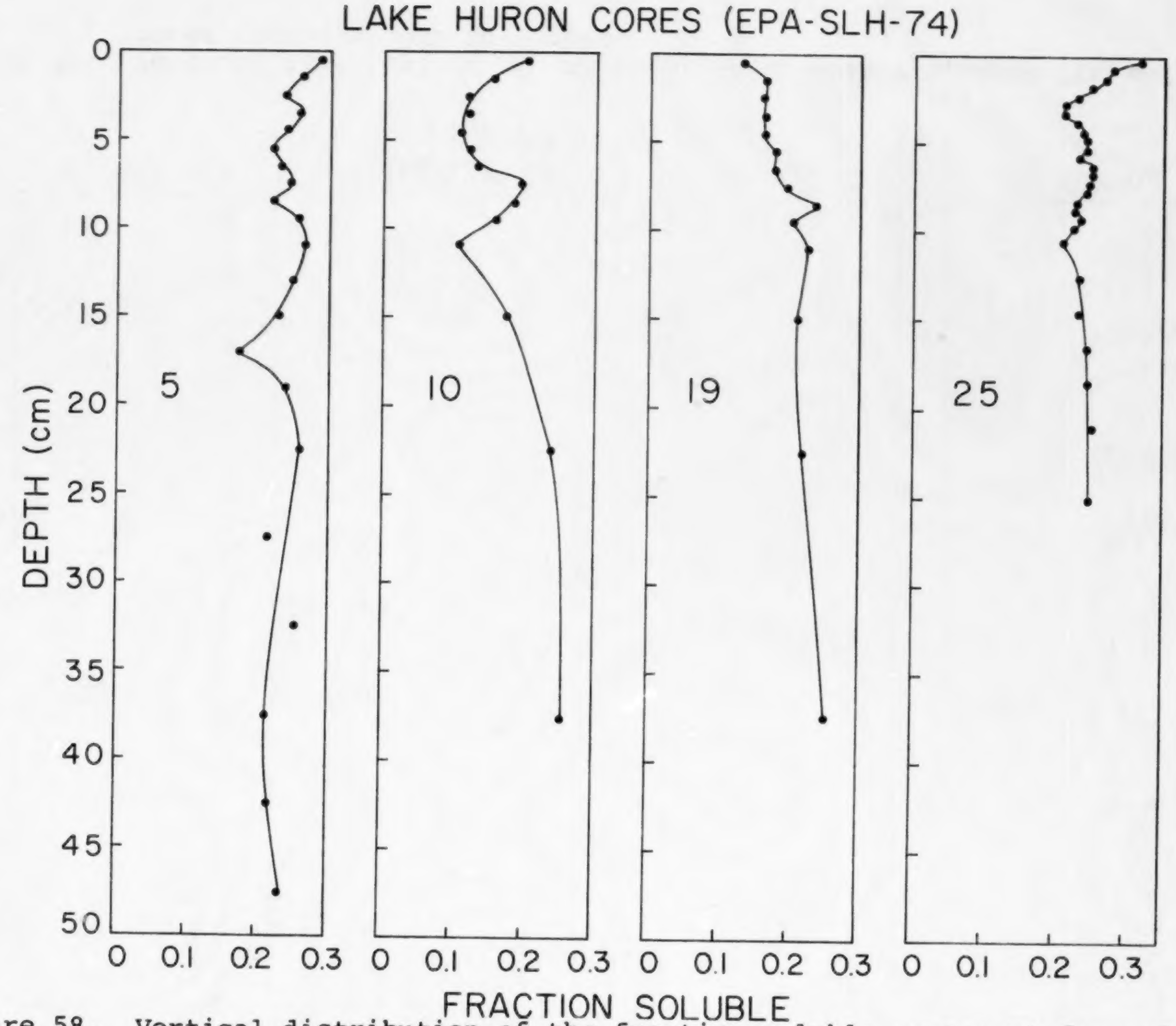

Figure 58. Vertical distribution of the fraction soluble component for selected cores from the Port Huron and Saginaw Depositional Basins.

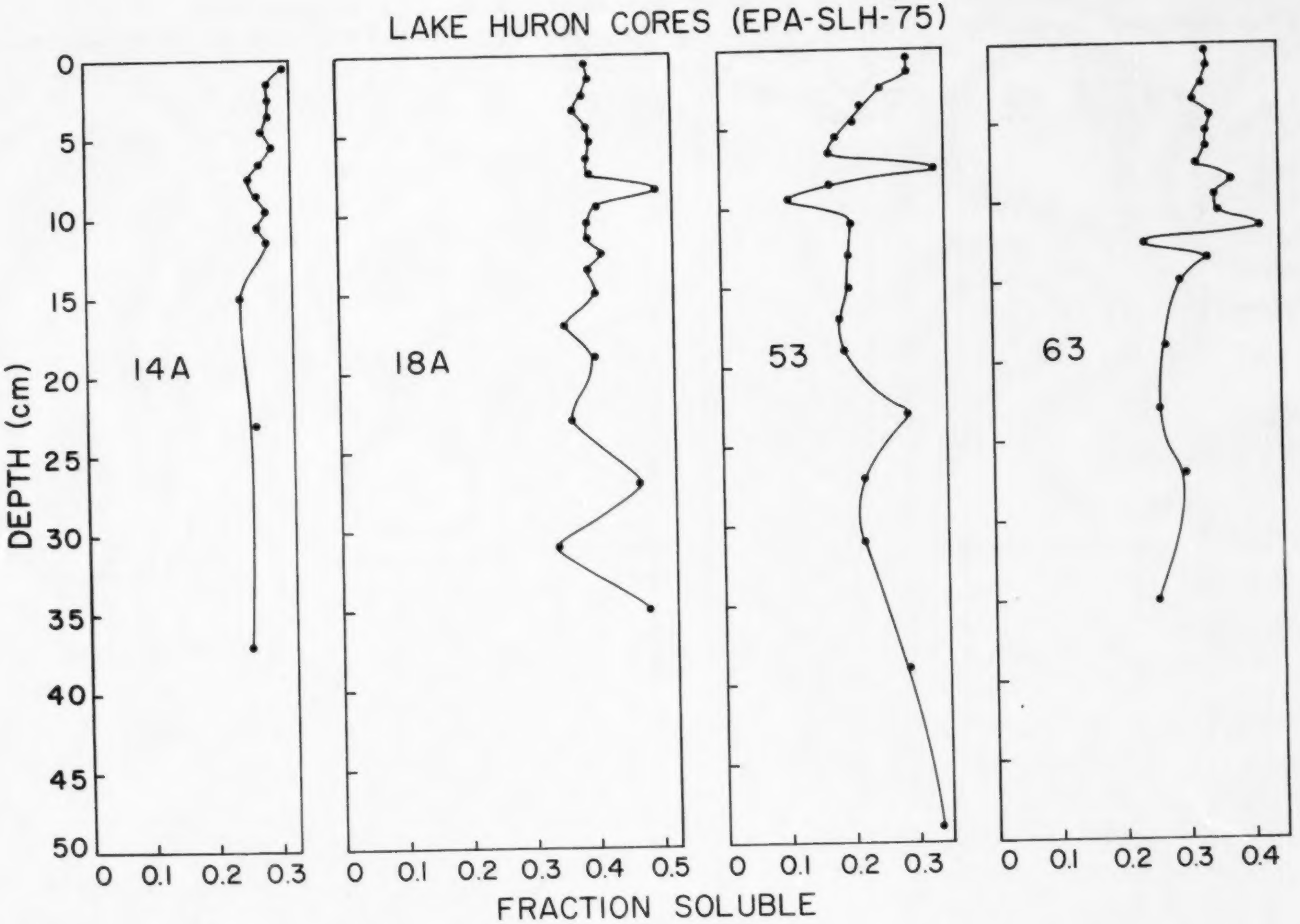

Figure 59. Vertical distribution of the fraction soluble component for selected cores from the Goderich Basin.

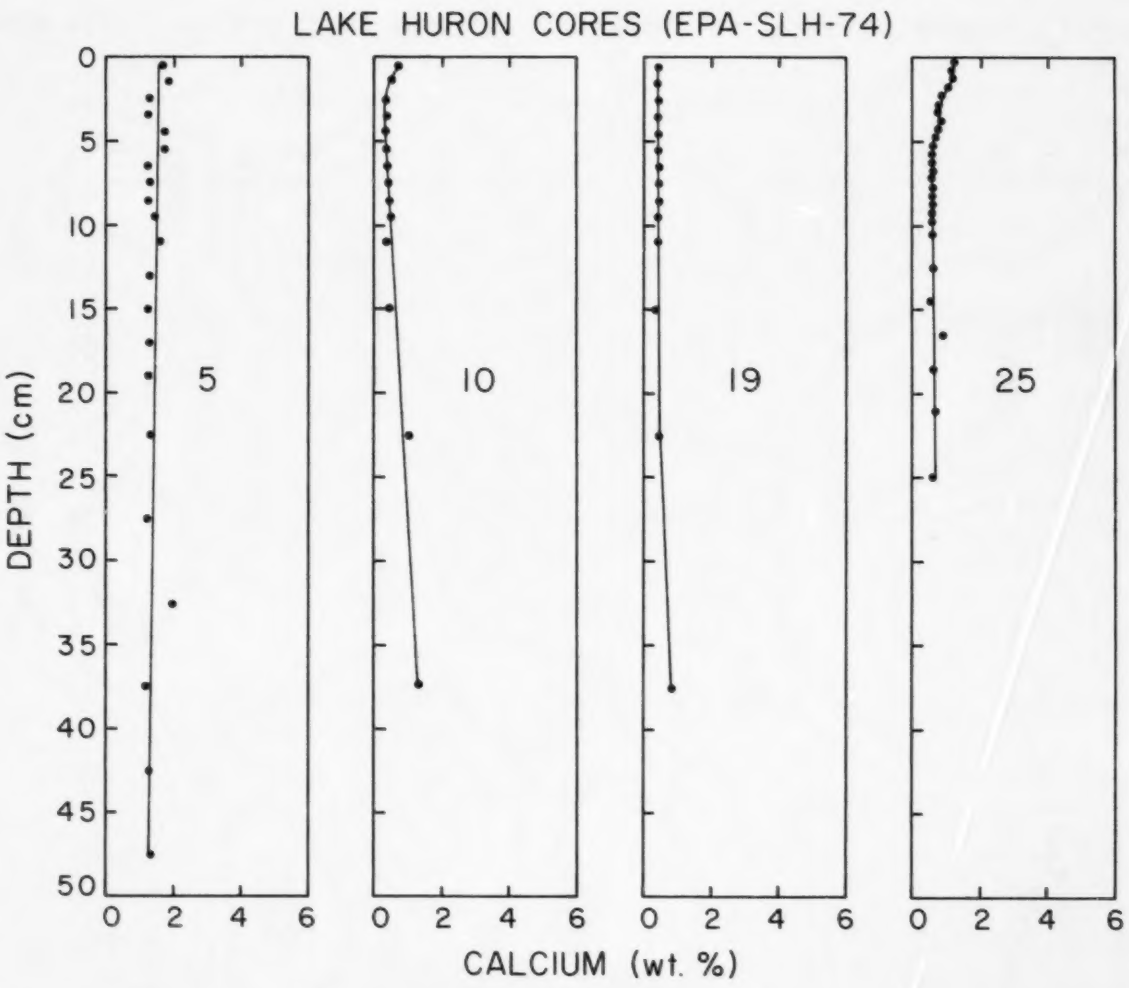

Figure 60. Vertical distribution of calcium in selected Port Huron and Saginaw Basin cores.

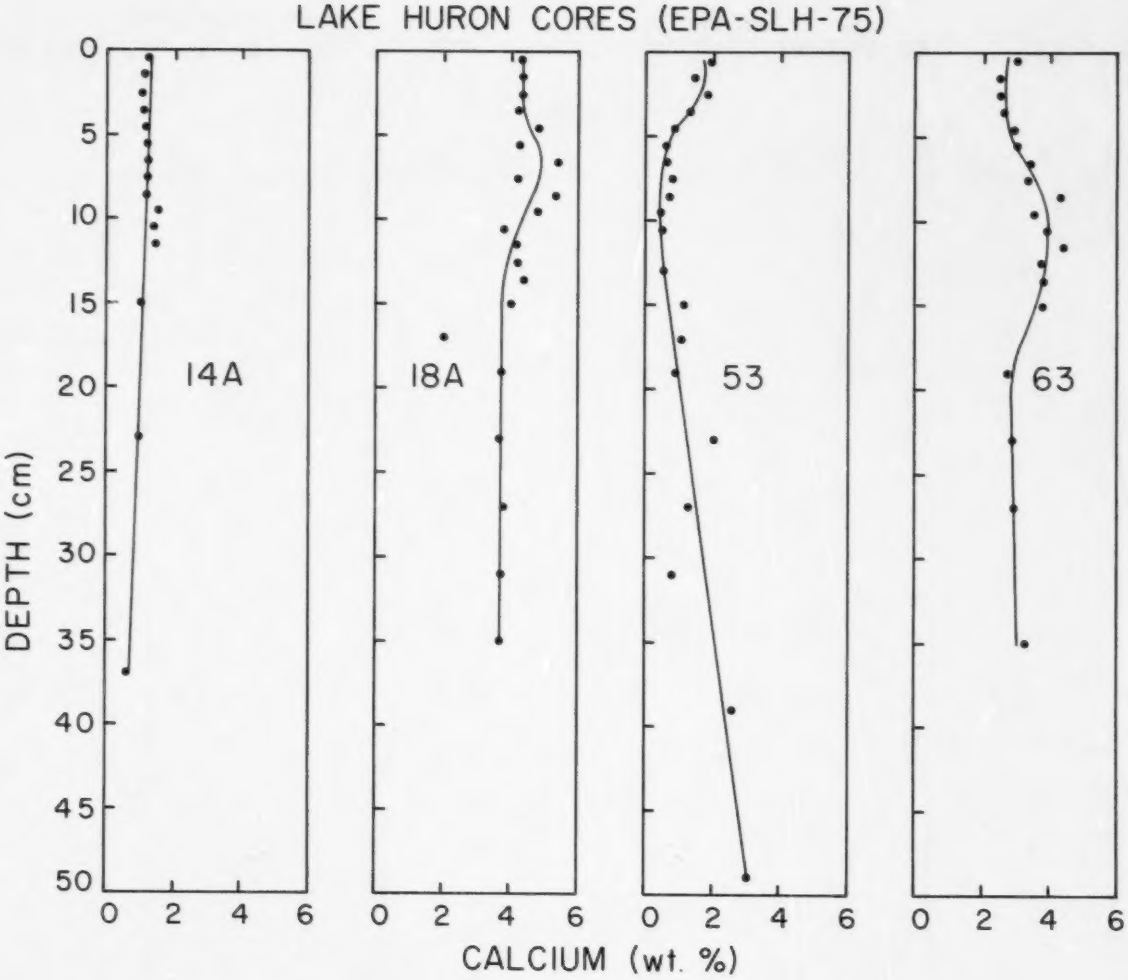

Figure 61. Vertical distribution of calcium in selected Goderich Basin cores.

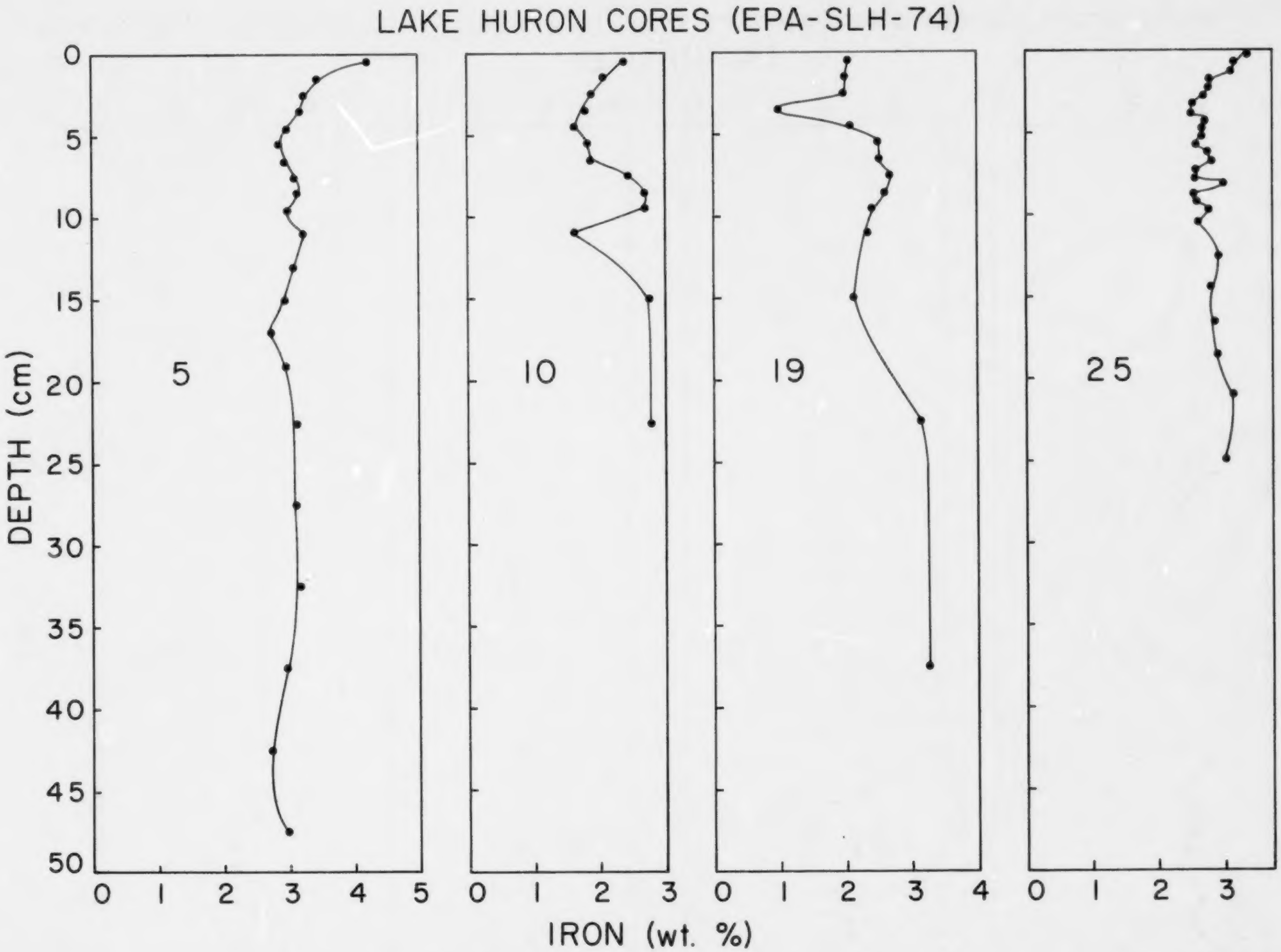

Figure 62. Vertical distribution of iron in selected Port Huron and Saginaw Basin cores.

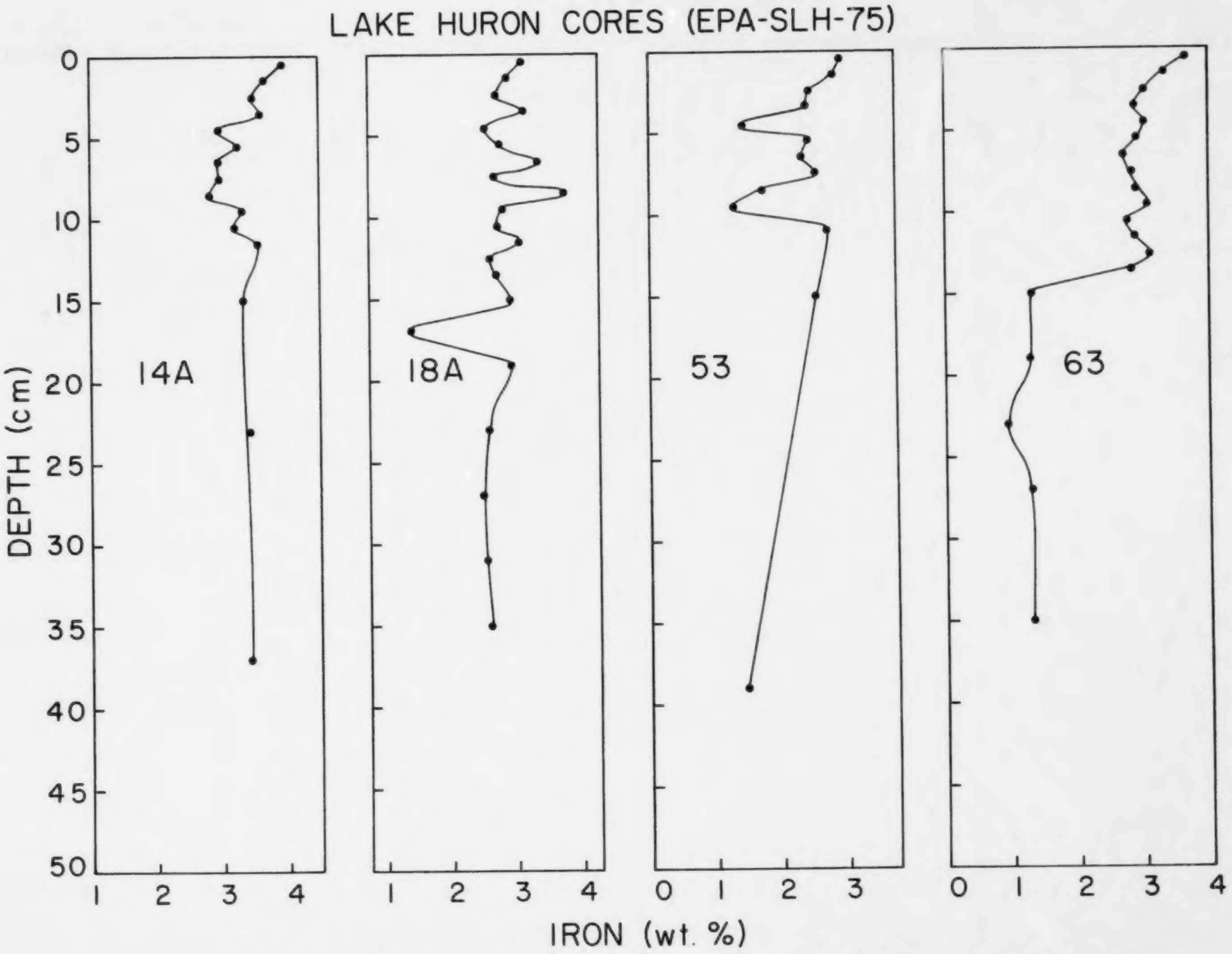

Figure 63. Vertical distribution of iron in selected Goderich Basin cores.

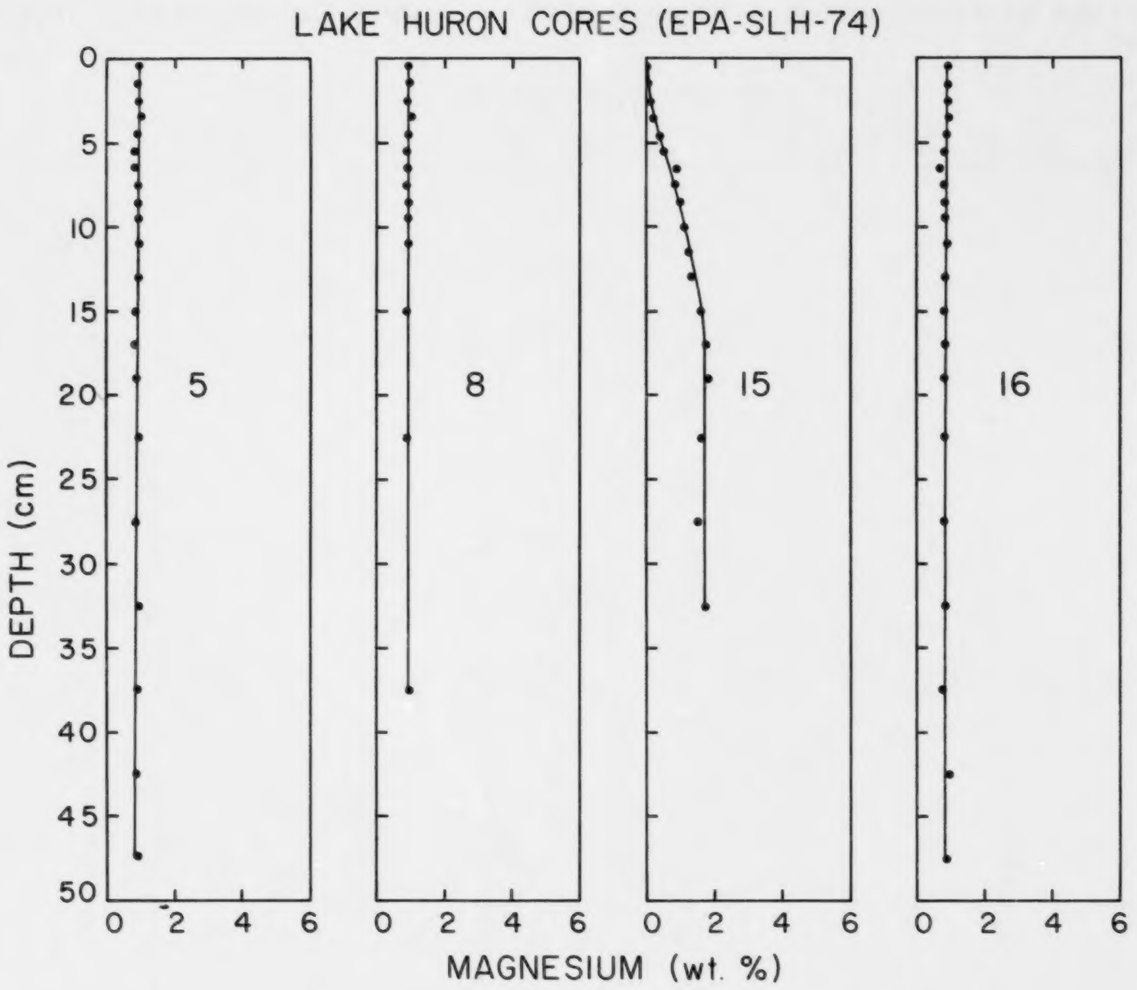

Figure 64. Vertical distribution of magnesium in selected Port Huron cores.

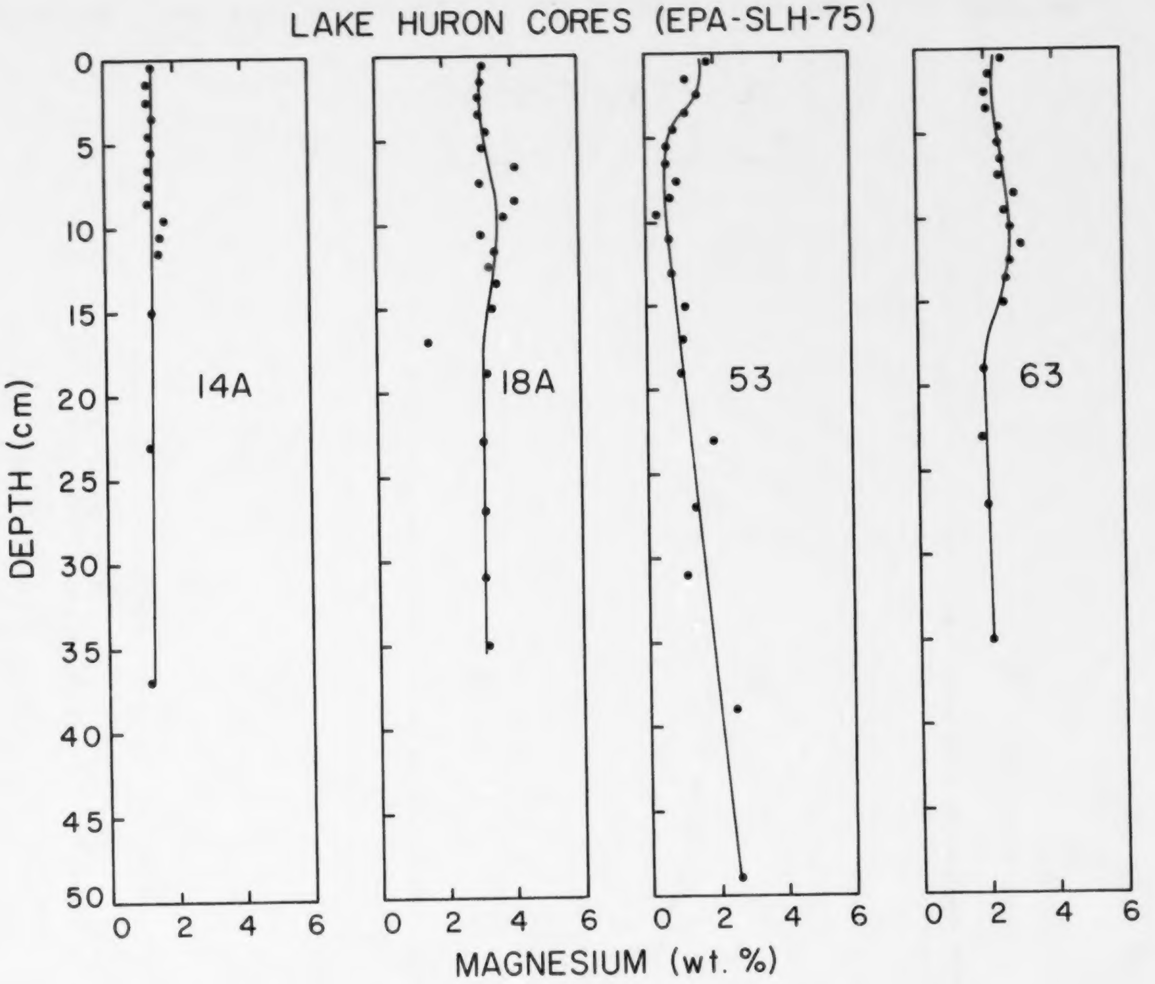

Figure 65. Vertical distribution of magnesium in selected Goderich Basin cores.

shift in sediment type is illustrated by the concentration profile of Mg (Fig. 64). On the average there is no significantly higher concentration of magnesium in surface sediments than there is in underlying sediments. It is therefore plausible that the reduction in Ca with increasing sediment depth is primarily the result of dissolution of non-dolomitic calcium, perhaps authigenic calcite. In contrast with other major element profiles, those of manganese are very strongly peaked at the sediment-water interface in every case including station 19, as can be seen in Figs. 67 and 68. Within the upper 3 cm or less, the concentration of Mn rises to a maximum in the uppermost sediment section and greatly exceeds underlying values. Very large near-surface Mn enrichment has now been widely observed in sediments of the Great Lakes and elsewhere (Robbins and Callender, 1975; Kemp et al., 1976) and is almost certainly due to diagenetic remobilization of the element. On the average the surface to depth concentration ratio is about 2.5 for Mn. This value is sensitive to the use of the 1-2 cm interval to define the ratio because of the rapid increase in Mn concentration toward the sediment surface. For the other elements including those which show enrichments due to anthropogenic loadings, concentration ratios and enrichment factors are not nearly as sensitive to the choice of the surface interval. The concentration of mercury (Fig. 66) shows a dramatic increase toward the sediment-water interface. Large surface enrichments have been observed earlier in cores from Lake Huron (Kemp and Thomas 1976), Lake Ontario (Thomas 1972), Lake Erie (Walters and Wolery 1974) and elsewhere and are attributed to anthropogenic additions of the element to the Lakes. For acid-soluble phosphorus (Figs. 69 and 70) there is a very slight increase in surface sediments except for the core at station 25 where there is a small but systematic decrease toward the sediment surface. On the average (Table 22) there is a small and marginally significant increase in acid soluble P, 7%. For potassium (Figs. 71 and 72) there are large excursions in the values of the concentration in individual sediment sections owing partly to experimental errors and to variable extractability of K from sediment matrix. As can be seen from Table 27, potassium is not on the average, enriched in surface sediments. Perhaps the most interesting major constituent is amorphous Si which in the four cores studied, shows a large increase in surface sediments (Fig. 73). Unlike Mn, the concentration of Si increases gradually from a depth of up to 15 cm toward the sediment water interface. Its profile is more closely related to those of the anthropogenically enriched elements than to Mn, showing concentration ratios on the average of 2 in these four cores (Table 27). Near-surface sediment enrichment of amorphorus Si first reported by Robbins et al. (1974) for Lake Michigan has subsequently been observed by Parker and Edgington (1976) and in other of the Great Lakes by Nriagu (1978). It is not yet clear whether the enrichment is a steady-state feature resulting from deposition of authigenic particulate silica and its progressive dissolution during burial in sediments or whether it is the result of recent increases in the rate of biological fixation of silicon and increased deposition of particulate forms.

Trace Constituents

The vertical distributions of minor elements are illustrated in Figs. 74-85. The only complete profile of cadmium is for a core at station 10 (Fig. 74). At this location there is a four-fold increase in Cd at the

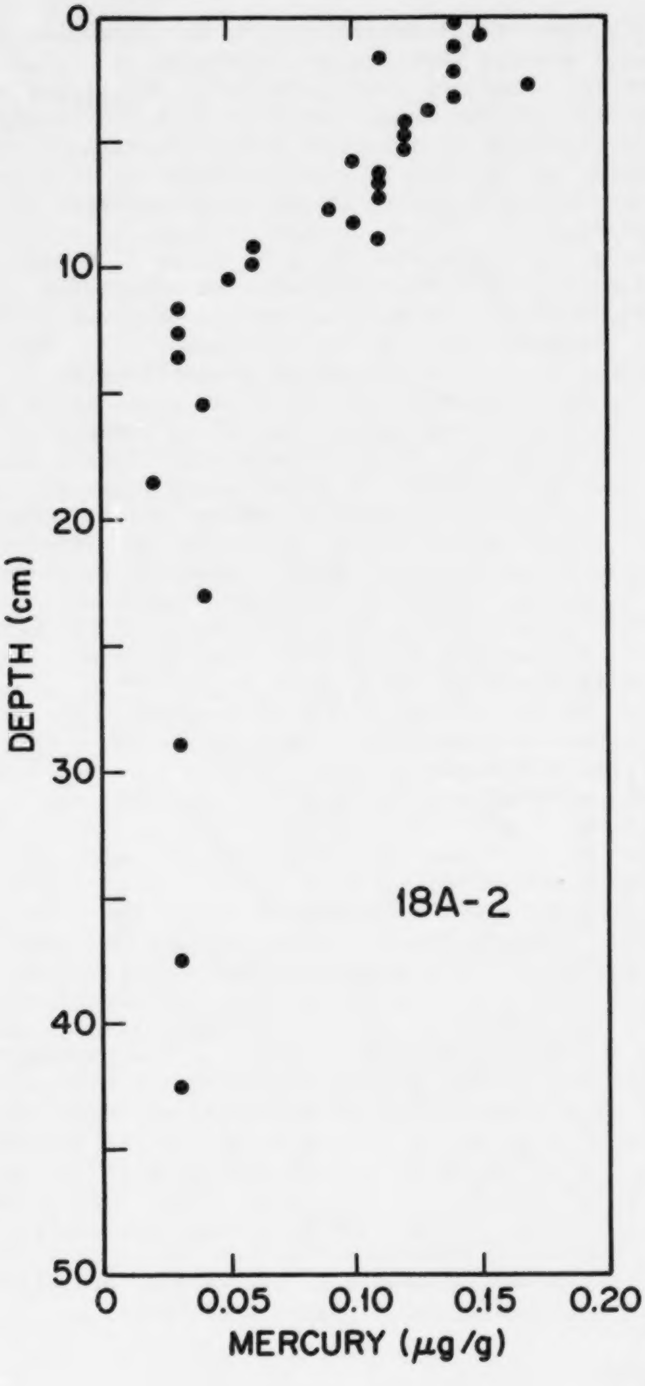

Figure 66. Vertical distribution of mercury in a Goderich Basin core.

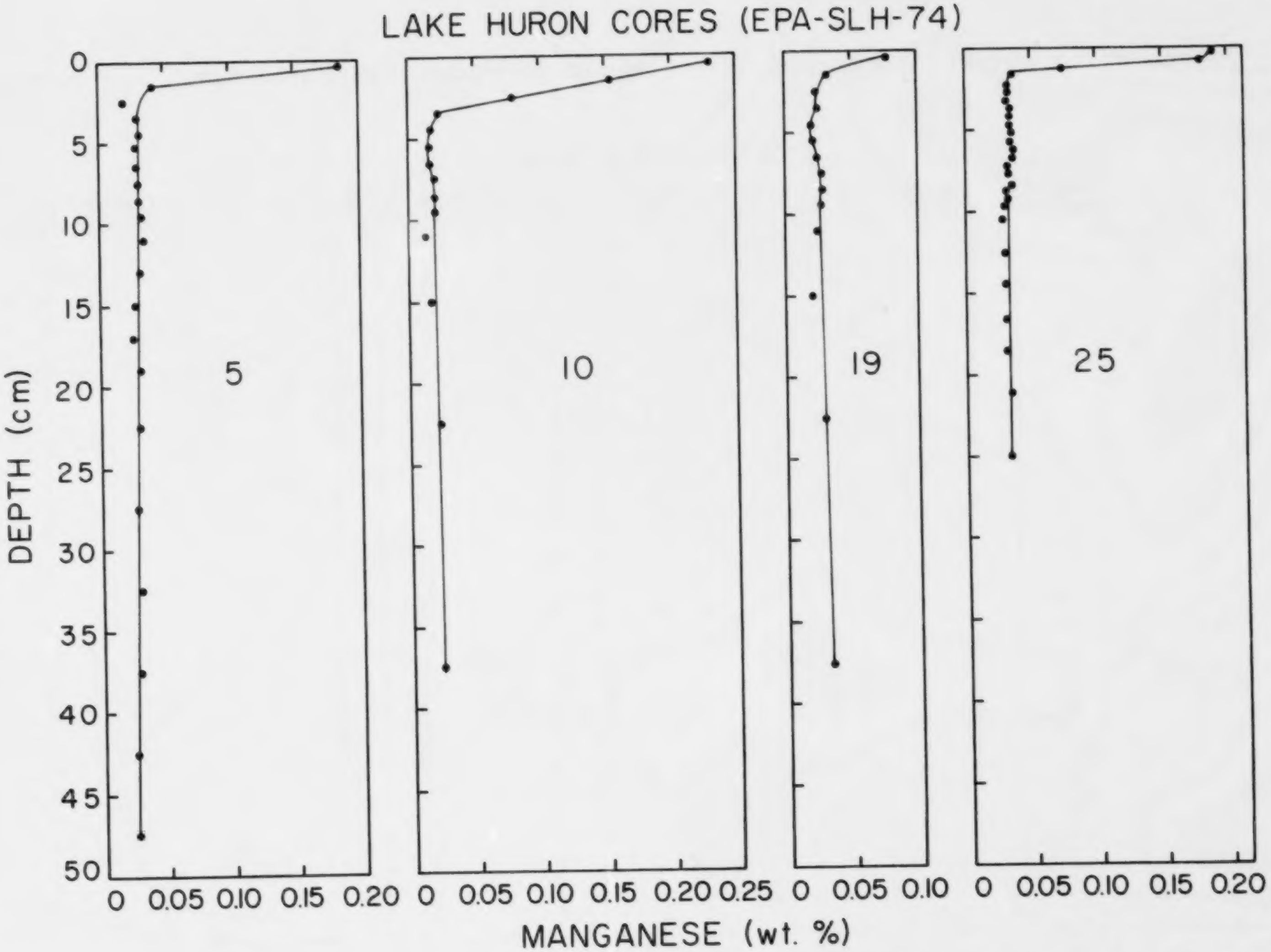

Figure 67. Vertical distribution of manganese in selected Port Huron and Saginaw Basin cores.

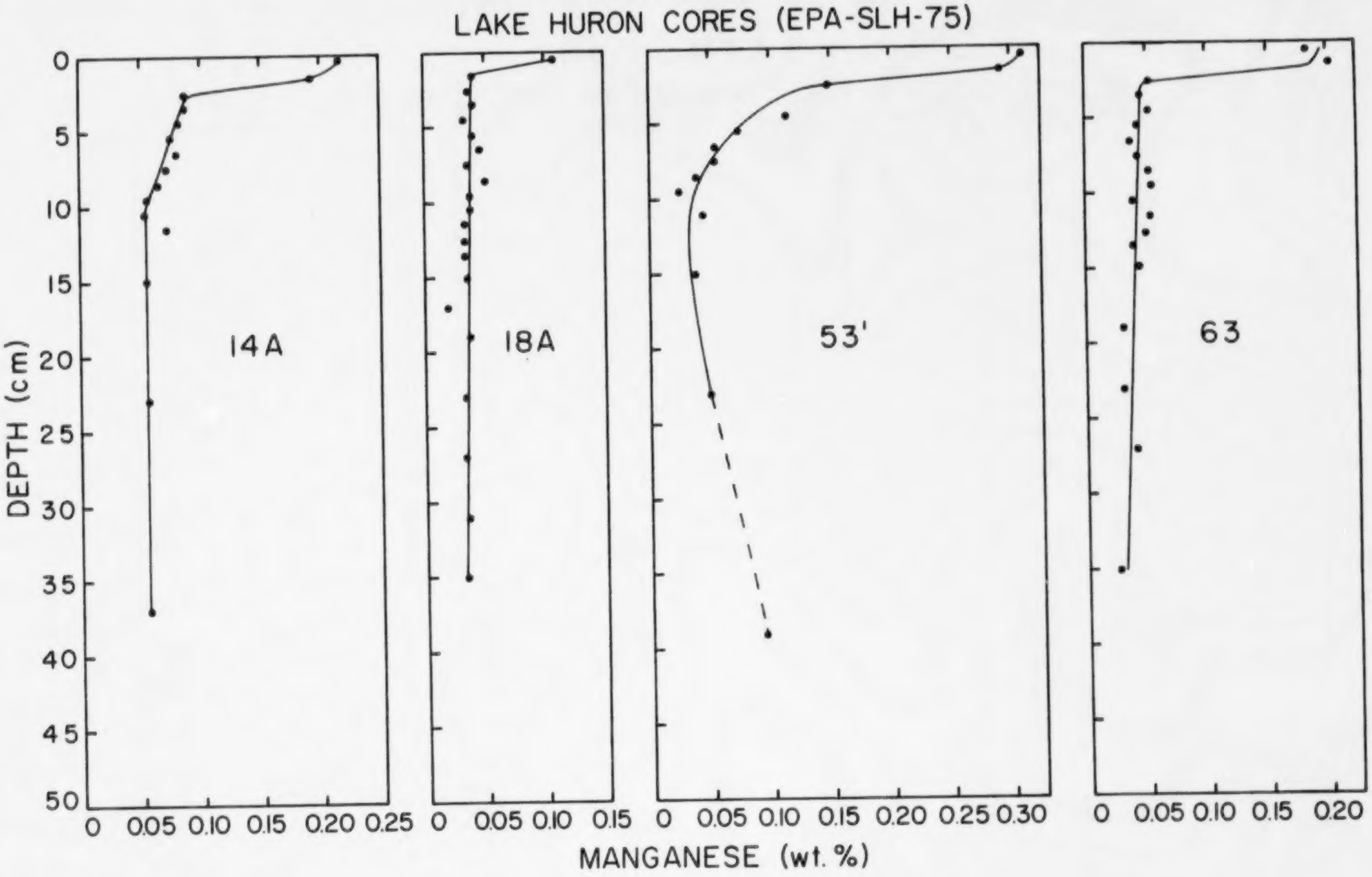

Figure 68. Vertical distribution of manganese in selected Goderich Basin cores.

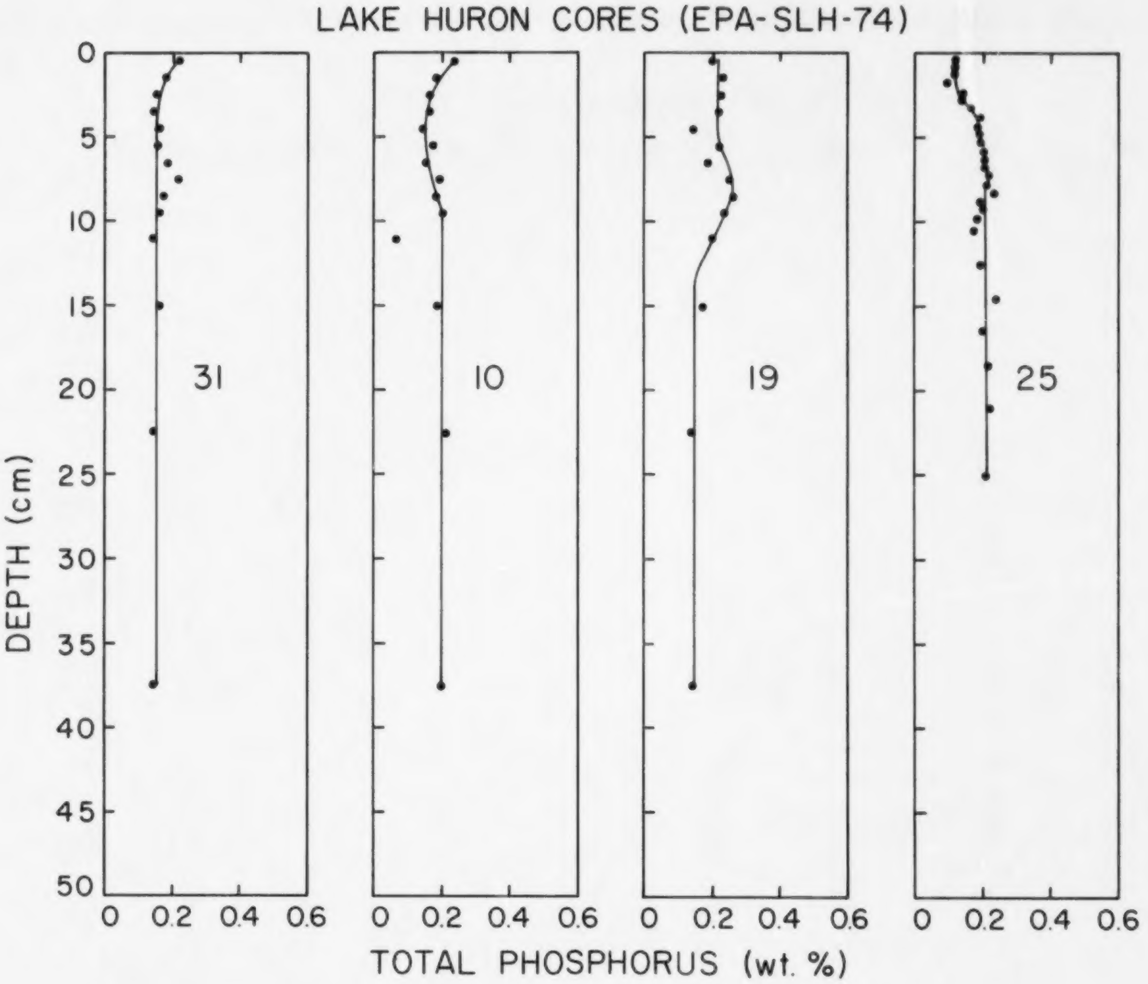

Figure 69. Vertical distribution of phosphorus in selected Port Huron and Saginaw Basin cores.

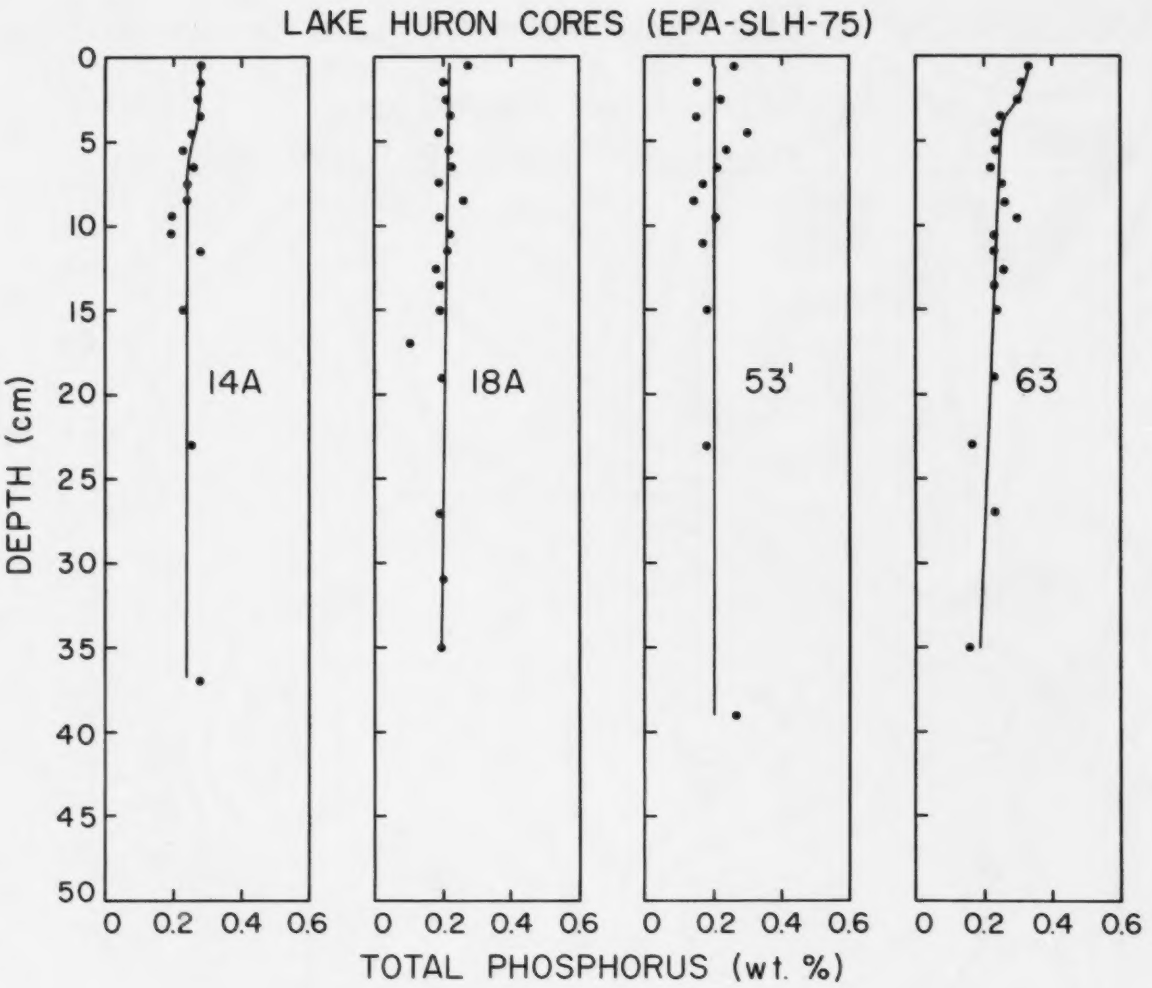

Figure 70. Vertical distribution of phosphorus in selected Goderich Basin cores.

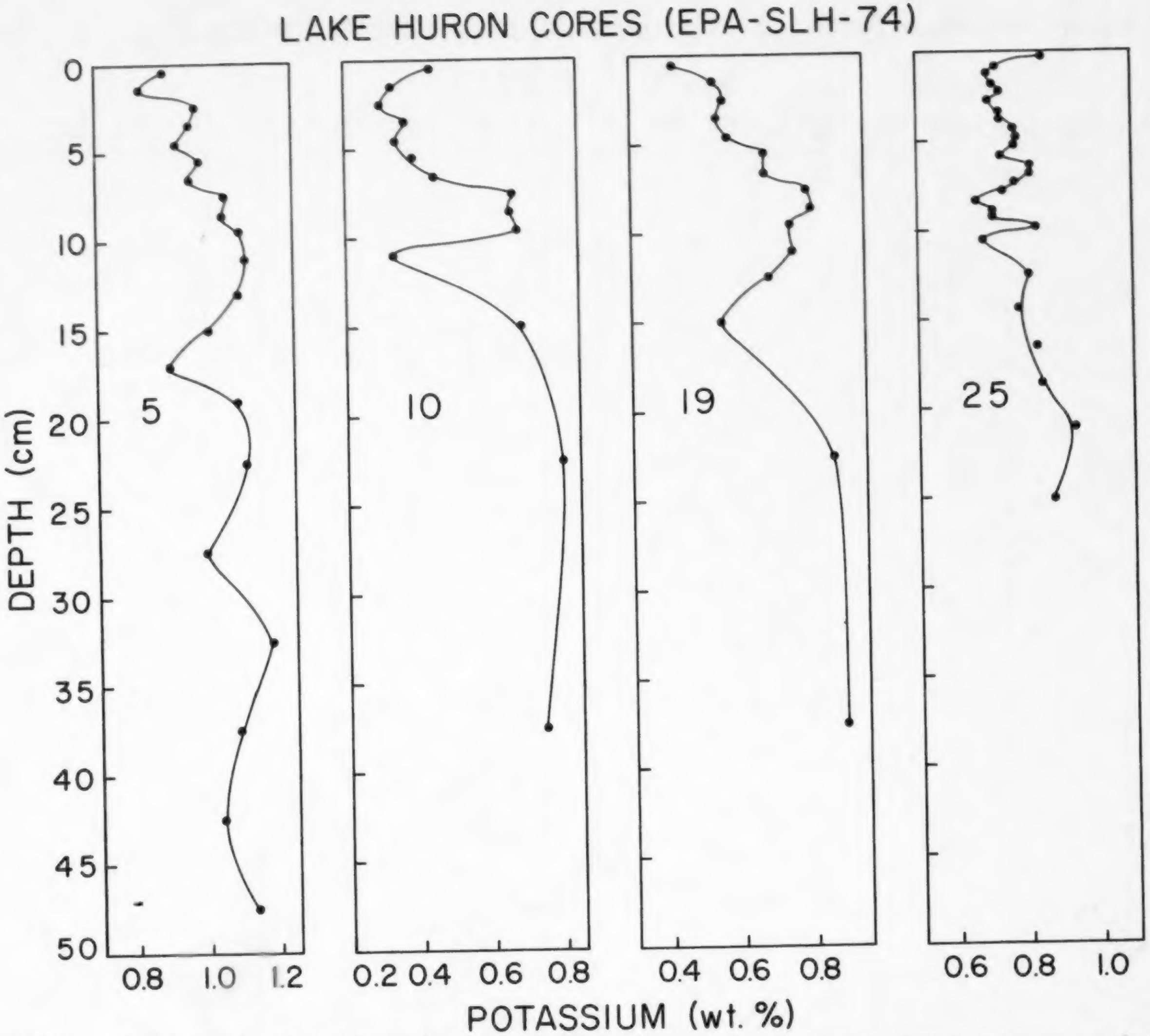

Figure 71. Vertical distribution of potassium in selected Port Huron and Saginaw Basin cores.

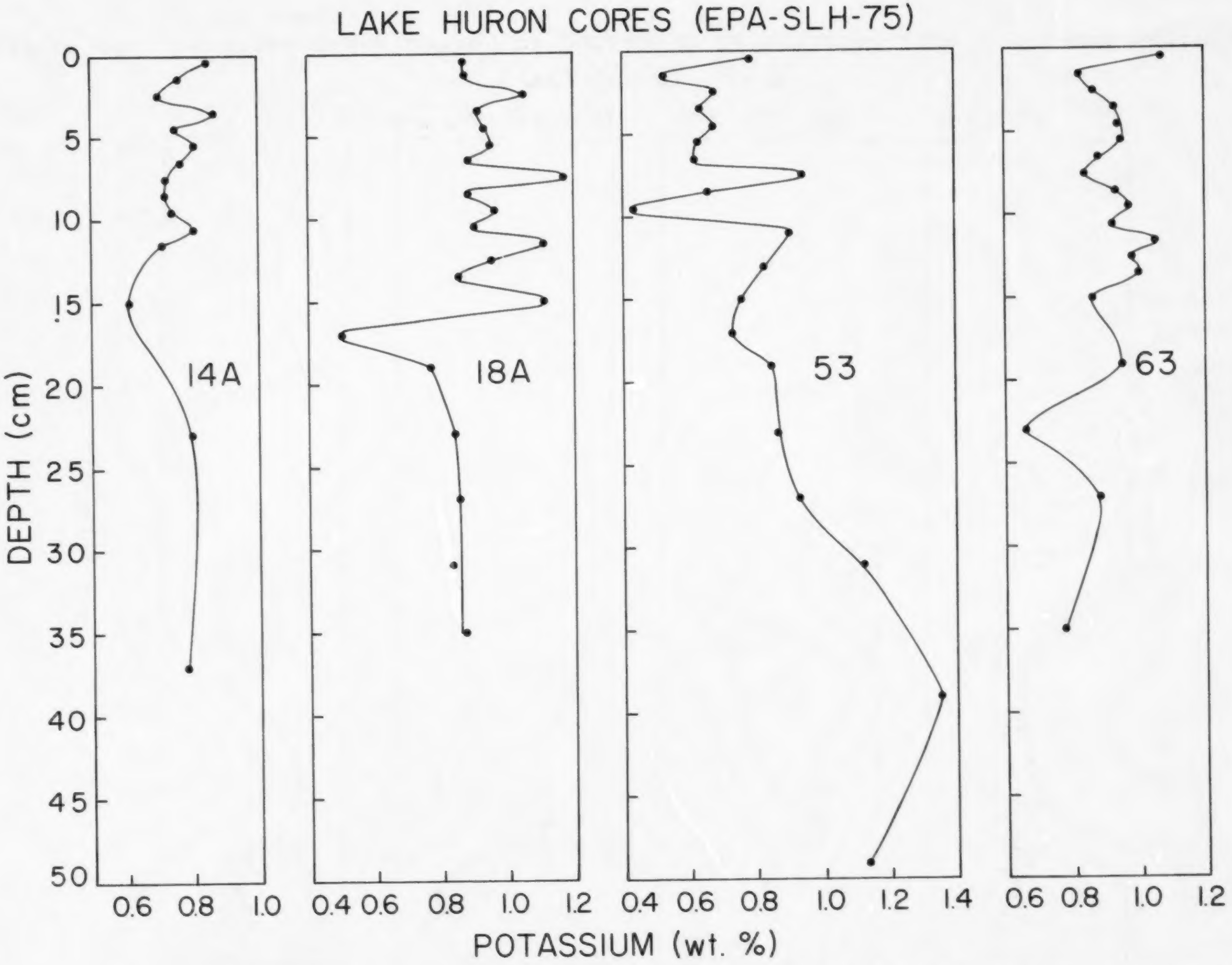

Figure 72. Vertical distribution of potassium in selected Goderich Basin cores.

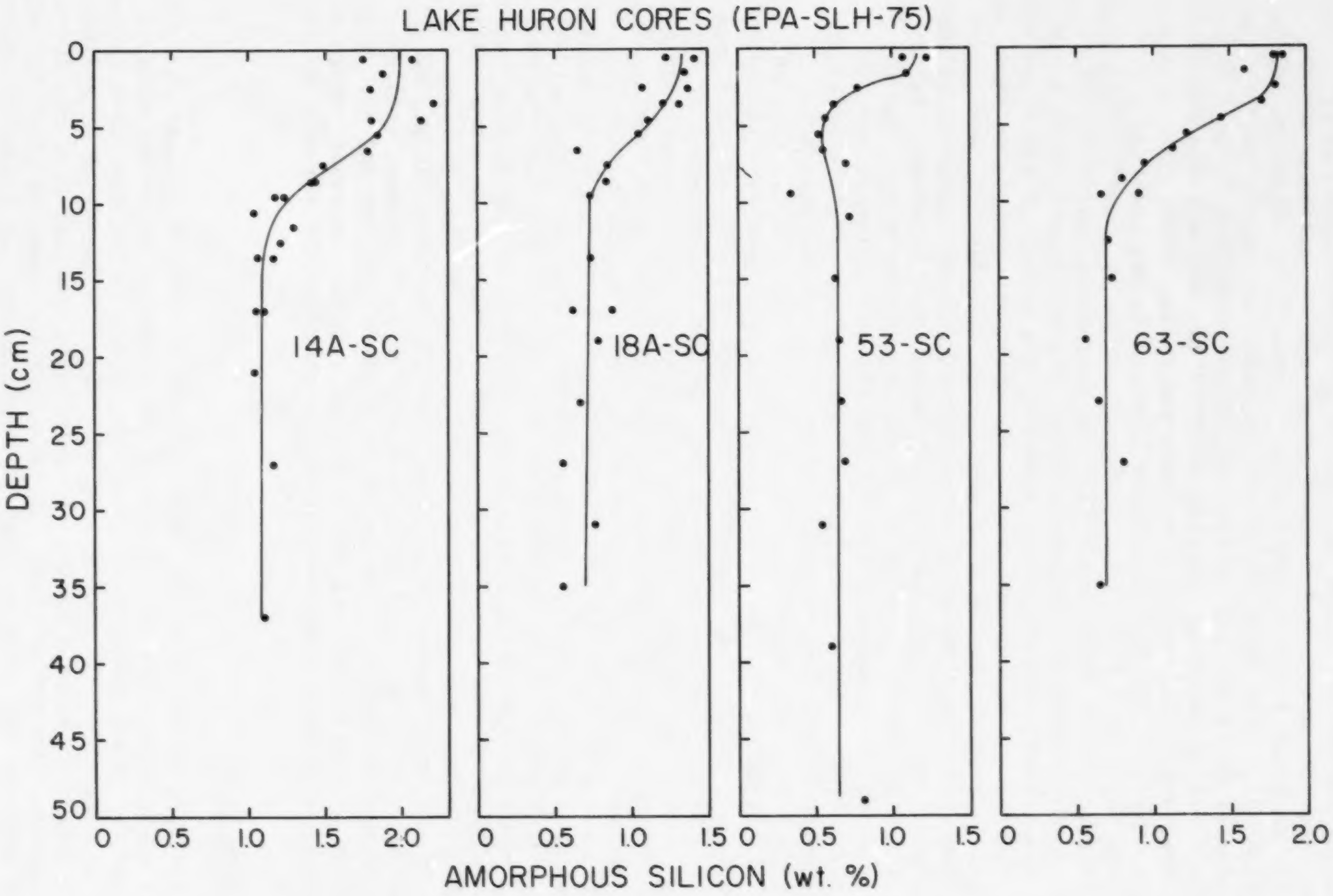

Figure 73. Vertical distribution of amorphous silicon in selected Goderich Basin cores.

sediment-water interface. While only one complete profile of Cd is available, concentration data for other cores includes not only surface values given in Table 9 but concentrations in underlying sediments (22-24 cm) given in Table 28. From Table 28, it can be seen that on the average the concentration of Cd in the 1-2 cm interval of sediment is 2.3 times higher than in the 22-24 cm section. Enrichment of Cd in surface sediments of Lake Huron has been previously reported by Kemp and Thomas (1976). In a core from the western margin of the Goderich Basin Kemp and Thomas observed a concentration ratio of 1.2 for Cd. While this value is significantly lower than the average, it is shown below that the enrichment factor itself is subject to large systematic variations within a given depositional basin, a result of considerable importance in assessing the impact of man's activities on the composition of recent sediments. The profiles of chromium shown in Figs. 75 and 76 suggest that this element is not significantly enriched. Apart from station 19 and 25 where Cr concentrations are depressed in surface sediments, profiles at other locations are essentially constant. As can be seen from Table 28, on the average Cr is not significantly enriched in surface sediments. For copper (Figs. 77 and 78) the sediments are consistently enriched near the surface. The exception is the profile at station 19 where sediments are inhomogeneous. On the average the surface-to-deep concentration ratio for Cu is 1.5 (Table 28). Kemp and Thomas (1976) observed a ratio of 1.7 in their single core from southern Lake Huron. Surface enrichment is even more pronounced for lead (Figs. 78 and 80). All profiles indicate a major increase in the concentration of lead (except 19) toward the sediment surface. In the one southern Lake Huron core described by Kemp and Thomas (1976) a six-fold increase in Pb concentration was found between the 20-30 cm section and 0-1 cm. Nickel is also consistently enriched in surface sediments located away from basin margins as can be seen in Figs. 81 and 82. The average surface to depth concentration ratio for this element is 1.7 (Table 28). The vertical distribution of tin (Fig. 83), exhibits a marked increase in the vicinity of the sediment-water interface. The more than five-fold enrichment of tin in core 18A-2 indicates that this is probably one of the most significantly enriched elements in sediments of the Great Lakes. Data below indicate that enrichments of this newly observed element probably are the result of anthropogenic loadings. Zinc is also appreciably enriched as can be seen in Figs. 84 and 85. With the exception of station 19, all profiles show a marked increase toward the sediment-water interface. The average concentration ratio for zinc is 2.2 (Table 28).

Cores at Station 18

All sections of the core (EPA-SLH-74-18-2) at station 18 were analyzed by neutron activation analysis. The data are given for major elements in Table 22 and for minor elements in Table 23. Profiles for the major elements are shown in Figure 86. It can be seen that with the exception of sodium, the concentration of major elements is essentially constant over the 50 cm length measured. The sodium (Na2) concentration increases by about 30% with increasing sediment depth and may reach a maximum value at around 30 cm depth.

In Figure 87 are shown examples of minor element (NAA) profiles while in Figure 88 are shown profiles of Zn, Pb, Ni, Cu (AAS) together with Cr and Sb

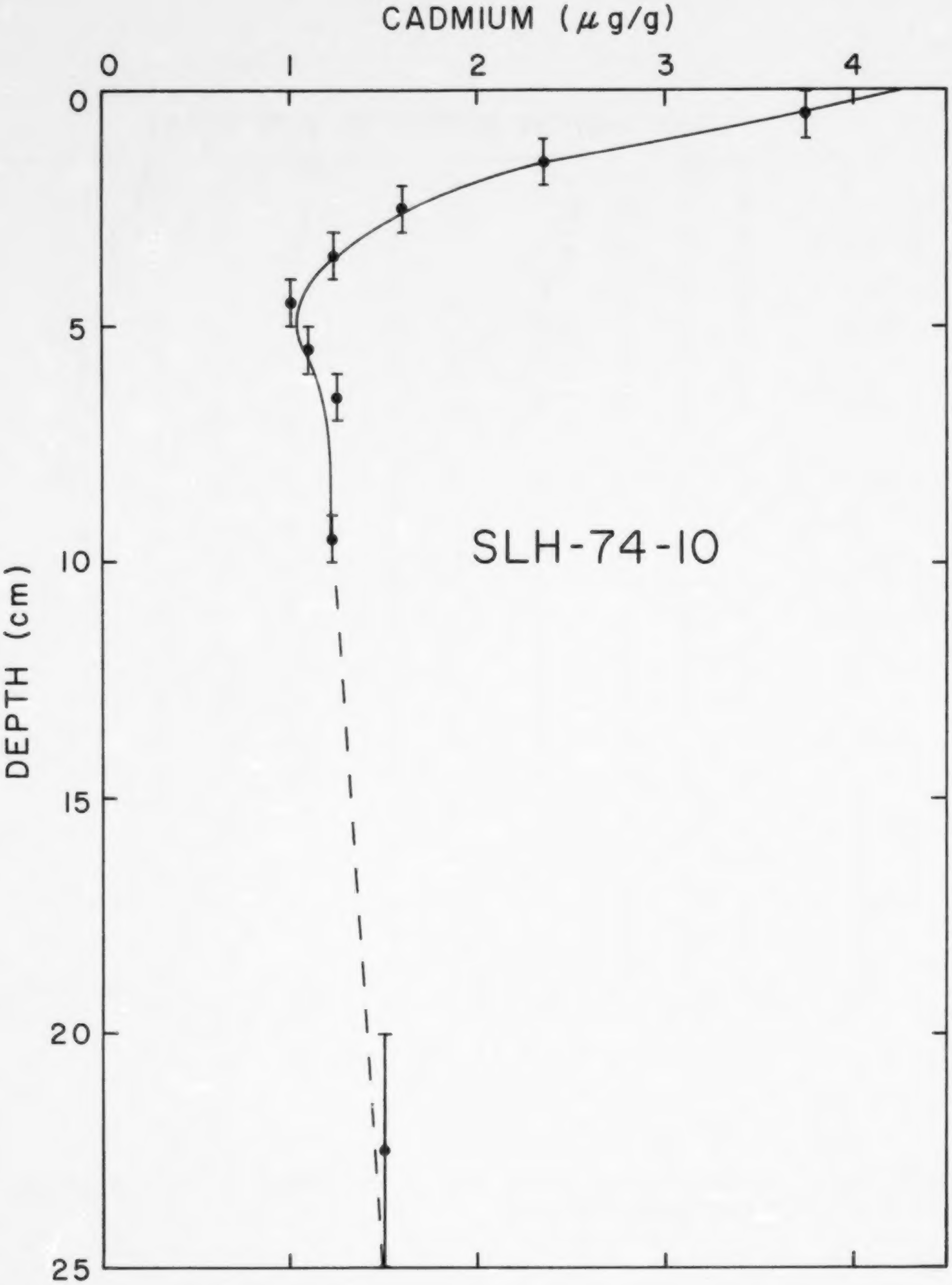

Figure 74. Vertical distribution of cadmium in a Port Huron Basin core.

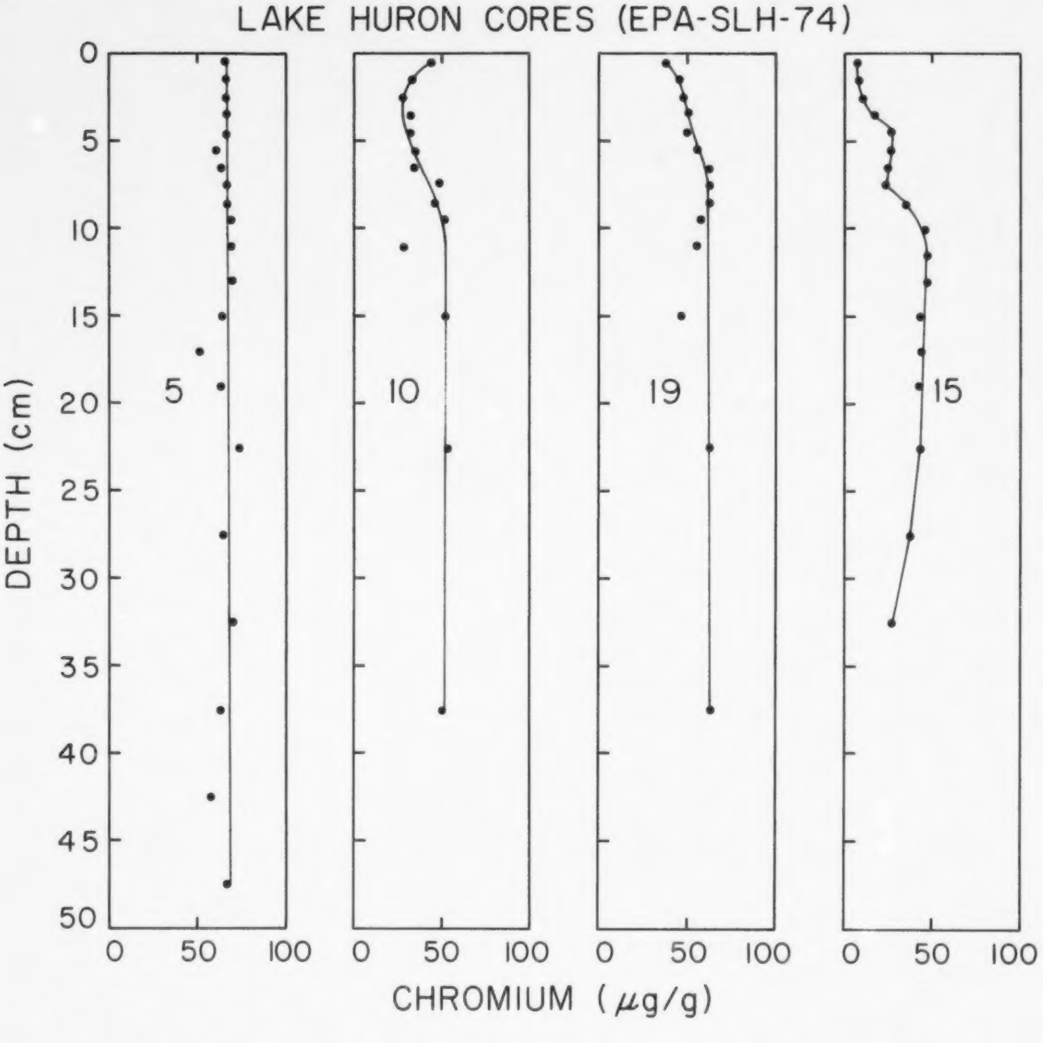

FIGURE 75. Vertical distribution of chromium in selected Port Huron Basin cores.

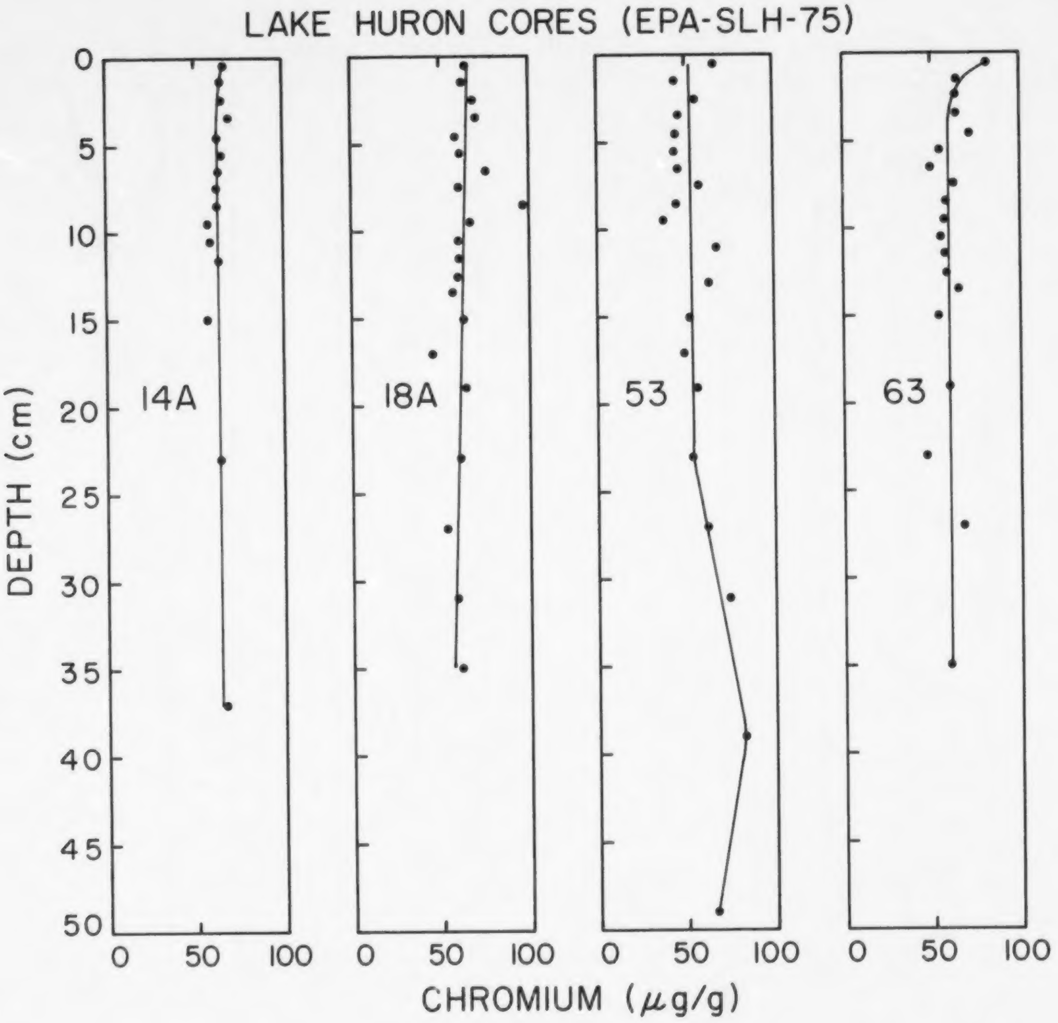

Figure 76. Vertical distribution of chromium in selected Goderich Basin cores.

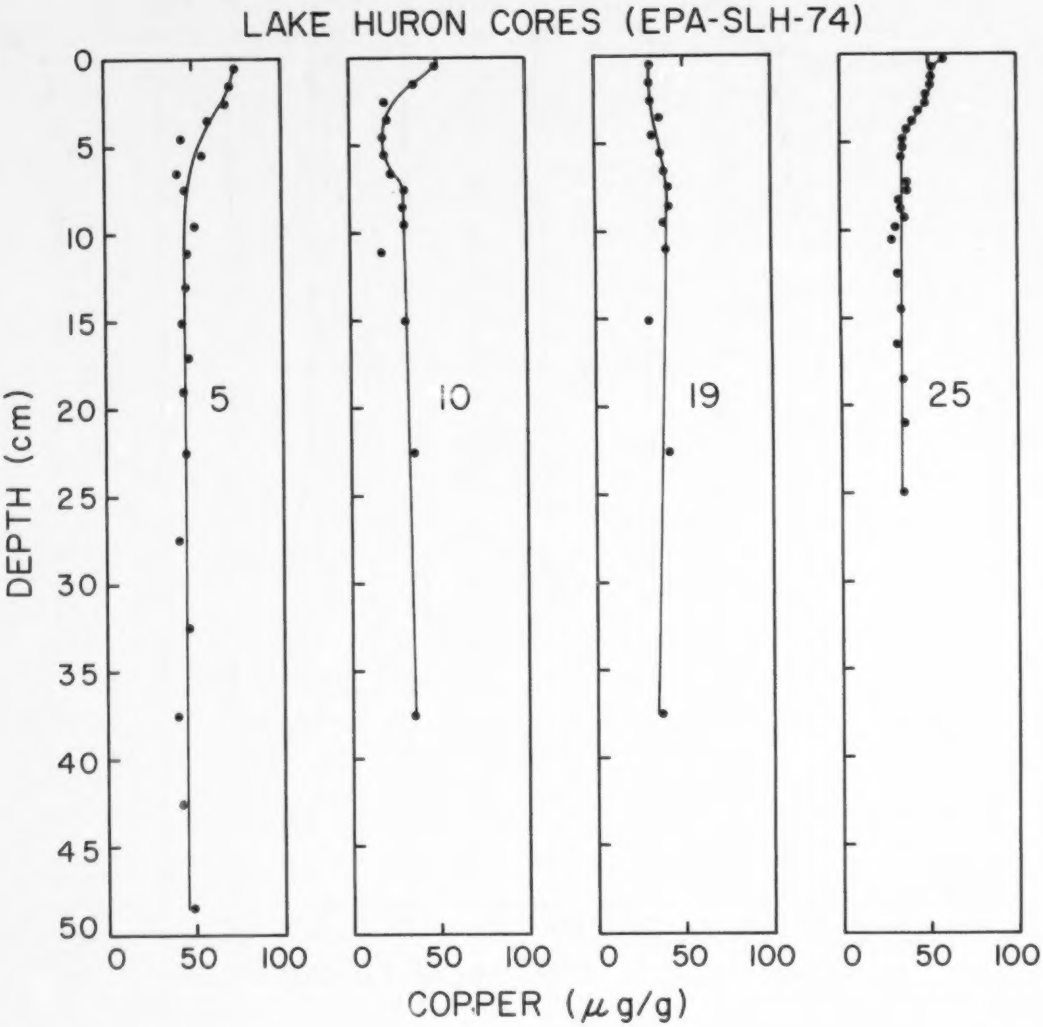

Figure 77. Vertical distribution of copper in selected Port Huron and Saginaw Basin cores.

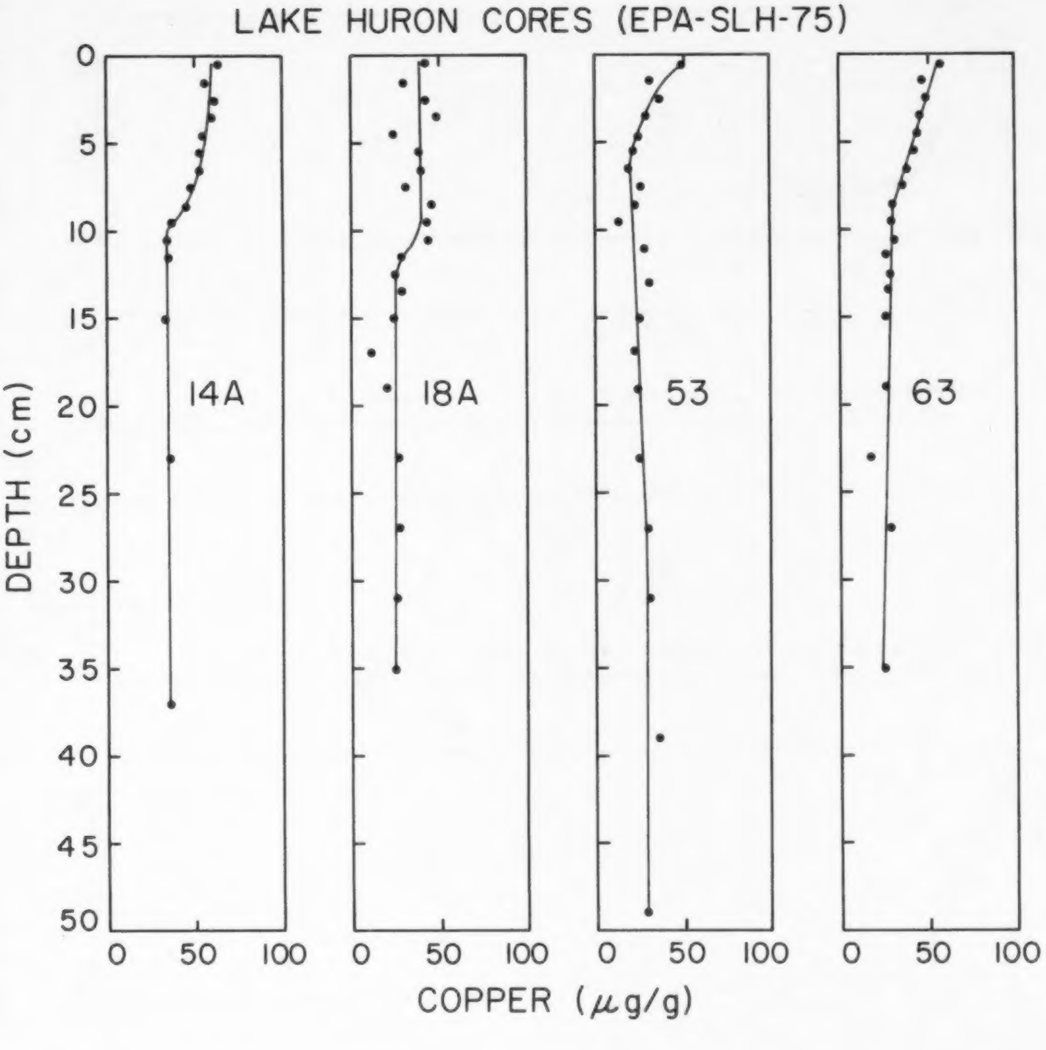

Figure 78. Vertical distribution of copper in selected Goderich Basin cores.

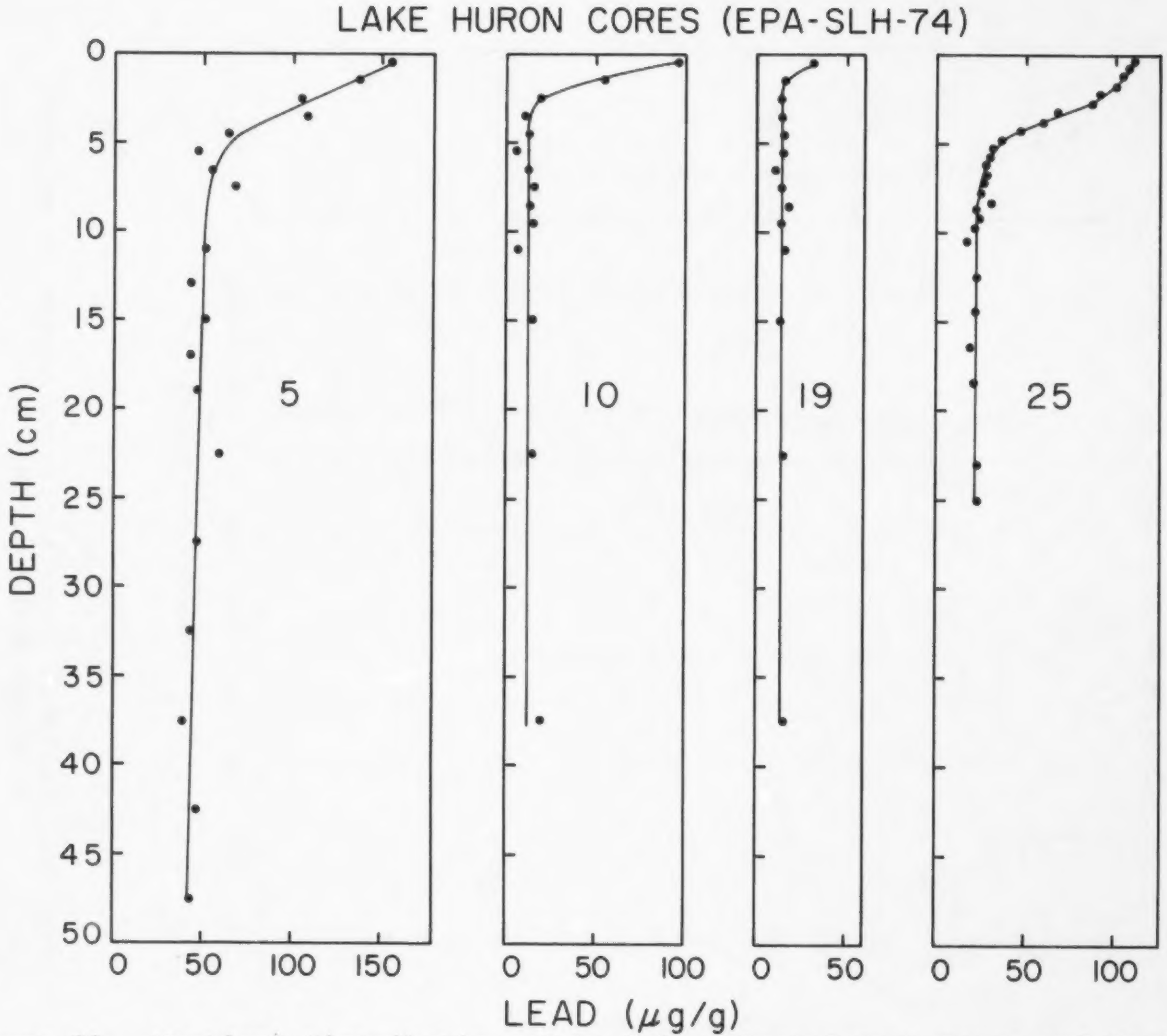

Figure 79. Vertical distribution of lead in selected Port Huron and Saginaw Basin cores.

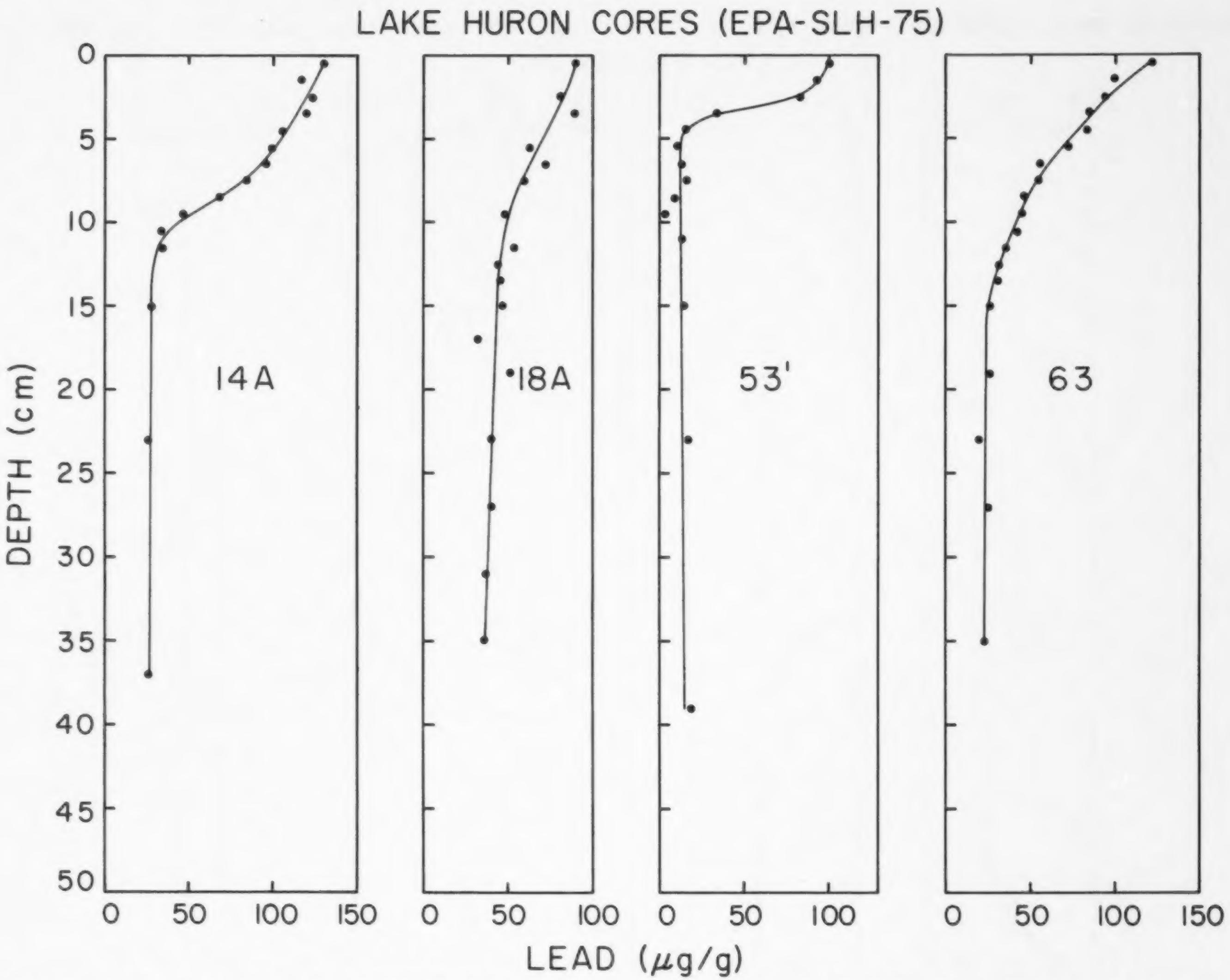

Figure 80. Vertical distribution of lead in selected Goderich Basin cores.

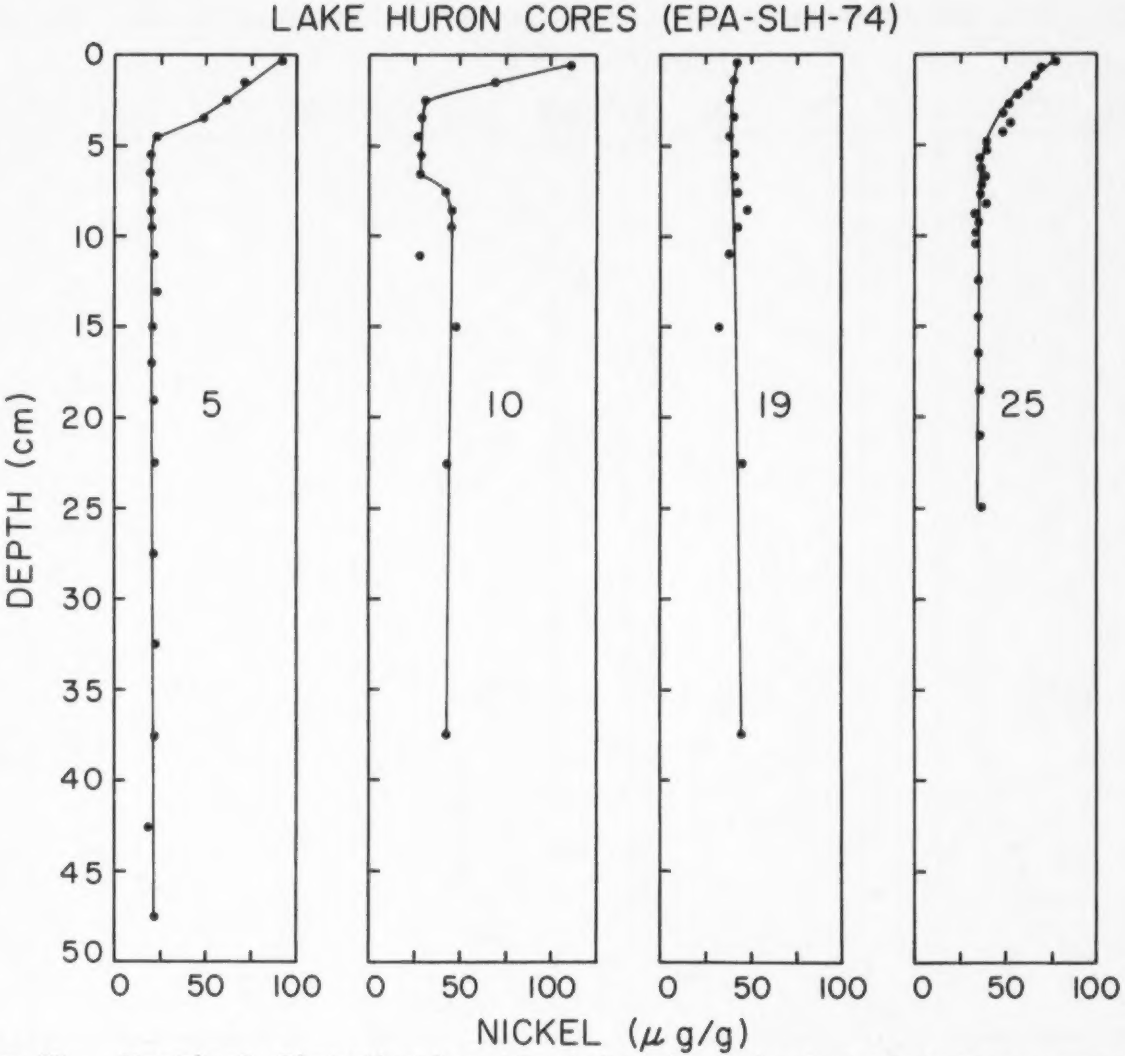

Figure 81. Vertical distribution of nickel in selected Port Huron and Saginaw Basin cores.

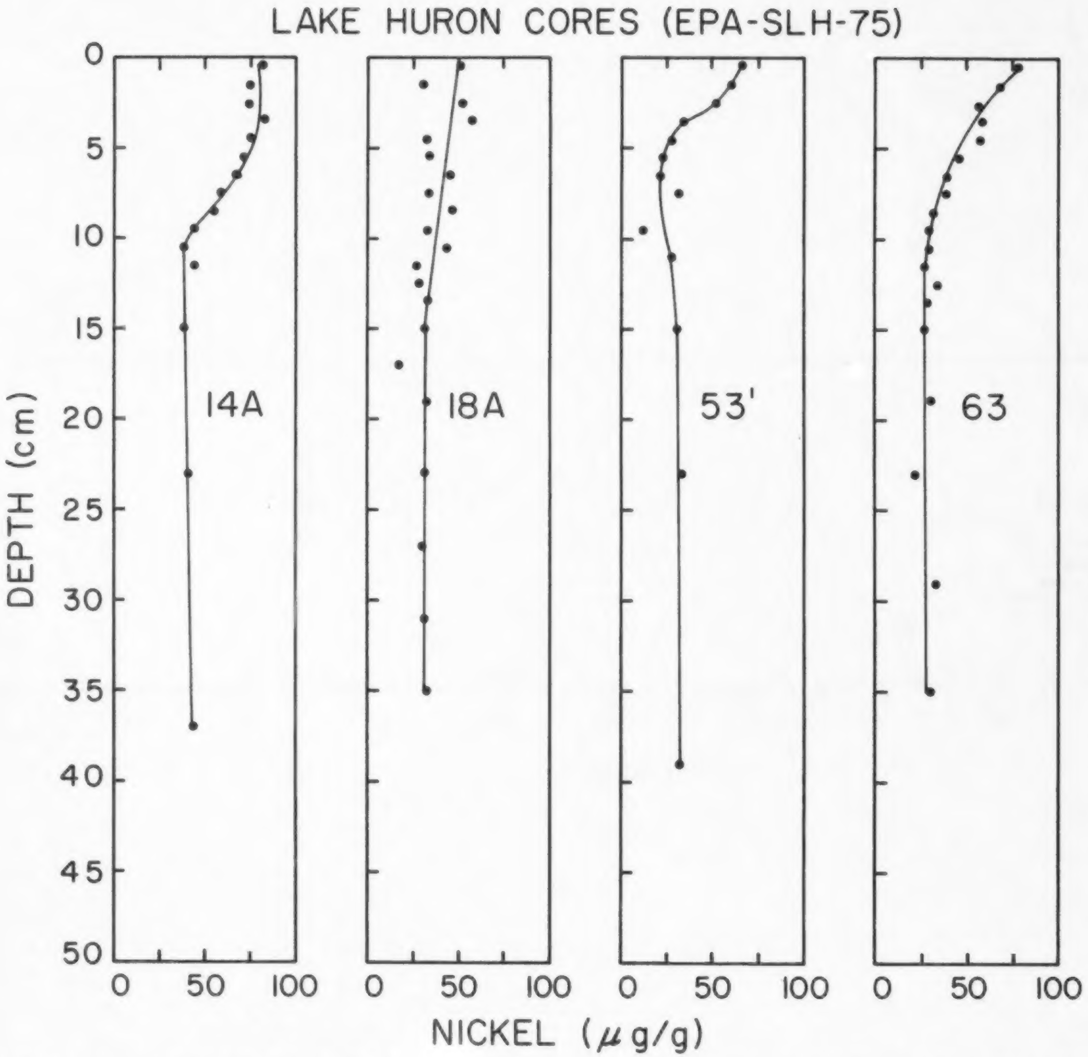

Figure 82. Vertical distribution of nickel in selected Goderich Basin cores.

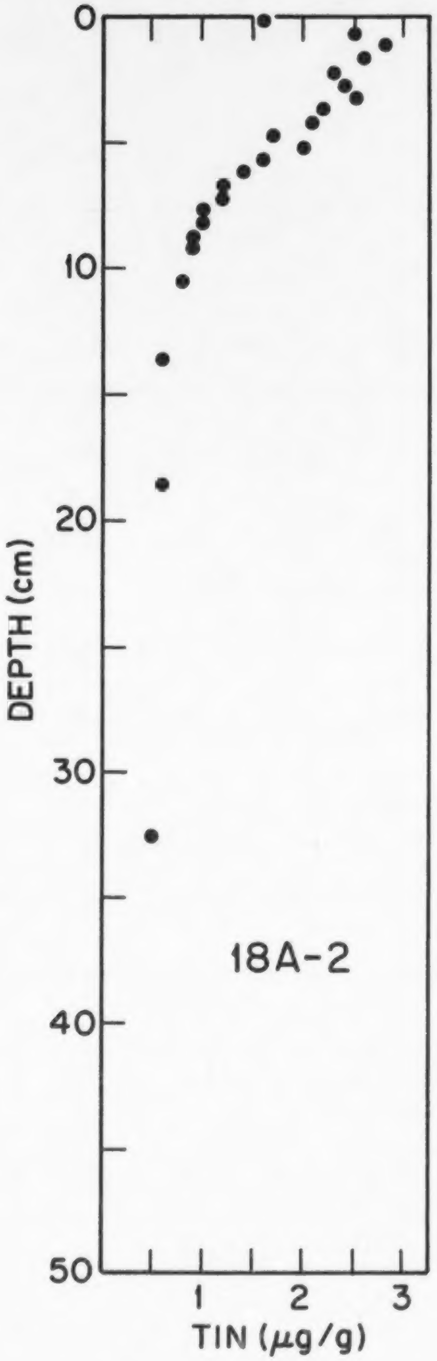

Figure 83. Vertical distribution on tin in a Goderich Basin core.

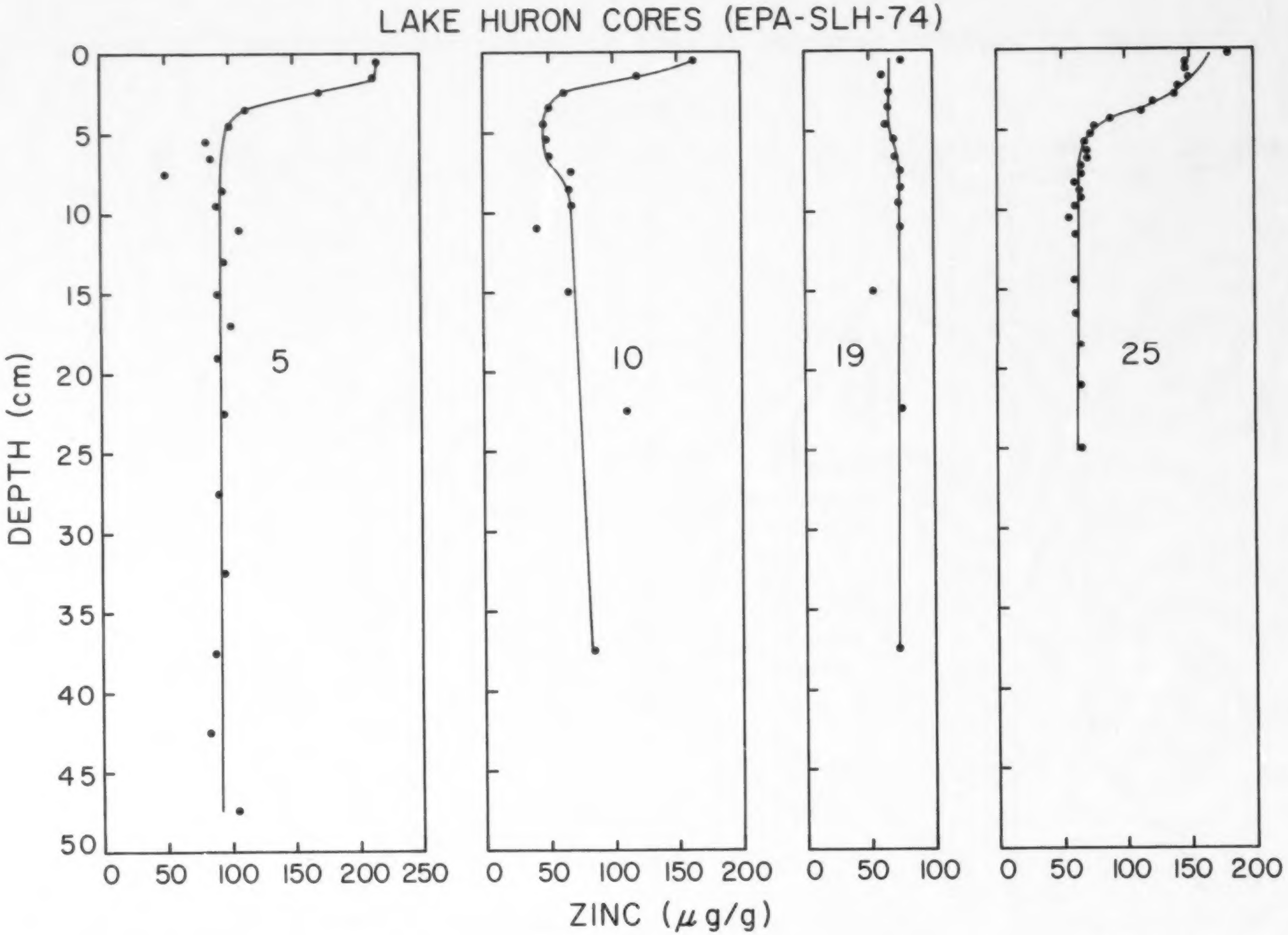

Figure 84. Vertical distribution of zinc in selected Port Huron and Saginaw Basin cores.

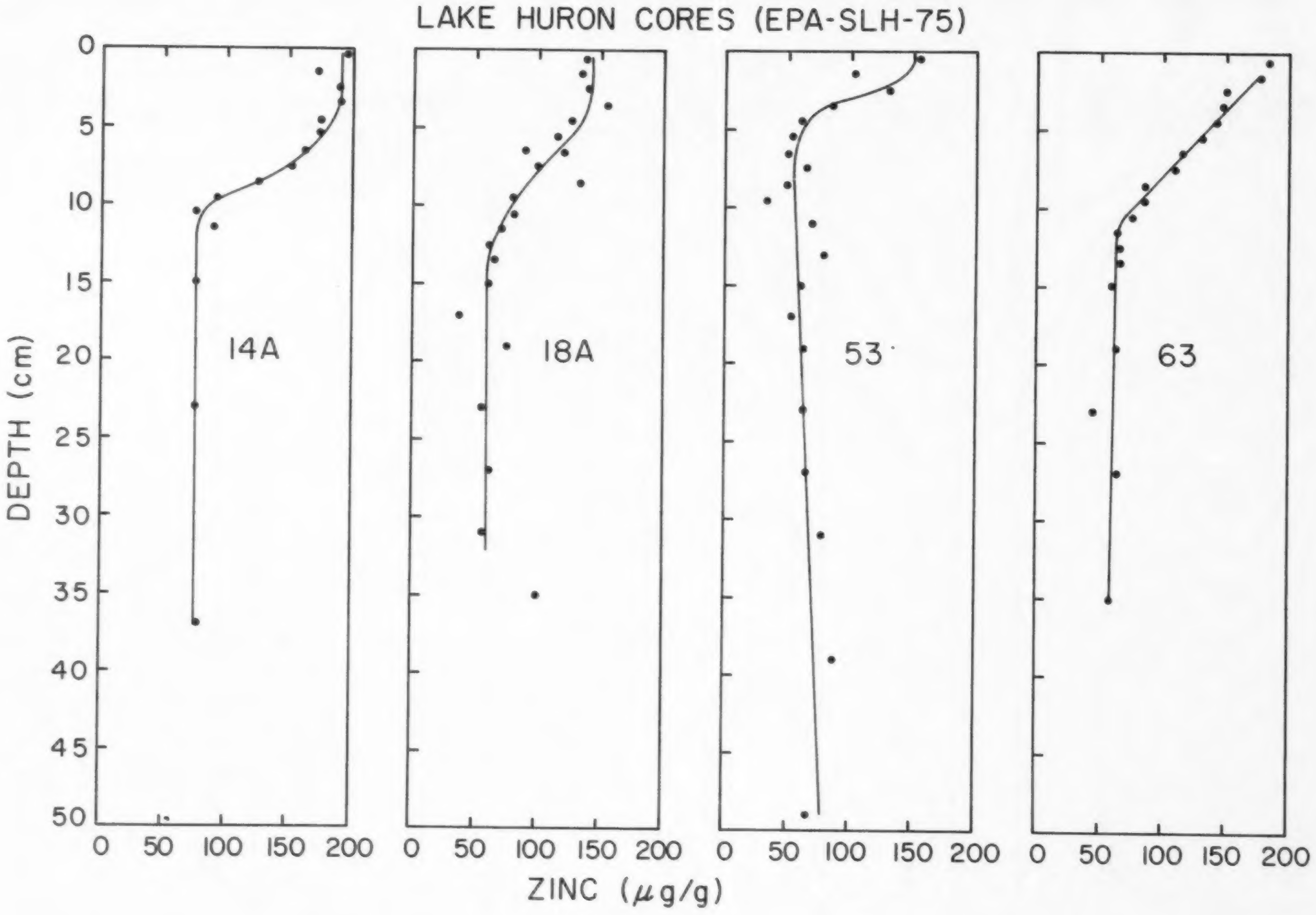

Figure 85. Vertical distribution of zinc in selected Goderich Basin cores.

TABLE 22. VERTICAL DISTRIBUTION OF MAJOR ELEMENTS IN WHOLE SEDIMENTS (NAA).
STATION EPA-SLH-74-18(2).

	Element (percent by weight)							
Depth (cm)	Al	Ca	Fe	K	Mg	Mn	Na	Ti
0.5-1	5.7	4.9	3.3	2.2	3.0	.130	0.70	0.38
1-2	5.9	4.9	3.0	2.0	2.3	.054	0.77	0.30
2-3	6.2	5.3	3.1	1.9	2.7	.054	0.71	0.45
3-4	5.6	4.7	3.0	2.6	3.4	.047	0.75	0.36
4-5	6.4	4.6	3.3	1.8	2.6	.050	0.64	0.39
5-6	5.9	4.9	3.2	2.4	3.1	.054	0.69	0.37
6-7	5.9	4.7	3.1	2.4	3.6	.052	0.73	0.31
7-8	6.9	5.5	3.0	-	3.2	.060	-	0.31
8-9	5.7	5.4	3.0	2.5	2.6	.048	0.76	-
9-10	6.5	5.5	3.2	2.3	2.7	.056	0.80	0.40
10-12	6.5	5.1	3.0	-	3.3	.060	-	0.34
12-14	5.9	5.3	3.0	1.9	2.8	.048	0.77	0.32
14-16	5.7	5.1	3.1	2.9	3.4	.048	0.80	0.32
16-18	-	-	-	-	-	-	-	-
18-20	6.0	5.7	2.9	2.6	3.6	.042	0.82	0.38
20-25	6.3	5.5	2.9	2.6	4.0	.045	0.88	0.25
25-30	-	-	2.9	-	-	-	-	-
30-35	5.6	4.5	2.8	3.0	2.1	.041	0.93	0.29
35-40	5.9	5.4	3.0	1.9	2.6	.039	0.75	0.37
40-45	6.1	4.8	2.9	-	2.1	.045	-	0.36
45-50	6.3	4.9	2.9	2.2	2.1	.039	0.72	0.44

TABLE 23. VERTICAL DISTRIBUTION OF MINOR ELEMENTS IN WHOLE SEDIMENT (NAA)
STATION EPA-SLH-74-18(2)

	Concentration (μg/g)											
Depth (cm)	As	Ag	Ba	Br	Ce	Co	Cr	Cs	Eu	Hf	Hg	La
0.5-1	16.1	<1.7	300	65.2	56.1	12.0	86.5	4.5	1.0	4.1	<1.0	29.1
1.2	10.6	<1.9	600	50.0	58.1	11.8	83.5	4.5	1.0	4.7	<1.0	31.2
2-3	9.5	<2.0	400	48.0	59.7	12.3	80.0	4.5	1.1	4.7	<1.2	32.1
3-4	9.7	<1.7	450	48.4	59.0	12.0	86.0	4.7	1.0	4.8	<1.1	31.1
4-5	8.9	<2.1	400	44.0	62.9	13.4	92.2	5.1	1.0	4.1	<1.2	34.3
5-6	3.6	<2.6	1200	51.8	62.7	13.0	92.2	4.2	1.0	4.7	<0.14	31.4
6-7	9.4	<1.7	300	46.2	60.0	12.0	81.4	4.7	1.0	4.6	<1.0	31.2
7-8	15.0±2	<2.0	900	38.5	58.9	11.9	67.3	3.9	1.0	3.9	<1.1	31.6
8-9	4.1	<2.3	900	46.2	59.4	11.7	76.4	3.7	0.95	4.3	<0.1	29.6
9-10	8.5	<2.1	600	43.6	62.2	12.9	71.6	4.5	1.1	4.9	1.3	35.2
10-12	<7.0	<2.1	800	47.1	56.9	11.7	69.5	3.8	1.9	3.8	<1.2	31.1
12-14	9.2	<1.9	500	44.9	58.2	11.8	79.8	4.2	1.0	4.3	<1.1	32.1
14-16	4.9	<2.5	500	52.8	62.1	12.3	79.7	3.5	1.1	4.3	<0.13	31.5
16-18	<7.1	<2.1	500	41.4	59.8	12.2	63.7	4.1	1.1	4.6	<1.3	32.0
18-20	7.5	<1.7	500	45.7	60.1	11.4	83.8	3.8	1.0	5.0	<1.0	32.4
20-25	4.0	<2.3	300	44.7	58.9	11.5	65.8	4.2	1.1	4.9	<0.1	29.3
25-30	<6.8	<2.1	400	45.4	58.7	11.6	69.6	4.1	1.0	4.3	<1.1	31.0
30-35	2.9	<2.5	800	43.5	60.3	11.7	75.0	3.7	0.96	4.5	<0.14	29.9
35-40	7.9	<2.0	500	45.5	63.0	12.3	73.8	4.3	1.1	5.1	<1.2	34.8
40-45	7.2	<2.1	700	40.7	60.6	11.7	69.6	4.0	1.0	4.3	<1.2	32.4
45-50	5.7	<2.4	300	42.0	61.4	12.2	66.9	4.2	1.2	4.9	<0.1	31.6
represent. uncertainty	±.6	±2	±150	±3	±1.0	±.2	±1	±.2	±.06	±.2	±1	±.8

(continued).

TABLE 23. (continued).

Depth (cm)	Concentration (μg/g)										
	Lu	Ni	Rb	Sb	Sc	Se	Sm	Th	U	V	Yb
0.5–1	0.34	<42.7	59.1	0.89	9.8	2.8	5.5	12.1	2.8	79	2.4
1–2	0.30	55.0	90.0	0.85	10.2	<3.1	5.1	8.0	4.8	90	2.5
2–3	0.41	<47.2	86.3	0.87	10.3	<3.2	5.6	9.0	2.7	95	2.2
3–4	0.32	68.7	55.8	1.10	10.4	<2.0	5.4	10.4	3.5	83	2.6
4–5	0.37	56.5	80.7	0.94	11.0	<2.6	5.7	10.9	3.7	102	2.6
5–6	0.40	<76.6	95.2	1.28	10.7	4.3	5.5	9.3	2.7	77	2.2
6–7	0.39	57.4	61.3	1.00	10.7	2.7	5.8	10.8	2.6	85	2.3
7–8	0.26	<57.7	95.5	0.79	10.0	<2.5	4.8	8.6	2.8	85	2.6
8–9	0.35	<69.9	77.6	1.10	10.0	3.7	5.2	9.1	2.1	73	1.9
9–10	0.41	<48.0	87.6	0.57	11.0	<3.3	5.8	9.0	3.7	93	2.7
10–12	0.30	<61.5	94.8	0.54	10.1	<2.6	4.5	7.9	3.4	99	2.4
12–14	0.21	50.7	70.8	0.56	10.4	<2.4	5.5	9.6	3.5	87	3.1
14–16	0.44	<76.1	85.7	0.41	10.8	<3.9	5.5	10.0	2.5	76	2.1
16–18	0.34	<75.6	96.3	0.46	10.8	<2.8	5.5	10.5	3.6	-	2.7
18–20	0.35	<42.9	60.4	0.35	10.6	<2.0	5.8	11.1	2.3	80	2.5
20–25	0.54	<62.0	114.0	0.23	10.2	<5.3	4.8	7.6	3.4	96	3.0
25–30	0.37	<60.0	103.0	0.41	10.1	<2.6	5.1	8.7	2.2	-	2.4
30–35	0.34	<75.0	80.0	0.59	10.2	<4.9	5.4	9.5	2.4	78	2.1
35–40	0.47	<46.0	81.9	0.27	10.8	3.9	6.0	8.3	2.9	85	2.1
40–45	0.41	66.0	95.8	0.35	10.5	<2.6	5.2	8.3	2.1	91	2.7
45–50	0.45	76.0	102.0	0.34	10.3	<5.7	5.6	8.0	2.2	120	2.6
represent. uncertainty	±.1	±60	±8	±.2	±.1	±2	±.1	±.9	±.8	±8	±.5

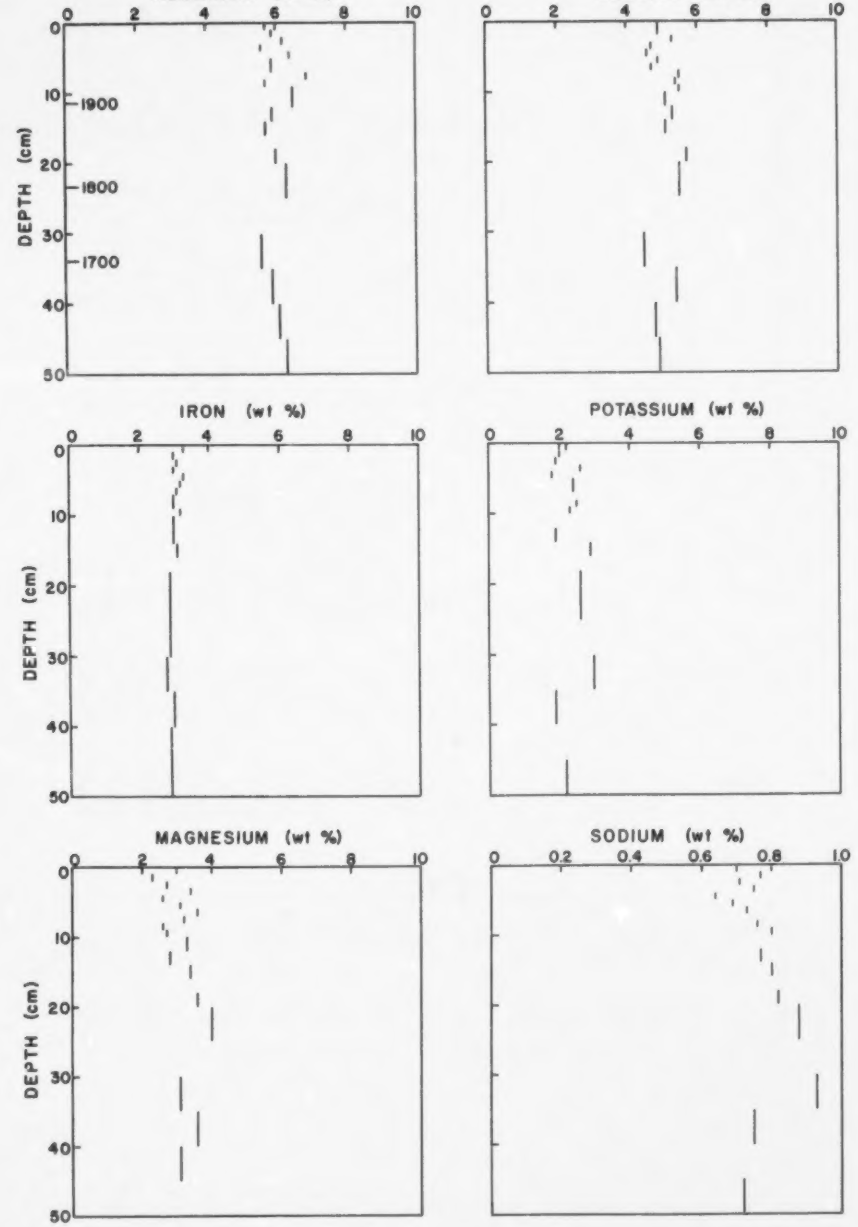

Figure 86. Vertical distribution of major elements (NAA) in Goderich Basin core (74-18-2).

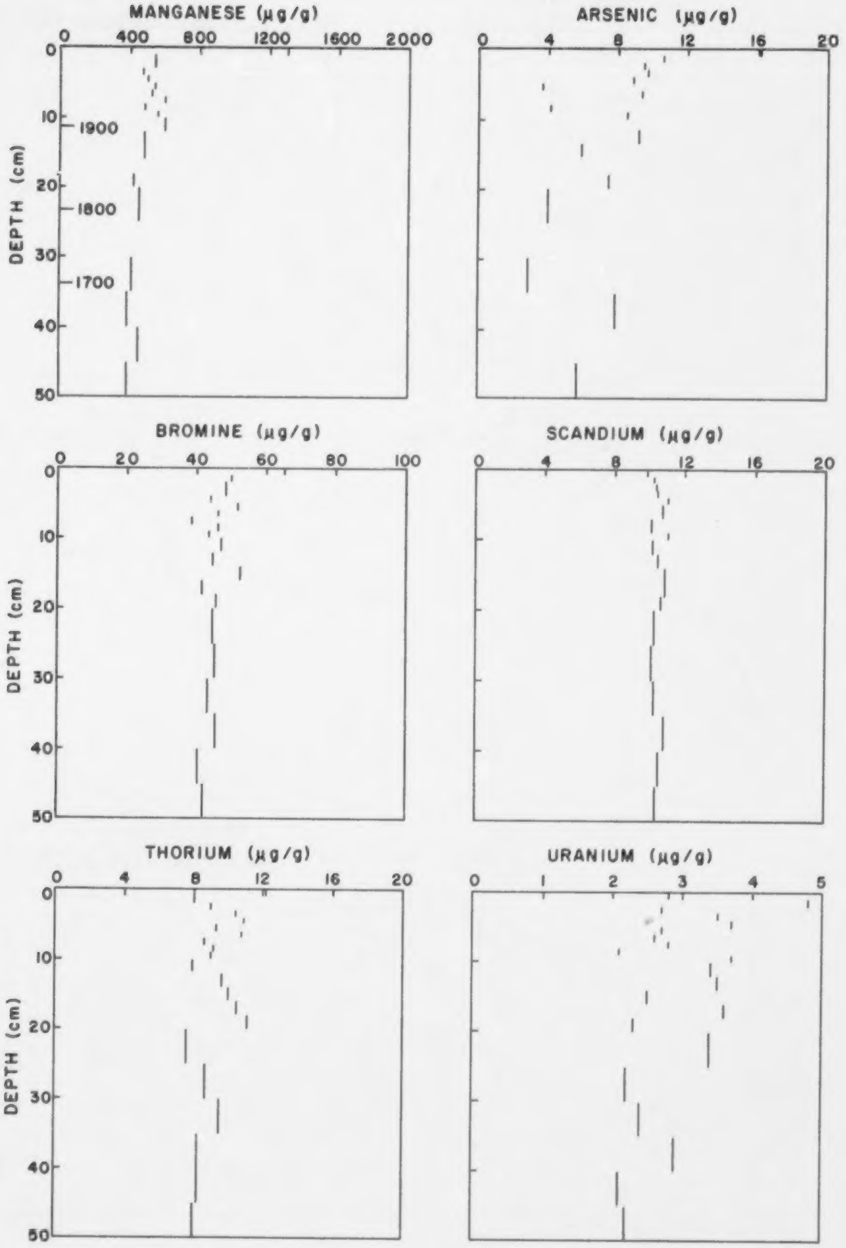

Figure 87. Vertical distribution of minor elements (NAA) in Goderich Basin core (74-18-2).

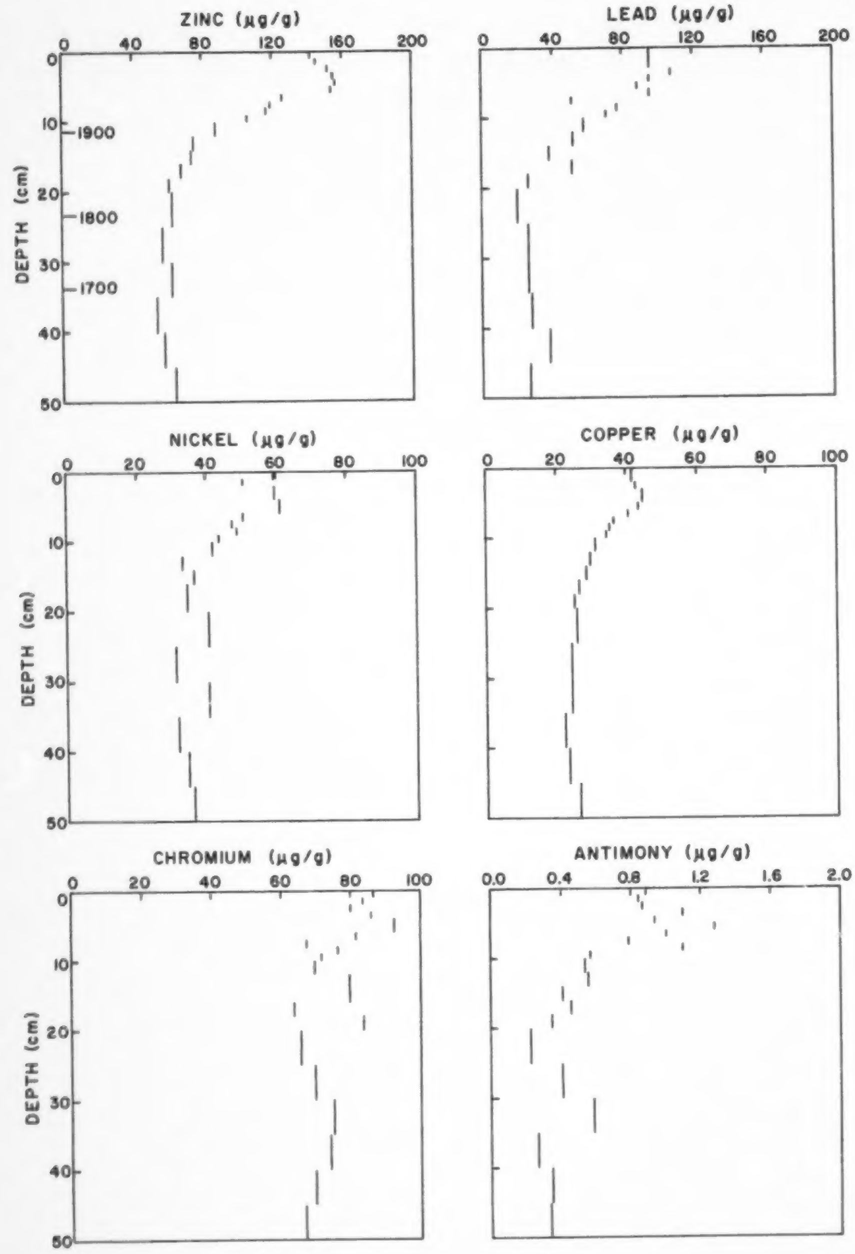

Figure 88. Vertical distribution of elements in Goderich Basin core (74-18-2) possessing a significant a significant degree of enrichment. (Cu, Ni, Pb, Zn: via AAS; Cr and Sb via NAA).

(NAA). From these figures it can be seen that Mn and perhaps Br are enriched only in the uppermost sediment layer while two elements determined via NAA show the characteristic anthropogenic profile, As and Sb. The mean ratio of element concentrations determined via AAS and via NAA for this core are given in Table 24. The ratios (extraction efficiencies) compare favorably with those determined for surface sediments (Table 18) and for standard mud samples (Table 6). The surface-to-depth concentration ratios and enrichment factors (defined below) are summarized in Table 25 for this core. Vertical distribution of elements determined via AAS in core 18A are given in Table 26.

ENRICHMENT FACTORS

This study as well as many others has shown that nearly all minor sedimentary constituents are associated with fine-grained materials. To eliminate the effect of small inhomogeneities in the distribution of fine or inert materials on measures of the degree of surface enrichment of trace elements, Kemp et al. (1976) introduced the concept of the sediment enrichment factor (SEF) defined in terms of the ratio of element concentrations to that of aluminum. Aluminum is taken as a measure of the clay mineral, or fine-grained sediment concentration. The SEF is defined as:

$$\mathrm{SEF} = \frac{(C_s/Al_s) - (C_d/Al_d)}{(C_d/Al_d)} \qquad (35)$$

where C_s = the observed elemental concentration in the surface cm of sediments (1-2 cm)

C_d = the precultural elemental concentration in a sufficiently deep layer

Al_s = the aluminum concentration in surface sediments (1-2 cm)

Al_d = the aluminum concentration in a sufficiently deep layer

Kemp et al (1976) took layers of sediment below the Ambrosia horizon (ragweed) corresponding to about 130 years b.p. for estimating C_d and Al_d. A simpler but valid technique is to choose these values as the average over an interval sufficiently deep that concentrations are constant. This approach has been taken in the construction of SEFs in Table 25. In this Table values of C_d and Al_d are calculated as the average of concentrations in the lowermost four sediment sections. When there is essentially no change in the concentration of aluminum with depth, as in the case of the core at station 18, the SEF reduces to $(C_s - C_d)/C_d$. When there is a significant variation in the concentration of Al with depth, the unnormalized enrichment factor might give a false picture of the extent of surface enrichment. As can be seen in Table 25 only a few elements (Fe, Mn, As, Br, Cr, and Sb) have any significant degree of enrichment in this core. The rest are not enriched and are "conservative" (Kemp et al., 1976) in that their relative proportion in sedimentary materials has not been changed as a result of mans' recent impact on the Lakes. (Sodium shows a slight negative "enrichment").

TABLE 24. MEAN RATIO OF ELEMENT CONCENTRATIONS DETERMINED VIA AAS AND VIA NAA FOR CORE EPA-SLH-74-18-2

Element	Ratio (± Standard Error)*
Ca	0.83 ± 0.01
Cr	0.71 ± 0.02
Fe	0.89 ± 0.01
K	0.31 ± 0.01
Mg	1.06 ± 0.04
Mn	0.96 ± 0.02
Na	0.14 ± 0.01

*Ratio = conc. via AAS/conc. via NAA averaged over all depth intervals.

TABLE 25. CONCENTRATION OF ELEMENTS DETERMINED VIA NAA IN SURFACE AND IN UNDERLYING SEDIMENTS, CONCENTRATION RATIOS AND ENRICHMENT FACTORS (BASED ON Al NORMALIZATION) FOR CORE EPA-SLH-74-18-2

Element	Concentration* Surface	Concentration* Deep	Ratio	Enrichment Factor**
Major				
Al	5.93	5.98	1.0	0
Ca	5.0	4.9	1.0	0
Fe	3.1	2.9	1.1	0.07
K	2.0	2.4	0.83	0
Mg	2.7	2.3	1.1	0
Mn	.08	.04	2.0	1.0
Na	.73	.82	0.89	-0.11
Ti	.38	.37	1.0	0
Minor				
As	12.1	5.9	2.1	1.1
Ba	433	580	.75	0
Br	54.4	42.9	1.30	0.27
Ce	58.0	61.3	0.95	0
Co	12.0	12.0	1.0	0
Cr	83.3	71.3	1.2	0.17
Cs	4.5	4.1	1.1	0
Eu	1.0	1.1	.91	0
Hf	4.5	4.7	.96	0
La	30.8	32.0	.96	0
Lu	35.0	34.3	1.0	0
Rb	78.4	90.0	.87	0
Sb	0.87	0.38	2.3	1.3
Sc	10.1	10.2	1.0	0
Sm	5.4	5.5	0.98	0
Th	9.7	8.5	1.0	0
U	3.4	2.4	1.4	∿ 0
V	88	94	0.94	0
Yb	24.0	23.0	1.04	0

* major elements in (wt %) minor elements in (μg/g). Surface concentration is the average over upper 3 cm. Deep concentration = average of values in deepest four sections.

**set = to zero if not statistically significant.

TABLE 26. VERTICAL DISTRIBUTION OF ELEMENTS (AAS) IN CORE EPA-SLH-75-18A-2

Interval (cm)	Fraction Soluble (g/g)	Major Elements (wt %)				Minor Elements (ppm)						
		Ca	Fe	Mg	Mn ($x10^{-2}$)	Cr	Cu	Hg	Ni	Pb	Sn	Zn
0.0-0.5	0.343	4.31	3.14	2.72	4.60	52.9	37.2	0.14	59.0	90.9	1.6	114
0.5-1.0	0.315	4.30	3.42	3.03	8.00	50.2	34.9	0.15	53.9	97.8	2.5	108
1.0-1.5	0.385	4.91	3.13	3.22	4.49	52.9	39.1	0.14	55.6	98.2	2.8	129
1.5-2.0	0.350	4.82	2.90	3.17	4.23	55.7	38.9	0.11	60.0	91.9	2.6	126
2.0-2.5	0.375	4.77	3.64	3.16	4.27	55.6	40.7	0.14	62.8	94.6	2.3	136
2.5-3.0	0.365	4.82	3.27	3.20	4.46	58.3	39.8	0.17	61.1	89.9	2.4	129
3.0-3.5	0.375	4.56	3.61	3.08	4.83	60.9	41.4	0.14	64.6	88.9	2.5	136
3.5-4.0	0.364	4.46	3.36	3.07	4.92	59.6	41.7	0.13	61.7	85.1	2.2	136
4.0-4.5	0.370	4.62	3.05	3.10	4.55	55.7	39.5	0.12	55.8	80.3	2.1	120
4.5-5.0	0.345	4.66	3.45	3.08	4.49	55.3	35.9	0.12	47.4	66.3	1.7	110
5.0-5.5	0.345	4.71	3.28	3.16	4.26	48.5	34.3	0.12	48.0	61.9	2.0	100
5.5-6.0	0.355	5.18	3.26	3.45	4.36	44.9	30.8	0.10	46.3	55.3	1.6	94.6
6.0-6.5	0.394	5.23	2.42	3.32	3.96	42.4	30.8	0.11	42.6	54.6	1.4	94.0
6.5-7.0	0.372	4.82	2.83	3.10	4.45	51.0	32.4	0.11	42.7	59.1	1.2	114
7.0-7.5	0.382	5.03	3.02	3.23	4.36	52.3	31.1	0.11	44.0	55.3	1.2	90.3
7.5-8.0	0.382	5.38	3.26	3.40	4.08	46.1	27.9	0.09	39.8	50.0	1.0	79.1
8.0-8.5	0.354	4.81	3.01	3.16	4.45	48.5	28.8	0.10	39.2	51.4	1.0	77.9
8.5-9.0	0.330	4.50	2.79	2.97	4.07	44.8	26.8	0.11	39.7	46.6	0.9	71.1
9.0-9.5	0.361	5.12	2.89	3.25	4.35	49.7	27.2	0.06	39.1	44.7	0.9	68.4
9.5-10	0.340	5.38	3.02	3.42	5.01	51.0	26.6	0.06	39.2	44.7	-	65.2
10-11	0.361	5.53	2.89	3.60	4.73	51.9	25.0	0.05	38.0	38.0	0.8	62.5
11-12	0.366	5.22	3.01	3.44	4.45	45.8	24.3	0.03	38.5	36.1	-	61.2
12-13	0.336	4.76	2.98	3.22	4.08	45.8	23.3	0.03	37.3	33.7	-	60.1
13-14	0.327	4.76	3.23	3.19	3.98	48.2	23.3	-	36.8	32.2	0.6	58.9
14-15	0.449	5.38	3.33	3.56	3.99	49.5	22.7	-	35.6	32.3	-	53.5
15-16	0.354	5.13	2.92	3.39	3.80	47.1	21.9	0.04	35.7	31.3	-	55.7
16-17	0.345	4.97	2.80	3.26	3.70	45.8	21.7	-	33.8	26.7	-	52.3

(continued)

TABLE 26. (continued)

Interval (cm)	Fraction Soluble (g/g)	Major Elements (wt %)				Minor Elements (ppm)						
		Ca	Fe	Mg	Mn ($x10^{-2}$)	Cr	Cu	Hg	Ni	Pb	Sn	Zn
17-18	0.227	4.97	2.40	3.26	3.71	42.3	21.1	-	33.9	29.4	-	50.2
18-19	0.340	4.87	2.86	3.22	4.40	49.5	23.3	0.02	38.6	30.3	0.6	54.6
19-20	0.372	4.81	2.92	3.28	4.21	53.0	24.3	-	40.3	31.2	-	56.7
20-22	0.358	5.08	3.58	3.39	3.89	47.1	23.0	-	37.4	31.3	-	52.4
22-24	0.366	5.28	3.20	3.51	4.17	50.7	23.5	0.04	38.0	29.4	-	56.8
24-26	0.243	4.81	2.08	3.13	3.42	47.0	21.4	-	32.7	27.4	-	47.9
26-28	0.342	5.16	2.58	3.38	3.74	47.0	22.6	-	35.0	28.4	-	53.4
28-30	0.362	5.64	2.55	3.64	4.04	48.3	23.0	0.03	36.2	30.3	-	52.4
30-35	0.351	5.07	3.01	3.32	3.89	49.5	23.3	-	35.6	30.8	0.5	53.5
35-40	0.380	5.64	2.58	3.67	3.80	49.5	24.0	0.03	36.2	30.3	-	53.5
40-45	0.376	5.38	2.71	3.51	3.66	53.1	23.0	0.03	36.8	30.4	-	53.5
45-50	0.348	4.90	2.52	3.26	3.62	50.8	24.3	-	35.7	30.9	-	56.4

In Tables 27 and 28 are listed the enrichment factors for 29 additional cores. Because Al concentrations were not determined for these cores, an alternative normalization was used. As shown previously, the fraction soluble (Fsol) is, as expected, a composite of carbonate materials and organic carbon and iron-associated constituents. Thus normalization to Fsol eliminates the effect of dilution of sediments by inert (non acid-soluble) materials on the estimate of the enrichment factor. A normalization to Fe rather than Fsol is probably somewhat more analogous to the Al normalization used by Kemp et al. (1976) but in the present case the values of the enrichment factors are largely independent of whether Fsol or Fe is used.

The degree of near-surface enrichment for the non-conservative elements varies strongly with location as can be seen in Figs. 89-95. The distribution of enrichment factors tends to follow the distribution of fine-grained constituents with highest values tending to occur toward the centers of the two depositional basins. However, the distribution patterns are generally not strongly correlated as can be seen in Table 29. Zn and Cu have the best correlated enrichment factors, with $r = 0.89$ ($N = 26$); those for Pb and Mn also are significantly correlated, with $r = 0.67$ ($N = 26$). The remaining correlations between enrichment factors are appreciably less. This study represents the first observation of the systematic spatial variability in enrichment factors. The degree of enrichment of surface sediments relative to background levels is not a unique characteristic of the lake or even of a given depositional basin but rather shows nearly as much spatial variability as do element concentrations themselves.

Mean surface-to-deep concentration ratios and enrichment factors for all elements measured in more than one core are given in Table 30. Also given in Table 30 is the coefficient of correlation between elemental concentrations in near-surface and in underlying sediments. Clearly when surface and deep concentrations are identical not only must $Ef = 0$ but the correlation coefficient must equal 1.00. On the other hand, for elements with a high degree of enrichment there is no a priori reason why the correlation between surface and deep concentrations should remain high. Defining the degree of unrelatedness as $-\ln r$, a linear regression of the enrichment factor versus this variable shows that the greater the degree of surface enrichment, the less related is the composition of underlying sediments. This relationship is illustrated in Figure 96. The regression line gives

$$Ef = 0.06 - 2.12 \ln r \text{ or } r \quad e^{-0.5Ef} \tag{36}$$

which satisfies the requirement that when $Ef = 0$ $r = 1$.

Table 31 provides a comparison of mean enrichment factors for each depositional basin. Only two elements show significant differences in enrichment factors between basins, Mn and Pb. Both elements are significantly more enriched in the Port Huron basin. Enhancement of enrichment factors in the Port Huron basin could be the result of generally lower sedimentation rates. In cores where the sedimentation rate is high, surface concentrations may be reduced as a result of higher deposition of inert material. Other anthropogenic elements such as Cd, Cu, Ni and Zn also have higher average enrichment factors in this basin but the differences

TABLE 27. CONCENTRATION OF MAJOR ELEMENTS IN SURFACE[1] AND IN UNDERLYING[2] SEDIMENTS, CONCENTRATION RATIOS, AND ENRICHMENT FACTORS

	Fraction Soluble (g/g)			Calcium (wt %)				Iron (wt %)			
Station	S	D	R[3]	S	D	R	E[4]	S	D	R	E[4]
3.	0.23	0.18	1.278	1.90	0.60	3.167	1.478	2.60	2.10	1.238	-0.031
4.	0.071	0.17	0.418*	0.40	1.60	0.250	-0.401	1.10	2.40	0.458	0.097
5.	0.26	0.23	1.130	1.80	1.30	1.385	0.225	3.60	3.10	1.161	0.027
7.	0.43	0.43	1.000	8.60	8.40	1.024	0.024	1.24	1.34	0.925	-0.075
8.	0.26	0.23	1.130	0.57	0.45	1.267	0.121	3.00	2.80	1.071	-0.052
9.	0.27	0.26	1.038	3.50	2.80	1.250	0.204	2.10	2.70	0.778	-0.251
10.	0.16	0.19	0.842*	0.49	0.40	1.225	0.455	1.90	2.20	0.864	0.026
12.	0.33	0.25	1.138	2.20	1.40	1.571	0.381	3.30	3.10	1.065	-0.065
13.	0.46	0.44	1.045	4.00	4.00	1.000	-0.043	1.74	1.58	1.101	0.053
14.	0.30	0.27	1.111	1.50	1.40	1.071	-0.036	3.60	3.10	1.161	0.045
15.	0.045	0.34	0.132*	0.16	2.60	0.064	-0.518	0.98	4.00	0.245	0.851
16.	0.25	0.23	1.087	0.61	0.41	1.488	0.369	3.50	2.90	1.207	0.110
17.	0.33	0.27	1.222	3.30	2.50	1.320	0.080	3.70	3.60	1.028	-0.159
18.	0.37	0.37	1.000	4.40	4.40	1.000	0.000	2.80	2.70	1.037	0.037
19.	0.15	0.21	0.714*	0.42	0.43	0.977	0.367	2.00	2.50	0.800	0.120
25.	0.29	0.24	1.208	1.12	0.56	2.000	0.655	3.20	2.80	1.143	-0.054
29.	0.32	0.26	1.231	1.60	1.02	1.569	0.275	3.60	3.50	1.029	-0.164
31.	0.19	0.19	1.000	0.62	0.46	1.348	0.348	2.40	2.40	1.000	0.000
33.	0.26	0.24	1.08	0.56	0.43	1.302	0.202	3.50	3.00	1.167	0.077
35.	0.07	0.26	0.269*	0.33	1.62	0.204	-1.266	1.51	3.01	0.502	0.863
39.	0.20	0.26	0.769*	1.50	2.20	0.682	0.114	1.20	0.98	1.224	0.592
50.	0.38	0.41	0.927	6.30	6.10	1.033	0.114	1.10	1.30	0.846	-0.087
53.	0.28	0.27	1.037	1.70	1.98	0.859	-0.872	2.60	3.30	0.788	-0.340
57.	0.23	0.22	1.046	0.73	0.59	1.237	0.184	3.30	3.20	1.031	0.031
61.	0.43	0.42	1.024	5.50	5.60	0.982	-0.041	2.00	1.80	1.111	0.085
63.	0.34	0.28	1.214	2.70	3.14	0.861	-0.292	3.40	1.25	2.720	1.240
69.	0.31	0.27	1.148	2.00	1.67	1.200	0.043	3.40	3.20	1.062	-0.075

(continued)

---

[1] Derived from vertical profiles. Average of upper 3 cm or 1-2 cm interval.

[2] Average of approximately the lower 20-50 cm.

[3] R = Surface concentration (C_s)/deep concentration (C_d).

[4]
$$E = \text{enrichment factor} = \frac{(C_s/F_s) - (C_d/F_d)}{(C_d/F_d)}$$

where F_s = the fraction soluble in surface sediments
F_d = the fraction soluble in underlying sediments

* inhomogeneous cores having significant departures of F_s/F_d from the mean are excluded in calculating mean ratios and enrichment factors.

TABLE 27. (continued)

Station	Magnesium (wt. %)				Manganese (wt %)				Phosphorus (wt %)			
	S	D	R	E	S	D	R	E	S	D	R	E
3.	--	--	--	--	0.073	0.030	2.433	0.904	0.12	0.15	0.800	-0.374
4.	0.24	1.922	0.125	-0.745	0.040	0.027	1.429	2.421	0.076	0.140	0.543	0.300
5.	0.89	0.85	1.047	-0.074	0.080	0.028	2.857	1.527	--	--	--	--
7.	5.40	5.40	1.000	0.000	0.032	0.022	1.231	0.231	--	--	--	--
8.	0.91	0.89	1.022	-0.096	0.085	0.034	2.500	1.212	0.23	0.15	1.533	0.356
9.	2.70	3.00	0.900	-0.133	0.070	0.026	2.692	1.593	0.14	0.13	1.077	0.037
10.	--	--	--	--	0.160	0.020	8.000	8.500	0.19	0.20	0.950	0.128
12.	1.90	1.60	1.187	0.044	0.170	0.053	3.208	1.819	--	--	--	--
13.	5.20	5.40	0.963	-0.079	0.052	0.028	1.857	0.776	--	--	--	--
14.	1.50	1.50	1.000	-0.100	0.180	0.056	3.214	1.893	0.33	0.27	1.222	0.100
15.	0.148	3.40	0.044	-0.671	0.034	0.048	0.708	4.352	--	--	--	--
16.	0.88	0.83	1.060	-0.025	0.170	0.046	3.696	2.400	--	--	--	--
17.	1.50	1.40	1.071	-0.123	0.160	0.044	3.636	1.975	--	--	--	--
18.	2.90	3.20	0.906	-0.094	0.067	0.040	1.675	0.675	0.22	0.17	1.294	0.294
19.	--	--	--	--	0.045	0.026	1.731	1.423	0.22	0.20	1.100	0.540
25.	--	--	--	--	0.150	0.033	4.545	2.762	0.11	0.20	0.550	-0.545
29.	1.50	1.50	1.000	-0.188	0.262	0.066	3.964	2.236	--	--	--	--
31.	0.78	0.73	1.068	0.068	0.049	0.027	1.815	0.815	0.18	0.15	1.200	0.200
33.	0.91	0.92	0.989	-0.084	0.100	0.036	2.778	1.564	0.21	0.19	1.105	0.020
35.	--	--	--	--	0.038	0.023	1.652	5.121	0.14	0.180	0.778	1.889
39.	--	--	--	--	0.038	0.017	2.235	1.865	0.106	0.096	1.104	0.435
50.	4.70	4.90	0.959	0.035	0.027	0.025	1.080	0.165	--	--	--	--
53.	1.50	1.90	0.790	-0.239	0.180	0.053	3.40	2.275	0.21	0.210	1.00	-0.036
57.	1.20	1.13	1.06	0.016	0.140	0.054	2.59	1.480	0.16	0.18	0.889	-0.111
61.	4.40	4.40	1.000	-0.023	0.048	0.035	1.371	0.340	0.13	0.14	0.929	-0.093
63.	2.20	2.09	1.053	-0.133	0.150	0.034	4.425	2.634	0.31	0.20	1.550	0.277
69.	--	--	--	--	0.170	0.050	3.400	1.961	0.24	0.24	1.000	-0.129

(continued)

TABLE 27. (continued)

Station	Potassium (wt. %)				Silicon (wt %)				Sodium (wt %)			
	S	D	R	E	S	D	R	E	S	D	R	E
3.	0.53	0.49	1.082	-0.154	--	--	--	--	--	--	--	--
4.	0.28	0.72	0.389	-0.069	--	--	--	--	--	--	--	--
5.	0.89	1.10	0.809	-0.284	--	--	--	--	--	--	--	--
7.	0.26	0.36	0.722	-0.278	--	--	--	--	0.10	0.10	1.00	0.00
8.	0.68	0.71	0.958	-0.153	--	--	--	--	--	--	--	--
9.	0.34	0.48	0.708	-0.318	--	--	--	--	--	--	--	--
10.	0.36	0.65	0.554	-0.342	--	--	--	--	--	--	--	--
12.	0.72	0.83	0.867	-0.238	--	--	--	--	0.14	0.10	1.40	0.23
13.	0.38	0.40	0.950	-0.091	--	--	--	--	0.110	0.106	1.04	0.00
14.	0.83	0.82	1.012	-0.089	1.9	1.1	1.73	0.56	--	--	--	--
15.	0.188	0.940	0.200	0.511	--	--	--	--	0.118	0.064	0.72	4.44
16.	0.560	0.570	0.982	-0.096	--	--	--	--	0.074	0.056	1.32	0.21
17.	0.85	1.100	0.773	-0.368	--	--	--	--	0.21	0.20	1.05	-0.14
18.	0.70	0.63	1.111	0.111	1.3	0.69	1.88	0.88	0.12	0.11	1.09	0.09
19.	0.50	0.75	0.667	-0.067	--	--	--	--	--	--	--	--
25.	0.76	0.77	0.987	-0.183	--	--	--	--	--	--	--	--
29.	0.90	0.78	1.154	-0.063	--	--	--	--	--	--	--	--
31.	0.45	0.51	0.882	-0.118	--	--	--	--	--	--	--	--
33.	0.70	0.75	0.933	-0.138	--	--	--	--	--	--	--	--
35.	0.17	0.83	0.205	-0.239	--	--	--	--	--	--	--	--
39.	0.28	0.28	1.000	0.300	--	--	--	--	--	--	--	--
50.	0.19	0.27	0.704	-0.241	--	--	--	--	--	--	--	--
53.	0.71	1.08	0.657	0.366	1.0	0.62	--	--	--	--	--	--
57.	0.43	0.47	0.915	-0.085	--	--	--	--	--	--	--	--
61.	0.57	0.52	1.096	0.071	--	--	--	--	--	--	--	--
63.	0.92	0.82	1.11	-0.087	1.7	0.68	2.50	1.35	--	--	--	--
69.	0.77	0.75	1.027	-0.106	--	--	--	--	--	--	--	--

TABLE 28. CONCENTRATION OF MINOR ELEMENTS IN SURFACE AND IN UNDERLYING SEDIMENTS, CONCENTRATION RATIOS AND ENRICHMENT FACTORS

	Barium (μg/g)				Cadmium (μg/g)				Chromium (μg/g)			
Station	S	D	R	E	S	D	R	E	S	D	R	E
3.	--	--	--	--	2.81	1.75	1.606	0.257	58.0	58.0	1.000	-0.217
4.	--	--	--	--	1.50	1.52	0.987	1.363	24.0	52.0	0.462	0.105
5.	152.	151.	1.00	-0.12	3.06	1.28	2.391	1.115	57.0	66.0	1.015	-0.102
7.	107.	120.	.89	-0.11	--	--	--	--	19.4	30.8	0.630	-0.370
8.	--	--	--	--	--	--	--	--	62.0	58.0	1.069	-0.054
9.	--	--	--	--	2.00	1.50	1.333	0.284	38.0	46.0	0.826	-0.205
10.	--	--	--	--	2.36	1.50	1.573	0.868	34.0	51.0	0.667	-0.208
12.	133.	62.	2.15	0.89	--	--	--	--	53.0	55.0	0.964	-0.153
13.	92.	80.	1.15	0.10	--	3.78	--	--	34.0	30.0	1.133	0.084
14.	213.	164.	1.30	0.17	3.22	1.89	1.704	0.533	65.0	58.0	1.121	0.009
15.	44.	200.	.22	0.56	3.02	--	--	--	16.8	82.6	0.203	0.537
16.	170.	96.	1.77	0.63	2.83	0.66	4.288	2.945	55.0	51.0	1.098	0.010
17.	167.	197.	.85	.30	3.22	1.04	3.096	1.533	67.0	66.0	1.015	-0.169
18.	181.	150.	1.21	0.21	1.61	0.95	1.695	0.695	59.0	53.0	1.113	0.113
19.	--	--	--	--	1.50	1.78	0.843	0.180	43.0	59.0	0.729	0.020
25.	--	--	--	--	2.86	2.03	1.409	0.166	--	--	--	--
29.	--	--	--	--	3.020	0.57	5.298	3.305	69.0	62.0	1.113	-0.096
31.	--	--	--	--	2.11	1.24	1.702	0.702	50.0	48.0	1.042	0.042
33.	--	--	--	--	3.86	1.79	2.156	0.991	62.0	60.0	1.033	-0.046
35.	--	--	--	--	--	--	--	--	16.	50.	0.320	0.189
39.	--	--	--	--	3.26	2.30	1.417	0.843	24.0	24.0	1.000	0.300
50.	--	--	--	--	--	--	--	--	31.0	33.	0.539	0.014
53.	172.	201.	0.856	-0.175	2.51	1.13	2.221	0.507	62.0	65.0	0.954	-0.080
57.	--	--	--	--	4.24	--	--	--	65.0	66.1	0.983	-0.058
61.	--	--	--	--	4.22	2.53	1.668	0.629	37.0	36.0	1.028	0.004
63.	203.	192.	1.06	-0.129	2.57	1.02	2.520	1.371	71.0	58.0	1.224	0.152
69.	--	--	--	--	2.93	1.91	1.534	0.336	--	--	--	--

(continued)

TABLE 28. (continued)

Station	Copper (µg/g)				Lead (µg/g)				Lead-210 (pCi/g)			
	S	D	R	E	S	D	R	E	S	D	R	E
3.	47.	31.	1.516	0.187	87.	14.	6.214	3.863	8.9	0.49	18.163	13.215
4.	15.0	32.6	0.460	0.102	13.7	22.0	0.623	0.497	0.55	0.26	2.115	4.065
5.	72.	44.	1.636	0.448	132.	44.	3.000	1.654	7.4	0.49	15.1	12.36
7.	16.2	15.2	1.066	0.066	74.2	37.9	1.958	0.958	2.4	0.33	7.27	6.27
8.	56.	34.	1.647	0.457	103.	20.	5.150	3.556	5.4	0.49	11.020	8.749
9.	33.	33.	1.000	-0.037	62.	25.	2.480	1.388	5.0	0.43	11.628	10.197
10.	35.	26.	1.346	0.599	57.	13.	4.385	4.207	4.6	0.46	10.000	10.875
12.	50.	31.	1.613	0.417	101.	22.	4.591	3.034	14.0	0.70	20.000	16.576
13.	24.0	14.6	1.644	0.572	78.	48.0	1.625	0.554	2.9	0.31	9.355	7.948
14.	59.	33.	1.788	0.609	122.	27.	4.519	3.067	12.6	0.78	16.154	13.538
15.	5.8	36.0	0.161	0.217	13.	50.9	0.257	0.930	--	--	--	--
16.	64.	41.	1.561	0.436	108.	17.	6.353	4.845	8.2	0.77	10.649	8.797
17.	65.	38.	1.711	0.400	143.	43.	3.326	1.721	8.2	0.66	12.424	9.165
18.	40.	26.	1.538	0.538	93.	33.	2.818	1.818	8.8	0.444	19.820	18.820
19.	31.	39.	0.795	0.113	20.	15.	1.333	0.867	1.6	0.62	2.581	2.613
25.	54.	34.	1.588	0.314	108.	21.	5.143	3.256	10.9	0.63	17.302	13.319
29.	60.	35.	1.714	0.393	128.	35.	3.657	1.971	--	--	--	--
31.	46.	34.	1.353	0.353	81.	21.	3.857	2.857	4.3	0.51	8.431	7.431
33.	53.	35.	1.514	0.398	92.	22.	4.182	2.86	7.9	0.57	13.860	11.79
35.	9.77	19.4	0.503	0.871	20.	15.	1.333	3.952	--	--	--	--
39.	12.0	8.4	1.524	0.981	40.	28.	1.429	0.857	2.7	0.27	10.000	12.000
50.	17.	17.	1.000	0.079	41.	27.	1.519	0.638	2.2	0.37	5.946	5.415
53.	42.	28.2	1.489	.446	93.	27.5	3.382	2.261	8.3	0.51	16.275	10.043
57.	59.	40.	1.480	0.411	118.	24.	4.917	3.917	6.2	0.35	17.714	16.714
61.	24.	18.	1.333	0.302	56.	31.	1.806	0.764	3.7	0.27	13.704	12.385
63.	51.	25.	2.040	0.920	105.	24.	4.375	3.118	11.4	0.67	17.015	15.014
69.	46.	29.	1.586	0.382	98.	25.	3.920	2.414	7.3	0.85	8.588	6.480

(continued)

TABLE 28. (continued)

	Molybdenum (μg/g)				Nickel (μg/g)				Strontium (μg/g)			
Station	S	D	R	E	S	D	R	E	S	D	R	E
3.	--	--	--	--	63.0	32.0	1.969	0.541	--	--	--	--
4.	--	--	--	--	19.6	41.4	0.473	0.134	--	--	--	--
5.	--	--	--	--	75.0	21.0	3.571	2.159	38.	33.	1.15	0.01
7.	--	--	--	--	28.0	28.0	1.000	0.000	48.	44.	1.10	0.09
8.	--	--	--	--	60.0	36.0	1.667	0.474	--	--	--	--
9.	--	--	--	--	41.0	33.0	1.242	0.196	--	--	--	--
10.	--	--	--	--	71.0	37.0	1.919	1.279	--	--	--	--
12.	6.7	6.9	0.97	-0.15	61.0	34.0	1.794	0.577	42.	31.	1.35	0.19
13.	11.0	8.2	1.3	0.25	38.0	28.0	1.357	0.298	54.	48.	1.13	0.08
14.	11.0	10.0	1.1	-0.01	75.0	39.0	1.923	0.731	46.	35.	1.31	0.18
15.	--	--	--	--	11.2	52.0	0.215	0.627	15.6	48.	0.32	1.45
16.	--	--	--	--	71.0	41.0	1.732	0.593	36.	24.	1.50	0.38
17.	--	--	--	--	80.0	46.0	1.739	0.423	45.	37.	1.22	0.00
18.	--	--	--	--	50.0	33.0	1.515	0.515	39.	41.	0.95	-0.05
19.	--	--	--	--	40.0	42.0	0.952	0.333	--	--	--	--
25.	--	--	--	--	71.0	36.0	1.972	0.632	--	--	--	--
29.	--	--	--	--	85.0	44.0	1.932	0.570	--	--	--	--
31.	--	--	--	--	52.0	37.0	1.405	0.405	--	--	--	--
33.	--	--	--	--	61.0	39.0	1.564	0.444	--	--	--	--
35.	--	--	--	--	21.0	29.3	0.717	1.662	--	--	--	--
39.	--	--	--	--	22.0	16.8	1.310	0.702	--	--	--	--
50.	--	--	--	--	26.0	26.0	1.000	0.079	--	--	--	--
53.	--	--	--	--	56.0	35.5	1.578	0.521	--	--	--	--
57.	--	--	--	--	78.0	44.0	1.773	0.696	--	--	--	--
61.	--	--	--	--	37.0	26.0	1.423	0.390	--	--	--	--
63.	--	--	--	--	68.0	29.0	2.345	1.207	--	--	--	--
69.	--	--	--	--	68.0	37.0	1.838	0.601	--	--	--	--

(continued)

TABLE 28. (continued)

Station	Zinc (μg/g)			
	S	D	R	E
3.	145.	62.	2.339	0.830
4.	42.	68.	0.618	0.479
5.	200.	85.	2.353	1.081
7.	50.	34.	1.471	0.471
8.	167.	67.	2.493	1.205
9.	94.	58.	1.621	0.561
10.	114.	60.	1.900	1.256
12.	157.	69.	2.275	1.000
13.	74.	34.	2.176	1.082
14.	186.	73.	2.548	1.293
15.	20.	80.	0.250	0.889
16.	195.	95.	2.294	1.111
17.	195.	86.	2.257	0.855
18.	146.	59.	2.475	1.475
19.	67.	70.	0.957	0.340
25.	156.	62.	2.516	1.082
29.	191.	70.	2.729	1.217
31.	133.	65.	2.046	1.046
33.	165.	72.	2.292	1.115
35.	46.4	49.	0.947	2.517
39.	60.	38.	1.579	1.053
50.	52.	38.	1.368	0.476
53.	139.	68.7	2.023	0.951
57.	178.	74.6	2.386	1.282
61.	85.	47.	1.809	0.766
63.	171.	58.	2.948	1.775
69.	150.	65.	2.308	1.010

TABLE 29. CORRELATIONS BETWEEN ENRICHMENT FACTORS FOR ELEMENTS WITH A SIGNIFICANT DEGREE OF ENRICHMENT

	Mn	Cd	Cu	Ni	Pb	Pb-210
Mn						
Cd	0.32					
Cu	0.29	0.26				
Ni	0.37	0.09	0.37			
Pb	0.67	0.14	0.21	0.24		
Pb-210	0.34	-0.18	0.31	0.37	0.45	
Zn	0.35	0.27	0.89	0.38	0.43	0.53

TABLE 30. SUMMARY OF MEAN SURFACE-TO-DEPTH CONCENTRATION RATIOS, ENRICHMENT FACTORS AND CORRELATION COEFFICIENTS FOR SOUTHERN LAKE HURON CORES (ALL DEPOSITIONAL BASINS COMBINED)

Element	Mean Ratio	Mean Enrichment Factor*	Correlation Coefficient (N)
Soluble fraction	1.09 ± 0.02	0.00 ± 0.00	0.96 (22)
Calcium	1.30 ± 0.11	0.18 ± 0.08	0.97 (22)
Iron	1.08 ± 0.03	- 0.01 ± 0.02	0.97 (22)
Magnesium	1.00 ± 0.02	- 0.07 ± 0.02	0.99 (17)
Manganese	2.48 ± 0.21	1.26 ± 0.17	0.87 (21)
Phosphorus	1.07 ± 0.07	0.00 ± 0.07	0.78 (14)
Potassium	0.99 ± 0.06	- 0.09 ± 0.05	0.88 (22)
Silicon	2.04 ± 0.24	0.93 ± 0.23	0.74 (3)
Sodium	1.15 ± 0.07	0.07 ± 0.06	0.97 (6)
Barium	1.22 ± 0.13	0.12 ± 0.12	0.87 (9)
Cadmium	2.31 ± 0.31	1.06 ± 0.26	0.50 (14)
Chromium	1.04 ± 0.03	- 0.03 ± 0.03	0.97 (20)
Copper	1.51 ± 0.06	0.39 ± 0.05	0.95 (2)
Lead	3.54 ± 0.32	2.21 ± 0.27	0.49 (22)
Lead-210	12.9 ± 1.0	10.9 ± 0.9	0.79 (21)
Molybdenium	1.12 ± 0.1	0.03 ± 0.12	0.96 (3)
Nickel	1.70 ± 0.11	0.55 ± 0.09	0.85 (22)
Stronium	1.21 ± 0.06	0.11 ± 0.05	0.78 (8)
Zinc	2.23 ± 0.08	1.05 ± 0.07	0.96 (22)

*Factors underlined are significantly greater than zero. (±2σ).

TABLE 31. COMPARISON OF MEAN ENRICHMENT FACTORS BY DEPOSITIONAL BASIN

Element	Depositional Basin		
	Port Huron (N = 4)	Goderich (N = 17)	Difference
Fraction Soluble	--	--	--
Calcium	0.23 ± 0.05*	0.14 ± 0.09	0.09 ± 0.10
Iron	0.04 ± 0.04	- 0.02 ± 0.03	0.06 ± 0.05
Magnesium	- 0.07 ± 0.02	- 0.07 ± 0.02	0.00 ± 0.03
Manganese	1.67 ± 0.25	1.06 ± 0.18	0.61 ± 0.31
Phosphorus	0.19 ± 0.17	0.02 ± 0.06	0.17 ± 0.18
Potassium	- 0.17 ± 0.04	- 0.06 ± 0.06	- 0.13 ± 0.07
Cadmium	1.68 ± 0.63	0.96 ± 0.29	0.72 ± 0.69
Chromium	- 0.05 ± 0.02	0.03 ± 0.04	- 0.02 ± 0.04
Copper	0.44 ± 0.01	0.38 ± 0.06	0.06 ± 0.06
Lead	3.11 ± 0.18	1.94 ± 0.29	1.17 ± 0.34
Lead-210	10.43 ± 0.96	10.83 ± 1.09	- 0.04 ± 1.5
Nickel	0.92 ± 0.42	0.46 ± 0.07	0.46 ± 0.43
Zinc	1.13 ± 0.03	1.03 ± 0.09	0.10 ± 0.09

* Mean ± standard error in estimate of mean.
Underlined values are significantly (±σ) different from zero.

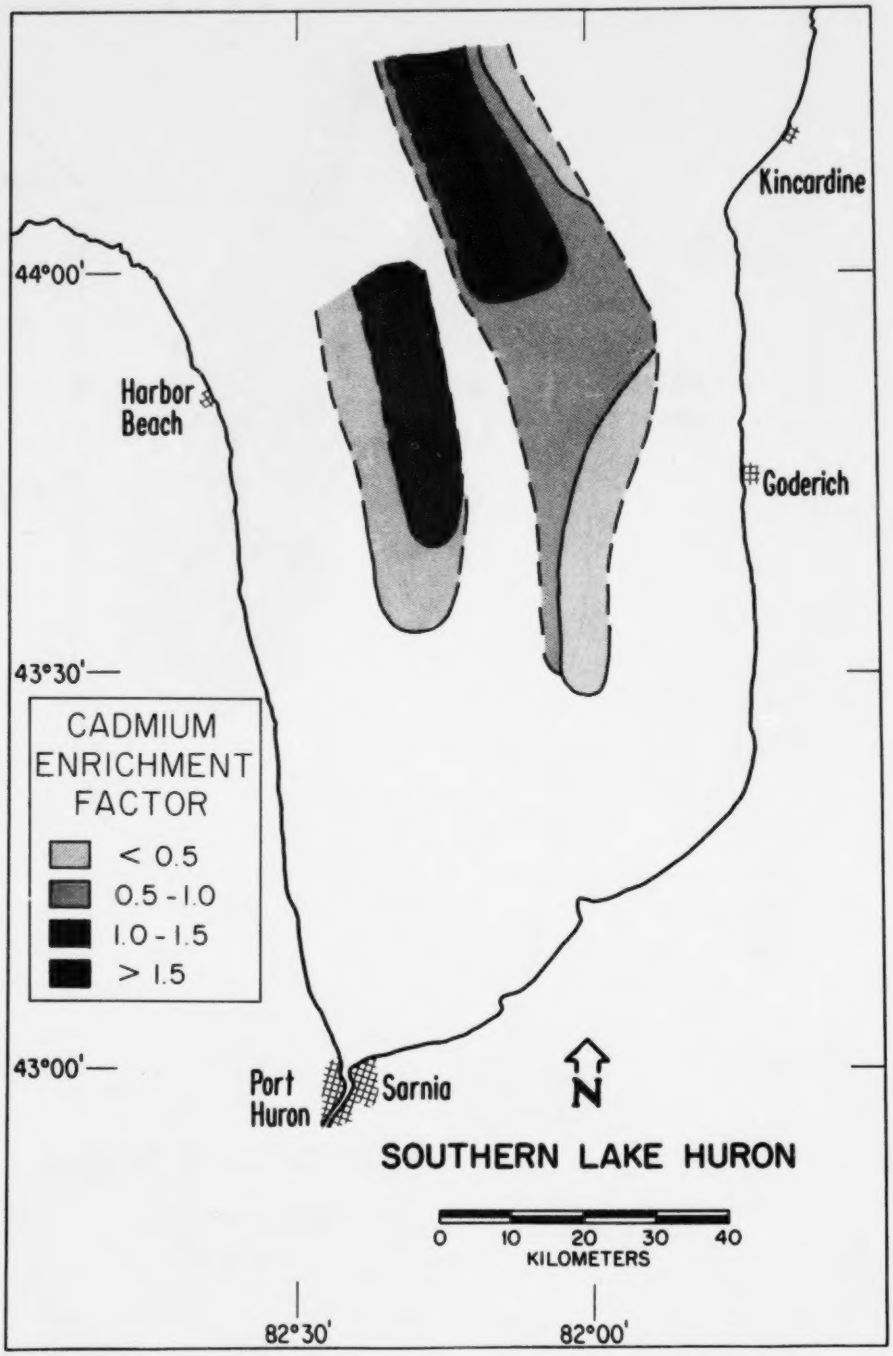

Kincardine
44°00'
Harbor Beach
Goderich
43°30'
CADMIUM ENRICHMENT FACTOR
< 0.5
0.5 - 1.0
1.0 - 1.5
> 1.5
43°00'
Port Huron
Sarnia
N
SOUTHERN LAKE HURON
0
10
20
30
40
KILOMETERS
82°30'
82°00'

Figure 89. Distribution of the cadmium enrichment factor.

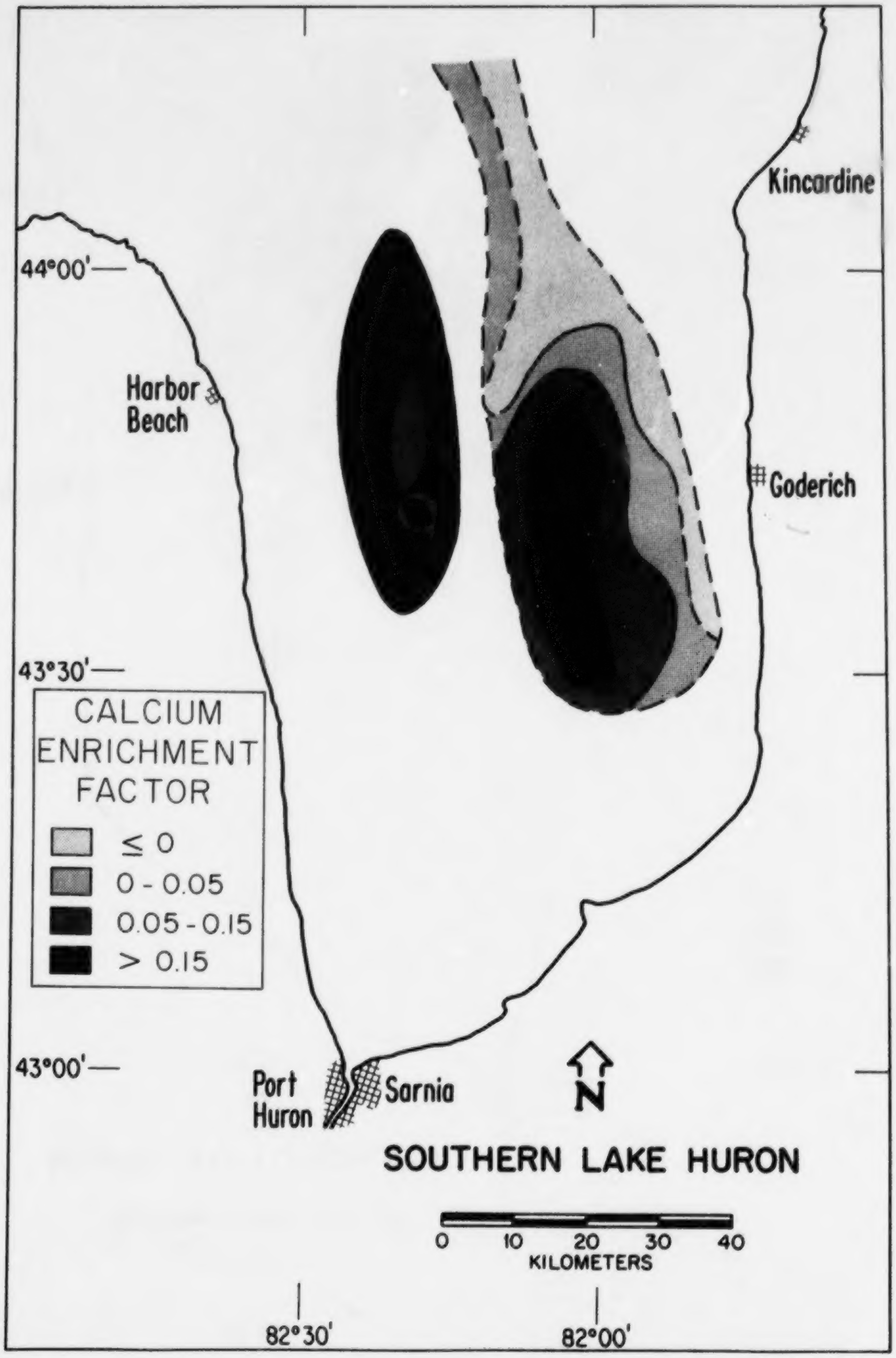
Kincardine
44°00'
Harbor Beach
Goderich
43°30'
CALCIUM ENRICHMENT FACTOR
≤ 0
0 - 0.05
0.05 - 0.15
> 0.15
43°00'
Port Huron
Sarnia
N
SOUTHERN LAKE HURON
0 10 20 30 40
KILOMETERS
82°30'
82°00'

Figure 90. Distribution of the calcium enrichment factor.

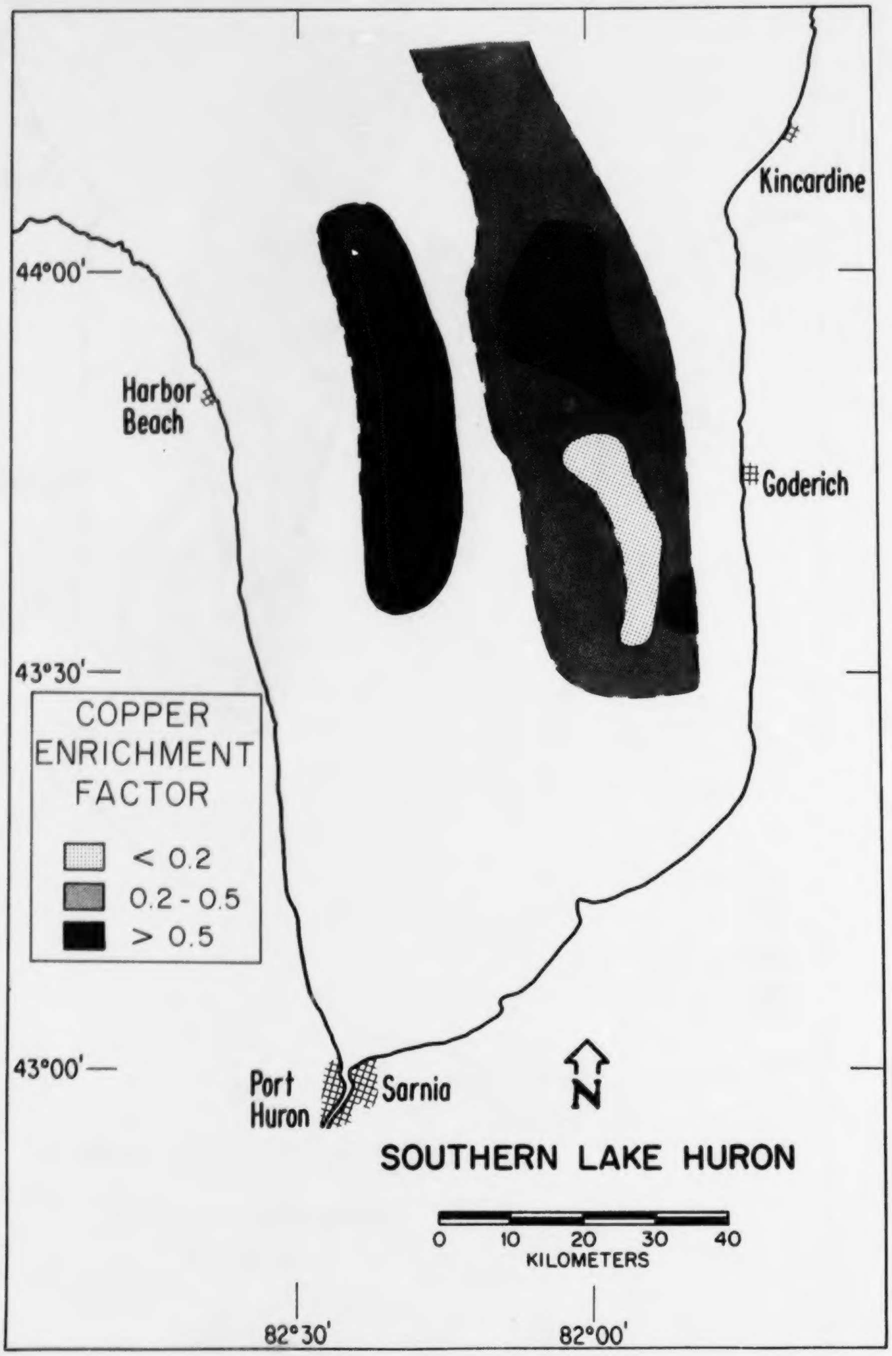
Kincardine
44°00'
Harbor Beach
Goderich
43°30'
COPPER ENRICHMENT FACTOR
< 0.2
0.2 - 0.5
> 0.5
43°00'
Port Huron
Sarnia
N
SOUTHERN LAKE HURON
0 10 20 30 40
KILOMETERS
82°30'
82°00'

Figure 91. Distribution of the copper enrichment factor.

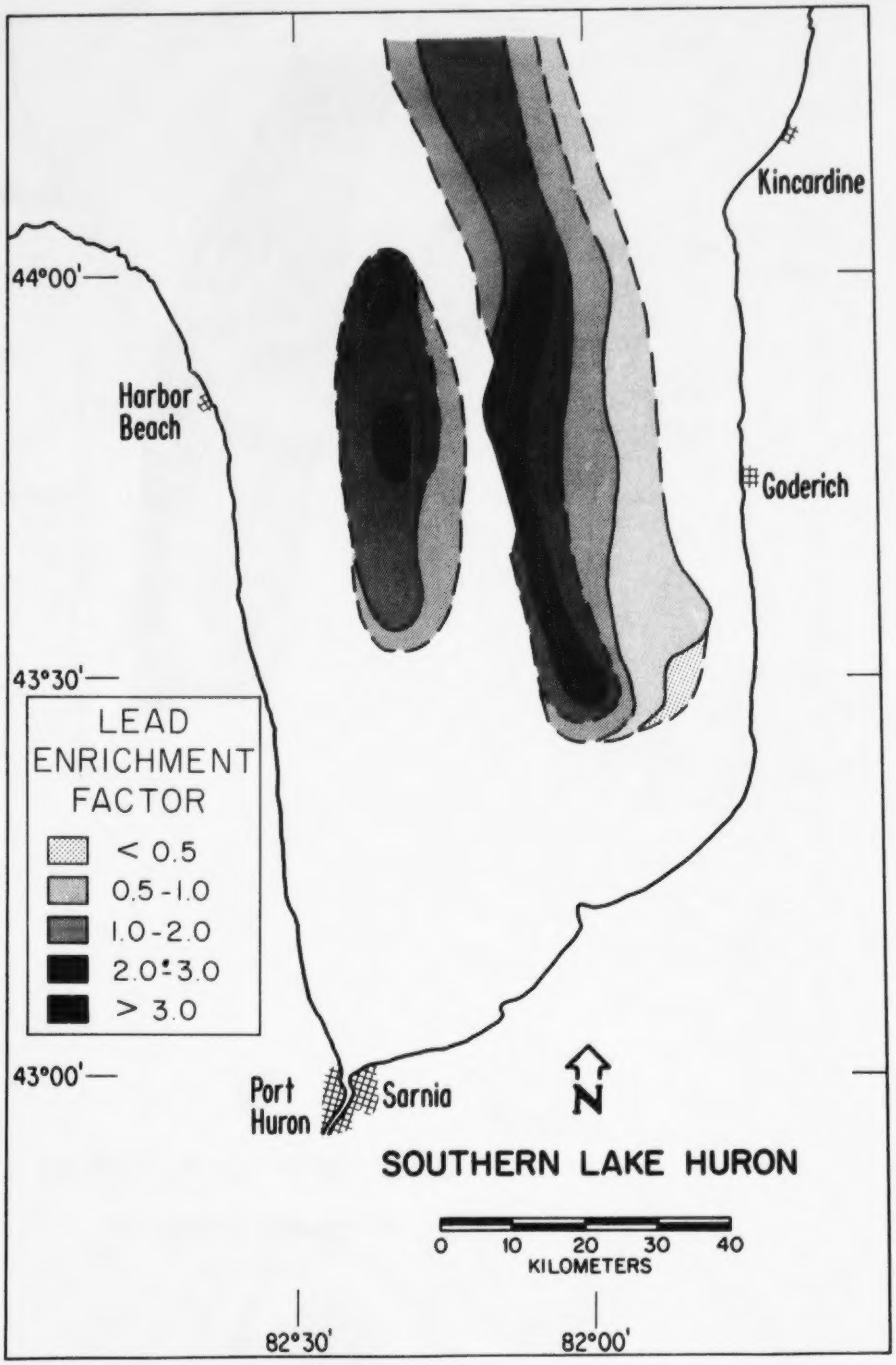
Kincardine
44°00'
Harbor Beach
Goderich
43°30'
LEAD ENRICHMENT FACTOR
< 0.5
0.5 - 1.0
1.0 - 2.0
2.0 - 3.0
> 3.0
43°00'
Port Huron
Sarnia
N
SOUTHERN LAKE HURON
0 10 20 30 40
KILOMETERS
82°30'
82°00'

Figure 92. Distribution of the lead enrichment factor.

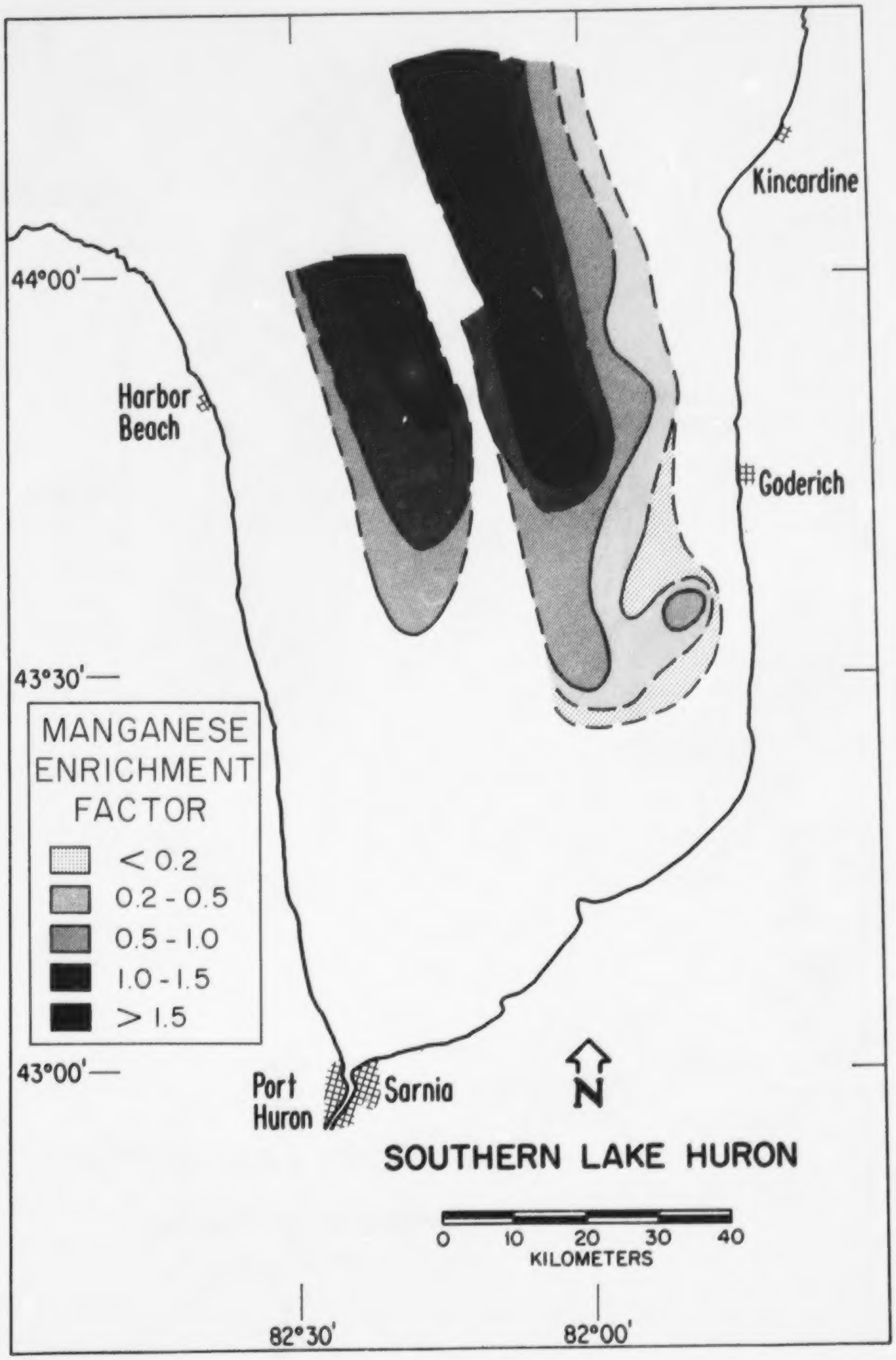
Kincardine
44°00'
Harbor Beach
Goderich
43°30'
MANGANESE ENRICHMENT FACTOR
< 0.2
0.2 - 0.5
0.5 - 1.0
1.0 - 1.5
> 1.5
43°00'
Port Huron
Sarnia
N
SOUTHERN LAKE HURON
0
10
20
30
40
KILOMETERS
82°30'
82°00'

Figure 93. Distribution of the manganese enrichment factor.

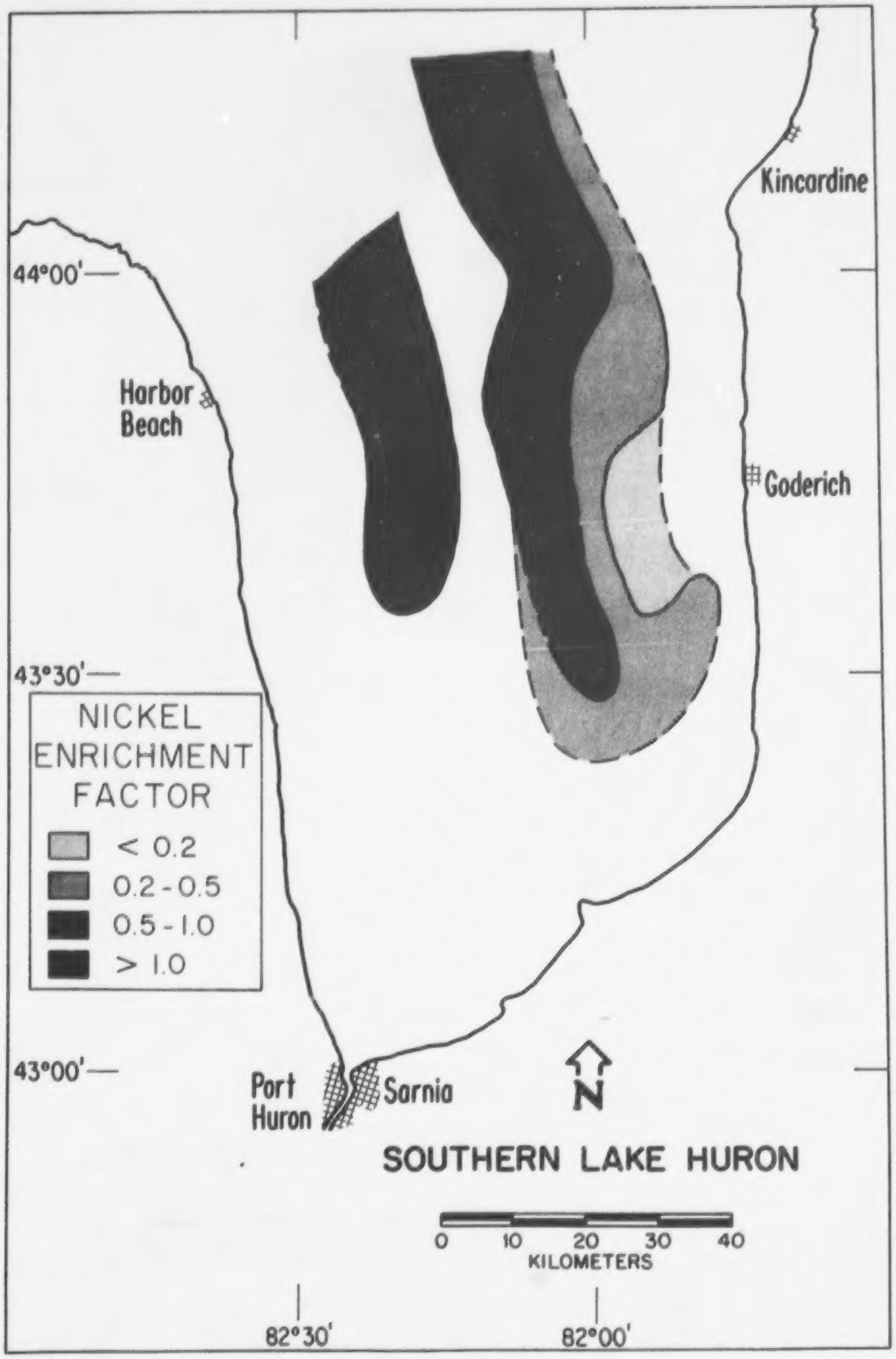
44°00'
43°30'
43°00'
82°30'
82°00'
Kincardine
Harbor Beach
Goderich
Port Huron
Sarnia
N
NICKEL ENRICHMENT FACTOR
< 0.2
0.2 - 0.5
0.5 - 1.0
> 1.0
SOUTHERN LAKE HURON
0 10 20 30 40
KILOMETERS

Figure 94. Distribution of the nickel enrichment factor.

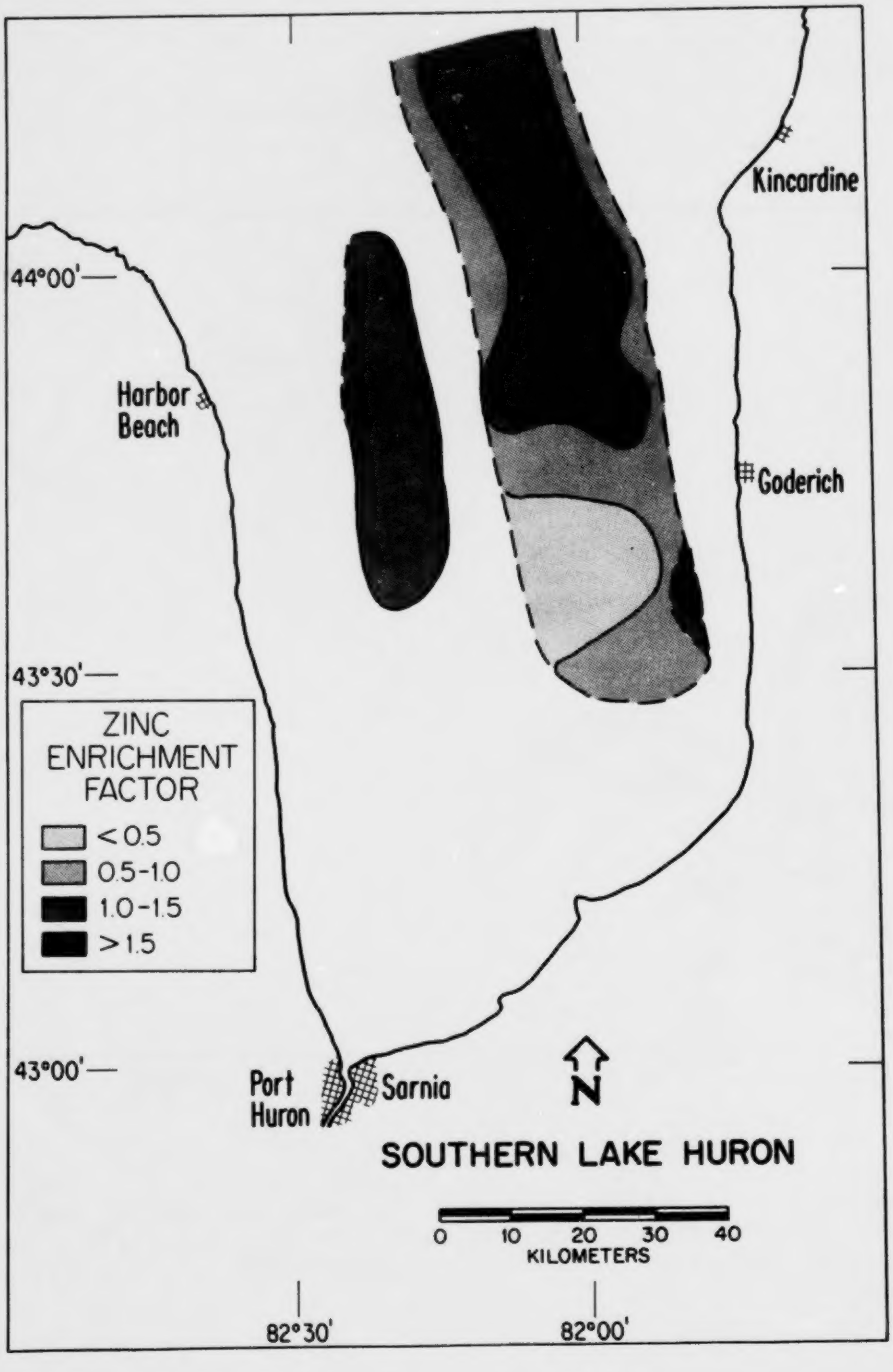

Kincardine
Goderich
Harbor Beach
Port Huron
Sarnia
44°00'
43°30'
43°00'
82°30'
82°00'
ZINC ENRICHMENT FACTOR
< 0.5
0.5-1.0
1.0-1.5
> 1.5
N
SOUTHERN LAKE HURON
0 10 20 30 40
KILOMETERS

Figure 95. Distribution of the zinc enrichment factor.

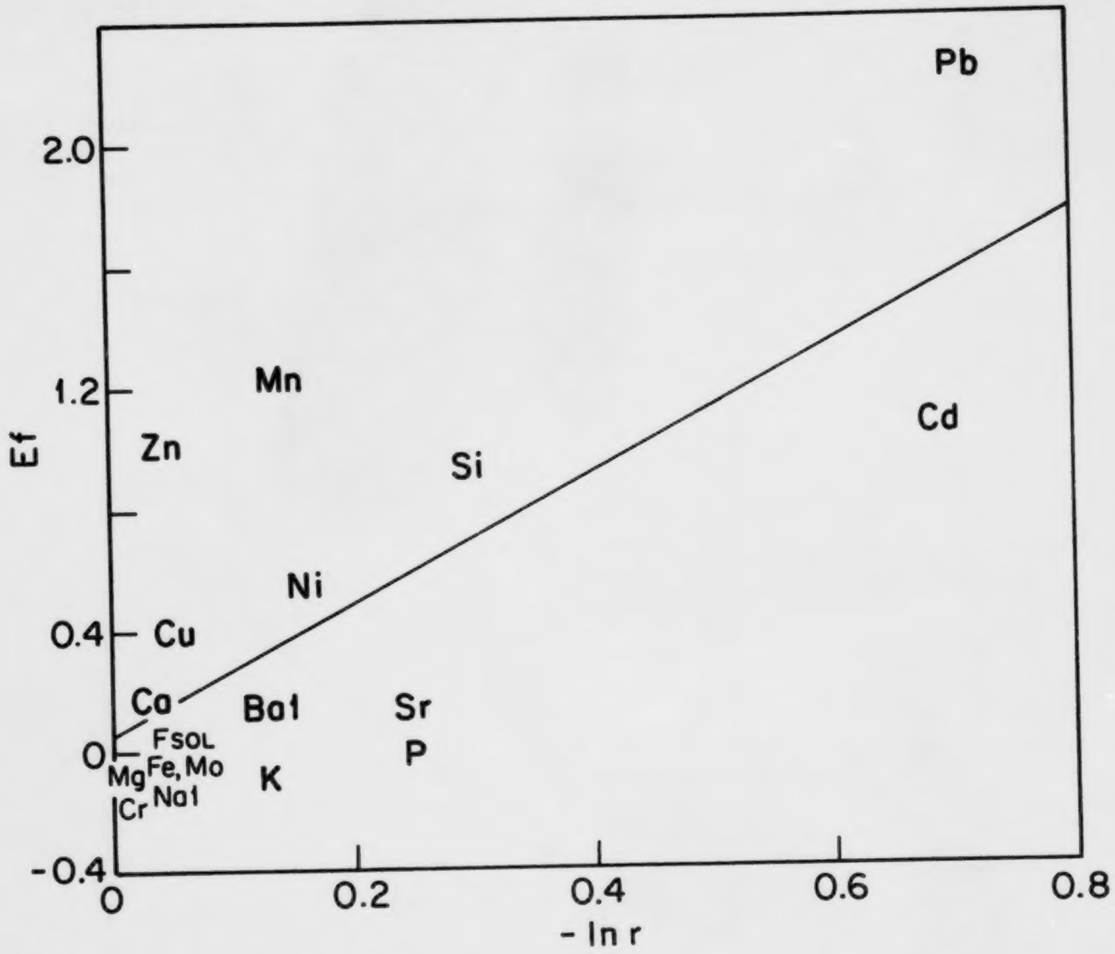

Figure 96. Relationship between the mean enrichment factor and the degree of unrelatedness between surface and underlying element concentrations.

between basins are only significant at the one sigma level as can be seen in Table 31.

In Fig. 97 the elements are ordered according to their degree of enrichment in core EPA-SLH-74-18-2. Of all the elements determined only a limited number show any significant degree of enrichment. Also shown in the same figure are the average values for the study area (shaded parts) and enrichment factors for additional elements based on the core taken by Kemp et al. (1976).

It should be kept in mind that the enrichment factors of the single Kemp et al. core could be very different from average values for the elements shown. Elements showing significant enrichment in southern Lake Huron include: Pb, Mn, Cd, Sn, Zn, Si, Ni, Cu, As, Sb, P, Br as well as Hg, IOC, OC, and N as determined by Kemp et al. (1976).

VERTICALLY INTEGRATED ELEMENT CONCENTRATIONS

The total anthropogenic loading of the sediments may be estimated by vertical integration of net concentration profiles. This integration is accomplished as follows:

$$\text{Total excess deposition } (\mu g/cm^2) = \sum_{i=1}^{N} (C_i - C_{bg}) \times dm_i \qquad (37)$$

where dm_i is the dry weight of sediment per unit area (g/cm^2) in the ith interval, C_i is the element concentration ($\mu g/g$) in the interval and C_{bg} is the mean background concentration ($\mu g/g$). Elements possessing enrichment factors of zero will have no significant total excess deposition (TED). Values for individual cores are given in Table 32. The element Mn is included for comparison although its excess is attributable to diagenetic effects rather than to cultural ones. Values reported in this table with the exception of Mn are estimates of the total amount of an element deposited at the given location as a result of man's activities to date (i.e. 1975). Part of the usefulness of these numbers lies in the fact that they are largely model-independent and therefore the estimate is not dependent on knowing the rate of sediment deposition.

The horizontal distribution of the TED for Mn, Cu, Ni, Pb and Zn are given in Figs. 98-102. Without exception, the greatest excess element accumulation occurs toward centers of the basins and patterns of the TED are very similar as can be seen from the correlation matrix given in Table 33.

Strong intercorrelations exist between all anthropogenic element pairs (Cu, Ni, Pb, and Zn) while Mn excess "deposition" patterns are not as well-correlated for reasons indicated previously. The particularly strong correlation between surface concentrations of Cu and Zn are also found in the TED values. Excess element deposition values for other elements such as As, Cd and Sb cannot be computed because of the lack of complete vertical profiles.

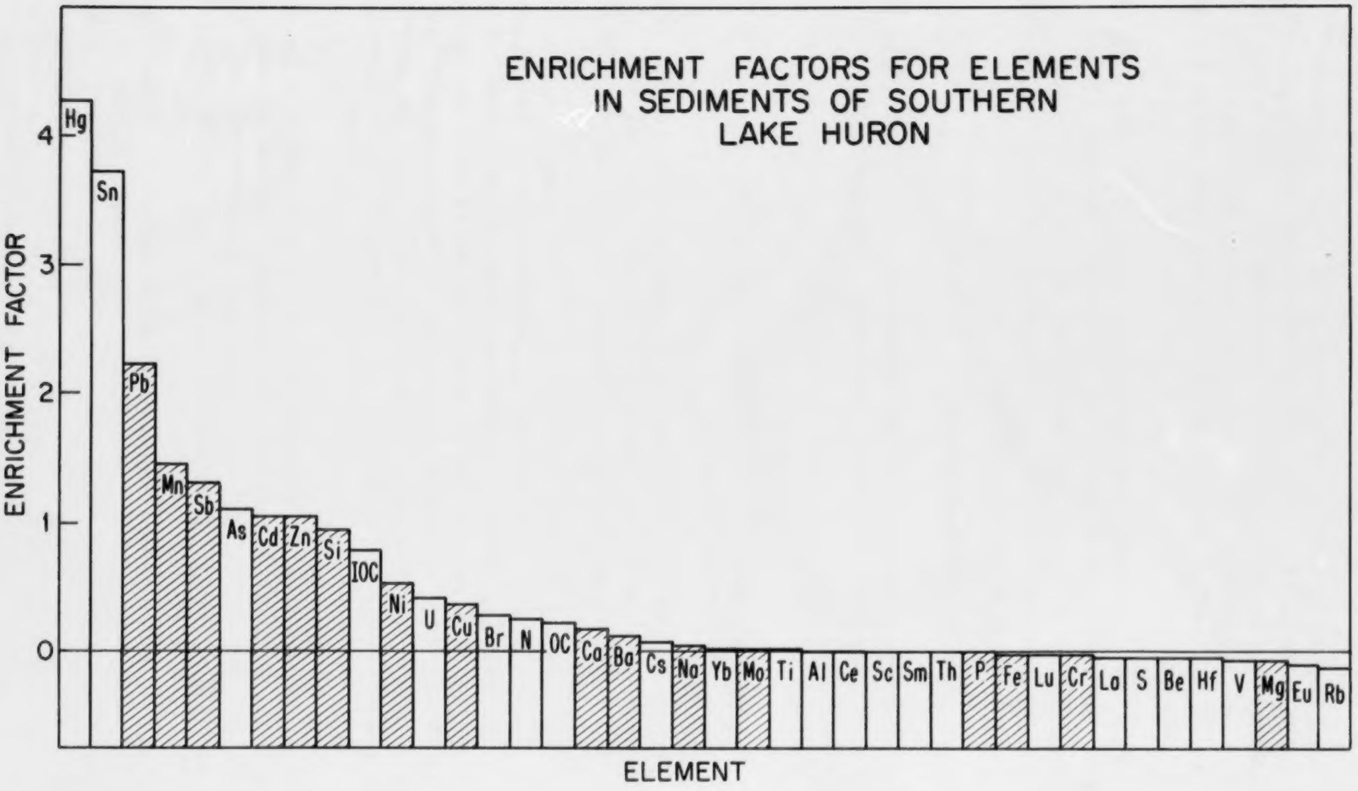

Figure 97. Enrichment factors for elements in the fine-grained sediments of southern Lake Huron. Values are either means (shaded regions) or based, where necessary, on individual cores.

TABLE 32. VERTICALLY INTEGRATED EXCESS ELEMENT CONCENTRATIONS (TOTAL EXCESS DEPOSITION)

	Total excess deposition (micrograms/cm^2)				
Station	Manganese*	Copper	Lead	Nickel	Zinc
3-2	370.	21.6	74.0	31.4	91.2
4-2	432.	0.0	0.8	0.0	0.0
5-2	255.	19.8	59.9	32.1	62.0
7-2	128.	3.0	135.0	1.6	47.8
8-2	201.	14.7	56.1	16.2	69.8
9-2	278.	4.9	34.2	7.7	31.7
10-2	1083.	7.3	30.9	24.7	40.5
12-2	895.	32.8	134.8	42.8	165.2
13-2	426.	24.0	55.0	22.7	102.2
14-2	1598.	59.2	233.2	82.3	282.1
14A-SC	1243.	56.5	198.5	60.4	239.2
14A-SC2	829.	36.3	133.4	54.5	170.9
15-2	0.	0.0	0.0	0.0	0.0
16-2	601.	13.9	57.1	18.2	68.2
17-2	583.	20.0	76.6	23.8	91.3
18-2	707.	59.0	241.7	62.0	274.9
18A-SC	263.	46.6	90.8	28.4	211.7
19	139.	0.0	4.1	0.13	1.55
25-1	255.	11.1	54.4	18.68	62.4
29-2	1410.	33.3	123.0	46.4	173.2
31-2	149.	9.1	42.4	10.9	47.0
33-2	334.	11.8	48.0	13.7	65.1
35-2	334.	0.0	14.0	0.0	7.6
38	277.	5.3	26.4	7.1	34.3
39	405.	10.5	31.6	13.4	54.7
41	279.	12.8	21.7	16.3	42.1
45	137.	3.0	29.0	16.0	36.7
50	108.	0.6	42.3	4.5	46.7
51	217.	9.9	36.5	10.9	44.3
53-SC	414.	13.3	58.6	18.9	57.5
53-SC2	561.	14.0	56.3	22.6	65.9
57	542.	27.5	116.6	32.9	146.2
61	139.	13.4	53.2	20.1	66.4
63-SC	717.	39.1	113.3	46.5	171.1
69	837.	42.7	147.3	62.9	211.7
Mean ± SD	504 ± 380	19.4 ± 18	75.2 ± 62	24.9 ± 21	93.8 ± 79

* Diagenetic excess

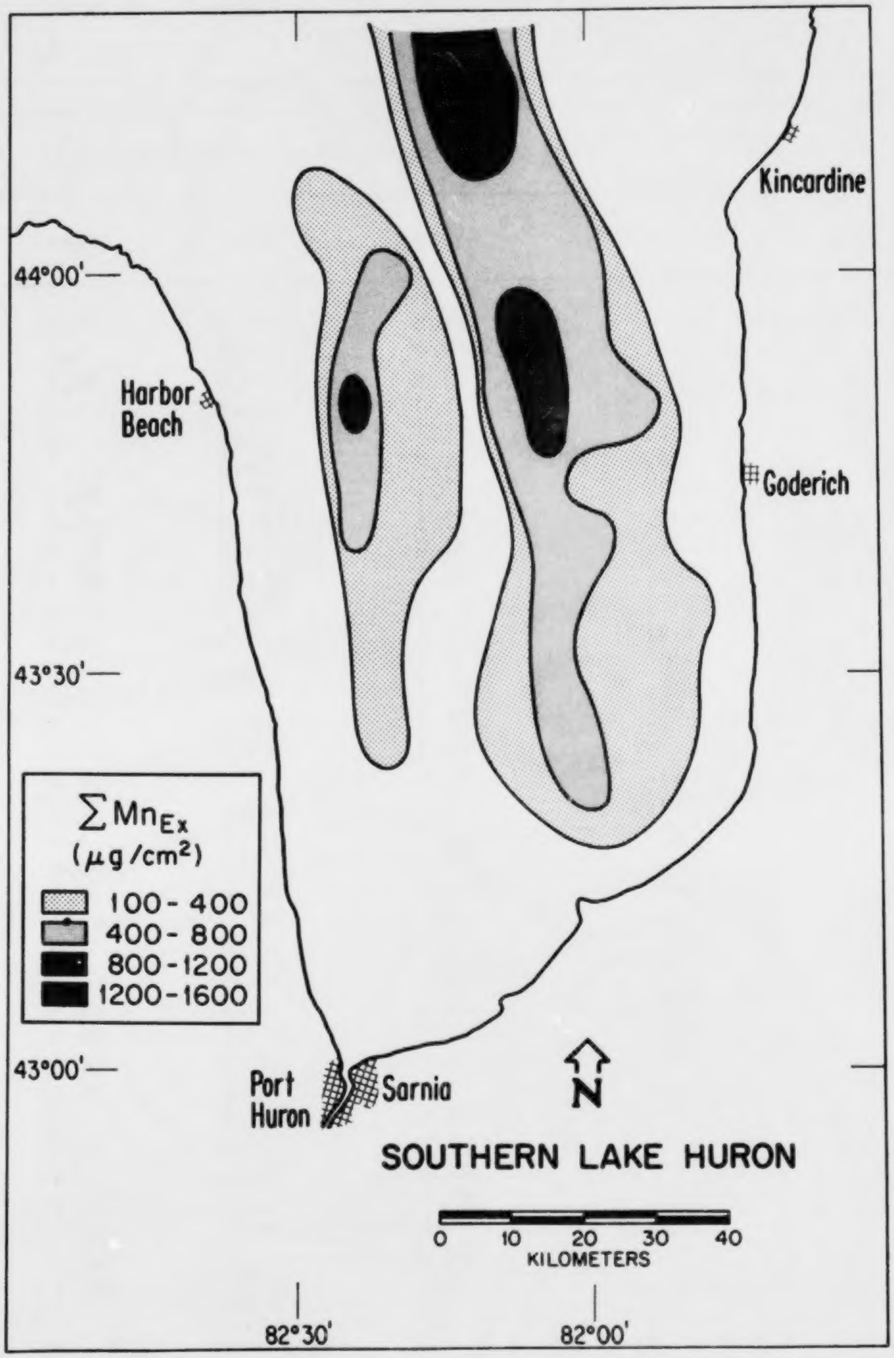

Kincardine
44°00'
Harbor Beach
Goderich
43°30'
$\sum Mn_{Ex}$
($\mu g/cm^2$)
100-400
400-800
800-1200
1200-1600
43°00'
Port Huron
Sarnia
N
SOUTHERN LAKE HURON
0 10 20 30 40
KILOMETERS
82°30'
82°00'

Figure 98. Distribution of vertically integrated excess manganese.

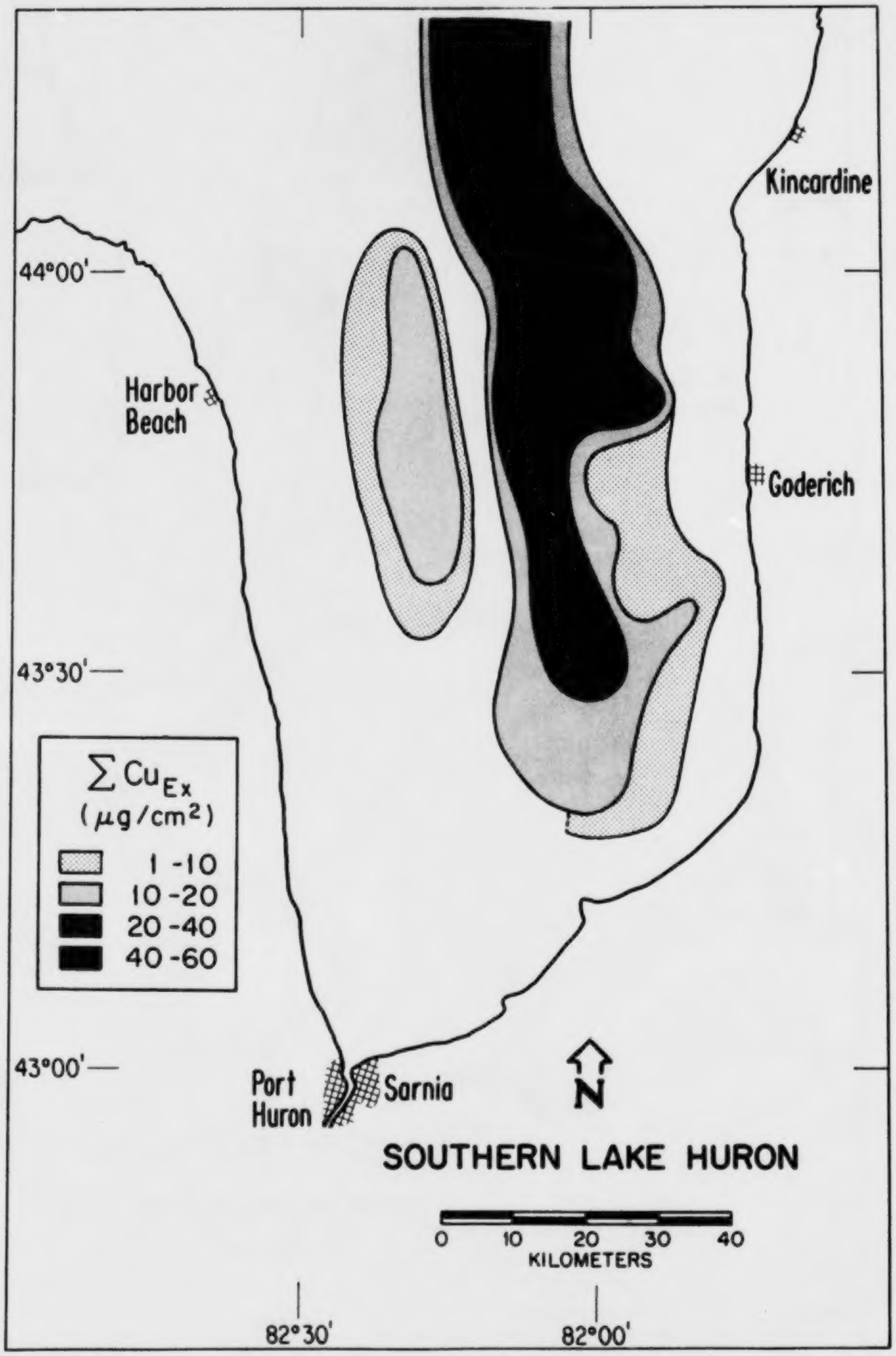
44°00'
43°30'
43°00'
82°30'
82°00'
Harbor Beach
Kincardine
Goderich
Port Huron
Sarnia
N
SOUTHERN LAKE HURON
$\sum Cu_{Ex}$
($\mu g/cm^2$)
1 -10
10 -20
20 -40
40 -60
0 10 20 30 40
KILOMETERS

Figure 99. Distribution of vertically integrated excess copper.

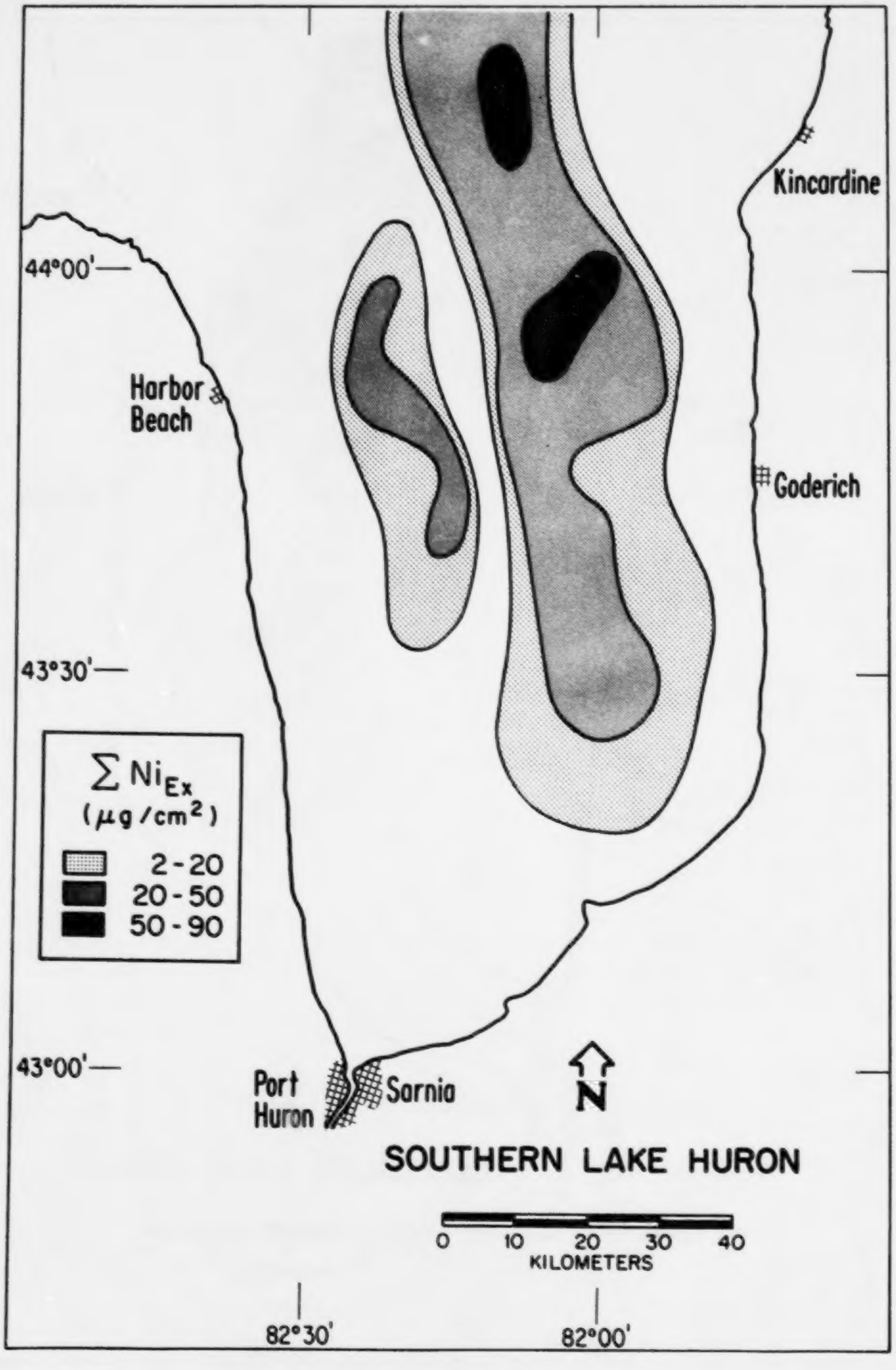
Kincardine
44°00'
Harbor Beach
Goderich
43°30'
∑ Ni$_{Ex}$ (μg/cm^2)
2-20
20-50
50-90
43°00'
Port Huron
Sarnia
N
SOUTHERN LAKE HURON
0 10 20 30 40
KILOMETERS
82°30'
82°00'

Figure 100. Distribution of vertically integrated excess nickel.

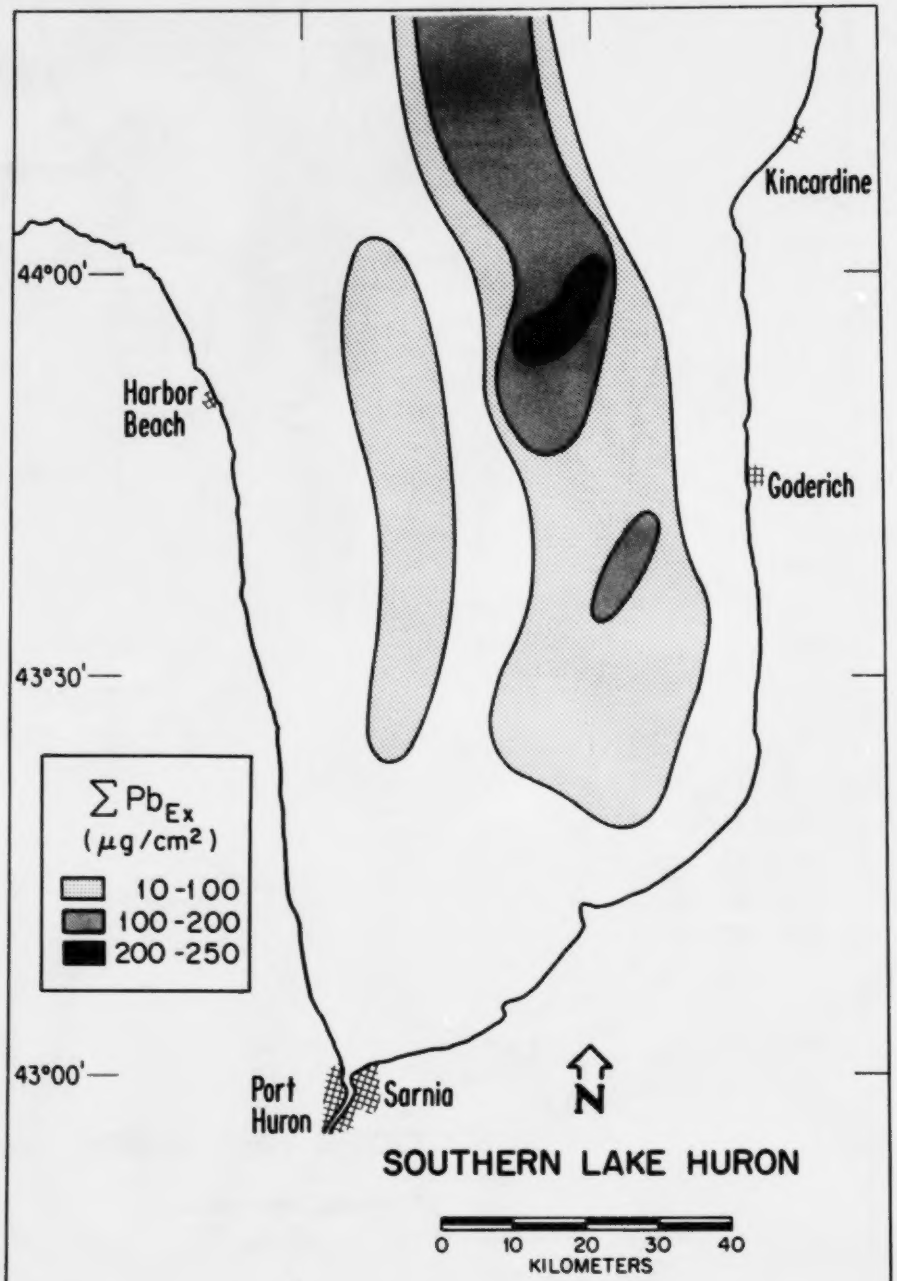
Kincardine
44°00'
Harbor Beach
Goderich
43°30'
∑Pb_Ex
(μg/cm²)
10-100
100-200
200-250
43°00'
Port Huron
Sarnia
N
SOUTHERN LAKE HURON
0 10 20 30 40
KILOMETERS
82°30'
82°00'

Figure 101. Distribution of vertically integrated excess lead.

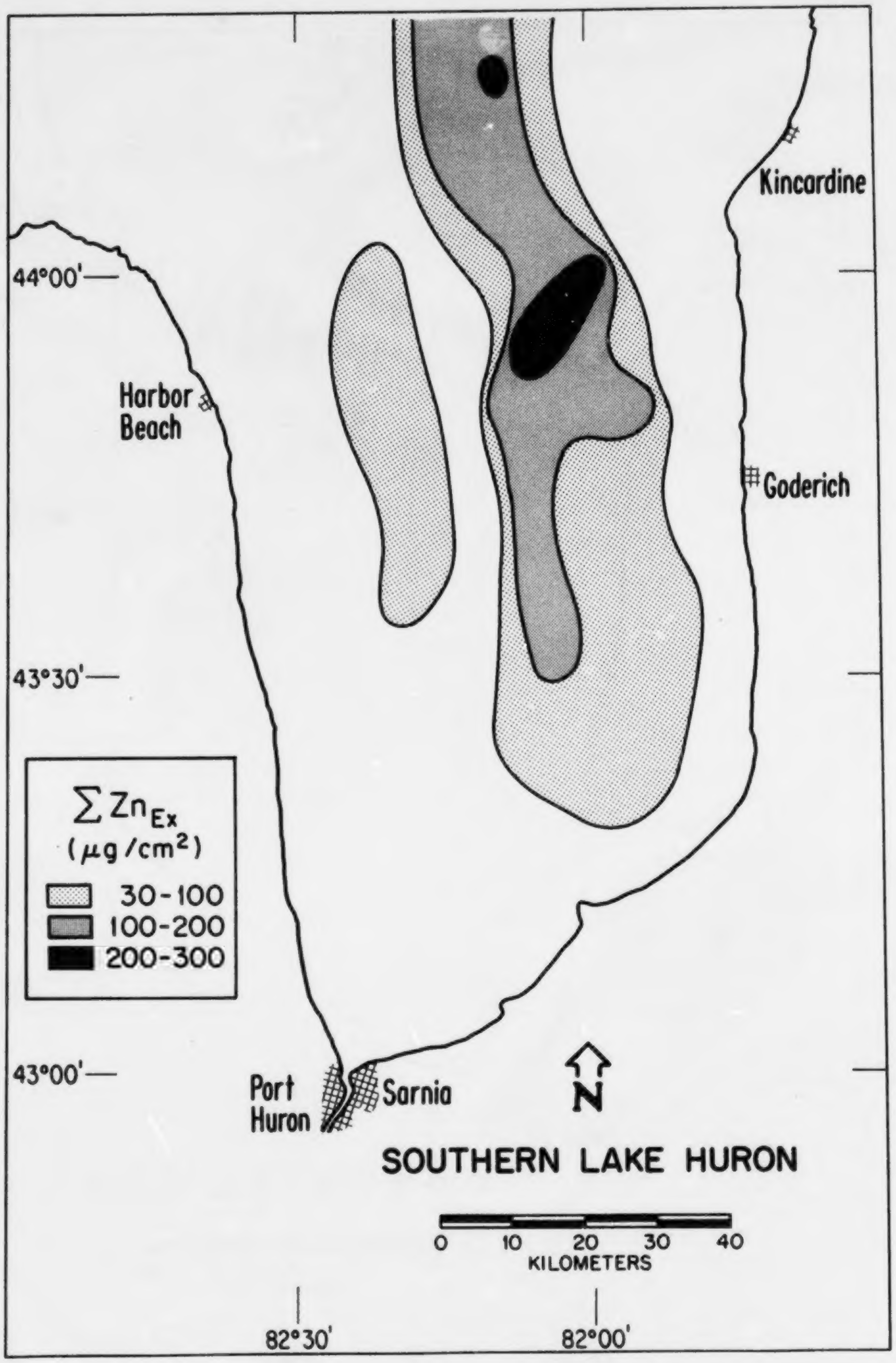
$\sum Zn_{Ex}$
($\mu g/cm^2$)
30-100
100-200
200-300
Kincardine
Harbor Beach
Goderich
44°00'
43°30'
43°00'
Port Huron
Sarnia
N
SOUTHERN LAKE HURON
0 10 20 30 40
KILOMETERS
82°30'
82°00'

Figure 102. Distribution of vertically integrated excess zinc.

TABLE 33. CORRELATIONS BETWEEN TOTAL EXCESS DEPOSITION (TED) OF SELECTED ELEMENTS

	Mn	Cu	Ni	Pb
Mn				
Cu	.71			
Ni	.81	.94		
Pb	.69	.90	.88	
Zn	.72	.99	.93	.93

N = 35 r = 0.43 at 0.01 level of significance.

On the basis of the distribution of TED values in each depositional basin, it is possible to arrive at an area-wide estimate of anthropogenic loadings. These loadings, expressed in metric tons (Table 34), are computed from the contour plots shown in Figs. 98-102. Values for As, Cd, and Sb are computed indirectly as follows: The mean surface concentrations of the four elements (Cu, Pb, Ni, and Zn) minus the mean "background" concentration or mean net concentrations are well-correlated with the total excess element stored ($r = 0.996$ for $N = 4$ significant at 0.01 level). Thus the regression of mean net surface concentrations on excess stored may be used to predict the excess storage of Cd, As and Sb from their mean net surface concentrations. Because of the limitations of this method of calculation, the values shown (in parentheses) in the table for these elements should be regarded as very approximate.

An important result of this study is the recognition that limited sampling of sediments can lead to considerable error in construction of materials budgets for the Lakes. As has all too often been the case in the past, sediment and contaminant budgets have been built on the analysis of an exceedingly limited number of sediment cores. In some cases inventories have been developed on the basis of a single core within a depositional basin. As can be seen from Table 32 there are up to order of magnitude differences in the total excess deposition from core to core within each depositional basin. There are sufficient data in this report to estimate the number of cores required per unit area of each depositional basin to arrive at a desired level of accuracy in estimating total inventory of a given contaminant. However, it is beyond the scope of this report to undertake such an analysis. It should be borne in mind that any relationship worked out for this study area is not generalizable to other parts of the lake.

Of particular interest is the total inventory of cesium-137 in southern Lake Huron. Integration of contours of vertically-integrated cesium-137 activity indicate a storage of about 60 Curies as of 1975 in the Port Huron Basin. In the Goderich Basin in 1975 there were about 320 Curies of cesium-137 present. At an aqueous concentration of about 0.02 pCi/l in 1975, inferred from the concentration-time model using the data of Barry (1973), the amount contained in the water in southern Lake Huron in 1975 was about 20 Curies. Thus the total stored in the water or in depositional basins amounted to about 400 Curies. In contrast the decay-corrected total deposition on this area of the lake is about 950 Curies (based on the data of Lerman 1970). Thus over half the cesium-137 deposited on the surface of southern Lake Huron did not end up in the underlying depositional basins. The hydraulic residence time of the lake is so long in comparison with the apparent residence time of cesium-137 in the water, that very little could have been lost by outflow. Hence either the numbers are wrong, or there has been a net export of the radionuclide out of the southern part of the Lake into other areas or there is storage of cesium-137 in non-depositional regions. The numbers are not likely to be off by a factor of two and until the inventory is made for the whole lake the second possibility cannot be ruled out. However, it does not take much mass per unit area overlying the non-depositional regions of the Lake to account for the missing cesium-137. Concentrations of cesium-137 in the very fine flocculent material overlying sediments has concentrations of cesium-137 approaching 30 pCi/g. One to two

TABLE 34. ANTHROPOGENIC ELEMENT STORAGE IN SEDIMENTS OF SOUTHERN LAKE HURON (METRIC TONS)

Element	Port Huron	Goderich	Combined	
			Regression*	Ratio**
Copper	100	611	710	600
Lead	410	2000	2400	2300
Nickel	157	788	950	1000
Zinc	344	2580	2900	3100
Antimony	-	-	(110)	40
Arsenic	-	-	(1000)	800
Bromine	-	-	-	600
Cadmium	-	-	(150)	60
Mercury	-	-	-	5
Tin	-	-	-	120

*Values in parentheses are approximates and based on regression of the net mean surface concentration vs. stored excess of Cu, Pb, Ni, and Zn

**Values based on the mean ratio of 1980 anthropogenic accumulation rates to the stored excess of Cu, Pb, Ni, and Zn.

TABLE 35. STORAGE OF CESIUM-137 IN SEDIMENTS OF SOUTHERN LAKE HURON

Region	Area ($\times 10^{13}$ cm^2)	Cesium-137 (1975) (Curies)
Water Column	9.5	(20)
Port Huron Basin	1.22	60
Goderich Basin	2.59	320
Non-depositional areas	5.93	(200)*
Total Cesium-137 in southern Lake Huron		600
Estimated time-integrated input decay-corrected to 1975		950
Unattributed cesium-137		350

*Arbitrarily assumes a 0.1 g/cm^2 flocculent/nephloid layer overlying non-depositional areas and having an average activity of 30 pCi/g.

cm of flocculent material may have a mass per unit area (dry weight) of 0.1 g/cm^2. This much mass per unit area if present over non-depositional areas could add 200 Curies to the cesium-137 inventory. Such calculations are summarised in Table 35. Such a layer of this characteristic mass per unit area could be present either in the form of a relatively well-defined layer in juxtaposition with non-depositional boundaries or in the form of a nephloid layer of some appreciable extent above the lake bottom. Evidence for the existence of such layers has been reported by Chambers and Eadie (1980) and confirms the sediment trap studies of Wahlgren et al. (1980). Whether it is necessary to postulate the existence of boundary-layer storage to realize accurate mass-balance calculations must remain a matter of speculation until critical experiments are performed.

SEDIMENT MIXING AND SEDIMENTATION RATES

In the preceding discussion, it has been possible to investigate patterns of contaminant metal deposition, inter-element associations and even total anthropogenic element loadings without reference to sedimentation rates. To gain information about the rates of contaminant deposition, however, it is necessary to associate a time scale with concentration profiles in individual cores. Three independent methods have been used for sediment geochronology in this report. The first relies on measurement of the vertical distribution of cesium-137 and the occurrence of a horizon corresponding to the onset of nuclear testing about 25 years ago. This method provides a measure on the average sedimentation rate over the past 25 years. The second method is based on the radioactive decay of lead-210 ($t_{1/2}$ = 22.26 years) following burial in sediments. In principle this method is capable not only of yielding average sedimentation rates over a period of roughly 100 years, but is capable of revealing changes in the rate of sedimentation over this period of time. The third method involves use of the anthropogenic element profiles themselves. The technique is based on the evidence that profiles of metals from diverse areas of a given lake or depositional basin reflect a common pollution history which is reconstructable in terms of regional contaminant loadings. The validity of this latter approach has been demonstrated by Edgington and Robbins (1976). Each of the three methods is investigated in this report and in combination, they lead to an internally consistent view of the local sedimentation process.

The computation of contaminant fluxes is sensitive to the interpretation given to individual profiles. This fact has been emphasized in a number of recent studies (Robbins et al., 1977, Robbins and Edgington, 1975, Edgington and Robbins, 1976, Robbins et al., 1978) which show that the mixing of surface sediments, probably by benthic organisms, has a significant influence on radioactivity and metal contaminant profiles and on the estimate of contaminant fluxes (Edgington and Robbins, 1976). In the section below on cesium-137, the effects of sediment mixing on radioactivity and contaminant profiles are discussed.

Cesium-137

Cesium-137 is a uniquely anthropogenic radionuclide first introduced into the environment as a result of atomic weapons testing which began roughly 25 years ago. Many studies have now demonstrated the utility of cesium-137 for investigation of sedimentation processes in aquatic systems such as lakes and reservoirs. Cesium-137 is an especially useful tracer because its input to the lakes may be accurately inferred from atmospheric and precipitation radioactivity measurements (Sr-90) made for about a 20 year period within the watershed of the Great Lakes and elsewhere. Shown in Figure 103 is the record of deposition of cesium-137 onto Lake Huron since about 1955. Two maxima are apparent, one in 1958-59 and a larger one in 1963-1964. In the middle panel of Fig. 103 is shown the average annual concentration of cesium-137 in waters of the Lake from about the mid 1960s (Barry, 1973). The smooth curve is the predicted concentration based on a time-dependent coupled-lakes model developed for this report and analogous to that used by Lerman (1970) for Sr-90. The theoretical fit is best in the least squares sense for an assumed residence time of 1.1 years for cesium-137 in the water column. Thus the radionuclide is rapidly removed from the water and changes in its aqueous concentration mimic the history of atmospheric deposition as a result. Since the hydraulic retention time of the Lake is long (about 30 years) in comparison with the overall residence time of the radionuclide, the dominant process for removal of cesium-137 is particle scavenging and sedimentation. This inference is consistent with the known high affinity of radiocesium for certain clay minerals present in the water column. It is therefore expected that the flux of cesium-137 to the sediments would follow the time-dependence of aqueous concentrations as well as that of atmospheric inputs. While the flux may do so, the profile of cesium-137 often does not as can be seen in the bottom panel of Fig. 103. In the core from station 18, dated by the lead-210 method, the cesium concentration is smeared out and details of the time-dependence of the input from the overlying water are entirely lost. This smeared-out character of the cesium-137 profiles is seen in other cores such as those shown in Figs. 104-108 for selected (1974) stations. The data for all cores are given in Table A-4 of the appendix. In most cases there is no detailed structure, and often there is a zone of nearly constant activity extending downward from the sediment-water interface. Subsurface maxima are sometimes but not always seen. These features are strikingly illustrated for a series of cores taken at station 14 (Fig. 109). At this location the reproducibility of profiles taken one year to the next is excellent. The open symbols in Fig. 109 refer to two cores collected in 1974 while the solid symbols refer to 1975 collections. In both cases there is a zone of nearly constant activity which extends down to about 4 cm, with a suggestion of a peak at around 5 cm, followed by a gradual decrease in activity below this point down to 10 cm.

As a part of this report, a model has been developed to account for the observed discrepancy between observed and expected cesium-137 profiles. The details are presented in Robbins et al. (1977). The smearing is assumed to occur only in the sedimentary column and as a result of the rapid steady-state mixing of sediments over a zone of fixed depths, at the sediment water interface. This depth is referred to as the mixing depth. It can be shown (Robbins et al., 1977) that if the activity of radiocesium added to the sediments at time t (with t = 0 corresponding to a very deep sediment layer) is $A^s(t)$, the expected cesium-137 distribution is given by:

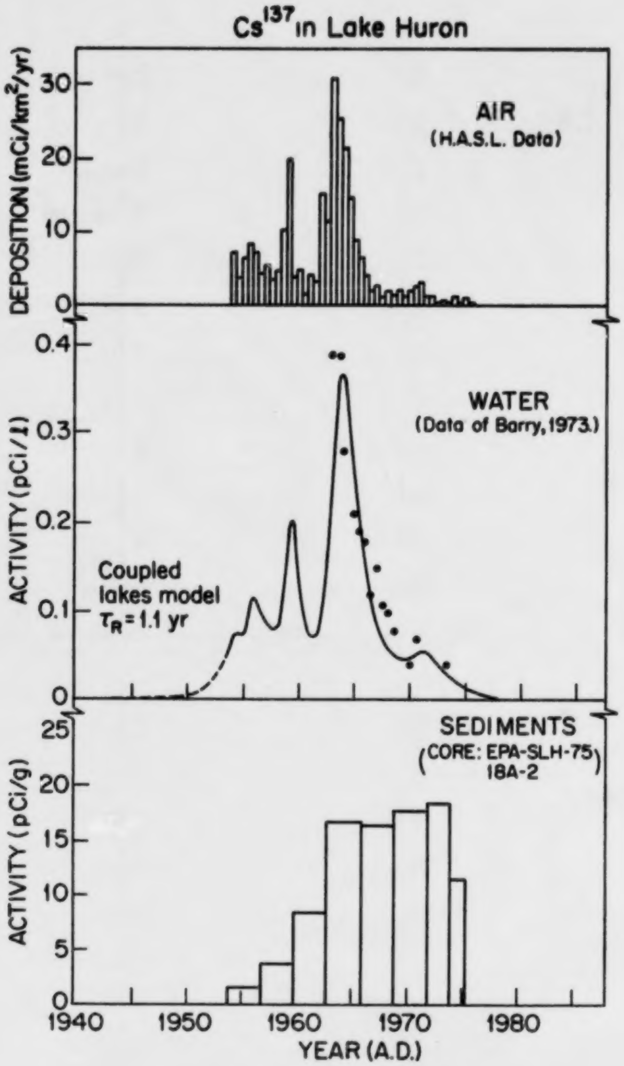

Figure 103. History of cesium-137 deposition in Lake Huron. (Upper panel: estimated flux to the lake surface; Middle panel: observed mean and predicted concentration in surface waters; Bottom panel: distribution observed in a dated sediment core.)

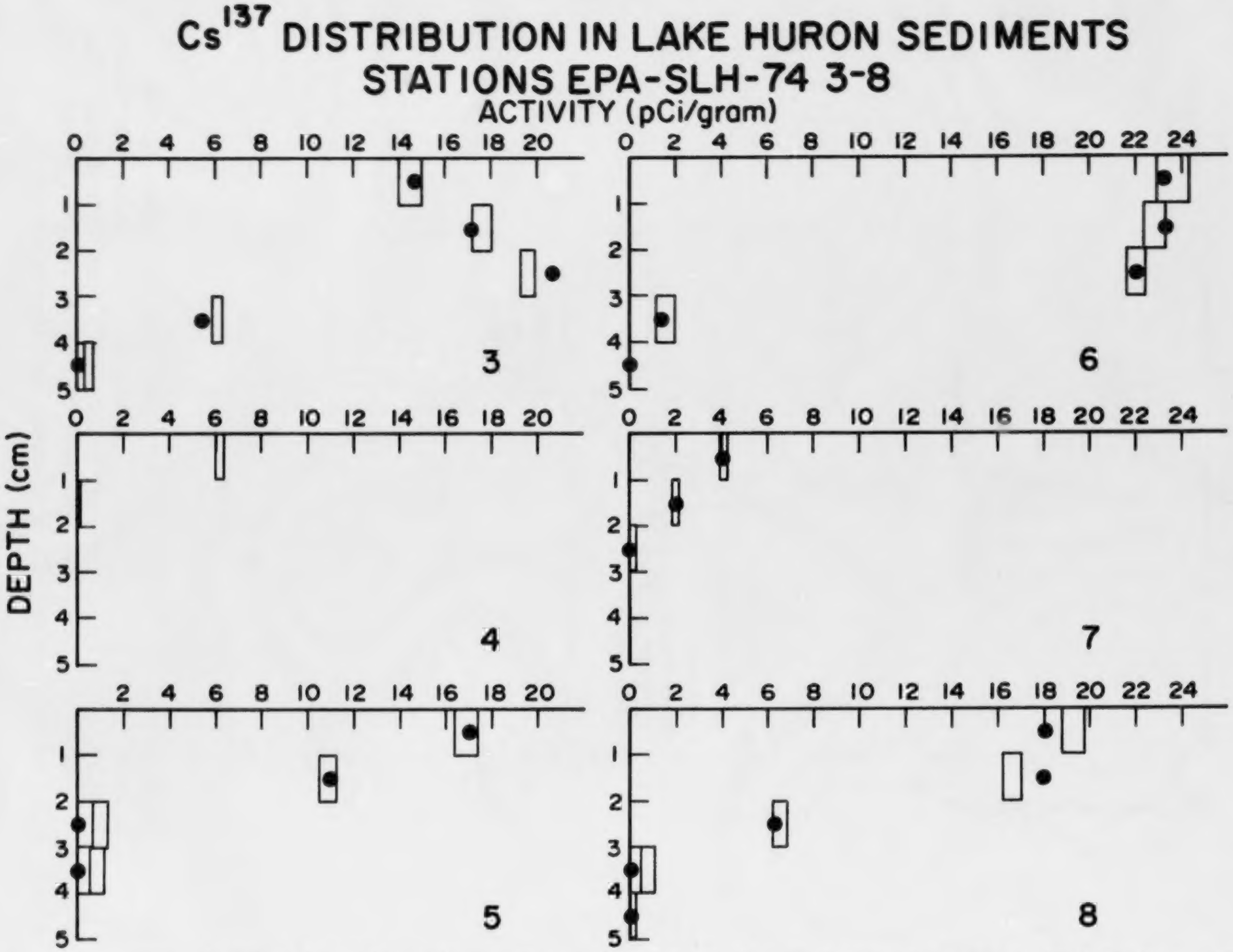

Figure 104. Vertical distribution of cesium-137 in selected cores (74:3-8). (Rectangular regions correspond to measured activities. Height indicates sampling interval, width represents analytical errors. Solid circles correspond to values predicted by steady-state mixing model.)

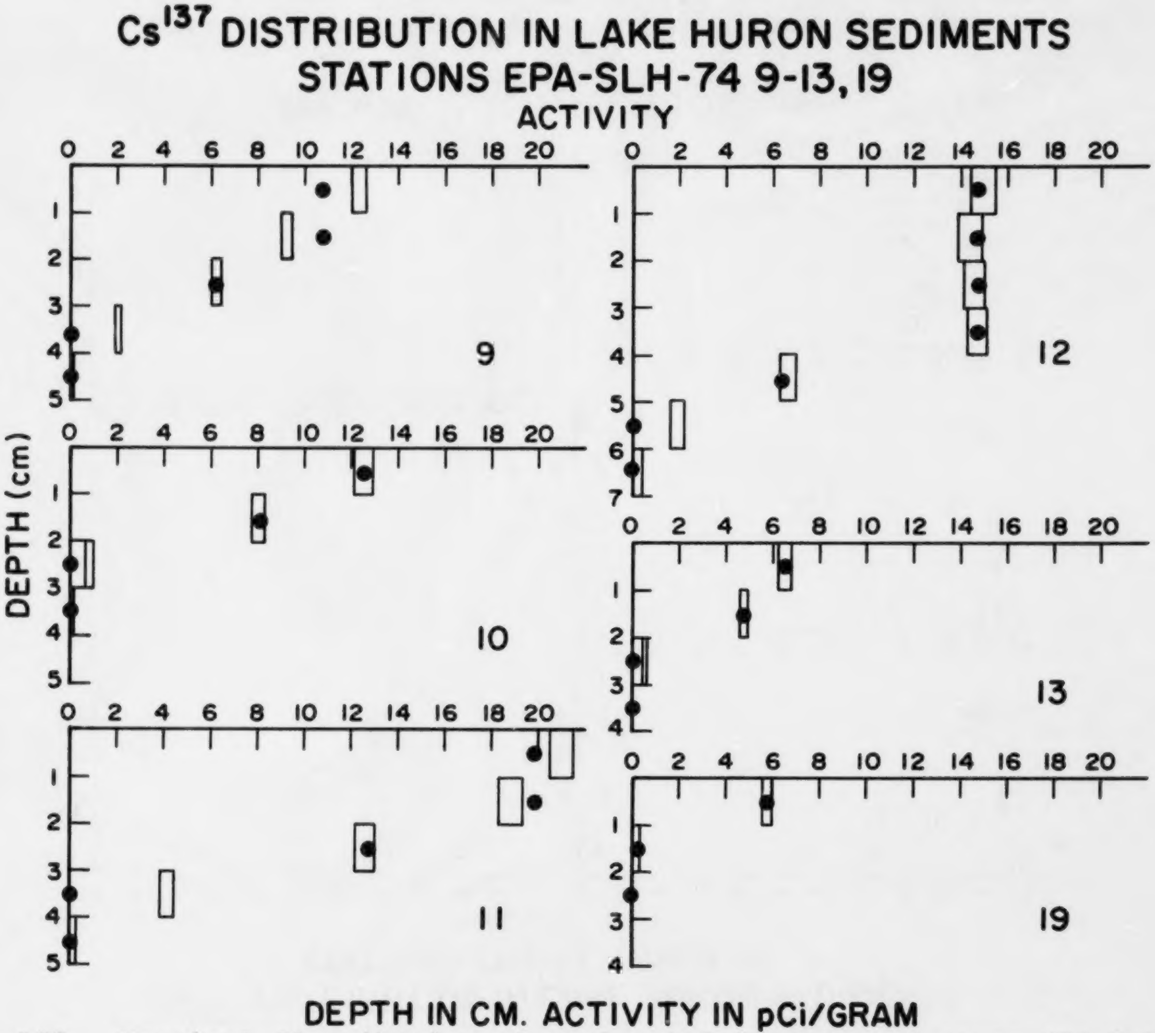

Figure 105. Vertical distribution of cesium-137 in selected cores (74:9-13,19)

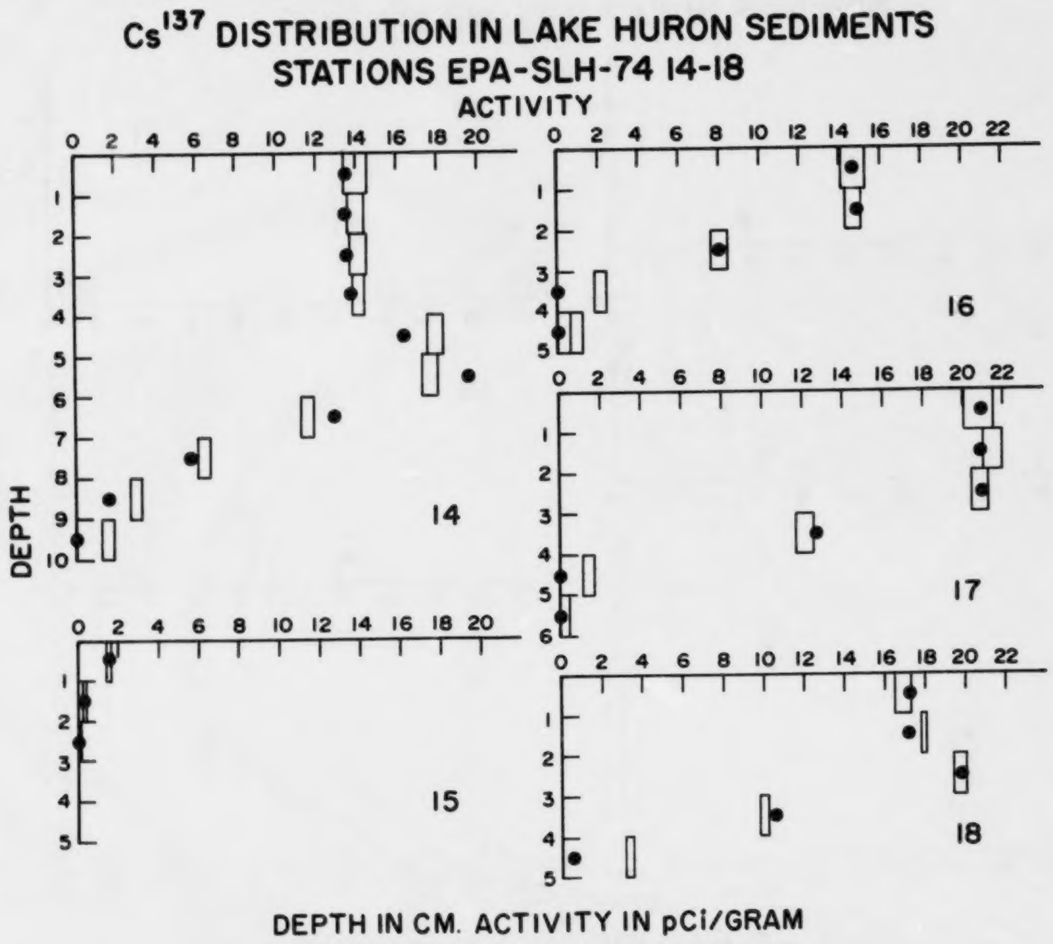

Figure 106. Vertical distribution of cesium-137 in selected cores (74:14-18).

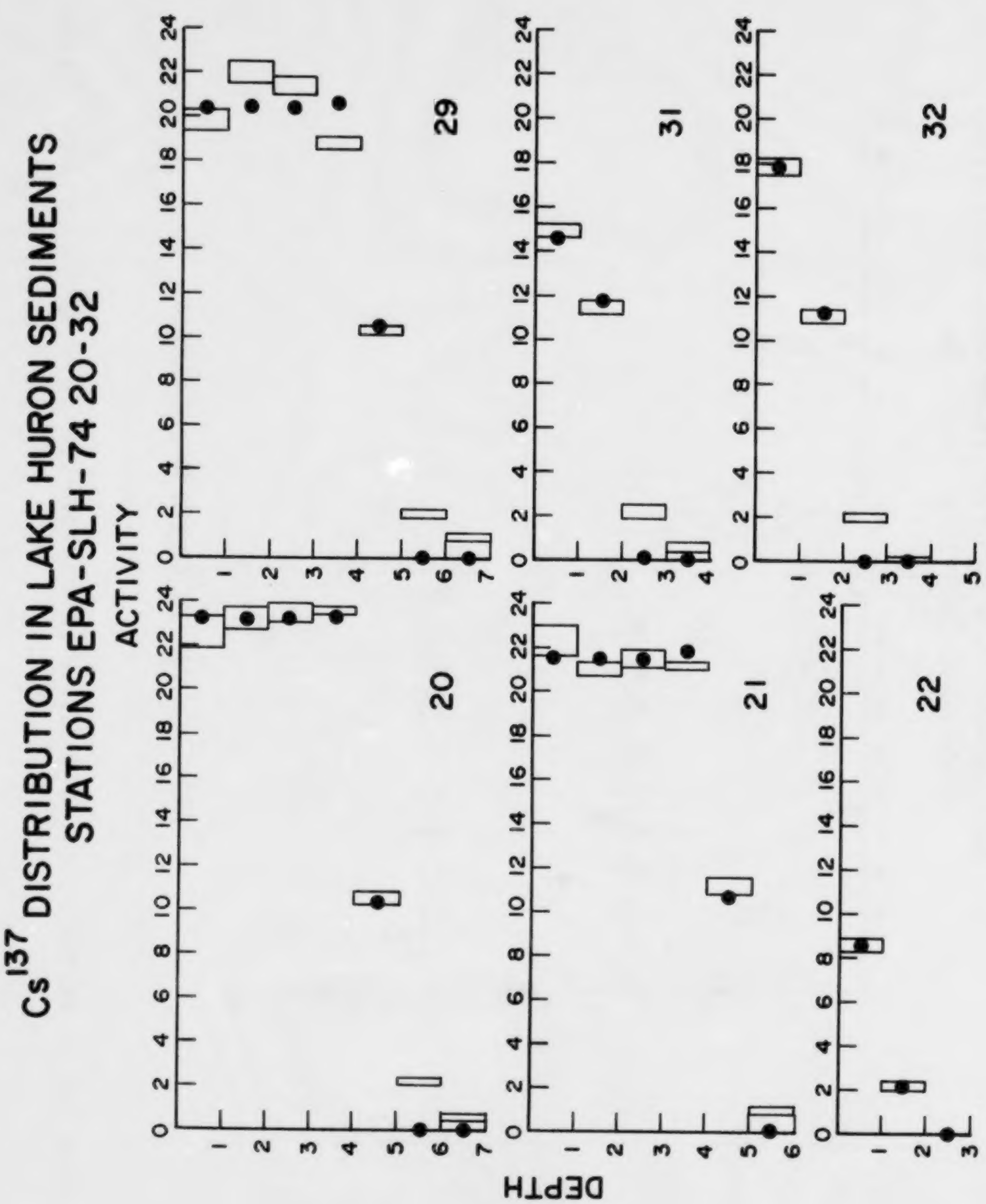

Figure 107. Vertical distribution of cesium-137 in selected cores (74:20-32).

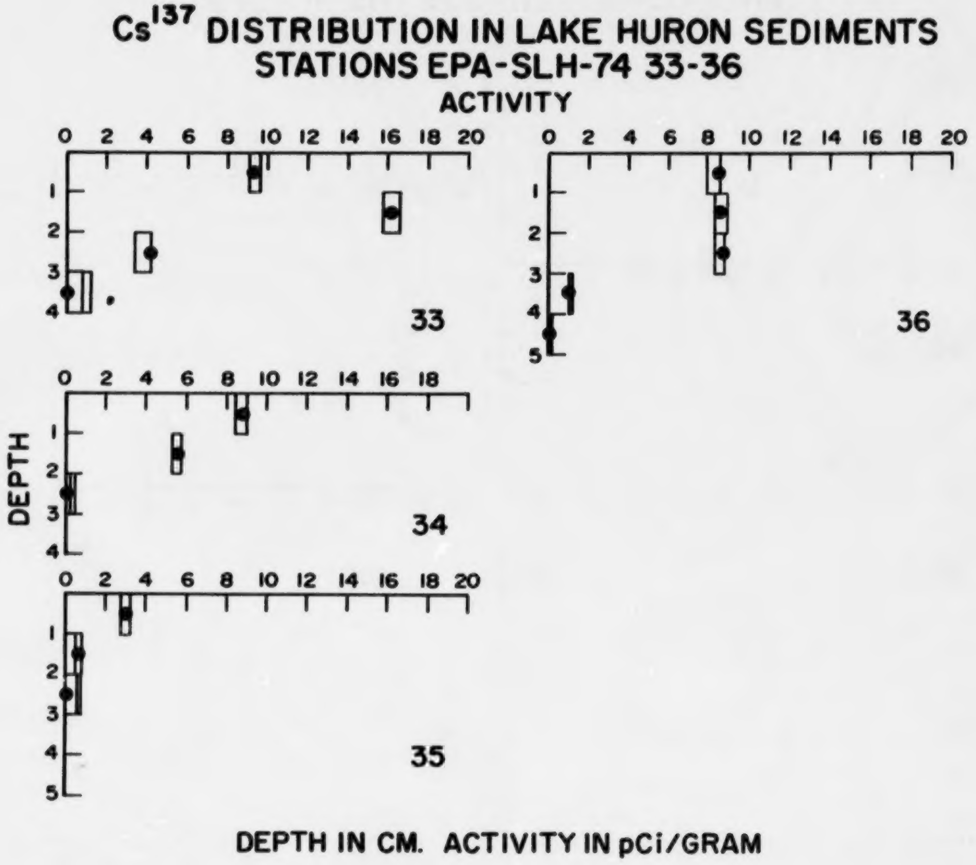

Figure 108. Vertical distribution of cesium-137 in selected cores (74:33-36).

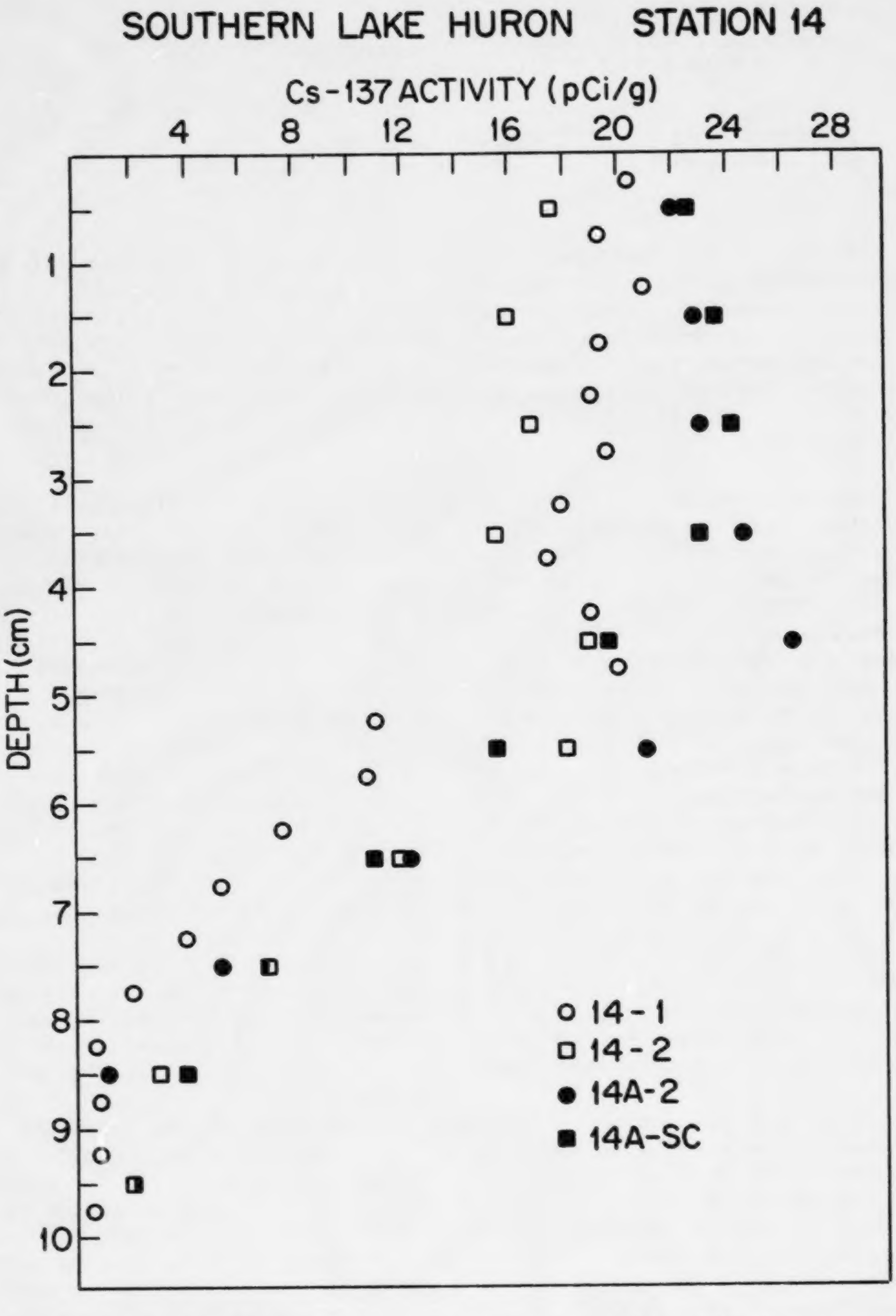

Figure 109. Vertical distribution of cesium-137 in a series of cores at station 14 collected in 1974(14-1,2) and in 1975(14A-2,SC).

$$A = Am(T) \qquad z \leq s$$

$$A = Am(T + (s - z) \,/\, \omega)\ e^{-\lambda(z-s)/\omega} \qquad z > s \tag{38}$$

and

$$Am(t) = \gamma\ e^{-(\gamma + \lambda)t} \int_{o}^{t} e^{+(\gamma + \lambda)\tau}\ A_s(\tau)\ d\tau$$

where $\gamma = r/s$, $t = T$ corresponds to the sediment water interface and $\bar{\omega}$ is the sedimentation rate (cm/yr) neglecting the effects of compaction. is the radioactive decay constant for cesium-137 ($\gamma = 0.69315/t_{1/2}$; $t_{1/2} = 30.0$ years) and z is the depth below the sediment-water interface. The effects of compaction are automatically taken into account by expressing z in terms of the cumulative mass per unit area and $\underline{\omega}$ in terms of the mass sedimentation rate (g/cm^2/yr). The mixing depth, in consistent units, is expressed in terms of mass/unit area.

A computer program was developed to find the value of the mixing depth, sedimentation rate and surface activity $A_s(T)$ giving the best least squares fit of the above equation to the observed profiles. The results are summarized in Table 36 and indicated in Figs. 104-108 in terms of the solid points of selected profiles. In general, the agreement is satisfactory but often, because of the limited range of penetration of radiocesium into these sediments, the inferred values, both the sedimentation rates and mixed depths, are subject to large uncertainties. The effect of steady-state mixing on the radio-cesium profile is illustrated in Fig. 110 which shows the distribution expected in a lead-210 dated core in the absence of mixing (left panel). With a short overall residence time in the Lake, radiocesium should have a sedimentary profile which corresponds to the history of atmospheric deposition. Because of mixing, however, the activity is found deeper in the core and is smoothly distributed as indicated in the right panel of Fig. 110. In most cores from the study area, the observed vertical distribution of radiocesium is largely the result of mixing rather than sedimentation. Thus limited reliable information is obtained on sedimentation rates via cesium-137 measurements. This is easily seen by examination of Fig. 107 for such stations as 20 and 21. In cores from these stations the activity is essentially constant over the upper 4 cm or so and drops abruptly in deeper sections. In such cores the sedimentation rate could be almost zero and yet, because of mixing, activity will appear at appreciable depths in the core.

Moreover both the sedimentation rate and mixing depth are sensitive to small losses of material from the tops of the cores. This may be illustrated by repeated analysis of the cesium-137 profile at station 14 via the mixing-model for progressive losses of sediment (i.e. the model was evaluated using the station 14 profile with top and successive layers of data left out and the surface (z=0) redefined). The results are shown in Table 37. As Cs-137 is found more deeply in this core than in most others, station 14 represents an optimal case. Cores in which Cs-137 is only a few cm deep will be far more sensitive to disturbances of the sediment-water interface. Thus, at best, cesium-137 can be used only as a rough indication of sedimentation rates in southern Lake Huron and an alternative measure of sedimentation

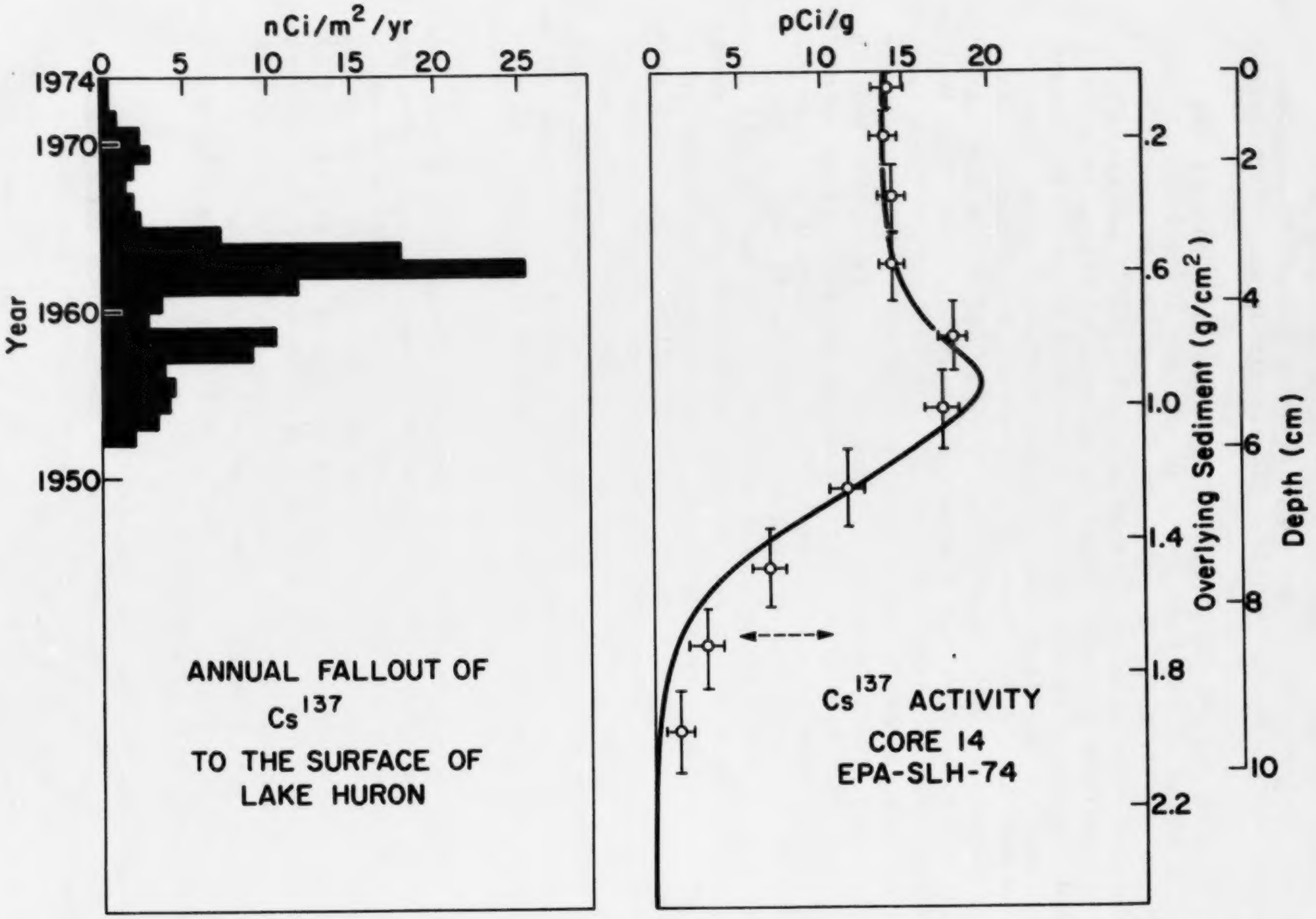

Figure 110. Relation between the expected and observed distribution of cesium-137 at station 14 (Core 14A-2). (Left panel: Distribution expected if transfer from air to sediments were instantaneous and if there were no sediment reworking. Right panel: Observed distribution and predicted profile using the steady-state mixing model.)

rates must be employed. Lead-210 is suitable in this respect partly because the average sedimentation rate determined by this method is almost completely insensitive to any realistic losses of sediment on coring or other short-range (cm) disturbances of the sediment-water interface. Sedimentation rates determined via cesium-137 and lead-210 are discussed further below.

As part of this report, the vertical distribution of benthos was determined in a series of replicate cores at stations 14A and 18A (Krezoski et al., 1978) to establish if their distribution and density could account for the inferred effects of mixing. Robbins et al. (1977) successfully showed that benthos were primarily found in the zone of mixing as defined by cesium-137 and lead-210 profiles and that they were present in sufficient numbers to account for estimated mixing rates. Further studies, sponsored by EPA in Saginaw Bay, have shown (Batac-Catalan et al. 1980) that the mixed depth is well-correlated with the depth above which 90% of the benthos occur. A summary plot for cores examined to date from this study area, from Saginaw Bay and from Lake Erie is given in Figure 111. The 90% cutoff depth is very well correlated with the depth of the mixed zone ($S = -0.2 + 1.16 Z$; $r = 0.91$, $N = 10$). Thus, there is strong circumstantial evidence that benthic organisms are primarily responsible for the mixing of near-surface sediments and the resultant alteration of radioactivity and contaminant metal profiles. Previously it had been suggested (Lerman & Lietzkie, 1975) that profiles of cesium-137 as well as those of strontium-90 might be affected or even largely determined by diffusional migration. However, Robbins et al. (1977) showed that cesium-137 cannot migrate significantly its sediments by molecular diffusion since it is strongly bound to sediment solids. This result cannot be generalized to include other contaminants, tracers, or sedimentary environments however. Cesium-137 can experience significant diffusional migration in sediments which do not contain minerals with a specific affinity for this radionuclide (cf. Alberts et al. 1979). Also a nearly conservative tracer such as Sr-90 undergoes considerable diffusion in sediments of the Great Lakes (Lerman & Lietzkie, 1975).

In Table 36 the mixing depth derived from the steady-state mixing model is given both in linear terms (cm) and in terms of mass per unit area. For both measures, there is a systematic variation within each depositional basin. A major increase in the depth of sediment mixing occurs toward the deepest, central region and northward within the Goderich Basin (Fig. 112). Values range from essentially zero to over 4 cm. Reasons for the observed distribution are not clear, but the depth of mixing is directly related to the porosity of surface sediments. Less consolidated sediments are mixed to a greater depth (compare Figs. 16 and 112). This trend may be related to the nature of benthos-sediment interactions.

Also given in Table 36 is the vertically integrated activity of cesium-137 (or total deposition), the analogue of TED for soluble elements and computed using Eq. 37 with $C_{bg} = 0$. Mean vertically integrated activities (pCi/cm^2) for the Port Huron and Goderich Basins are respectively 4.8 ± 2.6 ($N = 12$) and 11.2 ± 7.7 ($N = 47$). The horizontal distribution of the total cesium deposition is shown in Fig. 113. Highest deposition occurs toward the center of the Goderich Basin but values often do not exceed that expected from atmospheric fallout, decay-corrected to 1975 (about 10 pCi/cm^2).

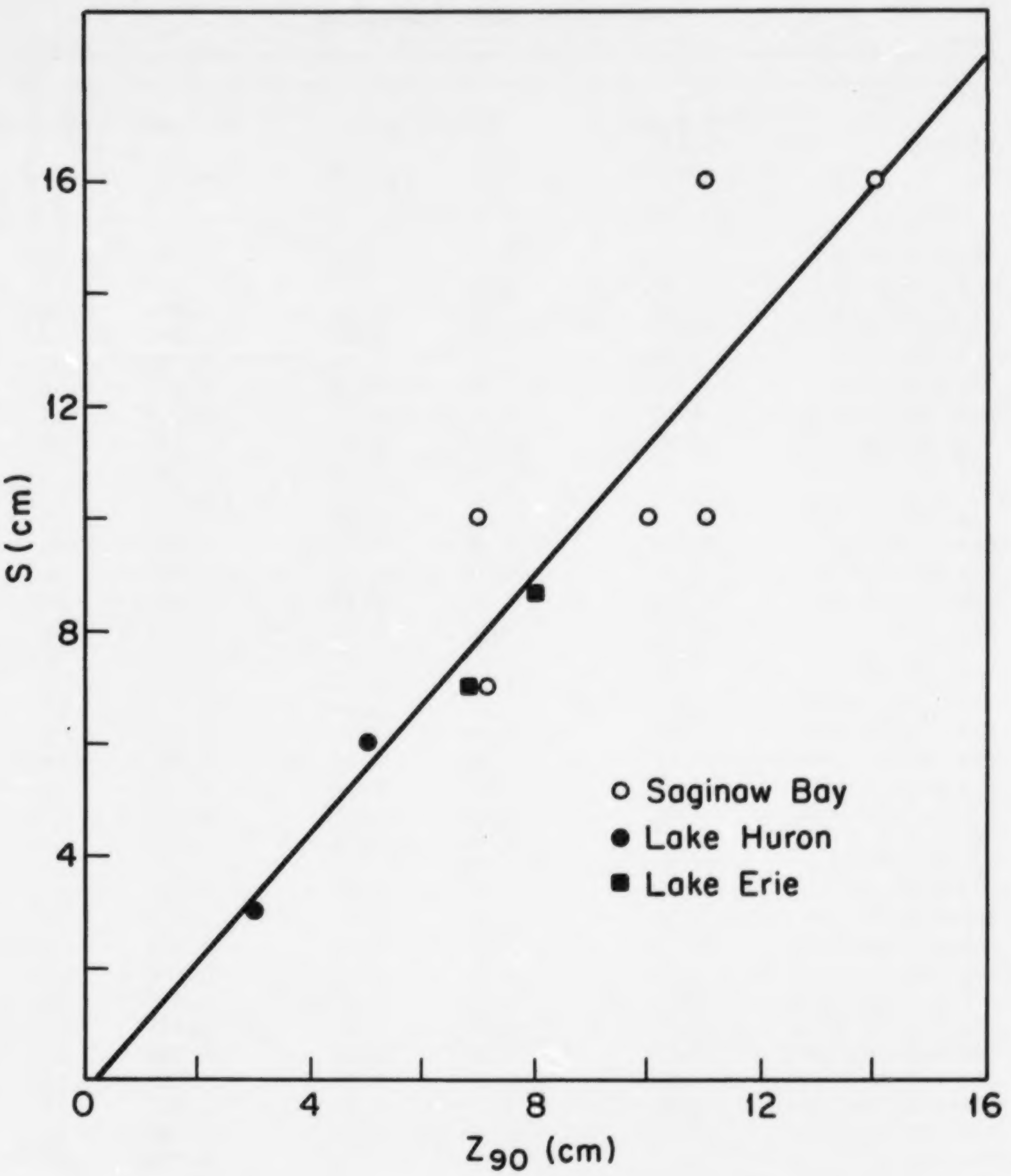

Figure 111. Relation between the depth of sediment mixing as indicated by either cesium-137 or lead-210 and the depth above which 90% of benthic macroinvertebrates occur (Z_{90}).

TABLE 36. VERTICALLY INTEGRATED ACTIVITY OF CESIUM-137 AND MIXING MODEL PARAMETERS

STATION	INTEGRATED CS-137 (pci/cm^2)	MIXING DEPTH		SEDIMENTATION RATE CS-137	
		(cm)	(g/cm^2)	(cm/yr)	(mg/cm^2/yr)
EPA-SLH-74-3-2	11.30	1.42	0.24	0.188	28.
EPA-SLH-74-4-2	1.45	0.00	0.00	--	0.
EPA-SLH-74-5-2	5.35	1.41	0.22	0.204	28.
EPA-SLH-74-6-2	10.01	2.52	0.36	0.069	7.
EPA-SLH-74-7-2	3.79	1.07	0.64	0.039	23.
EPA-SLH-74-8-2	7.30	1.96	0.28	0.051	6.
EPA-SLH-74-9-2	8.50	2.00	0.54	0.099	19.
EPA-SLH-74-10-2	4.83	1.08	0.22	0.057	11.
EPA-SLH-74-11-2	8.32	2.24	0.34	0.050	6.
EPA-SLH-74-12-2	14.91	3.80	0.72	0.085	11.
EPA-SLH-74-13-2	5.67	1.05	0.34	0.074	23.
EPA-SLH-74-14-1	22.57	3.79	0.65	0.500	49.
EPA-SLH-74-14-2	23.69	3.62	0.61	0.487	56.
EPA-SLH-75-14A-2	29.35	3.20	0.55	0.341	45.
EPA-SLH-75-14A-SC	28.20	5.28	0.95	0.152	20.
EPA-SLH-74-15-2	1.68	0.88	0.80	0.030	27.
EPA-SLH-74-16-2	7.11	1.69	0.22	0.093	10.
EPA-SLH-74-17-2	12.01	2.96	0.46	0.095	10.
EPA-SLH-74-18-2	15.25	2.05	0.48	0.340	32.
EPA-SLH-75-18A-SC	12.35	1.78	0.40	0.098	18.
EPA-SLH-75-18A-2	12.07	1.90	0.43	0.167	19.
EPA-SLH-74-19-2	1.00	0.18	0.04	0.044	10.
EPA-SLH-74-20-2	16.47	3.53	0.55	0.115	13.
EPA-SLH-74-21-2	15.91	3.38	0.52	0.156	17.
EPA-SLH-74-22-2	4.06	0.76	0.18	0.051	12.
EPA-SLH-74-25-1	9.30	1.72	0.25	0.123	13.
EPA-SLH-74-29-2	16.70	1.96	0.62	0.130	17.
EPA-SLH-74-30-2	3.60	0.35	0.07	0.077	12.
EPA-SLH-74-31-2	6.19	1.06	0.22	0.058	12.
EPA-SLH-74-32-2	5.78	1.04	0.17	0.063	10.
EPA-SLH-74-33-2	5.07	0.82	0.10	0.138	17.
EPA-SLH-74-34-2	5.13	1.17	0.36	0.060	16.
EPA-SLH-74-35-2	3.40	0.05	0.28	0.052	31.
EPA-SLH-74-36-2	9.21	2.40	0.70	0.090	20.
EPA-SLH-75-39	4.85	1.12	0.70	0.133	80.
EPA-SLH-75-40-2	3.18	1.40	1.25	0.056	45.
EPA-SLH-75-41-1	5.36	1.58	0.23	0.096	5.
EPA-SLH-75-42-1	11.92	2.81	0.68	0.140	20.
EPA-SLH-75-43	2.06	0.88	0.85	0.110	40.
EPA-SLH-75-44	0.33	0.85	1.13	0.026	35.

(continued).

TABLE 36. (continued).

STATION	INTEGRATED CS-137 (pci/cm^2)	MIXING DEPTH		SEDIMENTATION RATE CS-137	
		(cm)	(g/cm^2)	(cm/yr)	(mg/cm^2/yr)
EPA-SLH-75-45	2.42	1.42	1.70	0.071	80.
EPA-SLH-75-46	9.80	2.82	2.15	0.148	70.
EPA-SLH-75-47-2	26.80	4.84	0.72	0.318	28.
EPA-SLH-75-48	0.06	0.00	0.00	--	0.
EPA-SLH-75-49-2	11.24	1.64	0.30	0.088	14.
EPA-SLH-75-50	4.89	1.63	1.03	0.062	32.
EPA-SLH-75-51-1	4.09	1.54	1.40	0.106	90.
EPA-SLH-75-52	0.44	0.00	0.00	--	0.
EPA-SLH-75-53-SC	12.92	2.97	0.62	0.092	12.
EPA-SLH-75-54	15.33	3.72	1.52	0.238	54.
EPA-SLH-75-55	28.57	4.98	0.84	0.266	29.
EPA-SLH-75-56	2.26	0.78	0.21	0.041	11.
EPA-SLH-75-57	8.43	2.40	0.38	0.114	13.
EPA-SLH-75-58	5.59	1.10	0.19	0.075	11.
EPA-SLH-75-59	18.31	3.33	0.48	0.217	20.
EPA-SLH-75-60	22.63	0.70	0.67	0.327	55.
EPA-SLH-75-61	13.69	1.31	0.42	0.167	48.
EPA-SLH-75-62	9.92	1.14	0.28	0.117	27.
EPA-SLH-75-63-SC	15.16	2.26	0.39	0.167	22.
EPA-SLH-75-65	23.57	4.00	0.62	0.303	27.
EPA-SLH-75-66	17.79	3.27	0.60	0.216	24.
EPA-SLH-75-67	3.26	0.86	0.13	0.040	6.
EPA-SLH-75-68	22.90	3.10	0.66	0.264	29.
EPA-SLH-75-69	24.93	3.78	0.66	0.268	34.
EPA-SLH-75-70	15.99	3.80	0.58	0.106	9.
EPA-SLH-75-71	11.44	1.83	0.43	0.071	7.

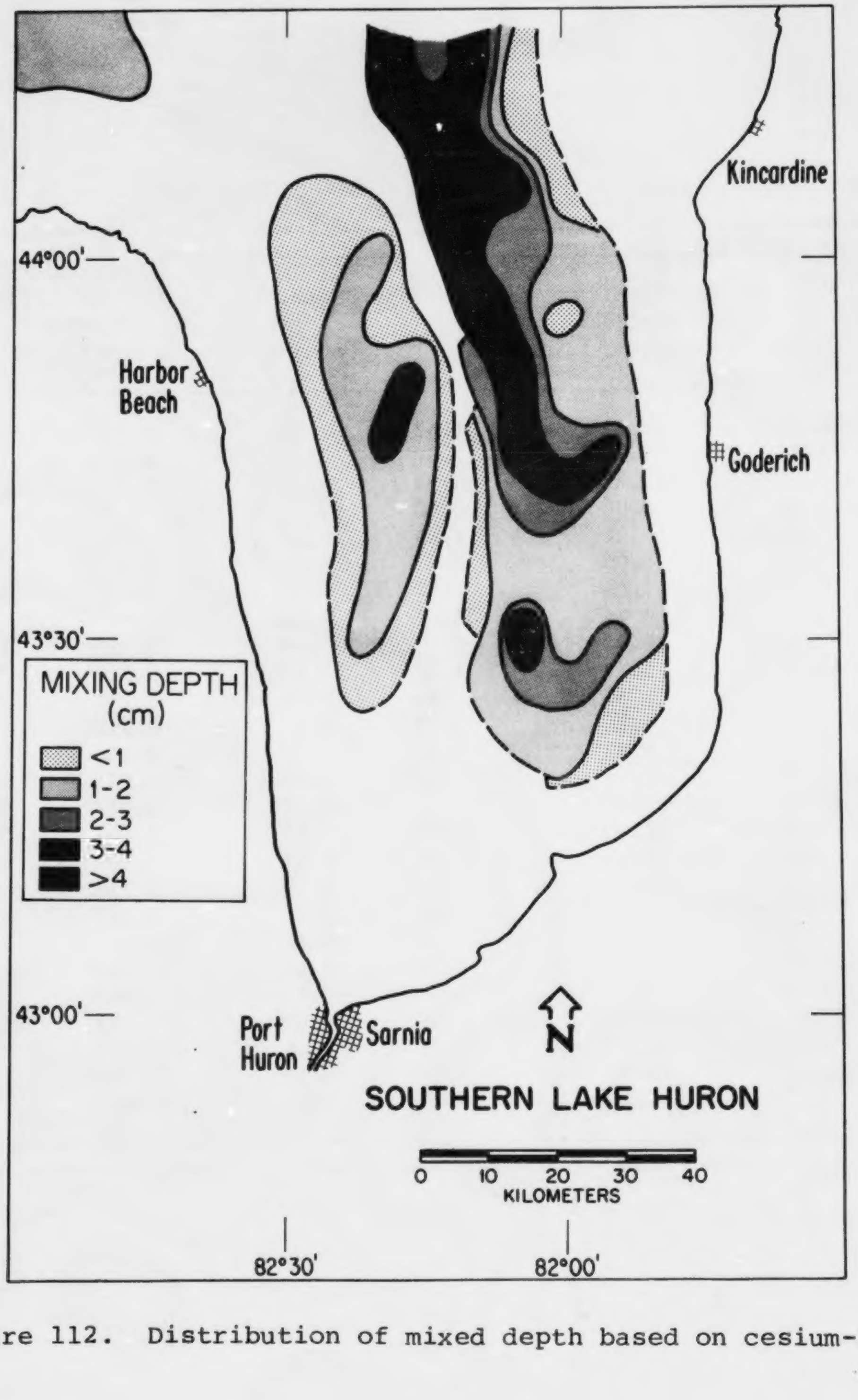
Kincardine
44°00'
Harbor Beach
Goderich
43°30'
MIXING DEPTH (cm)
<1
1-2
2-3
3-4
>4
43°00'
Port Huron
Sarnia
N
SOUTHERN LAKE HURON
0 10 20 30 40
KILOMETERS
82°30'
82°00'

Figure 112. Distribution of mixed depth based on cesium-137.

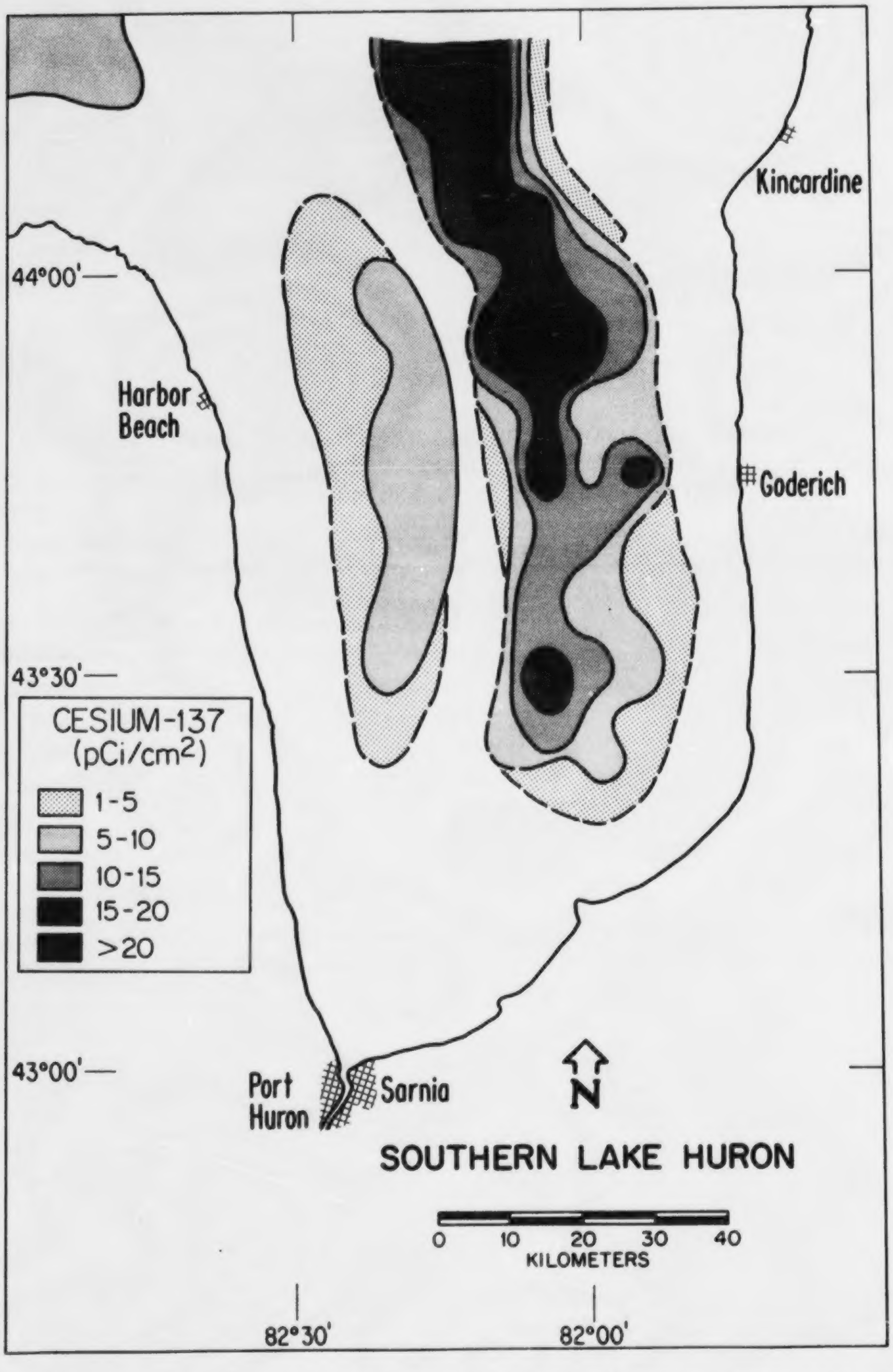
Kincardine
44°00'
Harbor Beach
Goderich
43°30'
CESIUM-137 (pCi/cm²)
1-5
5-10
10-15
15-20
>20
43°00'
Port Huron
Sarnia
N
SOUTHERN LAKE HURON
0 10 20 30 40
KILOMETERS
82°30'
82°00'

Figure 113. Distribution of vertically integrated cesium-137 activity.

TABLE 37. VALUES OF THE MIXING DEPTH AND SEDIMENTATION RATE VERSUS THE EXTENT OF SURFACE SEDIMENT LOSS DURING CORING

Loss (cm)	S (g/cm^2)	r (mg/cm^2/yr)
0	0.61	56
1	0.55	50
2	0.43	47
3	0.34	37

If the non-depositional areas within the study area contain insignificant amounts of cesium-137, then considerably less is stored at this part of the lake than expected on the basis of atmospheric fallout and estimated losses via outflow and storage of the radionuclide in the water column. This apparent mass balance discrepancy is considered in greater detail above.

Lead-210

The lead-210 method of dating coastal marine and lacustrine sediments has been used with increasing frequency since its first application by Krishnaswami et al. (1971). The extensive literature concerning radioactive lead isotopes and lead-210 in particular has been recently reviewed by Robbins (1978). The method has been shown to be of value in dating fine-grained sediments from all of the Great Lakes (Superior: Bruland et al. 1975; Michigan: Robbins and Edgington 1972, 1975; Edgington & Robbins 1976; Huron: Robbins et al. 1977; Robbins 1977; Erie and Ontario: Robbins et al. 1978; Farmer 1978). Generally, the method has been applied to a very limited set of cores. This report represents one of the first extensive applications of the method to determination of sedimentation rates in lakes. Only a brief account of the lead-210 method of dating sediments is given in this report. For a detailed discussion of the principles underlying the method, see Robbins (1978).

Lead-210 is produced as the indirect result of the decay of uranium present in crustal and sedimentary materials. The principal components in the decay scheme are:

$$\begin{array}{llll} U^{238} & \rightarrow Ra^{226}(t_{1/2} = 1620\ \mathrm{yr}) & \rightarrow Rn^{222}(t_{1/2} = 3.8\ \mathrm{d}) \\ & \rightarrow Pb^{210}(t_{1/2} = 22.26\ \mathrm{yr}) & \rightarrow Po^{210}(t_{1/2} = 138\ \mathrm{d}) \\ & \rightarrow Pb^{206} & \end{array}$$

Short-lived products in the decay scheme are not shown.

Some lead-210, present in sediments, is produced by in situ decay of radium-226. Generally this is a small and nearly constant activity referred to as supported lead-210. In addition to supported lead-210, there is an excess which is supplied to sediments from atmospheric deposition. Atmospheric lead-210 originates from a unique property of the uranium series decay scheme shown above. Radium-226 decays to form the radioactive noble gas, radon-222, which diffuses out of crustal materials into the atmosphere. Radon-222 decays through a series of very short-lived nuclides to lead-210 which has a high affinity for atmospheric particulate matter and is rapidly scavenged from the air. The flux of lead-210 over the Great Lakes has not yet been measured but is expected to be around 0.5 $pCi/cm^2/year$ and quite constant from year to year. Once in the water, lead-210 is rapidly transferred to sediments and this excess, not being supported by radium activity, decays toward supported levels during burial. In sediment cores from the Great Lakes excess lead-210 may be roughly twenty times higher than supported levels (cf. Robbins and Edgington, 1975).

In undisturbed cores where the sedimentation rate is constant, the activity of excess lead-210 is given by

$$A(m) = A_0 \, e^{-\lambda t} = A_0 \, e^{-\lambda m/r} \qquad (39)$$

where A_o is the excess activity at one surface ($m = o$), t is the time before collection (years), m is the cumulative dry weight of sediment (g/cm^2) and r is the mass sedimentation rate (g/cm^2/yr). The radioactive decay constant is given by $0.69315/22.26 = 0.0311$ yr^{-1}.

The total (observed) activity is given by

$$A_{tot} = A(m) + A_f \qquad (40)$$

where A_f is the activity of supported lead-210.

The above equations suffice to describe profiles in sediments where there is no mixing. Incorporation of the effects of rapid steady-state mixing is comparatively straight-forward for lead-210 (Robbins et al. 1977) since $A_s(t)$ in Eq. 38 is essentially constant over time. Using mass units rather than linear (cm) units and substituting A_o for $A_s(t)$ in that equation, the distribution of excess lead-210 is given by

$$\begin{aligned} A_m &= A_o \,/\, (1 + \lambda s/r) \\ A(m) &= A_m \qquad m < s \\ &= A_m e^{-\lambda(m-s)/r} \qquad r > s. \end{aligned} \qquad (41)$$

This is the equation used to obtain sedimentation rates and mixed depths from excess lead-210 profiles. Eq. 41 describes a theoretical profile in which the activity of lead-210 is constant from the sediment-water interface down to depths. Below that depth (mixed depth) the activity fall off exponentially.

Because of sediment compaction, the decrease in porosity with increasing sediment depth, the sedimentation rate in linear terms is not uniquely defined (Robbins and Edgington, 1975) even when the mass sedimentation rate is well-defined and constant. Layers of sediment are brought closer together on burial as a result of the loss of water so that the apparent linear sedimentation rate decreases with sediment depth. In an interval of thickness dz, the mass, dm, is given by

$$dm = (1 - \phi)\, \rho_s \, dz \qquad (42)$$

Thus the mass sedimentation rate r is related to the linear rate ω by

$$\begin{aligned} r &\equiv dm \,/\, dt \\ &= (1 - \phi(z))\, \rho_s \, dz/dt \\ &= (1 - \phi(z))\, \rho_s \, \omega \end{aligned} \qquad (43)$$

If the density of sediment solids, ρ_s, is constant for a given core and $\phi(z)$ is the porosity, then when r is constant

$$\omega = \omega_o \, (1 - \phi_o) \; / \; (1 - \phi(z)) \qquad (44)$$

where ω_o is the linear sedimentation rate at $z = 0$.

In the foregoing brief discussion of sedimentation rates based on cesium-137, $\bar{\omega}$ is computed (Table 38) as the average rate over the upper 5 cm or so while r remains uniquely but imprecisely defined. In the discussion of lead-210, $\bar{\omega}$, is defined as the average over the upper 10 cm ($\omega = 10/\Delta t$ where $\Delta t = m(10)/r$) and is given only to provide a rough indication in linear terms.

Vertical distributions of lead-210 and in some cases cesium-137 as well are given in Figures 114-117. The complete data set is given in Table 5A of the Appendix. In Fig. 114 (core EPA-SLH-74-13), it can be seen that excess lead-210 decreases in an essentially exponential way with increasing sediment depth as expected on the basis of simple radioactive decay, constant lead-210 flux and constant sedimentation rate. Total lead-210, indicated by the open circles, departs from excess lead-210 at around 10 cm depth and the supported level in this core is about 0.3 pCi/g, about an order of magnitude lower than excess lead-210 at Z = 0. Both lead-210 and cesium-137 profiles indicate essentially no (<1 cm) mixing at this location. In contrast, profiles of lead-210 and cesium-137 at station 12 (Fig. 115) both possess a zone of constant activity down to about 4 cm. In Figs. 116-117 are shown additional excess lead-210 profiles which illustrate the variety of profiles encountered in the study area. In core 19 (Fig. 116) excess lead-210 is measurable only over the upper two cm, and the rate is very poorly determined as a result. In contrast, in Core 25 (Fig. 116) there are many values down to 8 cm which fall on a well-defined line (log plot). There is also about 1-2 cm of mixing in this core. In each case the solid line is the theoretical (least squares fit) using Eq. 41. In Core 53 (Fig. 117) non-exponential features exist in the upper 3-4 cm which are not well-described in terms of rapid steady-state mixing. In this core there is a change in gross sediment composition at around 4 cm. Fig. 118 (upper panels) presents unsupported lead-210 (excess) and cesium-137 profiles for stations 14 and 18. In the lower panels are presented the vertical distribution of benthic organisms. This data set has been discussed in detail by Robbins et al. (1977). The mixed depths inferred from lead-210 in both cases is consistently higher than that determined from cesium-137.

Sedimentation rate, and mixing parameters derived from the steady-state mixing model are given in Table 38. The uncertainty in estimating the activity of excess lead-210 increases without limit as background (unsupported) levels are approached. For this reason, a weighted least squares analysis was used to extract parameter values from the model. Weights were chosen proportional to the reciprocal of the square of the error associated with the estimate of excess lead-210.

The distribution of vertically integrated excess lead-210 or standing crop shown in Fig. 119 illustrates the strong focusing effect seen as well (in greater detail) for the distribution of total cesium-137 (Fig. 113). If the excess lead-210 were deposited uniformly over the lake bottom and there were no transfers into or out of the study area, the expected standing crop would be given by the ratio of the atmospheric flux to the radioactive decay

TABLE 38. SUMMARY OF LEAD-210 DATA AND MODEL-DERIVED SEDIMENTATION RATES AND MIXED DEPTHS

	Activity (pCi/g)		Sedimentation Rate		Mixed Depth	
Station	Mean Surface	Mean Supported	($mg/cm^2/yr$)	(cm/yr)[a]	(cm)	(g/cm^2)
3	8.9	0.49	16.3	0.063	2.5	0.47
4	1.3	0.25	≤5	0	0	0
5	11.1	0.59	7.5	0.038	0	0
7	3.3	0.32	65.6	0.087	0	0
8	7.2	0.49	14.0	0.071	0	0
9	5.9	0.45	21.0	0.041	1.7	0.5
10	7.1	0.47	16.0	0.054	0	0
12	15.0	0.77	38.2	0.16	3.5	0.66
13	3.9	0.34	94.2	0.15	0	0
14ASC	11	0.7	24.0	0.12	4.5	0.71
16	9.4	0.76	11.2	0.060	1.5	0.2
17	8.6	0.65	13.5	0.066	2	0.3
18-2	7.5	0.45	53.2	0.20	3	0.75
18A2	8.8	0.55	41.4	0.13	2.5	0.78
19	3.5	0.62	<1.7	0	0	0
21[b]	-	-	11.6	0.072	3.5	0.5
25	10.2	0.70	13.4	0.067	1.5	0.2
31	5.8	0.50	11.4	0.054	0	0
33	10.3	0.57	11.9	0.062	0	0
35	2.4	0.51	<19	<0.02	1.0	0.5
38	2.8	0.29	<28	<0.02	0	0
39	3.1	0.26	≤27.8	≤0.029	2	1.5
41	11.7	0.19	12.3	-	0	0
45	2	0.18	49.4	-	0	0
50	3.0	0.36	61.0	0.084	0	0
51	2.8	0.25	114	0.088	0	0
53[c]	10.2	0.52	≤11.1	≤0.031	0	0
57	6.6	0.35	20.6	0.10	2	0.3
61	3.7	0.27	103	0.19	3	1.2
63	10.8	0.67	34.2	0.14	4.5	0.97
69	7.1	0.84	39.7	0.18	4	0.71

[a] mean sedimentation rate over the upper 10cm
[b] data only in counts/min/gram
[c] discontinuity around 4 cm

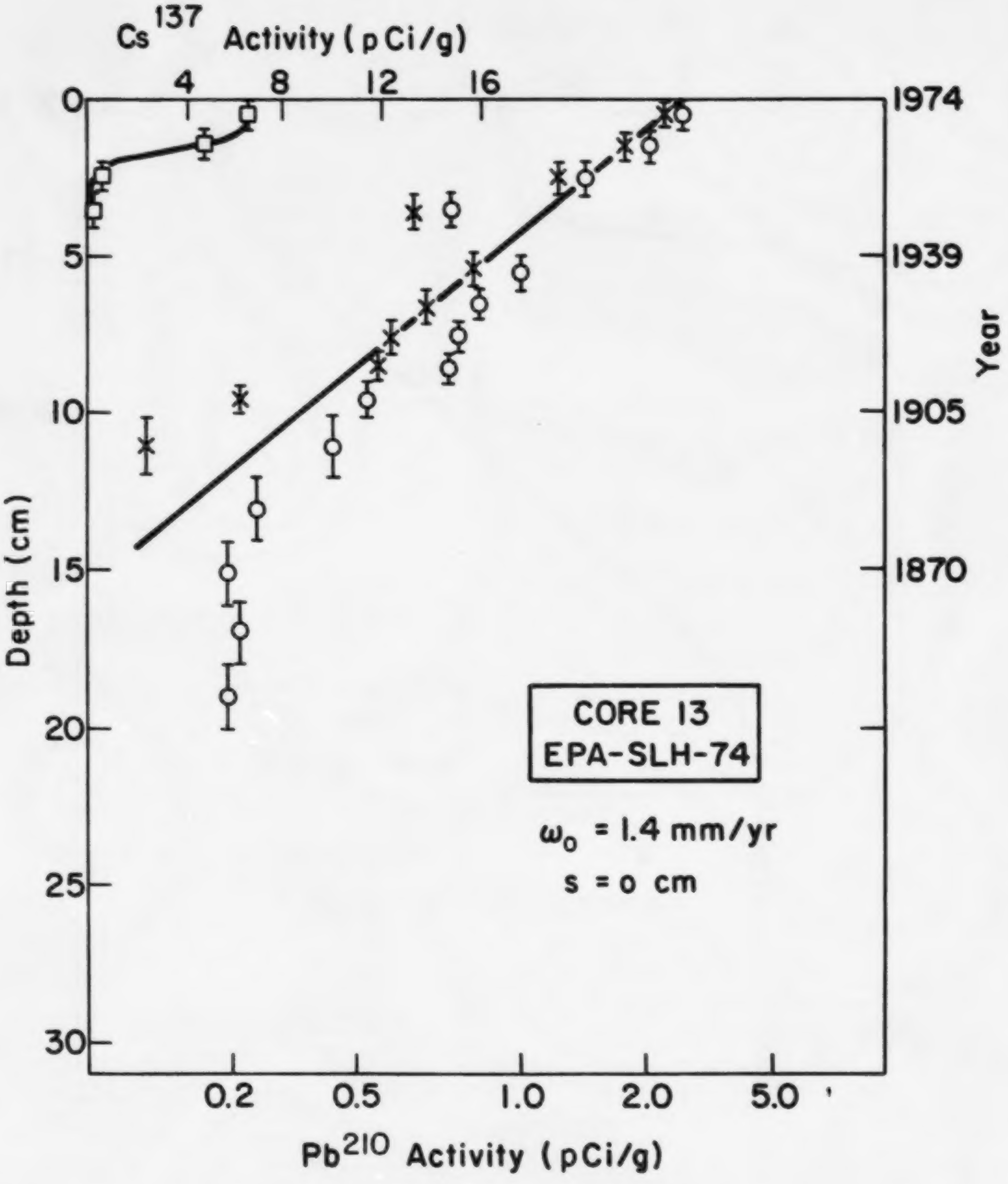

Figure 114. Vertical distribution of lead-210 and cesium-137 in core 74-13. (Open circles: total lead-210; X: excess lead-210.)

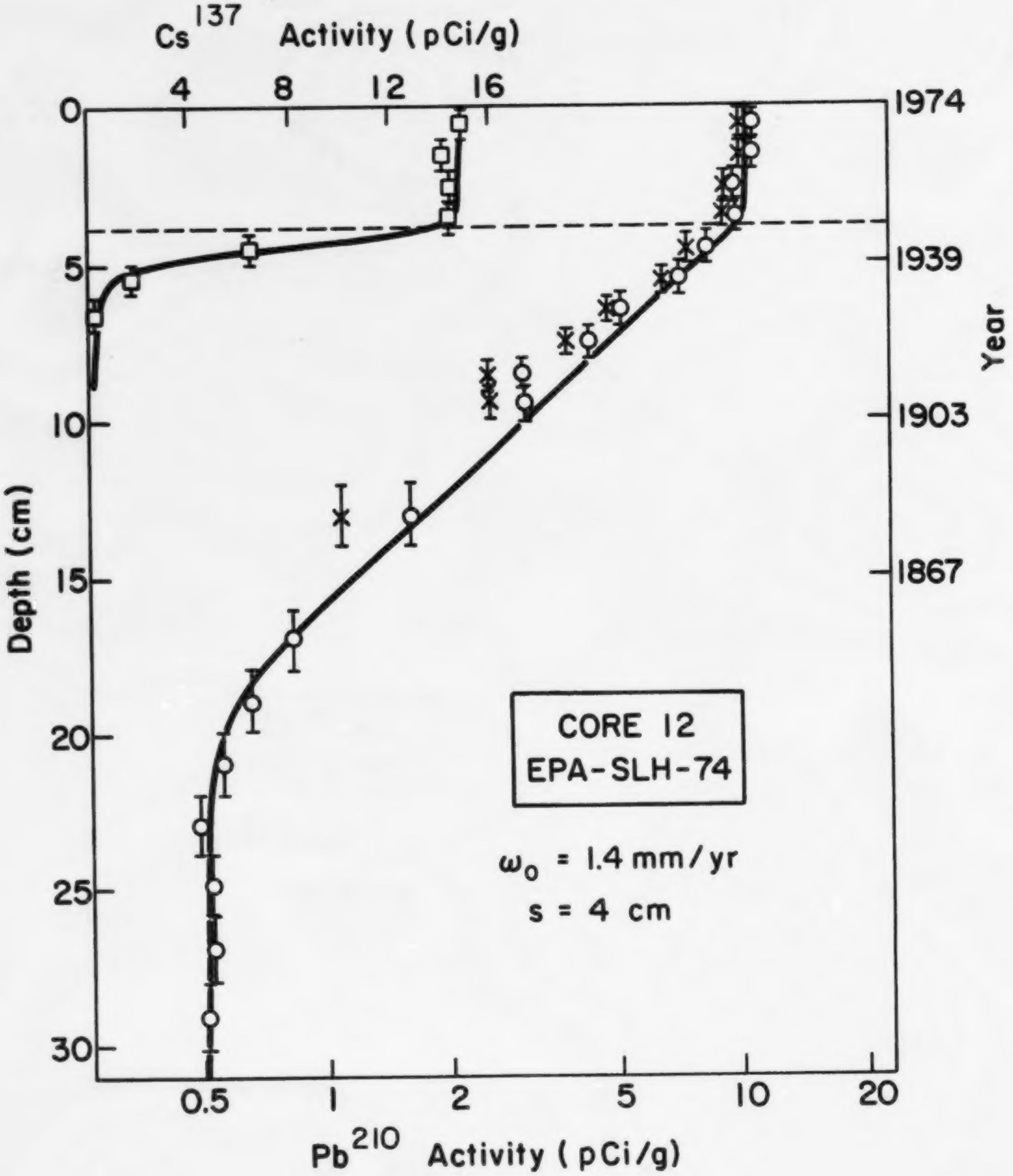

Figure 115. Vertical distribution of lead-210 and cesium-137 in core 74-12.

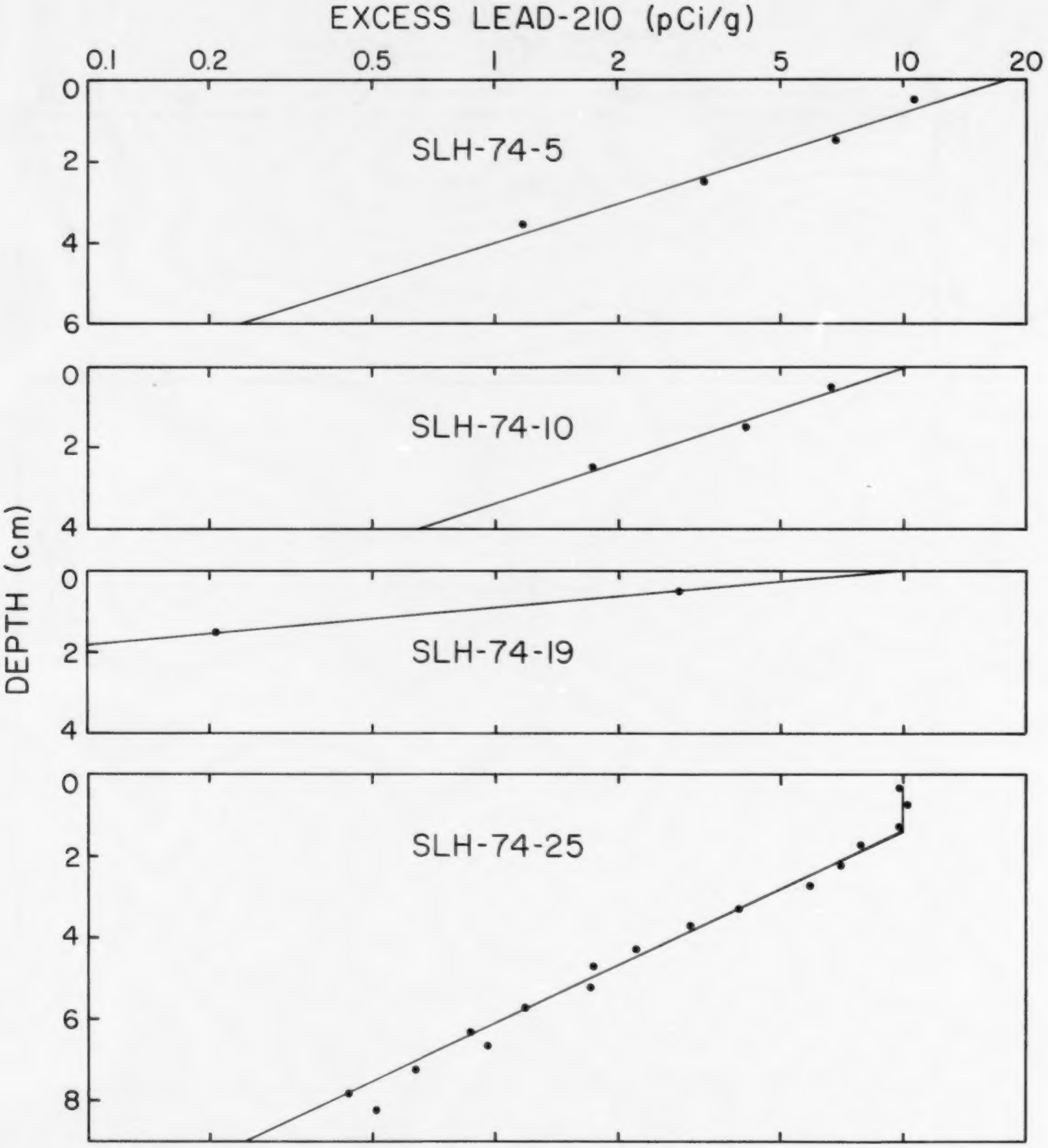

Figure 116. Vertical distribution of excess lead-210 in selected Port Huron and Saginaw Basin cores.

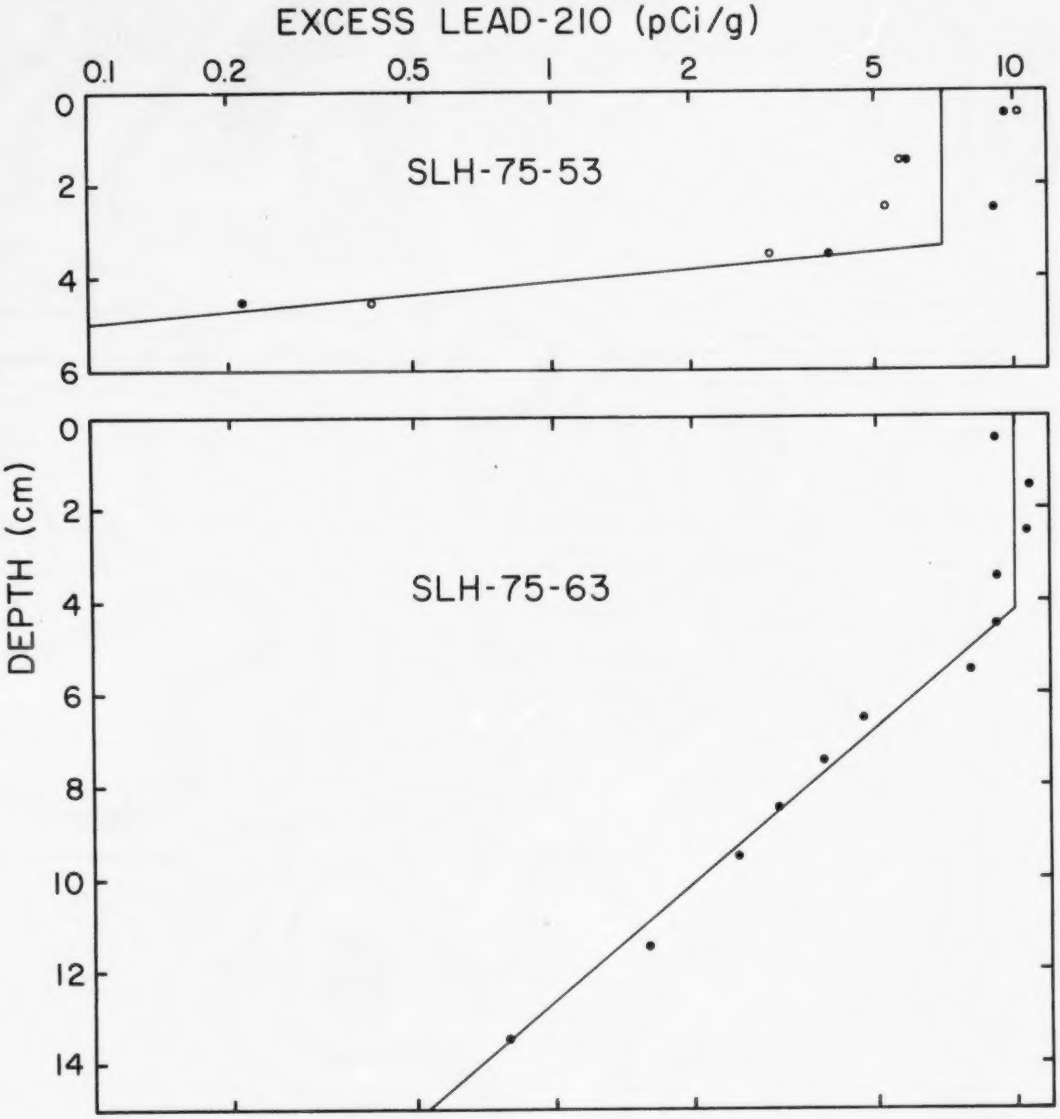

Figure 117. Vertical distribution of excess lead-210 in selected Goderich Basin cores (75-53,63).

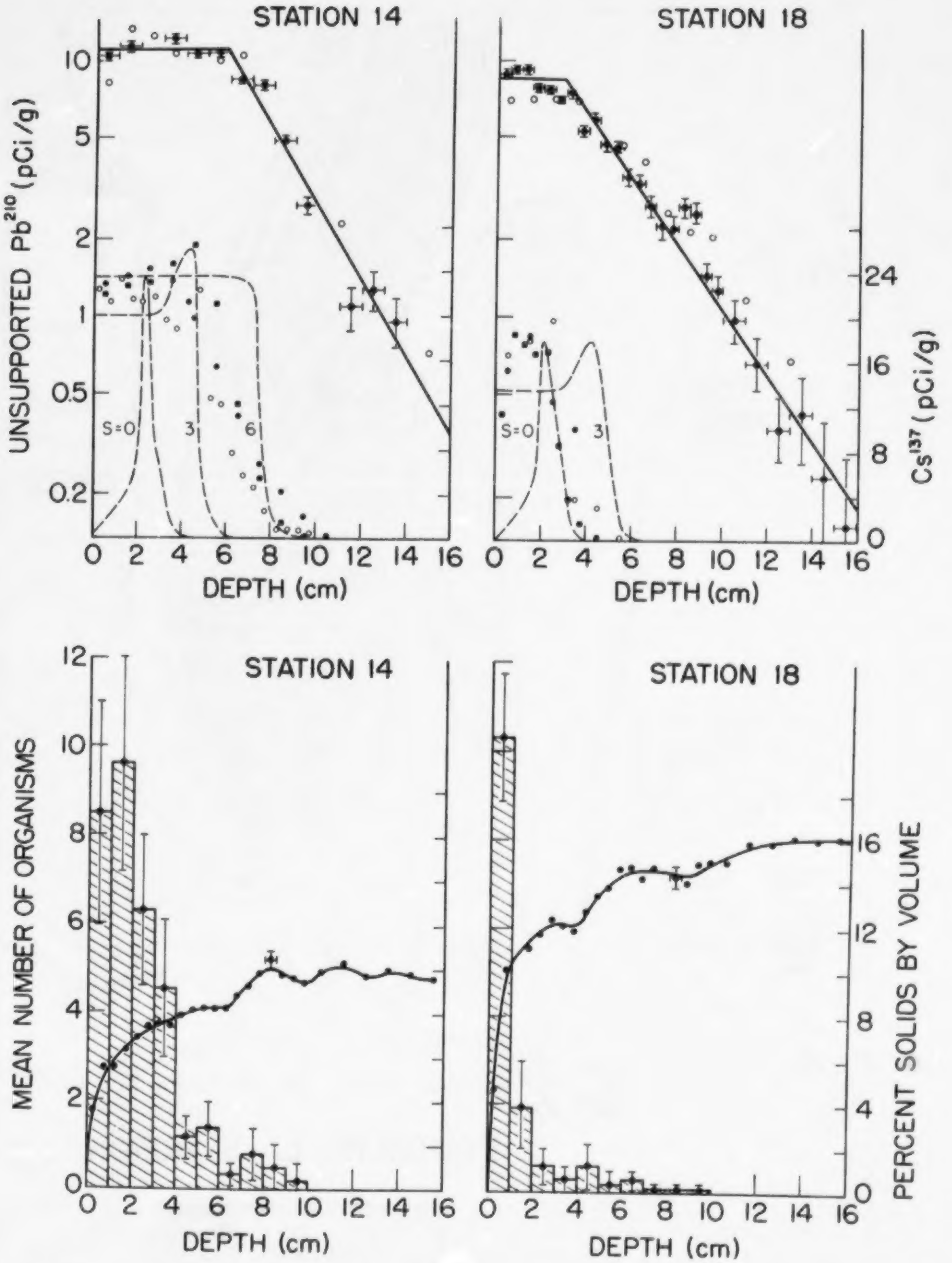

Figure 118. Vertical distribution of lead-210 and cesium-137 in cores from stations 14 and 18 (upper panel). Lower panel indicates the mean number of benthic macroinvertebrates vs depth at these two stations. Also shown is the percent solids by volume (For discussion see text and Robbins et al., 1977)

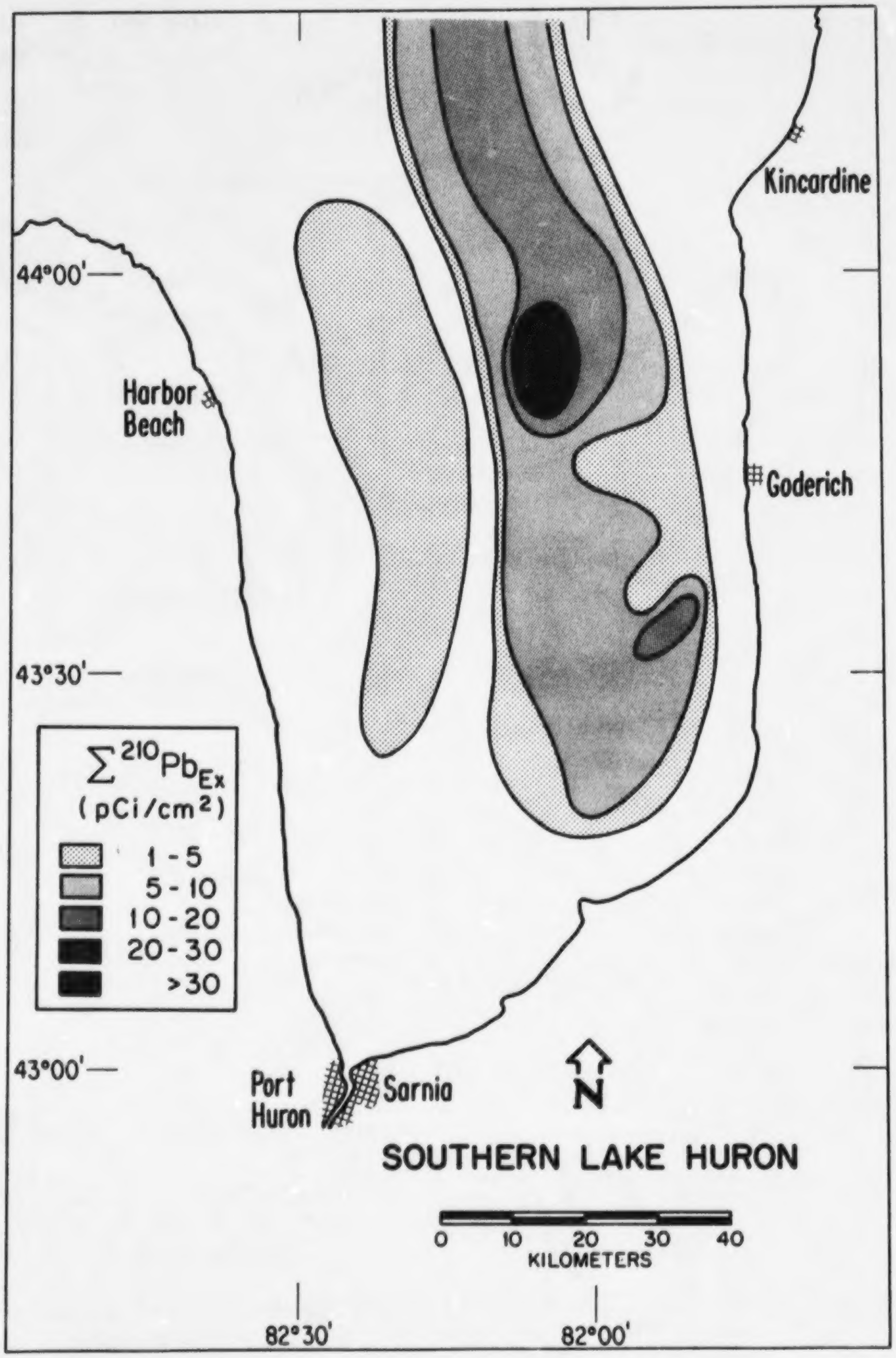
Kincardine
44°00'
Harbor Beach
Goderich
43°30'
$\sum {}^{210}Pb_{Ex}$
(pCi/cm²)
1 - 5
5 - 10
10 - 20
20 - 30
>30
43°00'
Port Huron
Sarnia
N
SOUTHERN LAKE HURON
0 10 20 30 40
KILOMETERS
82°30'
82°00'

Figure 119. Distribution of vertically integrated excess lead-210 (standing crop).

constant or about 0.5 pCi cm^{-2} yr^{-1} / 0.0311 yr^{-1} = 16 pCi/cm^2. Within the Goderich depositional basin this value is often exceeded as can be seen in Fig. 119. But on the average the standing crop is lower in this part of the lake than expected from atmospheric deposition. This result is consistent with that inferred from the cesium-137 analysis: the depositional basins do not store as much of either radionuclide as expected on the basis of known atmospheric inputs.

The comparison of sedimentation rates based on lead-210 and cesium-137 illustrates the difficulties in obtaining accurate estimates from cesium profiles in the study area. Shown in Fig. 120 is the relation between r_{Pb-210} and r_{Cs-137}. Regression analysis yields:

$$r_{Cs-137} = 3.24 + 1.08\ r_{Pb-210} \qquad (45)$$

with a correlation coefficient of 0.84 for N=25. While the relationship is highly significant there are none the less very large discrepancies in some cases between the two measures. Because of the uncertainties in the estimate from cesium-137 profiles, a simpler treatment of the data does equally well in predicting sedimentation rates. The first order effect of steady-state mixing on the cesium-137 profile is a downward displacement of the horizon by an amount equal to the depth of mixing. As a result, the sedimentation rate may be inferred from visual identification of the mixed depth and the location of the horizon, z_h. As cesium-137 was introduced into the environment in significant quantities just after 1952, the mixing-corrected horizon (z_h - s) should correspond to a time of 1975 - 1952 = 23 years so the sedimentation rate may be approximated as $r = (z_h - s)/23$ with s and z_h expressed in g/cm^2. Results of these two methods, least squares and simplified, are compared in Table 33 below. Also shown in Fig. 120 (open circles) is the relation between r_{Cs-137} and the mass sedimentation rate inferred from linear extrapolation or interpolation from lead-210 rates at nearby locations. Essentially the same degree of correlation (r_{corr} = 0.8, N = 22) exists for this set as for the lead-210/Cs-137 set. At locations where neither lead-210 nor stable lead data are available, sedimentation rate values are based on regression analysis of the two methods of treating cesium-137 profiles and on interpolation between grid points. (Table 40 below).

Stable Lead

An alternative means of determining sedimentation rates is based on analysis of pollutant metal concentration profiles. Walters and Wolery (1974) found that the mercury profiles in sediment cores from western Lake Erie possessed several horizons which tended to correspond to the development of local industrial mercury use over the past 40 years or so. In principle such features could be used to infer sedimentation rates. Edgington and Robbins (1976) showed that the vertical distribution of stable lead in the fine-grained sediments of Lake Michigan reflects the history of cultural lead inputs. Lead distributions in dated cores were quantitatively described by a universal time-dependent loading or source function taken to be a linear combination of the estimated annual inputs of atmospheric lead derived from the combustion of leaded gasoline and the burning of coal in the Great Lakes

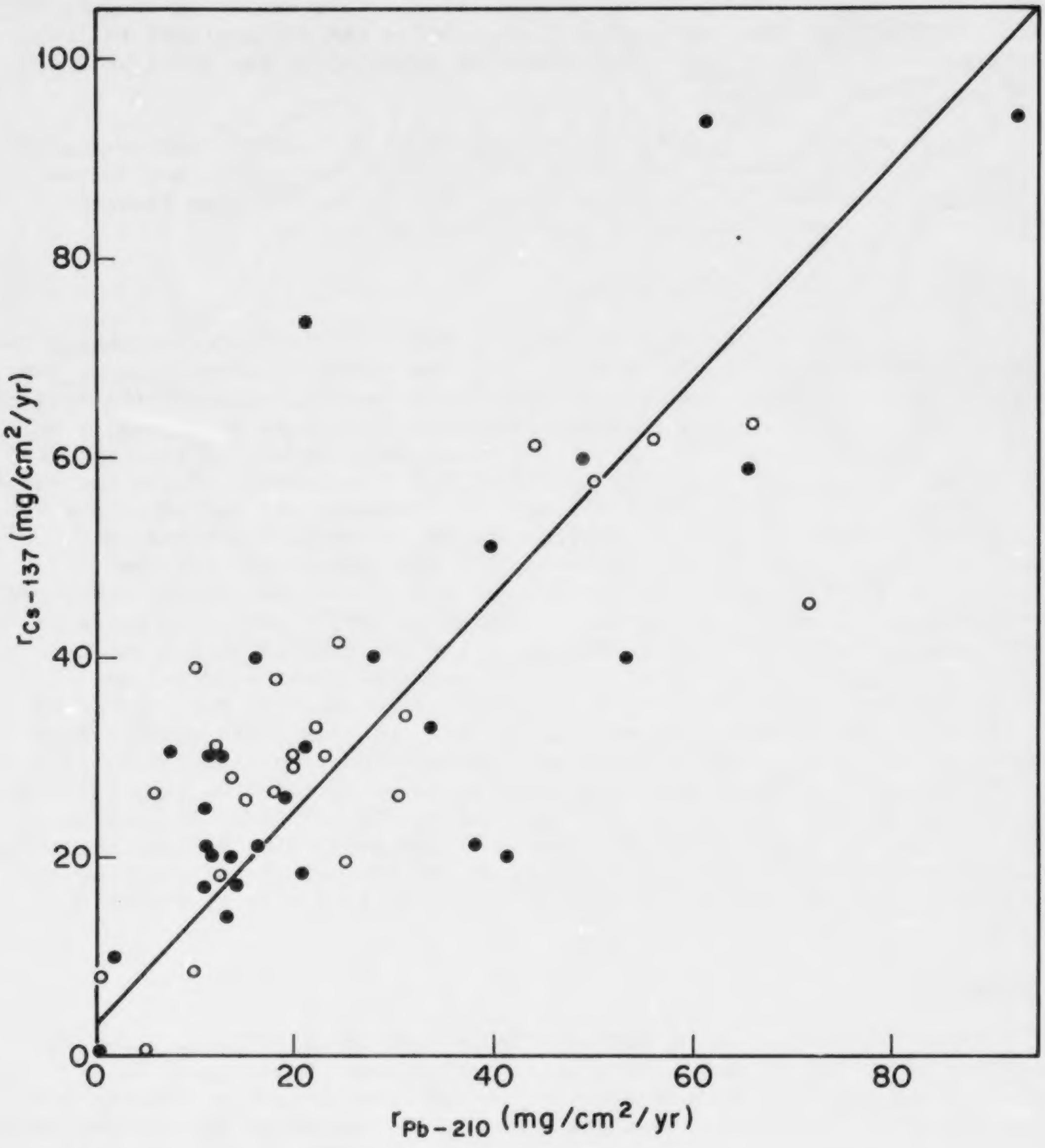

Figure 120. Relationship between the mass sedimentation rates estimated from cesium-137 and lead-210.

region since about 1800. Robbins and Edgington (1974) showed that application of this source function to lead profiles in other sediment cores from Lake Michigan yielded sedimentation rates consistent with rates inferred from seismic profiling data. The source function developed for Lake Michigan should be applicable to the entire Great Lakes region and therefore provide an alternative sediment dating method for Lake Huron as well.

The estimated loading of the lake in relative units (or source function) is shown in Fig. 121. Two sources have contributed most (>95%) of the anthropogenic lead in the environment today: coal and leaded fuel combustion (Winchester and Nifong, 1971). Until about the mid 1920's the dominant contributor was coal burning but not long after the introduction of leaded gasoline, combustion of this latter product became the principal source of lead pollution in the Great Lakes region. Details of construction of the source function are given by Edgington and Robbins (1976). It is assumed that non-atmospheric inputs are proportional to this source function (i.e. have the same time-dependence but different magnitude). Because of the presumed short residence time of lead in the lakes (cf. Nriagu et al. 1979) stable lead profiles should reflect this loading history apart from the effects of sediment mixing. The effects of mixing may be taken into account in the same way as done above for cesium-137 except that in the case of lead there is no radioactive decay so that in Eq. 41, $\lambda = 0$ while $A_s(t)$ is taken to be proportional to the source function. Details of the theoretical treatment are given by Edgington and Robbins (1976).

Values of the mixed depth and sedimentation rate are determined by trial and error and chosen to minimize the differences between observed and predicted lead concentration profiles in the least squares sense. The results for one of the most finely sectioned cores (EPA-SLH-75-18A-2) are given in Figures 122 and 123. The vertical distribution of major elements (Fig. 122) indicates that this core is of uniform composition with respect to many principal constituents. Dates assigned to sediment intervals in the figures are based on lead-210. In Fig. 124 vertical profiles of other elements are given in addition to lead for comparison. The solid line indicates the predicted lead profile corresponding to a sedimentation rate 41.5 mg/cm^2/yr as compared with a value of 41.4 mg/cm^2/yr based on lead-210. Clearly such close agreement is accidental in view of the over all relation between rates based on these two methods. The results of applying the method to lead profiles in the other cores are given in Table 39. Both lead and lead-210 profiles give a very consistent picture of sedimentation rates. Shown in Fig. 124 are other profiles of lead plotted against date as determined by lead-210. In each case the lead records indicate the onset of excess lead deposition as just prior to 1900. Shown in Fig. 125 is the relationship between sedimentation rates determined by the two methods. Regression analysis yields:

$$r_{\text{Pb-210}} = -.04 + 0.89\, r_{\text{Pb}} \tag{46}$$

with a correlation coefficient of 0.94 for N=24. This result indicates that 1) within the study area, profiles of stable lead are everywhere consistent with a lead loading history developed previously for Lake Michigan (note: not in absolute magnitude, however) and 2) stable lead may be used as an

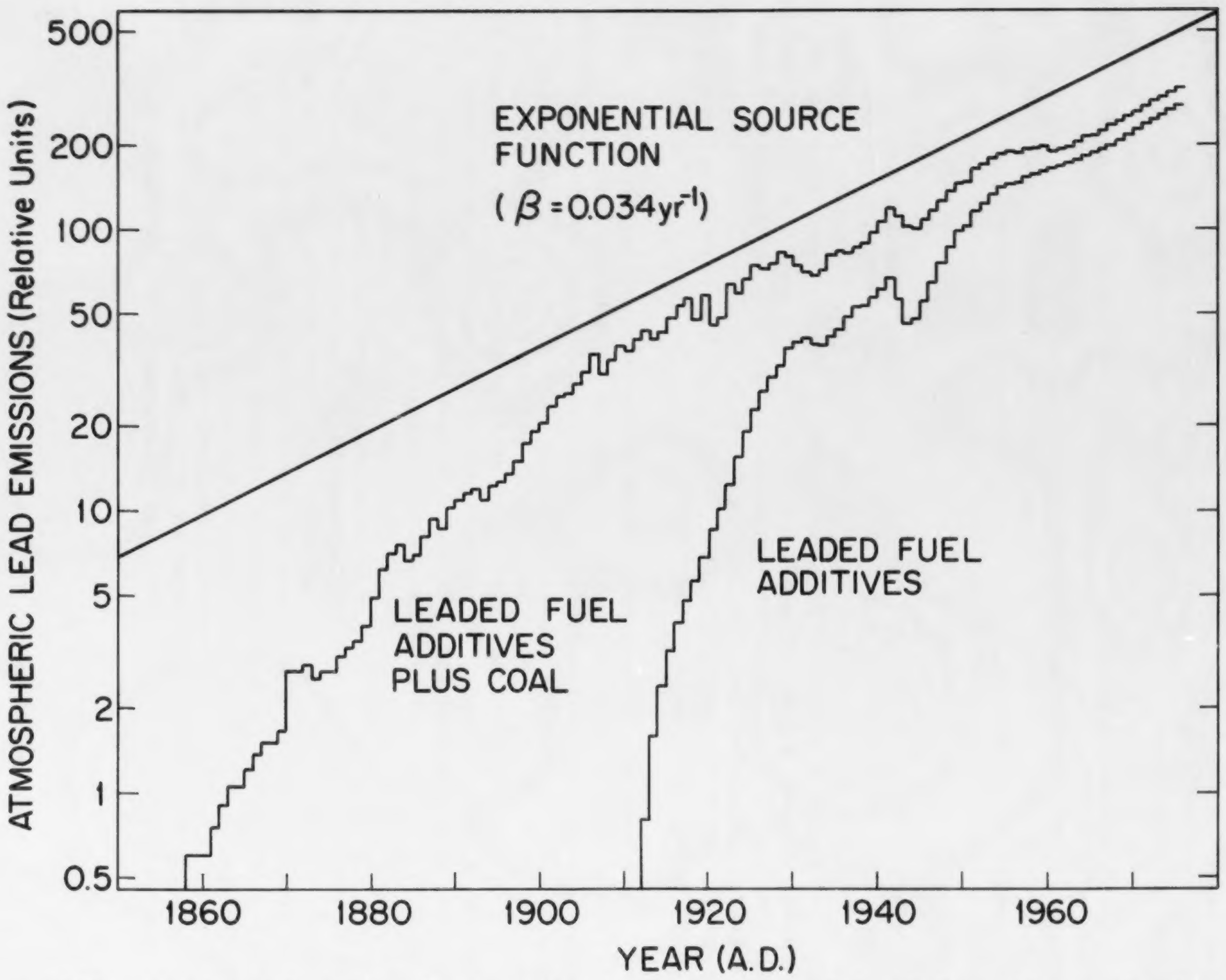

Figure 121. Estimated regional atmospheric emissions of lead from the combustion of coal and leaded fuel additives.

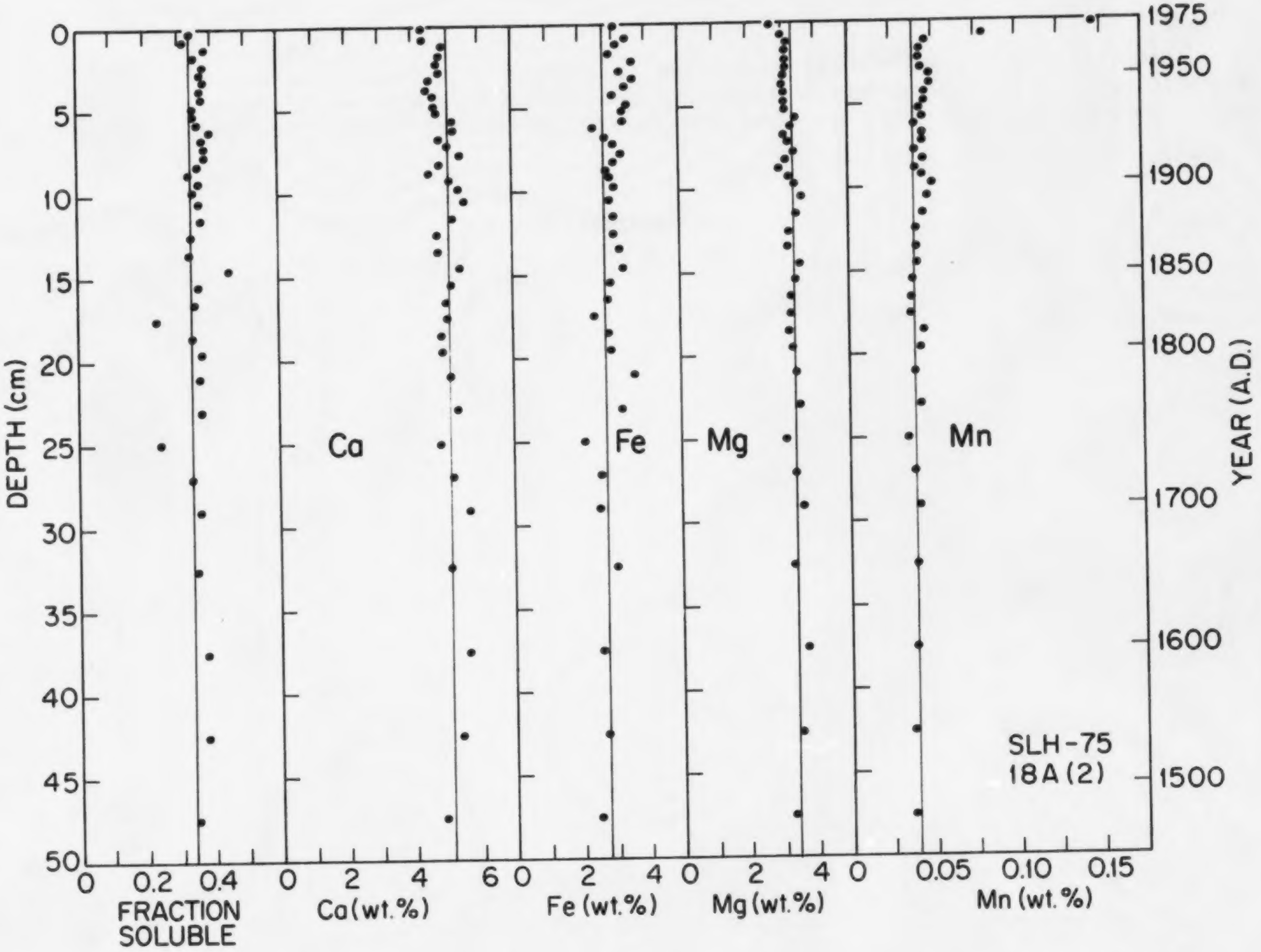

Figure 122. Vertical distribution of major elements in core EPA-SLH-75-18A.

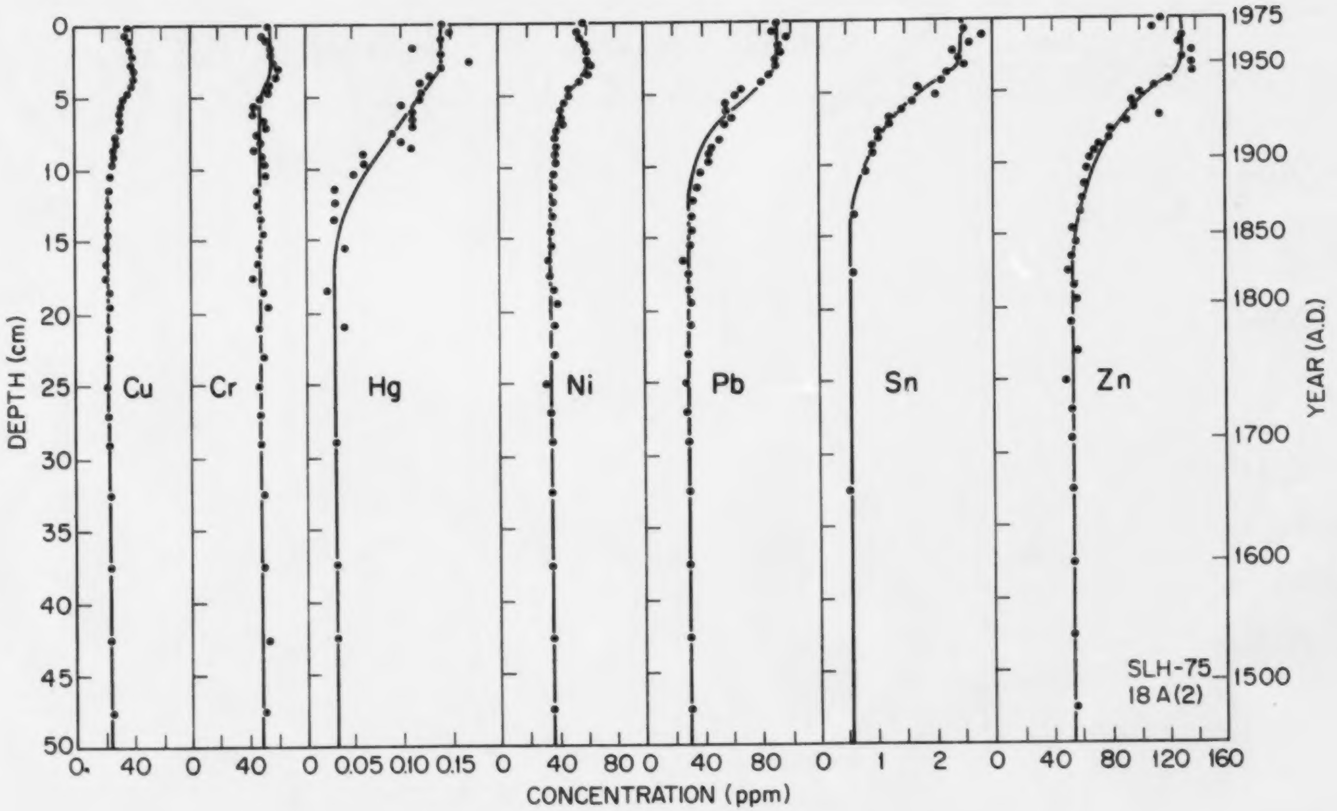

Figure 123. Vertical distribution of trace elements in core EPA-SLH-75-18A. The solid lines are the predicted concentrations based on the historical emissions inventory (lead) or exponential source function (other elements).

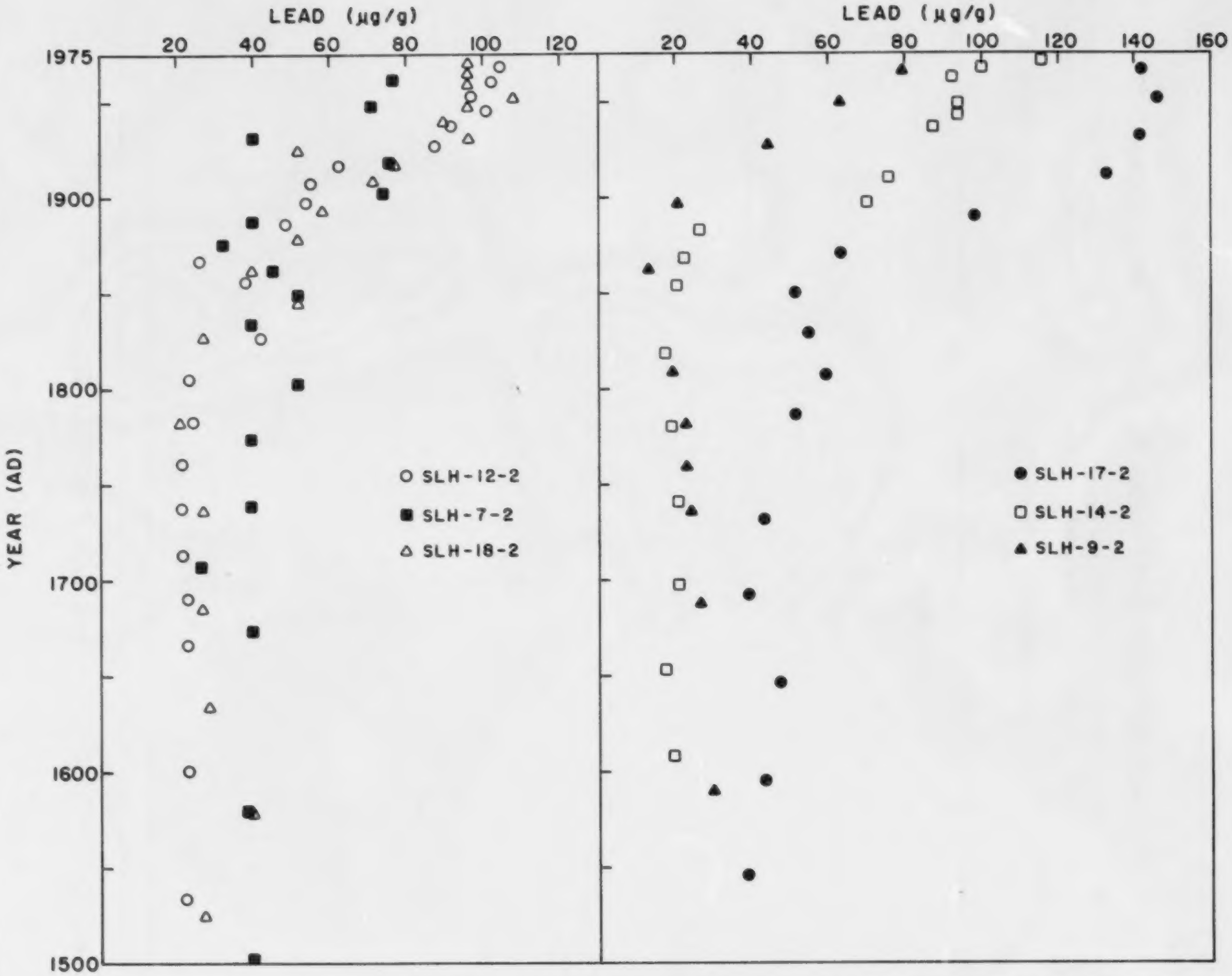

Figure 124. Vertical distribution of lead in selected radiometrically dated cores.

TABLE 39. SEDIMENTATION RATES BASED ON ANALYSIS OF LEAD PROFILES[a]

Station	Sedimentation Rate (mg/cm^2/yr)	Mixed Depth (g/cm^2) (cm)
3	21.0	3
4	0	0
5	12.9	2
7	100	2
8	14.4	2
9	17.0	0
10	6	0
12	36.4	4
13	14.0	0
14A-SC	38.0	4.5
16	12.3	3
17	12.0	3
18-2	60.0	5
18A2	41.5	3
19	<2	0
25	13.3	2
29	32.0	3
31	13.5	2
33	17.2	0
35	0	0
38	<25	0
39	37	0
50	78	0
51	110	0
57	32.0	2
61	90.0	2
63	38.0	3
69	40.0	6

[a] Using the source function shown in Fig. 121.

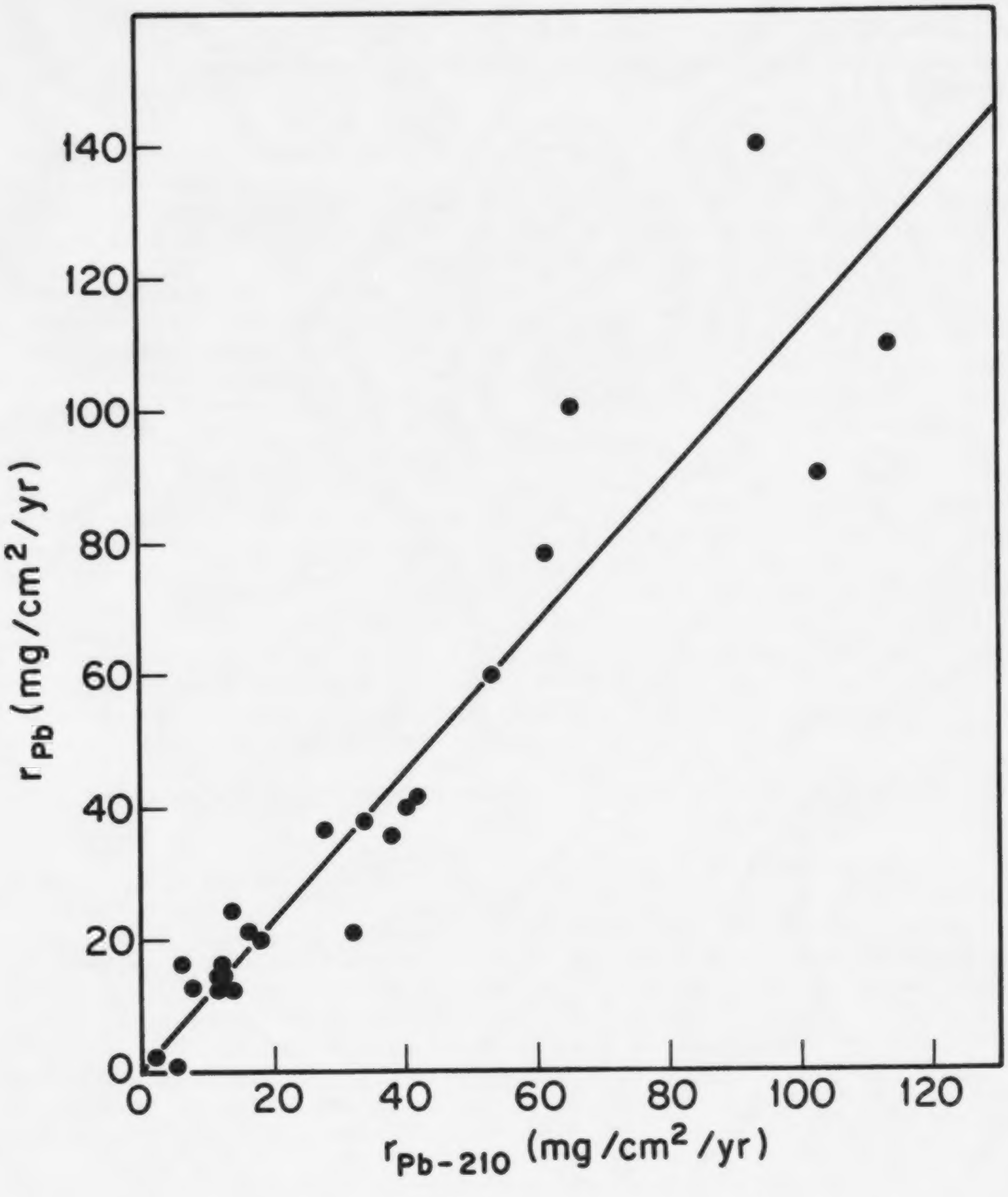

Figure 125. Relationship between the mass sedimentation rates calculated from stable lead and from lead-210 profiles.

alternative if not exclusive means of determining recent sedimentation rates in this and possibly other of the Great Lakes. This is an important result as it suggests the possibility of obtaining accurate sedimentation rate information for a considerably reduced expenditure of time and effort if lead-210 analysis may be discontinued. As suggested above, there are other reasons for retaining the analysis of lead-210 in sediments and in water, however.

It is important to note that excess concentration profiles of other elements such as copper, mercury, nickel, tin and zinc in core 18A-2 (Fig. 123) as well as in other cores imply a deposition history which is consistent with treating the excess as anthropogenic in origin and in fact is largely consistent with the source function developed for lead. It is possible to develop source functions for several of these elements based on historical records of regional population growth and metals usage but this approach is beyond the scope of this report. However, as a first approximation, the source function for the anthropogenic (excess) component of each element may be taken as essentially exponential. In such case the time-dependence is given by, $e^{-\beta t}$ where t is the time before present (1975). The increase in anthropogenic loading of the sediments can be expressed in terms of the doubling time = $0.69315/\beta$ which is analogous to the lead-210 half-life in terms of the treatment by the steady-state mixing model. If the exponential source function is used instead of the one based on historical records of lead usage, the best fit to the observed lead profile in core 18A-2 (which occurs for a β value of 0.034 yr^{-1} or doubling time of 20 years) is essentially indistinguishable from that based on the historical records. The reason for this is evident from inspection of Fig. 121. The exponential source function after 1900 has essentially the same time-dependence (slope) as that of the one based on historical records. Only before that date is the time-dependence of the exponential source function in error. But the pre-1900 contribution of anthropogenic lead is very small. As a result, lead profiles are dominated by post 1900 contributions which are essentially exponential in character.

Application of the exponential source function to other minor element profiles yields predicted distributions indicated as the solid lines in Figure 123. While there are some small systematic departures of theoretical from observed profiles the quality of the fits are generally excellent. Least squares values of β and the corresponding doubling time are given in Table 40. As can be seen from this table, the majority of elements have essentially the same doubling time, around 23 years (Cu, Pb, Sn and Zn), and very close to the half-life of lead-210 (22.6 years). The small enrichment of Cr seen in this, but not all cores, implies a smaller doubling time (roughly 7 years). The doubling time of Ni is also significantly shorter (14 years) and indicates a comparatively more recent onset of significant addition of anthropogenic Ni to the lake if this result can be generalized to other cores. Mercury is the only element with a significantly longer doubling time (40 years). This longer doubling time is probably inconsistent with historical records of mercury use and could arise from remobilization of the element within the core. It is beyond the scope of this report to consider this question in further detail.

TABLE 40. EXPONENTIAL SOURCE FUNCTION PARAMETERS DERIVED FROM APPLICATION OF THE STEADY-STATE MIXING MODEL TO MINOR ELEMENT PROFILES IN CORE EPA-SLH-75-18A-2

Element	β (yr^{-1})	Doubling time or half life (yr)
Cr	0.1	7
Cu	0.029	24
Hg	0.017	40
Ni	0.048	14
Pb	0.034	20
Pb-210	0.031	22
Sn	0.033	21
Zn	0.027	26

The use of the linear regression expressions for the relation between cesium-137 and lead-210 sedimentation rates (Eq. 45) and between stable lead and lead-210 sedimentation rates (Eq. 46) leads to a set of independent predictions of the sedimentation rate at each location. The values are summarized in Table 41. In most cases where there are lead-210 rates the adopted value is based on lead-210. In cases where there are no lead-210 or stable lead rates, the adopted value is based on cesium-137 rates in combination with values based on linear interpolation or extrapolation of lead-210 rates to the locations in question. The adopted value is generally taken as the approximate average of two of the three most similar measures of the sedimentation rate.

The mass sedimentation rate in southern Lake Huron is shown in Fig. 126, the numbers in parenthesis are approximate and derived from the cesium-137 profiles and grid interpolation as indicated above. The value enclosed by the square in Fig. 126 (33 $mg/cm^2/yr$) is based on analysis of the ragweed (Ambrosia) pollen profile in a core taken at the indicated location by Kemp et al. (1974). The sedimentation rate determined by Kemp et al. is very consistent with values determined at adjacent sites for this report.

It can be seen (Fig. 126) that there is a very systematic trend toward higher mass sedimentation rates on the eastern side of the Goderich Basin. Within this Basin rates toward the escarpment side are under 20 $mg/cm^2/yr$ while on the eastern side values may exceed 100 $mg/cm^2/yr$. The high sedimentation rates toward the eastern part are associated with the intense deposition of dolomitic materials. Because the materials are capable of relatively greater compaction than the organic and clay mineral phases, the high mass sedimentation rates are not generally accompanied by high linear rates. Values of the mean linear sedimentation rate (Fig. 127) have a very different distribution. They tend to follow a north-south trend with higher values occurring toward the northern part of the Goderich Basin. Mass sedimentation rates within the Port Huron Basin are very much lower and exhibit very limited spatial variability.

Time Resolution in Cores

The fidelity of sediments in recording events occurring in the lake is limited in part by postdepositional particle and solute movements. Several lines of evidence partly developed in this report indicate that there is a zone extending downward from the sediment water interface which is rapidly mixed probably by benthic invertebrates. Development of a model envisioning the mixing process as steady-state and confined to a precisely defined interval leads to self-consistent interpretation of metal and radioactivity profiles. Shapes are quantitatively and adequately described and within experimental uncertainties and sedimentation rates derived from application of the model are generally consistent. Values obtained for the mixed depth from application of the model are also consistent as can be seen from the summary in Table 42. Agreement is poorest for mixed depths under 2 cm because in this case the mixed depth is often comparable to the size of the sampling interval. Regression analysis of lead and lead-210 mixed depths yields $s_{Pb-210} = 0.13 + 0.72\ s_{Pb}$ with $r = 0.80$ and $N = 24$. While the correlation is highly significant, mixed depths derived from analysis of

TABLE 41. SEDIMENTATION RATES ESTIMATED FROM ANALYSIS OF CESIUM-137, LEAD-210, AND LEAD PROFILES

	Mass Sedimentation Rate (mg/cm²/yr)[a]						Mean Linear rate (cm/yr)	
	Cs-137							
Station	(d)	(e)	Pb	Pb-210	Grid[b]	Adopted Value	Adopted Value[c]	Intrinsic Resolution (yr)
3	17	38	125.1	16.3	(16.3)	16.3	0.063	22
4	0	0	0	<5	5.	0	0	-
5	25	38	11.5	7.5	(7.5)	7.5	0.038	47
6	5	14	-	-	0	0	0	>90
7	52	32	89.2	65.6	(65.6)	65.6	0.087	10
8	13	12	12.9	14.0	(14.0)	14.0	0.071	21
9	65	28	15.2	21.0	(21.0)	21.0	0.041	20
10	34	18	5	16.0	(16.0)	16.0	0.054	20
11	5	13	-	-	10	10	0.05	48
12	16	18	32.5	38.2	(38.2)	38.2	0.16	21
13	84	32	125	94.2	(94.2)	94.2	0.15	6
14ASC	52	29	34	24.0	(21.0)	30.0	0.17	30
15	0	37	0	0	0	0	0	-
16	20	17	11.0	11.2	(11.2)	11.2	0.060	24
17	15	17	10.7	13.5	(13.5)	13.5	0.066	35
18-2	34	43	53.5	53.2	(53.2)	53.2	0.20	9
18A-2	15	28	37.0	41.4	(41.4)	41.4	0.13	15
19	6	17	<2	<1.7	(<1.7)	0	0	-
20	14	21	-	-	13	14	0.07	46
21	15	25	-	11.6	(11.6)	11.6	0.072	43
22	55	20	-	-	56	55	0.08	9
25	10	21	11.9	13.4	(13.4)	13.4	0.067	30
29	21	25	28.6	-	15	28.6	0.14	30
30	39	20	-	-	12	40	0.03	17
31	25	20	12.1	11.4	(11.4)	11.4	0.054	20
32	23	17	-	-	14	20	0.064	11
33	16	25	13.6	11.9	(11.9)	11.9	0.06	15
34	33	24	-	-	10	25	0.02	18
35	21	42	0	<19	(<19)	<20	<0.02	24
36	28	29	-	-	22	25	0.05	38
38	45	-	<22	<28	(<28)	<30	<0.02	>40
39	38	99	33	≤28	(≤28)	≤30	<0.03	>82
40	<45	-	-	-	23	<20	<.02	-
41	26	11	-	12	(12)	12	-	18
42	33	29	-	-	17	25	0.05	15
43	-	<52	-	-	31	≤25	<0.02	38
44	51	47	-	-	50	50	0.04	27
45	58	99	-	49	(49)	50	-	50
46	-	87	-	-	33	0	0	-

(continued).

TABLE 4I. (continued).

	Mass Sedimentation Rate $(mg/cm^2/yr)$[a]						Mean Linear rate (cm/yr)	Intrinsic Resolution (yr)
	Cs-137							
Station	(d)	(e)	Pb	Pb-210	Grid[b]	Adopted Value	Adopted Value[c]	
47	15	38	-	-	24	20	0.1	48
49	21	6	-	-	31	20	0.07	20
50	34	43	69.6	61.0	(61.0)	61.0	0.084	12
51	52	110	98.2	110.	(110)	110	0.088	19
53	12	20	-	≤11.1	(41.1)	≤11.1	≤0.031	60
54	65	69	-	-	70	65	0.07	23
55	24	40	-	-	20	25	0.13	42
56	25	18	-	-	20	20	-	35
57	14	21	28.6	20.6	(20.6)	20.6	0.10	15
58	56	18	-	-	66	60	0.02	8
59	23	29	-	-	18	20	0.1	30
60	38	70	-	-	62	60	0.18	18
61	19	62	80.3	103	(103)	103	0.19	11
62	13	37	-	-	72	40	0.09	15
63	27	31	33.9	34.2	(34.2)	34.2	0.14	16
65	25	37	-	-	23	25	0.12	33
66	19	34	-	-	42	30	0.12	20
67	26	13	-	-	65	50	0.16	5
68	29	40	-	-	31	30	0.12	28
69	45	45	35.7	39.7	(39.7)	39.7	0.18	18
70	22	16	-	-	6	20	0.10	21
71	17	14	-	-	-	15	0.08	24

[a] Rates adjusted to lead-210 values by regression analysis (see text).

[b] Linear interpolation or extrapolation from values of r_{Pb-210} at neighboring locations. Values in parentheses are measured lead-210 rates.

[c] Mean sedimentation rate over 10 cm intervals = 10.0 cm / Δt where Δt = cumulative weight at 10 cm / mass sedimentation rate.

[d] Derived from the simplified treatment using the mixing-model (see text).

[e] Derived from mixing-model.

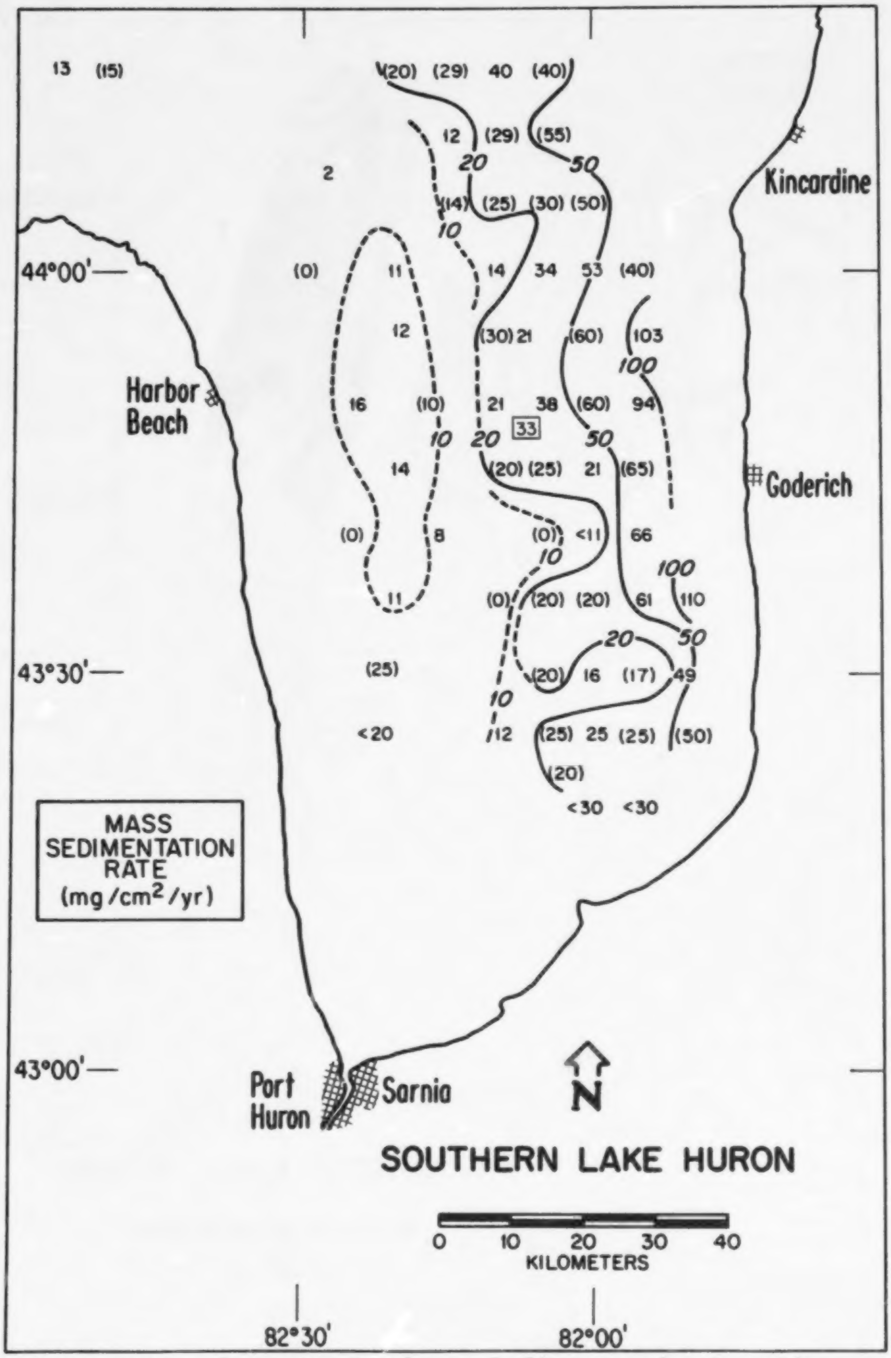
13 (15)
(20) (29) 40 (40)
12 (29) (55)
20
50
2
(14) (25) (30) (50)
10
Kincardine
44°00'
(0)
11
14 34 53 (40)
12
(30) 21
(60)
103
100
Harbor Beach
16
(10)
21 38 (60) 94
10 20
33
50
14
(20) (25) 21 (65)
Goderich
(0)
8
(0) <11 66
10
100
11
(0) (20) (20) 61 110
20
50
43°30'
(25)
(20) 16 (17) 49
10
<20
12 (25) 25 (25) (50)
(20)
<30 <30
MASS SEDIMENTATION RATE (mg/cm²/yr)
43°00'
Port Huron
Sarnia
N
SOUTHERN LAKE HURON
0 10 20 30 40
KILOMETERS
82°30'
82°00'

Figure 126. Rate of accumulation of fine-grained sediments in southern Lake Huron. Numbers in parenthesis are approximate estimates. The value enclosed by the square is based on analysis of an Amborsia (ragweed) pollen profile (Kemp *et al.*, 1974).

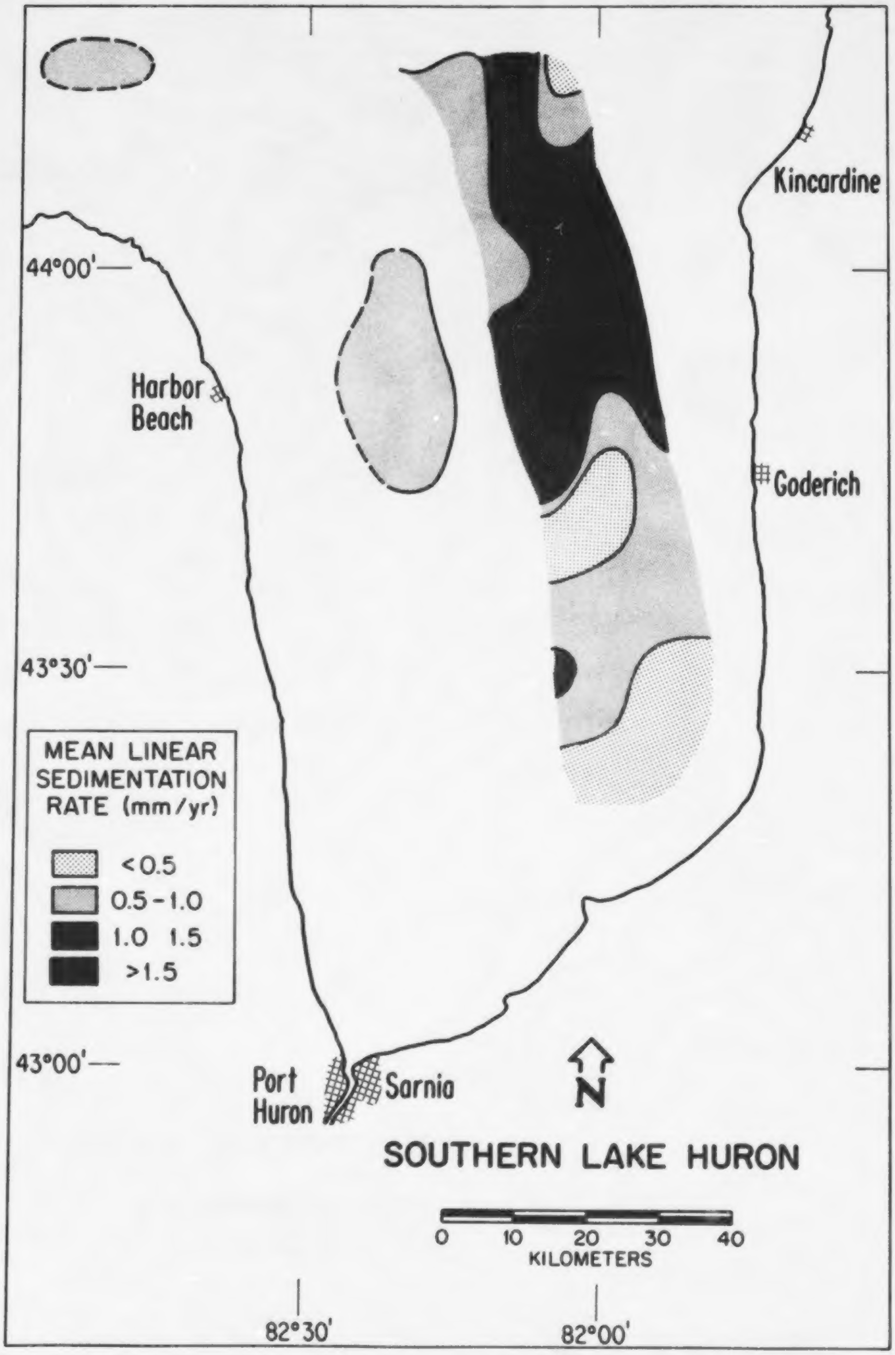
Kincardine
44°00'
Harbor Beach
Goderich
43°30'
MEAN LINEAR SEDIMENTATION RATE (mm/yr)
<0.5
0.5-1.0
1.0 1.5
>1.5
43°00'
Port Huron
Sarnia
N
SOUTHERN LAKE HURON
0 10 20 30 40
KILOMETERS
82°30'
82°00'

Figure 127. The average linear sedimentation rate in the upper ten centimeters of sediment in southern Lake Huron. Because of compaction, linear sedimentation rates are not uniquely defined in cores.

TABLE 42. MIXED-DEPTHS MEASURED OR CALCULATED FROM CESIUM-137, LEAD-210 AND LEAD PROFILES

	Mixed Depth (g/cm^2)				
	Cesium-137				
Station	(a)	(b)	Lead-210	Lead	Adopted Value
3	0.36	0.24	0.47	0.59	0.47
4	0	0	0	0	0
5	0	0.22	0	.32	0.27
6	0.45	0.36	-	-	0.4
7	0	0.64	0	1.4	0.5
8	0.29	0.28	0	.29	0.29
9	0	0.54	0.53	0.20	0.4
10	0	0.72	0	0	0
11	0.48	0.34	-	-	0.4
12	0.76	0.72	0.66	.76	0.73
13	0	0.34	0	0	0
14A-SC	0.95	0.95	.71	.71	0.71
15	0	0.8	-	-	0
16	0.27	0.22	0.2	.46	0.29
17	0.47	0.46	0.3	.47	0.43
18-2	.46	0.48	0.75	1.3	0.74
18A-2	0.61	0.43	0.78	.36	
19	0	0.04	0	0	0
20	0.64	0.55	-	-	0.60
21	0.64	0.52	0.5	-	0.55
22	0	0.18	-	-	0
25	.40	0.25	0.20	0.30	0.29
29	.60	0.62	-	-	.61
30	0	0.07	-	-	0
31	0	0.22	0	.45	0.17
32	0	0.17	-	-	0
33	.18	0.10	0	0	0.14
34	0	0.36	-	-	0.2
35	0	0.28	0.5	0	0.2
36	.94	0.70	-	-	0.8
38	0	-	0	0	0
39	2.45	0.70	1.5	-	1.6
40	0	1.3	-	-	0.7
41	.21	0.23	0	-	0.2
42	.38	0.68	-	-	0.5
43	1.5	0.85	-	-	1.2
44	0	1.13	-	-	0.6
45	2.49	1.70	0	-	2.1

(continued).

TABLE 42. (continued).

	Mixed Depth (g/cm^2)				
	Cesium-137				
Station	(a)	(b)	Lead-210	Lead	Adopted Value
46	3.2	2.15	-	-	2.7
47	.95	0.72	-	-	0.8
49	.38	0.30	-	-	0.3
50	0	1.0	0	0	0
51	2.06	1.4	0	0	0.8
53	.63	0.62	0	-	0.6
54	1.5	1.5	-	-	1.5
55	1.1	0.84	-	-	1.0
56	0	0.21	-	-	0.1
57	0.3	0.38	0.3	0.30	0.32
58	0	0.19	-	-	0
59	.6	0.48	-	-	0.5
60	1.1	0.67	-	-	0.9
61	1.2	0.42	1.2	0.71	0.9
62	0.59	0.28	-	-	0.4
63	0.55	0.39	0.97	0.56	0.6
65	0.82	0.62	-	-	0.7
66	0.78	0.60	-	-	0.7
67	0	0.13	-	-	0
68	0.85	0.66	-	-	0.8
69	0.71	0.66	0.71	1.2	0.82
70	0.42	0.58	-	-	0.5
71	0.36	0.43	-	-	0.4

[a] Derived from simplified model of mixing.
[b] Derived from least-squares fit or mixing model.

metals and radioactivity profiles are not as consistent as are sedimentation rates. In some cores, reported for Lakes Erie and Ontario (Robbins et al., 1978) profiles of Cs-137 are consistent with significant sediment mixing even when lead-210 profiles are not. While the concept of mixing is essentially established, it is clear that other factors such as areal resuspension effects (see Robbins et al., 1978), delayed watershed contributions, remobilization and particle-selective bioturbation may be important in the generation of observed profiles. Within these limitations an approximate mixed depth may be associated with each core based on the combined analysis of cesium-137, lead-210 and lead profiles. These values are provided in Table 39.

To the extent that steady-state mixing is a satisfactory representation of the principle postdepositional particle transport process in sediments, an intrinsic time resolution may be assigned to cores. The effect of steady-state mixing on the sedimentary record of two discreet events occurring ten years apart is illustrated in Fig. 128. For a hypothetical sedimentation rate of 2 mm/yr the expected distribution is shown for various assumed depths of sediment mixing. As the depth of sediment mixing increases, the record is increasingly smeared out and the events are essentially unresolvable for times greater than the residence time of the event record within the mixed zone. This time, which may be referred to as the intrinsic resolution, is given by the ratio of the mixed depth to sedimentation rate: $t(yr) = s\ (g/cm^2)\ /\ r\ (g/cm^2/yr)$. Thus, for example, an intrinsic resolution of 10 years corresponds to a mixed depth of 2 cm when the sedimentation rate is 2 mm/yr. For this intrinsic resolution the ten year discreet events produce a profile in which the full width at half maximum of the recorded peaks is approximately equal to their separation (Fig. 128).

Adding to the loss of sediment record fidelity is the practical size of sediment sections. While several cores were sectiond in half cm intervals, a practical limit is generally 1 cm. The resolution associated with this thickness is given by the ratio of mass per unit area corresponding to 1 cm to the sedimentation rate ($g/cm^2/yr$). Choosing whichever of the two measures above is largest, a practical intrinsic resolution may be estimated. These values are given in Table 40 and shown in Fig. 129 in terms of a contour map. This figure is useful as it provides an indication of the resolution which can be expected in reconstructing the pollution history of this lake by taking cores from various locations within the two depositional basins. Over much of the Goderich Depositional basin the practical intrinsic resolution is about twenty years while in a certain limited region toward the eastern margin of this basin the resolution may be under ten years and primarily limited by the 1 cm condition. This area is characterized by a combination of comparatively high sedimentation rates and small depth of sediment mixing. In the Port Huron basin the resolution is generally greater than twenty years.

Because of the time resolution inherent in sediments of these depositional basins, it is not likely that any recent improvements in water quality will as yet have had a measureable effect on sedimentary profiles. Another important aspect of this intrinsic resolution or characteristic integration time concept, is its bearing on the availability of pollutants

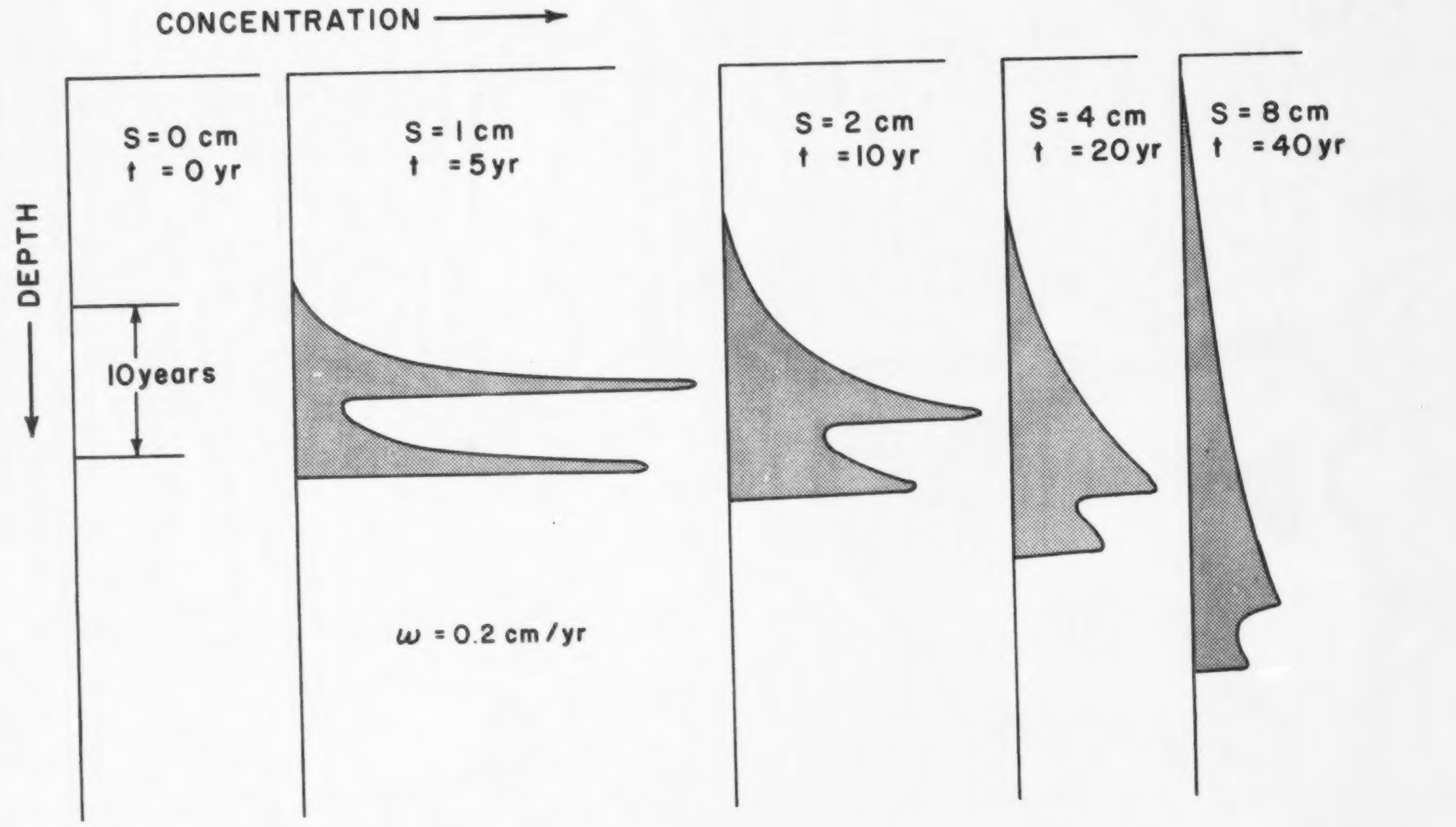

Figure 128. The effect of rapid steady-state mixing on the sedimentary record of two events occurring ten years apart.

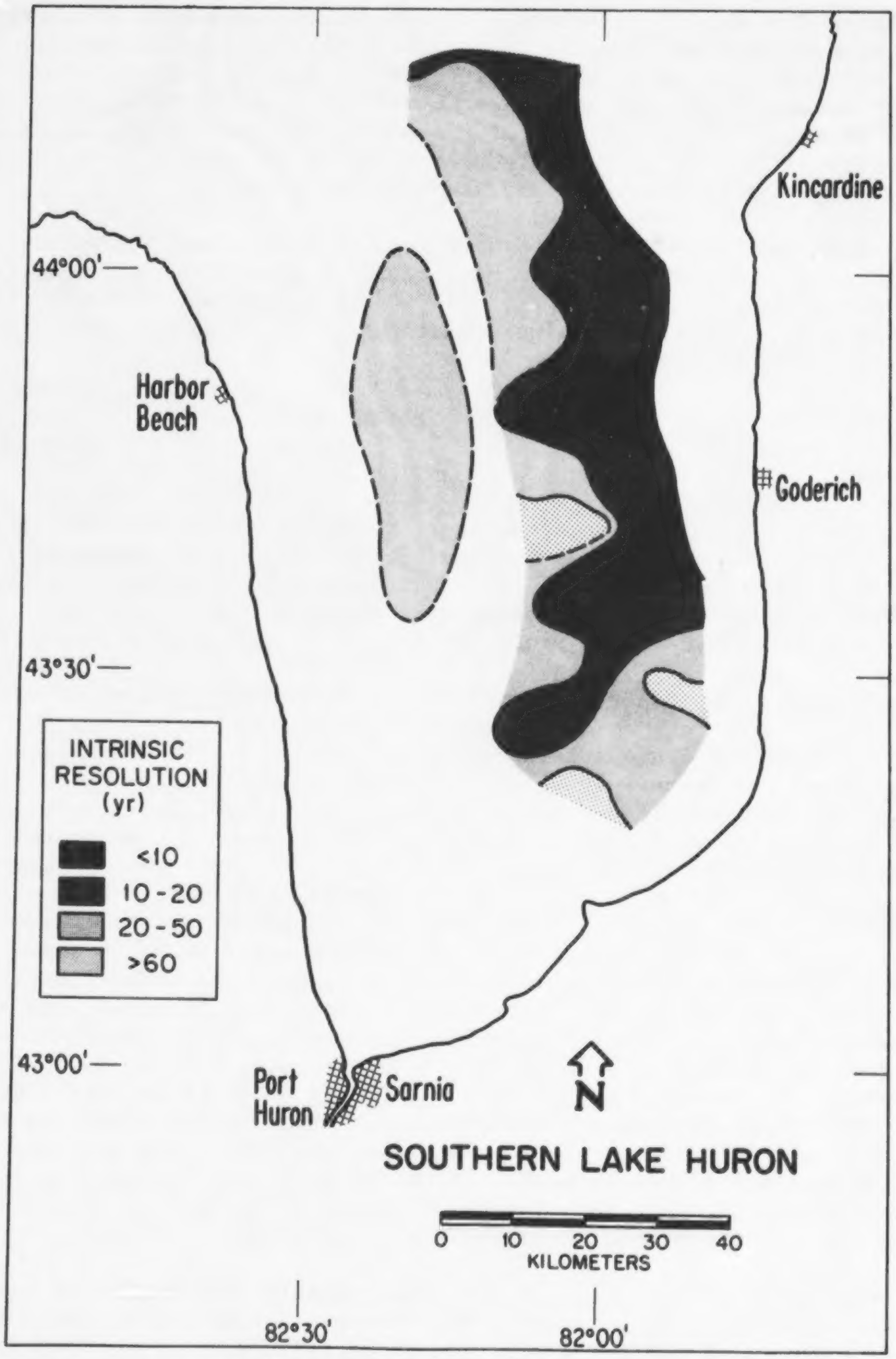
Kincardine
44°00'
Harbor Beach
Goderich
43°30'
INTRINSIC RESOLUTION (yr)
<10
10-20
20-50
>60
43°00'
Port Huron
Sarnia
N
SOUTHERN LAKE HURON
0
10
20
30
40
KILOMETERS
82°30'
82°00'

Figure 129. The approximate time-resolution expected in sampling cores in southern Lake Huron. The validity of the distribution depends on the correctness of the steady-state mixing model.

for exchange with overlying water. Sediment mixing serves to increase the contact time between water and polluted sediments. In the absence of any further anthropogenic metal additions to this area, the concentration of pollutant metals in surface sediments in contact with overlying water will decrease at a rate characteristic of the mean integration time, which for the two depositional basins in southern Lake Huron is on average about 20 years, corresponding to a rate constant of about 5% per year.

It should be emphasized that these results are strongly model-dependent and valid only to the extent that the concept of steady-state mixing is valid. Moreover, the results apply only to substances which remain strongly associated with sediment particles and are not subject to any appreciable post-depositional migration.

RATE OF ACCUMULATION OF SEDIMENTARY CONSTITUENTS

Computation

The rate of accumulation of non-enriched elements is computed as the product of the concentration of a given element in surface sediments (1-2 cm) and the mass sedimentation rate. For the non-enriched elements this value of the accumulation rate is both a measure of the most recent rate of accumulation ($z=0$) and of the precultural accumulation rate as well.

For elements possessing a significant degree of surface enrichment the rate of accumulation can be described in terms of two components, the background or natural rate and the portion attributable to anthropogenic loadings (Kemp and Thomas, 1976; Edgington and Robbins, 1976). The natural accumulation rate is computed as the product of the mass sedimentation rate and the average concentration of an element below the depth where there is any significant degree of enrichment. For sediment cores where the mean background concentration is not known, it can be adequately inferred from the regression relation between surface iron concentrations and background values in other cores. In some instances only one background value is known. In such cases approximate background levels are taken to be proportional to surface iron concentrations. (Note that there is very little ($\leq$ 8%) surface enrichment of iron.) Linear regression parameters used to determine missing background concentrations from surface iron data are given in Table 44. In the cases of the elements Cd, Cu, Mn, Ni, Pb and Zn there is very little uncertainty in the estimate of background data because (1) there are many measured values and (2) correlations between measured values and surface iron concentrations are generally high. In the case of such elements as Sn, Hg, As and Br where there are very few measurements of background concentrations, uncertainties in the method of background assignments are unknown.

The rates of accumulation of the anthropogenic components are time-dependent and should, in principle, be referred to a specific time. In most previous analyses of anthropogenic element profiles some sort of ambiguous time-averaging has introduced biases into reported anthropogenic accumulation rates. For example, in the core collected by Kemp et al. (1974) in 1970 from the Goderich Basin, the so-called surface concentration refers to an interval from 0-2 cm. As the sedimentation rate is about 0.14 cm/yr at this location, this interval corresponds to 2/0.14=14 years. Hence the anthropogenic concentrations and accumulation rates for this core actually refer to a mean date of (1970-7)±7 = 1963±7 years. In this regard, the values reported for rates of anthropogenic element accumulation in Lake Huron by the IJC (1977) are based on this and two other cores which were sampled in a way which leads to an assigned date of 1962±8 years.

In the present report the so-called surface concentration values refer to the 1-2 cm sections of cores. Because of the great variability of sedimentation rates within each depositional basin, this section does not have a uniquely defined date from core to core. Moreover, because of averaging over the 1 cm section, the 1-2 cm interval may correspond to an appreciable span of years as discussed above. Because both the sedimentation rate and source function have been determined as part of this study, it is possible to correct concentration data for the effect of finite interval sampling in the way indicated above. If C_o is taken as the net anthropogenic concentration (total-background) of a given element at the sediment surface (z=0 corresponding to 1974 or 1975) then the expected profile is:

$$C(m) = C_o e^{-\beta t} = C_o e^{-\beta m/r} \qquad (47)$$

where m is the cumulative mass per unit area and β is the source function parameter (see above). When the cores are sectioned in finite intervals, the expected concentration in the 1-2 cm interval, for example, is then

$$C_{1-2} = (C_o/(m_2 - m_1)) \int_{m_1}^{m_2} e^{-\beta m/r}\, dm \qquad (48)$$

or in terms of dates associated with depths m_1 and m_2 ($t_1=m_1/r$ and $t_2=m_2/r$)

$$\begin{aligned} C_{1-2} &= (C_o/(t_2 - t_1)) \int_{t_1}^{t_2} e^{-\beta t}\, dt \\ &= (C_o/\beta(t_2 - t_1))(e^{-\beta t_1} - e^{-\beta t_2}) \end{aligned} \qquad (49)$$

Therefore the expected concentration referred to z=0, C_o, is related to the observed concentration C_{1-2} by

$$C_o = C_{1-2}\, \beta (t_2 - t_1) / (e^{-\beta t_1} - e^{-\beta t_2}) \qquad (50)$$

Thus the concentration in the 1-2 cm interval may be used to infer the most recent accumulation rate (C_o x r) when the mass sedimentation rate and source function parameter are known.

In the tables below, the present accumulation rate is adjusted to the date of this report (1980). It is assumed that the values of the doubling times calculated above for the enriched elements hold as well for the period between the collection date 1974 or 1975 and 1980. As the source function parameter is approximately 0.034 yr^{-1} the correction is given by

$$C_o(1980) = C_o(1975)\ e^{+0.034(1980-1975)} = 1.18\ C_o(1975) \quad (51)$$

which represents an 18% increase during the 5 year period.

The above corrections apply to unmixed sediments (s=0). When there is a zone of rapid steady-state mixing greater than about 1 cm depth, the concentrations in the 1-2 cm interval may be affected primarily by the mixing process. The effect of mixing is to suppress the concentration in the mixed zone. It can be shown (Robbins, 1978) that provided the 1-2 cm interval falls within the mixed zone the observed concentration is given by,

$$C_{1-2} = C_o\ \gamma\ /\ (\gamma + \beta) \text{ so that} \quad (52)$$

$$C_o(1975) = C_{1-2}\ (\gamma + \beta)\ /\ \gamma \quad (53)$$

where $\gamma = r/s$ (yr^{-1}) and s is the depth of the mixed zone in g/cm^2. Hence in computing the present accumulation rates either Eq. 50 or Eq. 53 is used depending on whether s is zero or not. A more rigorous treatment of the combined effects of mixing and finite interval sampling is given by Edgington and Robbins (1976).

Distribution of Accumulation Rates

Examples of the distribution of the rate of accumulation of non-enriched elements are shown in Figures 130-135. To conserve space only a few examples are given. As expected from the previous discussion of interelement associations, there is considerable redundancy in patterns of accumulation. There are two primary patterns, that of organic carbon-iron and that of the calcium family elements. The patterns of accumulation representative of the first group are organic carbon (Fig. 130), iron (Fig. 131) and chromium (Fig. 132). In each case there is a systematic trend toward increased rates of accumulation in the northern part of the Goderich Basin. Also in the northern sector the rates increase toward the eastern margin of the basin. Accumulation rates of the organic carbon-iron group of elements are considerably lower in the Port Huron Basin and exhibit less spatial variability. The considerable variability in the organic carbon-iron group of elements in the Goderich Basin is brought about in part by the dramatic gradients in the deposition of the calcium family elements. In contrast however with the first group, the calcium family elements do not possess a significant north-south trend. Inorganic carbon (Fig. 133), calcium (Fig. 134) and magnesium (Fig. 135) all exhibit marked and systematic increases in rates of accumulation toward the eastern margin of the Goderich Basin. Within this basin more than an order of magnitude decrease in the rate of deposition of the calcium family elements occurs in traversing from east to west. In comparison with calcium family element accumulation rates in the

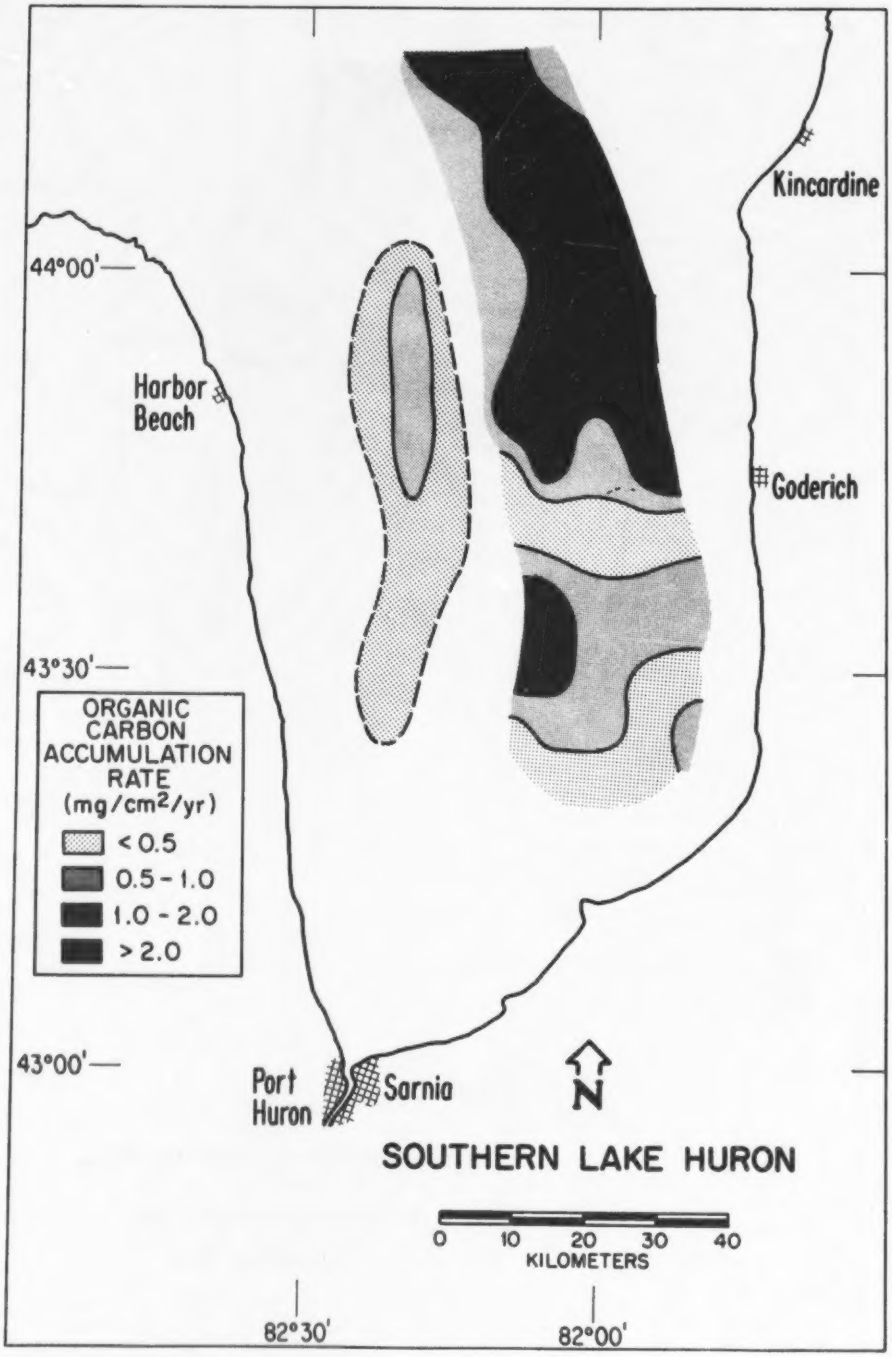
Kincardine
44°00'
Harbor Beach
Goderich
43°30'
ORGANIC CARBON ACCUMULATION RATE (mg/cm2/yr)
< 0.5
0.5 - 1.0
1.0 - 2.0
> 2.0
43°00'
Port Huron
Sarnia
N
SOUTHERN LAKE HURON
0
10
20
30
40
KILOMETERS
82°30'
82°00'

Figure 130. The rate of accumulation of organic carbon in surface sediments.

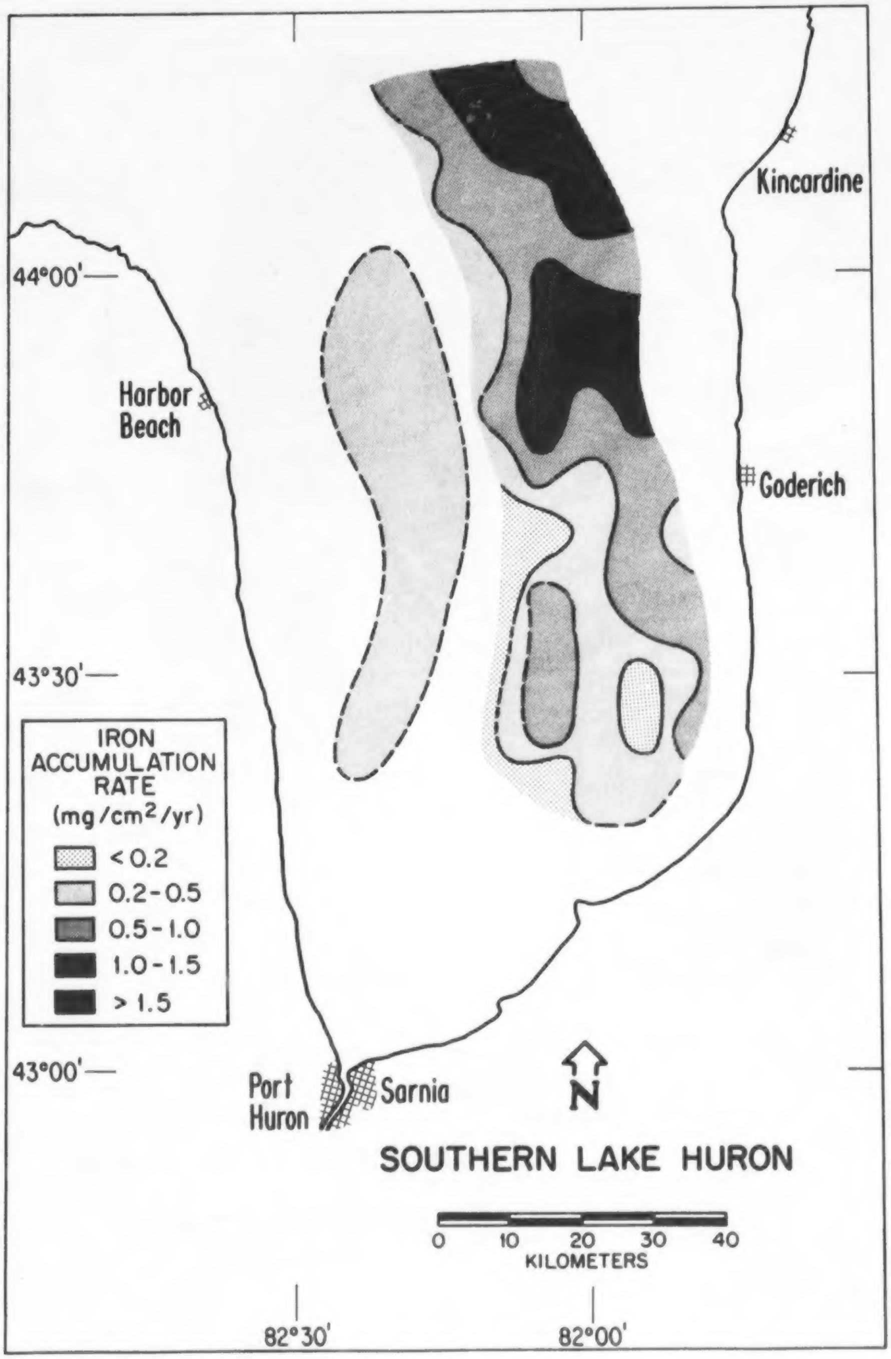
Kincardine
44°00'
Harbor Beach
Goderich
43°30'
IRON ACCUMULATION RATE (mg/cm²/yr)
< 0.2
0.2-0.5
0.5-1.0
1.0-1.5
> 1.5
43°00'
Port Huron
Sarnia
N
SOUTHERN LAKE HURON
0 10 20 30 40
KILOMETERS
82°30'
82°00'

Figure 131. The rate of accumulation of iron (AAS) in surface sediments.

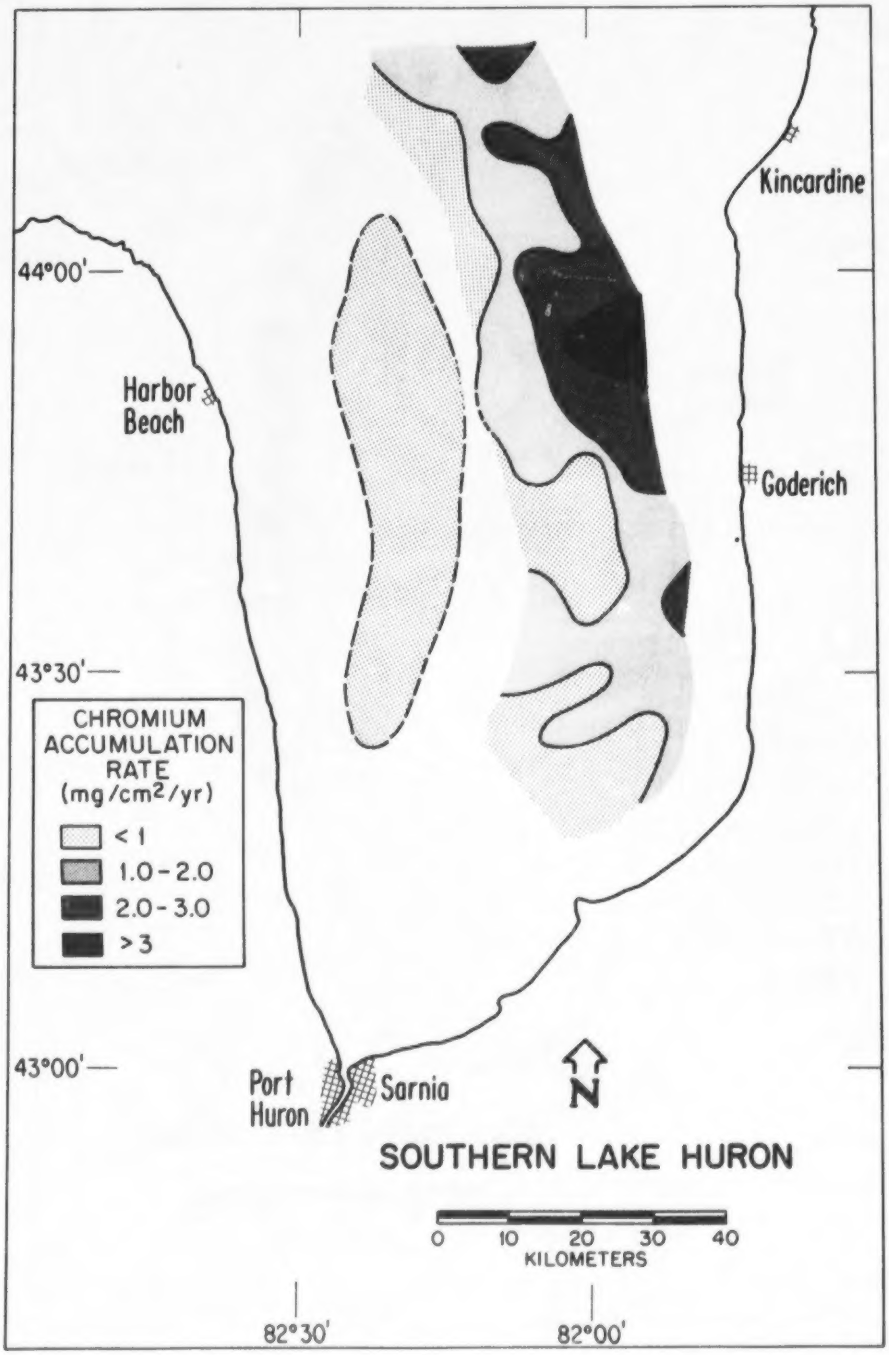

CHROMIUM ACCUMULATION RATE (mg/cm2/yr)
< 1
1.0 - 2.0
2.0 - 3.0
> 3
Kincardine
Harbor Beach
Goderich
Port Huron
Sarnia
N
SOUTHERN LAKE HURON
0 10 20 30 40
KILOMETERS
44°00'
43°30'
43°00'
82°30'
82°00'

Figure 132. The rate of accumulation of chromium (AAS) in surface sediments.

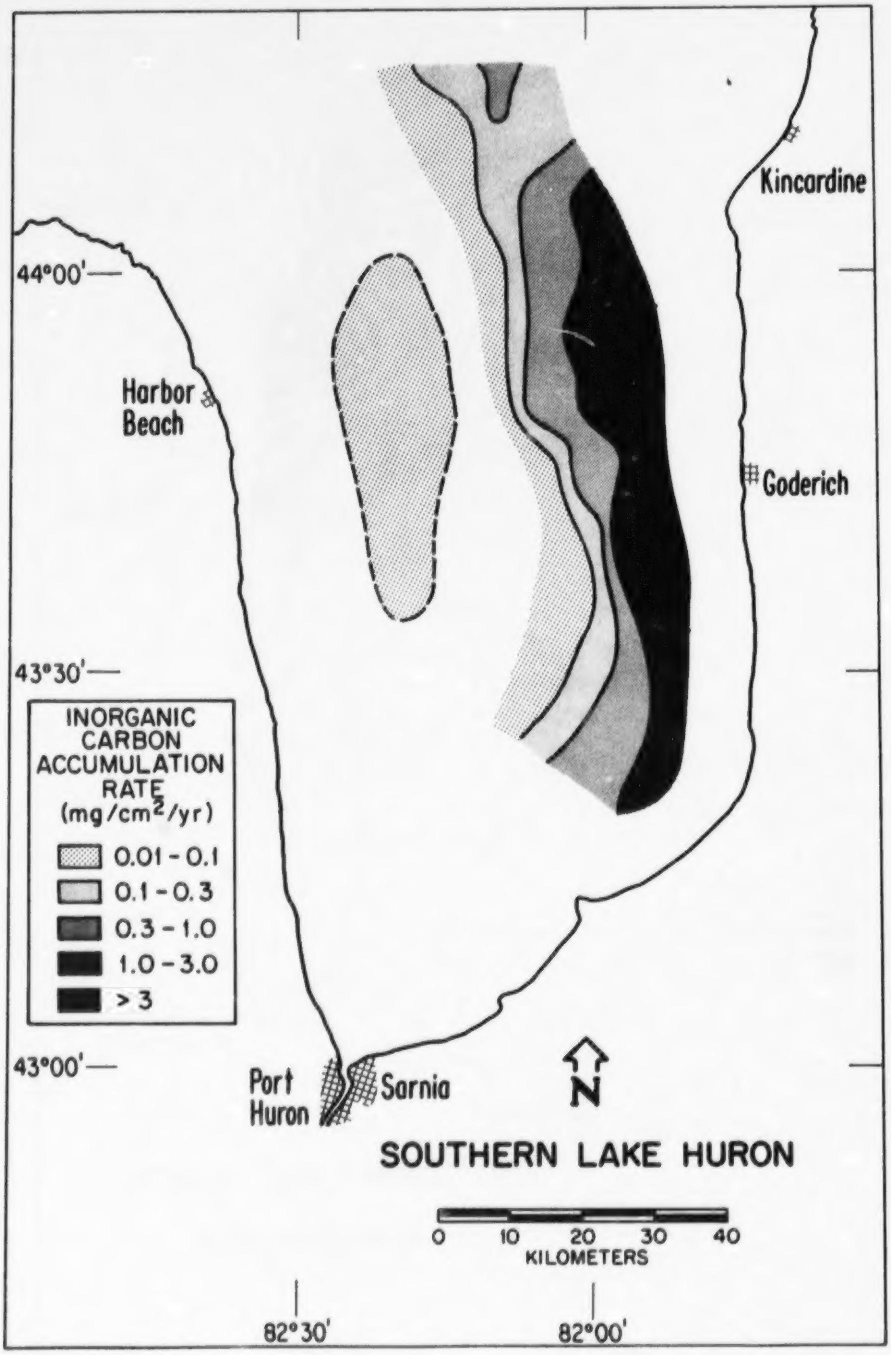

Kincardine
44°00'
Harbor Beach
Goderich
43°30'
INORGANIC CARBON ACCUMULATION RATE (mg/cm^2/yr)
0.01 - 0.1
0.1 - 0.3
0.3 - 1.0
1.0 - 3.0
> 3
43°00'
Port Huron
Sarnia
N
SOUTHERN LAKE HURON
0 10 20 30 40
KILOMETERS
82°30'
82°00'

Figure 133. The rate of accumulation of inorganic carbon in surface sediments.

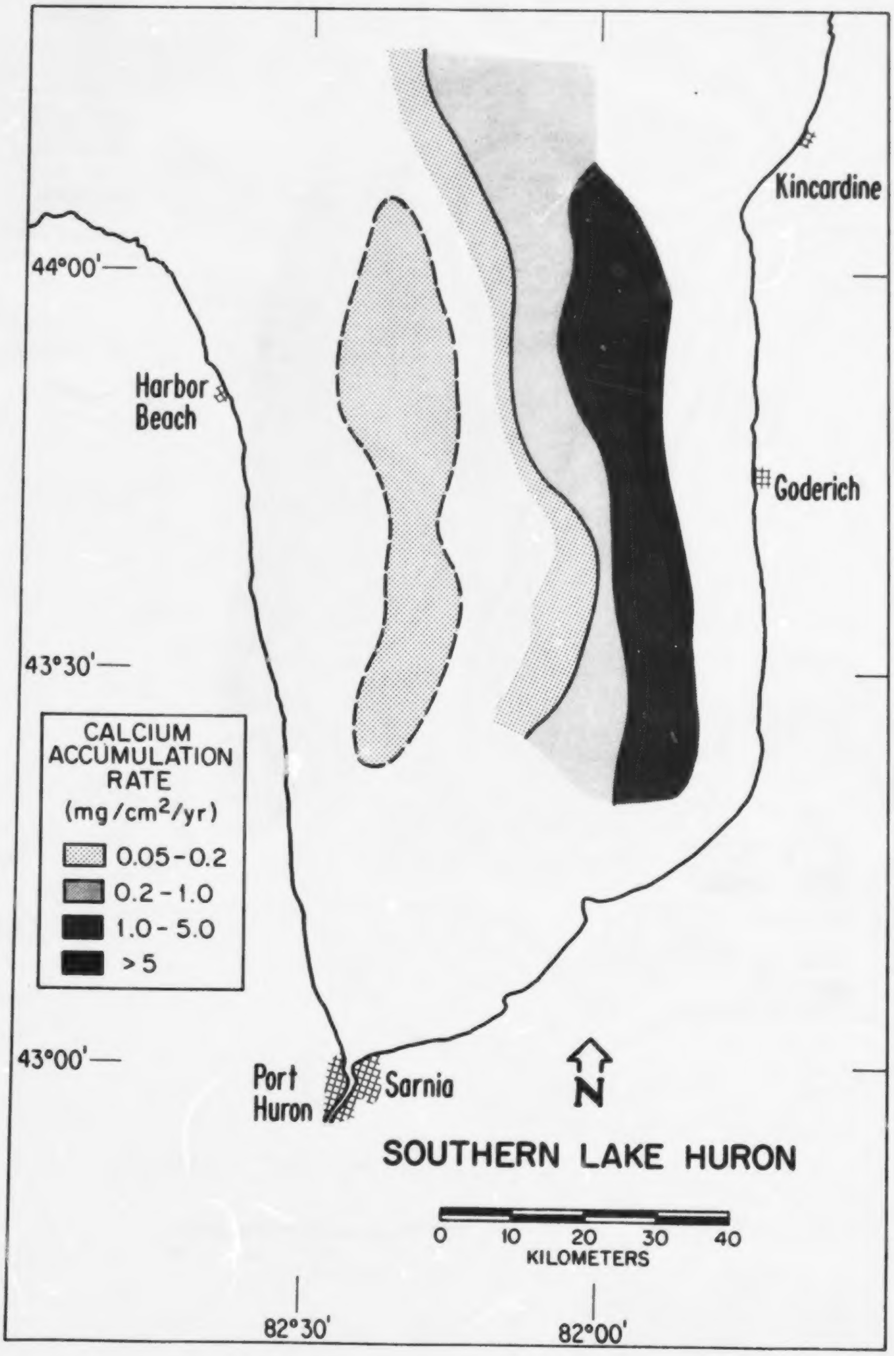

Kincardine
Harbor Beach
Goderich
44°00'
43°30'
43°00'
CALCIUM ACCUMULATION RATE (mg/cm2/yr)
0.05-0.2
0.2-1.0
1.0-5.0
>5
Port Huron
Sarnia
N
SOUTHERN LAKE HURON
0 10 20 30 40
KILOMETERS
82°30'
82°00'

Figure 134. The rate of accumulation of calcium in surface sediments.

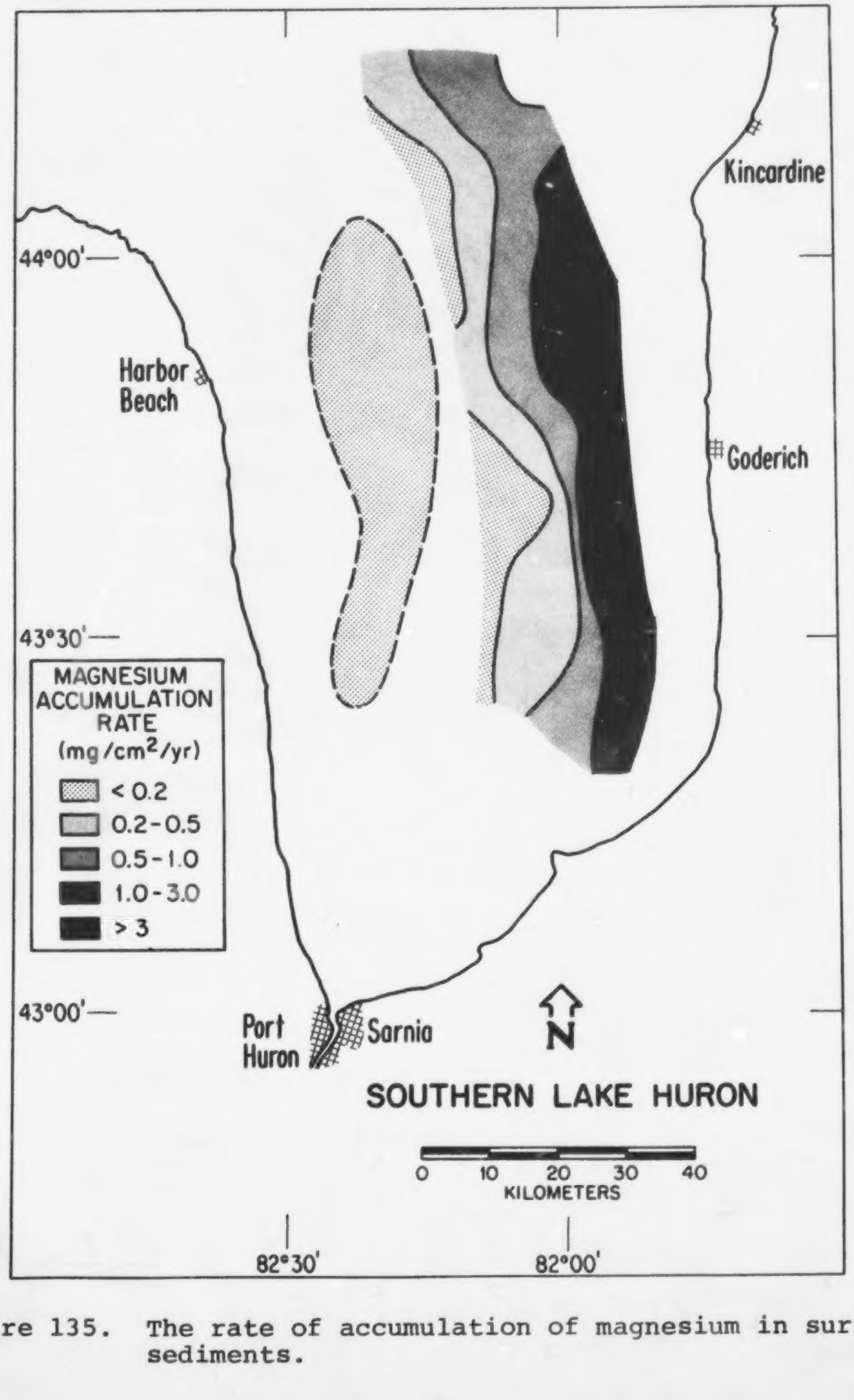

Kincardine
44°00'
Harbor Beach
Goderich
43°30'
MAGNESIUM ACCUMULATION RATE (mg/cm2/yr)
< 0.2
0.2-0.5
0.5-1.0
1.0-3.0
> 3
43°00'
Port Huron
Sarnia
N
SOUTHERN LAKE HURON
0
10
20
30
40
KILOMETERS
82°30'
82°00'

Figure 135. The rate of accumulation of magnesium in surface sediments.

Goderich Basin, those in the Port Huron Basin are virtually neglible.

The spatial distribution of the factor required to convert 1-2 cm anthropogenic concentration data to 1980 values is shown in Fig. 136. Highest values tend to occur toward the escarpment sides of the depositional basins. The mean conversion factor is 1.9 of which 18% (1.18) results from extrapolation of surface values in 1975 to those expected in 1980 (see above). That part of the factor associated with converting 1-2 cm concentrations to values at $z=0$ (1975) is on the average equal to $1.9/1.18=1.6$. Thus the use of the 1-2 cm section to represent surface concentrations of anthropogenic components, plus the effects of finite interval sampling and steady-state mixing combine to produce about a 60% average upward adjustment.

The present (1980) rates of accumulation of selected elements are shown in Figs. 137-143. The patterns are very similar for most of the elements and show highest values in the northern sector of the Goderich Basin and toward the western margin. Anthropogenic accumulation rates in the Port Huron Basin are substantially less and show less spatial variability.

Mean and Total Accumulation Rates

The mean and total accumulation rates of fine-grained sediments and non-enriched elements are summarized in Table 43. Mean rates for the two depositional basins have been computed as the mean of accumulation rates calculated for individual cores within each basin. Because of the large number of cores and their regular spacing within basins this method of estimation is not significantly different from that based on integration of isopleths.

In Table 43 the mean accumulation rates for southern Lake Huron are expressed in terms of the combined accumulation in the Goderich and Port Huron Basins divided by the total area of southern part of the Lake. Thus, for example, the mean accumulation rate of fine-grained sediment in southern Lake Huron, 11.4 $mg/cm^2/yr$, is calculated as follows: the total accumulation rate in the Port Huron Basin is $12.8\ mg/cm^2/yr \times 1.22 \times 10^{13}\ cm^2$. The total accumulation rate in the Goderich Basin is $35.7\ mg/cm^2/yr \times 2.59 \times 10^{13}\ cm^2$ while the total area of the southern Lake Huron is $9.5 \times 10^{13}\ cm^2$ (see Table 1). Therefore, the mean accumulation rate in the southern part of the Lake is $(12.8 \times 1.22 + 35.7 \times 2.59)/9.5 = 11.4\ mg/cm^2/yr$. Note that in Table 43, mean accumulation rates of the fine-grained sediments and major constituents are expressed in terms of $mg/cm^2/yr$ whereas for the trace constituents the units are micrograms/cm^2/yr. In the above calculation it is implicitly assumed that the areas of sand, till, glaciolacustrine clay and exposed bedrock are non-depositional. That is, at the present time there is no significant permanent accumulation of fine-grained sediments in those areas. Note that this assumption is open to question in view of the results obtained above for cesium-137 and lead-210. The utility of expressing accumulation rates in terms of the total per unit area of the southern part of the Lake is that, to the extent that there is no net export or import of particulate matter form the southern part of the lake, there is some basis for comparison of these mean rates with other loading data.

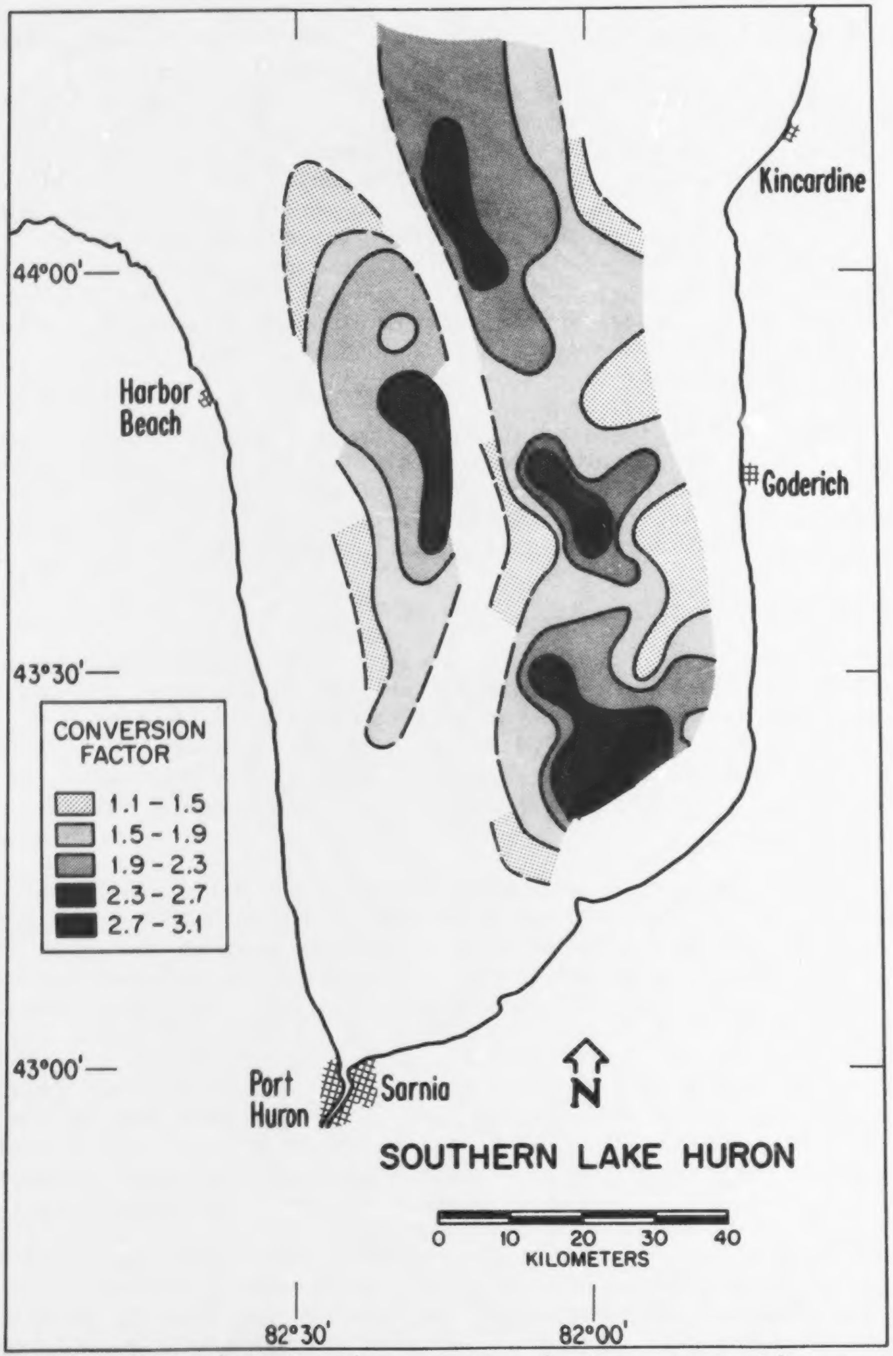
Kincardine
44°00'
Harbor Beach
Goderich
43°30'
CONVERSION FACTOR
1.1 - 1.5
1.5 - 1.9
1.9 - 2.3
2.3 - 2.7
2.7 - 3.1
43°00'
Port Huron
Sarnia
N
SOUTHERN LAKE HURON
0 10 20 30 40
KILOMETERS
82°30'
82°00'

Figure 136. The distribution of the factor converting surface concentrations to present (1980) values. Only 18% of the factor results from conversion from 1975 to 1980 values. The remainder results from sediment mixing and finite sampling corrections (see text).

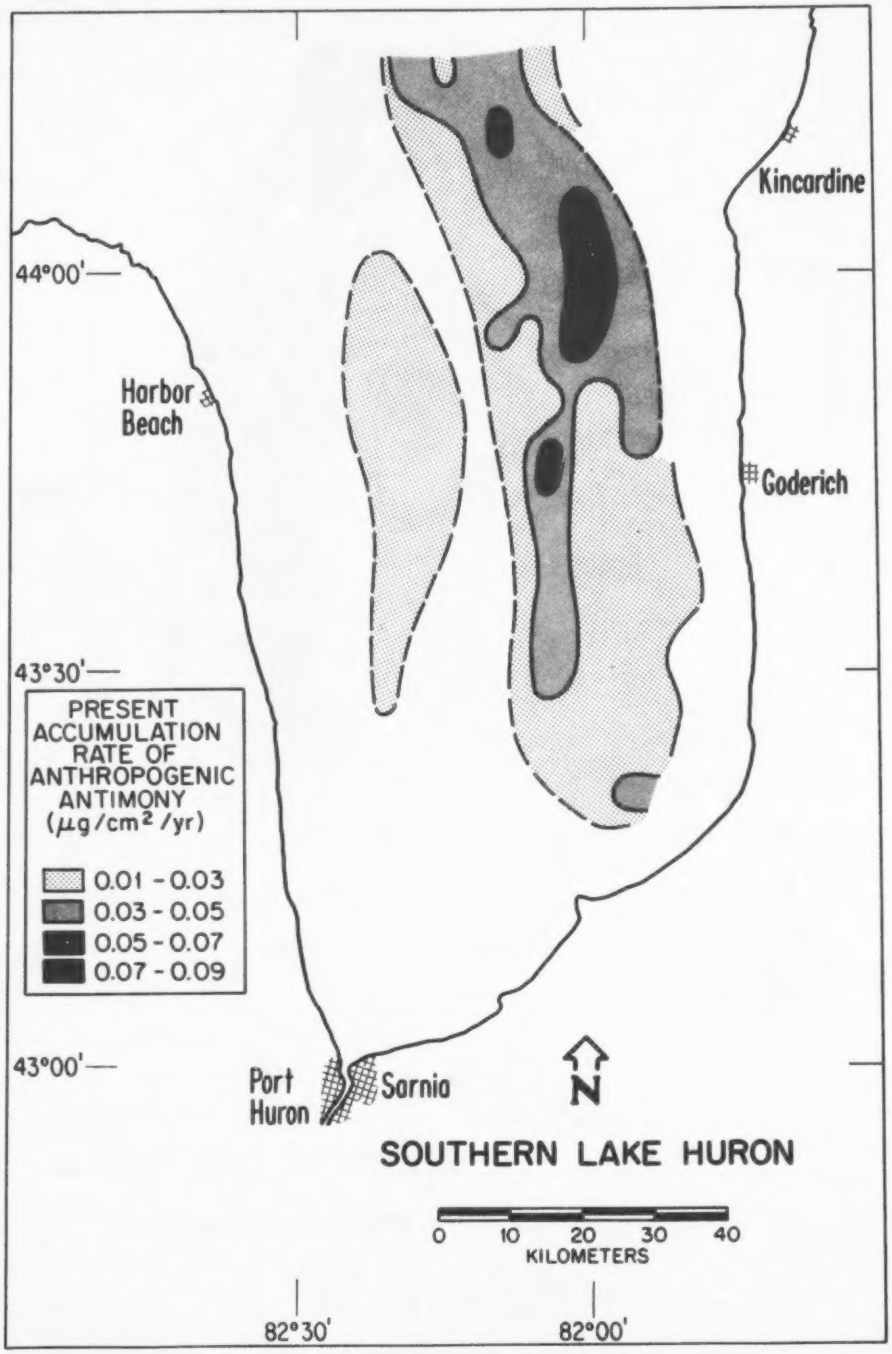
Kincardine
44°00'
Harbor Beach
Goderich
43°30'
PRESENT ACCUMULATION RATE OF ANTHROPOGENIC ANTIMONY (μg/cm² /yr)
0.01 - 0.03
0.03 - 0.05
0.05 - 0.07
0.07 - 0.09
43°00'
Port Huron
Sarnia
N
SOUTHERN LAKE HURON
0 10 20 30 40
KILOMETERS
82°30'
82°00'

Figure 137. Rate of accumulation of anthropogenic antimony (adjusted to 1980).

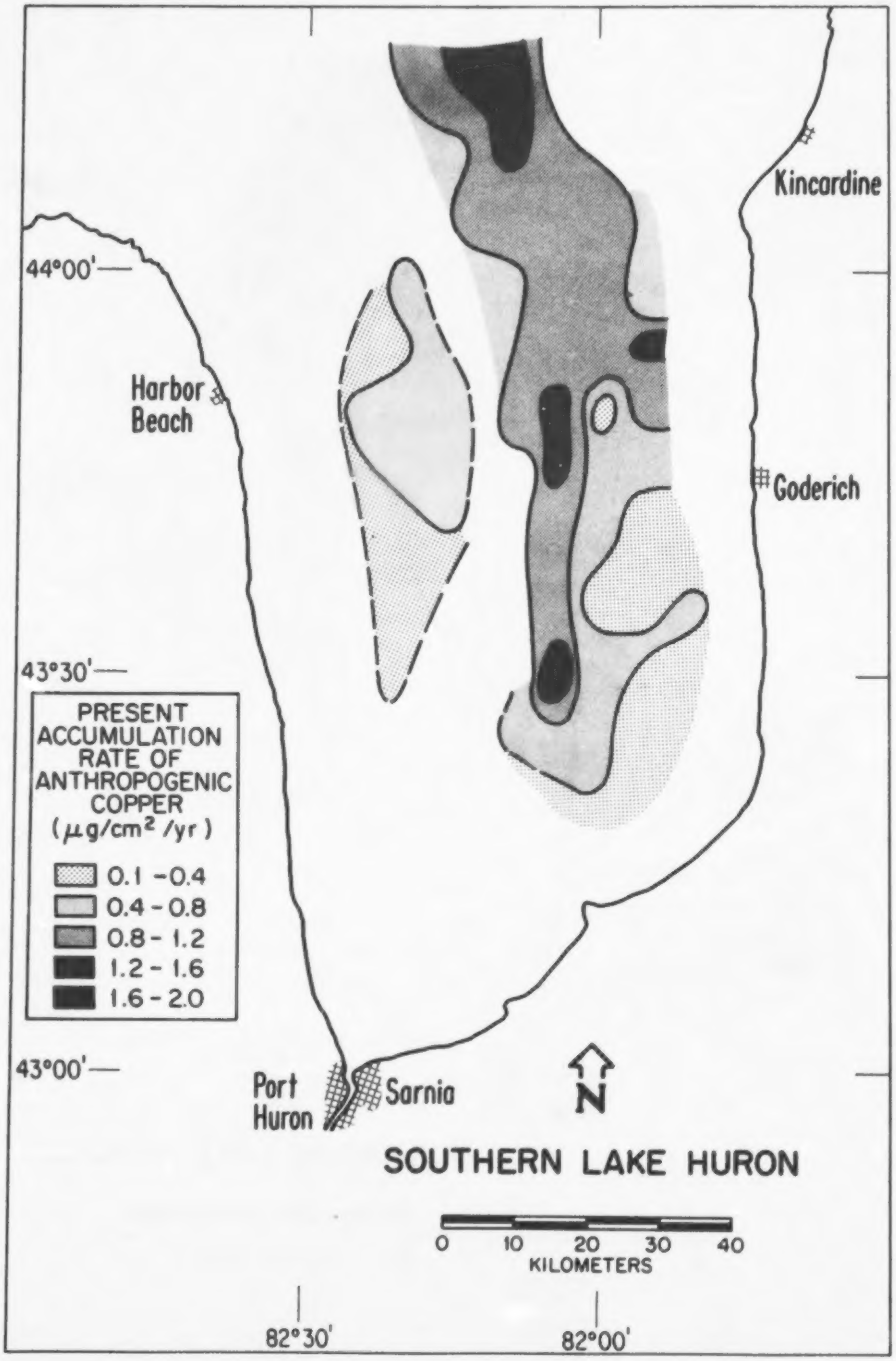

PRESENT ACCUMULATION RATE OF ANTHROPOGENIC COPPER (μg/cm² /yr)
0.1 - 0.4
0.4 - 0.8
0.8 - 1.2
1.2 - 1.6
1.6 - 2.0
Kincardine
Goderich
Harbor Beach
Port Huron
Sarnia
N
SOUTHERN LAKE HURON
0 10 20 30 40
KILOMETERS
44°00'
43°30'
43°00'
82°30'
82°00'

Figure 138. Rate of accumulation of anthropogenic copper (adjusted to 1980).

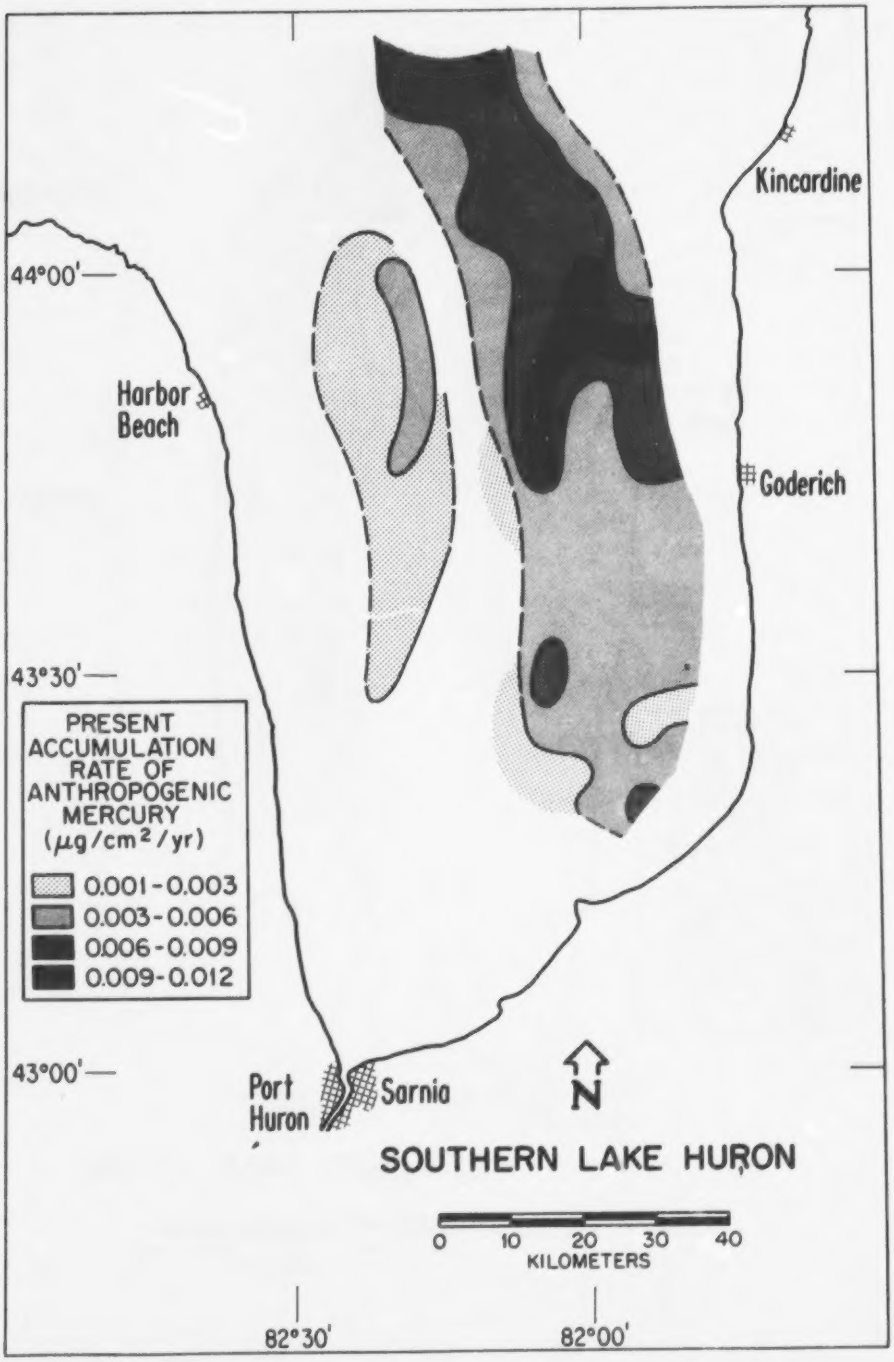
44°00'
43°30'
43°00'
82°30'
82°00'
Kincardine
Harbor Beach
Goderich
Port Huron
Sarnia
N
SOUTHERN LAKE HURON
0 10 20 30 40
KILOMETERS
PRESENT ACCUMULATION RATE OF ANTHROPOGENIC MERCURY (μg/cm² /yr)
0.001-0.003
0.003-0.006
0.006-0.009
0.009-0.012

Figure 139. Rate of accumulation of anthropogenic mercury (adjusted to 1980).

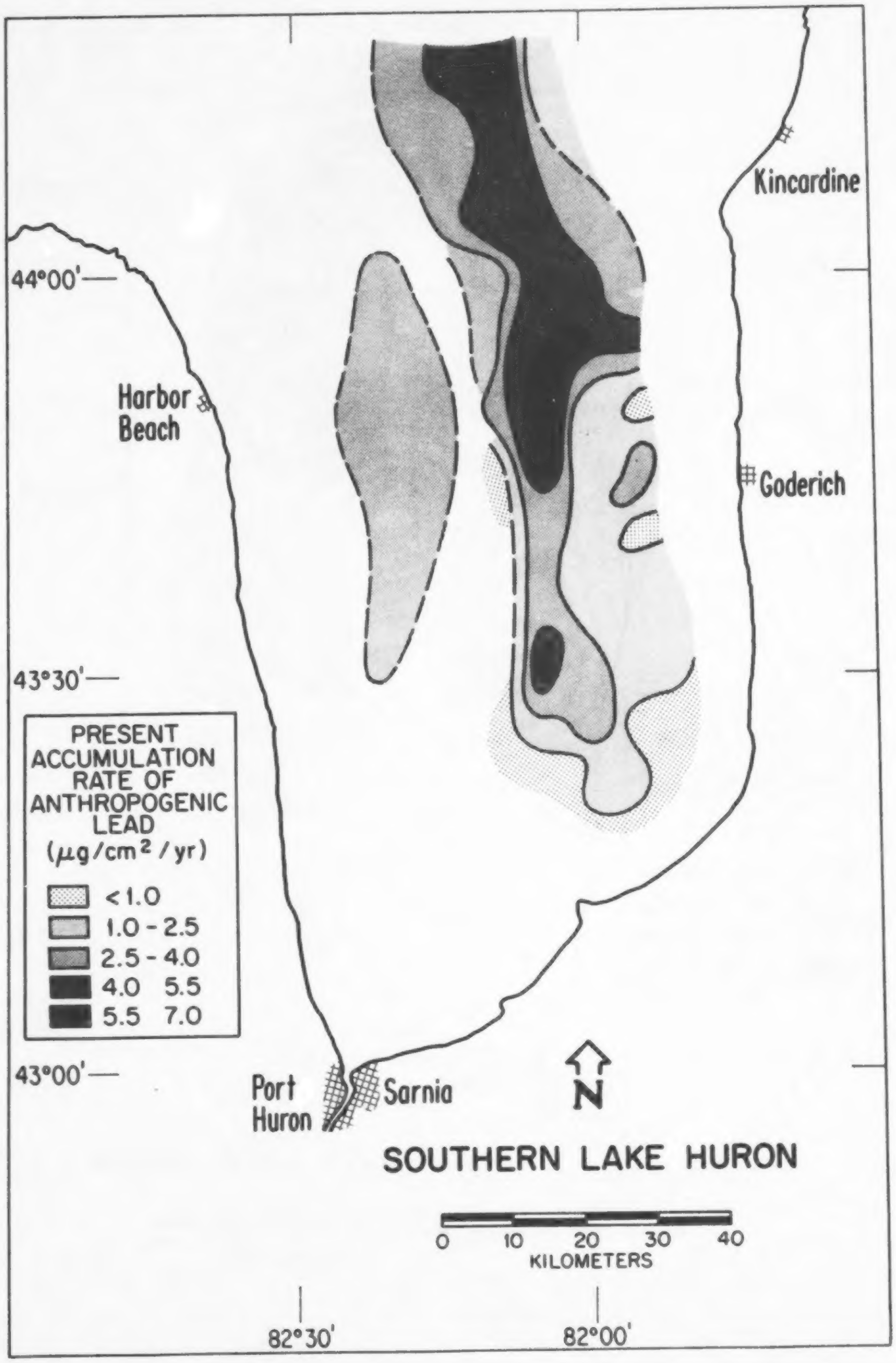
44°00'
43°30'
43°00'
82°30'
82°00'
Kincardine
Harbor Beach
Goderich
Port Huron
Sarnia
N
SOUTHERN LAKE HURON
0 10 20 30 40
KILOMETERS
PRESENT ACCUMULATION RATE OF ANTHROPOGENIC LEAD (µg/cm² / yr)
<1.0
1.0 - 2.5
2.5 - 4.0
4.0 5.5
5.5 7.0

Figure 140. Rate of accumulation of anthropogenic lead (adjusted to 1980).

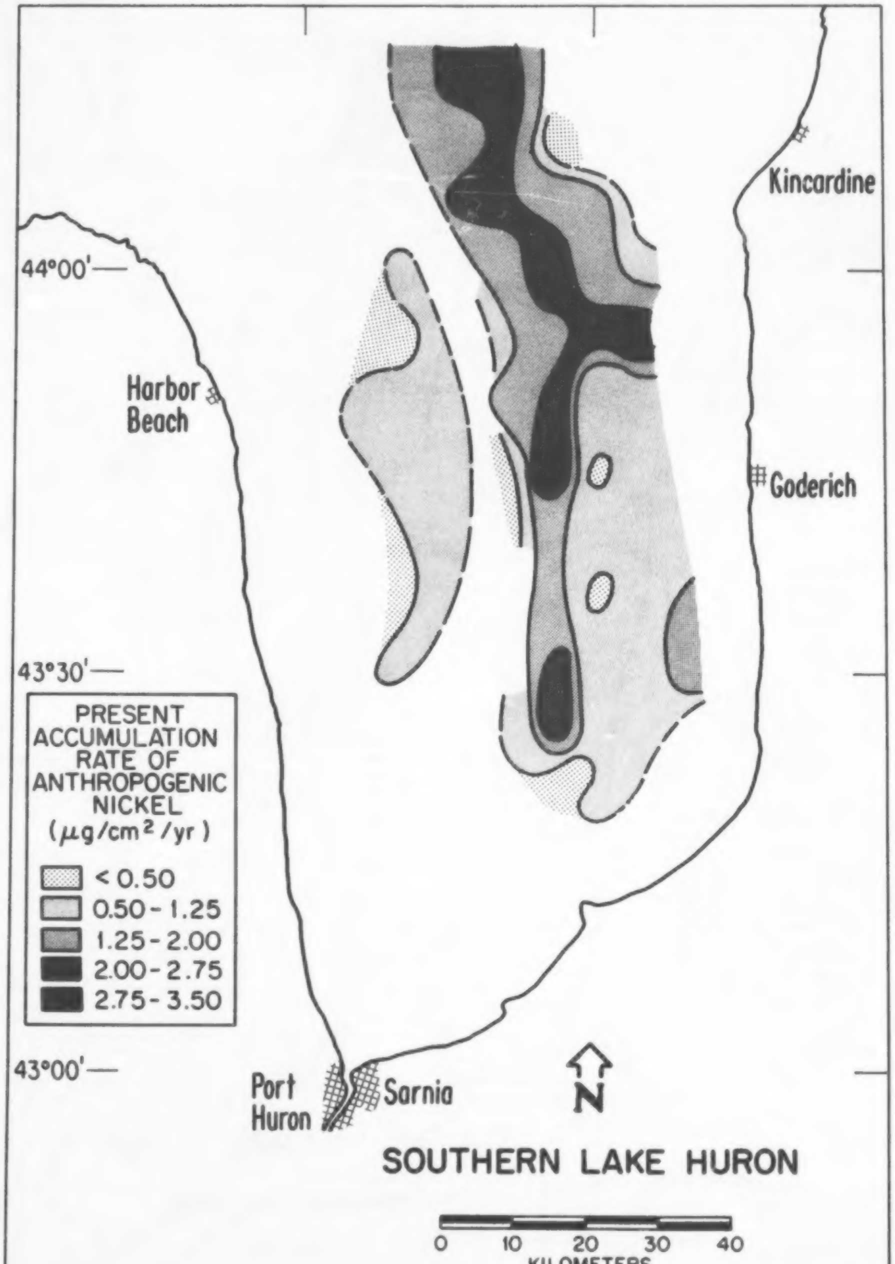
Kincardine
44°00'
Harbor Beach
Goderich
43°30'
PRESENT ACCUMULATION RATE OF ANTHROPOGENIC NICKEL ($\mu g/cm^2/yr$)
< 0.50
0.50 - 1.25
1.25 - 2.00
2.00 - 2.75
2.75 - 3.50
43°00'
Port Huron
Sarnia
N
SOUTHERN LAKE HURON
0 10 20 30 40
KILOMETERS
82°30'
82°00'

Figure 141. Rate of accumulation of anthropogenic nickel (adjusted to 1980).

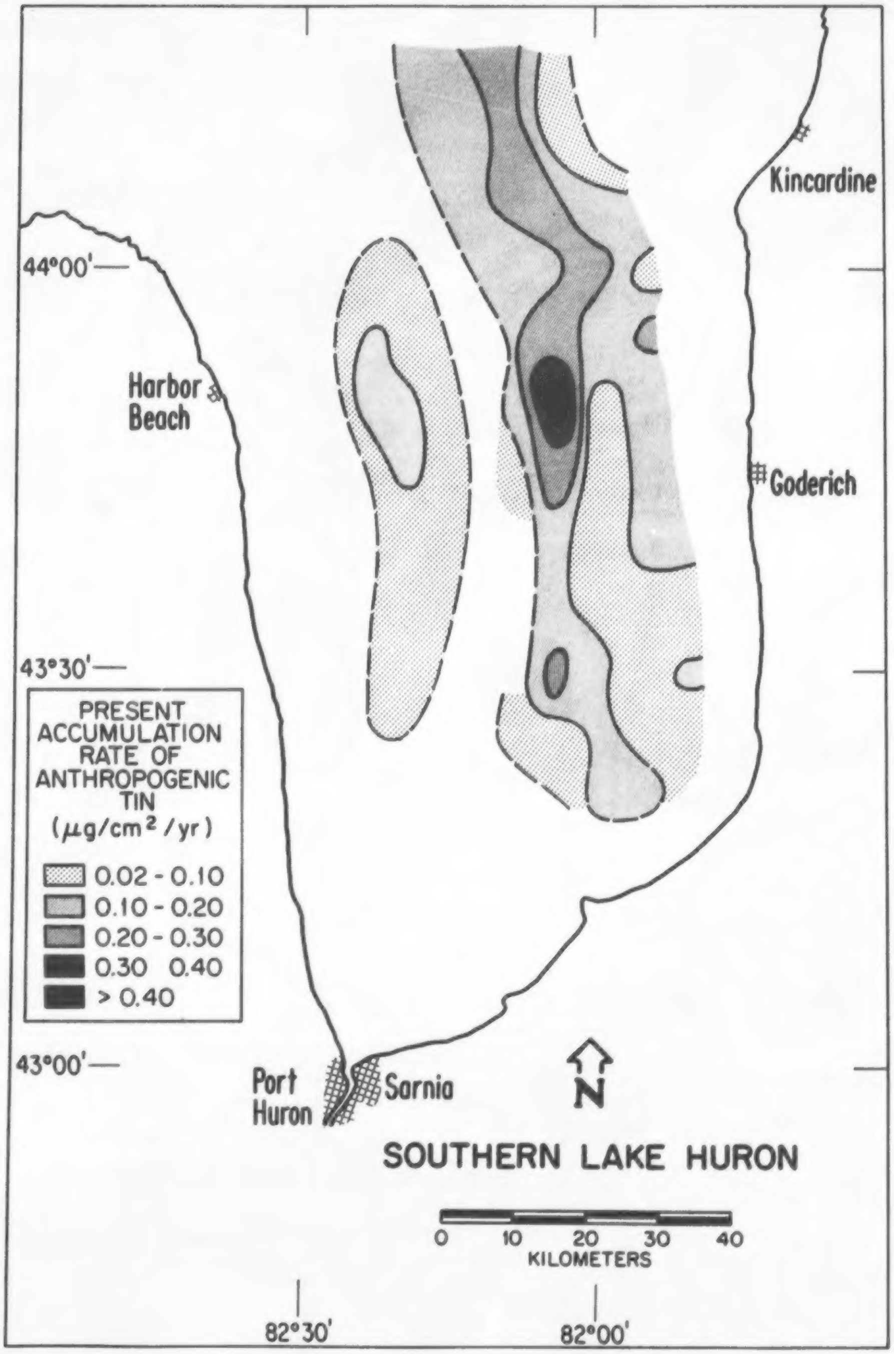
Kincardine
44°00'
Harbor Beach
Goderich
43°30'
PRESENT ACCUMULATION RATE OF ANTHROPOGENIC TIN
($\mu g/cm^2/yr$)
0.02 - 0.10
0.10 - 0.20
0.20 - 0.30
0.30 0.40
> 0.40
43°00'
Port Huron
Sarnia
N
SOUTHERN LAKE HURON
0 10 20 30 40
KILOMETERS
82°30'
82°00'

Figure 142. Rate of accumulation of anthropogenic tin (adjusted to 1980).

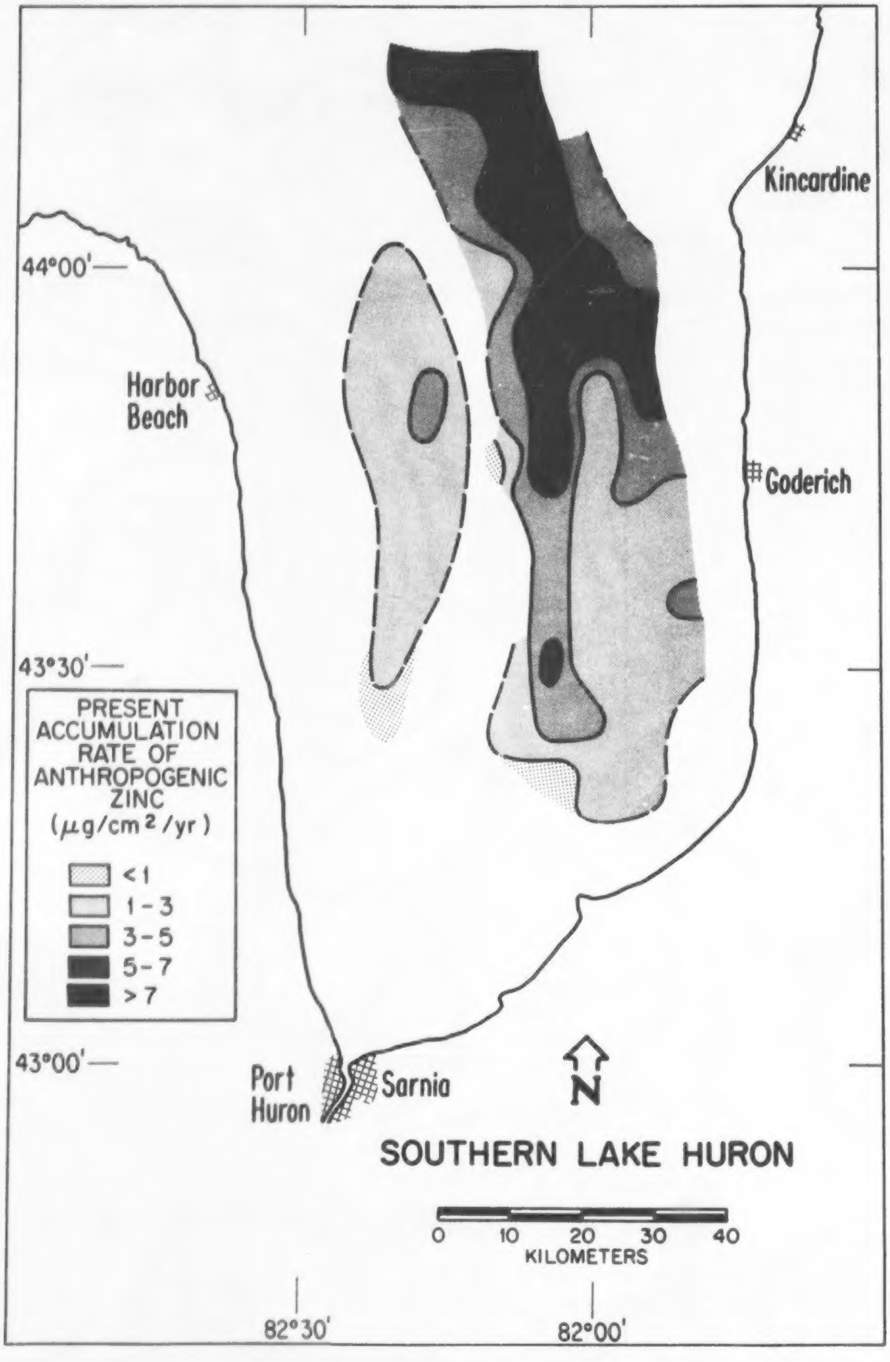
Kincardine
44°00'
Harbor Beach
Goderich
43°30'
PRESENT ACCUMULATION RATE OF ANTHROPOGENIC ZINC
(μg/cm²/yr)
<1
1-3
3-5
5-7
>7
43°00'
Port Huron
Sarnia
N
SOUTHERN LAKE HURON
0
10
20
30
40
KILOMETERS
82°30'
82°00'

Figure 143. Rate of accumulation of anthropogenic zinc (adjusted to 1980).

TABLE 43. MEAN AND TOTAL ACCUMULATION RATES OF FINE-GRAINED SEDIMENTS AND NON-ENRICHED ELEMENTS

	Port Huron Basin		Goderich Basin		Southern Lake Huron	
	Mean Accumulation Rate[a] (mg/cm^2/yr) or μg/cm^2/yr)	Total (metric tons/yr)	Mean Accumulation Rate[a] (mg/cm^2/yr) or μg/cm^2/yr)	Total (metric tons/yr)	Mean Accumulation Rate[b] (mg/cm^2/yr) or μg/cm^2/yr)	Total (metric tons/yr)
Mass						
(total)	12.8	1.6×10^5	35.7	9.3×10^5	11.4	1.1×10^6
(acid sol.)	3.5	0.43×10^5	12.6	3.3×10^5	3.9	0.37×10^6
Major Constituents						
OC	.47	5700	.93	24000	.31	30000
IOC	.24	2900	1.0	26000	.30	30000
Ca	.07	850	1.6	41000	.44	42000
Fe1	.35	4300	.77	20000	.25	24000
Fe2	.41	5000	.93	24000	.31	29000
K	.08	980	.21	5400	.068	6000
Mg	.08	980	1.1	28000	.31	29000
Na2	.11	1300	.27	7000	.088	8300
P	.021	250	.046	1200	.015	1000
Minor Constituents						
Ba2	∼6	70	∼15	390	4.9	460
Ce	.74	9	1.7	44	.56	53
Co	.14	1.7	.32	8.3	.10	10
Cr1	.59	7.2	1.6	41	.51	48
Cr2	.90	11	2.1	54	.69	65
Cs	.048	.59	.11	2.8	.036	3.4
Eu	.016	.19	.036	.93	.012	1.1

(continued).

TABLE 43. (continued).

	Port Huron Basin		Goderich Basin		Southern Lake Huron	
	Mean Accumulation Rate[a] (mg/cm^2/yr) or μg/cm^2/yr)	Total (metric tons/yr)	Mean Accumulation Rate[a] (mg/cm^2/yr) or μg/cm^2/yr)	Total (metric tons/yr)	Mean Accumulation Rate[b] (mg/cm^2/yr) or μg/cm^2/yr)	Total (metric tons/yr)
Minor Constituents						
La	.44	5.4	.96	25	.32	30
Lu	.0046	0.056	.011	.28	.0036	0.33
Sc	.15	1.9	.35	9.1	.11	11
Sm	.073	.89	.17	4.4	.056	5.3
Sr	.57	7	1.6	41	.51	48
Th	.12	1.4	.26	7.5	.086	8.9
U	$\sim$.04	.5	$\sim$.09	2.3	.030	2.8

[a] Sediment and major element accumulation rates in mg/cm^2/yr; minor element accumulation rates in μg/cm^2/yr

[b] Mean accumulation rate for all of southern Lake Huron = total accumulation/ total area of southern Lake Huron (9.5 x 10^{13} cm^2). Non-depositional areas (glacio-lacustrine clay and sand) are assigned zero accumulation rates.

TABLE 44. COEFFICIENTS USED IN THE REGRESSION RELATION TO DETERMINE ENRICHED ELEMENT BACKGROUND LEVELS FROM SURFACE IRON CONCENTRATIONS

Element	Coefficient[a] α	Coefficient[a] β	Correlation Coefficient	N
As	0	2.11	-	1
Br	0	15.32	-	1
Cd	3.0	-0.51	-0.52	17
Cu	5.0	8.87	0.84	24
Hg	0	0.0096	-	1
Mn	0.008	0.011	0.71	23
Ni	19.8	5.15	0.63	24
Pb	26.8	0	-	-
Sb	0	0.136	-	1
Si	-0.31	0.35	0.75	4
Sn	0	0.16	-	1
Zn	20.6	15.4	0.88	24

[a] $[\mathrm{Element}]_{BG} = \alpha + \beta\ [\mathrm{Fe}^{AAS}]$ 1-2.

Note: Fe, Mn and Si in wt. %, all others in μg/g.

The mean and total rates of accumulation of anthropogenic elements in the Port Huron and Goderich Basin and in southern Lake Huron are given in Tables 45, 46 and 47 respectively. Near-surface values are computed as the product of the mass sedimentation rate and uncorrected net surface concentrations in the 1-2 cm interval. This value is included both for completeness and because it is minimally dependent on model assumptions. Because of the necessity to construct some missing background values by regression analysis, the sensitivity of estimated mean concentrations was tested by varying calculated background levels by 20% while leaving known values unchanged. The results are given in Table 48 for the Goderich Basin data. For elements such as Hg, Sn, Zn, Pb where the degree of surface enrichment is high, a 20% change in calculated backgrounds results in only a 3-13 % change in mean accumulation rates. For other elements a 20% change results in approximately the same percent change in the estimate of mean accumulation rates.

From comparison of data in Tables 45 and 46 it can be seen that the mean accumulation rate of most elements is roughly twice (2.2) as high in the Goderich Basin as in the Port Huron Basin. This elevation occurs principally because sedimentation rates are considerably higher on the average in the Goderich Basin while mean concentrations of most elements other than the calcium family group are comparable in both basins. In addition to possessing a considerably higher average sedimentation rate, the Goderich Basin has roughly twice the area of the Port Huron Basin and therefore receives the lion's share of accumulating sedimentary constituents. On the average, the Goderich Basin receives 5 times more loading of most constituents than the Port Huron Basin. For the calcium family elements the Goderich Basin receives roughly 30 times as much per year as the Port Huron Basin.

Comparison with External Loading

It is premature to develop an accurate mass balance for Lake Huron which takes proper account of the accumulation of sedimentary materials, since the data for the northern part of the lake are not yet available. However, trends may be meaningfully examined by apportioning the loadings estimated by others for the main lake to the southern part. This approach is successful particularly in considering the accumulation of anthropogenic constituents since comparison of their accumulation rates with lake loadings does not depend on an accurate evaluation of the sources and composition of background constituents.

Fine-Grained Sediments -- The accumulation of fine-grained sediments in southern Lake Huron amounts to about 1 million metric tons annually and corresponds to a mean accumulation rate of 11.4 mg/cm^2/yr. This value is only slightly higher than the mean value for the main lake computed from the data of Kemp et al. (1976) as 10 mg/cm^2/yr corresponding to a lake-wide accumulation of 3.9 million metric tons annually. It therefore appears that the mean accumulation rate in the southern part of the lake is not greatly different from the lake-wide average. This is an important result in considering the representativeness of the southern lake for calculating

TABLE 45. ACCUMULATION RATES OF ENRICHED ELEMENTS IN THE PORT HURON BASIN

Element	Mean Accumulation Rate ($\mu g/cm^2/yr$)			Total Accumulation Rate* (metric tons/yr)		
	Natural	Anthropogenic		Natural	Anthropogenic	
		Near-Surface	Corrected to 1980		Near-Surface	Corrected to 1980
As	0.073	0.21	0.40	0.89	2.6	4.9
Br	0.53	0.12	0.22	6.5	1.5	2.7
Cd	0.023	0.017	0.034	0.28	0.21	0.41
Cu	0.41	0.19	0.38	5.0	2.3	4.6
Hg	$3x10^{-4}$	$13x10^{-4}$	$26x10^{-4}$	0.004	0.016	0.032
Mn	5	-	-	61	-	-
Ni	0.47	0.28	0.55	5.7	3.4	6.7
Pb	0.33	0.72	1.4	4.0	8.8	17
Sb	0.0047	0.0068	0.013	0.057	0.08	0.16
Si	78	60	120	950	730	1500
Sn	0.0055	0.033	0.065	0.067	0.40	0.79
Zn	0.87	1.0	2.0	11	12	24

* Mean accumulation rate x area of the Port Huron Basin.

TABLE 46. ACCUMULATION RATES OF ENRICHED ELEMENTS IN THE GODERICH BASIN

Element	Mean Accumulation Rate ($\mu g/cm^2/yr$) Natural	Mean Accumulation Rate ($\mu g/cm^2/yr$) Anthropogenic Near-Surface	Mean Accumulation Rate ($\mu g/cm^2/yr$) Anthropogenic Corrected to 1980	Total Accumulation Rate* (metric tons/yr) Natural	Total Accumulation Rate* (metric tons/yr) Anthropogenic Near-Surface	Total Accumulation Rate* (metric tons/yr) Anthropogenic Corrected to 1980
As	0.16	0.52	1.0	4.1	13	26
Br	1.18	0.39	0.78	30	10	20
Cd	0.074	0.033	0.064	1.9	0.85	1.9
Cu	0.81	0.36	0.69	21	9.3	17
Hg	7×10^{-4}	32×10^{-4}	61×10^{-4}	0.018	0.083	0.16
Mn	11	-	-	285	-	-
Ni	1.1	0.65	1.3	28	17	34
Pb	1.0	1.4	2.8	25	36	72
Sb	0.011	0.014	0.028	0.28	0.36	0.72
Si	156	117	235	4000	3000	6100
Sn	0.012	0.068	0.14	0.31	1.8	3.6
Zn	1.8	1.9	3.7	47	49	96

* Mean accumulation rate x area of the Goderich Basin.

TABLE 47. ACCUMULATION RATES OF ENRICHED ELEMENTS IN SOUTHERN LAKE HURON

	Mean Accumulation Rate* ($\mu g/cm^2/yr$)			Total Accumulation Rate (metric tons/yr)		
Element	Natural	Anthropogenic		Natural	Anthropogenic	
		Near-Surface	Corrected to 1980		Near-Surface	Corrected to 1980
As	0.053	0.17	0.32	5.0	16	30
Br	0.39	0.12	0.24	37	11	23
Cd	0.022	0.011	0.022	2.1	1.0	2.1
Cu	0.27	0.12	0.24	26	11	23
Hg	2.3×10^{-4}	10×10^{-4}	20×10^{-4}	0.022	0.10	0.19
Mn	3.6	-	-	350	-	-
Ni	0.36	0.21	0.42	34	20	40
Pb	0.32	0.47	0.94	30	45	89
Sb	0.004	0.005	0.014	0.34	0.44	1.3
Si	53	40	79	5000	3800	7500
Sn	0.004	0.023	0.047	0.38	2.2	4.5
Zn	0.60	0.64	1.3	57	61	120

* Total accumulation/area of southern Lake Huron. Non-depositional areas (sand and glaciolacustrine clay) assigned zero accumulation rates.

TABLE 48. SENSITIVITY OF CALCULATED ANTHROPOGENIC ACCUMULATION RATES* TO VARIATIONS IN THE ESTIMATE OF BACKGROUND CONCENTRATIONS

	Accumulation Rate (μg/cm^2/yr)		
Element	Optimal Background Estimate	20% increment	% change
As	1.0	0.96	4
Br	0.78	0.52	33
Cd	0.064	0.051	20
Cu	0.69	0.55	20
Hg	61×10^{-4}	59×10^{-4}	3
Ni	1.3	1.1	15
Pb	2.8	2.6	7
Sb	0.028	0.024	14
Si	235	180	23
Sn	0.14	0.13	7
Zn	3.7	3.22	13

* Goderich Basin. Note: only values based on the regression analysis were allowed to change. Known background levels were kept fixed.

anthropogenic loadings. Because of the absence of adequate information concerning the extent of contributions from shoreline erosions to the total accumulation of fine-grained sediments, a mass-balance calculation primarily gives information on the magnitude of shoreline erosion inputs. Contributions of particulate matter to the main Lake from municipal and industrial waste discharges calculated as part of the IJC (1977) report are 77,700 kg/day corresponding to a mean lake-wide loading of 0.075 mg/cm^2yr. Tributary inputs contribute about 2.2×10^6 kg/day corresponding to about 2.1 $mg/cm^2/yr$ while atmospheric inputs contribute about 0.55 $mg/cm^2/yr$. The combined inputs from the Lakes Michigan and Superior and from Georgian Bay amount to approximately 0.42 $mg/cm^2/yr$ while the outflow of suspended matter through the St. Clair River is about 0.53 $mg/cm^2/yr$ (assuming a mean particulate matter concentration of 1 mg/l). Hence the net loading of fine-grained materials from sources other than shoreline erosion is about $0.075 + 2.1 + 0.55 + 0.42 - 0.53 = 2.6$ $mg/cm^2/yr$. Comparison of this value with the mean accumulation rate, of 10 $mg/cm^2/yr$ indicates the relative importance of shoreline erosion as a source of fine-grained sediments. Roughly 2/3 of the material in the depositional basins are apparently derived from this source which remains to be adequately characterized.

Sodium -- An understanding of the difficulties in comparing the sedimentary accumulation data for natural components may be gained by considering the case of sodium. For Na2, neutron activation analysis sodium, the analytical method is interference-free and values represent the whole-sediment concentrations of the element. The total deposition in the southern part of the lake is about 3000 metric tons per year corresponding to a mean accumulation rate of about 0.9 $mg/cm^2/yr$ over the main lake area. This accumulation rate cannot be reproduced or even approximated by considering sodium inputs and outputs from the lake because most reported sodium values refer to dissolved sodium or, at best, to total sodium for which that contained in the particulate fraction is only a small part. The total loading of sodium to the lake is approximately equal to the mean concentration of total sodium in the lake water times the outflow of the St. Clair river or 1.6 mg/cm^2 of main lake area per year. Thus the mean accumulation of Na2 is only 0.09/1.6=6% of the total loss of sodium from the lake per year. Since Na2 is essentially a label of the fine-grained particulate fraction, the proper comparison is with concentrations of Na exclusively in the suspended solids fraction of lake loadings but these data are not yet available.

Calcium -- Another example of the difficulties in developing a mass-balance for non-anthropogenic constituents may be seen in considering the element calcium. Like sodium, calcium is primarily a conservative element in the lake and particulate calcium (neglecting authigenic $CaCO_3$ formation) is a minor fraction of the total calcium in the lake water. The estimated rate of loss of calcium from the lake is about 14 $mg/cm^2/yr$ whereas the rate of calcium accumulation in southern Lake Huron is only 0.44 $mg/cm^2/yr$. From the previous discussion it is clear that in southern Lake Huron (at least in the Goderich Basin) most of the calcium in sediments is derived from local erosion of shoreline material rich in dolomite. Hence for this element a lake-wide inventory of the particulate calcium loading would still not accurately reflect the accumulation in the Goderich Basin. A proper mass balance for this element could be constructed only if the extent of shoreline erosion were accurately known and in a fairly detailed way since the hydrodynamics of dolomitic materials (silt-size particles) is such that sedimentary dolomite tends to be locally-derived. Based on analysis of the calcium family elements (Ca, Mg and IOC), the annual rate of deposition of dolomite ($CaMg(CO_3)_2$) in southern Lake Huron is about 200,000 metric tons per year. This value could be usefully compared with the composition and rate of erosion of material from the Canadian shoreline adjacent to the Goderich Basin.

A comparison of the trace element composition of materials eroded from the Canadian shoreline generally is compared with the composition of dolomitic sediments collected for this report in Table 49. Values reported by the IJC (1977) do not include major constituents so it is impossible to tell whether the eroded materials are primarily dolomitic or not. However the minor element composition reported by IJC generally agrees with that found for sediments containing over 35% dolomite by weight.

Phosphorus -- According to the IJC report (1977), the total loading of total phosphorus to the main lake is 3720 tonnes per year while the amount lost by outflow was calculated to be 1080 tonnes per year. If the inventory of phosphorus is not increasing in the lake, the difference between these values which is 2640 tonnes must be deposited each year. This latter value corresponds to a mean accumulation rate of 0.006 mg $P/cm^2/yr$ on a lake-wide basis. This value is approximately 40% of the total, acid-soluble P, found to accumulate in the southern part of the Lake which is 0.015 mg $P/cm^2/yr$. Thus removal of phosphorus from the water via sedimentation is consistent with measured rates of acid-soluble phosphorus accumulation in this part of the lake. Further refinements of the comparison would necessitate careful identification of sedimentary phosphorus constituents perhaps via chemical separation techniques such as those employed by Williams et al. (1976).

Silicon -- Comparison of the accumulation rates of silicon with mass balance calculations is particularly intriguing. According to the IJC report (1977), there is a net annual increase in soluble reactive silica (SiO_2) of 183,000 tonnes in the main lake. This increase corresponds to a value of 200 micrograms $Si/cm^2/yr$ which is quite close to that expected as the anthropogenic plus natural (total) mean accumulation rate of amorphous silicon in southern Lake Huron (1980). The computed total from Table 47 for the natural plus anthropogenic mean accumulation rate is 53+79=132 micrograms $Si/cm^2/yr$. Such agreement would be expected if the dissolved reactive silicon in the lake is converted to the particulate form (either as diatoms or as other forms of amorphous silicon) and removed permanently from the water column. Because of the many uncertainties in the calculation the close agreement may be accidental. If not, that data suggest that the increases seen toward the sediment-water interface in the concentration of amorphous silicon in the cores examined for this report, may reflect the increased rate of conversion of soluble silicon to particulate form in the lake as a result of the stimulation of diatom growth by phosphorus additions. Note that the most satisfactory agreement between the net loading of soluble reactive silicon to the lake and the mean accumulation rate is obtained by adding the anthropogenic component to background levels. The favorable comparison

TABLE 49. COMPARISON OF THE COMPOSITION OF DOLOMITE SEDIMENTS WITH THE COMPOSITION OF CANADIAN LAKE HURON SHORELINE MATERIALS

Major Elements (wt %)	Dolomitic Sediments[a]	Shoreline Material IJC (1977)
Ca	7.5 ± 1.0	-
Fe	0.96 ± 0.2	-
K	0.18 ± 0.06	-
Mg	5.0 ± 0.3	-
Mn	0.024 ± 0.01	-
Nal	0.11	-
P	0.11 ± 0.04	-
Minor Elements (μg/g)		
As	-	3.1 ± 4
Cd	-	1.3 ± 0.5
Co	-	11 ± 6
Cr	23 ± 5	25 ± 23
Cu	12 ± 6	19 ± 50
Hg	0.05	0.025 ± 0.02
Mo	-	3.1 ± 3
Ni	20 ± 5	15 ± 9
Pb	36 ± 6	17 ± 12
Sr	49	183 ± 50
V	-	38 ± 20
Zn	35 ± 10	30 ± 26

[a] Dolomite ≥ 35% by weight, mean of 4 cores.

further suggests that the result of increased conversion of silicon to particulate form has on the average enhanced the accumulation rate of amorphous Si by 79/53=1.49 or about 50% since the onset of such changes. Were it not for the possibility, if not likelihood, that silicon undergoes significant dissolution in the sediments, this result would in turn imply corresponding changes in the water column. The alternative explanation for observed amorphous Si profiles, and one offered by Parker and Edgington (1976), is that they result from steady-state postdepositional dissolution of diatoms and possibly another amorphous materials and do not reflect changes in the diatom productivity of overlying waters. The truth may well lie between these extreme possibilities and further discussion is provided below in connection with an examination of profiles of dissolved silicon in selected cores.

In considering the mean accumulation rate of anthropogenic trace constituents, several features are apparent on inspection of Table 50. First, direct municipal/industrial runoff does not contribute significantly to anthropogenic element accumulation rates. Second, tributary inputs generally far exceed anthropogenic accumulation rates. This is likely to be due to a combination of effects. Both natural and anthropogenic components are typically present in tributary water samples and are lumped together in reporting concentration values. In addition, as noted before, concentrations refer to both soluble plus some fraction of the particular matter present depending on the sampling and analytical methods. As the form and amount of the anthropogenic components are not distinguished in reporting tributary loadings, it is difficult to properly compare such loadings with anthropogenic accumulation rates. In the discussion below, the relation between atmospheric inputs and anthropogenic accumulation rates is emphasized It is shown that generally these rates are comparable to the atmospheric loading rates. This result suggests that the anthropogenic loading by tributaries may be relatively unimportant for many elements considered. It should also be noted that even for a background-free contaminant like cesium-137 whose inputs to the Great Lakes are relatively well-known, there are factor of two discrepancies between the amount stored in sediments in the southern part of the lake and the time-integrated loading (see Table 35 above). Because of the many approximations inherent in making comparisons between anthropogenic accumulation rates in sediments and existing loading data, a factor of two agreements may be considered as a satisfactory comparison at this point.

Arsenic -- Information on atmospheric contributions of arsenic to the lakes is sparse. Zinc-normalized values obtained from the data of Gatz (1975) indicate a characteristic deposition rate of around 0.046 micrograms per cm^2/yr. To the degree that any valid comparison can be made with sediment accumulation data, indications are that atmospheric deposition cannot account for anthropogenic loadings to the sediments, which for southern Lake Huron are about 0.32 micrograms/cm^2/yr. Municipal and industrial runoff to the main lake also cannot account for the inferred accumulation rate. In contrast, tributary inputs (0.73 micrograms/cm^2/yr) are sufficient but as indicated above, there are problems with the tributary data as to how much of the element is in the soluble phase initially, how much is anthropogenic, and how much may be converted to particulate form or

TABLE 50. COMPARISON OF MEAN ANTHROPOGENIC ELEMENT ACCUMULATION RATES IN SOUTHERN LAKE HURON WITH VARIOUS MAIN-LAKE LOADING ESTIMATES[a] ($\mu g/cm^2/yr$)

	Mean Anthropogenic Accumulation Rate in Southern Lake Huron		Municipal & Industrial Runoff	Tributary Inputs	Atmospheric Inputs			
Element	This study[b]	Kemp & Thomas[c] (1976)	IJC (1977)	IJC (1977)	Lake Huron IJC (1977)	Lake Ontario Shiomi & Kuntz (1973)[d]	Lake Michigan Gatz (1975)[e]	Lake Michigan Fingleton & Robbins (1980)[e]
As	0.32	-	0.005	0.73	-	-	0.046	-
Br	0.24	-	-	-	-	-	-	0.50
Cd	0.022	0.01	0.002	1.2	0.12	0.085	0.045	-
Cu	0.24	0.56	0.02	2.1	1.1	0.42	0.59	0.21
Hg	0.002	0.002	0.0002	0.007	-	-	-	0.001
Ni	0.42	-	0.017	2.2	0.31	0.22	0.15	-
Pb	0.94	1.7	0.013	1.8	1.2	1.4	2.6	-
Sb	0.014	-	-	-	-	-	-	0.012
Si	79	-	-	-	-	-	-	-
Sn	0.047	-	-	-	-	-	-	-
Zn	1.3	2.2	0.26	2.0	-	5.2	1.3	1.3

[a] Whole lake loadings are expressed in terms of element weight per unit area of the main lake (excluding Saginaw and Georgian Bay).

[b] Values corrected to 1980 (18% increase since 1975) and based on approximately 60 cores.

[c] Values based on a single core from the Goderich Basin.

[d] Bulk precipitation measurements.

[e] Based on emissions inventories, and over-water sampling. Values are arbitrarily normalized to the observed value of the zinc accumulation rate for comparison.

become associated with particulate matter in the lake. Because of analytical uncertainties associated with determination of this element and the limited number of observations, the mean anthropogenic accumulation rate reported here should be regarded as very approximate.

Bromine -- Like arsenic there are limited observations of bromine, especially in underlying sediments and anthropogenic accumulation rates are very approximate. The limited data on atmospheric inputs derived on the basis of zinc normalization of the over-lake (Michigan) sampling of particulate matter by Fingleton and Robbins (1980), the rate of deposition of bromine is about 0.5 micrograms/cm^2/yr. This value is quite comparable to the calculated accumulation rate (0.24 micrograms/cm^2/yr) in southern Lake Huron. In continental air nearly all bromine as well as lead at the present time, originates from the combustion of leaded fuel additives which contain, among other ingredients, ethylene dibromide (cf. Robbins and Snitz, 1972). The ratio of bromine to lead in TEL Motor Mix (Ethyl Fluid) is 0.39 which compares very well with the mean ratio of Br to Pb observed in continental air. Fordyce (1975) reported a mean Br/Pb ratio in air sampled in Cleveland, Ohio for an entire year of 0.31. The ratio of mean anthropogenic accumulation rate of Br to that of Pb in southern Lake Huron is 0.24/0.94=0.26. Thus the mean rate of accumulation of bromine is consistent with the data for lead and indicates combustion of fuel additives as the primary source.

Cadmium -- Reported tributary loadings (IJC, 1977) exceed the anthropogenic accumulation rate by more than a factor of 50. For other elements, the contrast between tributary loads and anthropogenic accumulation rates is not nearly as pronounced, being generally a factor of 2 to 9. As cadmium is not found to any great degree in the soluble phase in natural waters, it is surprising that the values are so far apart. The atmospheric inputs are much closer to the mean anthropogenic accumulation rate of cadmium but both the IJC values and those reported for Lake Ontario (Shiomi and Kuntz, 1973) are still about a factor of four higher. The most consistent comparison is with the zinc-renormalized data of Gatz (1975).

Copper -- Values reported for atmospheric inputs by IJC (1977) are appreciably higher than the observed anthropogenic accumulation rate. In contrast, values derived from the three other studies are very consistent with the measured accumulation rate.

Mercury -- The measured accumulation rate of mercury 0.002 micrograms/cm^2/yr is consistent with the zinc-renormalized data of Fingleton and Robbins (1980) of 0.001 microgram/cm^2/yr. The values reported by Fingleton and Robbins, however, could well be low because significant amounts of Hg may be in the vapor phase and not collected by their sampling method.

Nickel -- The mean anthropogenic accumulation rate of nickel, 0.42 micrograms/cm^2/yr, is quite consistent with values derived from three studies including the IJC report.

Lead -- It is known that much of the lead entering the Great Lakes comes from atmospheric deposition. Therefore, the good agreement between the anthropogenic accumulation rate (0.94 micrograms/cm^2/yr) and several estimates of rates of atmospheric input (1.2, 1.4 and 2.6 micrograms/cm^2/yr) support the idea that the mean anthropogenic accumulation rates for southern Lake Huron are representative of the entire main lake. The rates of anthropogenic lead accumulation found in this study are very comparable to those found in Lake Ontario by Farmer (1978) ranging from 1.2 - 6.7 μg/cm^2/yr and in southern Lake Michigan by Edgington and Robbins (1976) (mean of 1.3 μg/cm^2/yr). Mean anthropogenic rates observed by Nriagu et al. (1979) in Lake Erie are significantly higher. Average accumulation of excess lead in the fine-grained sediments of the Western, Central and Eastern Basins of Lake Erie are 13, 2.5 and 16 μg/cm^2/ yr. The agreement supports the impression that for lead and for other trace contaminant metals, the mean anthropogenic accumulation in sediments is representative primarily of regional atmospheric loading (except possibly Lake Erie). To the extent that trace metal contaminants are atmospherically derived, the results of this study further underscore the importance strong focusing effects occurring on this and other of the Great Lakes. Constituents (including cesium-137 and lead-210 as well) which are deposited for the most part uniformly on the lake surface are eventually stored in very selective areas of the Lake bottom.

Antimony -- There are but very limited comparisons for antimony. The measured anthropogenic accumulation rate (.014 micrograms/cm^2/yr) is in excessively good agreement with the zinc-renormalized data of Fingleton and Robbins (1980), 0.012 micrograms/cm^2/yr.

Tin -- This element has not been previously reported for the Great Lakes and is identified in this report as a contaminant. There are no comparisons with loading data available. Because of the likelihood that tin is subject to methylation and partial remobilization out of sediments into the water column, it would be desirable to develop a better picture of the mass-balance for this element, its chemical forms and potential availability to the biota. The mean anthropogenic accumulate rate of tin in southern Lake Huron is 0.047 micrograms/cm^2/yr, corresponds to an annual total accumulation rate of about 4.5 metric tons per year as of this report date and represents a total sediment inventory of 120 metric tons.

Zinc -- The anthropogenic accumulation rate of zinc is comparable to that of lead. The data of Shiomi and Kuntz (1973) based on bulk precipitation measurements show zinc to have about a four-fold greater loading rate than that of lead. The zinc-renormalized data of Gatz (1975) show the opposite trend with lead loading from the atmosphere being twice as high as that of zinc. It is beyond the scope of this report to consider reasons for these differences in any great detail.

VERTICAL DISTRIBUTION OF DISSOLVED CONSTITUENTS

The vertical distribution of dissolved constituents in selected cores is shown in Figs. 144-153. The vertical distribution data are given in Table A7 of the Appendix. A summary of concentration data and information on concentration gradients is given in Table 51. In the discussion that follows, emphasis is placed on the possible exchange of dissolved species across the sediment-water interface. It is beyond the scope of this report to give much accord to geochemical factors affecting the distribution of dissolved constituents. Diffusional fluxes of solutes across the sediment-water interface are computed as the product of the diffusion coefficient and the concentration gradient at Z = 0, $(dC/dZ)_{Z=0}$. With the exception of Si the gradient is estimated by a linear least squares fit using data points near the sediment-water interface. Approximate values for the diffusion coefficients of ions in free solution are taken from the work of Li and Gregory (1974) unless otherwise indicated. With the exception of Si, the mass-balance calculations below are only approximate.

Barium -- The vertical distribution of barium (Fig. 144) is poorly defined because of the appreciable analytical uncertainties. There are indications in cores such as 18A and 63 of a gradient in concentration around z=0. However, the data are best summarized in terms of a mean pore water concentration (Table 51) which ranges from 0.32 ± 0.20 (ppm) for core 53 to 0.73 ± 0.22 (ppm) for core 63. Concentrations for cores 14A, 18A and 63 are not significantly different and average 0.61 ± 0.2 ppm.

Calcium -- In contrast with the barium data, the profiles of calcium (Fig. 145) are extremely well-defined because of the very low analytical uncertainties. The striking feature of these profiles is the linear increase in concentration with increasing sediment depth in each core. Such profiles may indicate a very slow approach of dissolved calcium toward saturation concentrations. In all of the cores the saturation value is not reached even in the deepest interval sampled. Therefore the values of C_f given in Table 51 are only approximate and probably are a lower limit. The average gradient in each of the cores is obtained from a linear least-squares fit and ranges from 0.16 (53) to 0.47 (63) micrograms/cm^4. Gradients at the sediment-water interface are essentially the same as the average in the cores. For a molecular diffusion coefficient of around (5×10^{-6} cm^2/sec or about 160 cm^2/yr) these gradients imply an outward flux at z=0 of about 25 to 75 micrograms Ca/cm^2/year.

Iron -- Profiles of dissolved iron (Fig. 146) increase greatly with increasing sediment depth in three of the four cores. In core 53 there is essentially no significant change with depth below 3 cm. Iron concentrations in this core remain constant and low. This core is collected from a low sedimentation area where sediments are perhaps less anoxic. In cores 53 and 63, concentrations reach undetectable limits appreciably below the sediment-water interface. Thus there is no appreciable gradient of dissolved Fe at z=0 for these two cores and the diffusional flux is essentially zero. If the profiles are steady-state, the existence of the large gradient in these two cores below the sediment-water interface implies the build-up of

TABLE 51. A SUMMARY OF PORE WATER CONCENTRATION DATA

		Concentration (μg/ml)			Gradient ($\mu g/cm^4$)	
Element	Core	$\bar{C}$	C_0	C_f	z=0	Average
Barium	14	0.61 ± 0.15	-	-	-	-
	18	0.50 ± 0.21	-	-	-	-
	53	0.32 ± 0.20	-	-	-	-
	63	0.73 ± 0.22	-	-	-	-
Calcium	14	-	26.2	~50	0.34	0.34
	18	-	26.2	~47	0.30	0.30
	53	-	27.2	~40	0.16	0.16
	63	-	~26	~55	0.47	0.47
Iron	14	-	<0.01	24	1.3	0.47
	18	-	<0.01	~11	1.9	0.34
	53	-	<0.01	~ 0.2	0	0
	63	-	<0.01	~11	~0	0.31
Magnesium	14	-	7.6	14.5	2.5	0.10
	18	-	7.2	11.8	4.0	0.12
	53	-	7.6	11.3	0.7	0.073
	63	-	7.5	~13.3	-	0.16
Manganese	14	-	<0.01	3.6	0.69	-
	18	-	<0.01	1.4	~0.7	-
	53	-	<0.01	0.24	0	-
	63	-	<0.01	1.6	~0	-
Phosphate (soluble reactive)	14	-	-	-	0.5	-
	18	-	-	-	0.6	-
	53	-	-	-	0	-
	63	-	-	-	0.8	-
Potassium	14	-	6.86	1.6	~0.44	-
	18	-	0.84	1.3	~0.8	-
	53	-	0.82	1.2	~0.3	-
	63	-	0.87	1.3	0.06	-
Silicon (soluble reactive)	14	-	0.96	19.2 ± 1.0	3.6	-
	18	-	0.97	18.0 ± 1.0	5.9	-
	53	-	0.94	9.0 ± 0.7	3.4	-
	63	-	1.1	17.2 ± 0.5	4.2	-

(continued).

$\bar{C}$ = the mean ± sd for elements with no significant gradients, C_0 = concentration in overlying water, C_f = mean concentration in deep sediments for sediments with significant gradients around z=0 or elsewhere.

TABLE 51. (continued).

Element	Core	Concentration (μg/ml) $\overline{C}$	C_0	C_f	Gradient (μg/cm^4) z=0	Average
Sodium	14	3.3 ± 0.4	-	-	-	-
	18	2.7 ± 0.2	-	-	-	-
	53	3.7 ± 0.3	-	-	-	-
	63	3.5 ± 0.5	-	-	-	-
Strontium	14	0.13 ± 0.02	-	-	-	-
	18	0.13 ± 0.01	-	-	-	-
	53	0.14 ± 0.01	-	-	-	-
	63	0.15 ± 0.01	-	-	-	-

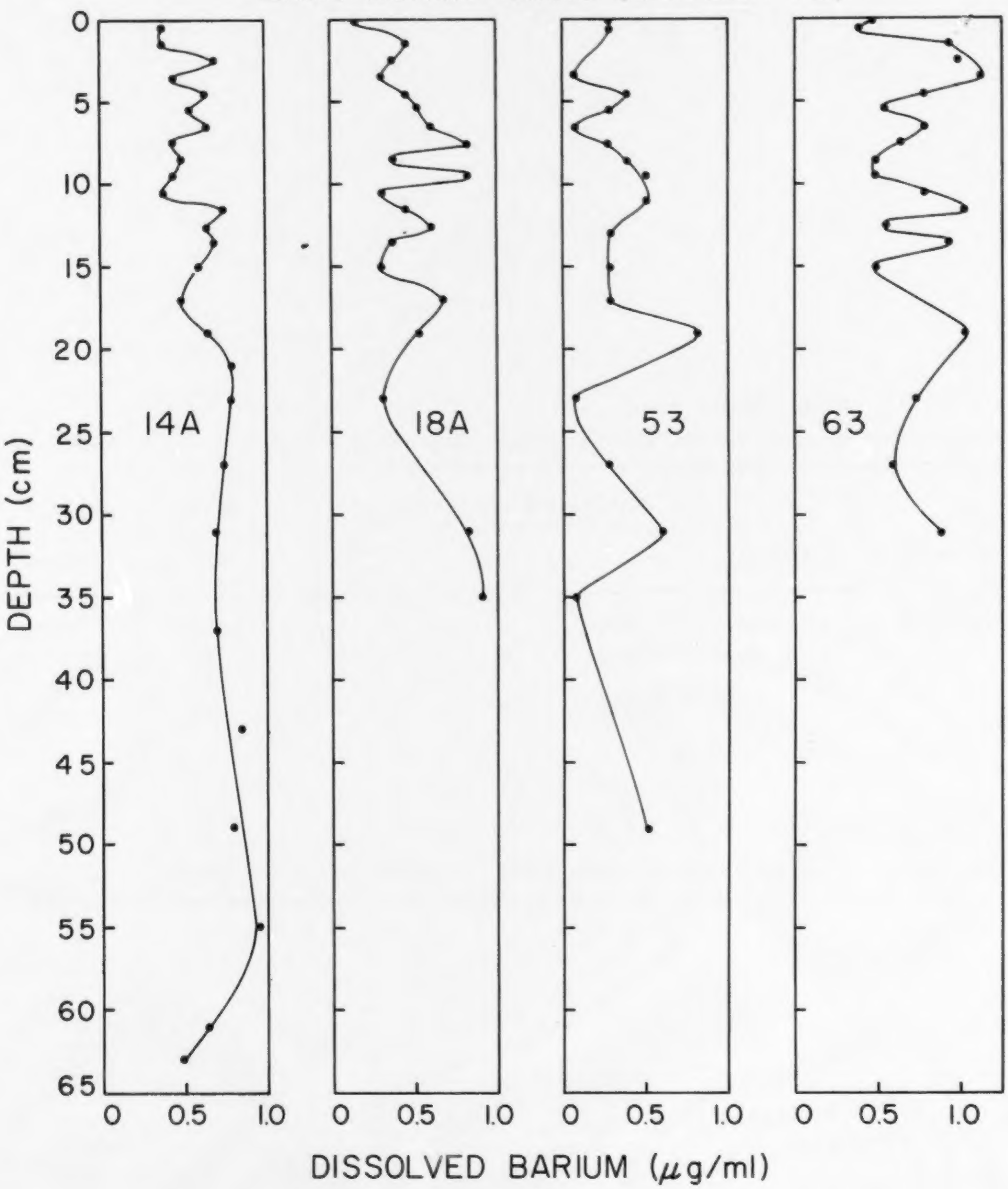

Figure 144. Vertical distribution of dissolved barium in selected cores.

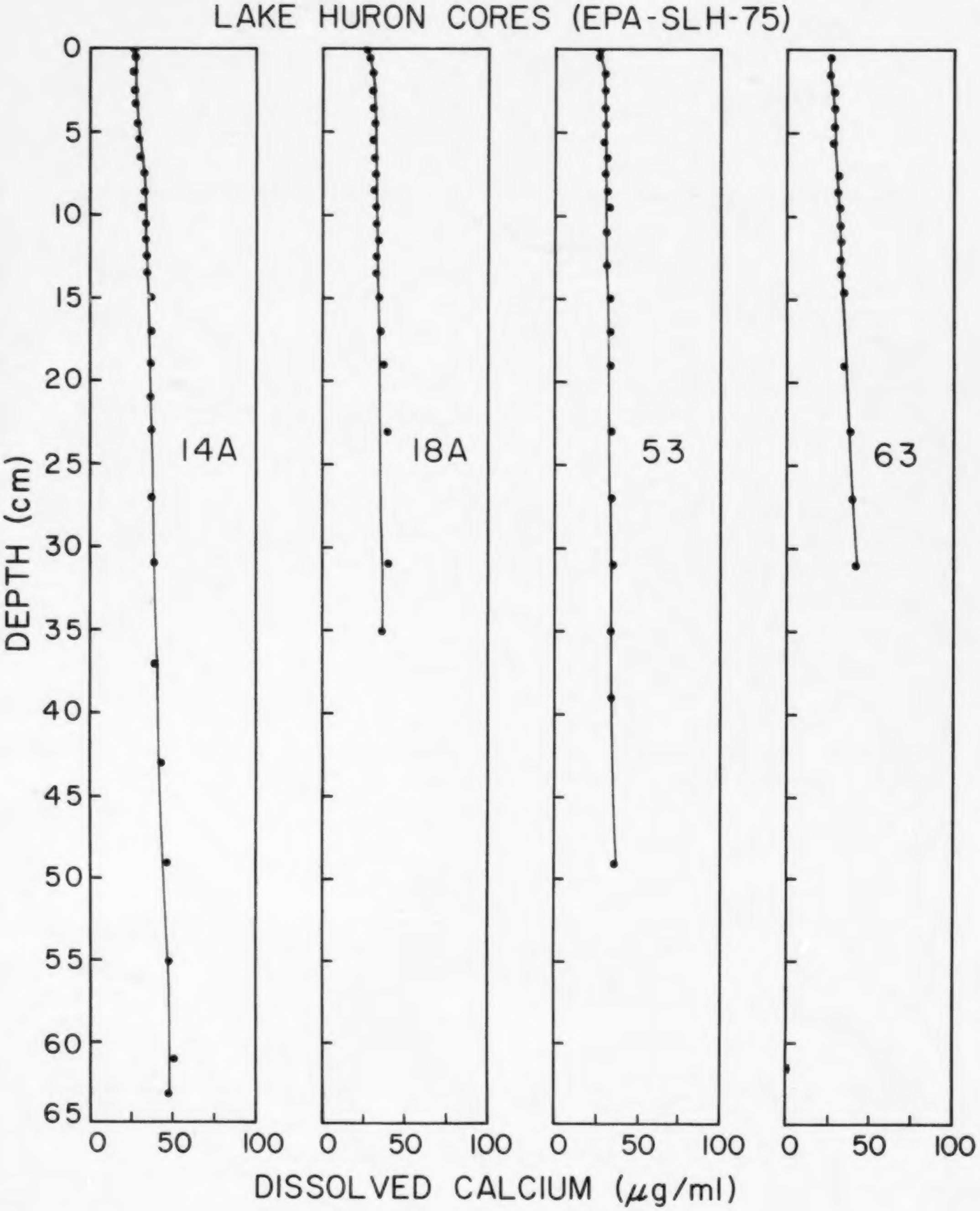

Figure 145. Vertical distribution of dissolved calcium in selected cores:

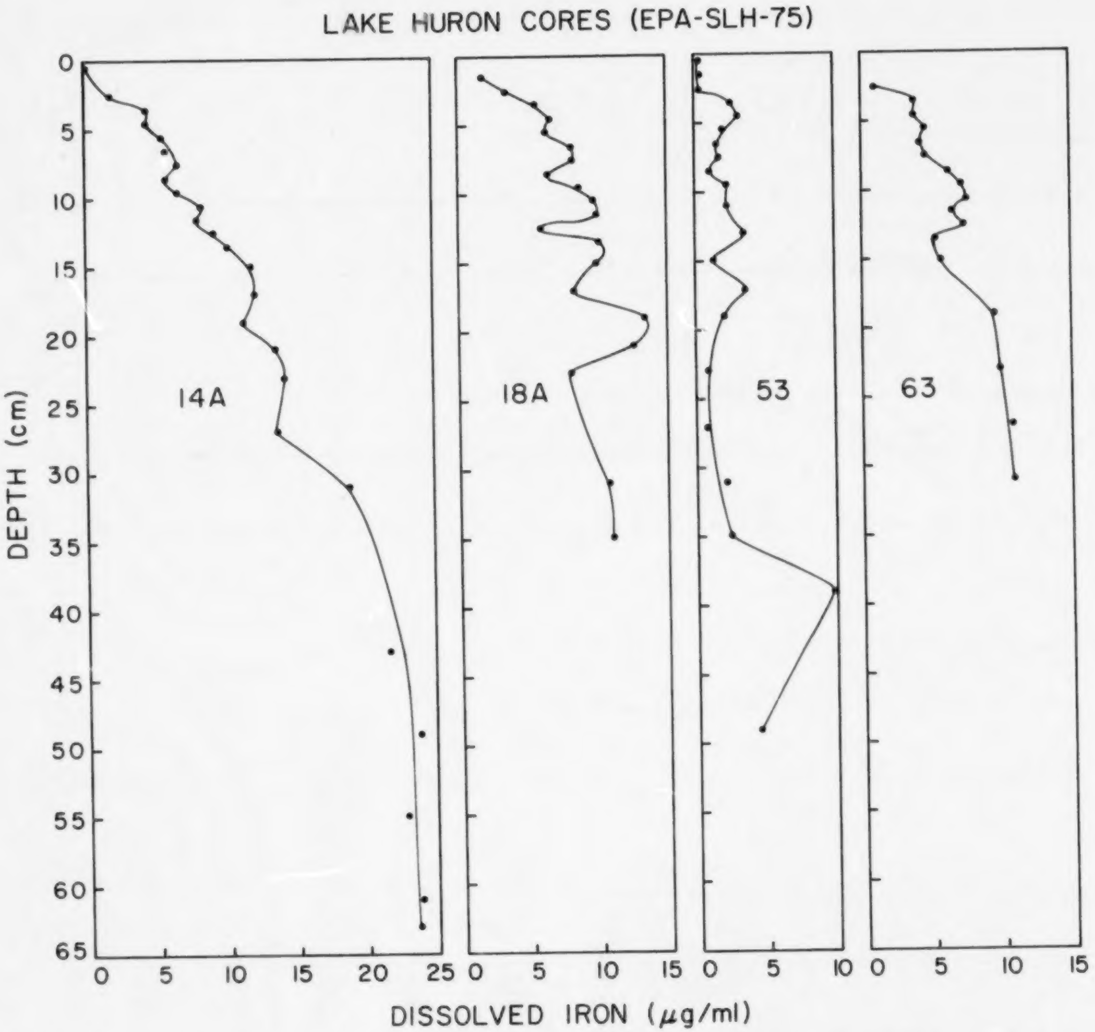

Figure 146. Vertical distribution of dissolved iron in selected cores.

iron in the solid phase in the same region. In cores 14A and 18A, concentrations approach the limits of detection at z=0 and gradients at this interface at 1.3 and 1.9 micrograms Fe/cm^4 respectively. These gradients imply a flux at the sediment-water interface of about 165 and 240 micrograms Fe/cm^2/yr in cores 14A and 18A respectively, assuming an effective molecular diffusion coefficient of about 4 x 10^{-6} cm^2/sec or 126 cm^2/yr. Because of the sensitivity of dissolved Fe concentrations on sedimentary redox conditions (see Fig. 11), it is likely that much of the dissolved iron transferred through the sediment-water interface is reprecipitated. Therefore, there should be a buildup of iron in near surface sediments. Inspection of Fig. 63 shows that there is a slight increase of Fe in the vicinity of the sediment-water interface which could be due to diagenetic remobilization. In core 18A, for example, the upward flux of 240 micrograms/cm^2/yr may be compared with the "excess" iron accumulation rate. The concentration at the surface is about 3.1 wt % while the average underlying concentration is 2.75±0.22 wt %. The iron enrichment amounts to about 3.1-2.75=0.35 wt % or 0.0035 g/g. As the sedimentation rate in this core is 0.0414 g/cm^2/yr, the steady-state rate of loss of iron on burial of solid phase iron is 0.0035 x 0.0414 = 140 micrograms/Fe cm^2/yr which is comparable (within a factor of two) to that given in the approximate flux calculation. Thus the loss of Fe on burial may be counter-balanced by that supplied to the surface by diffusion, as must be the case if the process of diagenesis is steady-state.

Magnesium -- The vertical profiles of dissolved magnesium (Fig. 147) exhibit a roughly linear increase with sediment depth. Average gradients found by linear least squares analysis, as in the case of calcium, range from 0.073 to 0.16 mirograms/cm^2/yr. In contrast with calcium, there is a significant decrease in the concentration of dissolved magnesium in the vicinity of the sediment-water interface, so that the average gradient does not well-represent the concentration gradient at z=0. Values at the interface are from 10 to 30 times higher at the interface than on average. This feature suggests that the overlying water is undersaturated with respect to certain forms of magnesium occurring in sediments and that, on burial, pore waters rapidly become saturated with respect to such components. In addition to this, there are other components which result in higher saturation levels after very long times. Diffusional fluxes implied by surface gradients range from 112 to 600 micrograms/cm^2/yr for Mg assuming an effective diffusion coefficient of 160 cm^2/yr.

Manganese -- Profiles of dissolved manganese, such as those shown in Fig. 148, have been found in the Great Lakes by Robbins and Callender (1975) and elsewhere by others. As is the case for iron, concentrations of Mn approach undetectable levels in cores 53 and 63 well below the sediment-water interface. In cores 14A and 18A, concentrations approach undetectable levels at the sediment-water interface. In each of these latter cores the gradient at z=0 is about 0.7 micrograms/cm^4, corresponding to a flux of 77 micrograms/cm^2/yr assuming a diffusion coefficient of 110 cm^2/yr. Using core 18A again as an example, the concentration of manganese at the surface is 0.11 wt % while the average concentration of Mn in underlying sediments is 0.0352 ± 0.003 wt %. Hence the net loss of Mn on burial is given by 0.11 - 0.0352 = 0.0748 wt % or 7.48 x 10^{-4} g/g. The rate of loss then is

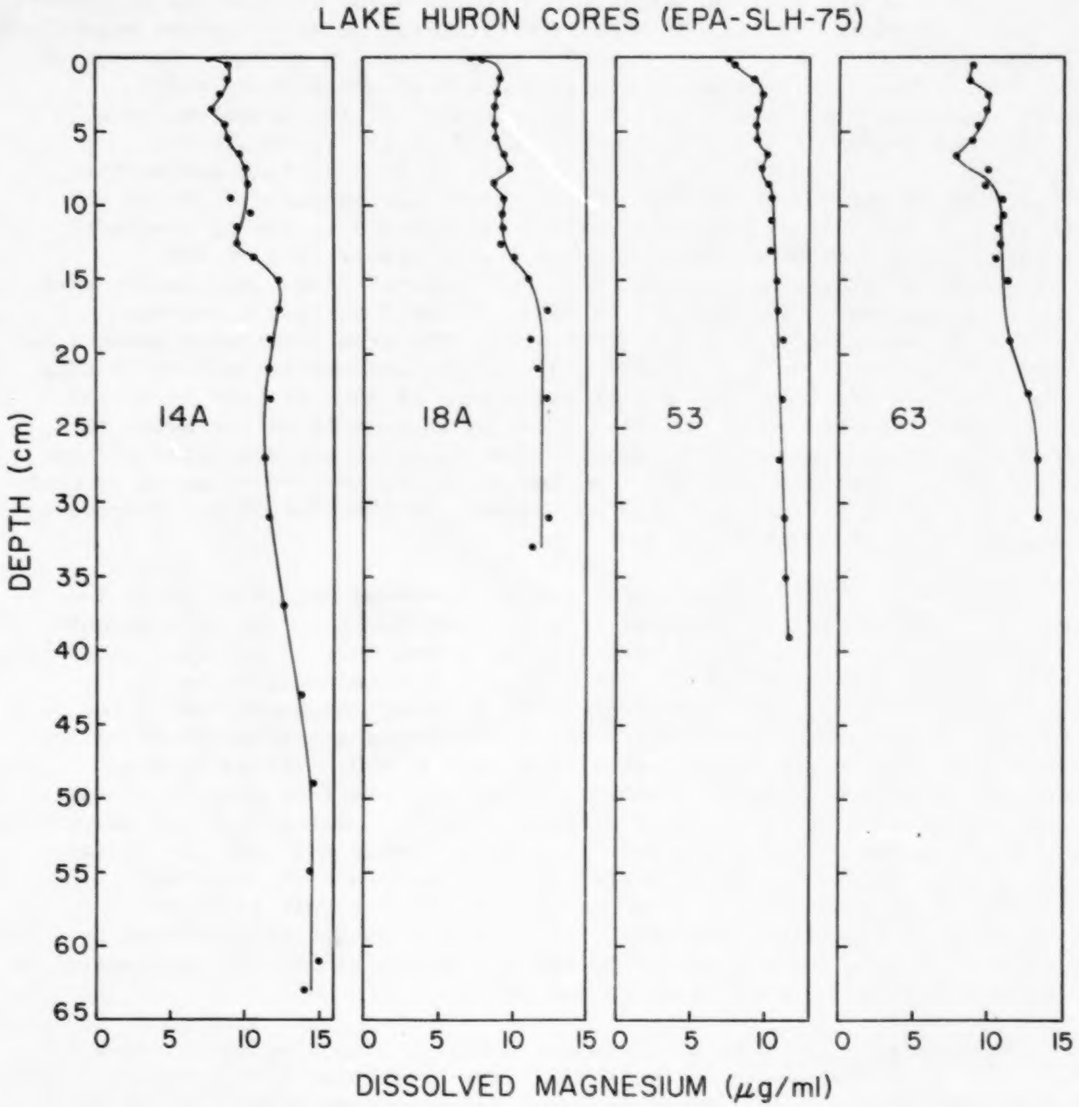

Figure 147. Vertical distribution of dissolved magnesium in selected cores.

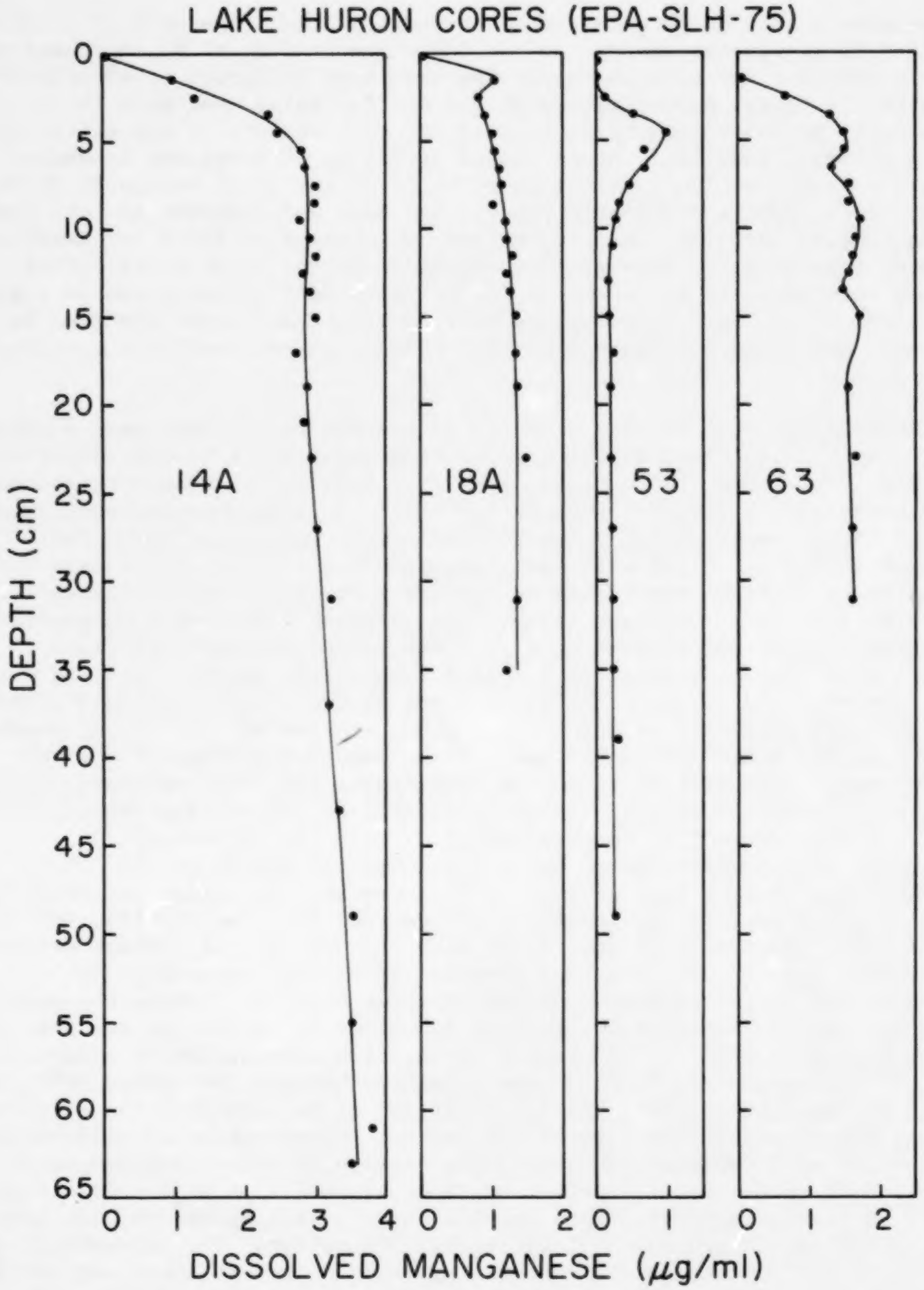

Figure 148. Vertical distribution of dissolved manganese in selected cores.

approximately this difference times the sedimentation rate or $7.48 \times 10^2 \times 0.0414 = 31$ micrograms/cm^2/yr. Since the concentration of Mn increases so rapidly toward $z = 0$ over the upper few cm, it is difficult to accurately estimate the actual concentration at $z = 0$. The value used here is undoubtedly an underestimate as it does not take account of the effect of finite interval sampling. Hence upward diffusion of manganese is essentially (within a factor of 2) counterbalanced by formation of an excess Mn in the solid phase. Such a diagenetic process has been well-documented (cf. Robbins and Callender, 1975) and leads to marked enhancement of Mn in the uppermost sediment layers in the fine-grained sediments of the Great Lakes. This surface enrichment is an invariant feature of intact cores as can be seen from Figs. 67 and 68. That surface enrichments of manganese are seen in virtually all cores attests to the fact that cores recovered are essentially undisturbed.

Phosphorus -- Of all the elements determined in sediment pore waters for this report, phosphorous exhibits an extreme sensitivity to contamination with air. The large fluctuations seen (Fig. 149) in the concentration of soluble reactive phosphate (SRP) versus depth in various cores, particularly 18A and 63, are most probably due to inadvertent contamination of the sediment squeezing system with small amounts of air. For this reason the lowest concentrations should almost certainly be discarded and higher levels should be regarded as minimum values. In contrast with Fe and Mn profiles, concentrations of SRP in each core decrease toward the sediment-water interface but not to undetectable levels. Actual values in overlying water should be essentially undetectable in terms of the analytic methods employed. Concentration gradients in three cores (14A, 18A and 63) are either nearly correct or are lower limits and are 0.5, 0.6 and 0.8 micrograms PO_4/cm^4 respectively. Assuming an effective diffusion coefficient of about 5×10^{-6} cm^2/sec or about 160 cm^2/yr, the apparent flux at the sediment-water interface is about 100 micrograms/cm^2/yr in core 18A (or greater). Inspection of the distribution of acid-soluble phosphorus in the corresponding cores (Fig. 70) shows that there are very small increases in concentrations near the sediment-water interface in cores 14, 18A, and 63 but not in 53. This result is consistent with the presence of surface gradients in all but core 53. The increase seen in 18A is very marginal. The concentration at the surface (0-1 cm) is about 0.267 wt % while the mean concentration in deeper layers is 0.20 ± 0.02 wt %. Hence the net loss of PO_4 on burial is $0.267 - 0.20 = 0.067$ wt % which corresponds to a rate of about 30 micrograms PO_4 cm^2/yr. Not enough to balance the upward diffusional flux. However, the numbers are too uncertain to be sure that the difference in this case is real. In core 63 the surface concentration of acid-soluble PO_4 is 0.33 wt %, whereas the mean concentration in underlying sediments is 0.236 ± 0.04 wt %. Hence, the net PO_4 lost on burial is $0.33 - 0.24 = 0.09$ wt %. As the sedimentation rate in this core is 34.2 mg/cm^2/yr, the loss rate is $0.09 \times 10^4 \times 0.034 = 31$ micrograms PO_4 cm^2/yr. The approximate flux is $0.8 \times 160 = 130$ micrograms/cm^2/yr. Again in this core there may not be enough loss of acid-soluble PO_4 to counter-balance the upward flux. The same result applies to core 14. Thus the indications are that although some phosphorus may be involved in diagenetic cycling, a significant amount may be contributed to overlying water as a result of interstitial diffusion. It should be emphasized that this indication is based on the assumption of

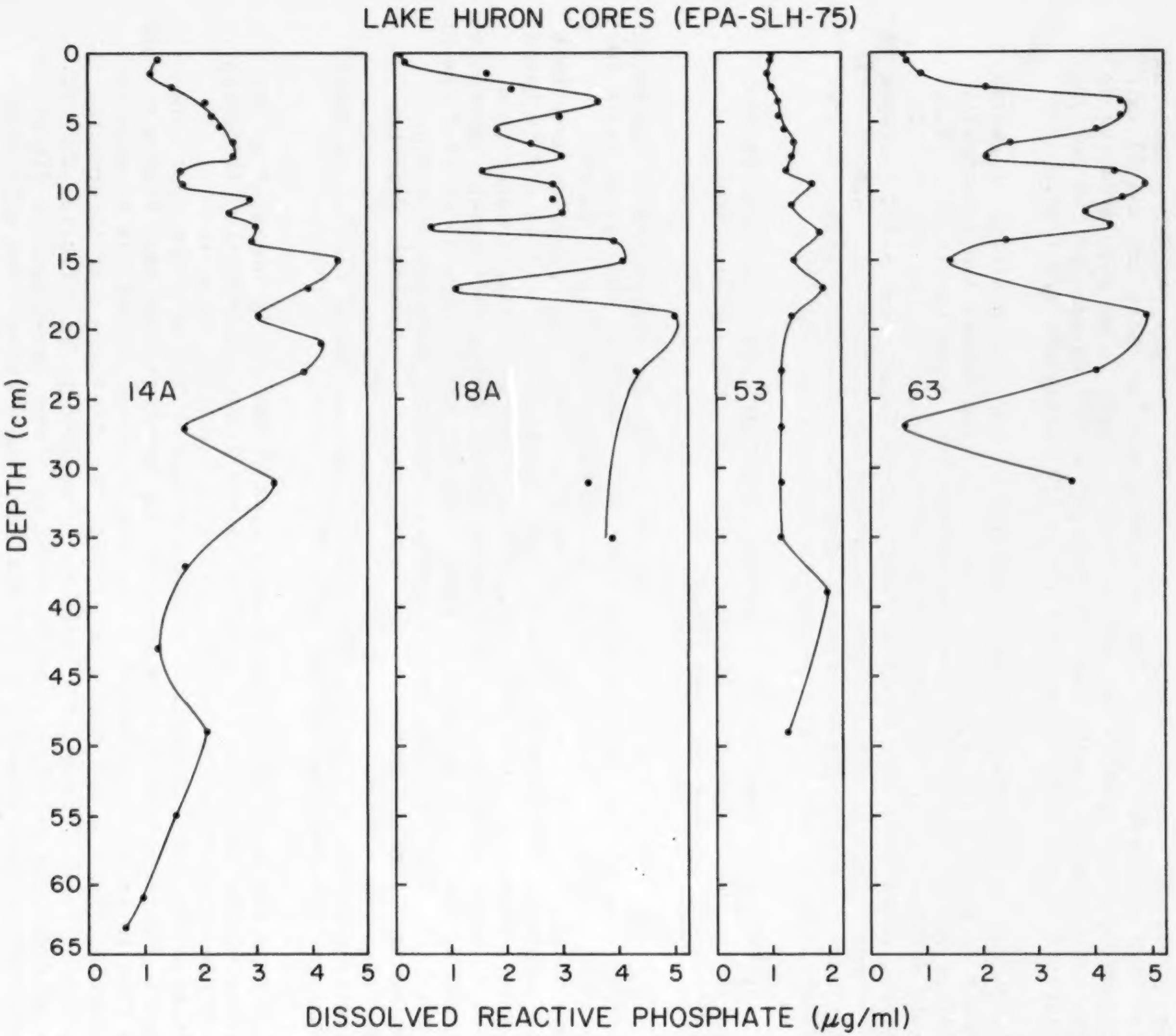

Figure 149. Vertical distribution of dissolved reactive phosphate in selected cores.

steady-state conditions and on phosphorus concentrations of very marginal quality.

Potassium -- In all cores there is a two-fold increase in equilibrium concentrations of dissolved potassium over concentrations in overlying water (Fig. 150). In general, equilibrium concentrations are reached within the upper five centimeters of the cores studied and for cores 18A and 53 this increase in concentration is confined to the upper cm or so. Assuming an effective diffusion coefficient of about 10×10^{-6} cm/sec, or 316 cm^2/yr, calculated fluxes range from about 20 to 250 micrograms K/cm^2/yr.

Sodium -- With the possible exception of core 63, profiles of sodium exhibit no significant gradients (Fig. 152). The values are essentially constant and average 3.30 ± 0.4 ppm for the four cores (Table 51). This result contrasts with the observations of Lerman and Weiler (1970). In sediment cores from Lake Ontario these authors found about a 20% increase in the concentration of sodium above background levels near the sediment-water interface. The increase was successfully attributed to increases in the concentration of sodium in Lake Ontario waters since the 1900s.

Strontium -- Profiles of dissolved strontium (Fig. 153) exhibit no significant variations with sediment depth. Concentrations average 0.14 ± 0.0.01 ppm for the four cores.

Silicon -- The data on dissolved and amorphous silicon are of sufficient quality and detail to warrant a more accurate treatment than given above for the other elements. Profiles of dissolved silicon (Fig. 151) exhibit dramatic gradients at the sediment-water interface. Such profiles have been seen before in sediments of Lake Michigan (Robbins et al. 1974) and in Lakes Superior, Erie, and Ontario (Nriagu 1978). Concentrations increase from about 1 ppm Si above $z = 0$ to saturation levels within each core. Saturation concentrations given in Table 51 range from 9.0 ppm in core 53 to 19.2 ppm Si in core 14. Concentration values increase smoothly with sediment depth showing very little scatter. Note that in contrast to soluble reactive phosphate, the concentration of soluble reactive silicon (SRS) is only slightly affected by exposure of sediments and pore water samples to small amounts of air (See Fig. 11 and Table 8).

As stated previously, the outward flux of SRS may be computed as the product of the concentration gradient as $z = 0$ and the effective diffusion coefficient, provided the release of SRS to overlying water is diffusion-limited. Recent direct measurements of the SRS flux from cores suggest that this method of calculation may underestimate real fluxes because the flux is in part determined by surface reactions as well as by transport properties (Robbins and Edgington, 1979). In the absence of information concerning actual fluxes, the exchange is assumed to be diffusion-limited. The gradient, in principle, can be found by linear least squares fit of the concentration data around $z = 0$ if the sampling intervals are sufficiently small. Values based on a linear fit are given in Table 52. However, this method can lead to a significant underestimate of the surface gradient of SRS because the concentrations increase so rapidly just below the sediment-water interface. Anikouchine (1967) and others have shown that for sediments

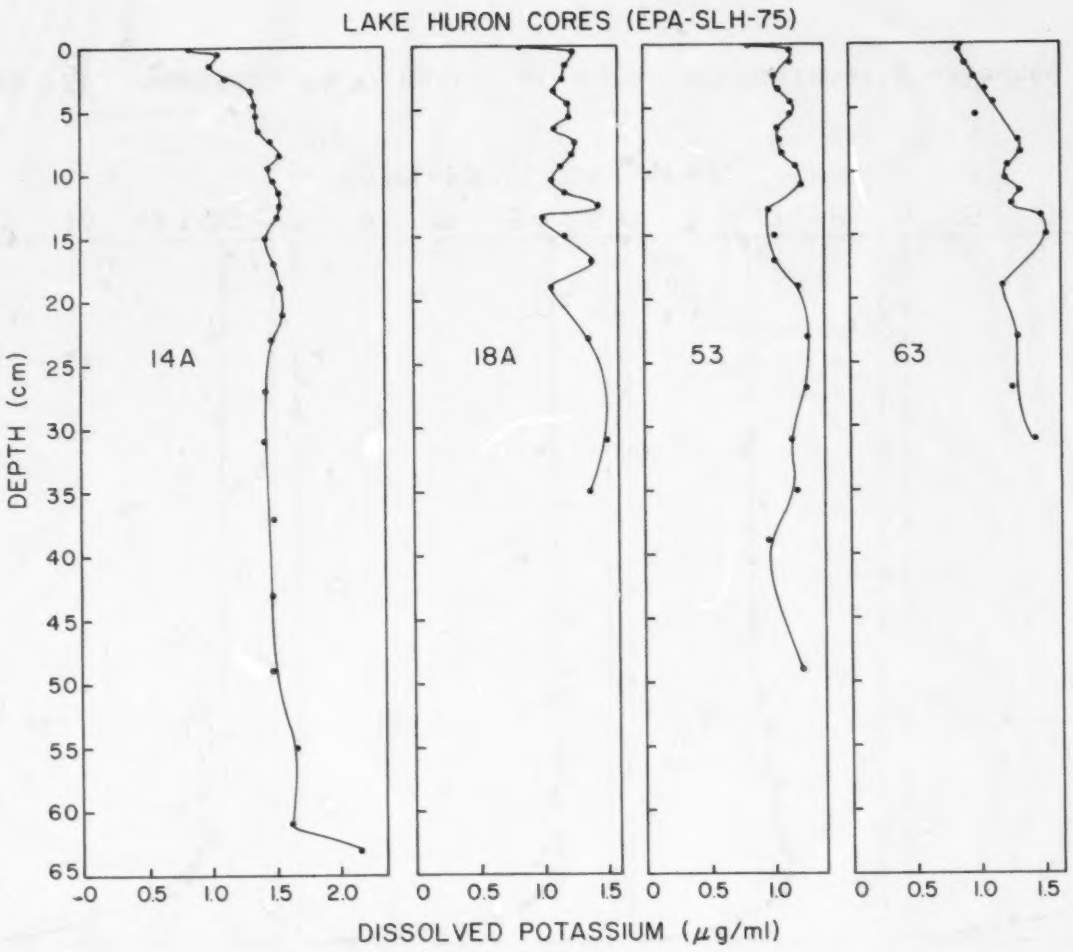

Figure 150. Vertical distribution of dissolved potassium in selected cores.

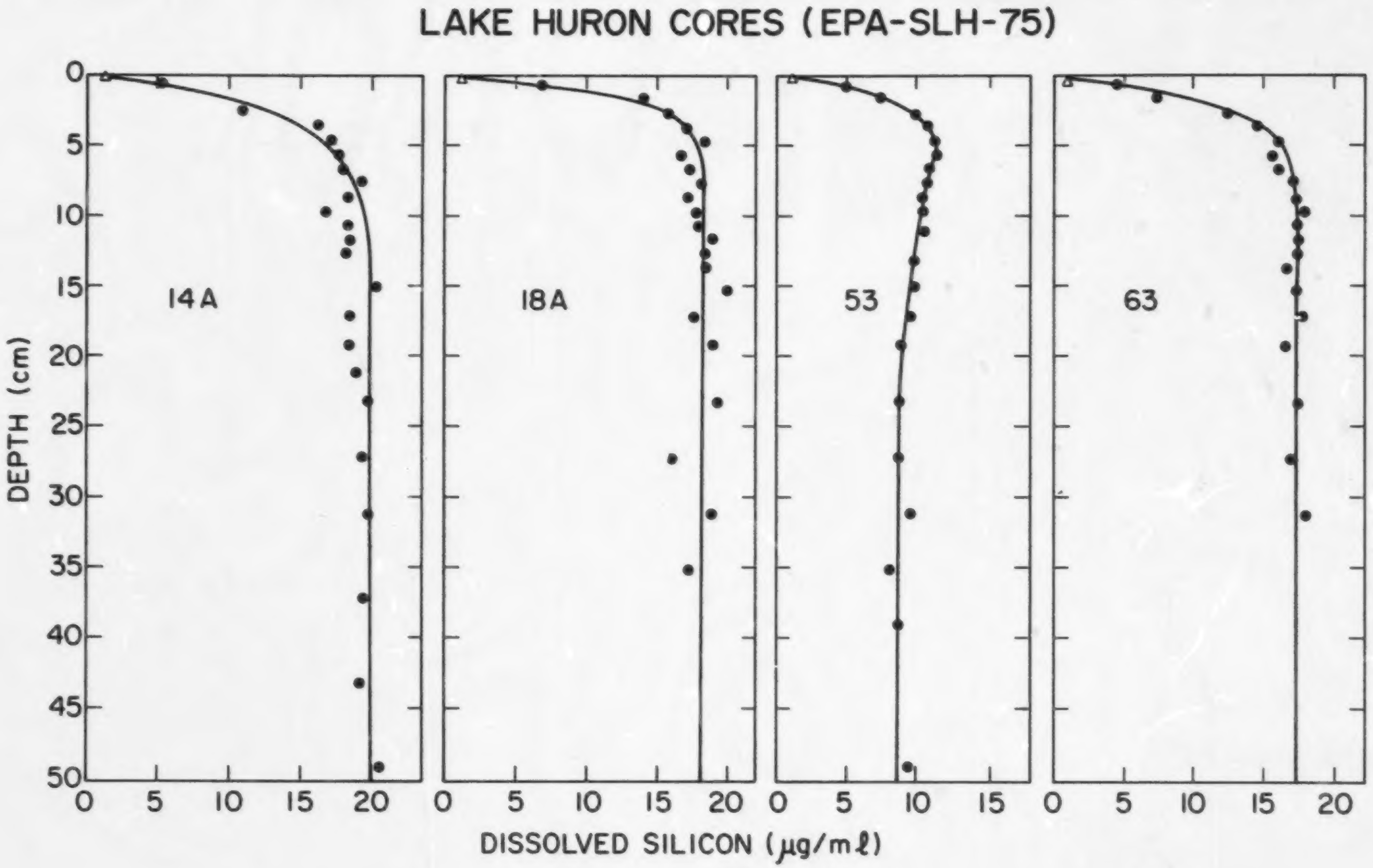

Figure 151. Vertical distribution of dissolved silicon in selected cores.

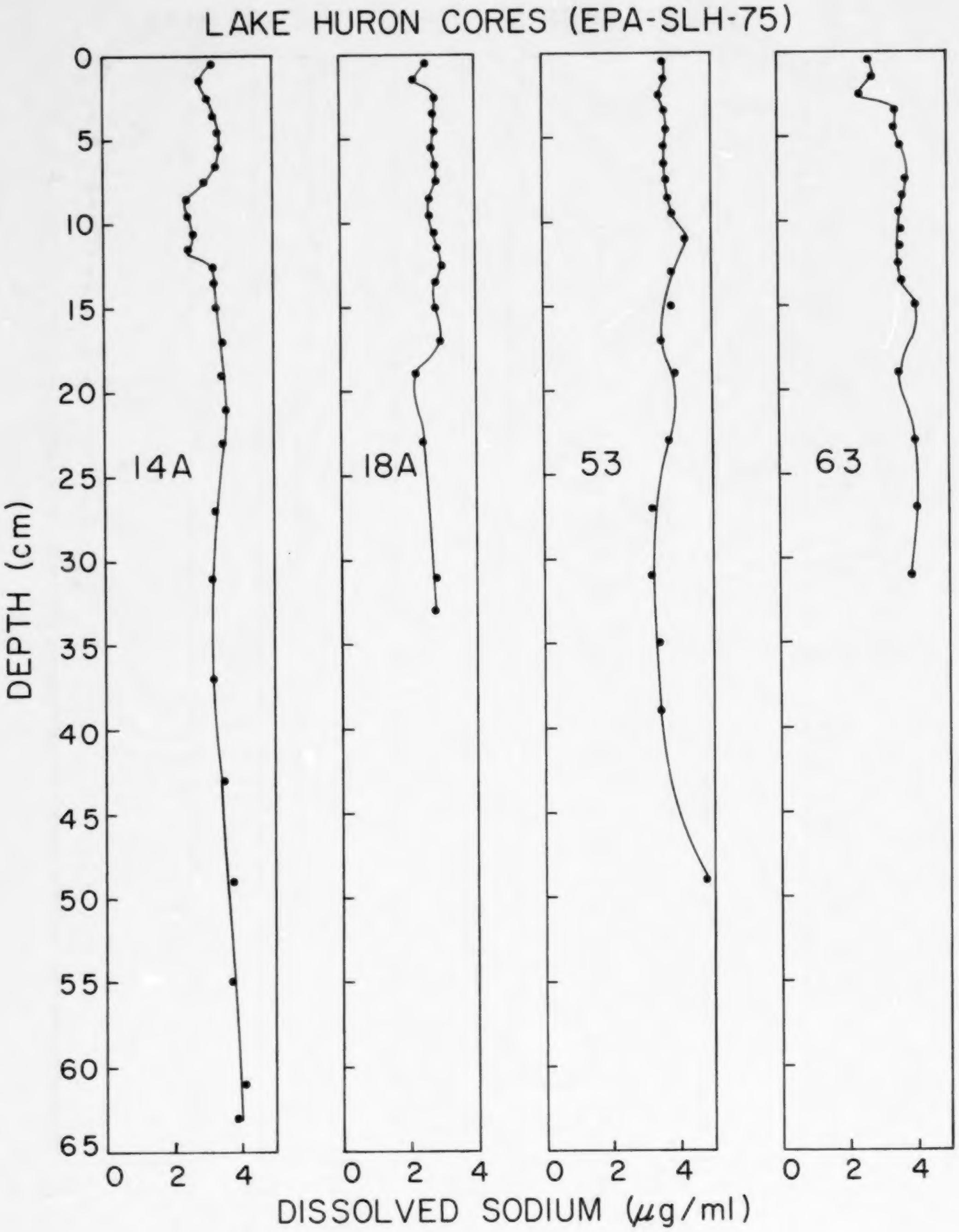

Figure 152. Vertical distribution of dissolved sodium in selected cores.

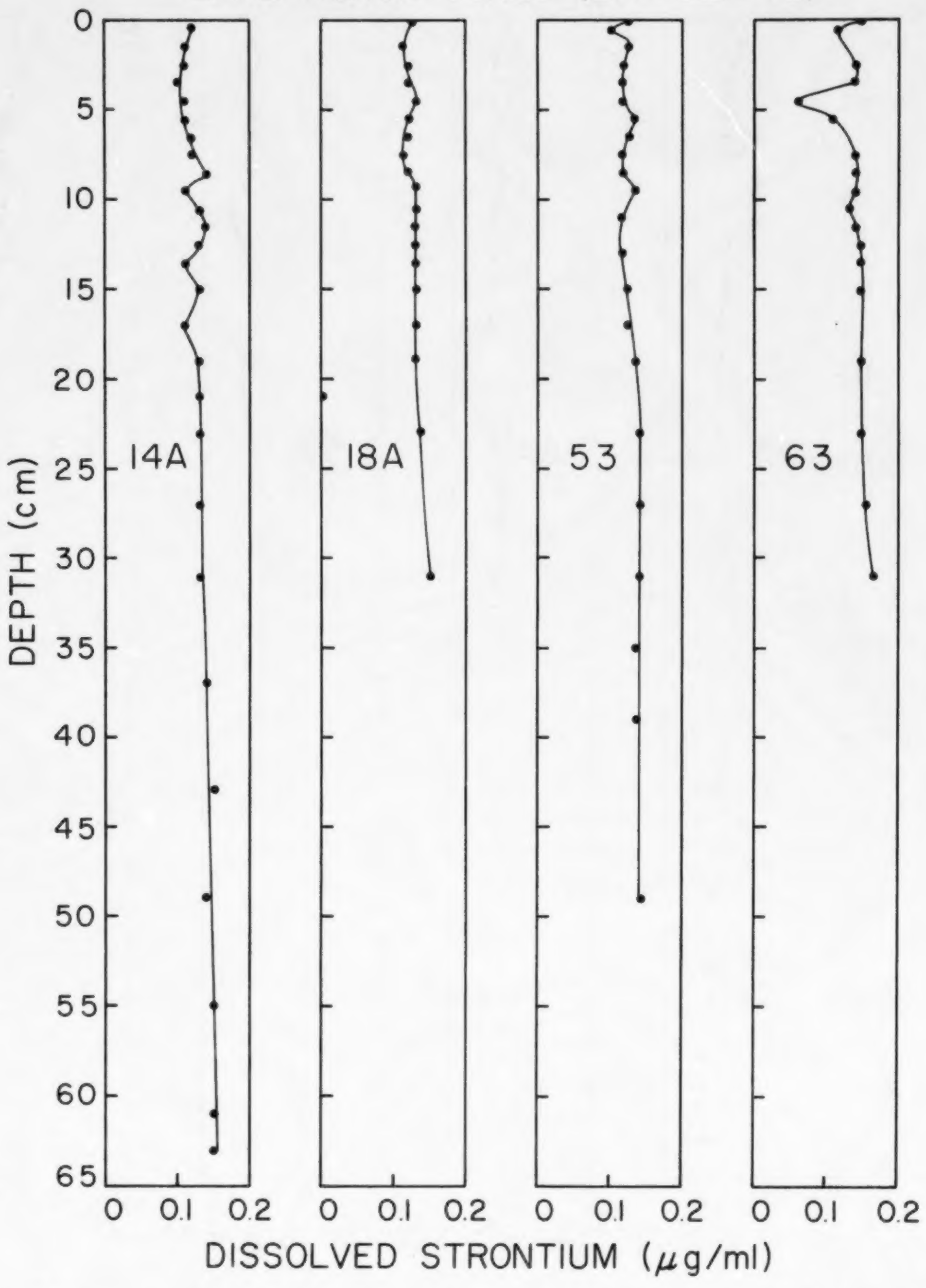

Figure 153. Vertical distribution of dissolved strontium in selected cores.

accumulating at a constant rate with a constant flux of silicon, and the solid phase dissolving according to first order kinetics, the steady-state distribution of SRS is approximately given by

$$D_e \frac{\partial^2 C}{\partial z^2} - k\,(C - C_f) = 0 \qquad (54)$$

where the effects of compaction and advection are neglected. D_e is the effective diffusion coefficient (cm^2/yr), k is the first-order rate constant (yr^{-1}), and C_f is the equilibrium concentration of SRS. Under such conditions the solution to the above equation is

$$C = (C_o - C_f)\,e^{-\beta z}, \qquad \beta \equiv \sqrt{k/D_e} \qquad (55)$$

Thus, even the most elementary model of silicon dissolution indicates that the increase in concentration with sediment depth is not linear but involves an exponential term over any appreciable sediment interval. Inspection of the distribution of amorphous silicon in the cores as well as the SRS profile in core 53 show that the above formalism is not sufficient for describing the overall relations between amorphous and dissolved silicon, but the above equation (55) is adequate for estimating surface gradients. A least squares fit of the above equation, using values of C_0 and C_f given in Table 51 and the first four data points below $z = 0$, gives a estimate of the parameter, β, and a second estimate of the gradient at $z = 0$ for each core is $\beta\,(C_f - C_o)$. The effect of finite sampling may be taken into account by averaging the theoretical profile (Eq. 55). Thus, the predicted of concentration is really the average of the theoretical concentration over the sampling interval or

$$C\,(z1,z2) = \frac{1}{z2-z1} \int_{z1}^{z2} [\,(C_o - C_f)\,e^{-\beta z} + C_f]\,dz \qquad (56)$$

Inclusion of the sampling effect leads to a second estimate of beta, β^*, and the gradient. Each of the estimates is given in Table 52, along with other relevant values.

From values given in Table 52, it can be seen that: (1) provided only the first two points ($z = 0$ and $z = 0$-1 cm) are used in a linear calculation the inferred gradients are generally consistent with those based on a theoretical distribution with inclusion of sampling effects; (2) the inclusion of four points in a linear fit leads to appreciable underestimates of the gradient; and (3) the effect of including sample averaging is to slightly increase the estimated gradient in three of the four cases. The values of the surface SRS gradients are very comparable to those obtained by Nrigau (1978) and Robbins et al. (1974). Re-analysis of Nriagu's Lake Ontario core data in terms of the theoretical profile, plus sample averaging (Eq. 56), shows that the four profiles of SRS in Lake Ontario sediments yield a gradient of 7.1 ± 0.5 $\mu g\ Si/cm^4$. Values in Table 52 range from 5.8 to 15.9 $\mu g\ Si/cm^4$.

TABLE 52. PARAMETERS DERIVED FROM ANALYSIS OF DISSOLVED AND AMORPHOUS SILICON PROFILES

Quantity	Core			
	14A	18A	53	63
Exponent coefficient (cm^{-1})				
β	0.31	0.86	0.66	0.44
β^*	0.32	0.94	0.68	0.42
Gradient at z=0 (μg Si/cm^2/yr)				
linear (two points)	8.4	11.6	7.1	7.0
linear (four points)	3.6	5.9	3.4	4.2
$\beta\ (C_f-C_o)$	5.7	14.6	7.2	7.0
$\beta^*(C_f-C_o)$	5.8	15.9	7.5	6.7
Mean porosity, ϕ	0.93	0.89	0.93	0.92
Apparent diffusion coefficient (cm^2/yr)				
$\phi\ D_e$	130	107	130	124
First order rate constant (yr^{-1})				
k	21	87	55	28
SRS Flux (μg Si/cm^2/yr)				
$F_{\uparrow}$	750	1700	980	830

(continued)

TABLE 52. (continued)

Quantity	Core			
	14A	18A	53	63
Amorphous Si Concentration (wt%)				
mean surface	1.91	1.28	1.13	1.75
mean deep	1.09	0.70	0.60	0.69
net (uncorrected)	0.82	0.58	0.53	1.06
net (corrected)	2.62	1.13	1.47	2.17
Sedimentation rate ($mg/cm^2/yr$)	30	41.4	~11	34.2
Available Si Flux ($\mu g\ Si/cm^2/yr$)				
$F_{\downarrow}$	790	470	160	740

Note: in core 53, C_f = 11.9 μg/ml for estimating the gradient at z=0.

The effective diffusion coefficient for silicon in pore water is not well known and should be measured for sediments of the Great Lakes. Nriagu (1978) adopted the value given by Lerman (1975) of 94.6 cm^2/yr in his treatment of SRS profiles. This value is certainly reasonable. The self-diffusion coefficient of SRS in seawater at 25° C is 1×10^{-5} cm^2/sec (Wollast and Garrels 1971). At the *in situ* temperature of 6° C this value should be about 5.5×10^{-6} cm^2/sec or 173 cm^2/yr (cf Li and Gregory 1974). This value characterizes diffusion in ocean water. In fresh water the diffusion coefficient should be about 5% higher because of a lower viscosity (Li and Gregory 1974) or about 183 cm^2/yr. The effective diffusion coefficient is smaller than that in free solution because of the interference of sediment particles with the movement of ions. While there are no absorption effects under steady-state conditions, there are sediment tortousity effects. The tortuosity is the average ratio of the actual tortuous diffusion path of ions around sediment particles to the straight distance of that path. Hurd (1973) used an empirical relationship derived from measurement with clays between the free solution, D_o, and effective diffusion coefficients, D_e:

$$\log_{10} (D_e/D_o) = 1.65 (\phi -1). \qquad (57)$$

This formula gives an adequate correction for tortuosity effect. ϕ is the sediment porosity which in the present case is around 0.9 in each core near the sediment-water interface. In calculating the flux, a correction must be made (Berner 1975) for the fraction of the area across which solutes diffuse which is not blocked by sediment particles. This fraction is simply ϕ. Thus, the best estimate of the flux if SRS is

$$F_{\uparrow} = 183 \times 10^{1.65\ (\phi-1)} \times \phi \times (dC/dz)_{z=0} \ . \qquad (58)$$

The term ϕD_e corresponds to the value used by Nriagu (1978) and generally is about 13-30% higher than his value. Nriagu did not attempt to adjust the value of D_e for the effects of sediment porosity and tortuosity. Values of ϕD_e are given in Table 52.

Values of the SRS flux (Table 52) range from 750 to 1700 μg $Si/cm^2/yr$. As has been noted by Robbins et al. (1974), Robbins (1976), and Nriagu (1978), if such fluxes are representative of the annual silicon release from sediments of the Great Lakes then regeneration of silicon from sediments is a major process in the cycling of silicon in the water column. The calculated fluxes reported here are very consistent with the values based on direct measurement of releases from eight cores taken in July 1976 from northern Lake Huron by Remmert et al. (1977). These authors report actual fluxes ranging from 1015 to 2050 μg $Si/cm^2/yr$. Their results suggest that measured release rates can be reconciled with values estimated from concentration gradients and thus that the process of exchange may be adequately described in terms of diffusional and advective transport.

In this regard, advective contributions to silicon exchange have been assumed to be small in comparison with diffusional transport in calculating the outward SRS flux above. The advective flux is given approximately by $\bar{\omega}C_o$ and is less than about 0.15 μg/cm^2/yr for each core, (Table 52) and thus indeed may be neglected.

The first-order rate constant, k, is computed from the value of beta. In the above calculations the value of beta was found using only points in the vicinity of the sediment water-interface in order to best infer the concentration gradient at z=0. For purposes of computing the rate constant it is appropriate to use all the data. Values of k given in Table 52 are based on least squares fit of Eq. 56 to all the data. The first-order rate constant is then given by

$$k=\phi D_e \beta^2 \tag{59}$$

Values listed in Table 52 range from 21 to 87 yr^{-1}. Less variation from core to core might be expected if an accurate formalism were used to describe solid phase Si dissolution and solute transport. An appropriate formalism which includes the effect of sediment mixing is provided below. Reanalysis of the SRS profiles in the Lake Ontario cores (Nriagu 1978) yields values of the first-order rate constant ranging from about 11 to 15 yr^{-1}.

Under steady-state conditions the upward flux of SRS is exactly matched by sedimentation of silicon. Comparison of the upward flux with sedimenting silicon is rendered difficult because of at least two important effects: (1) not all of the silicon reaching the sediments is available for dissolution. Therefore a means must be found for isolating or identifying that portion of the total silicon which participates in diagenetic transformations (i.e. available Si) and (2) while the downward flux is given as the product of the mass sedimentation rate and the concentration of available silicon in sedimenting material, this concentration is not necessarily the same as the concentration of available silicon in surface sediments. There are at least two reasons for possible differences: (1) rapid dissolution at and near z=0 causes the concentration of available silicon on incoming material to be different from material actually deposited at z=0 as practically defined and (2) post-depositional movement (such as that due to bioturbation) of sediment solids carrying available silicon can redistribute the initially-deposited silicon downward in the sediment core. In the absence of a unified formalism for these processes, an approximate calculation can be made which at least takes account of mixing. The available silicon may be taken as the concentration of amorphous silicon in surface sediments minus the amount which remains in deeper sediment layers. Because of sediment mixing the concentration at the surface will be reduced over that in initially deposited materials. The effects of mixing may be corrected approximately on the assumption that in the absence of mixing the profile of amorphous Si would be exponential. Thus, the theoretical profile is assumed to have the form

$$C(z)=C_o' e^{-\alpha z} + C_f' \tag{60}$$

where C_o' is the concentration at z=0 and C_f' is the concentration at sufficient depth. The coefficient α can in turn be expressed in terms of an apparent reciprocal life-time, so that α = "λ"/ω, and the correction for the effects of mixing takes the form

$$\frac{\gamma + "\lambda"}{\gamma} = \frac{(\omega/s) + \alpha\omega}{(\omega/s)} = 1 + \alpha s \qquad (61)$$

See Eq. 41 for comparison. The value of alpha is determined graphically from the exponential portion of each amorphous silicon profile. The downward flux of available silicon, $F\downarrow$, is taken to be

$$F_{\downarrow} = r\ (C'_o - C'_f)\ (1 + \alpha s) \qquad (62)$$

The values of the rate of sedimentation of available silicon, $F_{\downarrow}$, are given in Table 52. The product of the two terms in parentheses is referred to as the corrected available silicon.

A comparison of the downward flux of available silicon with the upward flux of SRS indicates that for cores 14A and 63 there is essentially a balance. In cores 18A and 53 there appears to be a considerably greater SRS flux than can be matched by the supply of available silicon. Because of the many uncertainties in the comparisons it is not possible to identify the probable reasons for the mismatch. It should be emphasized that the calculation of SRS fluxes based on surface gradients is extremely sensitive to small losses of sediment or other disturbances of sediment during coring. Thus, in a core such as 18A where the gradients at z=0 is very large, a loss of even a few mm of sediment can introduce a factor of two change (increase) in the computed value. In core 53 there is a stratigraphic discontinuity around 4 cm so that the formalism developed above may not be applicable at all to Si profiles in this core. In addition, the above formalism does not properly incorporate conservation of mass or solid/solution reaction kinetics and assumes steady-state conditions. A useful approach to rigorous quantitative modeling of the effect of bioturbation on the sediment-water interactions has been formulated specifically for the dissolution of silicon in marine sediments by Schink and Guinasso (1977) and Schink et al. (1975). The formalism is transferrable to the case of Great Lakes profundal sediments with certain modifications. While it is beyond the scope of the present report to actually develop solutions to a unified model for silicon dissolution, it is of value to provide an outline of the formalism as it emerges from the insights gained in this study.

In the original formulation of Schink et al. (1975) the non-steady state distributions of soluble reactive silicon and amorphous silicon were represented by two separate differential equations describing transport of these phases.

The equations given by Schink et al. (1975) are:

$$(\phi + K_D^*)\ \frac{\partial C}{\partial t} = \frac{\partial}{\partial z}\ (\phi D_e\ \frac{\partial C}{\partial z}) - v\ [\partial(\phi + K_D^*)\ C/\partial z] + K_B\ B\ (C_f - C)/C_f$$

$$\frac{\partial B}{\partial t} = \frac{\partial}{\partial z}\ (D_b\ \frac{\partial B}{\partial z}) - v\ (\frac{\partial B}{\partial z}) - K_B\ B\ (C_f - C)/C_f \qquad (63)$$

Where the terms have the following meaning:

ϕ = the porosity which is depth-dependent
K_D^* = the effective adsorption coefficient of dissolved species on associated solids
C = the concentration of SRS (μg Si/cm^3)
C_f = aqueous phase saturation concentration
C_o = concentration in overlying water
t = time in years
z = depth below the sediment-water interface (cm)
D_e = effective diffusion coefficient (cm^2/yr)
v = velocity of the sediment-water interface relative to incoming sediment particles (cm/yr)
K_b = first order dissolution rate constant (yr^{-1})
B = concentration of available silicon in the bulk phase (solids+fluids) of the sediment (μg Si/cm^3)
D_b = rate of vertical (biological) mixing of solid phases (cm^2/yr)

The most important boundary condition for the model is that the input flux of available silicon is equal to mixing redistribution plus advection, i.e.

$$F_{\downarrow} = - D_b \, (\partial B/\partial z)_o + v \, B_o \qquad (64)$$

Note that in the absence of mixing, $F_b = vB_o$ as assumed in the approximate calaculations above. For non-steady-state problems the time-dependence of the sediment silicon profiles results from the time-dependence of $F_{\downarrow}$ and C_o. Note that the mixing is described in terms of an eddy diffusion process. Robbins et al. (1977) have shown that this representation is acceptable for the action of the amphipod, Pontoporeia Hoyi, on sediments. The conveyor belt species such as Oligochaete worms transport sediment in a different way but the above formalism may still provide an adequate representation of their long-term interaction with sediments. The above formalism of Schink et al. (1975) assumes that the range of bioturbation is essentially infinite. In contrast, the results of the present study indicate that the range is quite limited in the Great Lakes, often not exceeding 3 or 4 cm depth. This is the principal modification required of the above set of equations. Another is that the advective terms are negligible. Thus, the equations above can be used as a basis for describing SRS and amorphous Si profiles if the proper depth-dependence of D_b is introduced. The simplest being that, below the depth of the mixed zone, D_b=0. It may also be necessary to introduce a depth-dependent effective diffusion coefficient D_e. Recent studies by Krezoski and Robbins (1980) using radiotracers have shown that the presence of benthos significantly enhances the value of D_e within the mixed zone.

Guinasso and Schink (1977) and Schink et al. (1975) assume that the change in SRS concentration in a given segment of sediment due to reactions with solid phases is given by a term which couples solid and solution phase concentrations, namely:

$$(\phi + K_D^*) \left.\frac{\partial C}{\partial t}\right|_{\text{reactions}} = K_b \, B \, (C_f - C)/C_f \qquad (65)$$

While this form is probably adequate to describe the SRS and amorphous silicon profiles, its validity needs to be ascertained for freshwater sediments under carefully controlled laboratory conditions.

LITERATURE CITED

Alberts, J. J., L. J. Tilly and T. J. Vigerstad. 1979. Seasonal cycling of Cesium-137 in a reservoir. Science 203: 649-651.

Anikouchine, W. A. 1967. Dissolved chemical substances in compacting marine sediments. J. Geophys. Res. 72: 505-509.

Barron, M. A. 1976. Concentration and distributive behavior of cadmium and other selected heavy metals in sediments of southern Lake Huron. University of Michigan, Ph.D. Thesis. 284 pp.

Barry, P. J. 1973. Estimating dose commitments to populations from radioactive waste disposals into large lakes. In Environmental Behavior of Radionolides Released in the Nuclear Industry. International Atomic Energy Agency, Vienna, Austria. IAEA-SM-172/43. pp.99-505.

Batac-Catalan, Z., J. R. Krezoski, J. A. Robbins, and D. S. White. 1980. Distribution and abundance of zoobenthos in the muddy deposits of Saginaw Bay, Lake Huron. 23rd Conf. on Great Lakes Research of the International Association for Great Lakes Research, Kingston, Ontario. May 19-22. Abstracts p. 63.

Bien, G. S. 1952. Chemical Analysis Method: Univ. California, Scripps. Inst. Oceanogr. Ann. Rept., Ref. 52-58. 9 pp.

Berner, R. A. 1975. Diagenetic models of dissolved species in the interstitial water of compacting sediments. Amer. Jour. Sci. 275: 88-96.

Bray, J. T., O. P. Bricker, and B. N. Troup. 1973. Phosphate in interstitial waters of anoxic sediments: Oxidation effects during sampling procedure. Science. 180: 1362-1364.

Bruland, K. W., M. Koide, C. Bowser, and E. D. Goldberg. 1975. Lead-210 and pollen geochronologies on Lake Superior sediments. Quater. Res. 5: 89-98.

Chambers, R. and B. Eadie. 1980. Nephloid layer and suspended particulate matter in southeastern Lake Michigan. Sedimentology (In press May, 1980).

Clay, E. M. and J. Wilhm. 1979. Particle size, percent organic carbon, phosphorus, mineralogy and deposition of sediments in Ham's and Arbuckle Lakes. Hydrobiologia 65: 33-38.

Eakins, J. D. and R. T. Morrison. 1974. Dating Lake sediments by the determination of Polonium-210. In J. E. Johnston and T. V. Sutter (eds.) United Kingdom Atomic Energy Authority Research Group, Environ. Med. Sci. Div., Progr. Rept. for 1973, Harwell. AERE-PR/EMS 1. pp. 10-12.

Edgington, D. N. and J. A. Robbins. 1976. Records of lead deposition in Lake Michigan sediments since 1800. Environ. Sci. Techol. 10: 266-274.

Elliott, J. M. 1971. Some methods for the statistical analysis of samples of benthic invertebrates. Freshwater Biol. Assoc. Sci. Publ. 25. 144 pp.

Farmer, J. G. 1978. Lead concentration profiles in lead-210 dated Lake Ontario sediment cores. Sci. Total Environ. 10: 117-127.

Fingleton, D. J. and J. A. Robbins. 1980. Trace elements in air over Lake Michigan near Chicago during September, 1973. J. Great Lakes Res. 6: 22-37.

Flanagan, F. J. 1973. 1972 Values for international geochemical reference samples. Geochim. Cosmochim. Acta. 37: 1189-1200.

Flynn, W. W. 1968. The determination of low levels of polonium-210 in environmental samples. Anal. Chim. Acta. 43: 221-227.

Fordyce, J. S. 1975. Air pollution source identification. In Proc. Second Federal Conf. on the Great Lakes. Prepared by Argonne National Laboratory for the Interagency Committee on Marine Science and Engineering, March 25-27, 1975. 525 pp.

Frye, J. C. and N. F. Shimp. 1973. Major, minor and trace elements in sediments of late Pleistocene Lake Saline compared with those in Lake Michigan sediments. Ill. State Geological Survey, Environmental Geology Notes, EGN-60, Jan. 1973. 13 pp.

Gatz, D. F. 1975. Wet deposition estimation using scavenging ratios. In Proc. First Specialty Symposium on Atmospheric Contribution to the Chemistry of Lake Waters. Internat. Assoc. Great Lakes Res. Sept. 28 - Oct. 1, 1975. pp. 21-32.

Hodge, V. F., S. L. Seidel, and E. D. Goldberg. 1979. Determination of tin (IV) and organotin compounds in natural waters, coastal sediments and macro algae by atomic absorption spectrometry. Anal. Chem. 51: 1256-1259.

Holtzman, R. B. 1963. Measurement of the natural contents of RaD (Pb^{210}) and RaF (Po^{210}) in human bone-estimates of whole-body burdens. Health Phys. 9: 385-400.

Hongve, D. and A. H. Erlandsen. 1979. Shortening of surface sediment cores during sampling. Hydrobiologia 65: 283-287.

Hurd, D. C. 1973. Interactions of biogenic opal, sediment and seawater in the central equatorial pacific. Geochim. Cosmochim. Acta. 37: 2257-2282.

International Joint Commission. 1977. The Waters of Lake Huron and Lake Superior. Volume II (Parts A and B). Editorial committee M. P. Bratzel, M. E. Thompson and R. T. Bowden, International Joint Commission, Upper Lakes Reference Group, Windsor, Ontario. 743 pp.

Kamp-Nielsen, L., and B. T. Hargrave. 1978. Influence of bathymetry on sediment focusing in Lake Esrom. Verh. Internat. Verein. Limnol. 20: 714-719.

Kemp, A. L. W. and R. L. Thomas. 1976a. Cultural impact on the geochemistry of the sediments of Lakes Ontario, Erie and Huron. Proc. of Symposium on the Great Lakes, Geol. Assoc. Can. and N.E. Section, Geol. Soc. America, Waterloo, 1975.

Kemp, A. L. W. and R. L. Thomas. 1976b. Cultural impact on the geochemistry of the sediments of Lakes Ontario, Erie and Huron. Geosci. Can. 3: 191-207.

Kemp, A. L. W. and R. L. Thomas. 1976c. Impact of man's activities on the chemical composition in the sediments of Lakes Ontario, Erie and Huron. Water, Air and Soil Pollution 5: 469-490.

Kemp, A. L. W., T. W. Anderson, R. L. Thomas, A. Mudrochova. 1974. Sedimentation rates and recent sediment history of Lakes Ontario, Erie and Huron. J. Sediment Petrol. 44: 207-218.

Kolpack, R. L. and S. A. Bell. 1968. Gasometric determination of carbon in sediments by hydroxide adsorption. J. Sed. Petrol. 38:620-623.

Krezoski, J. R. and J. A. Robbins. 1980. Radiotracer studies of solute and particle transport in sediments by freshwater macrofauna. 23rd Conference on Great Lakes Research of the International Association for Great Lakes Research. Kingston, Ontario. May 19-22. Abstracts p. 42.

Krezoski, J. R., S. C. Mozley, and J. A. Robbins. 1978. Influence of benthic macroinvertebrates of mixing of profundal sediments in southeastern lake sediments. Limnol. Oceanogr. 23: 1011-1016.

Krishnaswami, S., D. Lal, J. M. Martin, and M. Meybeck. 1971. Geochronology of lake sediments. Earth Plant. Sci. Lett. 11: 407-414.

Lawrence, K. E., M. White, and R. A. Potts. 1980. Cold-vapor determination of mercury. Anal. Chem. (In press. June, 1980).

Lehman, J. T. 1975. Reconstructing the rate of accumulation of lake sediment: the effect of sediment focusing. Quat. Res. 5: 541-550.

Lerman, A. 1970: Strontium-90 in the Great Lakes: concentration-time model. J. Geophys. Res. 77: 3256-3264.

Lerman, A. 1975. Maintenance of steady state in oceanic sediments. Am. J. Sci. 275: 609-635.

Lerman, A. and T. A. Lietzke. 1975. Uptake and migration of tracers in lake sediments. Limnol. Oceanogr. 20: 497-510.

Lerman, A. and R. Weiler. 1970. Diffusion and accumulation of chloride and sodium in Lake Ontario sediment. Earth Planet. Sci. Lett. 10: 150-156.

Li, Y. and S. Gregory. 1974. Diffusion of ions in sea water and in deep sea sediments. Geochim. Cosmochim. Acta. 38: 703-714.

McKyes, E., A. Sethi, and R. N. Young. 1974. Amorphous coatings in particles of sensitive clay soils. Clays and Clay Miner. 22: 427-433.

Nriagu, J. O. 1978. Dissolved silica in pore waters of Lakes Ontario, Erie and Superior sediments. Limnol. Oceanogr. 23: 53-67.

Nriagu, J. O., A. L. W. Kemp, H. K. T. Wong, and N. Harper. 1979. Sedimentary record of heavy metal pollution in Lake Erie. Geochim. Cosmochim. Acta. 43: 247-258.

Parker, J. I. and D. N. Edgington. 1976. Concentration of diatom frustules in Lake Michigan sediment cores. Limnol. Oceanogr. Note 21: 887-893.

Parker, J. I., H. L. Conway, and E. M. Yaguchi. 1977. Dissolution of diatom frustules and recycling of amorphous silicon in Lake Michigan. J. Fish. Res. Board Can. 34: 545-551.

Ramakrishna, T. V., J. W. Robinson, and P. W. West. 1969. Determination of phosphorus, arsenic or silicon by atomic absorption spectrometry of molybdenum heteropoly acids. Anal. Chim. Acta. 45: 43-49.

Reeburgh, W. 1967. An improved interstitial water sampler. Limnol. Oceanogr. 12: 163-165.

Remmert, K. M., J. A. Robbins, and D. N. Edgington. 1977. Release of dissolved silica from sediments of the Great Lakes. 20th Annual Conference on Great Lakes Research of the International Association for Great Lakes Research. May 10-12.

Robbins, J. A. 1976. The role of sediments in the silica budget of the Great Lakes. 10th Great Lakes Regional Meeting of the American Chemical Society, Northwestern University, Evanston, Il. June 17-19. Abstracts, pp. 206-207.

Robbins, J. A. 1977. Recent sedimentation rates in southern Lake Huron and in Saginaw Bay. 40th Ann. Meeting of the American Society of Limnology and Oceanography, Lansing, Michigan. June 20-23, 1977. Abstr.

Robbins, J. A. 1978. Geochemical and geophysical applications of radioactive lead. In J. O. Nriagu (ed), The Biogeochemistry of Lead in the Environment. Elsevier/North-Holland Biomedical Press, New York. pp. 285-393.

Robbins, J. A. and E. Callender. 1975. Diagenesis of manganese in Lake Michigan sediments. Am. J. Sci. 275: 512-533.

Robbins, J. A. and D. N. Edgington. 1974. Stable lead geochronology of fine-grained sediments in southern Lake Michigan. Radiological and Environmental Research Division Annual Report, Ecology, Argonne National Laboratory, Argonne, Ill. Jan.-Dec., 1974, ANL-75-3 Part III. pp. 32-39.

Robbins, J. A. and D. N. Edgington. 1975. Determination of recent sedimentation rates in Lake Michigan using Pb-210 and Cs-137. Geochim. Cosmochim. Acta. 39: 285-304.

Robbins, J. A., and D. N. Edgington. 1979. Release of dissolved silica sediment of Lake Erie. 22nd Annual Conference on Great Lakes Research of the International Association for Great Lakes Research, May 1-13. Abstracts, pp. 19.

Robbins, J. A. and J. Gustinis. 1976. A squeezer for efficient extraction of pore water from small volumes of anoxic sediment. Limnol. Oceanogr. 21: 905-909.

Robbins, J. A. and F. Snitz. 1972. Bromine and chlorine loss from lead halide automobile exhaust particulates. Environ. Sci. Technol. 6: 164-169.

Robbins, J. A., D. N. Edgington, and J. I. Parker. 1974. Distribution of amorphous, diatom frustule and dissolved silica in a lead-210 dated core from southern Lake Michigan. Radiological and Environmental Research Division Annual Report, Ecology, Argonne National Laboratory, Argonne, Ill. Jan.-Dec., 1974. ANL-75-3 pp. 14-31.

Robbins, J. A., J. R. Krezoski, and S. C. Mozley. 1977. Radioactivity in sediments of the Great Lakes: Post-depositional redistribution by deposit-feeding organisms. Earth Planet. Sci. Lett. 36: 325-333.

Robbins, J. A., D. N. Edgington and A. L. W. Kemp. 1978. Comparative lead-210, cesium-137 and pollen geochronologies of sediments from Lakes Ontario and Erie. Quater. Res. 10: 256-278.

Rossmann, R. 1975. Chemistry of nearshore surficial sediments from southeastern Lake Michigan. Great Lakes Res. Div., Spec. Rept. No. 57, Univ. of Michigan, Ann Arbor. 62 pp.

Ruch, R. R., E. J. Kennedy, and N. F. Shimp. 1970. Distribution of arsenic in unconsolidated sediments from southern Lake Michigan. Ill. State Geological Survey, Environmental Geology Notes, EGN-37. 16 pp.

Shimp, N. F., J. A. Schleicher, R. R. Ruch, D. B. Heck, and H. V. Leland. 1971. Trace element and organic carbon accumulation in the most recent sediments of southern Lake Michigan. Ill. State Geol. Surv., Environ. Geol. Notes, No. 41. 25 pp.

Schink, D. R. and N. L. Guinasso, Jr. 1977. Effects of bioturbation on sediment-seawater interaction. Marine Geol. 23: 133-154.

Schink, D. R., N. L. Guinasso, and K. A. Fanning. 1975. Processes affecting the concentration of silica at the sediment-water interface of the Atlantic Ocean. J. Geophys. Res. 80: 3013-3031.

Shiomi, M. T. and K. W. Kuntz. 1973. Great Lakes precipitation chemistry: Part I. Lake Ontario Basin. In Proc. 16th Conf. Great Lakes Res. of the Internat. Assoc. Great Lakes Res., pp. 581-602.

Strickland, J. D. H. and T. R. Parsons. 1960. A manual of sea water analysis. Fisheries Research Board, Canada, Bull. No. 125. Ottawa. 185 pp.

Sutherland, J. C., J. R. Kramer, L. Nichols, and T. D. Kurtz. 1966. Mineral-water equilibria, Great Lakes: Silica and phosphorus. In Proc 9th Conf. Great Lakes Res. of the Internat. Assoc. Great Lakes Res., pp. 439-445.

Thomas, R. L. 1972. The distribution of mercury in the sediments of Lake Ontario. Can. J. Earth Sci. 9: 636-651.

Thomas, R. L. 1973. The distribution of mercury in the surficial sediments of Lake Huron. Can. J. Earth Sci. 10: 194-204.

Thomas, R. L., A. L. Kemp, and C. F. M. Lewis. 1973. The surficial sediments of Lake Huron. Can. J. Earth Sci. 10: 226-271.

Troup, B. N., O. P. Bricker, and J. T. Bray. 1974. Oxidation effect on the analysis of iron in the interstitial water of recent anoxic sediments. Nature 249: 237-239.

Wahlgren, M. W., J. A. Robbins, and D. N. Edgington. 1980. Plutonium in the Great Lakes, In Transuranics in the Environment (W. C. Hanson, Ed.), U. S. Dept. of Energy (TID-22800). (In Press, April 1980).

Walters, L. J. and T. J. Wolery. 1974. Transfer of heavy metal pollutants from Lake Erie bottom sediments to the overlying water. State of Ohio Water Resources Center, Completion Report No. 421X. 84 pp.

Walters, L. J., T. J. Wolery, and R. D. Myser. 1974. Occurrence of As, Cd, Co, Cr, Fe, Hg, Ni, Sb and Zn in Lake Erie sediments. In Proc 17th Conf. Great Lakes Res. of the Internat. Assoc. Great Lakes Res. Part I. pp. 219-234.

Weiler, R. 1973. The interstitial water composition in the sediments of the Great Lakes. I. Western Lake Ontario. Limnol Oceanogr. 18: 918-931.

Williams, J. D. H., T. P. Murphy and T. Mayer. 1976. Rates of accomulation of phosphorus forms in Lake Erie sediments. J. Fish. Res. Board Can. 33: 430-439.

Winchester, J. W. and G. D. Nifong. 1971. Water pollution in Lake Michigan from pollution aerosol fallout. Water, Air and Soil Pollut. 1: 50-64.

Wollast, R. and R. M. Garrels. 1971. Diffusion coefficient of silica in sea water. Nature Phys. Sci. 229: 94-95.

Zobell, C. E. 1946. Studies of redox potentials of marine sediments. Bull. Am. Assoc. Petrol. Geologists. 30: 477-513.

ARTICLES PRESENTED OR PUBLISHED RECEIVING EPA SUPPORT

Robbins, J. A. The role of sediments in the silica budget of the Great Lakes. Invited paper for the 10th Great Lakes Regional Meeting of the American Chemical Society, Northwestern University, Evanston, Ill., June 17-19, 1976. Abstracts p. 206-207.

Burin, G. and J. A. Robbins. Polychlorinated byphenyls (PCBs) in dated sediment cores from southern Lake Huron and Saginaw Bay. 20th Annual Conferences on Great Lakes Research of the International Association for Great Lakes Research, Ann Arbor, Michigan. May 10-12, 1977.

Johansen, Kjell A. and J. A. Robbins. Fallout cesium-137 in sediments of southern Lake Huron and Saginaw Bay. Ibid.

Krezoski, J. R. and J. A. Robbins. Radioactivity in sediments of the Great Lakes: post-depositional redistribution by deposit-feeding organisms. Ibid.

Remmert, K. M., J. A. Robbins and D. N. Edgington. Release of dissolved silica from sediments of the Great Lakes. Ibid.

Robbins, J. A. Recent sedimentation rates in southern Lake Huron and Saginaw Bay. Ibid.

Ullman, W. and J. A. Robbins. Major and minor elements in sediments of southern Lake Huron and Saginaw Bay: patterns and rates of deposition, historical records and interelement associations. Ibid.

Robbins, J. A., Limnological applications of natural and fallout radioactivity in the Great Lakes, Symposium on limnology of the Great Lakes, 40th annual meeting of the American Society of Limnology and Oceanography, East Lansing, Michigan, June 20-23, 1977.

Robbins, J. A., McCall, P., Fisher, J. B. and Krezoski, J. R. Effect of deposit feeders on migration of radiotracers in lake sediments. American Society of Limnology and Oceanography, 41st Annual Meeting, Victoria, British Columbia, June 19-22, 1978.

Robbins, J. A., and Johansen, K. A., Cesium-137 in the sediments of Lake Huron. Ibid., p. 10.

Robbins, J. A. Radiotracer studies of sediment reworking by freshwater macrobenthos. Forty-second Annual Meeting of the American Society of Limnology and Oceanography, Inc. Marine Sciences Research Center, State University of New York, Stoney Brook, N. Y. June 18-21, 1979. Abstracts P. 100.

Robbins, J. A. Aspects of the interaction between benthos and sediments in the North American Great Lakes and effects of toxicant exposures. Invited paper for the Symposium on the Theoretical Aspects of Aquatic Toxicology, Borok, USSR, July 3-5, 1979.

Robbins, J. A. Accumulation of tin and other metal contaminants in sediments of southern Lake Huron. The XXIst Congress of the International Association of Theoretical and Applied Limnology, Kyoto, Japan, Aug. 24-31, 1980.

Robbins, J. A. and J. Gustinis, A squeezer for efficient extraction of pore water from small volumes of anoxic sediment. Limnol. and Oceanogr., 21, (1976) 905-909.

Robbins, J. A. Geochemical and geophysical applications of radioactive lead isotopes. In: Biogeochemistry of lead in the Environment, Part A., J. O. Nriagu (Ed.), Elsevier Scientific Publishers, Amsterdam, Netherlands. Vol. 1A. (1978) 285-393.

Robbins, J. A., J. R. Krezoski and S. C. Mozley. Radioactivity in sediments of the Great Lakes: postdepositional redistribution by deposit-feeding organisms. Earth Planet. Sci. Lett. 36, (1977) 325-333 .

Krezoski, J. R., S. C. Mozley and J. A. Robbins. Influence of benthic macroinvertebrates on mixing of profundal sediments in Lake Huron. Limnol. Oceanogr. 23 (1978) 1011-1016.

Robbins, J. A., P. L. McCall, J. B. Fisher and J. R. Krezoski, Effect of deposit feeders on migration of cesium-137 in lake sediments. Earth Planet. Sci. Lett. 42 (1979) 277-287.

Meyers, P. A., Takeuchi, N. and Robbins, J. A. Petroleum hydrocarbons in sediments of Saginaw Bay, Lake Huron. Environ. Sci. Technol. (submitted Aug. 1979).

Robbins, J. A. Aspects of the interaction between benthos and sediments of the North American Great Lakes and effects of toxicant exposures. In Proc. of the US-USSR Symposium on Theoretical Aspects of Aquatic Toxicology, Borok, Jaroslavl, USSR, July 3-5, 1979.